R-06-12

Hydrogeochemical evaluation

Preliminary site description Laxemar subarea – version 1.2.

Svensk Kärnbränslehantering AB

April 2006

Svensk Kärnbränslehantering AB
Swedish Nuclear Fuel
and Waste Management Co
Box 5864
SE-102 40 Stockholm Sweden
Tel 08-459 84 00
+46 8 459 84 00
Fax 08-661 57 19
+46 8 661 57 19

ISSN 1651-4416
SKB R-06-12

Hydrogeochemical evaluation

Preliminary site description
Laxemar subarea – version 1.2.

Svensk Kärnbränslehantering AB

April 2006

Preface

This work forms part of the Initial Site Investigation (ISI) stage of the hydrogeochemical evaluation carried out at the Simpevarp area leading to a Hydrogeochemical Site Descriptive Model version 1.2 of Laxemar subarea. SKB's ChemNet (former HAG) consisting of independent consultants and university personnel, carried out the modelling during the period November 2004 to September 2005. The INSITE and SIERG review comments on the earlier model versions of Simpevarp and Forsmark were considered where possible in this work. Several groups within ChemNet were involved and the evaluation was conducted independently using different approaches ranging from expert knowledge to geochemical and mathematical modelling including also transport modelling. During regular ChemNet meetings the results were presented and discussed. The ChemNet members contributing to this report where (in alphabetic order):

Luis Auqué, University of Zaragoza, Appendix 3
María Gimeno, University of Zaragoza, Appendix 3
Javier Gómez, University of Zaragoza, Appendix 3
Ioana Gurban, 3D-Terra, Montreal, Appenix 4
Lotta Hallbeck, Vita vegrandis, Göteborg, Appendix 2
Marcus Laaksoharju, Geopoint AB, Stockholm, Appendix 4
Jorge Molinero, University of Santiago de Compostela, Appendix 5
Teresita Morales, SKB, Oskarshamn, Appendix 1
Juan Raposo, University of Santiago de Compostela, Appendix 5
John Smellie, Conterra AB, Stockholm, Appendix 1
Eva-Lena Tullborg, Terralogica AB, Gråbo, Appendix 1
Nicklaus Waber, University of Bern, Appendix 1

The different modelling approaches applied on the same data set and the similarities in the results gave added confidence to the modelling results presented in this report.

Marcus Laaksoharju
ChemNet leader and editor

Summary

Siting studies for SKB's programme of deep geological disposal of nuclear fuel waste currently involves the investigation of two locations, Simpevarp and Forsmark, on the eastern coast of Sweden to determine their geological, hydrogeochemical and hydrogeological characteristics. Present work completed has resulted in Model version 1.2 for Laxemar subarea which represents the third evaluation of the available Simpevarp area groundwater analytical data collected up to November, 2004 (i.e. the third "data freeze" of the site). The ChemNet group (former HAG) had access to relatively few new samples from boreholes in the Laxemar subarea that were not already evaluated during the Simpevarp 1.2 phase. The Laxemar 1.2 hydrochemical evaluation involved data from five cored boreholes and 14 percussion boreholes from the Laxemar subarea, three cored boreholes and 4 percussion boreholes from the Simpevarp penninsula, and two cored boreholes and 10 percussion boreholes from Ävrö island.

Model version 1.2 focusses on improving the methodology and tools used for evaluating the hydrochemistry combined with a sensitivity and uncertainty analysis of the available data. The major goal has been to consolidate groundwater geochemical understanding and the models used at the site.

The complex groundwater evolution and patterns at Simpevarp are a result of many factors such as: a) the present-day topography and proximity to the Baltic Sea, b) past changes in hydrogeology related to glaciation/deglaciation, land uplift and repeated marine/lake water regressions/transgressions, and c) organic or inorganic alteration of the groundwater composition caused by microbial processes or water/rock interactions. The sampled groundwaters reflect to various degrees processes relating to modern or ancient water/rock interactions and mixing.

The groundwater flow regimes at Laxemar/Simpevarp are considered local and extend down to depths of around 600–1,000 m depending on local topography. Close to the Baltic Sea coastline where topographical variation is small, groundwater flow penetration to depth will subsequently be less marked. In contrast, the Laxemar subarea is characterised by higher topography resulting in a much more dynamic groundwater circulation which appears to extend to 1,000 m depth in the vicinity of borehole KLX02. The marked differences in the groundwater flow regimes between the Laxemar and Simpevarp are reflected in the groundwater chemistry where four major hydrochemical groups of groundwaters (types A–D) have been identified:

Type A: Shallow (< 200 m) at Simpevarp but deeper (down to ~ 800 m) at Laxemar subarea. Dilute groundwater (< 2,000 mg/L Cl; 0.5–3.5 g/L TDS); $\delta^{18}O$ = –11 to –8‰ SMOW. Mainly meteoric and Na-HCO_3 in type. Redox: Marginally oxidising close to the surface, otherwise reducing. Main reactions: Weathering; ion exchange (Ca, Mg); dissolution/precipitation of calcite; redox reactions (e.g. precipitation of Fe-oxyhydroxides); microbially-mediated reactions (SRB) which may lead to formation of pyrite. Mixing processes: Mainly meteoric recharge water at Laxemar subarea; potential mixing of recharge meteoric water and a modern sea component at Simpevarp subarea; localised mixing of meteoric water with deeper saline groundwaters at Laxemar and Simpevarp subareas.

Type B: Shallow to intermediate (150–600 m) at Simpevarp but deeper (down to ~ 500–950 m) at Laxemar subarea. Brackish groundwater (2,000–10,000 mg/L Cl; 3.5–18.5 g/L TDS); δ = –14 to –11‰ SMOW. B_L – Laxemar subarea: Meteoric, mainly Na-Ca-Cl in type; Glacial/Deep saline components. B_S – Simpevarp subarea: Meteoric mainly Na-Ca-Cl in type but some Na-Ca(Mg)-Cl(Br) types (± marine, e.g. Littorina); Glacial/Deep saline components. Redox: Reducing. Main reactions: Ion exchange (Ca, Mg); precipitation of calcite; redox reactions (e.g. precipitation of pyrite). Mixing processes: Potential residual Littorina Sea (old marine) component at Simpevarp, more evident in some fracture zones close to or under the Baltic Sea; potential glacial component at Simpevarp and Laxemar subareas; potential deep saline (non-marine) component at Simpevarp and at Laxemar subareas.

Type C: Intermediate to deep (~ 600–1,200 m) at Simpevarp but deeper (900–1,200 m) at Laxemar subarea. Saline (10,000–20,000 mg/L Cl; 18.5–30 g/L TDS); δ = ~ –13‰ SMOW. Dominantly Ca-Na-Cl in type at Laxemar but Na-Ca-Cl changing to Ca-Na-Cl only at the highest salinity levels at Simpevarp subarea; increasingly enhanced Br/Cl ratio and SO_4 content with depth at both

Simpevarp and Laxemar subareas; Glacial/Deep saline mixtures. Redox: Reducing. Main reactions: Ion exchange (Ca). Mixing processes: Poential glacial component at Simpevarp and Laxemar subareas; potential deep saline (i.e. non-marine) and an old marine component (Littorina?) at shallower levels at Simpevarp subarea; Deep saline (non-marine) component at Laxemar subarea.

Type D: Deep (> 1,200 m) only identified at Laxemar subarea. Highly saline (> 20,000 mg/L Cl; to a maximum of ~ 70 g/L TDS); δ = > –10‰ SMOW. Dominantly Ca-Na-Cl with higher BrCl ratios and a stable isotope composition that deviates from the GMWL when compared to Type C groundwaters; Deep saline/brine mixture; Diffusion dominant transport process. Redox: Reducing. Main reactions: Water/rock reactions under long residence times. Mixing processes: Probably long term mixing of deeper, non-marine saline component driven by diffusion.

Characterisation of pore water in core samples from the Laxemar borehole, KLX03, shows that chemical and isotopic pore water signatures have a characteristic variation of groundwater composition with rock type and depth that is in close agreement with the general trends in hydrochemistry of the adjacent formation (fracture) groundwaters. There is little apparent evidence of a glacial melt signature in the pore waters. Pore waters at depth show an affinity with deep brine evolution. Steady state conditions between pore water and formation groundwaters in the fractures are essentially only developed in the shallow zone of the Ävrö granite, while at depths greater than 450 m the chemical and isotopic composition of the pore water differs markedly from that of the fracture groundwaters in fractures. Diffusion between rock pore water and adjacent fracture groundwaters is identified as the dominant transport process; calculated diffusion coefficients agree well with current knowledge of conditions in the Laxemar site.

There are no new representative samples from repository depth from the Laxemar subarea so samples from earlier sampled boreholes were used to check if they meet the SKB chemical suitability criteria for groundwaters at repository depth for Eh, pH, TDS, DOC and Ca+Mg. The samples from from KLX01: 680–702 m (sampled in 1988) and KLX02: 798–803 m (sampled in 1993) were selected for this purpose. The evaluation shows that these samples can meet the SKB suitability criteria for the analysed parameters.

In this report the models and the site understanding have been consolidated. Despite relatively few new data from depth, the models have been updated and the further understanding gained of groundwater origin, groundwater evolution, reactions, studies of interaction between shallow and deep groundwater, pore water composition in bedrock, microbial depth variation, uncertainties of the mixing calculations, tritium variations with time and 3D visualisation of the spatial variability of groundwater properties. An updated Hydrogeochemical Site Descriptive Model version 1.2 for Laxemar subarea has evolved. The resulting description has improved compared with the 1.2 version for Simpevarp subarea by producing a more detailed process modelling, uncertainty analysis and 3D visualisation. The microbial characterisation gives direct support to, for example, the redox modelling. The coupled transport modelling can address processes questions from an advective point of view which is of importance for the site understanding.

Contents

1 Introduction 9
1.1 Background 9
1.2 Scope and objectives 9
1.3 Setting 10
1.4 Methodology and organisation of work 11
1.4.1 Methodology 11
1.5 This report 11

2 Evolutionary aspects of Laxemar subarea 13
2.1 Premises for surface and groundwater evolution 13
2.1.1 Development of permafrost and saline water 13
2.1.2 Deglaciation and flushing by meltwater 13

3 Bedrock hydrogeochemistry 17
3.1 State of knowledge at the previous model version 17
3.2 Hydrogeochemical modelling 19
3.2.1 Modelling assumptions and input from other disciplines 19
3.2.2 Conceptual model with potential alternatives 20
3.3 Hydrogeochemical data 20
3.3.1 Groundwater chemistry data sampled in boreholes 21
3.3.2 Representativeness of the data 22
3.4 Explorative analysis 24
3.4.1 Borehole properties 24
3.4.2 Examples of evaluation of scatter plots 24
3.4.3 Descriptive observations – main elements 27
3.4.4 Descriptive observations – isotopes 29
3.4.5 Microbes 32
3.4.6 Colloids 33
3.4.7 Gas 34
3.4.8 Pore water composition in the rock matrix 34
3.4.9 Fracture fillings 36
3.4.10 Investigations of the geohistory of fracture minerals 37
3.4.11 Origin of brine water 37
3.5 Massbalance, reaction path and mixing calculations 38
3.5.1 Sensitivity and uncertainty analysis of the mixing models 40
3.6 Modelling of tritium transport 45
3.7 Conclusions used for the site descriptive model 48
3.7.1 Visualisation of the groundwater properties 48
3.7.2 Hydrochemical suitability criteria 66
3.8 Evaluation of uncertainties 67
3.9 Comparison between the hydrogeological and hydrogeochemical models 68

4 Resulting description of the Laxemar subarea 71
4.1 Bedrock hydrogeochemical description 71
4.1.1 Summary of groundwater types 72

5 Conclusions 75
5.1 Overall changes since previous model version 75
5.2 Overall understanding of the site 75
5.3 Implication for further modelling 75

6 Acknowledgements 77

7 References 79

Appendix 1 Explorative analysis and expert judgement of major components and isotopes 83

Appendix 2 Explorative analyses of microbes, colloids and gases 271

Appendix 3 PHREEQC modelling 303

Appendix 4 M3 calculations 341

Appendix 5 Coupled hydrogeological and solute transport modelling 379

1 Introduction

1.1 Background

SKB is conducting thorough investigations at two candidate sites for the eventual disposal of spent nuclear fuel. These sites are located in the municipalities of Simpevarp/Laxemar and Forsmark. The main objective is aimed at providing detailed proposals of how a deep repository can be constructed and operated. The investigations at Simpevarp-Laxemar commenced in 2002 and will take between four and eight years to complete.

The site selection and investigation phases encompass a sufficiently large scale in terms of time, space and content to make a breakdown into different stages necessary. At the end of the initial selection phase the site that is considered most suitable for a deep repository will be chosen. A few boreholes are drilled as part of an Initial Site Investigation (ISI) stage and the data they generate enables a decision to be made as to whether the site is still deemed suitable. The site and its immediate surroundings should cover an area of 5–10 km^2 in areal extent.

Provided that the preconditions established are still good, a Complete Site Investigation (CSI) stage follows. The main aim is to collect sufficient knowledge about the rock and its properties to enable SKB to conduct a safety analysis and produce both a site description and a construction plant description.

The surface/near-surface hydrological and groundwater chemistry studies include charting water courses, measuring stream discharge and taking water samples. Drilling is the most intensive activity conducted in which some 10–20 percussion boreholes will be made to a maximum depth of 200 m and an equal number of cored boreholes to depths of 500–1,000 m. An extensive hydrochemistry programme together with other investigation programmes will be conducted during and after the drilling.

1.2 Scope and objectives

The work presented here forms part of the ISI stage and the derived model described here represents the second and final ISI model based on measured data from the site investigation programme. As the investigations progress over the next years, several updated models (version 2.1, 2.2 and 2.3 within the CSI program) will be derived based on supplementary analytical data and groundwater samples from new boreholes at the Laxemar subarea and repeated sampling of existing boreholes.

The aim of the site modelling is to develop a hydrogeochemical Site Descriptive Model (SDM) according to the strategy described in /Smellie et al. 2002/. The first such model for Simpevarp was the “version 0” model /SKB 2002/ followed by Simpevarp 1.1 /Laaksoharju et al. 2004/ and Simpevarp 1.2 /SKB 2005/. The model presented in this report is Laxemar model version 1.2 which represents the first evaluation of the available Laxemar groundwater data collected up to November 2004 (i.e. the time of the “data freeze”).

ChemNet had access to water samples collected from the surface and subsurface environment (e.g streams and lakes and soil pipes in the overburden,); together with samples collected from drilled boreholes in the Simpevarp subarea and new and old boreholes from the Laxemar subarea. The deepest samples from Laxemar subarea reflected conditions down to about 1,700 m. At the time of modelling, many of the samples either lacked important analytical information that restricted their evaluation or the sampling or analytical quality was in question. The new samples reflected conditions down to about 200 m depth. Sampling from old boreholes reflects deep borehole conditions down to 1,700 m and beyond. Laxemar model version 1.2 focuses on consolidation of models constructed during Simpevarp 1.2 work, uncertainty evaluation of, for instance, mixing models and further integration with hydrogeological modelling.

1.3 Setting

The Laxemar subarea is situated about 350 km south of Stockholm and is located within the confines of the Oskarshamn nuclear power plant facility. The candidate area selected for the site investigations is divided into the Simpevarp area (regional area) and Laxemar and Simpevarp subareas (local areas). The Laxemar subarea is shown on an areal photograph in Figure 1-1 and as a map in Figure 3-2.

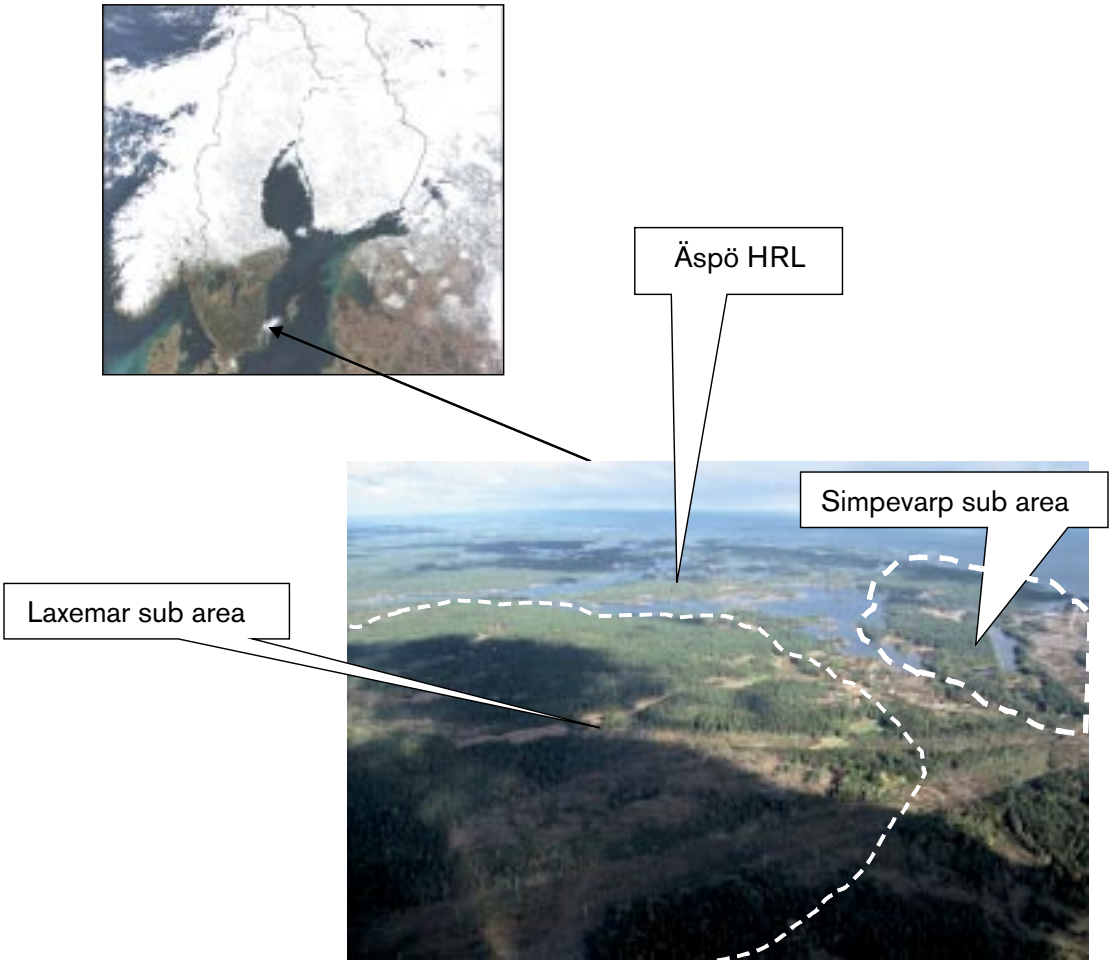

Figure 1-1. *Overview of the Laxemar sub area showing the area for detailed site investigation (dashed line).*

1.4 Methodology and organisation of work

1.4.1 Methodology

The main objectives of the Hydrogeochemical Site Descriptive Model for the Simpevarp area are to describe the chemistry and distribution of the groundwater in the bedrock and overburden and the processes involved in its origin and chemical evolution. The SKB hydrogeochemistry programme /Smellie et al. 2002/ is intended to fulfil two basic requirements: 1) to provide representative and quality assured data for use as input parameter values in calculating long-term repository safety, and 2) to understand the present undisturbed hydrogeochemical conditions and how these conditions will change in the future. Parameter values for safety analysis include pH, Eh, S, SO_4, HCO_3, PO_4 and TDS (mainly cations), together with colloids, fulvic and humic acids, other organics, bacteria and dissolved gases. These values will be used to characterise the groundwater environment at, above and below repository depths. When the hydrogeochemical environment has been fully characterised, this knowledge, together with an understanding of the past and present groundwater evolution, should provide the basis for predicting future changes. The site investigations will therefore provide important source material for safety analyses and the environmental impact assessment of the Simpevarp region.

1.5 This report

Chapters 1–6 of this report summarise the hydrogeochemical results collated and interpreted by ChemNet. These results will serve as input for the final Site Descriptive Model report which will integrate the results from all the geoscientific disciplines.

The main aim of this report is to attempt to integrate the different approaches of ChemNet to arrive at an overall interpretation of the presently available hydrogeochemical data from the Laxemar subarea. Chapter 2 describes the present ideas concerning the palaeoevolution of the Simpevarp region. Chapter 3 covers the integrated evaluation of the primary hydrogeochemical data and the quantitative modelling for the different modelling approaches attempted, the assumptions made, an evalua-tion of the uncertainties involved, and how such modelled results can best be visually presented. Chapter 4 summarises the hydrogeochemical description of the Laxemar subarea and Chapter 5 presents the main conclusions.

The detailed contributions of the three ChemNet modelling groups are presented in Appendices 1–5. Appendix 6 gives references to all the groundwater analytical data available at the ‘data freeze’ point. Appendix 7 gives references to the Nordic data used as background information for the modelling.

2 Evolutionary aspects of Laxemar subarea

2.1 Premises for surface and groundwater evolution

The first step in the groundwater evaluation is to construct a conceptual postglacial scenario model for the site (Figure 2-1) based largely on known palaeohydrogeological events from Quaternary geological investigations. This model can be helpful when evaluating data since it provides constraints on the possible groundwater types that may occur. Interpretation of the glacial/postglacial events that might have affected the Simpevarp area is based on information from various sources including /Fredén 2002, Påsse 2001, Westman et al. 1999/ and /SKB 2002/. This recent literature provides background information which is combined with more than 10 years of studies of groundwater chemical and isotopic information from sites in Sweden and Finland in together with various hydrogeological modelling exercises of postglacial hydrogeological events /Laaksoharju and Wallin, 1997, Luukkonen 2001, Pitkänen et al. 1998, Svensson 1996/. The presented model is therefore based on Quaternary geological facts, fracture mineralogical investigations and groundwater observations. These facts have been used to describe possible palaeo events that may have affected the groundwater composition in the bedrock.

2.1.1 Development of permafrost and saline water

When the continental ice sheet was formed at about 100,000 BP permafrost formation ahead of the advancing ice sheet probably extended to depths of several hundred metres. According to /Bein and Arad 1992/ the formation of permafrost in a brackish lake or sea environment (e.g. similar to the Baltic Sea) produced a layer of highly concentrated salinity ahead of the advancing freezing front. Since this saline water would be of high density, it would subsequently sink to lower depths and potentially penetrate into the bedrock where it would eventually mix with formational groundwaters of similar density. Where the bedrock was not covered by brackish lake or sea water, similar freeze-out processes would occur on a smaller scale within the hydraulically active fractures and fracture zones, again resulting in formation of a high-density saline component which would gradually sink and eventually mix with existing saline groundwaters. Whether the volume of high salinity water produced from brackish waters by this freeze-out process would be adequate to produce such widespread effects is presently under debate.

With continued evolution and movement of the ice sheet, areas previously subjected to permafrost would be eventually become covered by ice accompanied by a rise in temperature and slow decay of the underlying permafrost layer. Hydrogeochemically, this decay may have resulted in distinctive signatures being imparted to the groundwater and fracture minerals.

2.1.2 Deglaciation and flushing by meltwater

During subsequent melting and retreat of the ice sheet the following sequence of events is thought to have influenced the Simpevarp area (see Figure 2-1).

During the recession and melting of the continental ice sheet, glacial meltwater was hydraulically injected into the bedrock (> 14,000 BP) under considerable pressure close to the ice margin. The exact penetration depth is still unknown, but depths exceeding several hundred metres are possible according to hydrodynamic modelling /e.g. Svensson 1996/. Some of the permafrost decay groundwater signatures may have been disturbed or destroyed during this stage.

Different non-saline and brackish lake/sea stages then transgressed the Simpevarp area during the period c. 14,000–4,000 BP. Of these, two periods with brackish water can be recognised; Yoldia Sea (11,500 to 10,800 BP) and Littorina Sea starting at 9,500 and continuing to the present. The Yoldia period has probably resulted in only minor contributions to the subsurface groundwater since the water was very dilute to brackish because of the large volumes of glacial meltwater it contained. Furthermore, this period lasted only for 700 years. The Littorina Sea period in contrast had a maximum salinity of about twice that of the present Baltic Sea and this maximum prevailed at least from 6,500 to 5,000 BP; during the last 2,000 years the salinity has remained almost equal to the present

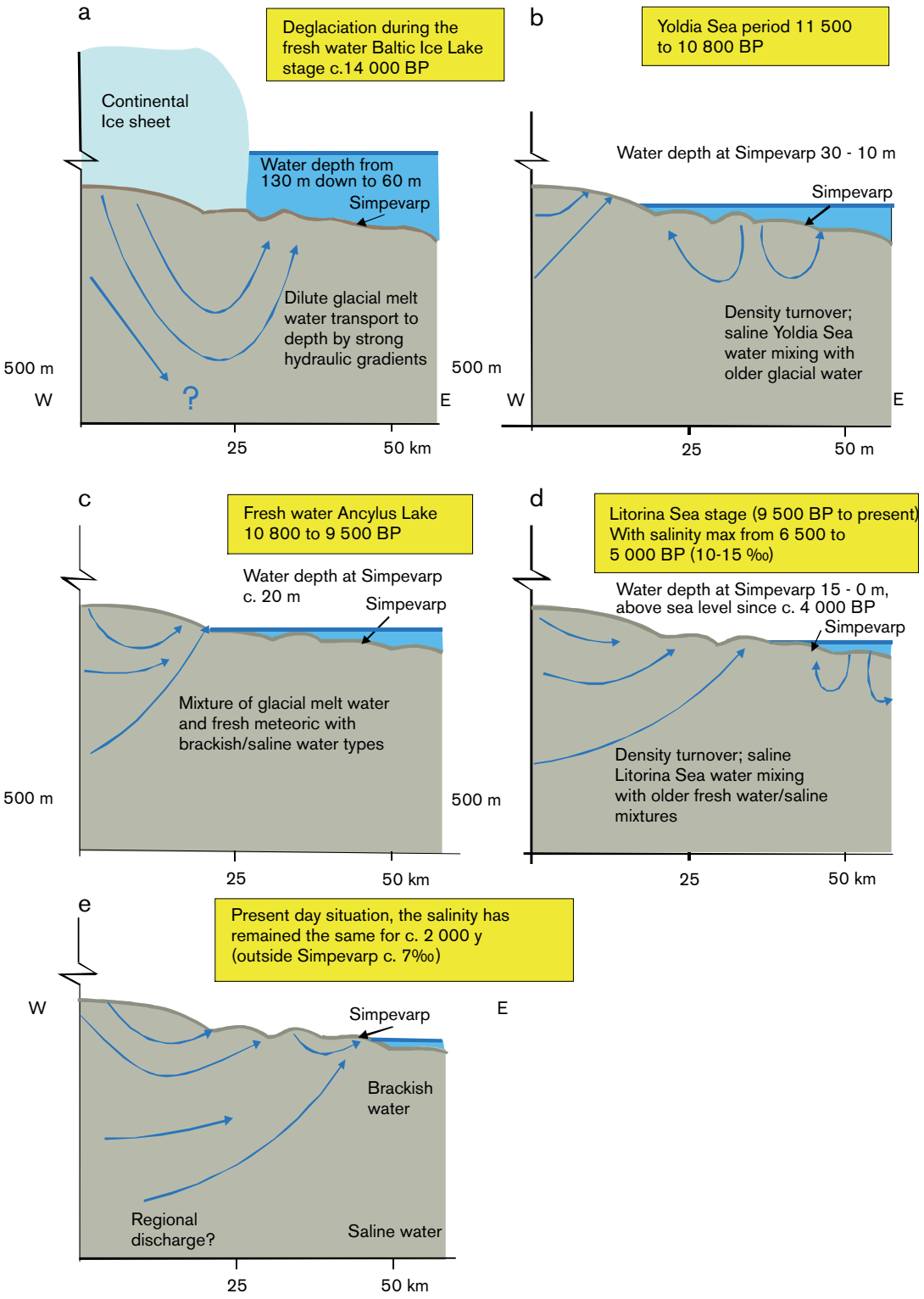

Figure 2-1. *Conceptual postglacial scenario model for the Simpevarp area. The figures show possible flow lines, density driven turnover events and non-saline, brackish and saline water interfaces. Possible relation to different known postglacial stages such as land uplift which may have affected the hydrochemical evolution of the site is shown: a) deglaciation of the continental ice, b) Yoldia Sea stage, c) Ancylus Lake stage, d) Littorina Sea stage, and e) present day Baltic Sea stage. From this conceptual model it is expected that glacial melt water and deep and marine water of various salinities have affected the present groundwater. Based on the shoreline displacement curve compiled by /Påsse 2001/ and information from /Fredén 2002, Westman et al. 1999/ and /SKB 2002/.*

Baltic Sea values /Westman et al. 1999 and references therein/. Because of increased density, the Littorina Sea water was able to penetrate the bedrock resulting in a density turnover which affected the groundwater in the more conductive parts of the bedrock. The density of the intruding seawater in relation to the density of the groundwater determined the final penetration depth. As the Littorina Sea stage contained the most saline groundwater, it is assumed to have had the deepest penetration depth, eventually mixing with the glacial/brine groundwater mixtures already present in the bedrock.

When the Simpevarp region was subsequently raised above sea level 5,000 to 4,000 years ago, fresh meteoric recharge water formed a lens on top of the saline water because of its low density. However, local hydraulic gradients resulting from higher topography to the west of the Simpevarp area may have flushed out varying amounts of these older waters, at least to depths of 100–150 m, with the freshwater lens mostly occupying these depths today depending on local hydraulic conditions.

Many of the natural events described above may in the future be repeated several times during the lifespan of a repository (thousands to hundreds of thousands of years). As a result of these events, brine, glacial, marine and meteoric waters are expected to be mixed in a complex manner at various levels in the bedrock, depending on the hydraulic character of the fracture zones, groundwater density variations and borehole activities prior to groundwater sampling. For the modelling exercise which is based on the conceptual model of the site, groundwater end members reflecting, for example, Glacial meltwater and Littorina Sea water composition, were added to the data set /cf Appendix 4/.

The uncertainty of the updated conceptual model increases with modelled time. The largest uncertainties are therefore associated with the stage showing the flushing of glacial melt water. The driving mechanism behind the flow lines in Figure 2-1 is the shore level displacement due to the land uplift.

3 Bedrock hydrogeochemistry

There are relatively few new groundwater samples from boreholes in the Laxemar subarea that were not already evaluated during the Simpevarp 1.2 modellingphase. Therefore, this work has focused more on improving the methodology and tools used for evaluating the hydrochemistry combined with a sensitivity and uncertainty analysis of the available data. The major goal has been to consolidate groundwater geochemical understanding and the models used at the site.

Evaluation of the hydrogeochemical data has been carried out by considering not only the samples from the Laxemar subarea, but also in relation to those from the Simpevarp subarea, Äspö and, in some cases, also related to the entire Fennoscandian hydrochemical dataset. Information from hydrogeochemical model versions based on previously investigated sites in Sweden and elsewhere, and information from ongoing geological and hydrogeological modelling in the Simpevarp subarea, were included in the evaluation when possible.

The evaluation and modelling of the hydrogeochemical data consist of manual evaluation and expert judgment (section 3.4) and mathematical modelling (sections 3.5 and 3.6), all of which must be combined when evaluating groundwater information. Visalisation techniques have been used to show the 3D geographical distribution of the different groundwater characteristics seen in the Simpevarp area (section 3.7).

The results of the detailed hydrogeochemical modelling described in this present chapter are used to produce an updated hydrogeochemical site descriptive model (section 4). The outcome of the hydrogeochemical modelling is used in, for example, the hydrogeological modelling, transport modelling and safety assessment modelling.

The results presented herein is a product of the collective effort made by the ChemNet analysis group.

3.1 State of knowledge at the previous model version

The first model of the Simpevarp area was the Site Descriptive Hydrogeochemical Model version 0 /SKB 2002/. Although there were few data from the Simpevarp regional model area to support a detailed hydrogeochemical site descriptive model, postglacial events believed to have affected the groundwater evolution and chemistry at Simpevarp were described in a conceptual model.

The model versions Simpevarp 1.1 /Laaksoharju et al. 2004/ and Simpevarp 1.2 /SKB 2004/ represented the evaluation of the available groundwater analytical data from the Simpevarp area with special emphasis on the Simpevarp subarea. The complex groundwater evolution and patterns at Simpevarp are a result of many factors such as: a) the present-day topography and proximity to the Baltic Sea, b) past changes in hydrogeology related to glaciation/deglaciation, land uplift and repeated marine/lake water regressions/transgressions, and c) organic or inorganic alteration of the groundwater composition caused by microbial processes or water/rock interactions. The sampled groundwaters reflect to various degrees processes relating to modern or ancient water/rock interactions and mixing.

The groundwater flow regimes at the Laxemar and Simpevarp subareas are considered local and extend down to depths of around 600–1,000 m depending on local topography. Close to the Baltic Sea coastline, where topographical variation is small, groundwater flow penetration to greater depth will subsequently be less marked. In contrast, the Laxemar subarea is characterised by higher topography resulting in a much more dynamic groundwater circulation which appears to extend to 1,000 m depth in the vicinity of borehole KLX02. The marked differences in the groundwater flow regimes between the Laxemar and Simpevarp subareas are reflected in the groundwater chemistry where four major hydrochemical groups of groundwaters (types A–D) have been identified (further development and visualisation of this modelling is discussed in Chapter 4):

Type A: This type comprises dilute groundwaters (< 2,000 mg/L Cl; 0.5–2.0 g/L TDS) of Na-HCO_3 type present at shallow (< 200 m) depths at Simpevarp, but at greater depths (0–900 m) at Laxemar. At both localities the groundwaters are marginally oxidising close to the surface, but otherwise reducing. Main reactions involve weathering, ion exchange (Ca, Mg), surface complexation, and dissolution of calcite. Redox reactions include precipitation of Fe-oxyhydroxides and some microbially-mediated reactions (SRB). Meteoric recharge water is mainly present at Laxemar whilst at Simpevarp potential mixing of recharge meteoric water and a modern sea component is observed. Localised mixing of meteoric water with deeper saline groundwaters is indicated at both Laxemar and Simpevarp.

Type B: This type comprises brackish groundwaters (2,000–6,000 mg/L Cl; 5–10 g/L TDS) present at shallow to intermediate depths (150–300 m) at Simpevarp, but at greater depths (approx. 900–1,100 m) at Laxemar. At Simpevarp the groundwaters are mainly Na-Ca-Cl in type but some Na-Ca(Mg)-Cl(Br) types also occur. At Laxemar there is a transition to more Ca-Na-Cl types with depth. The main reactions involve weathering, ion exchange (Ca, Mg) and dissolution/ precipitation of calcite. Redox reactions include precipitation of sulphides and some microbially-mediated reactions (SRB). At Simpevarp there is potentially some residual Littorina Sea (old marine) component, commonly in fracture zones close to or under the Baltic Sea. At both the Simpevarp and Laxemar sites there is a glacial component and also a deep saline (non-marine) component.

Type C: This type comprises reducing saline groundwaters (6,000–20,000 mg/L Cl; 25–30 g/L TDS) present at intermediate to deep (> 300 m) levels at Simpevarp, and at even greater depths (approx. 1,200 m) at Laxemar. At Simpevarp the groundwaters are mainly Na-Ca-Cl with increasingly enhanced Br and SO_4 with depth. At Laxemar they are mainly Ca-Na-Cl also with increasing enhancements of Br and SO_4 with depth. The main reactions involve calcite precipitation and ion exchange(Ca-Na). At both sites a glacial component and a deep saline component are present. At Simpevarp the saline component may be potentially non-marine and/or non-marine/old Littorina marine in origin; at Laxemar it is more likely to be non-marine in origin.

Type D: This type comprises reducing highly saline groundwaters (> 20,000 mg/L Cl; to a maximum of ~ 70 g/L TDS) and only has been identified at Laxemar at depths exceeding 1,200 m. It is mainly Ca-Na-Cl with higher Br but lower SO_4 compared to Type C groundwaters. The main reactions involve water/rock interaction for long residence times. Groundwater mixing at these depths probably involves long term mixing of deep non-marine brines driven by diffusion.

The redox state of groundwaters appears to be well described by sulphur redox pairs in agreement with some previous studies in this area and in other sites from the Fennoscandian Shield. Furthermore, the CH_4/CO_2 is another important redox pair in determining the redox state.

A modelling approach was used to simulate the composition of the highly saline or brine groundwaters and, for the Simpevarp area, concluded that mixing is the main irreversible process. It controls chloride concentration that, in turn, determines the re-equilibrium path (water-rock interaction) triggered by mixing.

Coupled transport modelling was used to model the groundwater age, tritium content and calcite dissolution/precipitation processes at shallow groundwater depths at both the Laxemar and Simpevarp subareas. The modelled results provide additional support to hydrogeological models by using independent hydrochemical information and added support to the general hydrogeochemical understanding of the site.

The modelling also indicated that the groundwater composition at repository depths is such that the representative samples from KSH01A: 548–565 m and KSH02: 575–580 m can meet the SKB chemical stability criteria for Eh, pH, TDS, DOC and Ca+Mg.

3.2 Hydrogeochemical modelling

3.2.1 Modelling assumptions and input from other disciplines

The main modelling assumption is that the measured groundwater compositions are a result of mixing and reactions including different water types. The water types are a result of palaeohydrogeological events and recent hydrodynamic conditions (see Figure 2-1). A schematic presentation of how a site evaluation/modelling is performed, its components and the interaction with other geoscientific disciplines, is shown in Figure 3-1. The methodology applied in this report is described in detail in the SKB strategy report for hydrogeochemical modelling /Smellie et al. 2002/.

Hydrogeochemical modelling involves the integration of different geoscientific disciplines such as geology and hydrogeology. This information is used as background information, supporting information or as independent information when models are constructed or compared.

Geological information is used in hydrogeochemical modelling as direct input in mass-balance modelling, but also to judge the feasibility of the results from, for example, saturation index modelling. For this particular modelling exercise, geological data were summarised, the information was reviewed and the relevant rock types, fracture minerals and mineral alterations were identified (cf Appendix 1).

The underlying geostructural model provides important information on water-conducting fractures used for the understanding and modelling of the hydrodynamics. The cross section used for visualisation of groundwater properties is generally selected with respect to the geological model and the hydrogeological simulations (cf Appendix 1 and 5). The available hydrogeological information and the results of hydrogeological modelling are used in the coupled flow and transport modelling (cf Appendix 5). The measured values of Cl, ^{18}O, ^{2}H, ^{14}C and the results from the M3 mixing calculations were provided as input data for hydrodynamic modelling simulations (cf Appendix 4). In addition a more comprehensive data table was provided to the hydromodellers where additional samples where indicated as useful for hydrogeological modelling purposes (Appendix 8). The mixing models used are descriptive and do not include advection or diffusion processes. However, these models can indicate effects of transport processes or reactions in a simplified way.

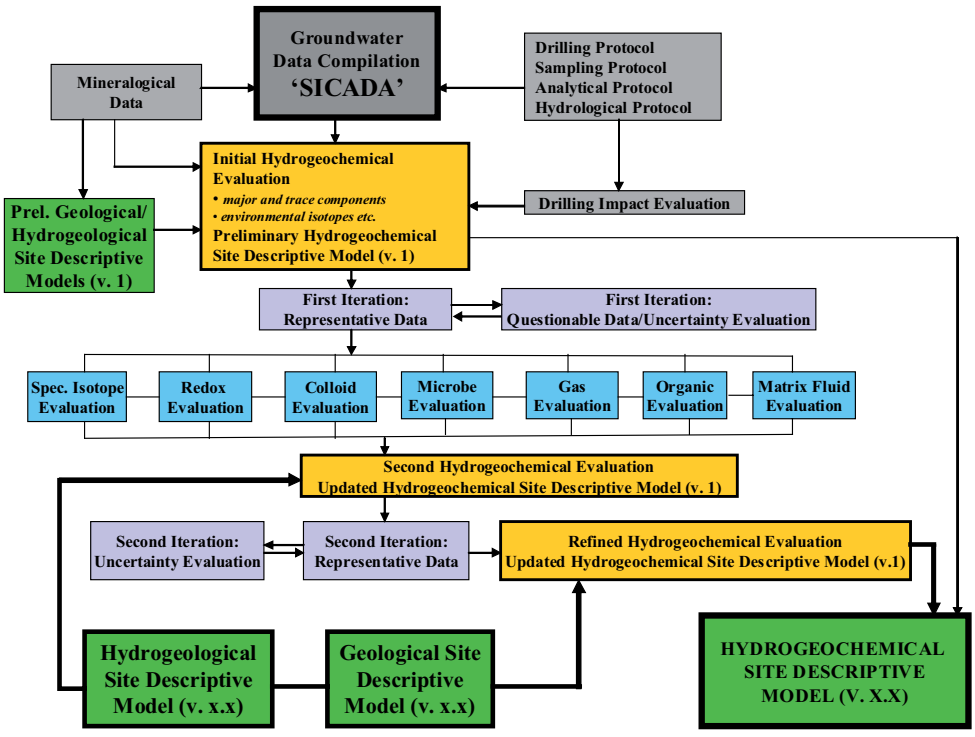

Figure 3-1. *The evaluation and modelling steps used for Laxemar model version 1.2 (after /Smellie et al. 2002/).*

3.2.2 Conceptual model with potential alternatives

The conceptual hydrogeochemical model for the Simpevarp area is the paleohydrogeological model shown in Figure 3-15. Much of the hydrogeochemical work focuses on tracing effects of the paleohydrogeological events, but also on assessing how mixing and reactions have altered the ground-water composition. The alternative conceptual models tested included different reference waters and local and regional models and different mathematical solutions to calculate the mixing proportions (cf Appendix 3 and 4); various modelling tools (associated with explorative analyses, PHREEQC, M3 and M4) and approaches were applied on the data set. In addition, the concept by which the water composition is modelled by using PHREEQC and the M4 approach is discussed in Appendix 3. M4 is a new method to calculate mixing proportions in the multivariate space. The uncertainties of the mixing models have been evaluated and discussed in Appendicies 3 and 4.

3.3 Hydrogeochemical data

The approach chosen has been to include all relevant data in the Simpevarp and Laxemar subareas together with the available information from the islands of Äspö (before the time of tunnel construction) and Ävrö.

The new samples in the version 1.2 “data freeze” for the Laxemar subarea(all collected in 2004) include:

30 samples from the Ävrö island:

- 8 samples from percussion boreholes (two samples from each of the following boreholes HAV11, HAV12, HAV13 and HAV14).
- 22 samples from the cored borehole KAV04: 20 tube samples (from 0 to 1,000 m depth) and 2 packed-off samples (729–805 m and 729–819 m).

112 samples from the Laxemar subarea:

- 10 samples from percussion boreholes: 4 samples from borehole HLX14 (one of them selected as representative sample for modelling purposes), two samples from HLX18, two from HLX20 (one of them of limited suitability; to be used with caution), one from HLX22 and one from HLX24.
- 102 samples from cored boreholes:
  - 26 samples from KLX03: 20 tube samples (from 0 to 990 m depth) and 6 packed-off samples (12–60 m, 12–100 m, 103–218 m [1 representative sample], 497–600 m, 600–695 m and 693–761 m).
  - 69 samples from KLX04: 21 tube samples (from 0 to 985 m depth) and 48 packed-off samples (104–109 [3], 103–213 [1 representative sample], 210–329 [1], 329–404 [1], 401–515 [1], 510–515 [25], 614–701 [1], 698–850 [1], 849–993 [1], 971–976 [13]).
  - 7 packed-off samples from KLX06 (103–202 [1], 200–310 [1], 260–268 [2], 307–415 [1], 331–364 [1], 514–613 [1]).

360 samples from Simpevarp:

- 44 groundwater samples:
  - 4 samples from percussion boreholes: 2 samples each from boreholes, HSH04 and HSH05.
  - One sample from KSH02 cored borehole (422.3–423.3 m).
  - 39 shallow groundwater (0–10 m depth) samples from soil pipes (one of them selected as limited suitability; to be used with caution for modelling).
- 296 surface water samples:
  - 92 sea water samples (56 selected as limited suitability; to be used with caution).
  - 64 lake water samples (48 selected as limited suitability; to be used with caution).
  - 140 stream water samples (65 selected as limited suitability; to be used with caution).
- 20 samples of precipitation (13 selected as limited suitability; to be used with caution).

Altogether, there are 502 new water samples, but not all of them with a complete chemical analysis at the time of the data Laxemar 1.2 freeze. Some of them have been considered representative for modelling purposes, see Appendix 6. There are relatively few new samples from boreholes in the Laxemar subarea that were not already evaluated during the Simpevarp 1.2 phase.

3.3.1 Groundwater chemistry data sampled in boreholes

The Laxemar 1.2 hydrochemical evaluation involved data from five cored boreholes (KLX01–KLX04 and KLX06) and 14 percussion boreholes (HLX01–HLX08 and HLX10, 14, 18, 20, 22, 24) from the Laxemar subarea, three cored boreholes (KSH01A, KSH02 and KSH03A) and 4 percussion boreholes (HSH02–HSH05) from the Simpevarp penninsula, and two cored boreholes (KAV01 and KAV04A) and 10 percussion boreholes (HAV04–HAV07 and HAV09–HAV14) from Ävrö island. The borehole sampling locations are shown in Figure 3-2. The analytical programme included: major cations and anions (Na, K, Ca, Mg, Si, Cl, HCO_3^- SO_4^{2-}, S^{2-}), trace elements (Br, F, Fe, Mn, Li, Sr, DOC, N, PO_4^{3-}, U, Th, Sc, Rb, In, Cs, Ba, Tl, Y and REEs) and stable (^{18}O, ^{2}H, ^{13}C, ^{37}Cl, ^{10}B, ^{34}S) and radioactive-radiogenic (^{3}H, ^{226}Ra, ^{228}Ra, ^{222}Rn, ^{238}U, ^{235}U, ^{234}U, ^{232}Th, ^{230}Th and ^{228}Th) isotopes, microbes, gases and colloids (cf Appendix 6).

The different analytical results obtained using contrasting analytical techniques for Fe and S have been confirmed with speciation-solubility calculations and checking their effects on the charge balance. The values selected for modelling were those obtained by ion chromatography (SO_4^{2-}) and spectrophotometry (Fe) assuming no colloidal contribution. The selected pH and Eh values correspond to available downhole data (cf Appendix 6).

Figure 3-2. *The groundwater sampling locations in the Simpevarp area. Location of hydrogeochemically prioritised boreholes KLX01, KLX02, KLX03, KLX04 and KLX06 (Laxemar subarea) and KAV01, KAV04A, KSH01A, KSH02 and KSH03 (Simpevarp subarea). Also indicated are the percussion boreholes, many of which are included in the Laxemar v. 1.2 evaluation.*

3.3.2 Representativeness of the data

A careful evaluation of the representativeness is described in Appendix 1. It has been criticised by some of the field staff and reviewers that the evaluation approach employed for borehole groundwaters is too rigorous, revealing that less than 20% of the total number of water samples are considered to be representative or suitable for the Laxemar v. 1.2 modelling, inferring that there is a large number of water samples that are not used and correspondingly much information lost. This is a common and understandable misconception. In reality all data provided by the SICADA database are available for use for all interested ChemNET analysis groups. However for each analysis group to familiarise themselves with all the data is not practical given the time constraints. Furthermore, because of the different modeling approaches, not all data are used by all the modelling groups.

The selection of 'representative' or 'suitable' values is, therefore, severalfold, for example as an aid to help provide a degree of confidence or support (or otherwise) when using or interpreting other data which may be less reliable for different reasons (e.g. incomplete analyses; lack of chemical stability during sampling; contamination etc). It is important also to point out that to arrive at 'representative' or 'suitable' values requires using **all** the available hydrochemical data, and that these data are evaluated as much as possible with reference to known hydraulic conditions in: a) the borehole, b) the fracture zone sections being sampled, and c) the surrounding host bedrock. The reliability of these data is therefore judged as much as possible on prevailing hydraulic and geologic conditions during borehole drilling, monitoring and sampling.

Without the integration of hydrochemistry, geology, hydrogeology and borehole activities there is a great danger that data can be misrepresented. An important example of this is the open hole tube sampling carried out in KLX02 in 1993 and 1997 where the hydrochemical and isotopic data collected along the borehole has been accepted and modelled as representing the evolution of formation groundwater with depth in the surrounding host rock, despite reservations related to open hole mixing as noted by /Laaksoharju et al. 1995a, Ekman 2001/, and more recently has been criticised during internal review. Other examples have included the use of tritium and radiocarbon data without considering closely enough: a) the possibility of induced mixing during borehole activities, b) natural dilution and radioactive decay of tritium with time when combining and comparing old and newly collected samples, c) the potential surface input of tritium from the nearby nuclear power facilities, and d) successive lowering of detection levels throughout the years.

The representativity check of the borehole groundwater samples from the Laxemar 1.2 data freeze revealed that there is only a very limited set of groundwater data suitable to be quality checked, and only very few of these available data are considered representative or suitable (highlighted in orange in Appendix 6), or of limited suitability but useable with caution (highlighted in green in Appendix 6). Most data have been deemed as unsuitable. Of course data judged to be of limited suitability may still provide valuable information, for example: a) the use of some of the major ion analyses in hydrochemical plots, and b) observed compositional changes with time which may reflect groundwater mixing, either artificially induced by pumping and/or sampling or due to natural flow.

The absence of suitable data is attributed mainly to the very high portions of drilling fluid in many or the analysed groundwaters sampled during drilling, during pumping and injection tests, and during subsequent tube sampling. Furthermore, there are no complete sets of data comprising major elements, stable deuterium and ^{18}O, and tritium, which are the minimum requirement to evaluate the representativeness of the groundwaters in terms of, for example, charge balance and the inmixing of drilling water and near-surface groundwaters. However, even though no complete Class 5 analyses are available, groundwaters that have major ions, TOC, D and ^{18}O, tritium and ^{14}C are rated as suitable if the charge balances are $< \pm 5\%$ and the drilling fluid $< 1\%$.
Table 3-1 refers to the Laxemar and Simpevarp subareas where the above criteria have been applied to establish the number of groundwater samples that fall into these categories. Only seven groundwater samples from the Laxemar and Simpevarp subareas are considered suitable or of limited suitability, and six of these are all from the upper part of the bedrock (0–218 m) and of dilute groundwater character. These shallow groundwaters mainly represent a recent meteoric/older meteoric (tritium free) origin, except for KLX03: 103–218 m which is tritium free and shows inmixing of a cold climate recharge water component. One sample included is from greater depth

(KAV04A: 245–293 m) and is of brackish character although it contains a substantial drilling water component (12.3%). It is suitable for major ion chemistry use but, for example, is not recommended for tritium analysis use since the sample has been influenced by the drilling water.

All tube samples from KLX03 and KLX04 are lacking stable isotope data and tritium which means that even young dilute groundwaters with a relatively low percentage of drilling fluid (< 10%), can consist of modern meteoric, older meteoric or glacial water of unknown proportions.

Groundwaters with higher chloride contents are detected at depth in all the boreholes but these samples are characterised by: a) excessive amounts of drilling water, or b) an incomplete set of analyses, and c) mixing of different groundwater types along the borehole lengths (e.g. KAV04A).

In conclusion, the tube samples from all four sampled cored boreholes (KAV01, KAV04A, KLX03 and KLX04) are judged as unsuitable due reasons given above. In addition, the KLX03 and KLX04 tube samples, based on information from the differential flow measurements, show significant differences in the behaviour of the electrical conductivity profiles versus depth. The difference in values resulting from pumping compared to without pumping indicate generally higher electrical conductivity during pumping. The tube samples, which are collected under natural flow conditions (i.e. equivalent to without pumping) in the open borehole, therefore do not reflect the maximum salinity recorded during pumping. Instead, the tube samples indicate mixing of groundwaters of different origin, especially inmixing of near-surface groundwaters and, in many cases, extremely high portions of drilling water. It is therefore strongly recommended not to use the tube samples in the detailed modelling exercises as they probably reflect a perturbed groundwater system and may give, for example, erroneous indications of near-surface groundwaters at great depth that do not reflect initial, undisturbed conditions. The tube samples are helpful when comparing the representativity and checking the temporal variability and for reflecting the general geochemical depth trends.

The general uncertainty surrounding tube sampling has also been extended to borehole KLX02. Tube hydrochemical data from KLX02 have been consistently used over many years in several of the evaluation and modelling exercises. Even though there is a reasonably close correlation with some of the data from packed-off borehole sections, and a general absence of drilling water, there are some discrepancies (e.g. tritium; sulphate) which can be attributed to open hole mixing. Consequently, selected tube hydrochemical data have been highlighted green in the Laxemar 1.2 data freeze table indicating limited suitability but to be used with caution. For example, in the majority of the ion-ion plots and for much of the water/rock geochemical equilibrium modelling these data have been excluded altogether.

Table 3-1. Groundwater samples from the Laxemar and Simpevarp subareas rated with regards to suitability for detailed groundwater modelling (se also Appendix 6).

Water sample (metres depth)	Suitable	Limited suitability	Comment
HLX10: 0–85	Yes		Class 3
HLX14: 0–115.90	Yes		Class 5
HLX20: 0–200.20		Yes	Class 5 No ^{2}H and ^{18}O available
KLX03: 103–218	Yes		Class 3
KLX04: 103–213		Yes	Class 3 Drilling fluid 7.76%
KAV04: 0–100	Yes		Class 5
KAV04: 245.85–295.05		Yes	Class 3 Drilling fluid 12.37%

3.4 Explorative analysis

A commonly used approach in groundwater modelling is to commence evaluation by explorative analysis of different groundwater variables and properties. The degree of mixing, the type of reactions and the origin and evolution of the groundwater can be indicated by applying such analyses. Also of major importance is to relate, as far as possible, the groundwaters sampled to the near-vicinity geology and hydrogeology.

3.4.1 Borehole properties

Figure 3-3 show an example of integrated geology, fracture frequency, hydraulic conductivity and chemistry plot of borehole KLX03. The results from drillcore mapping, BIPS measurements, differential flow measurements and electrical conductivities, together with groundwater quality and representativeness of the samples, are discussed in detail for all investigated boreholes in Appendix 1.

3.4.2 Examples of evaluation of scatter plots

The hydrochemical data have been expressed in several X-Y plots to derive trends that may facilitate interpretation. The hydrogeochemical evaluation presented below shows only a few examples of the chain of analysis employed in the systematic approach described in Appendix 1 in with traditional plots to group the main groundwater types characterising the Simpevarp area and to identify general evolution or reaction trends. A complete and detailed evaluation of the major components and isotopes can be found in Appendicies 1 and 3. Discussion of many of the reactive elements is presented in the modelling part of this report and also in Appendix 3.

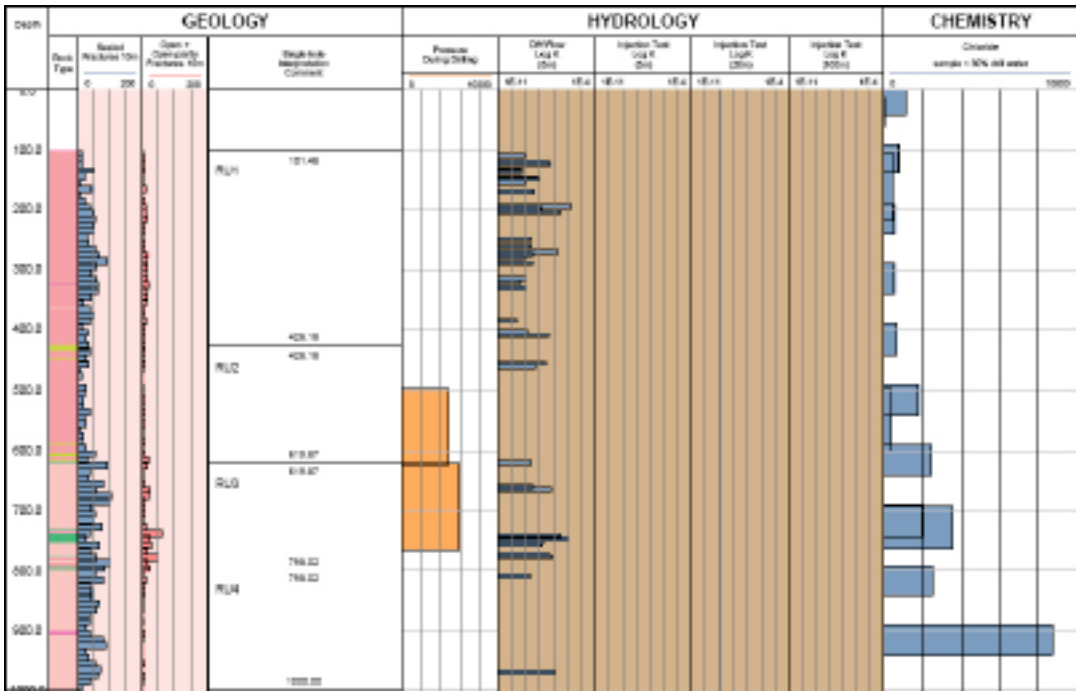

Figure 3-3. *Integrated geology, fracture frequency, hydraulic conductivity and chemistry (Cl) along borehole KLX03.*

Chloride depth trends

The Laxemar subarea data show mostly dilute groundwaters (< 2,000 mg/L Cl) extending to at least 275 m in KLX01 and to around 500–600 m for boreholes KLX03 and KLX04 situated in the central part of the Laxemar subarea. In borehole KLX02 dilute groundwater was detected down to 800 m before a rapid increase in salinity to maximum values of around 47 g/L Cl at 1,700 m (Figure 3-4). The Simpevarp subarea data shows a higher level of salinity at shallow depths (brackish to around 5,000 mg/L Cl at approx. 300 m depth), more saline at intermediate depths (up to 10,000 mg/L Cl at 700 m) and also a more systematic increase to around 850 m (to a maximum of ~ 17,000 mg/L Cl) when compared to the Laxemar subarea.

Bicarbonate versus depth

Figure 3-5 shows bicarbonate plotted against depth. The plot shows the expected rapid decrease in bicarbonate derived from organic decomposition with increasing depth and correspondingly with increasing chloride. The small deviations or scatter in the depth trends caused by some of the cored boreholes in the Laxemar subarea reflect on one hand the differing hydrogeology at the borehole locations sampled and on the other hand possibly some open hole mixing effects.

Magnesium versus chloride

Figure 3-6 shows the relationship of magnesium against chloride and underlines the generally higher magnesium contents in samples from the Simpevarp subarea (to ~ 70 mg/L) corresponding to more brackish conditions (3,000–7,000 mg/L Cl) and possibly suggesting a small Littorina Sea or older seawater component. Over the same range of salinity the Laxemar groundwaters show generally very low Mg values (≤15 mg/L) except for a small magnesiun increase to 30 mg/L Cl recorded in borehole KLX01, before decreasing to near zero values at higher salinities (~ 15,000 mg/L Cl).

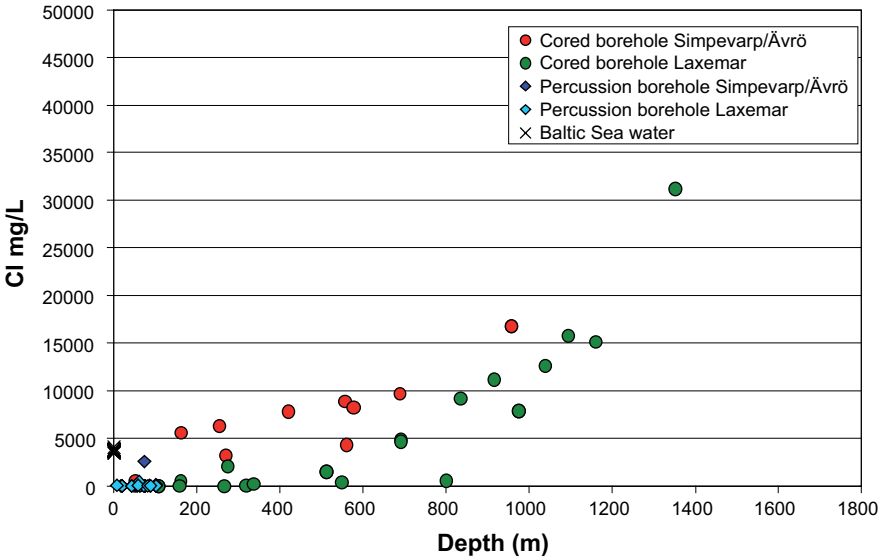

Figure 3-4. Depth (depth along boreholes) variation of chloride in the Simpevarp and Laxemar subareas.

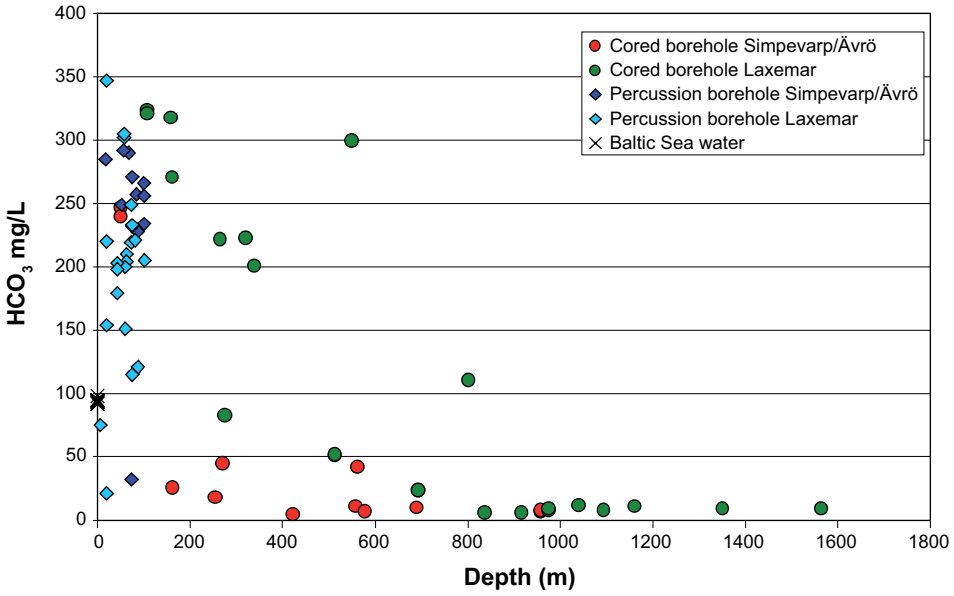

Figure 3-5. *Plot of HCO_3 vs depth (depth along boreholes) for the Simpevarp and Laxemar subareas.*

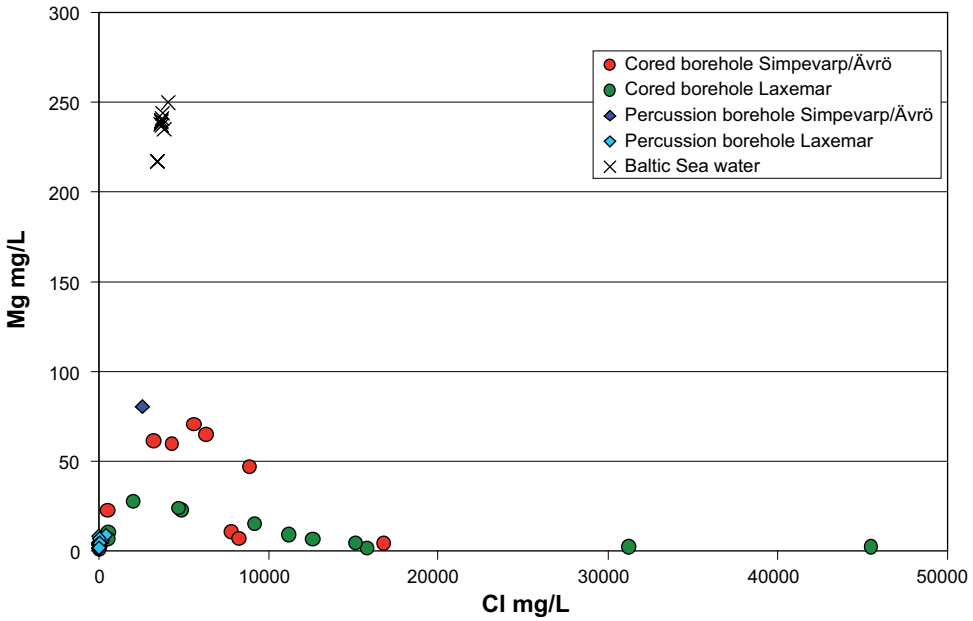

Figure 3-6. *Plot of Mg vs Cl for the Simpevarp and Laxemar subareas.*

Oxygen-18 versus deuterium and Cl

Figure 3-7 details the stable isotope data most of which plot on or close to the Global Meteoric Water Line indicating a meteoric origin. In accordance with much of the other hydrochemical data, three main groundwater groups are indicated: a) shallow dilute groundwaters ranging from $\delta^{18}O$ = –10.9 to –9.8‰ SMOW, δD = –78.7 to 67.1‰ SMOW, b) brackish to saline groundwaters ranging from $\delta^{18}O$ = –14.0 to –11.7‰ SMOW, δD = –100.0 to –86.2‰ SMOW, and c) highly saline from $\delta^{18}O$ = –11.7 to –8.9‰ SMOW, δD = –78.6 to –47.4‰ SMOW. The lighter isotopic values of the brackish groundwater group (b) indicate the presence of a cold recharge meteoric component (glacial melt water?). This is further illustrated by Figure 3-8 by plotting $\delta^{18}O$ against chloride, especially the brackish nature of the groundwaters characterised by light isotope cold climate signatures. The limited data suggest there is no major Baltic Sea influence on the sampled groundwaters. One distinguishing feature is the characteristic deviation trend from the GMWL (i.e. the two highly saline groundwaters from –9.7 to –8.9‰ SMOW, δD = –61.7 to –47.4‰ SMOW) which appears to increase with increasing salinity. A similar deviation has been reported from the deep Canadian basement brines which has been discussed, among others, by /Frape and Fritz 1987/ who considered this as an indication of very intensive water/rock interactions over long residence times.

3.4.3 Descriptive observations – main elements

The site descriptive observations described in this section are based on the detailed data evaluation presented in Appendix 1. The overall depth trends show increasing TDS with increasing depth. There are significant differences in "depth trends" between the two subareas; in Simpevarp the upper fresh water regime (mostly Na-HCO_3) reaches only to approx. 150 m whereas in the central parts of the Laxemar subarea fresh water is found down to 500 m and in some cases as deep as 800 m.

Ca/Na ratios increase markedly with depth and also illustrate differences between the two subareas down to around 1,000 m. The Simpevarp subarea saline groundwaters (~ 10,000–20,000 mg/L Cl) show a more Na-rich trend (Na-Ca-Cl dominant) compared with the Laxemar groundwaters which are more Ca-rich (Ca-Na-Cl dominant). Generally, at depths exceeding 1,000 m, higher saline Ca-Na-Cl groundwaters dominate in both areas.

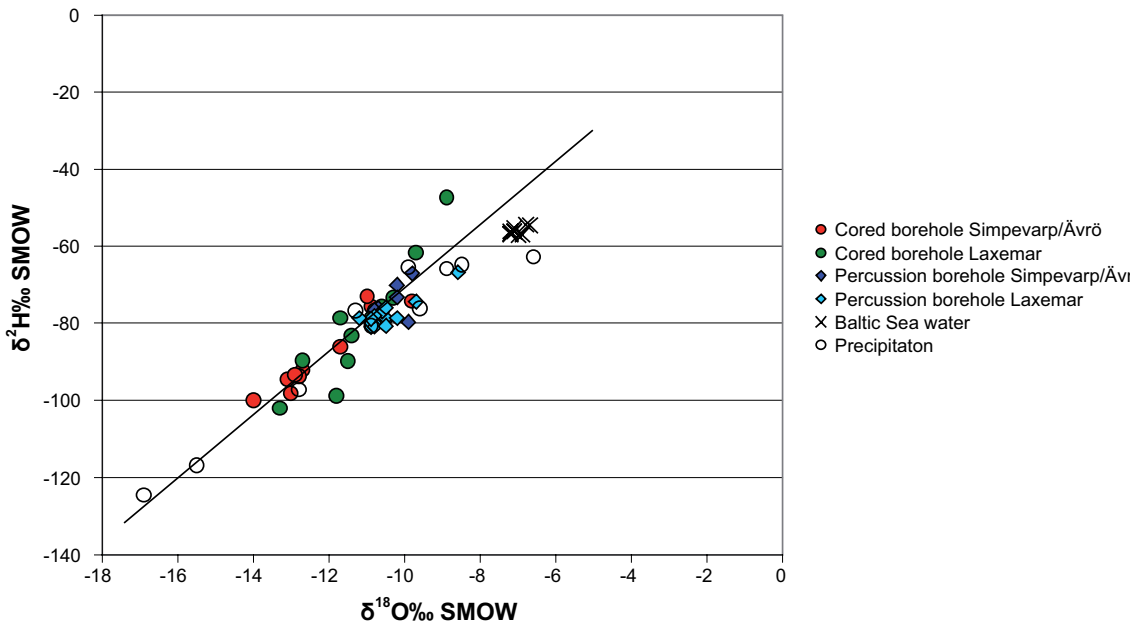

Figure 3-7. *Plot of $\delta^{18}O$ vs $\delta^{2}H$ for the Simpevarp and Laxemar subareas (Global Meteoric Water Line is indicated).*

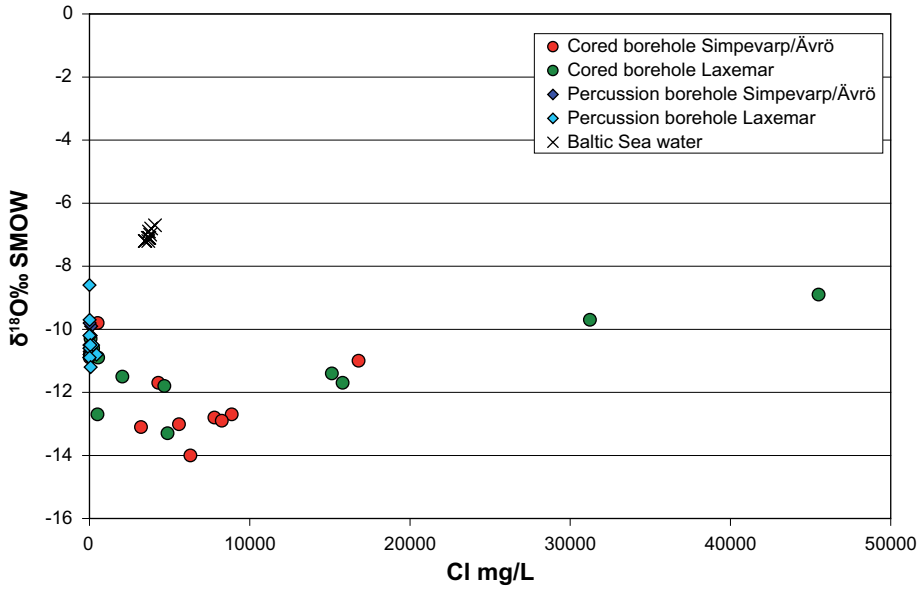

Figure 3-8. *Plot of $\delta^{18}O$ vs Cl for the Simpevarp and Laxemar subareas.*

At a more regional scale, deep groundwaters in the Simpevarp subarea and Äspö HRL (down to 1,000 m) are Na-Ca-Cl in type; deep groundwaters at a borehole drilled in the town of Oskarshamn (KOV01; 1,000 m) and in the Laxemar subarea (1,300 to 17,000 m) are Ca-Na-Cl in type. Since Laxemar is inland and Oskarshamn is close to the coast, this should be an indication of discharging very deep groundwater at Oskarshamn. At greater depths below the Simpevarp subarea and Äspö HRL than presently sampled, Ca-Na-Cl groundwaters are expected to dominate.

Br/Cl ratios indicate an absence of marine signatures in the Laxemar subarea; all ratios are significantly higher than marine. Contrastingly, in the Simpevarp' subarea, lower ratios indicate a weak but significant marine signature. Borehole KLX01 (the easternmost of the Laxemar boreholes) shows, however, values close to marine Br/Cl ratio at 272–277 m.

A clear marine signature (in terms of high Mg values, marine Br/Cl ratios and relatively high $\delta^{18}O$ values) is rare, but a small set of samples with a possible Littorina Sea signature do exist from 150–300 m depth sampled in fracture zones close to the Baltic Sea. In addition, there also seems to be a small marine input (Littorina or older), distinguished by slightly higher Mg values and lower Ca/Na ratios, in the Simpevarp subarea waters which is absent in the Laxemar subarea (with the exception of the upper 700 m in KLX01 which shares similarities to the Simpevarp samples).

The plot of $\delta^{18}O$ versus Cl indicates a contribution of cold climate or glacial melt waters to the brackish (i.e. 2,000–10,000 mg/L Cl) and deeper saline (i.e. 10,000–20,000 mg/L Cl) groundwater samples.

The SO_4 contents vary considerably within the brackish and saline groundwaters. Microbially mediated sulphate reduction, (indicated by $\delta^{34}S > 20‰$ CDT), is taking place not only in brackish waters but also in some fresh waters (i.e. KLX03 and HLX 14). The SO_4 contents in the more highly saline groundwaters indicate mixing with SO_4 from deep brine waters, which in turn may have reached their high SO_4 content through leaching of sediments and/or dissolution of gypsum previously present in fractures. The presence of gypsum in sealed fractures in a few places at the site supports gypsum as a possible source for SO_4 in the deep groundwaters.

3.4.4 Descriptive observations – isotopes

The isotope data from borehole samples are still relatively few and not very much new information has been forthcoming since the Simpevarp 1.2 model version; see Appendix 1. However, tritium has been given much attention together with ^{14}C since they represent isotopes of great interest for groundwater modelling. Furthermore they also provide the possibility to assess potential contamination from the nearby power plants.

Tritium

Tritium data from precipitation, surface stream and lake waters, and sea water localities were studied with respect to their distribution, content and origin. It can be concluded that:

Generally there is a spread in values between 8.5 to 19 TU for surface water localities which is almost equal to the variation in the precipitation (9–19 TU), i.e. the input term.

The highest mean value is found in the Baltic Sea samples, with the highest contents (mean of 15.1 TU) in the samples east of Kråkelund, north of Simpevarp.

The highest values for the lake and stream waters are found in the eastern part of the Simpevarp area even though mean values only deviate by 1–1.3 TU (11.4 compared with the highest value of 12.6 TU).

The question now to be addressed is how much of the tritium is due to fall-out contamination from the nuclear power plant? Present day contamination, although small, should be more apparent following the systematic decrease of global tritium values during the past five decades. Consequently, continued sampling of surface waters for tritium analyses is recommended with particular attention to surface water samples taken: a) close to the cooling water outlet of the nuclear power plant, b) close to the power plant, and c) some 100 km away, preferably down-wind from the power plant.

The tritium values from the cored boreholes are few and only two values from the Laxemar subarea are available, representing relatively shallow sampling sections; KLX03: 103–218 m and KLX04: 103–213 m. The KLX04 sample shows values similar to HLX10; tritium close to 4 TU and $\delta^{18}O$ values around –11‰ SMOW. Both are dilute meteoric waters. The KLX03 sample, in contrast, shows tritium levels close to the detection limit (0.8 TU) and with a significantly lower $\delta^{18}O$ value (–12.7‰ SMOW) indicating a possible older cold climate meteoric water component. This water is less dilute, having a Cl content of 507 mg/L.

All the new samples analysed for tritium with chloride contents > 5,000 mg/L from the Simpevarp peninsula showed values below detection limit when tube samples and samples with high contents of drilling fluid are excluded (cf Figure 3-9). These samples are from depths of 150 m and deeper. This indicates that modern water (< 45 years) has reached a depth of about 150 m at the Simpevarp peninsula. Other analysed groundwaters (0–218 m) show low chloride contents and variable tritium contents. Old values analysed before year 2000 from Laxemar at depths > 200 m show tritium contents less than 10 TU which inidicate that these values are lower than modern recharge values. The increased tritium is an indication of water portions from 1960.

Unfortunately the number of new suitable groundwater samples analysed for tritium to date are very few and the possibility of evaluation is therefore highly restricted.

Tritium and carbon-14

Tritium was also related to the regional distribution of carbon-14 in the analysis presented in Appendix 1. This indicated that Baltic Sea samples show the highest ^{14}C values (around 105 to 110 pmC) which means that they have either some residual bomb test ^{14}C or, in common with the tritium values, contain a modern contribution from the nuclear power plant emissions resulting in higher than background values. Most of the lake and stream waters show values ranging from 60 to 100 pmC, accompanied by high tritium values (~ 8–15 TU). With the exception of two samples (45 and 55 pmC) the soil pipes show values within the same interval as the surface waters. The percussion and cored boreholes show decreasing tritium contents with decreasing ^{14}C, i.e. waters with very low tritium reflect also the lowest ^{14}C values (around 30 pmC).

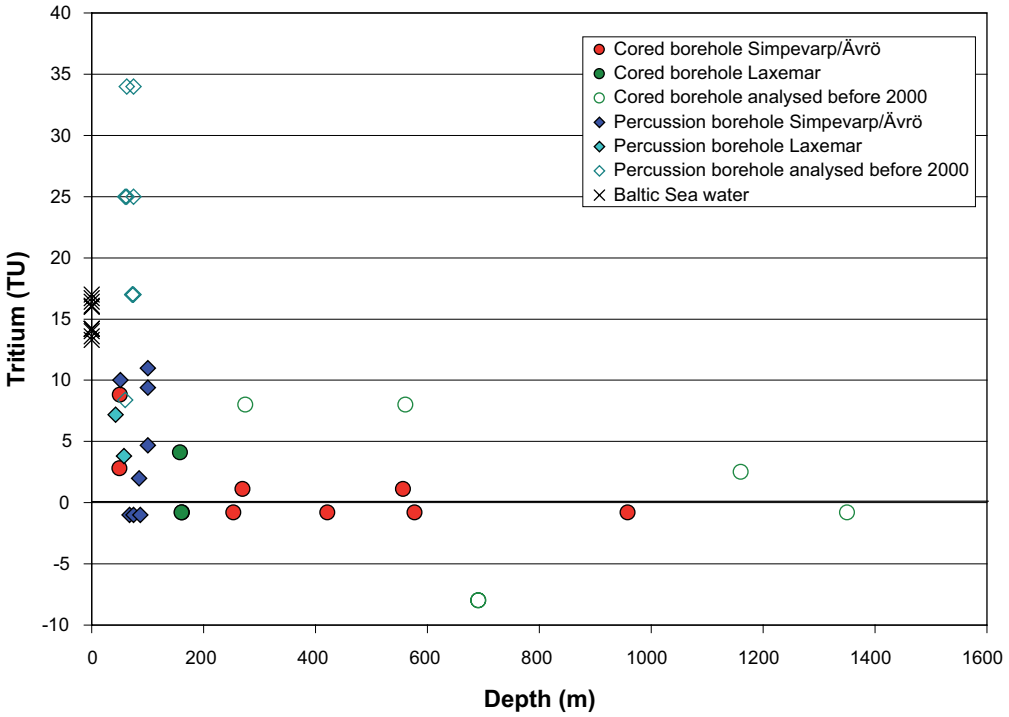

Figure 3-9. *Tritium (TU) versus borehole depth (m) for surface waters and groundwaters from the Simpevarp and Laxemar subareas. Tritium values below detection limit (0.8 TU) are shown as negative values. Old analytical values from Laxemar with an detection limit of 8 TU are shown for comparison.*

Carbon

All samples analysed for ^{14}C were also analysed for stable carbon isotope ratios (given as $\delta^{13}C$‰ PDB) (Appendix 1). These $\delta^{13}C$ ratios, together with HCO_3 contents, are commonly used to evaluate possible processes that have taken place resulting in ^{14}C changes in the groundwater.

Waters in equilibrium with atmospheric CO_2 show high $\delta^{13}C$ values (0 to –3‰ PDB); this is exemplified by the Baltic Sea samples.

Incorporation of biogenic CO_2, produced by breakdown of organic material of variable age, lowers the $\delta^{13}C$ values significantly; this is well illustrated by the surface waters which show significantly lower $\delta^{13}C$ values (–12 to –24‰).

The ^{14}C values of most of these waters are relatively high (although somewhat lower than the Baltic Sea values) and it is probable that the organic source for the CO_2 is young, although some dilution with 'dead carbon' (^{14}C free) has occurred. Some surface waters and most of the percussion and cored boreholes show similarly low $\delta^{13}C$ values but significantly lower ^{14}C values.

In particular, the shallow groundwaters from the percussion boreholes and the two samples from KLX03: 103–218 m and KLX04 103–213 m show high HCO_3 contents (174 to 318 mg/L) and ^{14}C contents in the range of 70 to 40 pmC. Several explanations for the decrease of ^{14}C are possible: 1) dissolution of calcite has contributed ^{14}C free carbon to the HCO_3, or 2) CO_2 has been produced from older organic material, or 3) these waters are old and very little ^{14}C has been contributed during a long period of time. The combination of all these processes is possible for the groundwater samples. The fracture calcites show no homogeneous $\delta^{13}C$-values and it is therefore not possible to model calcite dissolution as a mixing of two end members.

Sulphur

Sulphur isotope ratios, expressed as $\delta^{34}S‰$ CDT, have been measured in dissolved sulphate in Baltic Sea waters, surface waters and groundwaters from the Simpevarp and Laxemar subareas (Appendix 1). The recorded values were found to vary within a wide range (–1 to +48‰ CDT) indicating different sulphur sources for the dissolved SO_4^{2-}, for example:

- For the surface waters and most of the near-surface groundwaters (soil pipes) the SO_4^{2-} content is usually below 25 mg/L and the $\delta^{34}S$ is relatively low but variable (–7 to +15‰ CDT) with most of the samples in the range 0–10‰ CDT. These relatively low values indicate that atmospheric deposition and oxidation of sulphides in the overburden is the origin for the SO_4^{2-}. There is a tendency towards lower $\delta^{34}S‰$ CDT with higher SO_4^{2-} contents in these waters but the variation is large.
- The Baltic Sea waters cluster around the 20‰ CDT marine line but show a relatively large spread (+16 to +23‰ CDT). The reason for this is not fully understood but suggestions include: a) contribution from land discharge sources (e.g. streams) to various degrees (low values), and b) potential bacterial modification creating high values in the remaining SO_4^{2-}.
- The borehole groundwaters show $\delta^{34}S$ values between +11.8 to + 48.2‰ CDT with most of the samples in the range +15 to +25‰ CDT. Values higher than marine (< 20‰ CDT) are found in samples with Cl contents < 6,500 mg/L Cl. These latter values are interpreted as a product of sulphate reduction taking place in situ. The two highest values (+32 and +48‰ CDT) are detected in waters where SO_4^{2-} contents are low (around 30 mg/L) and the Cl contents 70 and 503 mg/L, respectively. Such extreme $\delta^{34}S$ values as +48‰ CDT are strong indicators of closed, stagnant conditions and biological activity.
- The groundwaters with higher salinities, all from the Simpevarp peninsula, share lower $\delta^{34}S$ but higher SO_4^{2-} contents. The reasons are uncertain and more information is needed. Possible explanations include dissolution of, for example gypsum, or mixing with very deep saline water which in turn has received contributions of sulphate from leaching of sediments etc. The deep and intermediate groundwaters are very reducing and non-corroded pyrite is present in the fractures so that oxidation of sulphides in these groundwaters seems not to be a plausible explanation.

Strontium

Available Sr isotope information from the Baltic Sea waters, near-surface waters and groundwaters, show two or possibly three separate correlations between Sr isotopes and 1/Sr and Cl contents (Appendix 1):

- Large variation in Sr ratios but relatively small variation in Sr content for the near-surface groundwaters indicating interaction (leaching) from overburden of different mineralogical compositions.
- Large variation in Sr content but small variation in Sr isotope ratios for the fresh groundwaters indicating homogenisation of the Sr isotope ratios due to mineral/water interactions along the flow paths (mainly ion exchange).
- Tendency towards higher Sr isotope ratios with increasing Sr content for the saline samples possibly as a result of more stagnant conditions and rock-water interaction.

Boron

Enhanced $\delta^{11}B$ has been used as an indicator of permafrost conditions as it appears to become isotopically enriched in the fluid phase during freeze-out conditions (Appendix 1). For example, deep saline groundwaters characterised by negative $\delta^{18}O$ values tend to correlate with high ^{11}B values, see Appendix 1.

Since the boron isotope data are limited, initial scoping plots have been made using all data where both $\delta^{11}B$ and $\delta^{18}O$ have been analysed. Almost all of the $\delta^{11}B$ data in the Simpevarp area plot between 20–60‰ which is in agreement with earlier published data (see Appendix 1) from Fennoscandia including the Äspö HRL. Of interest are groundwaters from three anomalously high $\delta^{11}B$ (80–110‰) cored borehole outliers from the Simpevarp subarea (KSH01A: 556 m, KSH02: 422 m and KSH02: 578 m). Otherwise the remaining borehole data fall within the same $\delta^{11}B$ range.

Plotting $\delta^{11}B$ against $\delta^{18}O$ couples these three Simpevarp cored borehole groundwaters, high $\delta^{11}B$, to somewhat lighter $\delta^{18}O$ values (–12.9 to –12.7‰ SMOW). According to the literature, this is consistent with the possibility that these groundwaters might reflect freeze-out processes which occurred under permafrost conditions.

3.4.5 Microbes

Microbes have been evaluated from the Simpevarp area (Appendix 2). There are still rather few data from the Laxemar subarea and therefore the model reflects only the regional scale Simpevarp area. The model predicts (Figure 3-10), that the dominating microbial process in 'The anaerobic subsurface zone' is heterotrophic sulphate reduction. This zone is found at depths from 100 to 500 m, 'The deep sulphate reducing zone' is found at about 600 to 900 m, and 'The deep autotrophic zone' is found from 1,000–1,400 m. There are indications of possible ongoing iron reduction and hetero-

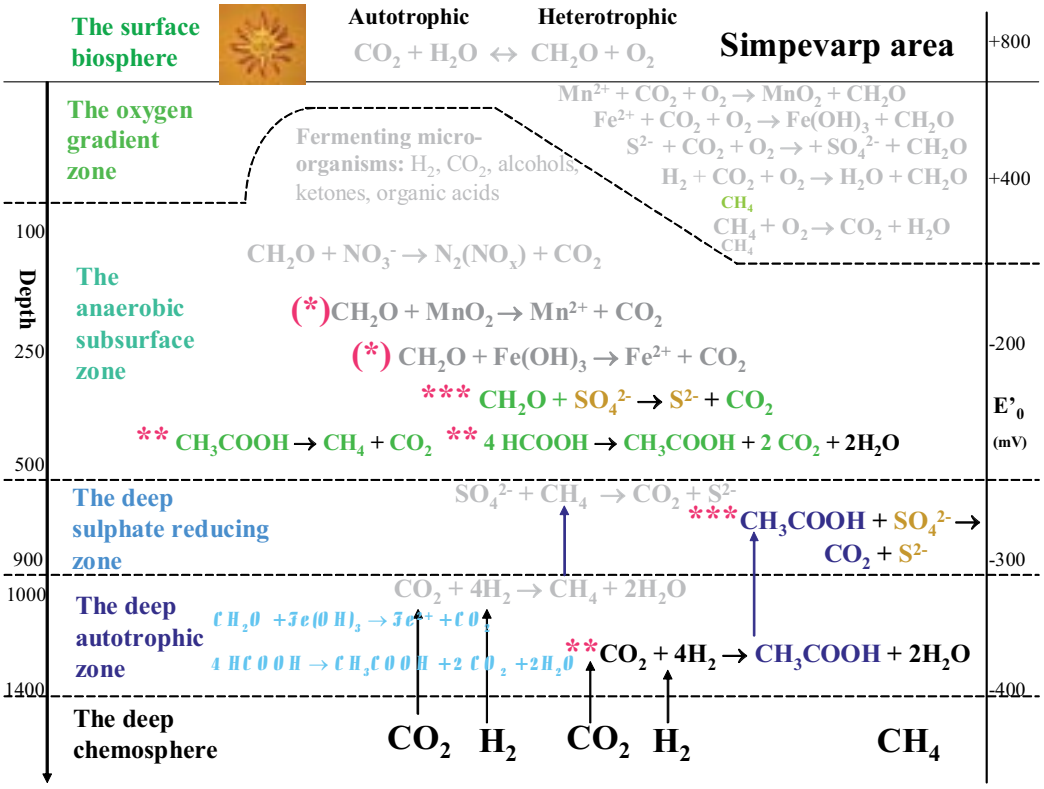

The colours in the model are used as listed below:

, light grey:	The process is not yet studied.
, dark grey:	The process is present but without influence
, green:	The carbon compounds originate from the surface biosphere
, blue:	The carbon compounds originate from the deep autotrophic zone
,black:	Compounds from the deep chemosphere
,turquoise:	Processes found but not anticipated and not yet confirmed

The star symbols in the figure illustrate the MPN values and influence by the microbial groups on the geochemistry.

(*)	1-10 ml^{-1}	Present without influence[1]
*	11-50 ml^{-1}	Present with putative influence if growth promoting changes occur
**	51-1000 ml^{-1}	Present with influence
***	>1000 ml^{-1}	Dominating with high influence

[1] influence here means that the organism group has an effect on the geochemistry of the ground water

Figure 3-10. *The microbial model of the Simpevarp area based on data available at the time of the Laxemar 1.2 data freeze. The star symbols before the reactions depict the significance of the reaction.*

trophic acetogenesis but this must be verified by thorough MPN-studies (most probable number of microorganisms study). The origin of carbon dioxide and hydrogen gas in this zone from 'The deep chemosphere' also requires to be verified with stable isotope studies of the gas in the groundwater.

The following conclusions can be drawn (from the work in Appendix 2):

- In the (regional scale) Simpevarp area three of the proposed zones in the subsurface microbial model has been identified: the anaerobic subsurface zone at least from 100 to 500 m, the deep sulphate-reducing zone between 600 and 900 m and the deep autotrophic zone from 1,000 to at least 1,400 m. The depths have to be seen as preliminary.
- In the anaerobic subsurface zone, sulphate-reducing bacteria, heterotrophic methanogens and heterotrophic acetogens are the dominating microorganisms.
- In the deep sulphate-reducing zone, acetate oxidation has been observed but no methane oxidation.
- In the deep autotrophic zone, autotrophic acetogens have been observed.
- The very few available data microorganisms attached to the bedrock and production of hydrogen sulphide under optimal conditions indicate that the attached microorganisms in a 1 mm wide fracture produce up to 1,000 times more hydrogen sulphide per day than unattached micro-organisms.

3.4.6 Colloids

Colloid compositional data have been evaluated from the Simpevarp area (Appendix 2). Particles in the size range 10^{-3} to 10^{-6} mm are regarded as colloids; their small size prohibits settling and renders them as a potential radionuclide transport mechanism in groundwater. The aim of the colloid study was to quantify and determine the composition of colloids in groundwater from boreholes, and to include the results in the hydrochemical modelling of the site.

In evaluating the background colloid values of the groundwaters the amount of colloids versus depth was studied. It can be seen in Figure 3-11 that the amount of colloids was greatest in borehole KLX01: 458.5 m with 92.03 µg l^{-}1, due to high amounts of aluminium colloids. The most plausible explanation is contamination from drilling activities when aluminium silicate colloids are released

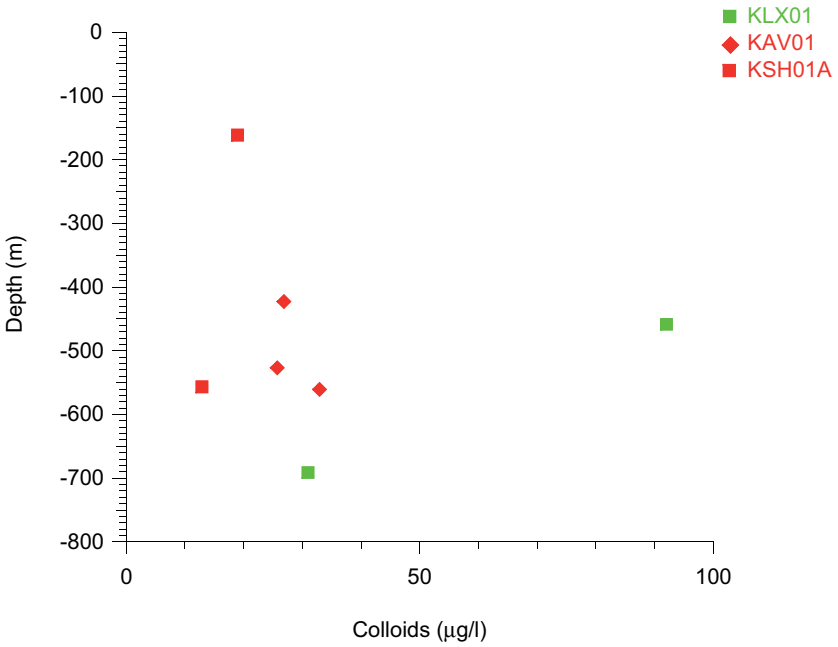

Figure 3-11. *Colloids (µg l^{-1}) plotted versus depth in samples from boreholes KLX01, KAV01 and KSH01A in the Simpevarp area*

from the bedrock during the grinding and pumping. The other data range from around 13 to 33 µg l^{-1} with the most recent data from borehole KSH01A recording the lowest amounts. Since there are only two samples from this study it is difficult to speculate on an explanation for this, but an improved sampling technique is a possible suggestion.

Generally, the average amount of colloids in this study was 23.1 ± 7.14 µg l^{-1} if the value from KLX01: 458.5 m is omitted. These values agree very well with data reported from colloid studies in Sweden (20–45 µg/l) and Switzerland (30 ± 10 and 10 ± 5 µg l^{-1}) /Laaksoharju et al 1995b, Degueldre 1994/ but about ten times lower than reported from Canada (300 ± 300 µg l^{-1}) /Vilks et al. 1991/.

3.4.7 Gas

No new gas analyses are available at present.

3.4.8 Pore water composition in the rock matrix

In crystalline rocks the pore water resides in the low-permeability zones (rock matrix) between principal water-conducting zones related to regional or local fracture networks. Depending on the residence time of water in these hydraulically active zones, interaction with water present in the pore space of the low-permeability zones might become significant. In addition, the pore water present in the low-permeability zones will be the first to interact with any artificial construction made in such zones (i.e. repository). For safety assessment considerations it is therefore important to know the composition of such pore water. The latter can be assessed by combining the information gained from pore water profiles determined over a low-permeability zone, with the chemical and isotopic data of water circulating in the fractures. The pore water studies are described in detail in Appendix 1).

Pore water that resides in the pore space between minerals and along grain boundaries in crystalline rocks of low permeability has been extracted successfully by laboratory out-diffusion methods using drillcore samples from borehole KLX03 from the Laxemar subarea. The experiment solutions obtained have been characterised chemically and isotopically and related to the in situ pore water composition of the rock, which in turn was related to the present and past formation groundwater evolution of the site. In addition, the method of extraction, together with interfaced measurements of interconnected porosity, provided the opportunity to derive diffusion coefficient values of potential use in predicting future rates of solute transport. Because of the very small volumes of pore water extracted and the possibility of rock stress release occurring during drilling which might lead to contamination by drilling fluid and also affect the derivation of rock porosity values, great care was taken to avoid such problems or, at least further understand the repercussions.

The results show that chloride concentrations in pore water and formation groundwater of the Ävrö granite are similar down to about 500 m depth suggesting steady state conditions between pore water and groundwater (Figure 3-12). This situation would change slightly at shallow levels when taking into account an assumed arbitrarily decreased water content due to stress release, in that the pore water at the most shallow levels would have higher chloride concentrations than the formation groundwater sampled at the same depth. Unfortunately, no formation groundwater could be sampled from the interval around 600 m where the pore water chloride concentrations are highest in the entire profile.

At increasing depth in the borehole (i.e. near the top of the quartz monzodiorite) the pore water becomes more dilute than the formation groundwaters in the fractures suggesting that the pore water retains an older signature. Interestingly, this dilute pore water is not associated with an isotopic composition of glacial melt water, which might initially be expected. Below about 800 m the chloride concentration of the pore water once again becomes similar to the formation groundwaters in the fractures (as does the overall chemical type), in common with the shallower levels described above and also in conjuction with an increase in transmissivity at around 750 m. The pore water differs significantly, however, in chloride content and chemical type from the deepest formation groundwater sampled. Chloride concentrations similar to this deep formation groundwater could be approx. attained if the very low water content of the samples is arbitrarily decreased by 50% assuming stress release.

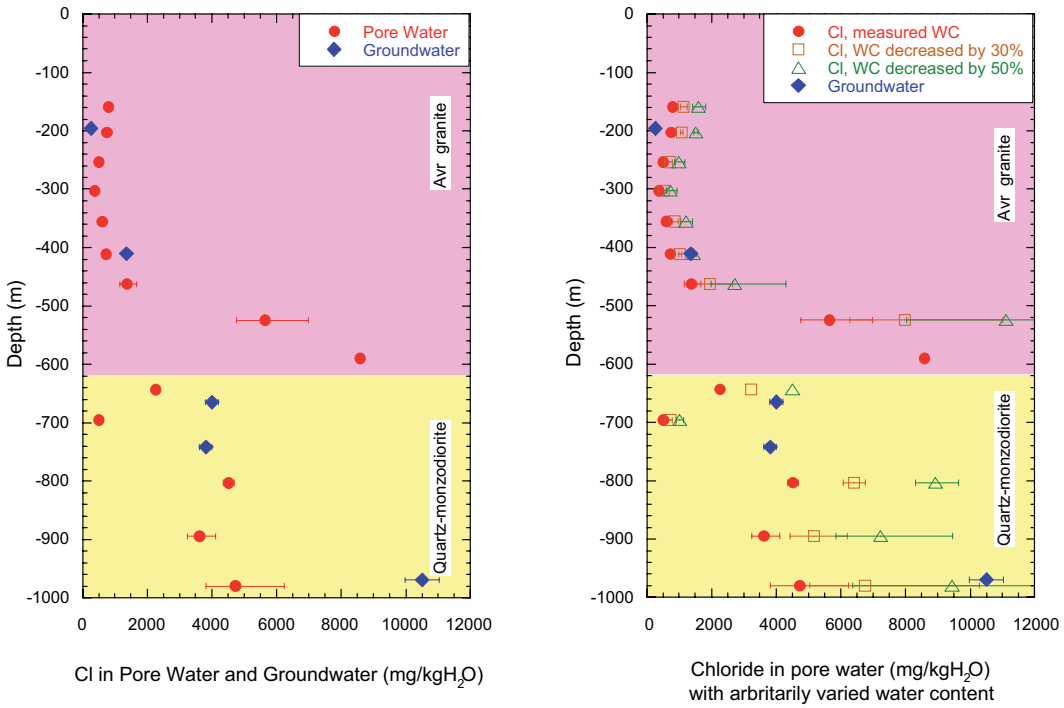

Figure 3-12. *Chloride concentrations of rock pore water from borehole KLX03 compared with groundwaters sampled from adjacent fractures as a function of sampling depth (left) and the same comparison with pore water chloride concentration calculated with arbitrarily decreased water contents to evaluate stress release effects (right; WC = water content).*

The characterisation of pore water in rocks from the Laxemar borehole KLX03 resulted in the following main conclusions (from the work in Appendix 1):

- Independent derivation of water content (to calculate (water content) porosity) by drying and isotope diffusive exchange methods gave consistent results excluding artefacts such as desaturation of the samples.
- There is multiple evidence that no significant stress release and its potential effect on water content porosity values and related drilling water contamination has affected the rock samples. Although quantitative proof cannot be given with the present data at hand, several qualitative arguments against such events happening have been discussed.
- The uncertainties surrounding the possibility of stress release effects were addressed by calculating the hypothetical variation in water content using a change of 50% by stress release; this would essentially increase the pore water chloride by a factor of 2. It is shown that such an increase would be inconsistent with determined parameters independent from water content measurements.
- Diffusion between rock pore water and adjacent formation groundwater bearing fractures and fracture zones, and vice versa, is identified as the dominant transport process; calculated diffusion coefficients agree well with present-day knowledge from the Laxemar site.
- Chemical and isotopic pore water signatures are characteristic and show a variation of groundwater composition with rock type and depth. In the Ävrö granite a shallow (< 450 m) and intermediate (450–600 m) zone can be distinguished. The pore water in the quartz monzodiorite indicates three zones (600–750 m, 750–850 m, and 850–1,000 m); this is in close agreement with the general trends in hydrochemistry of the adjacent formation groundwaters.
- There is little apparent evidence of a glacial melt signature in the pore waters; this could indicate that such waters had not diffused to the sampling location, or, they could have been subsequently removed, as suspected from the present steady state existing at shallower levels in the bedrock (to ~ 450 m).

- Pore waters at depth show a similarity with deep brine evolution.
- Steady state between pore water and formation groundwaters in the fractures is essentially only developed in the shallow zone of the Ävrö granite, while at depths greater than 450 m the chemical and isotopic composition of the pore water differs markedly from those of the formation groundwaters in fractures.

3.4.9 Fracture fillings

Available mineralogical information is based on Boremap data and more detailed investigations of cores from borehole KSH01A + B (cf Appendix 1). Even though most of the work reported so far has been carried out on core samples from the Simpevarp subarea, it can already be concluded that the sequences of minerals identified in the Simpevarp drillcores are recognised also in the Laxemar subarea boreholes and are very similar to earlier observations made at the Äspö HRL /cf e.g. Landström and Tullborg 1995, Andersson et al. 2002/.

From the perspective of groundwater chemistry the presence of four minerals, calcite ($CaCO_3$), gypsum ($CaSO_4$), barite ($BaSO_4$) and fluorite (CaF_2), are worthy of attention as their solutbility has an impact/control on the behaviour of some of the major ions.

Calcite is the most common of these minerals. It occurs frequently at all depths except in the upper tens of metres and below approx. 1,000 to 1,100 m were it is less common. A number of calcite generations have also been identified ranging from hydrothermal to possibly recent /Bath et al. 2000, Drake and Tullborg 2004/.

Barite occurs as very small grains but is relatively frequently observed (microscopically; not during the core logging) together with calcite, pyrite and the Ba-zeolite harmotome. In saline groundwater samples with very low SO_4 contents anomalously high Ba contents have been identified. For example, this was the case for the deepest saline groundwater from the KOV01 borehole at Oskarshamn, pointing towards a possible barite solubility control on the Ba and SO_4 content in the water.

Fluorite occurs in several hydrothermal mineral associations with epidote and later prehnite, and also occurs in a lower temperature (150°C) generation with calcite, barite and pyrite. Fluorite can be assumed to partly control the fluorite content in the groundwaters.

Gypsum is identified in relatively few fractures which in turn are usually situated in borehole sections showing a lowdegree of fracturing and low (or not measurable) transmissivity. Grondwater modelling /Laaksoharju et al. 2004/ suggests dissolution of gypsum as an explanation for the relatively high SO_4 contents in the saline Laxemar groundwaters but, sofar, it has not been possible to identify any gypsum in fractures from the Simpevarp area?. For example, gypsum has not been identified during the extensive work in the Äspö HRL. However, even though it can not be ruled out that it has been overlooked, a more probable explanation is that it is only present in some of the low-transmissive, relatively unfractured parts of the rock.

Other fracture fillings of particular interest for the hydrogeochemical interpretation are the redox-sensitive minerals. These consist mainly of Fe-minerals which in the fractures are dominantly haematite and pyrite. Some goethite may be present but is subordinate to haematite. In the very near-surface fractures, some less crystalline Fe-oxyhydroxides may be present, usually referred to as ‘rust’. These are likely to be related to recent oxidation and are usually associated with calcite dissolution.

In the fractures, several generations of haematite and pyrite are present. The observation of small pyrite grains in the outermost layers of the fracture coatings is in agreement with the groundwater chemistry, indicating reducing conditions.

From a redox buffer perspective, the main Fe-host in the fractures is, however, chlorite and clay minerals. Mössbauer analyses of fracture chlorites from Äspö HRL showed that 70–85% of the Fe present in fracture chlorites was Fe(II) /Puigdomenech et al. 2001/. In the bedrock, Fe(II) is dominantly found in biotite but also in magnetite, a common accessory mineral in the Ävrö granite and quartz monzodiorite.

Other redox sensitive phases may include Mn minerals but these are very rare and have not been identified in the area. However, Mn is present in the calcites (up to 1 or 2 weight %, although usually less than 0.5%) and also in some of the chlorites (less than 1 weight %).

3.4.10 Investigations of the geohistory of fracture minerals

Hydrogeological interpretations rely normally on borehole groundwater data and describe the present groundwater situation. This may, include the influence of perturbations such as groundwater short-circuiting through the surrounding bedrock and also along single boreholes under open hole conditions. Helping to unravel the influence of these perturbations (and other artefacts from borehole activities) to achieve an understanding of the 'undisturbed' formation groundwaters and their palaeo-evolution, is an integral part of the on-going hydrogeochemical evaluation process at the candidate sites.

Insight into the palaeoevolution of the groundwater systems is greatly aided by the fracture mineralogy which, in the best of cases, can help to evaluate the hydrogeochemical stability over timescales of interest for repository safety and performance assessment. Calcite is the mineral most frequently used for palaeohydrogeological interpretations as it can form during different temperature and pressure conditions including present low temperature ambient groundwater environments. Stable isotope analyses of O, C and Sr and trace element compositions can provide information about the groundwater from which the calcite precipitated. Under ideal conditions inclusions of formation groundwater are trapped within the developing calcite phases providing important information about the salinity and temperature of the in situ formation groundwaters. Moreover, many calcites show zonation and the character and succession of the different zones can provide information about changes in the groundwater chemistry with time.

Within the EU project PADAMOT a number of samples from borehole KLX01 have been analysed in detail for the purpose of palaeohydrogeological interpretation. This work has now been compiled and reported /Milodowski et al. 2005/, and the analyses will be made available for the Laxemar 2.1 modelling. Furthermore, stable isotope analyses (including not only O and C but also Sr) and chemical analyses of calcites from KLX03 and KLX04 have been carried out, which also will be included in the forthcoming Laxemar 2.1 model version.

Uranium-series analyses on fracture coatings from boreholes KSH01, KSH02 and KSH03 (in total 12 analyses) have been carried out and will be presented in the Laxemar 2.1 model version. Additional analyses from the Laxemar subarea are planned (samples are partly collected) and will be available for later model versions. The uranium-series analyses provide very useful palaeohydrogeological information in that they not only provide information about redox conditions and uranium transport, but may also provide time constraints on these processes.

3.4.11 Origin of brine water

The possible origin of the deep brine is discussed in detail in Appendix 1. It was concluded that there are several sources of salts that may combine to form highly saline groundwaters and ultimately hypersaline brines at great depth. However the fact that these deep saline groundwaters and brines are extremely old, have been subject to mixing, exist under near-stagnant hydraulic conditions and therefore long residence times, they have undergone intensive water/rock interactions which have served to mask any evidence of their original source and origin. Several hydrochemical and isotopic indicators are available to help unravel their hydrogeochemical evolution, but these have had only limited success and there is still much debate.

Considerable literature has been produced from the Canadian Shield brine occurrences /e.g. Frape and Fritz 1982, Gascoyne et al. 1989, Herut et al. 1990, Bottomley et al. 1999 and references within/ and although there is no dispute that the brine salinity is of marine basin origin, there is on-going debate as to the main mechanism responsible for concentrating fluids into hypersaline brine; evidence exists for both evaporative and cyrogenic processes.

In the Fennoscandian Shield the origin of the salinity is less clear; much evidence points to non-marine sources such as residual metamorphic/igneous fluids and fluid inclusions /Nordstrom et al. 1989/ accompanied by intensive meteoric water/rock interactions. The problem with these interactions is that they may mask any evidence of whether non-marine/old marine mixing has occurred at some period of time in the distant past. A marine origin for the brine salinity has been invoked by /Fontes et al. 1989/ and suggested also by /Louvat et al. 1999/ and /Casanova et al. 2005/. Therefore it is still an open question.

3.5 Massbalance, reaction path and mixing calculations

Hydrogeochemical modelling has been carried out with PHREEQC /Parkhurst and Appelo 1999/ using the WATEQ4F thermodynamic database. The main goal of the modelling is to investigate the processes that control water composition at the Simpevarp area based on a small subset of selected samples from the two main subareas (Laxemar and Simpevarp). The samples selected from boreholes KLX02 and KSH01A have a wide depth distribution and are representative of the depth evolution of the system (cf Appendix 3).

Modelling was carried out using the mass balance and mixing approach implemented in PHREEQC. The calculation procedure consists of assuming that each selected water is the result of: (a) mixing with the water immediately above the sampling location and with several end members (old waters already present in the rock system), and (b) reaction according to a preselected set of chemical reactions (only the simplest ones).

Once the samples have been selected, the next step involves the selection of the end members to be used in the calculations. The end members available for the modelling are Brine (B), Glacial (G), Littorina (L) and Precipitation. However, as in this specific modelling only groundwater samples are modelled, a new end member, "Dilute Granitic Groundwater (DGW)", representing shallow input into the system, was introduced.

After the samples and the end members had been selected, the mass balance calculations following two evolutionary trends with depth were conducted, one in the Laxemar subarea (borehole KLX02) and the other in the Simpevarp subarea (borehole KSH01A). In both cases, the trend starts by "evolving" a precipitation water into a diluted granitic groundwater. In this case the final solution is explained only by chemical reactions (no mixing) representative of the intense weathering in the overburden. The next step in both trends is the evolution from the representative diluted groundwater to the first real sample along the borehole. Now, apart from pure water-rock interaction, the potential mixing with "old" waters (B, G, L and DGW) is also taken into consideration in the balance. From this point on, all the subsequent steps include mixing of five end members (Previous Sample + DGW + G + L + B, as initial solution) and reactions involving calcite, silica, $CO_{2(g)}$, organic matter, cation-exchange (+ eq. gypsum in Laxemar) to reproduce the chemical and isotopic composition of the new sample. Results are shown in Figure 3-13 and Figure 3-14.

In both cases the mixing proportions evolve from dominant DGW proportions towards a more saline signature (Brine end member), more obvious in the Laxemar trend as the depth interval is three times greater than in the Simpevarp example.

Reactions are also similar although the amount of mass transfer is different. In general there is a clear dissolution process of the rock forming minerals (except for iron oxyhydroxides precipitation and CO_2 ingassing in the overburden) in the shallow part of the system, and a trend towards equilibrium with the selected minerals as depth increases (precipitation with progressively lower mass transfers). Cation exchange can play an important role in the balance including Ca, Na, Mg and K (Figure 3-13 and Figure 3-14).

For this exercise, the considered reactions are the simplest ones. A better understanding of the actual chemical processes operating in the system could be obtained when more data about the fracture minerals dominating at each depth and when the modelled hydrogeological flow lines in the system become available.

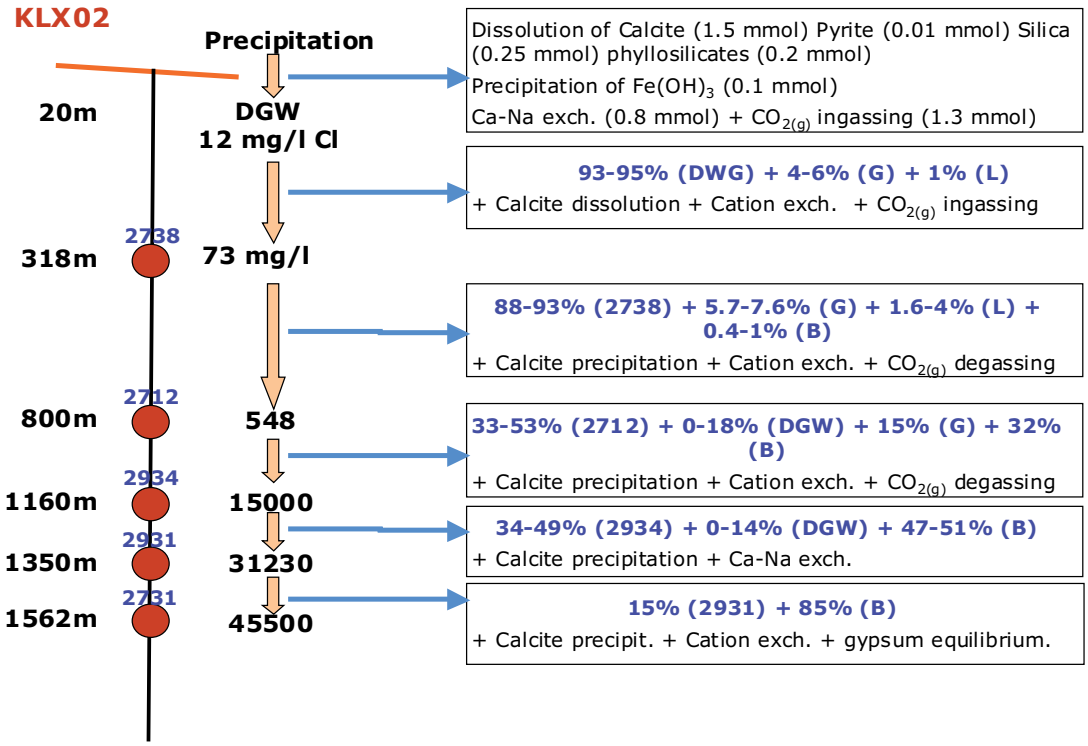

Figure 3-13. *Mixing and mass balance calculations obtained in the depth evolution trend represented by KLX02 (Laxemar subarea).*

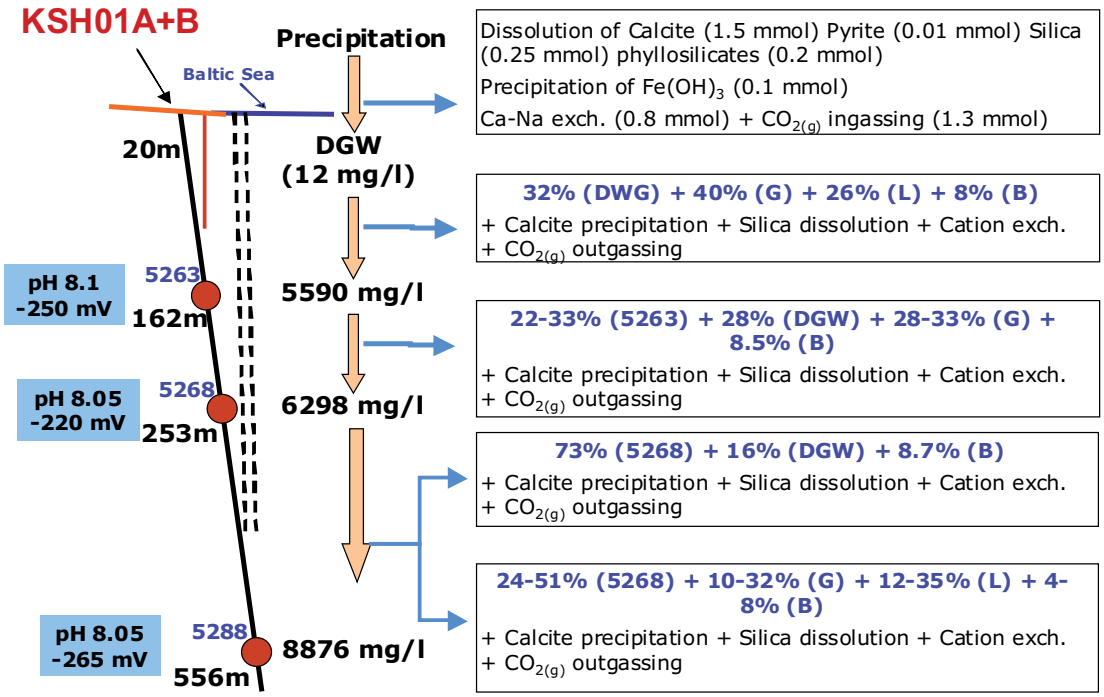

Figure 3-14. *Mixing and mass balance calculations obtained in the depth evolution trend represented by KSH01A (Simpevarp subarea).*

3.5.1 Sensitivity and uncertainty analysis of the mixing models

A sensitivity and uncertainty analysis was performed on results from PHREEQC, M4 and M3 applications (cf Appendix 3 and 4). The analysis has three parts:

1. Checking the inverse approach methodology implemented in PHREEQC by means of synthetic waters created with PHREEQC built-in direct-approach capabilities.
2. Checking the effects of the compositional variability of the end members on the mixing proportions calculated with M4 and M3.
3. Using synthetic samples, to check the effects of chemical reactions on the mixing proportions calculated by M4.

Inverse approach

In order to check the inverse approach implemented in PHREEQC (and to cross-check M4) several synthetic waters have been composed representative of groundwaters affected by two broad geochemical processes: mixing with old waters and reaction with the rock forming and fracture filling minerals. This procedure was carried out with the direct approach implemented in PHREEQC. With the knowledge of the processes responsible for the chemical composition of these waters, the inverse approach has been used to account for the processes (cf Appendix 3).

The mixing and mass balance calculations performed with PHREEQC, give a reasonable estimate of the end members mixing proportions. The use of at least three conservative species (Cl, δ^2H, $\delta^{18}O$) provides extra robustness to the calculated proportions independently of the reactions or phases included in the calculations.

First, all these results start with a selection of the end members to be used in the calculations. The effects of a different selections were already checked elsewhere /Laaksoharju 1999, Luukonen 2001/ and can dramatically modify the mixing proportions and mass transfers obtained. Several calculations were made in the present work with two additional end members (Sea Sediment and Baltic) in the inverse modelling, not used in the direct calculations. The results indicate that Littorina proportions were the most affected, either lowering its proportions or transfering of its proportion to one of the two new end members, Baltic or Sea Sediment. Therefore, the selection of end members is a fundamental component in this methodology and it requires a very careful hydrogeological and hydrogeochemical study of the system.

Second, sulphate-reduction in waters with high sulphate contents produces additional variations, mainly in the mixing proportions of the end members which supply this component to the waters (Brine and Littorina). Therefore, the real presence of this process must be clearly established before the mass balance calculations are performed. Alternatively, the inclusion of a higher number of parameters in the model should be taken into account.

Finally, with the analytical data used in the mass balance calculations, the chemistry of groundwaters can be explained by invoking the action of different reactions, mainly ionic exchange and equilibrium with different mineral phases (mainly aluminosilicates and calcite). However, the lack of aluminium data in the studied groundwaters and exchange capacity constants in the fracture filling minerals, are two important limitations, both in assessing the feasibility and extent of these processes before the balance calculations are carried out, and in the overall performance of the approach.

Compositional variability of end-members

A procedure has been developed to assess the impact of the compositional variability of water end members on the calculated mixing proportions (cf Appendix 3). This scheme is based on a PCA analysis performed with the M4 code.

The procedure starts from a pre-selected number of end members (i.e. no attempt is made here to define which end members to be use in the analysis) and has the following steps: (1) Define the compositional variability of the end-members; (2) Construct a probability density function (input

probability) from the compositional ranges; (3) Generate, according to the chosen input probabilities, a large number of end member compositions; (4) For each run, compute the mixing proportions of selected samples; (5) Bin mixing proportions to construct the output probability distributions.

For the definition of the input probability density functions (pdfs) that characterise the compositional variation of each end member (step 2 above) the following two assumptions are adopted: (1) all compositional variables follow a *log-normal distribution* except those expressed as delta-values (^{2}H and ^{18}O), which follow a *normal distribution;* and (2) the input ranges are equated to the 99th *percentile* of the chosen probability function, which means that, with a probability of 1%, end-member compositions outside the reported range are allowed. The ranges are defined by expert judgment, taking into account all the geochemical and hydrological knowledge of the system. Table 3-2 summarised the ranges used for the modelling in Laxemar 1.2.

Once a probability function has been chosen and the statistical meaning of the empirical compositional range defined, the input probability functions are completely characterised. Figure 3-15 shows, as an example, the input pdfs for SO_4 (a lognormal distribution) and ^{2}H (a normal distribution) for five end-members used in the Laxemar 1.2 modelling (Brine, Glacial, Littorina, Rain and Dilute groundwater). The pdfs have been constructed binning 10,000 values for each compositional variable and normalising to ensure that the area under each curve is equal to unity.

Table 3-2. Compositional ranges of the end members used in Laxemar 1.2 PCA mixing modelling.

End member	Na (mg/l)	K (mg/l)	Ca (mg/l)	Mg (mg/l)	HCO_3 (mg/l)	Cl (mg/l)	SO_4 (mg/l)	^{2}H (dev)	^{3}H (TU)	^{18}O (dev)
Brine 1	8,500	45.5	19,300	2.12	14.1	47,200	906	–44.9	0.00	–8.9
Brine 2	9,540	28	18,000	130	8.2	45,200	8.4	–49.5	0	–9.3
Glacial 1	0.17	0.4	0.18	0.1	0.12	0.5	0.5	–158	0.00	–21
Glacial 2	0.17	0.4	0.18	0.1	0.12	0.5	0.5	–125	0	–17
Littorina 1	3,674	134	151	448	93	6,500	890	–38	0.00	–4.7
Littorina 2	1,960	95	93.7	234	90	3,760	325	–53.3	0.00	–5.9
Rain 1	0	0	0	0	0	0	0	–125	0	–17
Rain 2	0	0	0	0	0	0	0	–44	168	–6.9
DGW 1	19.2	3	38.5	3.8	162	12	21.5	–68.4	11.913	–9.9
DGW 2	237	4	25	6	370	119	118	–73.8	0.775	–9.9

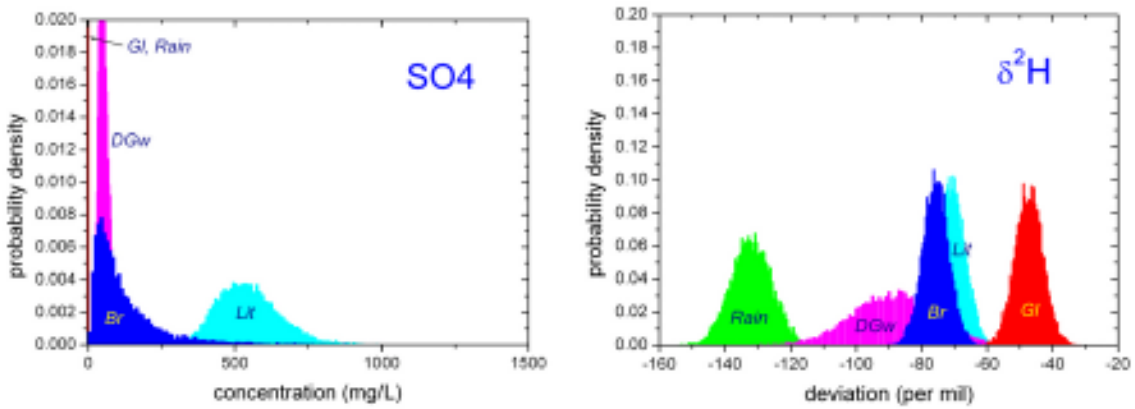

Figure 3-15. *Input probability density functions for SO_4 and ^{2}H, as constructed from the compositional ranges of the end-members Brine (blue), Glacial (red), Littorina (cyan), Rain (green) and Dilute Groundwater (magenta).*

The output probabilities (the ones that give the uncertainty in the mixing proportions) are calculated by running the PCA-mixing step a large number of times, each one with a different composition of the end-members. The composition is chosen at random based on the input probability distributions. Each sample in the dataset has its own output pdf, reflecting the impact of the compositional variability of the end-members on the mixing proportions. Figure 3-16 shows the output pdfs for three selected samples from borehole KSH01A. The calculations were done using the 158 groundwater samples in the Laxemar 1.2 dataset and the end-members Brine, Glacial, Littorina and Dilute groundwater. As can immediately be appreciated, the range of mixing proportions for each of the selected samples is quite narrow, considering the a priori compositional variability of the end members. This is a strong indication that the computed mixing *proportions are indeed a robust estimator of the mixing behaviour of the waters.*

The important conclusion that can be drawn from the above results is that, *once the number and type of end members are known,* the inclusion of the compositional variability of the reference waters in the PCA analysis gives a robust estimation of the mixing proportions, in the sense that the output probability functions are narrow, predicting mixing proportions tightly concentrated around a mean value. The bonus of this analysis, apart from the robustness itself, resides in the statistical bracketing of the variability of the mixing proportions, which is a fundamental issue when "exporting" these results for hydrogeological modelling.

Several M3 modelling concerns were identified during the stage 1.1 and 1.2 of the site modelling project (cf Appendix 4). The following concerns were adressed:

- *Can a better resolution be obtained by using only site specific data in the modelling?* In order to optimise the statistical modelling used in the M3 calculations, as many observations as possible are required. Therefore, data from as many Nordic sites as possible are analysed and the information compiled together. The dataset is called "All Nordic Sites" containing data from the sites: Finnsjön, Fjällveden, Forsmark, Gideå, Karlshamn, Klipperås, Kråkemåla, Oskarshamn, Svartboberget, Taavinunnanen (all from Sweden), Olkiluoto, Kivetty and Romuvaara (from Finland).
- *Are all variables useful in the PCA?* As many meaningful variables as possible are used in the M3 modelling. A fixed set of variables will, for example, allow comparisons between the groundwater characteristics of the Laxemar and Forsmark sites. The variables used are the major components (Na, K, Ca, Mg, Cl, HCO_3 and SO_4) and the isotopes ^{2}H, ^{18}O and ^{3}H. Although the inclusions of all variables makes the model sensitive to effects from reactions (see next section) An important concern was the use of tritium. Samples collected at different years are difficult to compare directly because the radioactive decay. The tritium values can also be affected by the nearby nuclear power plant. The tritium values for some of the analyses were time corrected in order to be more comparable. Later on this approach has been questioned (see Appendix 5). The reason is that tritium is affected by transport and decay and a simple time correction cannot be used on the obtained data.
- *Should samples from the surface and bedrock be analysed together in the same PCA?* There are no clear indications of direct flow connections between the surface and the bedrock system. Global models included all type of data and were analysed separately from data containing only data from bedrock (bedrock models).

Based on the above concerns, five test runs were performed where the data and the variables were modified. The tests show that in most cases the model is robust and is not affected to any large extent by changes in data set or removal of some variables or changes in the end-member selection in agreement with the M4 tests. In any case, the effects have to be tested carefully before accepting the changes in the final models to be used for site description. An example of the outcome is shown in Figure 3-17, where the removal of surface waters and tritium and changing the end-member from rain water to shallow groundwater did not change to any large extent the calculated mixing proportions.

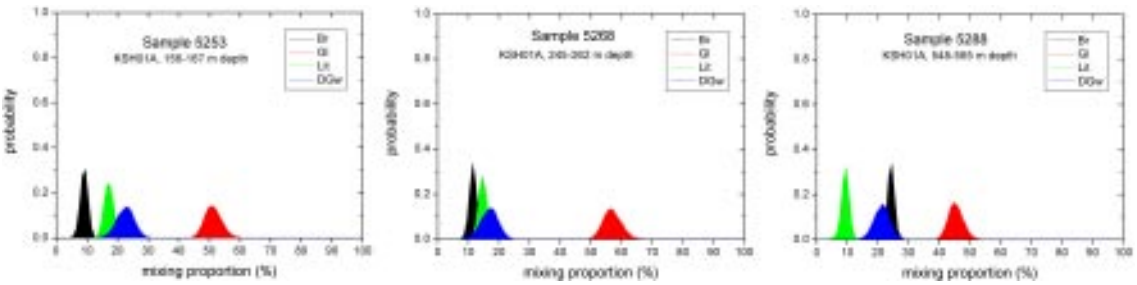

Figure 3-16. *Mixing proportions for three samples from borehole KSH01A (Simpevarp area). End members used for the calculations are Brine + Glacial + Littorina + Dilute Groundwater. For the PCA analysis only groundwater samples from Laxemar 1.2 iteration were used (158 samples).*

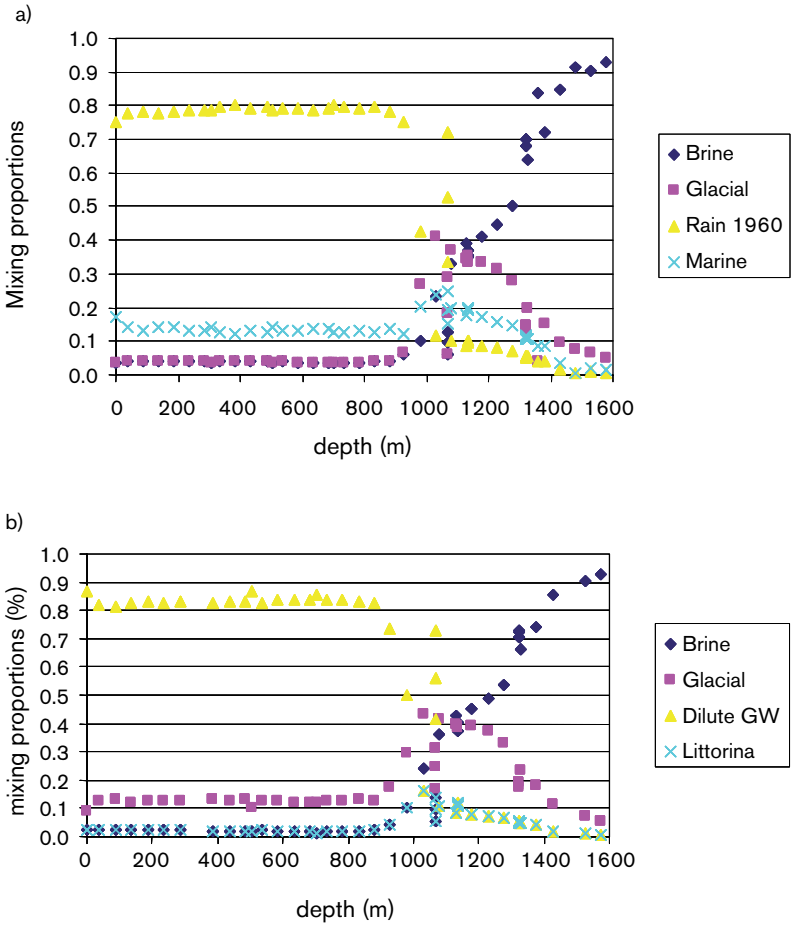

Figure 3-17. *Mixing proportions along KLX02 calculated using: a) all data, and b) omitting surface samples and tritium and changing the end member from rain to shallow groundwater in the M3 analysis.*

Effects of chemical reactions on the mixing proportions

Synthetic waters created by PHREEQC with known mixing proportions and reaction processes have been used for verifying the M4 performance (cf Appendix 3).

Ideally, M4 should provide mixing proportions as close as possible to the synthetic ones, independently of the compositional variability introduced by reactions. Only then the chemical differences between the synthetic waters and the waters obtained from the M4-calculated mixing proportions can be used, via a mass balance step, for inferring the reactions that could have taken place in the system.

In order to verify this, several synthetic waters have been included in the Laxemar 1.2 dataset (Local Model, groundwaters only, 158 samples). Mixing proportions have been calculated considering Brine, Glacial, Littorina and Precipitation (= Rain) as end members. The variables used for these calculations are: Na, K, Ca, Mg, HCO_3. SO_4, Cl, δ^2H, $\delta^{18}O$, ^3H. The tests were performed on samples representing: pure mixing, mixing + ionic exchange, and mixing + sulphate reduction. A set of simulations were also run considering only conservative elements (Cl, Br, δ^2H, $\delta^{18}O$) to check the influence of non-conservative elements in the mixing proportions.

The main results can be summarised as follows: When chemical reactions produce only minor compositional changes (lower than 2%) with respect to the chemical composition of samples created by conservative mixing, M4 gives mixing proportions in very good agreement with the measured ones.

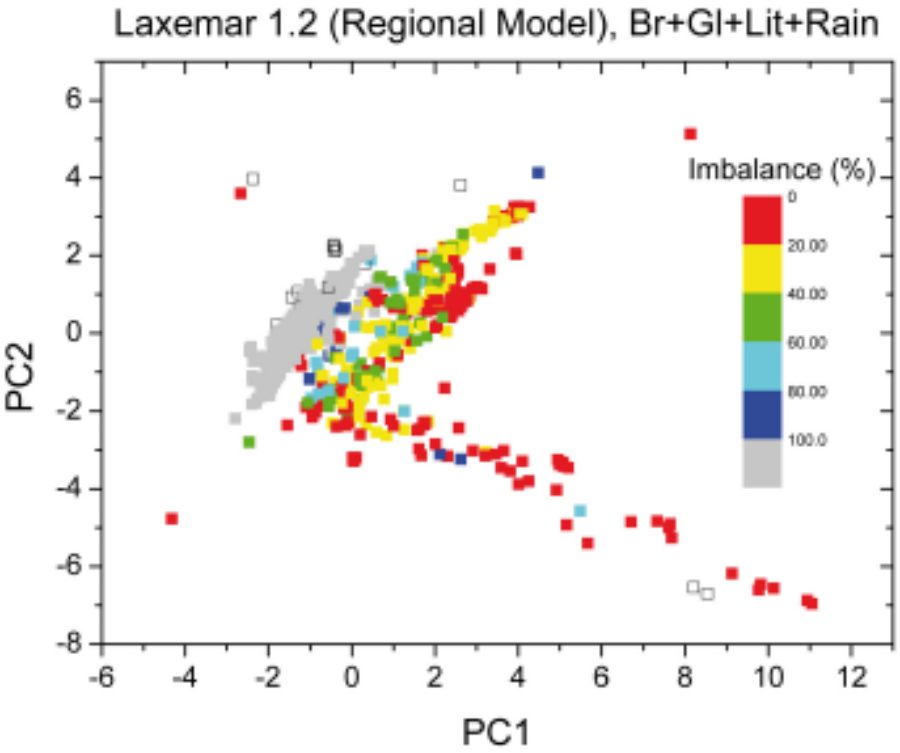

Figure 3-18. *Chlorine imbalance (measured as an absolute percent deviation from the real Cl content) in the Laxemar 1.2 Regional Model consisting of 1,088 samples. Grey samples have Cl imbalance greater than 100% and mainly correspond to superficial waters with very low Cl content. Open squares are samples not explained by mixing (outside M4 hyper-tetrahedron).*

When chemical reactions produce an important compositional change (higher than 10% for the studied samples) M4 mixing proportions do not in general reproduce the original values, and the amount of bias depends on both the chemical reaction and the type of water. For example, a simple reaction like sulphate-reduction (affecting only two of the elements included as variables in the calculations, SO_4 and HCO_3) can be responsible for important deviations in the calculated mixing proportions. The reason for this is that the noise introduced by the non-conservative elements in this kind of statistical analysis readily propagates to the mixing proportions calculated by the code. Preliminary tests carried out using only conservative elements suggest that mass balances are more robust that the ones computed using conservative and non-conservative elements. Further testes have to be conducted in order to see if the calculation in multidimensional space (M4) is more sensitive than calculations in 2D (M3).

Nevertheless, once the mixing proportions are calculated, mass balances provided by the code (with respect to the conservative elements, especially chloride), can easily detect those samples in which reactions have produced the biggest departure from the calculated mixing proportions (Figure 3-18). Waters with a high Cl imbalance are likely to be affected by reactions and should be checked independently because their mixing proportions are biased. An analysis of this sort should be considered a basic tool when assessing the reliability of the mass balance calculations and also of the calculated mixing proportions.

All the above uncertainties are taken into account in M3 in a lumped way when reporting that mixing proportions less than 10% are under the detection limit of the method and that the accuracy of the mixing proportion is ± 10% from the reported values. The detection limit and accuracy values will be further checked in future calculations with M3 and M4.

As mentioned above, the alternative could be the use of M4 only, with conservative elements. The scoping calculations performed with this methodology indicate that the calculated mixing proportions agree very well with the synthetic ones and are not affected by the reduction in the number of compositional variables used as input data. The main drawback of this approach is that it cannot be implemented if the number of conservative elements is low, specifically if lower than the number of end-members. In other words, the applicability of the method depends on the number of end members to be considered, the availability of conservative elements and ultimately the complexity of the groundwater system.

The uncertainty evaluations described above represent a major step forward in the uncertainty evaluation of the methods used and will help in judging the feasibility of the results calculated as well as future integration work with the hydrogeological modelling.

3.6 Modelling of tritium transport

The final aim is to perform coupled modelling of flow and reactive transport, in order to support the hydrochemical interpretation of field data. It is expected that reactive transport modelling will provide a quantitative framework for testing alternative hydrochemical hypotheses and conceptual models of key hydrochemical processes. The first step was to simulate conservative species (e.g. salinity, chloride). Tritium transport has now been included in order to have an independent source of information about the behaviour of the fresh water hydrogeological system.

The SUTRA /Voss and Provost 2003/ and CORE /Samper et al. 2000/ codes have been slightly modified to be compatible to solve, in two-steps, density dependent flow and reactive solute transport problems (Appendix 5).

Groundwater recharged in the past decades and taking part in an active hydrological cycle is referred to as modern groundwater /Clark and Fritz 1997/). Tritium has become a standard tool for the definition and study of modern groundwater systems. The era of thermonuclear bomb testing in the atmosphere (1951–1976), provided the tritium input signal that defines modern water. Due to its natural decay, pre-bomb tritium input cannot normally be detected; such tritium-free groundwater is considered “sub-modern” or “old water” /Clark and Fritz 1997/.

A two-dimensional domain has been simulated along a large-scale profile perpendicular to the coastline. Its total length is 35 km, 28 km of which correspond to land surface whereas the remaining 7 km are under the sea. The model domain is 2 km deep. A density-dependent groundwater flow model has been calibrated by comparing computed salinity against measured profiles in the Laxemar and Simpevarp subareas (see Figure 3-19). Hydraulic and transport parameters are based on previously available information from the Simpevarp area /Rhen et al. 1997/. Subsequent model versions (2.1) are being updated by using the latest hydraulic information presented in this report (including depth dependency of permeability).

Tritium evolution within the modelled profile through the Simpevarp area can be simulated as a natural tracer test. Its behaviour is not conservative since it is affected by radioactive decay, with a half-life of 12.43 years, and matrix diffusion (not included in this modelling). A step-wise time function, which mimics the Ottawa time series IAEA 2001 of atmospheric tritium, has been used as a time-varying condition at the top boundary, associated with the recharged (infiltrated) water. Initial conditions of tritium contents have been generated by a long-term run of the model from year 0 to year 1950. Figure 3-20 shows simulated tritium contents in groundwater at year 1951. This distribution corresponds to the steady state prior to the nuclear bomb tests performed during the period 1951–1976.

Figure 3-21. Shows the simulated tritium content in year 1993. The advective front of "modern" water infiltrated during the 1950's–1970's can be seen in the Laxemar subarea at a depth of about 800–900 m.

A certain overestimation of tritium content is observed when comparing model results with measured values (Figure 3-22). The discrepancy can be attributed to the fact that the upper soil layer is not considered in the model, thus imposing effective recharge directly on the bedrock top boundary. As a result, the travel time from the surface to the bedrock is neglected, which gives rise to a lesser degree of radioactive decay. In addition, matrix diffusion is also neglected in the current version

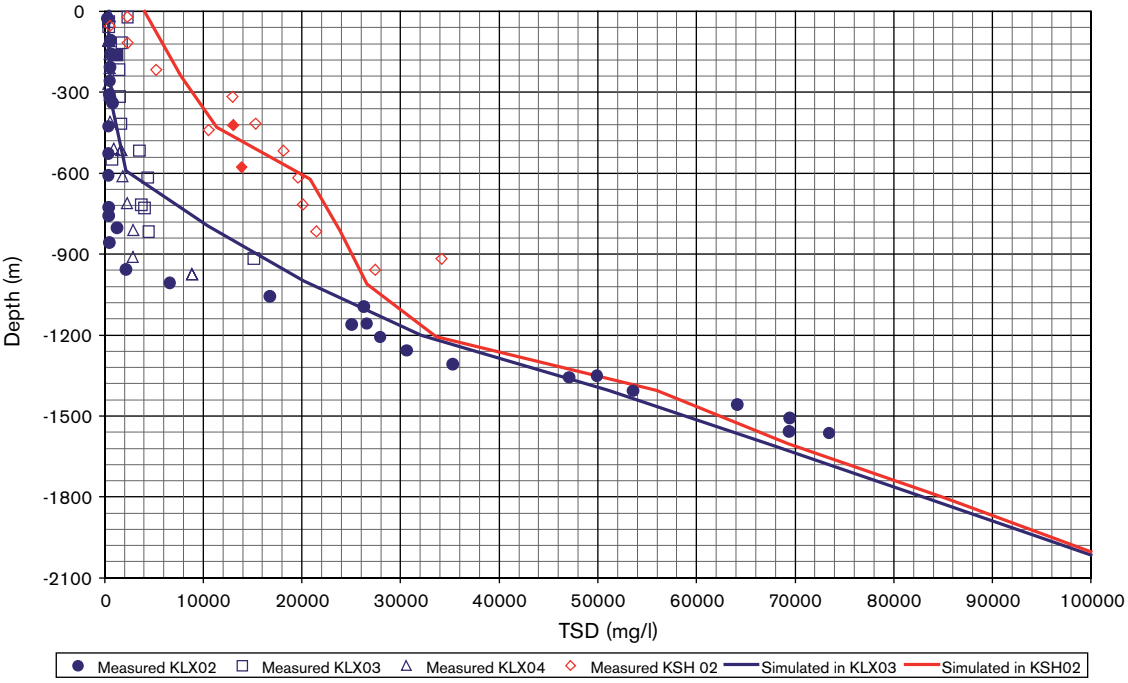

Figure 3-19. *Measured and computed salinities (TDS) versus depth in KLX02, KLX03, KLX04 (Laxemar subarea) and KSH02 (Simpevarp subarea). Unfilled symbols correspond to unrepresentative samples. Filled symbols correspond to representative samples.*

of the model which can also explain an overestimation of computed tritium activities. It is worth noting that even with a rough representation of the natural hydrogeological system, the model is able to provide patterns of tritium concentration which are qualitatively comparable to those measured at borehole KLX02, with a concentration peak located at approx. 900 m of depth. However, the representativity of the tritium values in KLX02 at year 1993 have been questioned (cf Appendix 1). The above modelling exercise will be updated and subject to additional testing when more data and updated hydrogeochemical models for the Laxemar subarea become available.

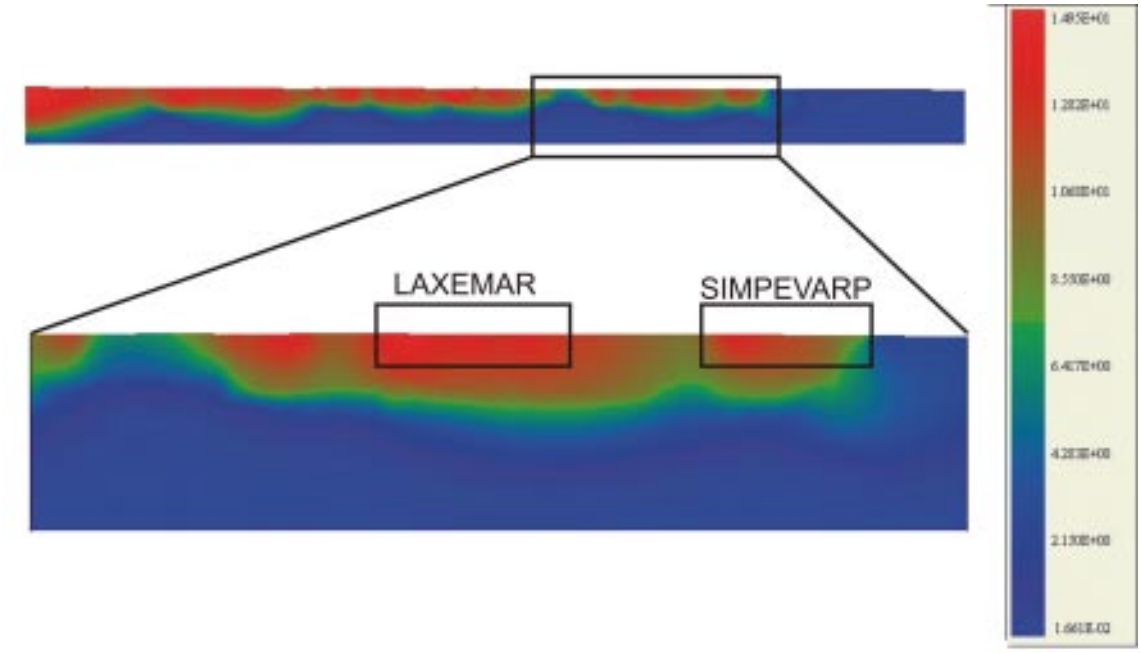

Figure 3-20. *Simulated tritium contents in the Laxemar and Simpevarp subareas at year 1951 (repreenting pre-bomb test conditions).*

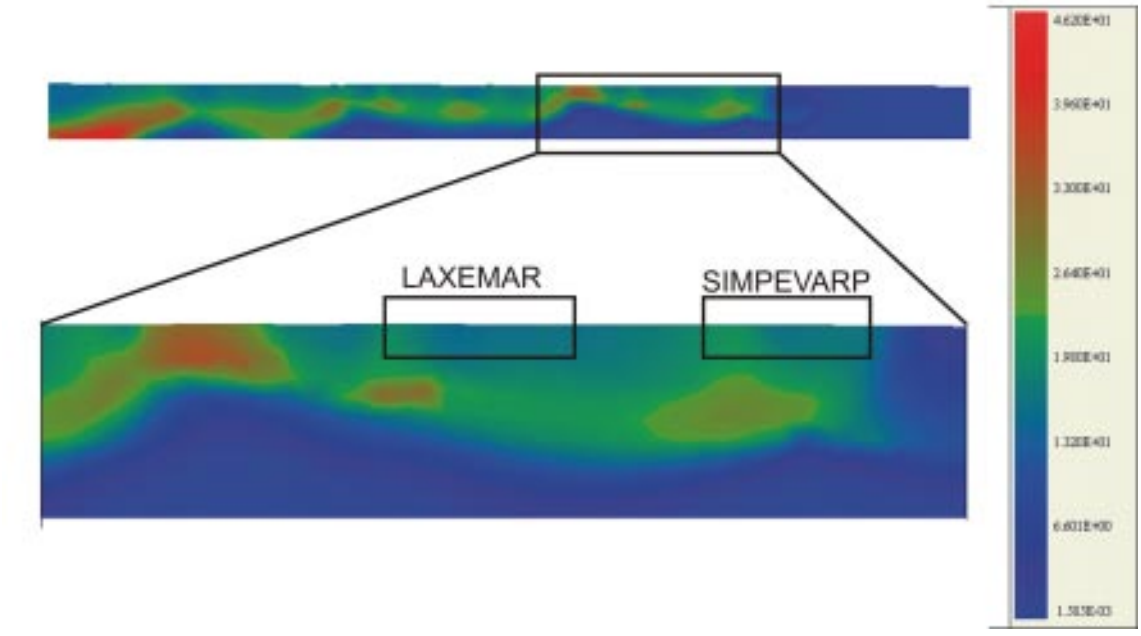

Figure 3-21. *Simulated tritium contents in the Laxemar and Simpevarp subareas at year 1993.*

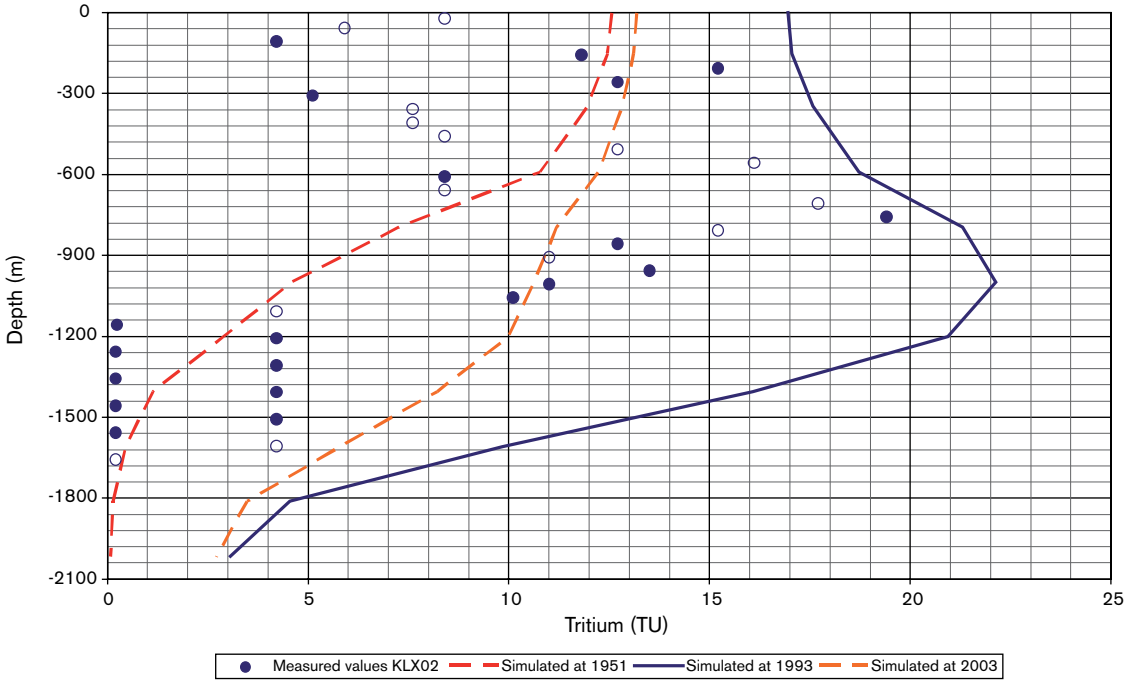

Figure 3-22. *Measured and computed tritium activitiy (TU) versus depth in KLX02. Computed tritium at 1951 (previous to bombs) and 2003 is also shown). Filled symbols correspond to representative samples and unfilled symbols to non epresentative samples.*

3.7 Conclusions used for the site descriptive model

The descriptive and modelled observations described in the preceding sections are included in the hydrogeochemical site descriptive model (see Chapter 4) and they are fundamental to the overall hydrochemical understanding of the site. The basic groundwater evolution and origin of the groundwater is now fairly well established. The possibility to characterise the pore water chemistry in bedrock is an important improvement for the undersanding of the interaction between the rock matrix and groundwater chemistry in fractures. The understanding of the groundwater system such as redox conditions has evolved both from a hydrochemical and microbial point of view. The uncertainty issues related to mixing modelling have been further detailed. Important features, summarised in previous sections are discussed and visualised below.

3.7.1 Visualisation of the groundwater properties

An important tool for site understanding, i.e. constructing a conceptual model and for integration of the results with hydrogeology, is the spatial representation and visualisation of available data. Hydrochemical modelling is usually made on a “water sample basis” with relatively little analysis of the spatial distribution of the information. Hydrochemical information is normally treated either by x-y plots (a given variable against chloride or depth, etc) or more sophisticated methods such as mass balance and statistical mixing models. These kinds of analyses often make it difficult to obtain an impression of information which corresponds to different hydrogeological and geographical settings, such as inland-coastal or recharge-discharge zones. This is why a specific visualisation application has been developed with the aim of representing “objectively” (i.e. without interpolation) the available hydrochemical information. The visualisation tool has been programmed using the IBM Open Visualization environment, known as OpenDX (cf Appendix 5).

Modelling and visualisation of the near surface properties

The interactions between the surface and deep groundwaters were described in detail in Appendix 1). All original data used are stored in the primary databases (SICADA and/or GIS). The evaluation strategy is based on a large amount of background information which was systematically incorporated:

- Elevation maps showing the locations of the cored and percussion boreholes and soil pipes.
- Regional hydrological identification of recharge/discharge areas and their relation to the locations of cored and percussion boreholes.
- Hydrological characterisation of soil pipe locations in terms of potential recharge/discharge areas.
- Correlation of soil pipe groundwater hydrochemistry with the hydraulically identified recharge/discharge areas; selection of areas showing a positive correlation.

Based on geological and hydrological information and the distribution of soil types in the overburden, a preliminary classification of the soil pipe data in terms of recharge/discharge could be carried out. Prior to this, however, an initial classification was conducted based on the hydrogeological modelling (in turn based on topography).

Using the overburden soil pipe hydrochemical data a preliminary series of anomalous ('hot spot') chemical distribution maps were made (see Appendix 1). The available data (most of the data points) at this initial stage included only chloride, sulphate, pH and alkalinity.

When available, the following background data were used when studying shallow groundwater from percussion drilled boreholes:

- Geophysical logs (BIPS, resistivity, fracturing).
- Recorded observations of groundwater flow.
- Hydraulic tests and flow measurements.
- Hydraulic conductivity and transmissivity.

Using this information the hydrochemical data were, when possible, allocated to the following shallow depth intervals: 0–25 m, 25–50 m, 50–75 m, 75–100 m, 100–150 m, 150–200 m and 200–250 m. Selected ion and isotopic plots versus depth were then produced (see Appendix 1). The data were plotted to identify any shallow groundwater trends that might, together with the Soil Pipe evaluation, give some indication of recharge/discharge features.

The conclusion is that this preliminary evaluation of groundwater data representing the geosphere/biosphere interface has shown promising results. This has involved overburden data from Soil Pipes and upper bedrock (0–200 m) data from percussion boreholes. Integration of these data has identified areas of recharge/discharge which will be further investigated and quantified when more data become available. This will help to characterise the chemical and isotopic composition of the recharge water end member into the bedrock and, also, the evolution of groundwaters at points of discharge from the bedrock into the overburden in future model versions.

The overall picture from the evaluation in Appendix 1 is that discharge locations, at one area characterised by tritium free water, have been identified in the Simpevarp subarea (Ävrö), whereas near-surface groundwaters from Laxemar (only percussion borehole data are available so far) are mainly characterised by recharge or shallow discharge (except for HLX20) characteristics.

The soil pipe data described above were used for visualisation (cf Appendix 5) and Figure 3-23 shows the location of all the available soil pipes in the Laxemar and Simpevarp subareas (cf Appendix 4).

Only those samples categorised as “representative samples” in the database have been included in the visualisation of near-surface hydrochemistry. The amount of data is different depending on the type of element to be visualised (i.e. there are more representative samples with chloride or bicarbonate data than tritium or ^{14}C data, for instance).

Figure 3-24 shows chloride concentrations in soil pipes. It can be seen that near surface groundwater samples are diluted, with chloride concentrations always lower than 150 mg/L. However, there is a clear influence of Baltic water in those soil pipes located close to the coast line (such as SSM00034 and SSM0040). An apparent anomaly to this general trend is observed in soil pipe SSM00022, located on Ävrö. This particular soil pipe is not located close to the coast line but more “inland” on the Ävrö Island. However it shows the highest chloride concentration of all the representative samples of soil pipes. This soil pipe also shows the highest concentrations of strontium, sodium and sulphates.

Figure 3-25 shows the spatial distribution of bicarbonate in soil pipes. Bicarbonate is the dissolved component having the largest number of representative samples. It can be seen in Figure 3-25 that there is not an easily recognisable spatial trend for this component. The highest concentration of bicarbonate corresponds to soil pipe SSM00034, which is located on the coast, opposite to Äspö, but other soil pipes located in the vicinity of the coast line show low concentrations. At inland positions in Laxemar subarea, there are a number of soil pipes with low bicarbonate concentrations (such as SSM00031, SSM00009, SSM00011, SSM00019 and SSM00017) and other soil pipes located even further inland (SSM00030, SSM00037 and SSM00021) which show relatively high concentrations. Dissolved bicarbonate can be related to two main processes: calcite dissolution and oxidation of organic matter. Thus the spatial distribution of bicarbonate concentrations could be correlated with local abundance of calcite and/or organic matter. It can be expected that both compounds will be more abundant where Quaternary deposits and organic soils are thicker.

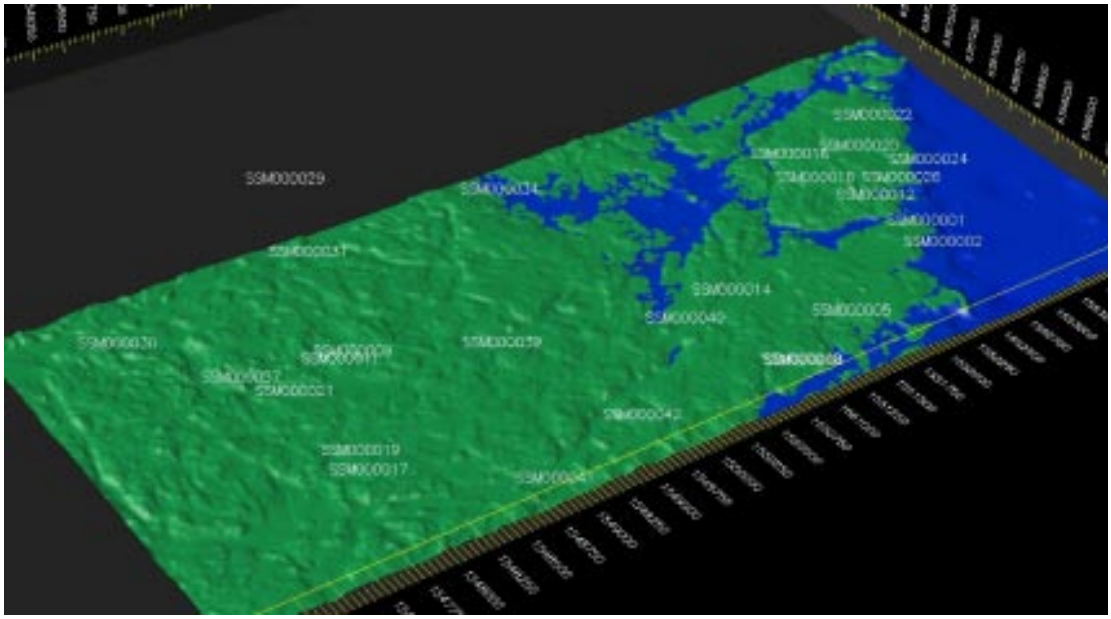

Figure 3-23. *Spatial location of soil pipes included in the Laxemar v. 1.2 work.*

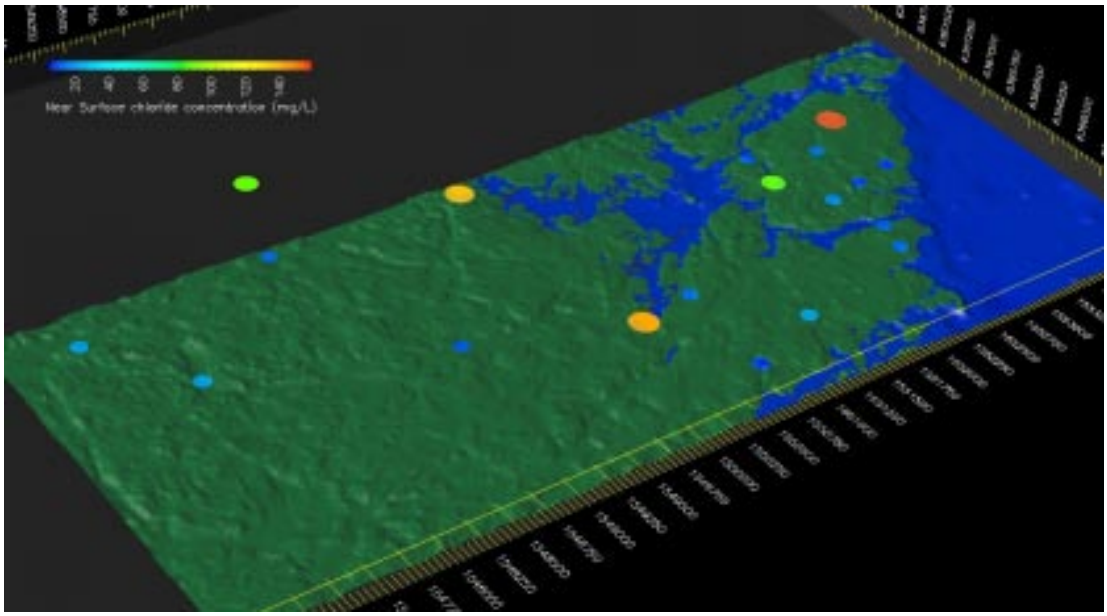

Figure 3-24. *Spatial distribution of chloride concentration in soil pipes. The highest value is located in soil pipe SSM00022 at Ävrö.*

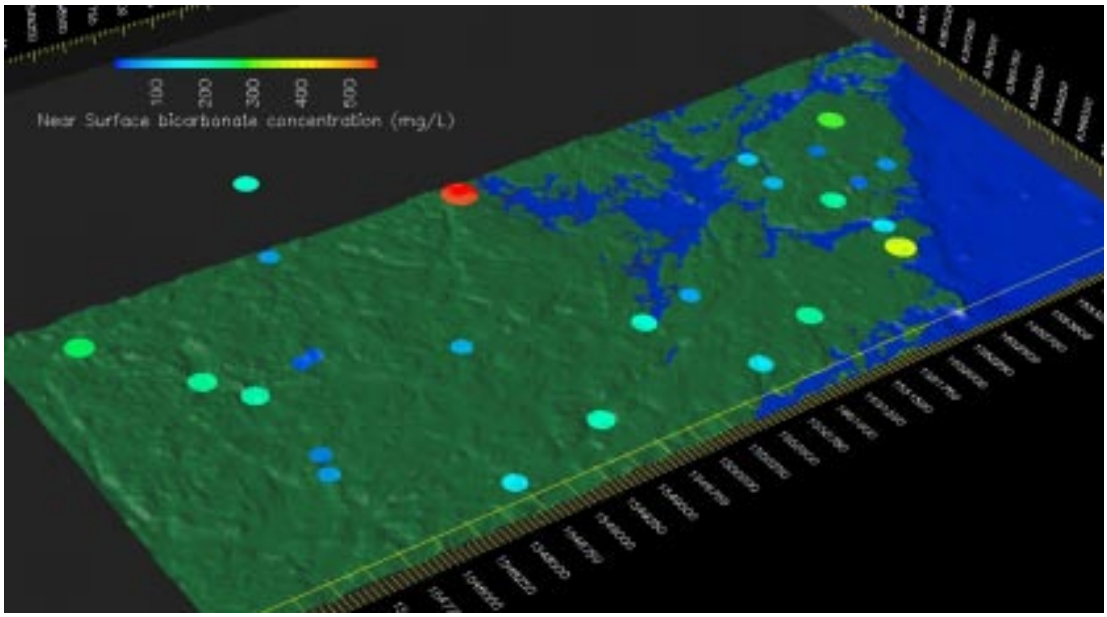

Figure 3-25. *Spatial distribution of bicarbonate concentration in soil pipes. There is not an easily recognisable spatial trend for this component.*

There are few representative samples in soil pipes that have been analysed for radioactive isotopes. Figure 3-26 and Figure 3-27 show the spatial distribution of available measurements of ^{14}C and tritium, respectively. It can be recognised that soil pipe SSM00022 (Ävrö) shows clearly the lowest modern carbon contents and tritium activities.

From the above analyses it can be seen that soil pipe SSM0022 on Ävrö shows hydrochemical signatures consistent with the influence of older and more saline groundwater than the representative samples from other soil pipes. These hydrogeochemical signatures, typical of the near-surface environment, could provide an indication of a groundwater discharge zone or stagnant older water that has been preserved under a low-permeable soil cover. At the present time, there is no available isotopic information for soil pipes in the Laxemar subarea.

Modelling and visualisation of the groundwater properties

Figure 3-28 shows a top view for the location of the main cored boreholes (from the point of view of the number of representative samples) available in the Laxemar and Simpevarp subareas, as they are included in the Laxemar 1.2 data freeze (Appendix 5).

The main available cored boreholes are KLX01, KLX02, KLX03 and KLX04 in the Laxemar subarea and KSH01, KSH02, KSH03, KAV01, KAV04, KAS02, KAS03, KAS04 and KAS06 in the Simpevarp subarea. It is worth noting that several percussion boreholes also contribute to the hydrochemical database with representative samples. The geometry of the percussion boreholes has not been included yet in the visualisation program, but all the representative samples available in the database, including percussion boreholes, have been taken into account for the hydrochemical visualisation.

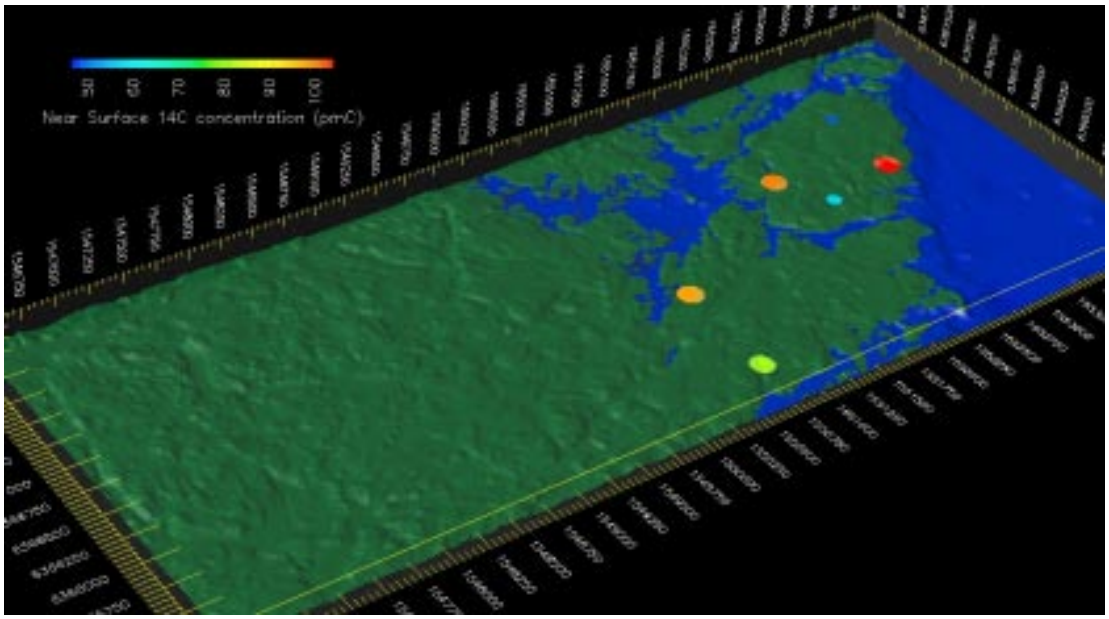

Figure 3-26. *Spatial distribution of ^{14}C (pmC) in soil pipes. The minimum value is located in soil pipe SSM00022 at Ävrö.*

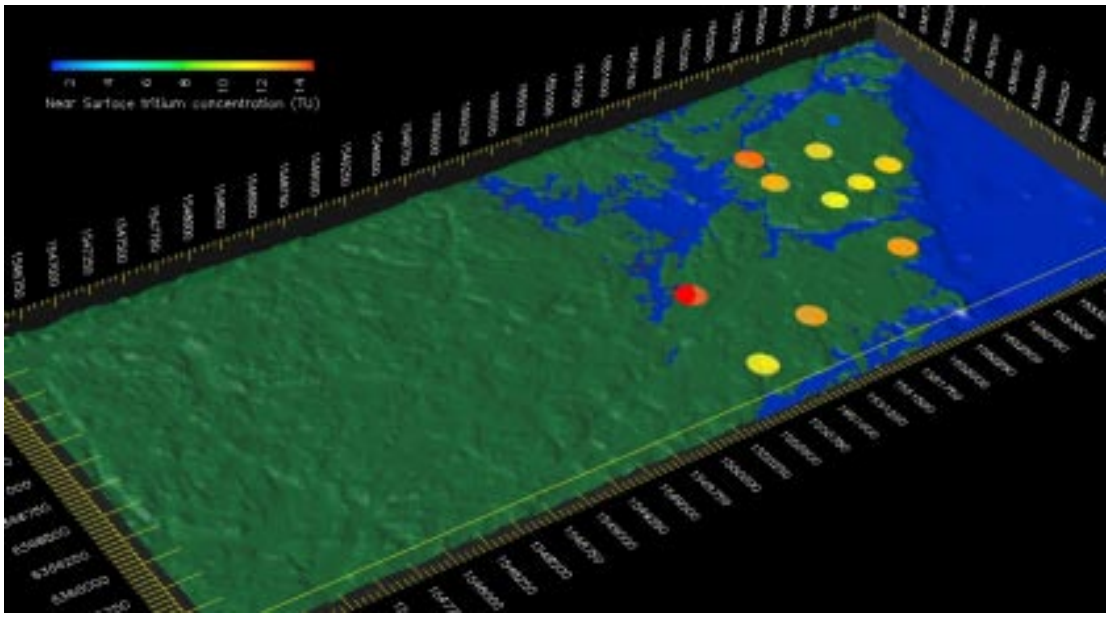

Figure 3-27. *Spatial distribution of tritium (TU) in soil pipes. The minimum value is located in soil pipe SSM00022 at Ävrö.*

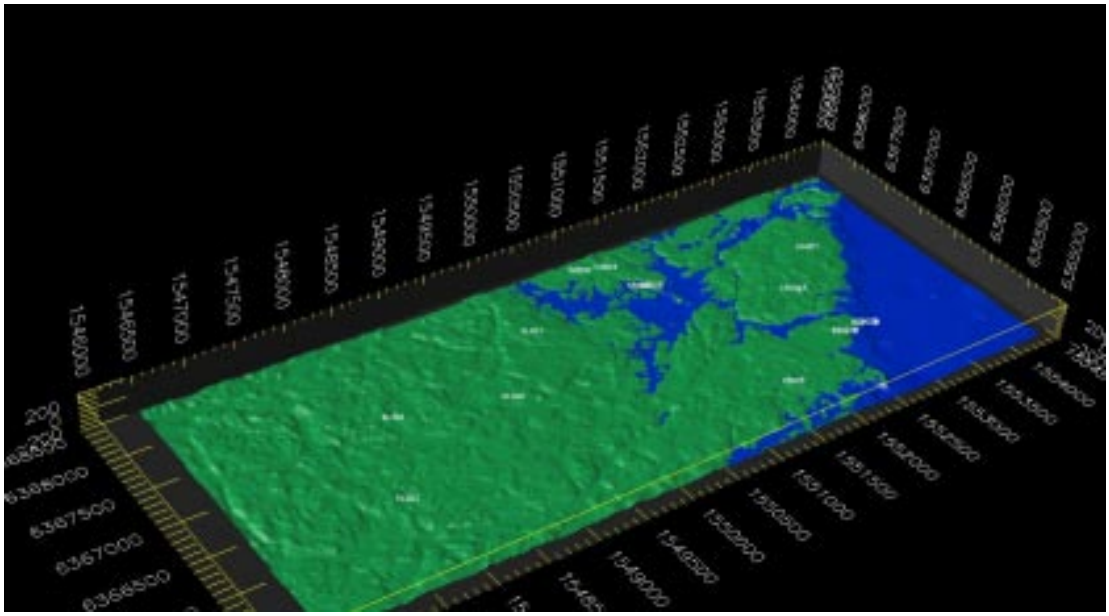

Figure 3-28. *Top-view showing the spatial location of the main cored boreholes in the Laxemar v. 1.2 database.*

Figure 3-29 shows a basal view (from the southwest) of the Laxemar and Simpevarp subareas, including the geometry of the main cored boreholes and the Äspö tunnel. Both the boreholes and the tunnel are very useful geographical references for 3-D visualisation of bedrock hydrochemistry. It is worth noting that the geometry of the boreholes is not accurate but has been approximated from the coordinates of some water samples. This is the reason why Äspö boreholes do not reach the surface in the present version of the modelling.

Figure 3-30 shows all the available representative chloride data in the bedrock samples, except for boreholes KLX03 and KLX04, where all available samples (only for chloride visualisation) have been included (and some of them should be considered with caution).

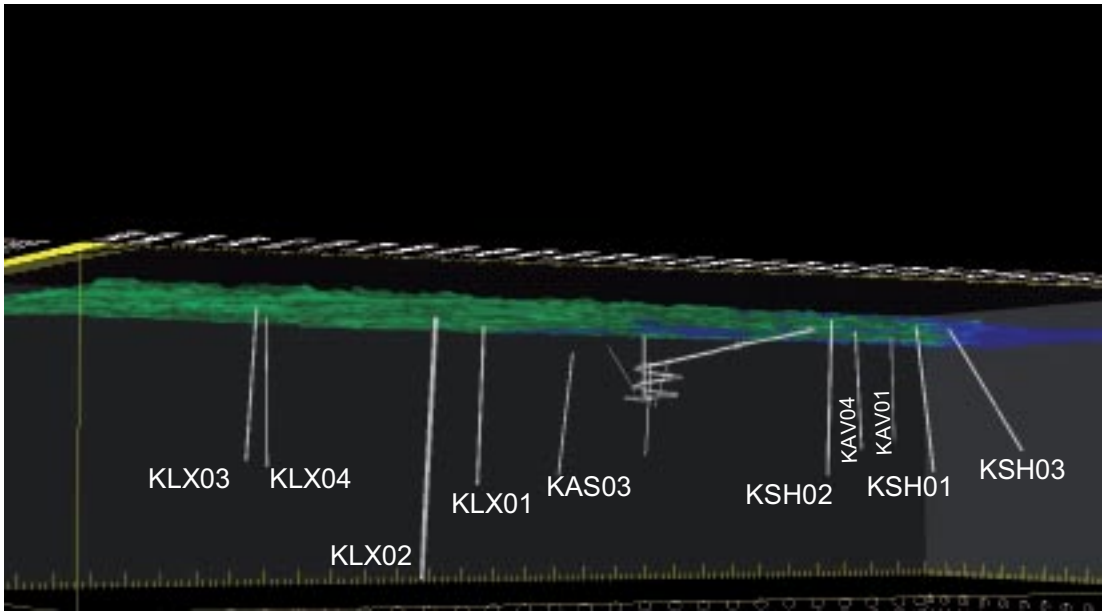

Figure 3-29. *Bottom-view (from the southwest) of the Laxemar and Simpevarp subareas. Main cored boreholes, as well as the Äspö tunnel, have been included as geographical references in the visualisation.*

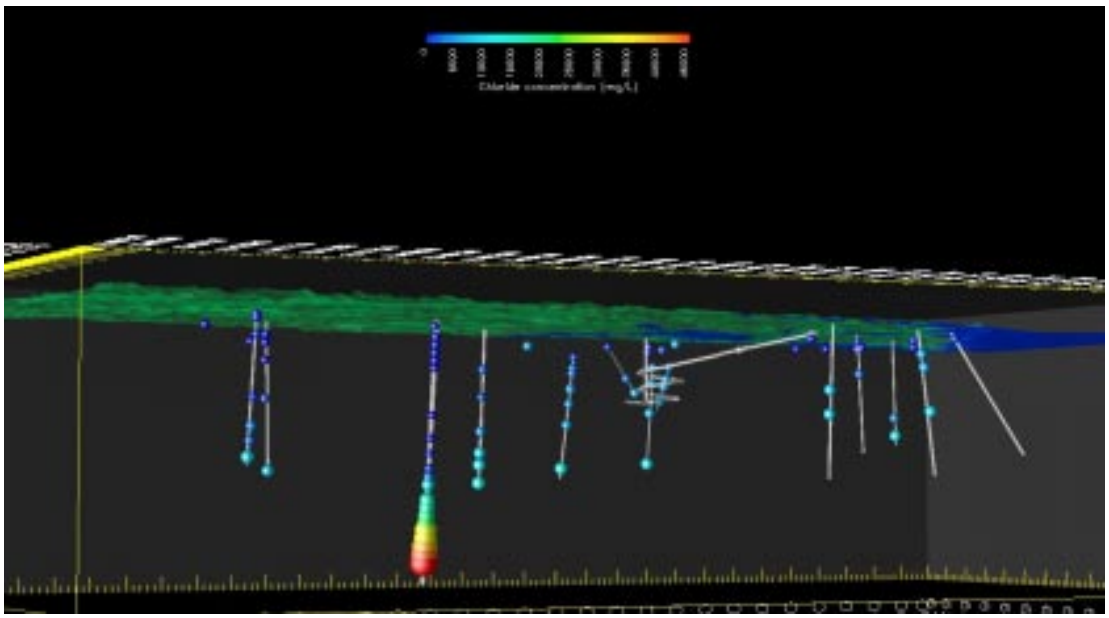

Figure 3-30. *Distribution of chloride concentrationsint the bedrock of the Laxemar and Simpevarp subareas. Symbol size is proportional to the chloride concentration.*

The reason for including non-representative dissolved chloride concentrations in KLX03 and KLX04 is to have a "first guess" of the salinity distribution at Laxemar subarea (note that all the "representative knowledge" available up to now comes from KLX01 and KLX02). Figure 3-30 shows the occurrence of brine water at depth in the Laxemar subarea. The brine has been detected in water samples of borehole KLX02 at a depth greater than 1,100 m. Figure 3-31 shows the same distribution of chloride concentration excluding the most saline waters of KLX02 boreholes. In this new visualisation of chloride, it is easier to notice the difference in salinity between the groundwater of the Laxemar and Simpevarp subareas. The Laxemar subarea represents a continental (inland) hydrogeological framework with a thick fresh water body reaching maximum depths of nearly 1,000 m. On the contrary, the Simpevarp subarea represents a coastal hydrogeological framework where fresh water bodies are confined to the first 100–200 m of the bedrock.

According to the water classification used by /Laaksoharju et al. 2004/, four main hydrochemical water types have been identified in the Simpevarp area: type A through to type D /Laaksoharju et al. 2004/.

Water Type A. This type comprises dilute groundwaters (< 2,000 mg/L Cl; 0.5–2.0 g/L TDS) of Na-HCO_3 type present at shallow (< 200 m) depths at the Simpevarp subarea, but at greater depths (0–900 m) at the Laxemar subaraea. At both subareas the groundwaters are marginally oxidising close to the surface, but otherwise reducing. Figure 3-32 shows a visualisation of the spatial distribution of water type A (diluted). This type of water is interpreted as related with a meteoric origin, and shows higher bicarbonate contents. Figure 3-33 shows the spatial distribution of bicarbonate concentrations. It can be seen that the higher values of bicarbonate concentrations coincide almost exactly with the diluted groundwater (type A). The high bicarbonate concentration can be mainly attributed to the occurrence of oxidation of organic matter of the soil layers at emerging land.

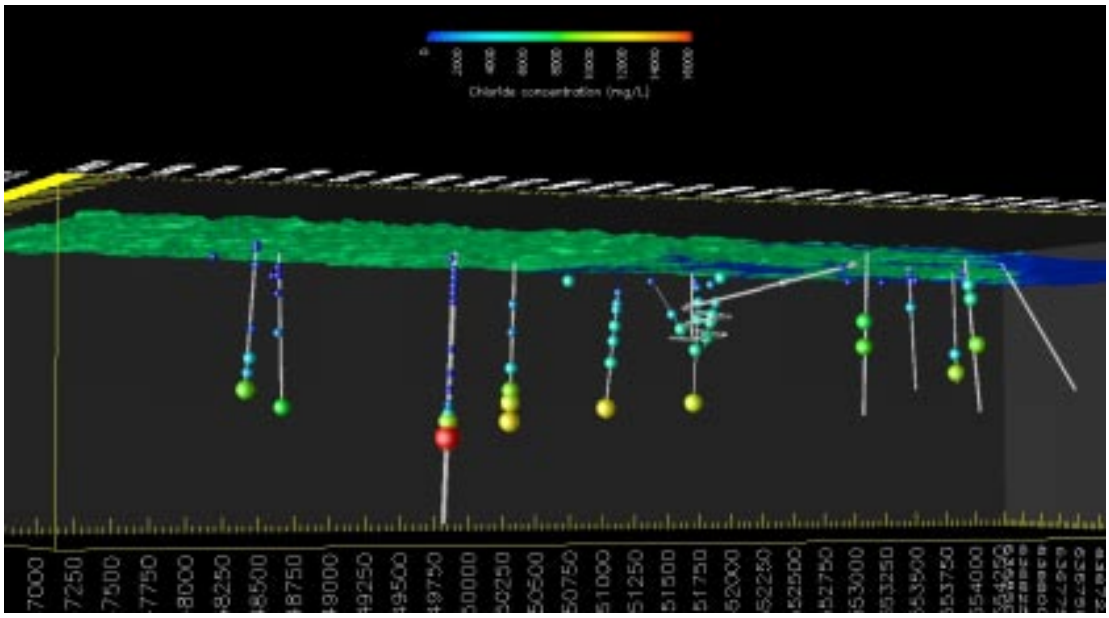

Figure 3-31. *Distribution of chloride concentrations in the bedrock of the Laxemar and Simpevarp subareas above 1,100 m (excluding the most saline waters in KLX02). Symbol size is proportional to the chloride concentration.*

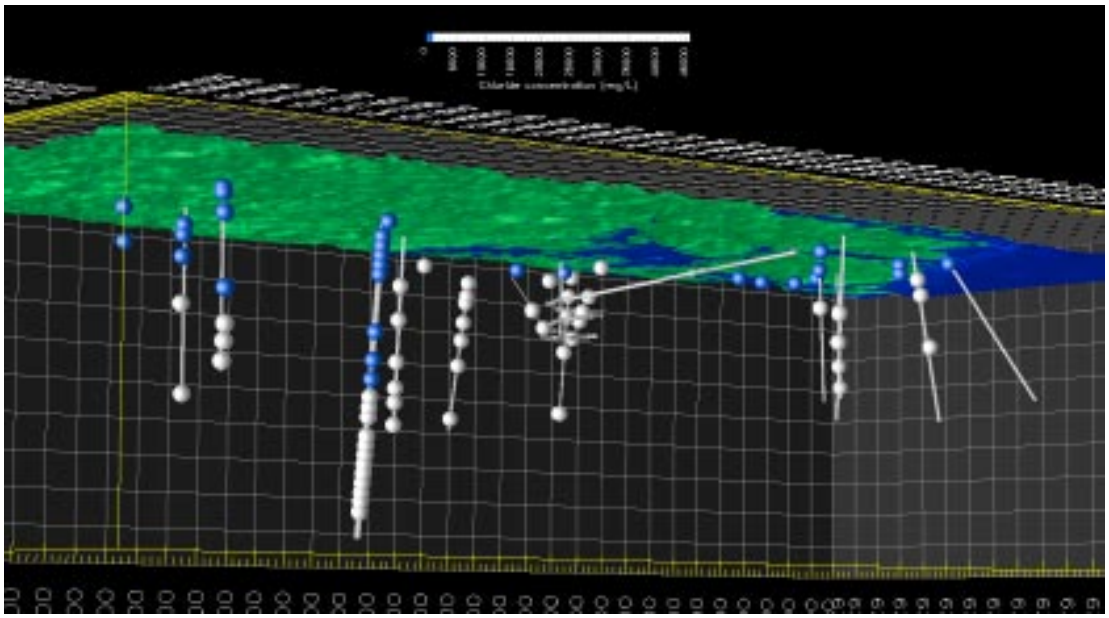

Figure 3-32. *Spatial distribution of water type A (diluted), which can be related to a meteoric origin. Note that this type of water reaches much greater depths at the Laxemar subarea than in the Simpevarp subarea.*

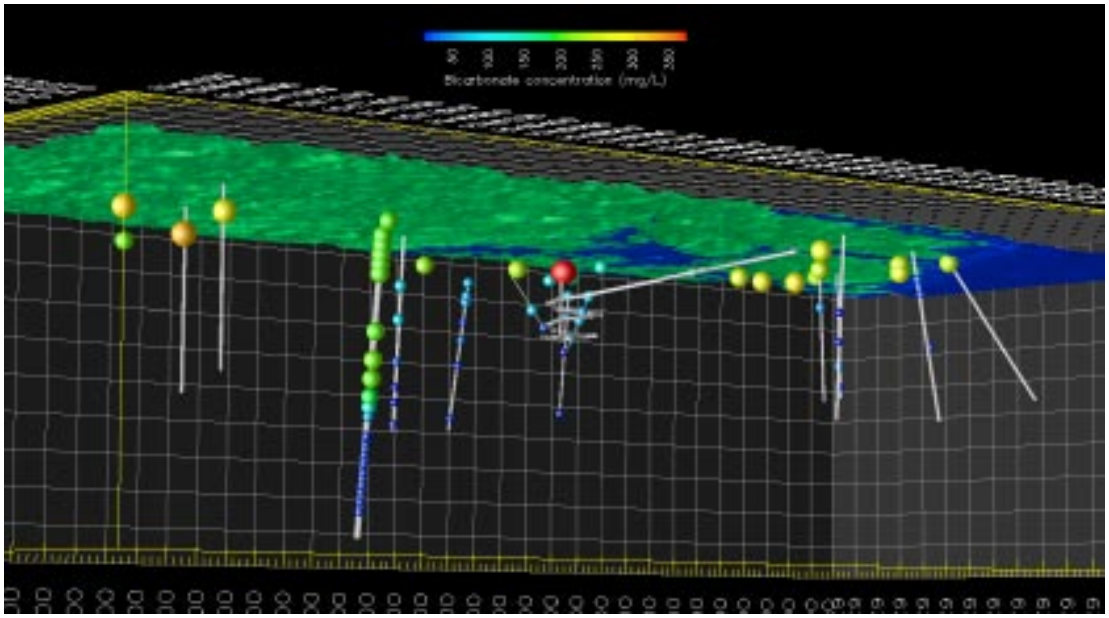

Figure 3-33. *Spatial distribution of bicarbonate concentrations. By comparing this figure with Figure 3-32 it can be seen that dilute water (type A) shows the highest bicarbonate concentrations, probably related to oxidation of organic matter in the surface soil layers.*

Water Type B. This type comprises brackish groundwaters (2,000–6,000 mg/L Cl; 5–10 g/L TDS) present at shallow to intermediate (150–300 m) depths in the Simpevarp subarea, but at greater depths (approx. 900–1,100 m) in the Laxemar subarea. The origin of this water type could be different from one place to another. In the Simpevarp subarea there is potentially some residual Littorina Sea (old marine) influence. On the contrary, at the Laxemar subarea the saline component of this water type could mainly be attributed to the influence (dispersion/diffusion) of deep brine water. Figure 3-34 shows a visualisation of the spatial distribution of water type B (brackish).

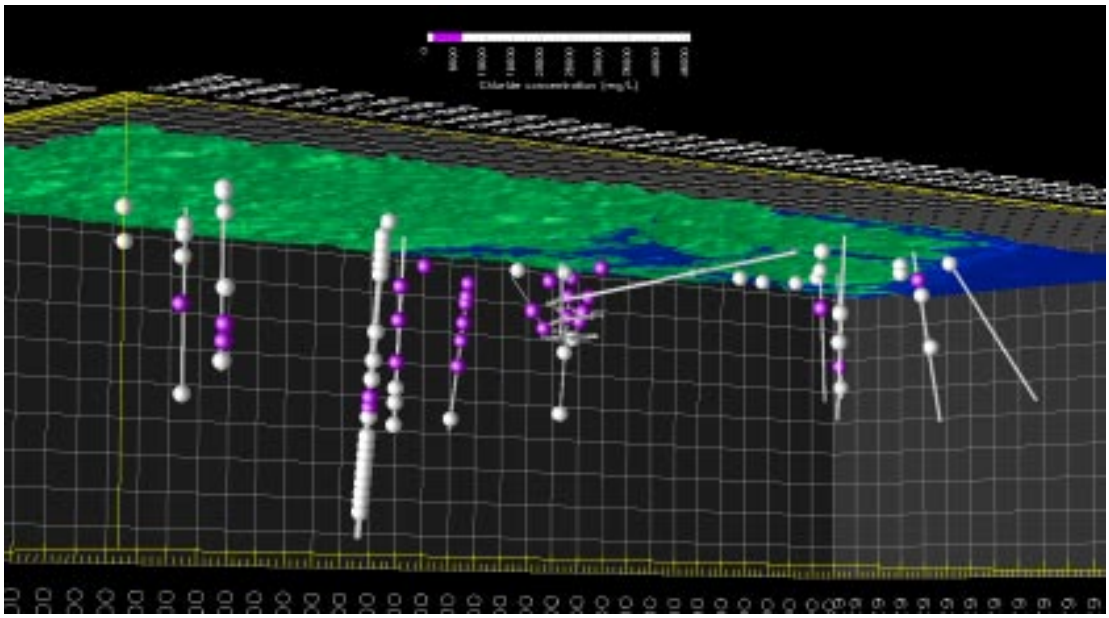

Figure 3-34. *Spatial distribution of water type B (brackish). This type of water is found at relatively shallow depths in the Simpevarp subarea (mainly under Äspö), but also in Laxemar subarea close to the coast (KLX01). Inland (KLX0, KLX03 and KLX04) this type of water is found at greater depth, from 600 to 1,100 m.*

The complex origin of water type B can be better understood by analysing other hydrochemical information. Figure 3-35 shows the spatial distribution of magnesium in groundwater. High magnesium concentrations are found in the Simpevarp subarea associated with the same waters corresponding to water type B (brackish). However, water type B in the Laxemar subarea shows low magnesium contents compared to the Simpevarp subarea. It is worth noting that magnesium is not a conservative element. On the contrary, it is well known that it can be involved in cation exchange processes, mainly in fractures and fracture zones with some clay content. However, according to /Laaksoharju 1999/ the average magnesium concentration in Baltic Sea water is 234 mg/L, while deep brine waters at KLX02 show very low concentrations of magnesium (about 2 mg/L). This high contrast therefore could be qualitatively useful to establish a difference between the salinity of brackish waters at the Laxemar and Simpevarp subareas. By comparing Figures 2-19 and 2-20 it can be stated that brackish waters at Laxemar are most likely related to the occurrence of a dispersion zone between deep saline waters and shallow diluted water of meteoric origin, while brackish waters of the Simpevarp subarea show an influence of marine waters. This is in accordance with /Laaksoharju et al. 2004/. These marine waters must be older than the Baltic Sea, since nowadays there is no driving force for marine water to penetrate in the bedrock. It has been postulated that this old marine water was introduced into the bedrock during the Littorina Sea stage, due to density-driven flow caused by the presence of low density relict fresh glacial water deeper in the bedrock.

Water Type C. This water type comprises saline groundwaters (6,000–20,000 mg/L Cl; 25–30 g/L TDS) present at intermediate depths (> 200–300 m) at the Simpevarp subarea, and at greater depths (> 1,000 m) at the Laxemar subarea. Similarly to water type B, this type C water could show different hydrochemical signatures from one place to another. In the Simpevarp subarea (but also at coastal Laxemar locations; e.g. KLX01) signatures of old marine influence can be recognised (see magnesium concentrations in Figure 3-35), together with glacial signatures (as will be shown below). On the contrary, in the Laxemar subarea this water type could mainly be attributed to the influence (dispersion/diffusion) of deep brine water. Figure 3-36 shows a visualisation of the spatial distribution of water type C (saline).

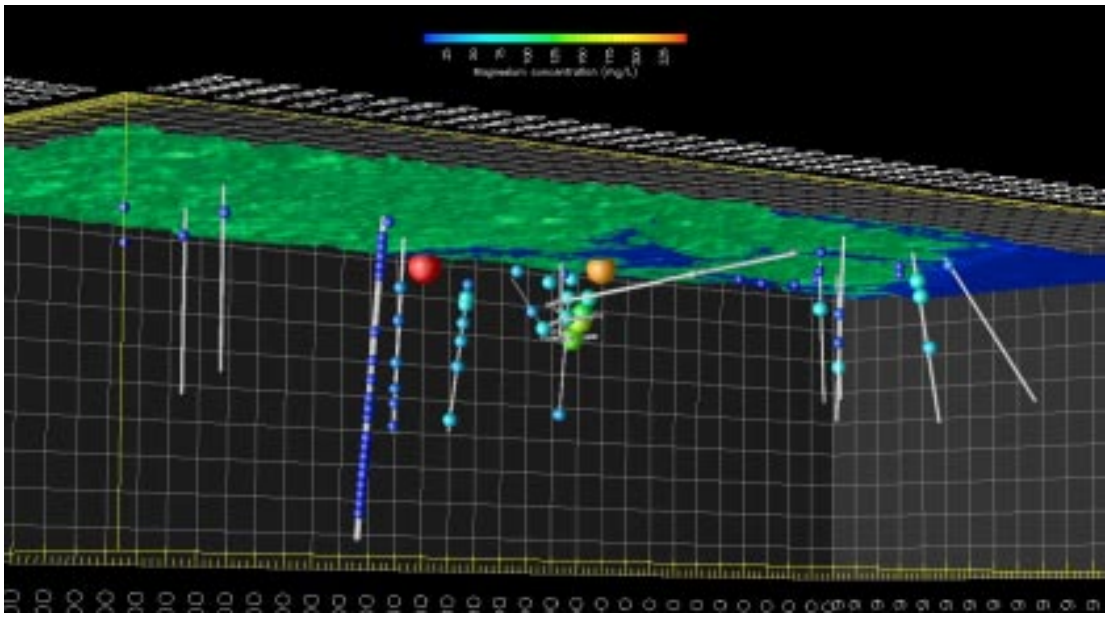

Figure 3-35. *Spatial distribution of dissolved magnesium in groundwater. It can be seen that highest magnesium concentrations are found in the Simpevarp subarea, indicating a possible influence of older marine waters.*

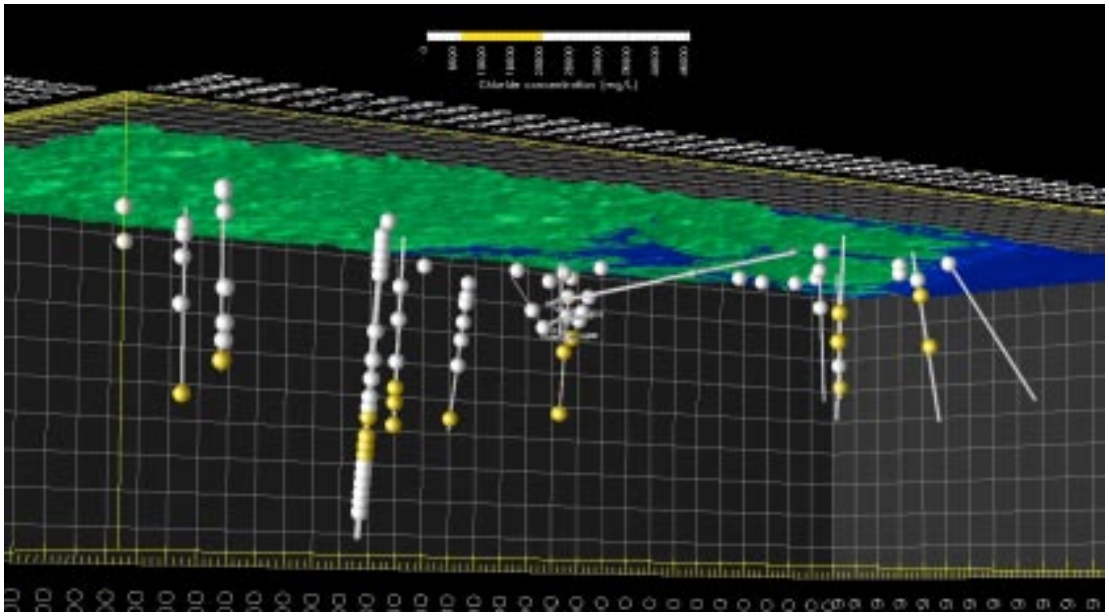

Figure 3-36. *Spatial distribution of water type C (saline). This type of water is found at shallow to intermediate depths in Simpevarp subarea, and deeper in the Laxemar subarea (at a depth of 800–1,200 m).*

Glacial isotopic signatures have been postulated to be present in groundwater at different places in Scandinavian bedrock. According to /Laaksoharju 1999/, glacial meltwater was hydraulically injected under considerable head pressure into the bedrock when the continental ice melted and retreated (about 13,000 years ago),. The exact penetration depth of glacial water is uncertain but, according to /Svensson 1996/ and /Jaquet and Siegel 2003/, depths of several hundreds metres can be expected according to hydrodynamic models.

The best tracers for glacial water signatures are considered to be ^{18}O and ^{2}H stable isotopes. According to /Laaksoharju 1999/, the isotopic composition for a Glacial end-member water is –21‰ SMOW for ^{18}O, and –158‰ SMOW for ^{2}H. The clearest glacial signature in the Simpevarp area was found below the Äspö island (KAS03) during the site characterisation process and before the construction of the tunnel. Figure 3-37 and Figure 3-38 show the spatial distribution of $\delta^{18}O$ and $\delta^{2}H$, respectively, for all the representative samples available in the Laxemar 1.2 database.

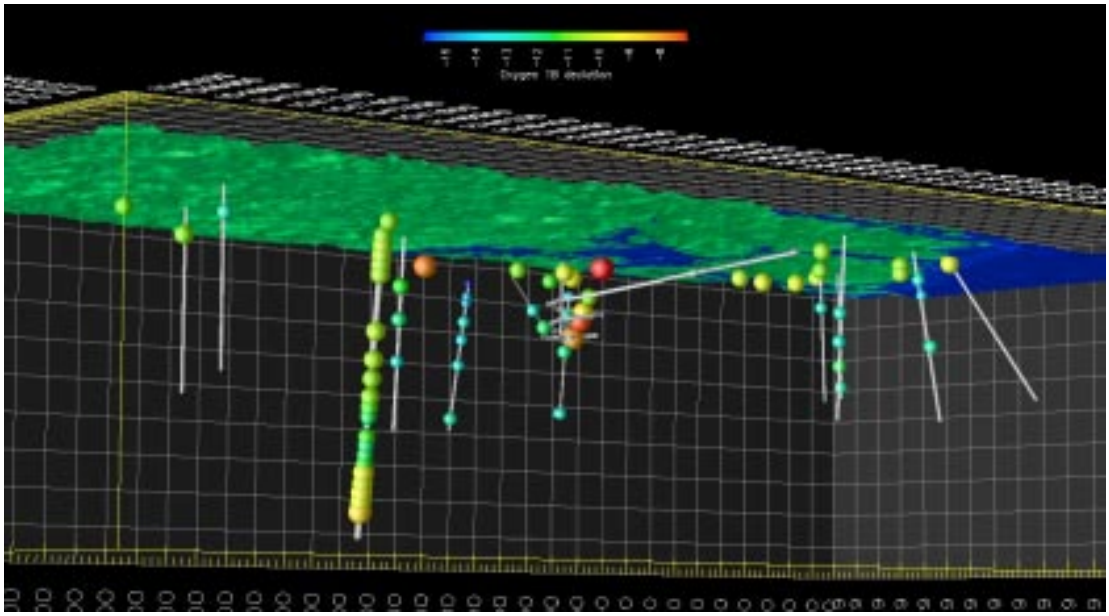

Figure 3-37. *Spatial distribution of ^{18}O deviations at the Laxemar and Simpevarp subareas. It can be seen that a clear minimum value in KAS03 (below Äspö) corresponds to the Glacial Reference Water /Laaksoharju 1999/.*

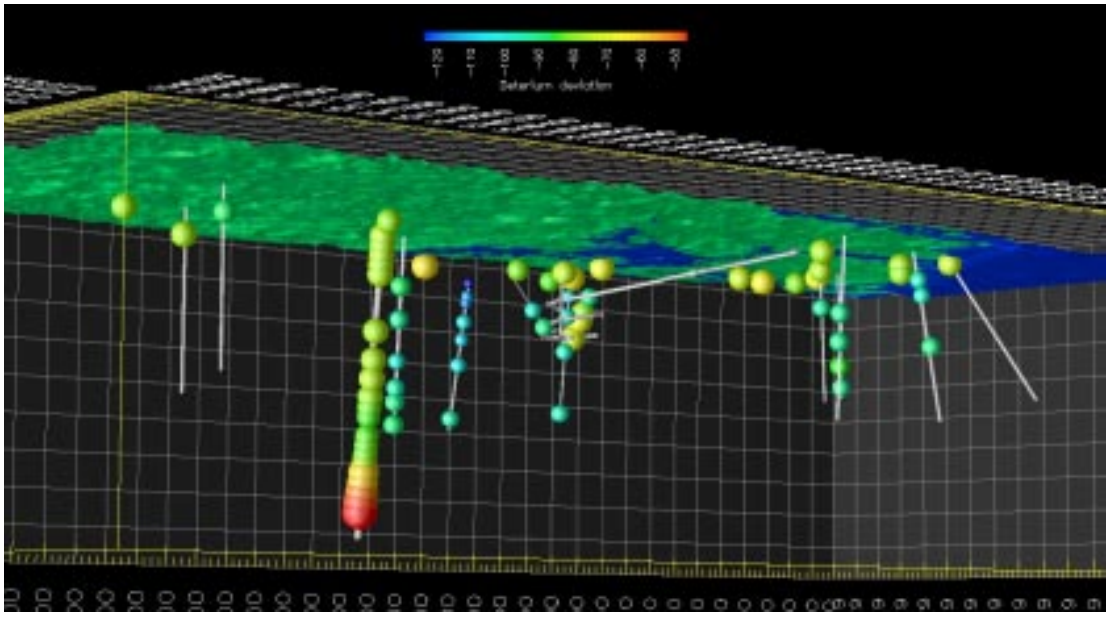

Figure 3-38. *Spatial distribution of ^{2}H deviations in the Laxemar and Simpevarp subareas. It can be seen that a clear minimum value in KAS03 (under Äspö) corresponds to the Glacial Reference Water /Laaksoharju 1999/.*

Figure 3-39 and Figure 3-40 show the spatial distribution of water samples with $\delta^{18}O$ lower than –13‰ SMOW and $\delta^{2}H$ lower than –90‰ SMOW respectively. These truncation values are set arbitrarily, but could help to visualise glacial signatures in brackish and saline groundwaters.

According to Figure 3-39 and Figure 3-40, glacial isotopic signatures can be recognised clearly in the Simpevarp subarea, especially under Äspö island and below the Simpevarp peninsula. The clearest signature corresponds to borehole KAS03 at a shallow depth (about –120 m above sea level). In the Laxemar subarea, glacial signatures appear to be evident only close to the coast (KLX01) and deeper than in Simpevarp subarea. It is worth noting that all glacial signatures are found in samples of groundwater types B and C (brackish or saline).

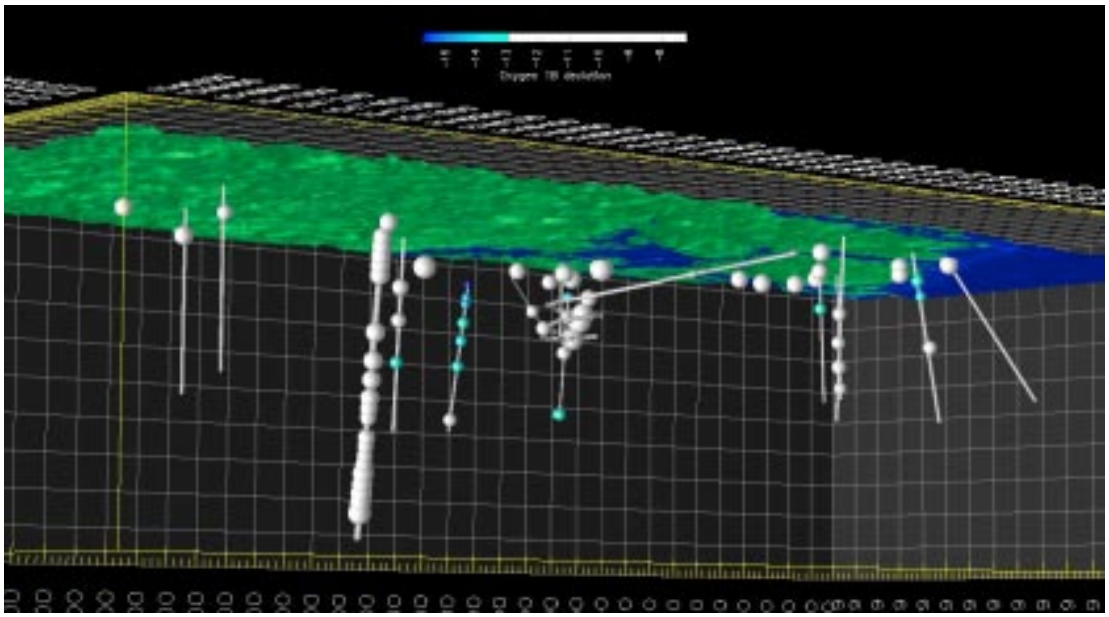

Figure 3-39. *Spatial distribution of $\delta^{18}O$ deviations lower than –13‰ SMOW.*

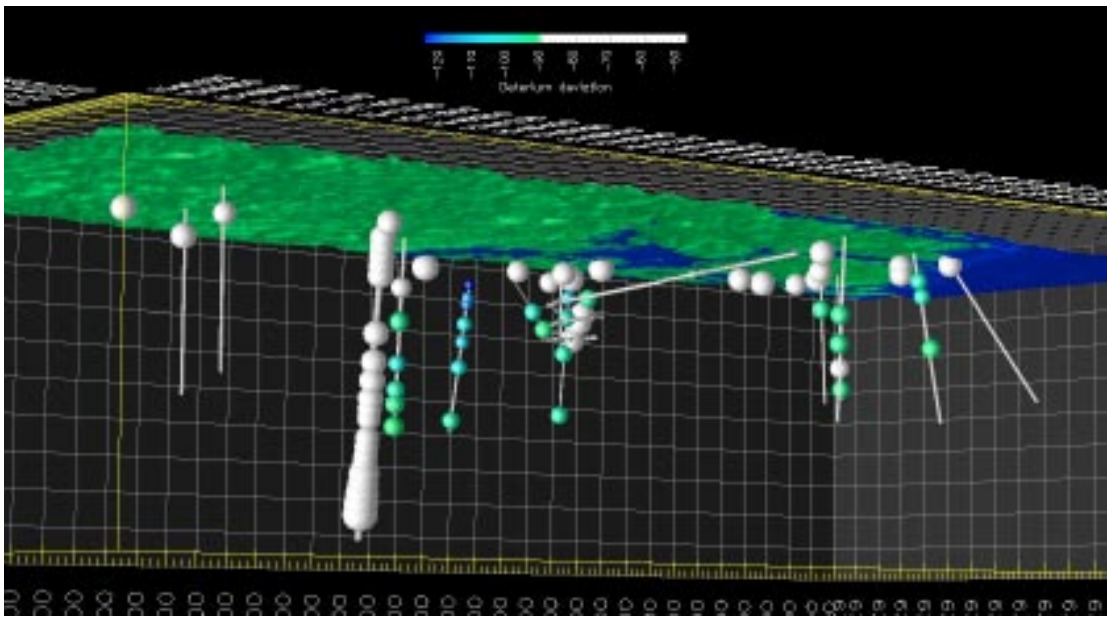

Figure 3-40. *Spatial distribution of $\delta^{2}H$ deviations lower than –90‰ SMOW.*

Water Type D. This type comprises highly saline groundwaters (> 20,000 mg/L Cl; to a maximum of ~ 70 g/L TDS) and has only been identified in one borehole in the Laxemar subarea (KLX02) at depths exceeding 1,200 m. Figure 3-41 shows a visualisation of the spatial distribution of water type D (highly saline, also referred to as "brine"). Water samples of type D (highly saline) show the highest concentrations of most dissolved species (see Appendix 5).

Water samples of type D (highly saline) also show the highest concentrations of sulphates in bedrock groundwaters (Figure 3-42).

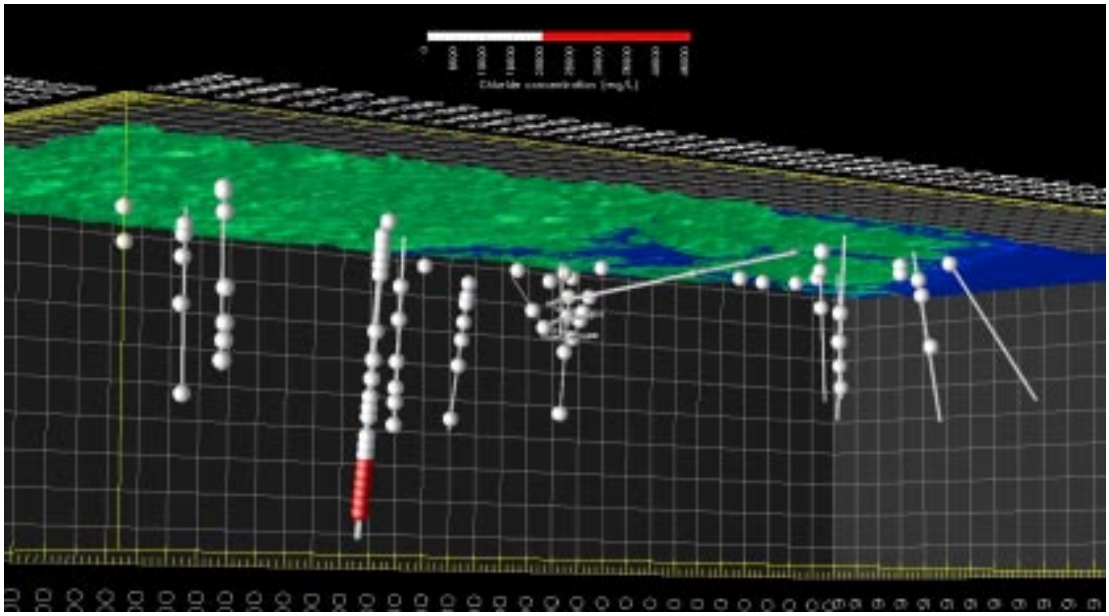

Figure 3-41. *Spatial distribution of water type D (highly saline). This type of water has only been found in borehole KLX02 (Laxemar subarea), at depths from –1,200 to –1,600 metre above sea level.*

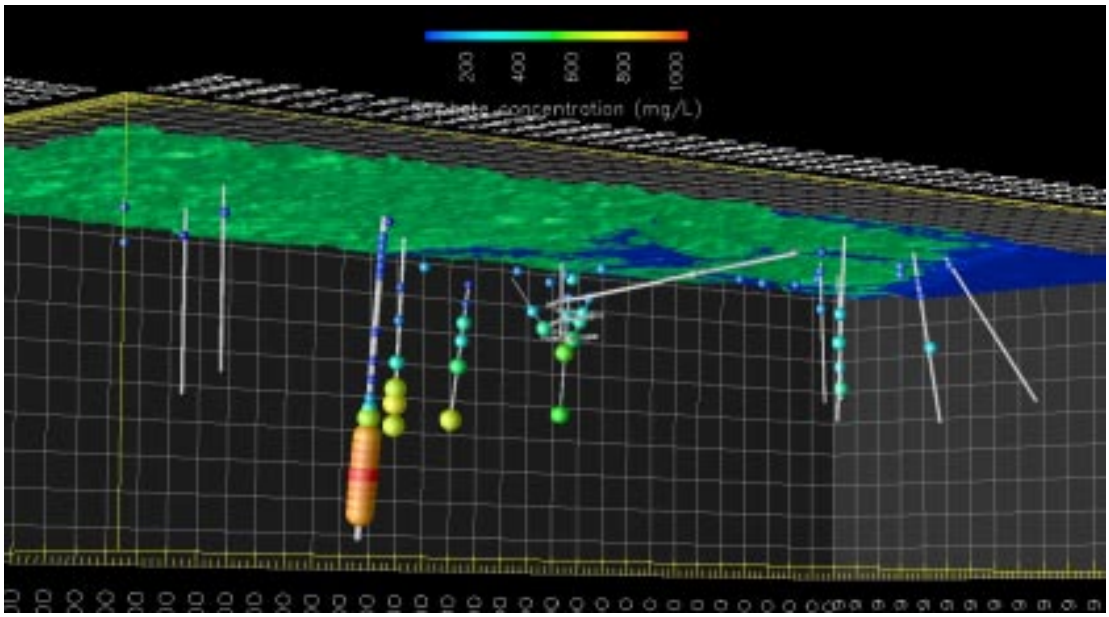

Figure 3-42. *Spatial distribution of dissolved sulphates in the Laxemar and Simpevarp subareas.*

Figure 3-43 and Figure 3-44 show two different visualisations of the spatial distribution of the four water types characterising the Laxemar and Simpevarp subareas. It can be seen that dilute water (type A) extends deeper at inland Laxemar locations compared to Laxemar coastal positions and the Simpevarp subarea in general, where dilute waters are only found at very shallow depths in the bedrock. On the contrary, brackish and saline waters (types B and C) are predominant in the Laxemar subarea coastal areas (KLX01) and in the Simpevarp subarea. Within the Simpevarp subarea, saline waters (type C) are found at much shallower depths below the Simpevarp peninsula than below the islands of Äspö and Ävrö.

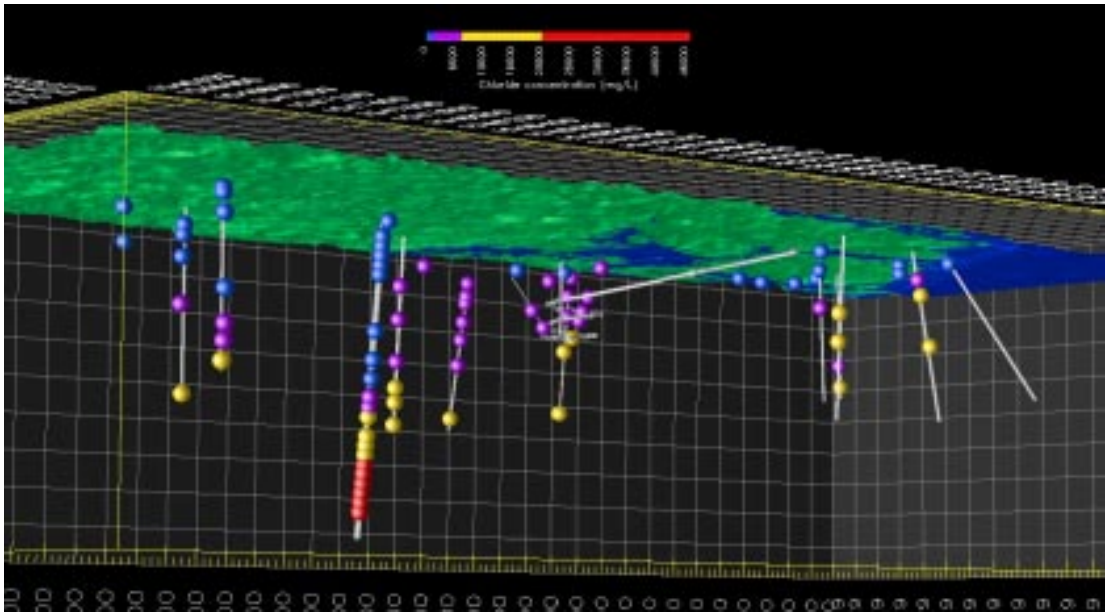

Figure 3-43. *Bottom view from the southwest of the spatial distribution of water types in the Laxemar and Simpevarp subareas. Water type A (blue), B (purple), C (yellow) and D (red).*

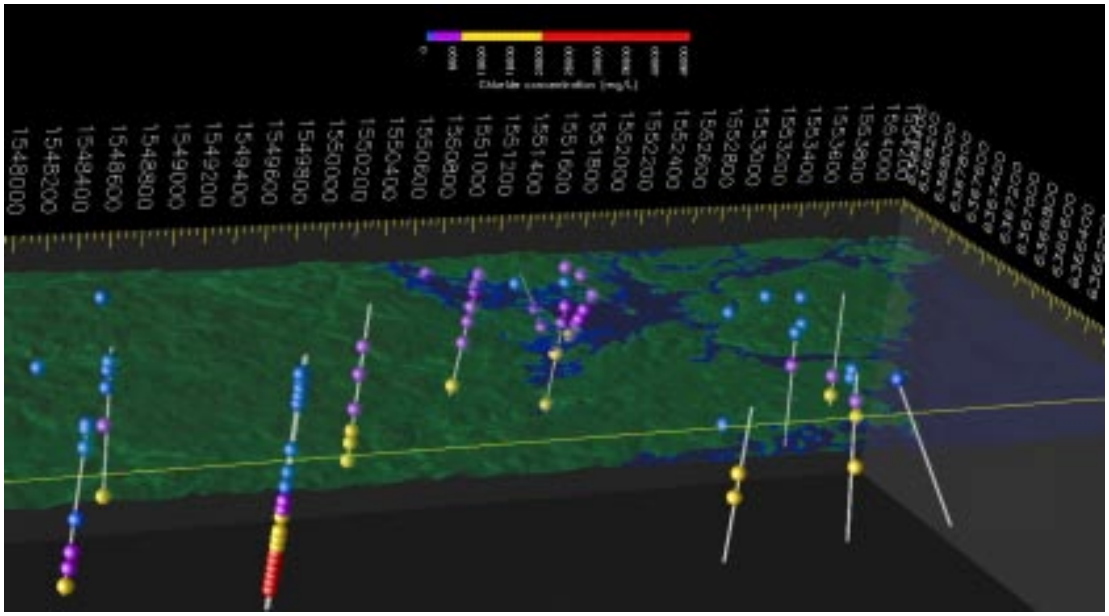

Figure 3-44. *Top view (with transparent terrain model) of the spatial distribution of water types in the Laxemar and Simpevarp subareas. Water type A (blue), B (purple), C (yellow) and D (red).*

It can be seen in the previous figures that water type classification based on chloride does not distinguish between the different origins of the B and C type of waters since the same chloride content in a water can have different origins (e.g. mixtures with marine or deep saline water). On the other hand, most of the dissolved species show qualitative trends very similar to chlorides. This could be taken as an indication of the important role of physical transport processes (e.g. dispersion-diffusion; i.e. mixing) in determining the hydrochemical nature of bedrock groundwater in the Laxemar and Simpevarp subareas. Even the concentrations of some of the hydrochemical components which are known to be clearly involved in geochemical processes (such as calcium) are obviously masked by the influence of the mixing between different waters. It is thought that the concentration contrast between highly saline waters and the rest is so large, that very little mixing involving this end-member water would produce mass transfers higher than those involved in some geochemical processes. However, this is not always the case. Some dissolved components, such as magnesium (see Figure 3-35), bicarbonate, iron and manganese show a very different spatial distribution. As discussed above, it has been postulated that magnesium is a good tracer for the marine influence of groundwater samples (even though it is not a conservative solute), due to the fact that highly saline deep waters (type D) show very low concentrations compared with Baltic Sea waters.

Figure 3-45 shows the spatial distribution of dissolved (total) iron.Unfortunately there is no representative sample at Laxemar fulfilling two requisites: a) being of type A (dilute), and b) having measurements of total dissolved iron. However, many of the representative samples available in the Simpevarp subarea fulfil both requisites. By comparing Figure 3-45 and Figure 3-33, it is possible to notice that highest concentrations of dissolved iron have been measured at the shallowest positions in the bedrock, coinciding with dilute water samples and showing higher concentrations of bicarbonates. Hydrogeochemical /Banwart et al. 1995, 1996/ and microbiological /Pedersen et al. 1995/ studies at the Äspö HRL provide significant evidence in support of Fe(III) reduction as a respiration pathway for the oxidation of organic carbon. This process is mostly similar to what has been happening at shallower depths in the Laxemar and Simpevarp subareas, following the emergence of the land during the last c. 2,000 years. Then, according to the observed concentrations of bicarbonate and iron in the dilute groundwater samples (Type A) of the Simpevarp subarea, microbially mediated oxidation of organic matter through the reduction of ferric minerals seems to be the most plausible hypothesis to explain the high bicarbonate concentrations of these groundwater samples. Both soil pipes and some shallow bedrock groundwater samples at Simpevarp are undersaturated with respect to calcite /Gimeno et al. 2004, Molinero and Raposo 2004/ and, therefore, dissolution of calcite could also contribute to the observed bicarbonate concentrations in dilute groundwater.

Groundwater samples in relation to major deformation zones

The visualisation tool has also the capability of representing structural objects such as deformation zones. This capability is important for the construction of conceptual models in a bedrock environment which is affected by the presence of such structures. Figure 3-46 shows a top view of the Simpevarp area with the main deformation zones considered up till now; these include deformation zones EW002A, EW007A, NE040A, NE005A and EW013A. The selection of these 5 interpreted deterministic deformation zones was made by considering the actual definition of the target area and the location of the boreholes in which representative hydrochemical information is available. In fact, for the case of the Laxemar subarea, deformation zones EW002A and EW007A are very important and constitute “high confidence” zones. NE040A is also a relevant structure due to the fact that it crosses the Laxemar subarea.

Inclusion of deformation zones in the visualisation tool allows for analysing the possibility of “direct” hydraulic connection between the loci of different groundwater samples available in the database. Deformation zone EW002A (white in Figure 3-46) is intersected by the KAS03 borehole below Äspö Island and runs very close to the locations where deeper saline water samples were collected in KLX02 in the Laxemar subarea (see Figure 3-47).

Figure 3-48 shows deformation zone EW007A which intersects boreholes KLX02 and KLX04. It is worth noting that the chloride concentration of samples from KLX04 does not correspond to representative samples and should be treated with caution.

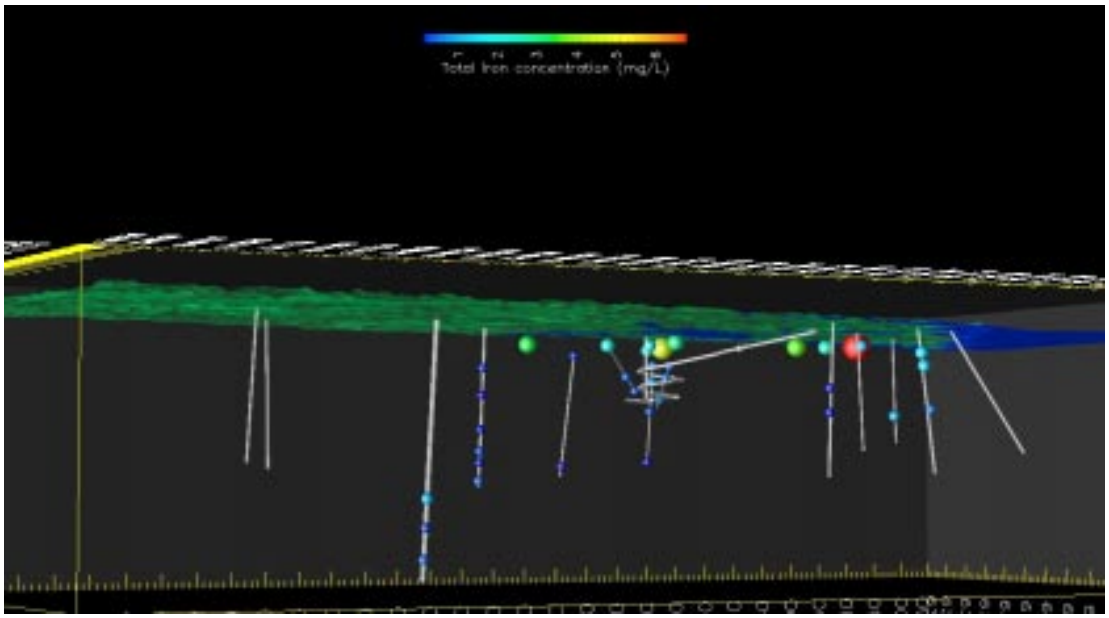

Figure 3-45. *Spatial distribution of iron (total) in the Laxemar and Simpevarp subareas.*

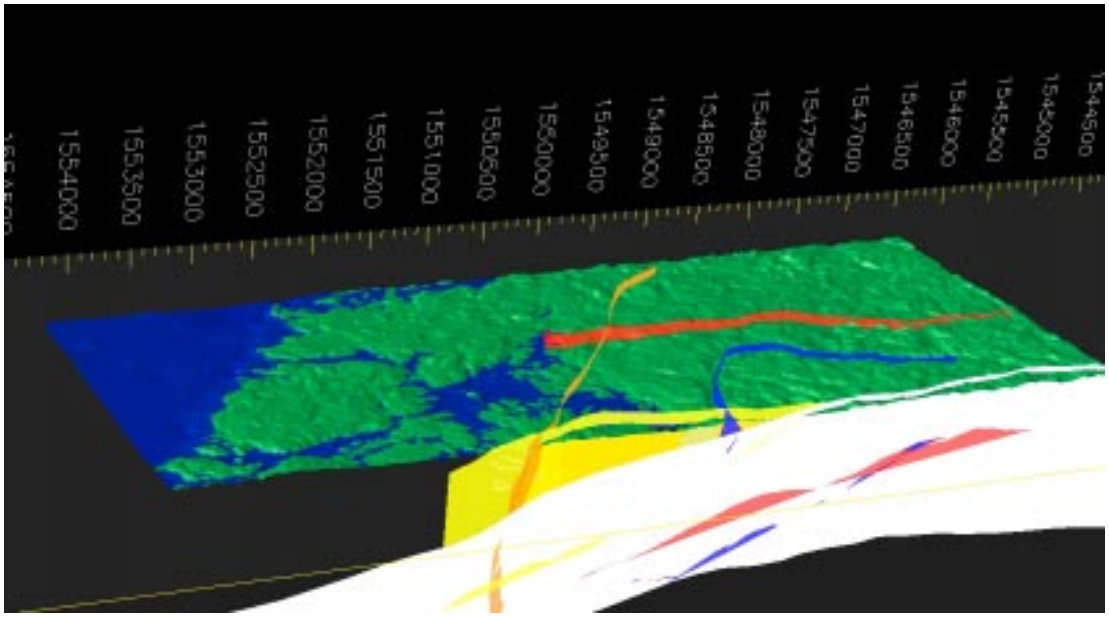

Figure 3-46. *Top view (from the north) of the Simpevarp area showing the key deformation zones. EW002A (white), EW007A (red), NE040A (blue), NE005A (orange) and EW013A (yellow).*

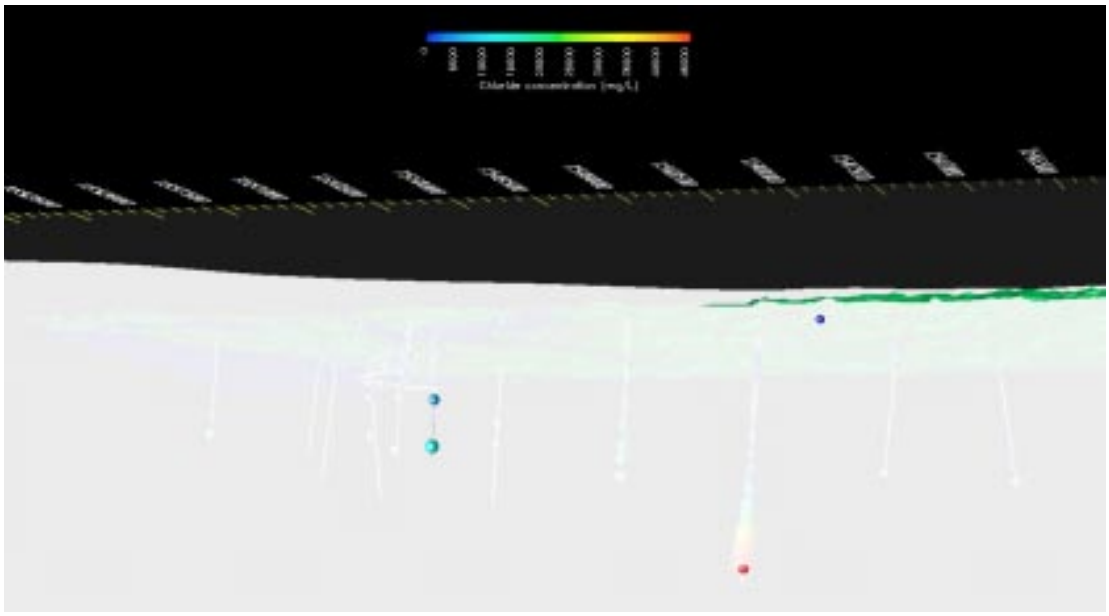

Figure 3-47. *Bottom view (from the north) of deformation zone EW002A and chloride concentrations in boreholes. This fracture zone intersects borehole KAS03 under Äspö island and runs very close to the deeper part of the KLX02 borehole in Laxemar.*

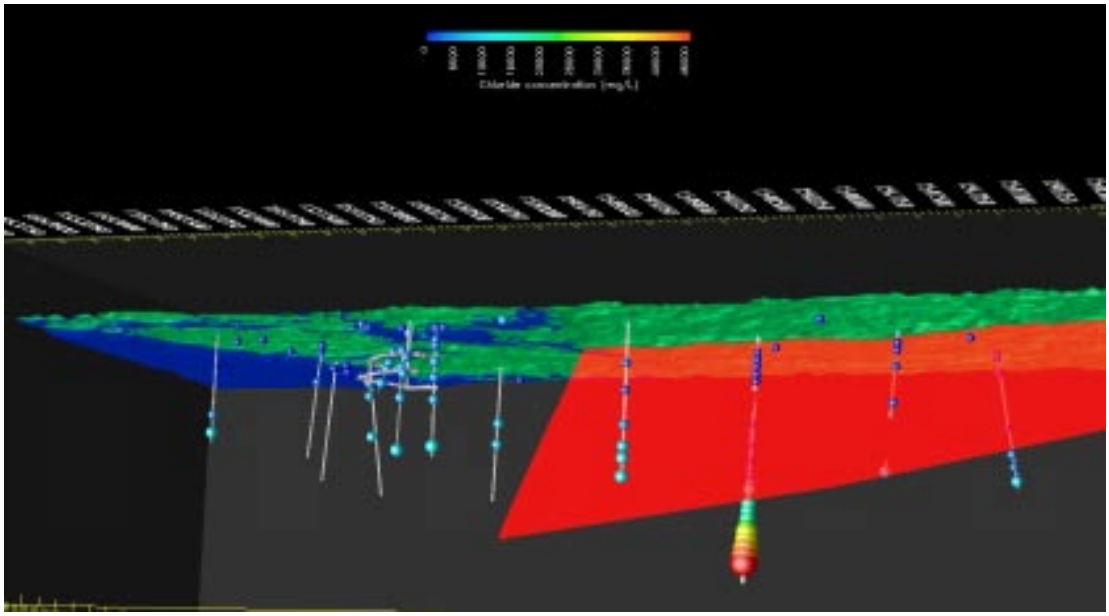

Figure 3-48. *Bottom view (from the north) of deformation zone EW007A and chloride concentrations in boreholes. This deformation zoneis currently interpreted to intersect boreholes KLX02 and KLX04 at a deeper section. The measured chloride concentrations in KLX04 do not correspond to representative samples and should be treated with caution.*

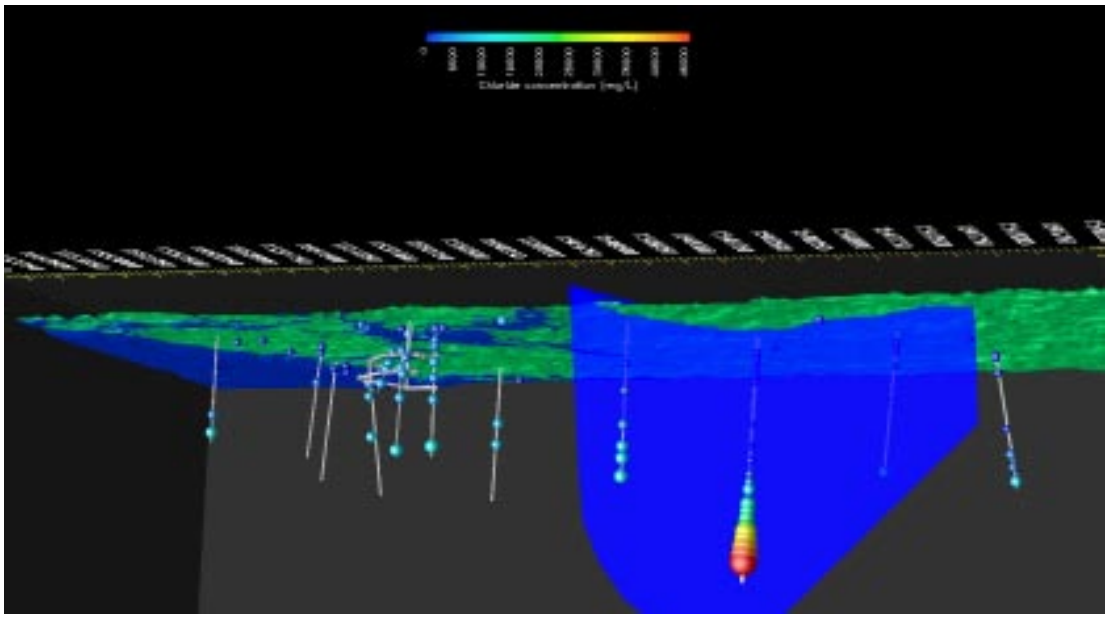

Figure 3-49. *Bottom-north view of deformation zone NE040A and chloride concentrations in boreholes. This fracture zone intersects boreholes KLX02 (deeper and inland) and KLX01 (more shallow and nearest to the coast).*

Figure 3-49 illustrates an interesting point. According to the current geometrical definition of deformation zones (deformation zone model of Simpevarp 1.2 /SKB 2005/), deformation zone NE040A intersects boreholes KLX02 and KLX01. It can be observed that both boreholes have a representative sample corresponding to the intersection with the deformation zone. The interesting point is that borehole KLX02 intersects the fracture zone at a greater depth than KLX01 and both representative samples are relatively dilute, so they can be assumed as being part of the current dynamic fresh water body at Laxemar. The geographical location of both boreholes, i.e. KLX02 (inland) and KLX01 (closer to the coast), is consistent with a topographically-driven flow from the first to the second borehole. It is therefore recommended that these two representative groundwater samples fulfil the requisites to be further analysed by means of inverse geochemical models and reactive solute transport models.

3.7.2 Hydrochemical suitability criteria

There are no new representative samples from repository depth from the Laxemar subarea so samples from earlier sampled boreholes were used to check if they meet the SKB chemical suitability criteria for Eh, pH, TDS, DOC and Ca+Mg (/Anderson et al. 2000/). The samples from from KLX01: 680–702 m (sampled in 1988) and KLX02: 798–803 m (sampled in 1993) where selected for this purpose despite the fact that they reflect conditions below repository depth. Table 3-3 show that these samples can meet the SKB suitability criteria for the analysed parameters.

Table 3-3. The hydrochemical suitability criteria defined by SKB are satisfied by the analysed values of the samples KLX01: 680–702 m and KLX02: 798–803 m.

	Eh (mV)	pH (units)	TDS (g/L)	DOC (mg/L)	Colloids (mg/L)	Ca+Mg (mg/L)
Criterion	**< 0**	**6–10**	**< 100**	**< 20**	**< 0.5**	**> 40**
KLX01: 680–702 m	–275	8.1	8.2	1.2	0.03	1,423
KLX02: 798–803 m	–125*	7.6	0.9	5	n.a.	134

* Measured during a sampling event in year 2002. n.a.= not analysed.

3.8 Evaluation of uncertainties

During every phase of the hydrogeochemical investigation programme – drilling, sampling, analysis, evaluation, modelling – uncertainties are introduced which have to be accounted for, addressed fully and clearly documented to provide confidence in the end result, whether it will be the site descriptive model or repository safety analysis and design /Smellie et al 2002/. Handling the uncertainties involved in constructing a site descriptive model has been documented in detail by /Andersson et al. 2002/. The uncertainties can be conceptual uncertainties, data uncertainties, spatial variability of data, chosen scale, degree of confidence in the selected model, and error, precision, accuracy and bias in the predictions. The results of the different evaluations and modelling carried out within hydrogeochemistry are summarised in Chapter 11. Many of the uncertainties are difficult to judge, since they are results of different steps ranging from expert judgement to mathematical modelling and not the result of a single model, such as in hydrogeology. Some of the identified uncertainties recognised during the modelling exercise are discussed below.

The following data uncertainties have been estimated, calculated or modelled for the Laxemar data based on models used for the 1.2 model versions and also based on the Äspö modelling where similar uncertainties are believed to affect the present modelling:

- temporal disturbances from drilling may be ± 10–70%,
- effects from drilling during sampling is < 5%,
- sampling; may be ± 10%,
- influence associated with the uplifting of water may be ± 10%,
- sample handling and preparation; may be ± 5%,
- analytical errors associated with laboratory measurements are ± 5% (the effects on the modelling were tested in Appendix 1 in /SKB 2004/),
- mean groundwater variability during groundwater sampling (first/last sample) is about 25%,
- M3 model uncertainty is ± 0.1units within 90% confidence interval (the effects on the modelling were tested in Appendix 4 in /SKB 2004/.

Conceptual errors can occur in, for example, the palaeohydrogeological conceptual model. The occurrence and influence of old water end members in the bedrock can only be indicated by using certain element or isotopic signatures. The uncertainty therefore generally increases with the age of the end member. The relevance of an end member participating in groundwater formation can be tested by introducing alternative end member compositions or by using hydrodynamic modelling to test if old water types can reside in the bedrock during prevailing hydrogeological conditions. In this model version, a measure of validation is obtained by comparison with results of hydrogeological simulations.

Uncertainties in the PHREEQC code depend on which code version is being used. Generally the analytical uncertainties and uncertainties concerning the thermodynamic data bases are of importance (in speciation-solubility calculations). Care also is required to select mineral phases which are realistic (even better if they have been positively identified) for the systems being modelled. These errors can be addressed by using sensitivity analyses, alternative models and descriptions. A sensitivity analysis was performed concerning the calculations of activity coefficients in waters with high ionic strength, this analysis and also the uncertainties of the stability diagrams and redox modelling are discussed in Appendix 3 in /SKB 2004/.

The uncertainties were evaluated using the inverse modelling approach used in PHREEQC, and by investigating the compositional variability of end-members and by checking the effects of chemical reactions on the mixing proportions calculated by M4. The test showed that PHREEQC is sensitive to the selection of end-member composition in contrast to M3 and M4 which are less sensitive. M4 showed sensitivity to effects resulting from reactions; such effects will have to be further tested for both M3 and M4.

The uncertainty due to 3D interpolation and 2D/3D visualisation depends on various aspects, i.e. data quality, distribution, model uncertainties, assumptions and limitations introduced. The uncertainties are therefore often site specific and some of them can be tested such as the effect of 2D/3D interpolations. The site-specific uncertainties can be tested by using quantified uncertainties, alternative models, and comparison with independent models such as hydrogeological simulations.

The discrepancies between different modelling approaches can be due to differences in the boundary conditions used in the models or in the assumptions made. The discrepancies between models should be used as an important opportunity to guide further modelling, including including validation efforts and confidence building. In this work, the use of different modelling approaches starting from manual evaluation to advanced coupled modelling can be seen as a combined tool for confidence building. The same type of process descriptions independent of the modelling tool or approach increases confidence in the modelling.

3.9 Comparison between the hydrogeological and hydrogeochemical models

Since hydrogeology and hydrogeochemistry deal with the same geological and hydrodynamic properties, these two disciplines should be able to complement each other when describing/modelling the groundwater system. Testing such an integrated modelling approach was the focus of a SKB project (Task 5) based on the Äspö HRL /Wikberg 1998, Rhén and Smellie 2003/. The advantages with such an approach were identified as follows:

- Hydrogeological models will be constrained by a new data set. If, as an example, the hydrogeological model, which treats advection and diffusion processes in highly heterogeneous media, cannot produce any Meteoric water at a certain depth and the hydrogeochemical data indicate that there is a certain fraction of this water type at this depth, then the model parameters and/or processes have to be revised.
- Hydrogeological models are fully three dimensional and transient processes such as shoreline displacement and variable-density flow can be treated, which means that the spatial variability of flow-related hydrogeochemical processes can be modelled, visualised and communicated. In particular, the role of the nearby borehole hydraulic conditions for the chemical sampling can be described.
- Hydrogeochemical models generally focus on the effects of reactions on the groundwater obtained rather than on the effects of transport. An integrated modelling approach can describe flow directions and hence help to understand the origin of the groundwater. The turnover time of the groundwater system can indicate the age of the groundwater and, knowing the flow rate, can be used to indicate the reaction rate. The groundwater chemistry obtained is a result of reactions and transport, and therefore only an integrated description can be used to correctly describe the measurements.
- By comparing two independent modelling approaches, a consistency check can be made. As a result greater confidence in active processes, geometrical description and material properties can be gained.

The present 1.2 modelling has further developed the comparison and integration between hydrochemistry and hydrogeology /SKB 2006/. The conceptual model for groundwater flow is a double porosity description, with flow taking place in a connected fracture network and with immobile water in the rock mass between the flowing fractures. Solutes can access the immobile water through diffusion into deadend fractures and by matrix diffusion. The salinity of the water implies that density driven flow needs to be considered. Thus, the salt both affects the groundwater flow characteristics in the mobile water phase, and diffuses into the immobile water phase. Conservative and reactive tracer transport as well as transport of water types can be modelled, but reactive tracer transport has not been considered in the hydrogeological modelling for Laxemar 1.2, see /SKB 2006/. The hydrogeological model can thus provide predictions of the concentrations of groundwater components and isotopes, such as Cl, ^{18}O and ^{2}H, in the connected rock matrix and in the flowing groundwater. It can also be used for dynamic predictions over time for the different water types

(meteoric, marine, glacial and brine). Furthermore, the groundwater flow model, independent of chemistry, can predict the salinity features at any point within the modelled rock volume, and the predictions can be compared with direct hydrogeochemical measurements or calculations. More detailes are given in the SDM report for Laxemar 1.2 /SKB 2006/.

The following conclusions were made in /SKB 2006/:

- There is potentially too much flushing of the Brine in the reference case suggesting that the calibration could benefit from decreasing the conductivities at depth. A variant case suggests reducing the fracture transmissivity by half an order of magnitude below –600 m elevation is sufficient to significantly improve the representation of palaeo-hydrogeology at depth. This well within the limits of uncertainty in hydraulic properties.
- The distribution of salinity (TDS) is broadly supported by the conceptual view given by ChemNet (see Chapter 4) of the distribution of the brine and adds credibility to the modelling results.
- Further integration is required where e.g. the salinity distribution is used by ChemNet to further explore the similarities/differences but also used for constructing a 3D hydrogeochemical conceptual model of the site and to describe the spatial variability of the site.
- Calculated mixing proportions from the hydrogeological model can be used to calculate a water composition in the 3D bedrock volume. If process modelling is coupled to the predicted water composition the spatial variability of SKB's suitability criteria can be calculated for the whole rock volume and important questions concerning spatial variability can be addressed.

Compared with model version 1.1, great progress has been made in the integration of hydrogeology and hydrochemistry. Hydrogeological modelling has shown that it is possible to simulate the observed water composition in the bedrock at Laxemar by assuming different initial conditions for Brine and Glacial end-members and boundary conditions of infiltration of Littorina and Sea water, in accordance with the conceptual palaeohydrogeological model of the site (Figure 2-1). This gives support to the conceptual model used within the hydrogeochemical modelling work.

Integrated models will increase the understanding of the origin, transport, mixing and reactions processes in the groundwater and will also provide a tool for predicting future chemical changes due to climate changes.

4 Resulting description of the Laxemar subarea

4.1 Bedrock hydrogeochemical description

The results of the hydrogeochemical modelling, as described in Chapter 3, have been used to produce a hydrogeochemical site descriptive model. This is a conceptual hydrochemical model of the site that summarises most of the important findings. The approach to construct the conceptual model is described in Appendix 1. Based on existing geological and hydrogeological information and in collaboration with the site hydrogeologists and geologists, schematic manual versions of these transects were produced to facilitate illustrating the most important structures/deformation zones and their potential hydraulic impact on groundwater flow. This hydraulic information was then integrated with the results of the hydrogeochemical evaluation and modelling results to show the vertical and lateral changes in the groundwater chemistry.

The marked differences in the groundwater flow regimes between the Laxemar and Simpevarp subareas are reflected in the groundwater chemistry. Along the main WNW-ESE transect Figure 4-1 shows the four major recognised groups of groundwaters and their interpreted spatial extent, denoted by A–D. The 'B' type groundwaters are subdivided into 'B_L' and 'B_S' types referring to Laxemar and Simpevarp respectively.

Figure 4-2 is oriented perpendicular to the main groundwater flow direction which is indicated by the encircled black dots. Only KLX03 has sufficient data (with some from KLX04) to give a good estimation of the depth extent of the various groundwater types A–D, and only B_L groundwaters are present as the transect is within the Laxemar subarea.

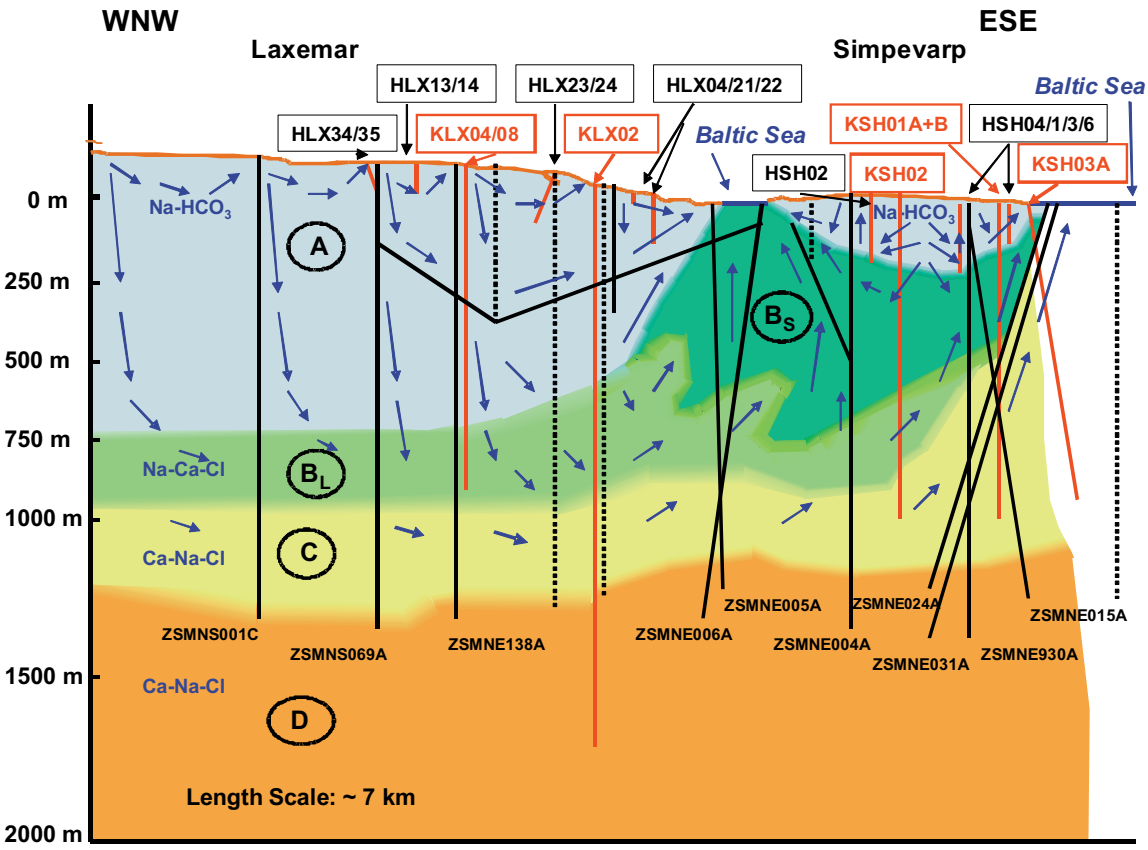

Figure 4-1. *Schematic 2-D visualisation along the WNW-ESE transect integrating the major structures, the major groundwater flow directions and the variation in groundwater chemistry from the sampled boreholes. Sampled borehole sections are indicated in red, major structures are indicated in black (full lines = confident; dashed lines = less confident), and the major groundwater types A–D are also indicated. The blue arrows are estimated groundwater flow directions.*

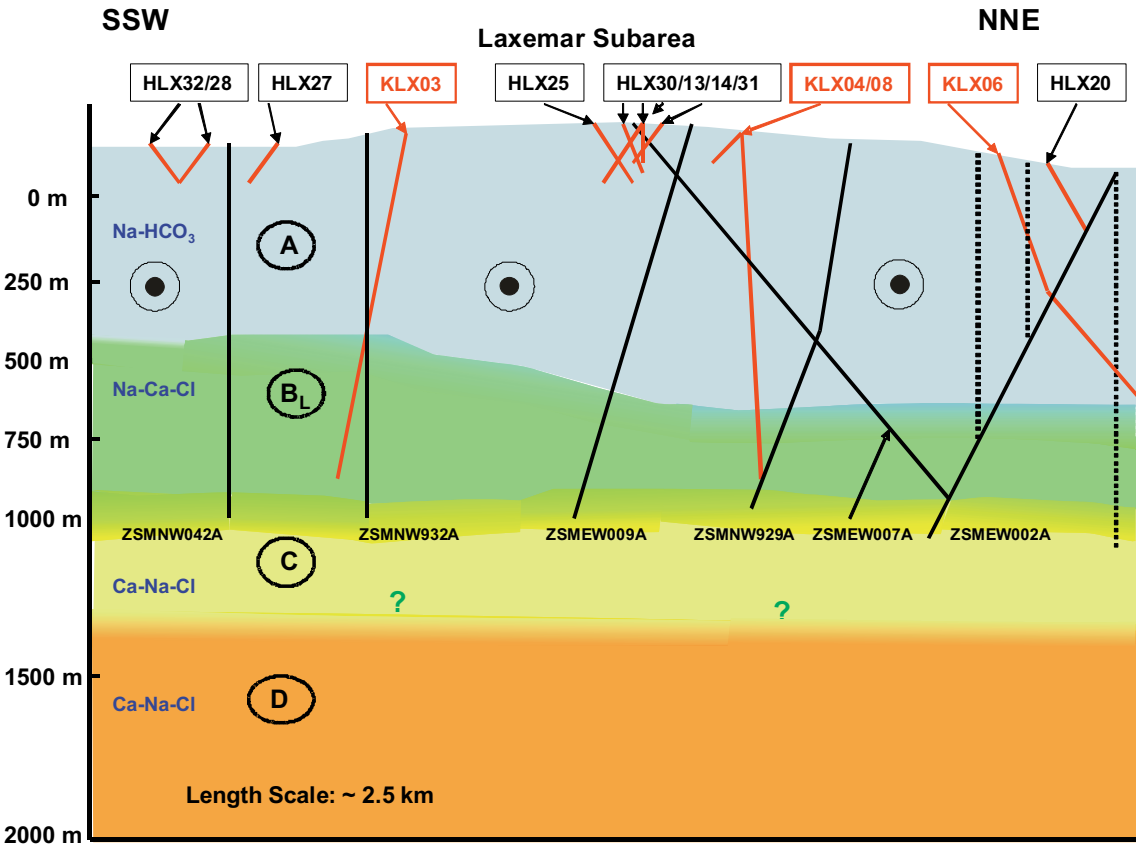

Figure 4-2. *Schematic 2-D model along the SSW-NNE transect integrating the major structures, the major groundwater flow directions and the variation in groundwater chemistry from the sampled boreholes. Sampled borehole sections are indicated in red, major structures are indicated in black (full lines = confident; dashed lines = less confident), and the major groundwater types A–D are also indicated. The encircled black dot symbol indicates the dominant horizontal/subhorizontal groundwater flow direction is out from the page.*

4.1.1 Summary of groundwater types

In terms of approximate depth, chemistry, major reactions and main mixing processes, the general features of these four groundwater types are summarised below.

Type A – Shallow (< 200 m) at Simpevarp but deeper (down to ~ 800 m) at Laxemar subarea

Dilute groundwater (< 2,000 mg/L Cl; 0.5–3.5 g/L TDS); δ = –11 to –8‰ SMOW.

Mainly meteoric and Na-HCO_3 in type.

Redox: Marginally oxidising close to the surface, otherwise reducing.

Main reactions: Weathering; ion exchange (Ca, Mg); dissolution/precipitation of calcite; redox reactions (e.g. precipitation of Fe-oxyhydroxides); microbially-mediated reactions (SRB) which may lead to formation of pyrite.

Mixing processes: Mainly meteoric recharge water at Laxemar subarea; potential mixing of recharge meteoric water and a modern sea component at Simpevarp subarea; localised mixing of meteoric water with deeper saline groundwaters at Laxemar and Simpevarp subareas.

Type B – Shallow to intermediate (150–600 m) at Simpevarp but deeper (down to ~ 500–950 m) at Laxemar subarea

Brackish groundwater (2,000–10,000 mg/L Cl; 3.5–18.5 g/L TDS); δ = –14 to –11‰ SMOW.

B_L – Laxemar subarea: Meteoric, mainly Na-Ca-Cl in type; Glacial/Deep saline components.

B_S – Simpevarp subarea: Meteoric mainly Na-Ca-Cl in type but some Na-Ca(Mg)-Cl(Br) types (± marine, e.g. Littorina); Glacial/Deep saline components.

Redox: Reducing.

Main reactions: Ion exchange (Ca, Mg); precipitation of calcite; redox reactions (e.g. precipitation of pyrite).

Mixing processes: Potential residual Littorina Sea (old marine) component at Simpevarp, more evident in some fracture zones close to or under the Baltic Sea; potential glacial component at Simpevarp and Laxemar subareas; potential deep saline (non-marine) component at Simpevarp and at Laxemar subareas.

Type C – Intermediate to deep (~ 600–1,200 m) at Simpevarp but deeper (900–1,200 m) at Laxemar subarea

Saline (10,000–20,000 mg/L Cl; 18.5–30 g/L TDS); δ = ~ –13‰ SMOW (? few data).

Dominantly Ca-Na-Cl in type at Laxemar but Na-Ca-Cl changing to Ca-Na-Cl only at the highest salinity levels at Simpevarp subarea; increasingly enhanced Br/Cl ratio and SO_4 content with depth at both Simpevarp and Laxemar subareas; Glacial/Deep saline mixtures.

Redox: Reducing.

Main reactions: Ion exchange (Ca).

Mixing processes: Potential glacial component at Simpevarp and Laxemar subareas; potential deep saline (i.e. non-marine) and an old marine component (Littorina?) at shallower levels at Simpevarp subarea; Deep saline (non-marine) component at Laxemar subarea.

Type D – Deep (> 1,200 m) only identified at Laxemar subarea

Highly saline (> 20,000 mg/L Cl; to a maximum of ~ 70 g/L TDS); δ = > –10‰ SMOW.

Dominantly Ca-Na-Cl with higher BrCl ratios and a stable isotope composition that deviates from the GMWL when compared to Type C groundwaters; Deep saline/brine mixture; Diffusion dominant transport process.

Redox: Reducing.

Main reactions: Water/rock reactions under long residence times.

Mixing processes: Probably long term mixing of deeper, non-marine saline component driven by diffusion.

Compared to the Simpevarp 1.2 visualisation /Laaksoharju 2005/ one of the major differences is the extent of the brackish ‘B’ type groundwaters, especially in the Simpevarp subarea. This is in part due to the absence of borehole KLX01, omitted because: a) it is located too far from the transects to be satisfactorily projected, and b) it has a marine component which makes it more representative for the NE ‘close to the Baltic Sea’ part of the Laxemar subarea but anomalous in the ‘total’ Laxemar subarea context. The ‘B’ type groundwaters in the Laxemar subarea therefore become meteoric and brackish, containing a mixture of glacial/deep saline groundwaters but devoid of an old marine (i.e. Littorina) component. They are referred to as ‘B_L’ type groundwaters. In the Simpevarp subarea the ‘B’ type groundwaters differ in that there is a weak but significant component of Littorina present, and these are referred to as ‘B_S’ type groundwaters. As indicated in Figure 4-1 the B_L groundwaters are continuously moving into the Simpevarp subarea at depth, mixing with the B_S groundwaters and gradually discharging to shallower levels.

5 Conclusions

5.1 Overall changes since previous model version

In this report the models and the site understanding has been consolidated. Despite relative few new data from depth the models have been updated and further understanding achieved concerning groundwater origin, evolution, reactions, pore water composition, microbial depth variation, uncertainties in the mixing calculations, tritium variations with time, and visualisation of the spatial variability of groundwater properties. An updated Hydrogeochemical Site Descriptive Model version 1.2 for the Laxemar subarea has evolved. The resulting description has improved compared to the 1.2 version for the Simpevarp subarea by producing a more detailed process modelling and 3D visualisation. The microbial characterisation gives direct support to the redox modelling. The coupled transport modelling can address processes questions from a transport point of view which is of importance for the site understanding. Further integration with the hydrogeological modelling has been achieved.

5.2 Overall understanding of the site

The overall understanding of the site describes the major processes taking place at the surface and to depth which includes the expected repository levels. The confidence in this description is relatively high since independent model approaches were utilised in the work. The origin, the postglacial evolution and the major reactions in the waters are fairly well understood. However the confidence concerning the spatial variation is low due to relatively few observations at depth. The continuation of the ongoing sampling programme at Laxemar will provide better spatial information and thus will increase confidence.

5.3 Implication for further modelling

Comparison and integration between geological and hydrogeological models in this model version was based on interactions concerning the structural model, fracture mineralogy, postglacial scenario models, concentrations of chloride, oxygen-18 and tritium, and mixing proportion calculations. The integration and comparison with hydrogeology should continue and the results have to be compared using 3D visualisation techniques. This will be an efficient support for the production of conceptual models of the site but also should be used for describing the spatial variability of the chemistry at the site.

The use of independent modelling approaches within the ChemNet group provided the possibility to compare the outcome of the different models and to use discrepancies between models to guide further modelling efforts. The many similarities resulting from the ChemNet modelling has given confidence in the results obtained. The use of independent but also new modelling approaches, such as modelling of the interaction between pore water chemistry and fracture groundwater, have to be further developed.

6 Acknowledgements

This study forms part of the SKB site investigation programme, managed and supported by the Swedish Nuclear Fuel and Waste Management Company (SKB), Stockholm. The support and advice from Anders Ström, SKB and Anders Winberg, Conterra AB are acknowledged. The helpful comments by the internal reviewers Mel Gascoyne, GGP Inc.; Bill Wallin, Geokema AB and Gunnar Buckau, FZK improved the work. The helpful interaction with the site chemist Liselotte Ekström is acknowledged.

7 References

Andersson J, Berglund J, Follin S, Hakami E, Halvarson J, Hermanson J, Laaksoharju M, Rhén I, Wahlgren C-H, 2002. Testing the methodology for site descriptive modelling, Application for the Laxemar area. SKB TR-02-19, Svensk Kärnbränslehantering AB.

Banwart S (ed.), Laaksoharju M, Skårman C, Gustafsson E, Pitkänen P, Snellman M, Landström O, Aggeryd I, Mathiasson L, Sundblad B, Tullborg E-L, Wallin B, Pettersson C, Pedersen K, Arlinger J, Jahromi N, Ekendahl S, Hallbeck L, Degueldre C, Malmström M, 1995. Äspö Hard Rock Laboratory. The Redox Experiment in Block Scale. Final reporting of results from the three year project. SKB PR 25-95-06, Svensk Kärnbränslehantering AB.

Banwart S, Tullborg E-L, Pedersen K, Gustafsson E, Laaksoharju M, Nilsson A-C, Wallin B, Wikberg P, 1996. Organic carbon oxidation induced by large-scale shallow water intrusion into a vertical fracture zone at the Äspö Hard Rock Laboratory (Sweden). Journal of Contaminat Hydrology, 21, 115–125.

Bath A, Milodowski A, Ruotsalainen P, Tullborg E-L, Cortés Ruiz A, Aranyossy J-F, 2000. Evidences from mineralogy and geochemistry for the evolution of groundwater systems during the quaternary for use in radioactive waste repository safety assessment (EQUIP project). EUR 19613 EN, Luxembourg.

Bein A, Arad A, 1992. Formation of saline groundwaters in the Baltic region through freezing of seawater during glacial periods. Journal of Hydrology, 140, Elsevier Science B.V., pp75–87.

Bottomley D J, Katz A, Chan L H, Starinsky A, Douglas M, Clark I D, Raven K G, 1999. The origin and evolution of Canadian Shield brines: evaporation or freezing of seawater? New lithium isotope and geochemical evidence from the Slave craton. Chem. Geol., 155, 295–320.

Casanova J, Négrel P, Blomqvist R, 2005. Boron isotope fractionation in groundwaters as an indicator of past permafrost conditions in the fractured crystalline bedrock of the fennoscandian shield. Water Res., 39, 362–370.

Clark I, Fritz P, 1997. Environmental Isotopes in Hydrogeology. Lewis Publishers. Boca Raton, Florida. 328 pp.

Degueldre C, 1994. Colloid properties in groundwater from crystalline formation. Paul Scherrer Institute, Villigen, Switzerland.

Drake H, Tullborg E-L, 2004. Fracture mineralogy – results from XRD, microscopy, SEM/EDS and stable isotopes analyses. SKB- P-report, in press.

Ekman L, 2001. Project Deep Drilling KLX02, Phase 2.Methods, scope, summary and results. Summary Report. SKB TR-01-11, Svensk Kärnbränslehantering AB.

Fontes J-Ch, Louvat D, Michelot J-L, 1989. Some constraints on geochemistry and environmental isotopes for the study of low fracture flows in crystalline rocks – The Stripa case. In: International Atomic Energy Agency (eds.) Isotopes techniques in the study of the Hydrology of Fractured and Fissured Rocks. IAEA, Vienna, Austria.

Frape S K, Fritz P, 1982. The chemistry and isotopic composition of saline groundwaters from the Sudbury Basin, Ontario. Canad. J. Earth Sci., 19, 645–661.

Frape S K, Fritz P, 1987. Geochemical trends from groundwaters from the Canadian Shield. In: (eds.) P. Fritz and S.K. Frape. Saline waters and gases in crystalline rocks. Geol. Assoc. Canada Spec. Paper 33, 19–38.

Fredén C, 2002. Berg och Jord, Sveriges Nationalatlas. 208 pp.

Gascoyne M, Ross J D, Purdy A, Frape S K, Drimmie R J, Fritz P, Betcher R N, 1989. Evidence for penetration of sedimentary basin brines into an Archean granite of the canadian Shield. WRI, (ed.) Miles. Balkema, Rotterdam.

Gimeno M J, Auqué L, Gómez L, 2004. Explorative analyses and mass balance modelling. In: Hydrochemical evaluation of the Simpevarp area, model version 1.2. Appendix 2. SKB R-04-74, Svensk Kärnbränslehantering AB.

Herut B, Starinsky A, Katz A, Bein A, 1990. The role of seawater freezing in the formation of subsurface brines. Geochim. et Cosmochim Acta, 33, 1321–1349.

Jaquet O, Siegel P, 2003. Groundwater flow and transport modelling during a glaciation period. SKB R-03-04, Svensk Kärnbränslehantering.

Laaksoharju M, Smellie J, Nilsson A-C, Skårman C, 1995a. Groundwater sampling and chemical characterisation of the Laxemar deep borehole KLX02. SKB TR 95-05, Svensk Kärnbränslehantering AB.

Laaksoharju M, Degueldre C, Skårman C, 1995b. Studies of colloids and their importance for repository performance assessment SKB TR-95-24, Svensk Kärnbränslehantering AB.

Laaksoharju M, Wallin B, 1997. Evolution of the groundwater chemistry at the Äspö Hard Rock Laboratory. Proceedings of the second Äspö International Geochemistry Workshop, June 6–7, 1995. SKB International Cooperation Report 97-04, Svensk Kärnbränslehantering AB.

Laaksoharju M, 1999. Groundwater characterisation and modelling: problems, facts and possibilities. Ph. D. Dissertation, Royal Institute of Technology, Stockholm, 144 p.

Laaksoharju M (ed.), 2004. Hydrogeochemical evaluation of the Simpevarp area, version 1.2. R-04-74, Svensk Kärnbränslehantering AB.

Laaksoharju M (ed.), Smellie J, Gimeno M, Auqué L, Gomez, Tullborg E-L, Gurban I, 2004. Hydrochemical evaluation of the Simpevarp area, model version 1.1. SKB R 04-16, Svensk Kärnbränslehantering AB.

Laaksoharju M (ed.), 2005. Hydrogeochemical evaluation of the Forsmark area, version 1.2. SKB R-05-17, Svensk Kärnbränslehantering AB.

Landström O, Tullborg E-L, 1995. Interactions of trace elements with fracture filling minerals from the Äspö Hard Rock Laboratory. SKB TR-95-13, Svensk Kärnbränslehantering AB.

Louvat D, Michelot J L, Aranyossy J-F, 1999. Origin and residence time of salinity in the Äspö groundwater system. Appl. Geochem., 14, 917–925.

Luukkonen, 2001. Groundwater mixing and geochemical reactions. An inverse-modelling approach. In: Luukkonen, A. and Kattilakoski, E. (eds.) Äspö Hard Rock Laboratory. Groundwater flow, mixing and geochemical reactions at Äspö HRL. Task 5. Äspö Task Force on groundwater flow and transport of solutes. (Progress Report SKB IPR-02-41), Svensk Kärnbränslehantering AB.

Milodowski A E, Tullborg E-L, Buil B, Gômez P, Turrero, M-J, Haszeldine S, England G, Gillespie M R, Torres T, Ortiz J.E, Zacharias J, Silar J, Chvátal M, Strnad L, Šebek O, Bouch J E, Chenery S R, Chenery C, Shepherd T J, McKervey J A, 2005. Application of mineralogical petrological and geochemical tools for evaluating the palaeohydrogeological evolution of the PADAMOT Study sites. PADAMOT PROJECT Technical Report WP2. EU FP5 Contract nr FIKW-CT2001-20129.

Molinero J, Raposo J, 2004. Coupled hydrogeological and reactive transport modelling In: Hydrochemical evaluation of the Simpevarp area, model version 1.2. Appendix 6. SKB R-04-74, Svensk Kärnbränslehantering AB.

Nordstrom D K, Lindblom S, Donahoe R J, Barton C C, 1989. Fluid inclusions in the Stripa granite and their possible influence on the groundwater chemistry. Geochimica Cosmochimica Acta, 53, 1741–1755.

Parkhurst D L, Appelo C A J, 1999. User's Guide to PHREEQC (Version 2), a computer program for speciation, batch-reaction, one-dimensional transport, and inverse geochemical calculations. U.S. Geological Survey Water-Resources Investigations Report 99-4259, 312 p.

Påsse T, 2001. An empirical model of glacio-isostatic movments and shore-level displacement in Fennoscandia. SKB R-01-41, 59 pp. Svensk Kärnbränslehantering AB.

Pedersen K, Arlinger J, Jahromi N, Ekendahl S, Hallbeck L, 1995. "Microbiological investigations". In: The Redox Experiment in Block Scale. Final Reporting of Results from the Three year Project. Chapter 7. Steven Banwart (ed). SKB Progress Report 25-95-06.

Pitkänen P, Luukkonen A, Ruotsalainen P, Leino-Forsman H, Vuorinen U, 1998. Geochemical modelling of groundwater evolution and residence time at the Kivetty site. POSIVA Report 98-07, Helsinki, Finland, 139 p.

Puigdomenech I, Ambrosi J-P, Eisenlohr L, Lartigue J-E, Banwart S, Bateman K, Milodowski A E, West J M, Griffault L, Gustafsson E, Hama K, Yoshida H, Kotelnikova S, Pedersen K, Michaud V, Trotignon L, Morosini M, Rivas Perez J, Tullborg E-L, 2001. O_2 depletion in granitic media. SKB TR-01-05, Svensk Kärnbränslehantering AB.

Rhén I, Bäckbom G, Gustafson G, Stanfors R, Wikberg P, 1997. Results from pre-investigations and detailed site characterization. Summary report. SKB TR 97-03, Svensk Kärnbränslehantering AB.

Rhén I, Smellie J, 2003. Task force modelling of groundwater flow and transport of solutes. Task 5 summary report. SKB TR-03-01, Svensk Kärnbränslehantering AB. (ISSN 1404-0344).

Samper J, Delgado J, Juncosa R, Montenegro L, 2000. CORE^{2D} v 2.0: A Code for non-isothermal water flow and reactive solute transport. User's manual. ENRESA Technical report 06/2000.

SKB, 2002. Simpevarp – site descriptive model version 0. SKB R-02-35, Svensk Kärnbränslehantering AB.

SKB, 2004. Hydrogeochemical evaluation for Simpevarp model version 1.2. Preliminary site description of the Simpevarp area. SKB R-04-74, Svensk Kärnbränslehantering AB.

SKB, 2005. Preliminary site description. Simpevarp subarea version 1.2. SKB R-05-08, Svensk Kärnbränslehantering AB.

SKB, 2006. Preliminary site description Laxemar subarea – version 1.2. SKB R-06-10, Svensk Kärnbränslehantering AB.

Smellie J, Laaksoharju M, Tullborg E-L, 2002. Hydrochemical site descriptive model – a stategy for the model development during site investigation. SKB R-02-49, Svensk Kärnbränslehantering AB.

Svensson U, 1996. SKB Palaeohydrogeological programme. Regional groundwater flow due to advancing and retreating glacier-scoping calculations. In: SKB Project Report U 96-35, Svensk Kärnbränslehantering AB.

Vilks P, Miller H, Doern D, 1991. Natural colloids and suspended praticles in Whiteshell Research area, Manitoba, Canada, and their potential effect on radiocolloid formation. Applied Geochemistry 8, 565-574.

Voss C I, Provost A M, 2003. SUTRA, A model for saturated-unsaturated variable-density groundwater flow with solute or energy transport. U.S. Geological Survey Water-Resources Investigations Report 02-4231, 250 p.

Westman P, Wastegård S, Schoning K, Gustafsson B, 1999. Salinity change in the Baltic Sea during the last 8,500 years w: evidence causes and models. SKB TR 99-38, Svensk Kärnbränslehantering AB.

Wikberg P, 1998. Äspö Task Force on modelling of groundwater flow and transport of solutes. SKB progress report HRL-98-07, Svensk Kärnbränslehantering AB.

Appendix 1

Explorative analysis and expert judgement of major components and isotopes

Contribution to the model version 1.2

John Smellie[1] Eva-Lena Tullborg[2] Niklaus Waber[3] Teresita Morales[4]

Conterra AB, Stockholm[1]

Terralogica AB, Göteborg[2]

University of Bern[3]

SKB, Oskarshamn[4]

September 2005

Contents

1	**Geological and hydrogeological setting**	89
1.1	Regional geology	89
1.2	Regional hydrogeology	90
1.3	Borehole locations and drilling	91
1.4	Fracture filling studies	92
2	**Groundwater quality and representativeness**	95
2.1	Background	95
2.2	Borehole data	96
2.3	Shallow soil pipe data	97
2.4	Baltic Sea water samples	98
2.5	Lake and stream water samples	98
2.6	Precipitation	98
2.7	Nordic sites	98
2.8	Organisation of evaluation	98
3	**The Laxemar site**	99
3.1	Cored Borehole KLX01	99
	3.1.1 Geological and hydrogeological character	99
	3.1.2 Groundwater quality and representativeness	100
3.2	Cored Borehole KLX02	101
	3.2.1 Geological and hydrogeological character	102
	3.2.2 Groundwater quality and representativeness	103
3.3	Cored Borehole KLX03	104
	3.3.1 Geological and hydrogeological character	104
	3.3.2 Groundwater quality and representativeness	106
3.4	Cored Borehole KLX04	110
	3.4.1 Geological and hydrogeological character	110
	3.4.2 Groundwater quality and representativeness	113
3.5	Borehole KLX06	115
	3.5.1 Geological and hydrogeological character	115
	3.5.2 Groundwater quality and representativeness	118
3.6	Percussion Borehole HLX10	119
3.7	Percussion Borehole HLX14	119
3.8	Borehole HLX18	119
3.9	Borehole HLX20	120
3.10	Borehole HLX22	120
3.11	Borehole HLX24	120
4	**The Ävrö site**	121
4.1	Cored Borehole KAV01	121
	4.1.1 Geological and hydrogeological character	121
	4.1.2 Groundwater quality and representativeness	123
4.2	Cored Borehole KAV04A	125
	4.2.1 Geological and hydrogeological character	125
	4.2.2 Groundwater quality and representativeness	127
4.3	Percussion Borehole HAV09	130
4.4	Percussion Borehole HAV10	131
4.5	Borehole HAV11	131
4.6	Borehole HAV12	131
4.7	Borehole HAV13	132
4.8	Borehole HAV14	132

5 The Simpevarp Site 133
5.1 Cored Borehole KSH01A 133
5.2 Cored Borehole KSH02A 133
5.3 Cored Borehole KSH03A 133
5.4 Percussion Borehole HSH02 133
5.5 Percussion Borehole HSH03 134
5.6 Percussion Borehole HSH04 135
5.7 Percussion Borehole HSH05 135

6 Summary of the evaluation 137

7 Additional input 139

8 Hydrogeochemical evaluation 141
8.1 Updated major ion and isotope plots for the Simpevarp area 141
8.1.1 Chloride depth trends 141
8.1.2 Calcium versus chloride and sodium 141
8.1.3 Magnesium versus chloride 142
8.1.4 Sulphate versus chloride and depth 143
8.1.5 Bicarbonate versus depth and chloride 144
8.1.6 Bromide/chloride versus chloride, magnesium and lithium 145
8.1.7 Oxygen-18 versus deuterium 147
8.1.8 Oxygen-18 versus depth and chloride 148
8.2 Updating of specific isotope plots for the Simpevarp area 149
8.2.1 Tritium 149
8.2.2 Carbon 152
8.2.3 Sulphur 155
8.2.4 Strontium 157
8.2.5 Uranium 158
8.2.6 Boron 158
8.3 Evidence of redox indicators 161

9 Bedrock-overburden interface 163
9.1 Introduction and background 163
9.2 Factors affecting sub-surface groundwater quality 163
9.2.1 General 163
9.2.2 Areas of recharge and discharge 163
9.3 Geology and hydrology, and soil and vegetation cover 165
9.3.1 Elevation and topography 165
9.3.2 Geology 165
9.3.3 Soil type distribution 165
9.3.4 Hydrology and hydrogeology 165
9.4 Sampled surface water and near-surface groundwater locations and present status 167
9.4.1 Sub-surface groundwaters: Soil Pipes < 10 m depth 167
9.4.2 Shallow bedrock groundwater: Percussion boreholes (0–200 m) 174
9.5 Recommended issues for Laxemar 2.1 178

10 Pore water studies of Borehole KLX03 179
10.1 Rock Porosity 180
10.2 General chemical characteristics of the pore water 182
10.3 Chloride concentration of the pore water 184
10.3.1 Sensitivity of derived chloride concentration 185
10.3.2 Preliminary modelling of chloride breakthrough 186
10.4 Comparison of pore water and groundwater compositions 187
10.4.1 Chloride content 187
10.4.2 Isotope composition 188
10.5 Summary 191

11 Palaeohydrogeochemistry 193

12 Conclusions 195
12.1 Major ions 195
12.2 Isotope sytematics 196
12.2.1 Tritium 196
12.2.2 Tritium and carbon-14 196
12.2.3 Carbon 197
12.2.4 Sulphur 197
12.2.5 Strontium 198
12.2.6 Boron 198

13 Visualisation of the Simpevarp area data 199
13.1 Construction of 2-D models 199
13.2 Hydrochemistry 202
13.3 Summary of groundwater types 203
13.3.1 Type A – Shallow (< 200 m) at Simpevarp but deeper (down to ~ 800 m) at Laxemar 203
13.3.2 Type B – Shallow to intermediate (150–600 m) at Simpevarp but deeper (down to ~ 500–950 m) at Laxemar 204
13.3.3 Type C – Intermediate to deep (~ 600–1,200 m) at Simpevarp but deeper (900–1,200 m) at Laxemar 204
13.3.4 Type D – Deep (> 1,200 m) only identified at Laxemar 204

14 Note on the origin of brines and their relevance to site characterisation studies 205
14.1 Background 205
14.2 Deep brines and origin of salts 205
14.2.1 The Swedish context 205
14.2.2 Measured salinities 205
14.2.3 Sources of salinity 206
14.2.4 Origin of salinity: Chemical and isotopic indicators 207
14.2.5 Application to the Swedish basement groundwaters 207
14.2.6 Summary and conclusions 213
14.3 Shallow freeze-out brines 214
14.3.1 Formation and evolution 214
14.3.2 Isotopic indicators 214
14.3.3 Summary and conclusions 216
14.4 Origin of the brine end member 218

15 References 219

Appendix 1 Borehole activities prior to, during, and subsequent to groundwater sampling 223

Appendix 2 Laxemar subarea: Upper bedrock hydrochemistry 231

Appendix 3 Laxemar: Pore water data from borehole KLX03 265

1 Geological and hydrogeological setting

1.1 Regional geology

The Simpevarp area is located at the Baltic coast some 30 km north of Oskarshamn (Figure 1-1). The area forms part of the TransScandinavian Igneous Belt of Precambrian basement rocks (dated to around 1.8 Ga) dominated by granitoids which, in the Simpevarp area, comprise porphyritic rocks ranging from red/grey granites to quartz monzodiorite. The granites are referred to as the Ävrö granites and the grey, medium-grained monzodiorites are dominantly quartz monzodiorite. A weak foliation is mostly observed. These rocks are usually medium-grained but with some fine-grained and porphyritic varieties. Along the south-east part of the Laxemar subarea and the Simpevarp peninsula, a grey-coloured, fine-grained variety of quartz monzodiorite occurs with a possible sub-volcanic origin. Because of its close relationship with the quartz monzodiorite and similarity in composition, the term dioritoid has been suggested. A thin belt of this rock type is also identified in the central part of Ävrö island. Small amounts of aplitic (named fine-grained granite) and dioritic and gabbroic rock-types also occur sporadically in smaller bodies, and are much more common in an E-W belt in the southern part of the Simpevarp area.Transecting all above-named rock-types are dykes characterised by fine- to medium-grained granite and pegmatites.

All rock-types have also been subjected to alteration (red staining caused by disseminated micro-grains of haematite) largely due to post-crystallisation penetration of hydrothermal fluids along pre-existing zones of weakness (e.g. fractures).

On a regional scale NE-SW oriented deformation zones are dominant (Figure 1-2). Completing the structural network are mostly discontinuous E-W and NW-SE oriented regional deformation zones. At the local scale, the Simpevarp site is bounded to the west and east by the large-scale regional NE-SW deformation zones aligned sub-parallel to the coast, and to the north and south by the approx. NW-SE and NE-SW oriented deformation zones.

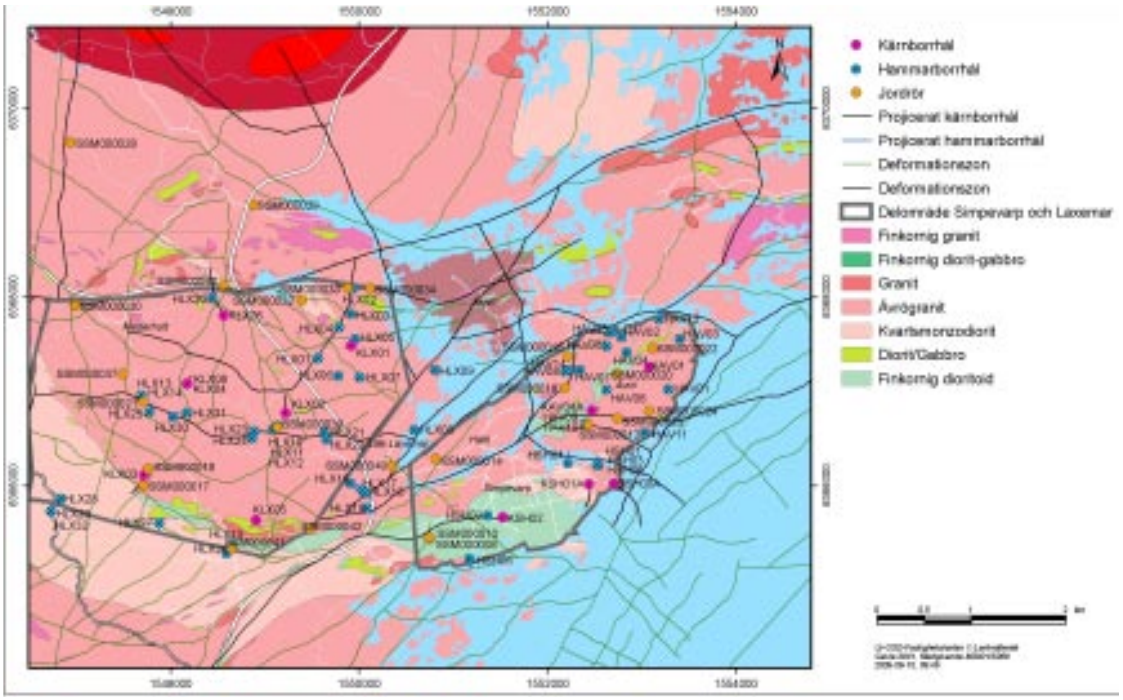

Figure 1-1. *Geological setting and borehole locations in the Simpevarp area.*

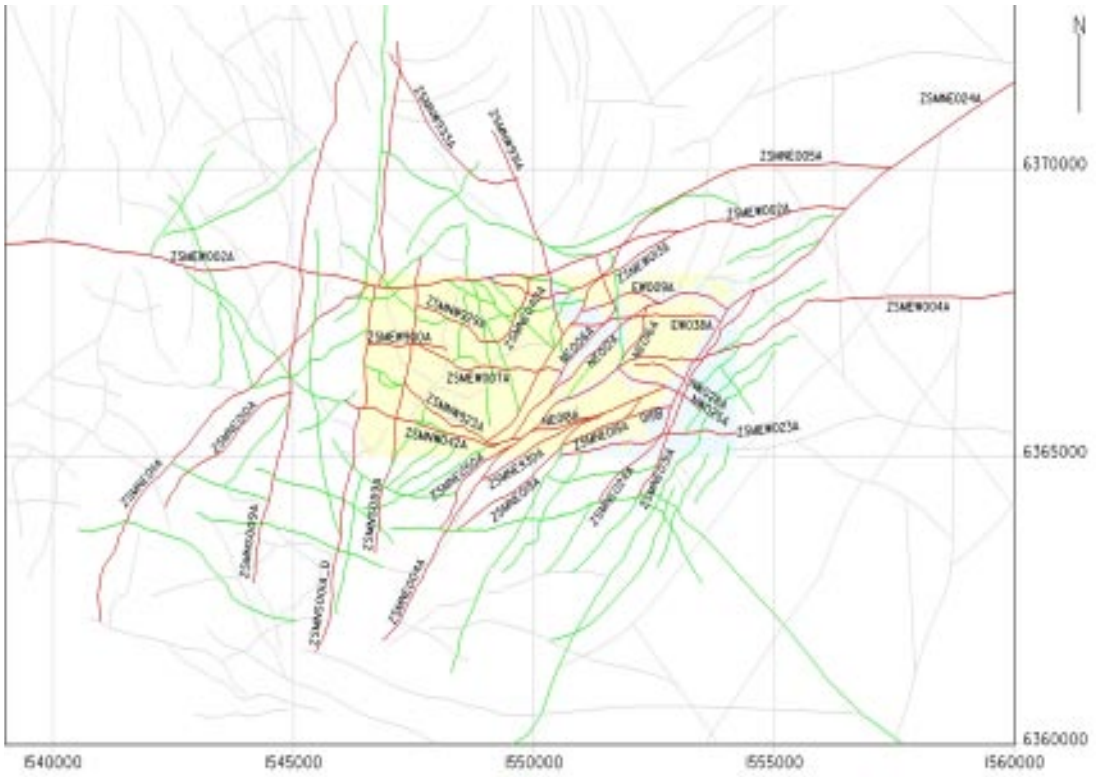

Figure 1-2. *Regional scale deformation zones that characterise the Simpevarp area (major zones in red).*

Three dimensional representations of the structural fabric are shown in Figure 1-3 (regional scale) and Figure 1-4 (local site scale). These further clarify the approx. E-W and NE-SW trends of the major deformation zones and the structural complexity of the Simpevarp penninsula and Ävrö/Äspö island localities.

1.2 Regional hydrogeology

The Simpecarp area is characterised by small-scale topographical undulation (< 50 m above sea level) and can be considered consisting of a large number of small catchments and mostly small water courses. The calculated annual run-off is 150–160 mm. Near-surface recharge/discharge is largely determined by the local topography and is sensitive to seasonal fluctuations in precipitation. Lakes are considered to be permanent discharge locations, streams sporadic discharge points during wet periods and wetlands/marshes/bogs can be either typical discharge areas in contact with groundwaters, or represent closed surface systems with no underlying hydraulic contact.

Since the last glaciation hydrological conditions have changed markedly due to shoreline displacement and changing salinity in the Baltic sea region (fresh to brackish). This has resulted in the present spatial distribution of groundwater types /SKB 2005/.

In common with the surface environment, topography appears to control much of the groundwater flow pattern in the upper part of the rock mass, possibly down to 1,000 m depth; increasing salinity with depth will reduce the flow rates. Discharge areas are located to the extreme east of the Simpevarp area along the Baltic Sea coastline and also onshore in conjunction with fracture zones. Results from the Simpevarp 1.2 evaluation /SKB 2005/ indicate that the Laxemar subarea is predominantly subjected to recharge conditions and that the Simpevarp subarea is an area of mainly groundwater discharge.

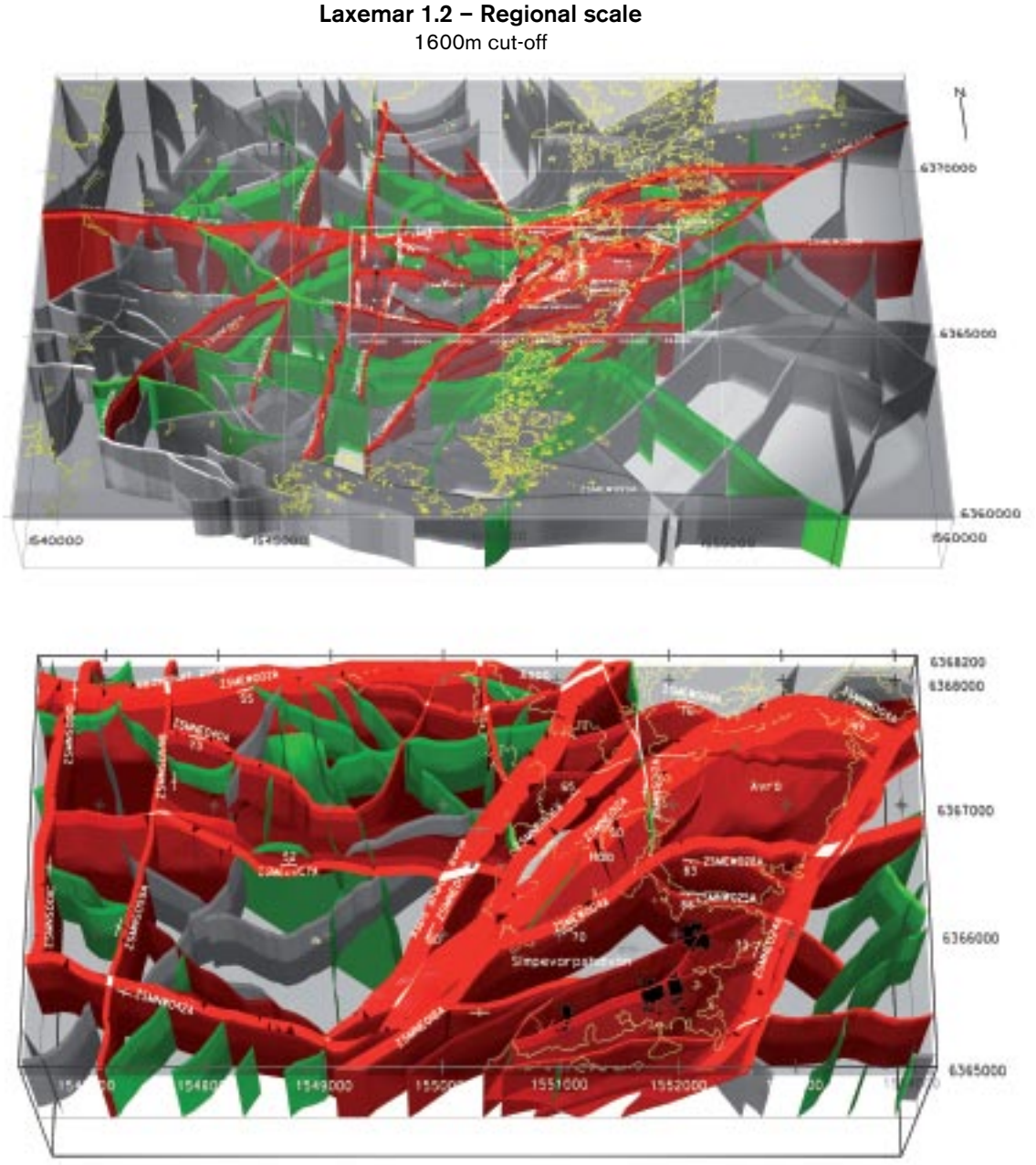

Figure 1-3. *3-D representation of the major deformation zones characterising the Simpevarp area on a regional scale (obove figure) and on a local scale (lower figure). Red coloured zones represent high confidence interpreted zones; green colouration representslower confidence interpreted zones.*

1.3 Borehole locations and drilling

The Laxemar 1.2 hydrochemical evaluation involved five cored boreholes (KLX01–KLX04 and KLX06) and 14 percussion boreholes (HLX01–HLX08 and HLX10, 14, 18, 20, 22, 24) from the Laxemar subarea, three cored boreholes (KSH01A, KSH02 and KSH03A) and 4 percussion boreholes (HSH02–HSH05) from the Simpevarp penninsula, and two cored boreholes (KAV01 and KAV04A) and 10 percussion boreholes (HAV04–HAV07 and HAV09–HAV14) from Ävrö island. These are shown in Figure 1-4.

Figure 1-4. *Location of hydrogeochemically prioritised boreholes KLX01, KLX02, KLX03, KLX04 and KLX06 (Laxemar subarea) and KAV01, KAV04A, KSH01A, KSH02 and KSH03 (Simpevarp subarea). Also indicated are the percussion boreholes, many of which are included in the Laxemar v. 1.2 evaluation.*

1.4 Fracture filling studies

Fracture minerals are determined macroscopically and are mapped within the Boremap system. However, since many of the minerals are difficult to identify and small crystals are easily overlooked, fracture mineral analyses have been carried out on additional samples for quantitative identification. Fracture samples have also been selected for sampling because they can provide information on the sequence of events that have resulted in fracturing and fracture mineralisation in the area. A number of samples have been taken from boreholes KLX02, KLX03, KLX04 and KLX06 for microscopy, in must cases including SEM/EDS, chemical analyses and stable isotope analyses of calcites. Results from these studies are not included in the Laxemar 1.2 data freeze but will be reported in the Laxemar 2.1 evaluation and later model versions.

Available mineralogical information is based on the Boremap data and the more detailed investigation of borehole KSH01A + B reported by /Drake and Tullborg 2004/. Even though most of the work reported so far has been carried out on core samples from the Simpevarp subarea, it can already be concluded that the sequences of minerals identified in the Simpevarp drillcores are recognised in the Laxemar subarea boreholes and are very similar to earlier observations made at the Äspö HRL /cf e.g. Landström and Tullborg 1995, Andersson et al. 2002/.

However, the order of frequency and the amounts of certain minerals can vary considerably throughout the Simpevarp subarea. It can however be speculated that the muscovite present in fractures north of the fracture zone ZSMEW002A (the Mederhult zone; Figure 1-2) is related to the

near vicinity of the Götemar granite and has not been observed in other boreholes in the central part of the Laxemar subarea.

Based on Boremap data and the hitherto available detailed information it can be concluded that:

- The most common fracture minerals are chlorite and calcite, which occur in several different varieties and are present in most of the open fractures. Other common minerals are epidote, prehnite, laumontite, quartz, adularia (low-temperature K-feldspar), fluorite, haematite and pyrite. A barium-zeolite named harmotome has been identified in some fractures and apophyllite has been identified in a few diffractograms. Baryte has been identified as small grains often together with calcite and pyrite. Gypsum has been identified in a few fractures from KSH03 east of the large fracture zone ZSMNE024A (Figure 1-2), in a section with very few open fractures in borehole KLX03 (around 500–600 m core length), and also in a few fractures at depth in borehole KLX06 (i.e. north of fracture zone ZSMEW002A).
- Clay minerals identified are, in addition to chlorite, made up of corrensite (mixed-layer chlorite/smectite or chlorite/vermiculite clay, the smectite or vermiculite layers are swelling), illite, mixed-layer illite/smectite (swelling) and a few observations of smectites.
- The red-staining of the wall rock around many fractures and mapped fractures zones, corresponds to hydrothermal alteration/oxidation, which has resulted in saussuritisation of plagioclase, breakdown of biotite to chlorite and oxidation of Fe(II) to form haematite, mainly present as micrograins giving rise to the red colour. The wall rock alteration has been subjected to a larger study focussing on the mineralogical and chemical changes in the altered wall rock compared with fresh host rock with special attention to redox reactions. This alteration sequence will be included in the Laxemar 2.1 data set.

It has, so far, not been possible to link different fracture minerals to different fracture orientations. The same difficulty was experienced in a corresponding analysis of a larger data set from Äspö /Munier 1993, Mazurek et al. 1997/. One explanation for this is that the core mapping is not, and cannot be, detailed enough to produce such precise data that is needed for correlation between orientations and mineralisations. There is, however, a possibility that the use of some minerals, for example that are produced only during one event and, in addition, can easily be identified during the core logging (like e.g. gypsum), can be used in the future.

The sequence of minerals from epidote facies, in combination with ductile deformation, over to brittle deformation and breccia sealing during prehnite facies, and subsequent zeolite facies and further decreasing formation temperature series, indicates that most of the fractures were initiated early in the geological history of the host rock and have been reactivated during several different periods of physiochemical conditions.

The locations of the hydraulically conductive fractures are mostly associated with the presence of gouge-filled faults produced by brittle reactivation of earlier ductile precursors or hydrothermally sealed fractures. The outermost coatings along the hydraulically conductive fractures consist mainly of clay minerals, usually illite and mixed layer clays (corrensite = chorite/smectite and illite/smectite) together with calcite and minor grains of pyrite.

In the perspective of groundwater chemistry the presence of the four minerals, calcite ($CaCO_3$), gypsum ($CaSO_4$), barite ($BaSO_4$) and fluorite (CaF_2), are worth attention as their solutbility has an impact/controls the behaviour of some major ions.

Calcite is as mentioned above the most common of these minerals. It occurs frequently at all depths except in the upper tens of metres and below approx. 1,000 to 1,100 m were it is less common. A number of calcite generations have also been identified ranging from hydrothermal to possible recent /Bath et al. 2000, Drake and Tullborg 2004/.

Barite occurs as very small grains but is relatively frequently observed (microscopically; not during the core logging) together with calcite, pyrite and the Ba-zeolite harmotome. In saline groundwater samples with very low SO_4 contents anomalously high Ba contents have been identified. For example, this was the case for the deepest saline groundwater from the KOV01 borehole at Oskarshamn, pointing towards a possible barite solubility control on the Ba and SO_4 content in the water. Solubility has an impact/controls the behaviour of some major ions.

Fluorite occurs in several hydrothermal mineral associations; together with epidote and the later prehnite but also together with the lower temperature (150°C) generation with calcite, barite and pyrite. Fluorite can be assumed to partly control the F content in the groundwaters.

Gypsum is identified only in relatively few fractures (Figure 1-5) which in turn are usually situated in borehole sections showing low a degree of fracturing and low (or not measurable) tranmissivity. Grondwater modelling /Laaksoharju 2004/ suggests dissolution of gypsum as an explanation for the relatively high SO_4 contents in the saline Laxemar groundwaters, but until this stage of the fracture filling studies it has not been possible to identify any gypsum in fractures from the area. For example, gypsum has not been identified during the extensive work in the Äspö HRL. It can not be ruled out that it has before been overlooked but a more probable explanation is that it is only present in some of the low transmissive relatively unfractured parts of the rock.

Other fracture fillings of certain interest for the hydrogeochemical interpretation are the redox sensitive minerals. These are mainly Fe-minerals which in the fractures are dominantly haematite and pyrite. Some goethite may be present but is subordinate compared with haematite. In the very near-surface fractures some less crystalline Fe-oxyhydroxides may be present, usually referred to as 'rust'. These are likely to be related to recent oxidation and are usually combined with dissolution of calcite.

In the fractures, several generations of haematite and pyrite are present. The finding of small pyrite grains in the outermost layers of the fracture coatings is in agreement with the groundwater chemistry, indicating reducing conditions.

In a redox buffer perspective the main host of Fe in the fractures is, however, chlorite and clay minerals. Mössbauer analyses of fracture chlorites from Äspö showed that 70–85% of the Fe present in fracture chlorite analysed was Fe(II) /Puigdomenech et al. 2001/. In the bedrock Fe is dominantly hosted in biotite but also in magnetite which is a common accessory mineral in the Ävrö granite and quartz monzodiorite

Other redox sensitive phases can be Mn minerals but these are very rare (not identified in the area) However, Mn is present in the calcites up to 1 or 2 weight % although usually less than 0.5% and also in some of the chlorites (less than 1 weight %).

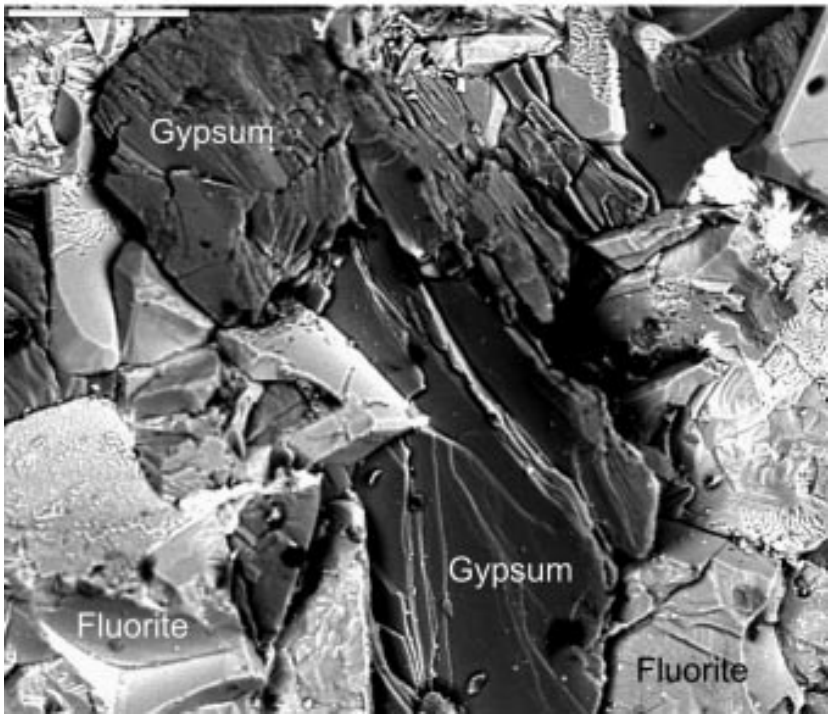

Figure 1-5. *Example of gypsum and fluorite in a fracture from KLX06: 789 m /Drake and Tullborg, in manuscript/.*

2 Groundwater quality and representativeness

2.1 Background

The hydrogeochemical evaluation approach used in the Simpevarp area, the uncertainties involved and one of the objectives to identify representative or suitable hydrochemical data, are addressed in the methodology outlined in /Smellie et al. 2002b/.

Prior to any hydrochemical evaluation is the necessity to judge the quality and the representativeness (or suitability) of the hydrochemical data derived from the site characterisation investigations. This should apply equally to borehole groundwaters (i.e. cored and percussion boreholes), to near-surface waters (shallow soil pipes and domestic wells) and to surface waters (i.e. Baltic Sea, streams, lakes and precipitation). However evaluating each location requires a different set of criteria and varying degrees of flexibility depending on the complexity of the sampled site. For example, surface waters may be subject to rapid seasonal fluctuations in chemistry and volume (and potentially microbial reactions) which contrasts to the deeper, more isolated bedrock groundwaters, although sampling at greater depth introduces additional problems. To evaluate representative or suitable data from all the sampled localities it is necessary therefore to consider a whole range of uncertainties of differing origin and importance.

The thoroughness of the data evaluation exercise will vary depending on the eventual use of the data and its origin, for example, high quality and complete borehole groundwater data are required to detect sensitive mixing or palaeoevolutionary trends (especially in the upper 300–500 m of the bedrock) and as input to geochemical equilibrium reaction modelling, whilst semi-quantitative (less complete) data may suffice to model large-scale lateral and vertical variations in groundwater chemistry or generally to distinguish time-series chemical trends during presampling monitoring and/or during the sampling interval. In contrast, for the reasons given above, hydrochemical data from surface and near-surface localities must be interpreted in more general terms because of the complex nature of the hydrochemical evolution through mixing and reaction.

It has been criticised by some of the field staff and reviewers that the evaluation approach employed for borehole groundwaters is too rigorous, revealing that less than 20% of the total number of water samples are considered to be representative or suitable for the Laxemar v. 1.2, inferring that there are large numbers of water samples that are not used and correspondingly much information lost. This is a common and understandable misconception. In reality all data provided by the SICADA database are available for use for all interested groups. However for each group to familiarise themselves with all the data is not practical given the time constraints. The selection of ‘representative’ or ‘suitable’ values is, therefore, severalfold, for example as an aid to help provide a degree of confidence or support (or otherwise) when using or interpreting other data which may be less reliable for different reasons (e.g. incomplete analyses; lack of chemical stability during sampling; contamination etc). It is important also to point out that to arrive at ‘representative’ or ‘suitable’ values requires using all the available hydrochemical data, and that these data are evaluated as much as possible with reference to known hydraulic conditions in: a) the borehole, b) the fracture zone sections being sampled, and c) the surrounding host bedrock. The reliability of these data is therefore based as much as possible on prevailing hydraulic and geologic conditions during borehole drilling, monitoring and sampling. The fact that all the data are not used by all the groups is due more to a lack of time and resources and also the general need for a major input of hydrogeological expertise and modelling at the borehole scale to aid hydrochemical interpretation for which there is yet no adequate provision.

Without the integration of hydrochemistry, hydrogeology and borehole activities there is a great danger that data can be misrepresented. A good example of this is the open hole tube sampling carried out in KLX02 in 1993 and 1997 where the hydrochemical and isotopic data collected along the borehole have been accepted and modelled as representing the evolution of formation groundwater with depth in the surrounding host rock, despite reservations of open hole mixing noted by /Laaksoharju et al. 1995/ and /Ekman 2001/, and more recently has been criticised during internal review. Other examples have included the use of tritium and radiocarbon data without considering closely enough: a) the possibility of induced mixing during borehole activities, b) natural dilution and radioactive decay of tritium with time when combining and comparing old and newly collected

samples, c) the potential surface input of tritium from the nearby nuclear power facilities, and d) lowering of detection levels throughout the years.

Of course there will be data which may be representative but will lack the full range of completed analyses or lack adequate background information to make a full evaluation possible. These data are also indicated in the database with the proviso that they should be used with caution.

The effect of borehole activities (Point (a) above) can be illustrated by the present Laxemar 1.2 evaluation. Figure 2-1 shows the relationship of tritium against depth using both representative/-limited suitability borehole groundwater values (red symbols), unrepresentative borehole groundwater samples (open symbols), and percussion boreholes which could not be fully assessed (in blue). As shown in the figure, there is a clear demarcation at depths > 200 m between tritium-free representative/limited suitability groundwaters and unrepresentative tritium contaminated samples. This provides confidence in the rigorous asessment approach applied. However, due to the very limited number of available analyses for the Laxemar 1.2. modelling, some analyses showing drilling fluid content up to 10% were selected as being of "limited suitability", i.e. highlighted in green in the SICADA table. However one of these samples indicated in the plot (KLX04: 103–213 m) shows a tritium content of ~ 4 TU and a drilling fluid content of 7.8%. The only tritium analysis of the drilling fluid (HLX10) available showed a content of 7.2 TU which means that the portion of drilling fluid in the sample can not alone explain the tritium content in the sample from KLX04: 103–213 m. This underlines the fact that a rigorous assessment of representativeness is only as good as the quality of the data available. With respect to this particular example which was collected from a long borehole length at shallow levels, the only way to improve the quality and representativeness of the data is to conduct a systematic and full analyses of the drilling fluids and close monitoring of these fluids (at least 3–4 samples) during the entire drilling period.

2.2 Borehole data

The majority of representative or suitable hydrochemical data have been selected from borehole sampling where the borehole activity record is well documented and degrees of contamination and/or induced mixing can be evaluated at least semi-quantitatively. Contamination can be judged,

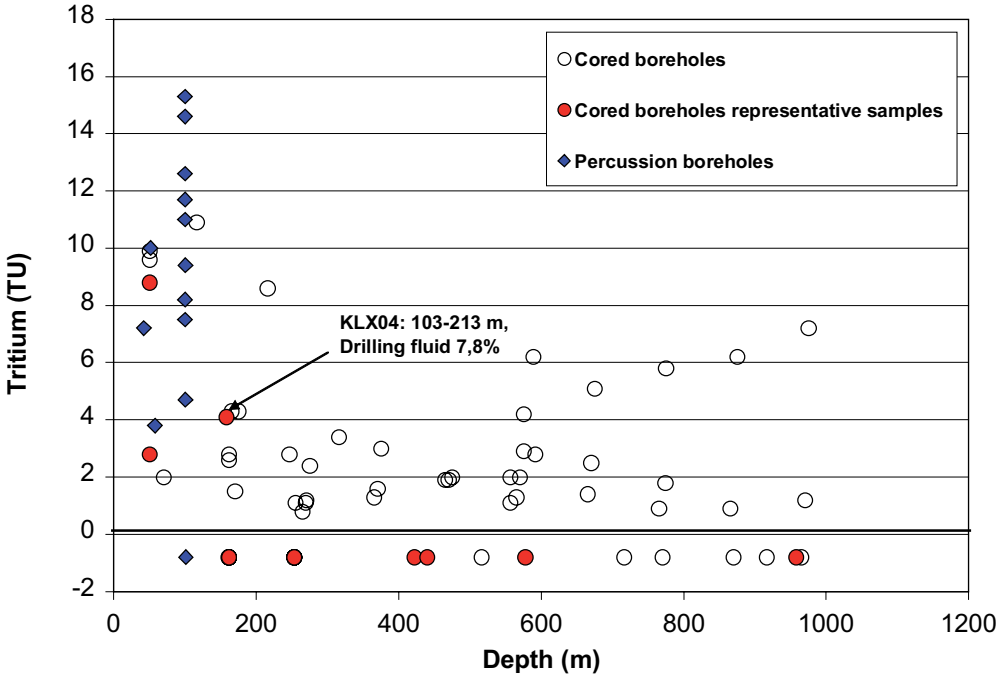

Figure 2.1. *Tritium versus depth for representative/limited suitability (red infilled symbols) and non-representative samples (open symbols) of groundwaters from percussion and cored boreholes at the Simpevarp and Laxemar subareas. (Negative tritium values indicate below detection).*

for example, by plotting tritium against percentage drilling water, and using measured values with specifically defined limits, i.e. charge balance (± 5%) and drilling water component (< 1%), and supported qualitatively by expert judgement based on detailed studies of the distribution and behaviour of the major ions and isotopes.

The final selection of data which best represents the sampled borehole section is based on identifying as near as possible a complete set of major ion and isotope (particularly tritium, ^{18}O and deuterium) analytical data. This is not always the case, however, and a degree of flexibility is necessary in order to achieve an adequate dataset to work with. For example:

- A charge balance of ± 5% was considered acceptable. In some cases groundwaters were chosen when exceeding this range to provide a more representative selection of groundwaters. These groundwaters should be treated with some caution if used quantitatively.
- In many cases the drilling water content was either not recorded or not measured. Less than 1% drilling water was considered acceptable. In some cases groundwaters were chosen when exceeding this range to provide a greater selection of groundwaters. Again these groundwaters should be treated with some caution if used quantitatively.
- Some of the older tritium data (before 2002) were analysed with a higher detection limit of 0.8TU; the present detection limit lies around 0.02TU. For some groundwaters an approx. tritium value is suggested where no recorded value is available. This value is selected normally from the same borehole section but representing an earlier or later sample from the same sampling campaign.

Resulting from this assessment, two groundwater sample types are highlighted in the SICADA database; one type considered representative or suitable (in orange), the other type less representative but suitable if used with caution (in green).

Open hole tube sampling has been carried out in many of the cored boreholes listed in the Laxemar 1.2 data freeze. This approach can be very useful in evaluating borehole groundwater circulation pathways and groundwater budgets (e.g. water in and water out between the borehole and surrounding bedrock). Understanding these processes helps greatly in assessing water quality and representativeness. However, since these groundwaters are mixed to varying degrees due to borehole hydraulics, the borehole activities prior to sampling, and also perturbation during lowering of the tube system into the borehole, their representativeness (or suitability) to describe the bedrock formation waters is questionable. Only at greatest depths where highly dense and saline groundwaters are typical, might they be considered more representative.

No representative groundwaters samples have therefore been selected from the SICADA tube sampling data contained in the Laxemar 1.2 data freeze. Some values of limited suitability from KLX02 have been highlighted in green, but need to be used with caution. These have been selected on the basis of more quantitative data from restricted borehole sections also from KLX02.

2.3 Shallow soil pipe data

Some of the soil pipes have been drilled in locations to monitor changes in the near-surface groundwater chemistry during percussion and core drilling of nearby deep boreholes. The remaining soil pipes have been located solely to monitor the natural undisturbed near-surface groundwater system.

An attempt was made to choose early or ‘First-Strike’ samples provided that there was no recorded major contamination with soil particles, that there were adequate analytical data and that the charge balance was within the ± 5% range. The analytical data considered most important are the major ions and the environmental isotopes: tritium, ^{14}C (pmC), ^{18}O and deuterium.

In addition, when a time-series of samples from the same campaign are available from a location and show no systematic variation in chemistry, the most suitable sample is selected with respect to analytical data, i.e. not necessarily from the final sample collected. When only a single sample is available, this is chosen if the analytical data listed above are complete, but is recommended to be used with caution since the chemistry may not have been stable when the sampled was collected.

2.4 Baltic Sea water samples

A large number of samples have been collected over a period of approx. 24 months ranging from the open Baltic Sea, to coastal areas comprising bays and coves, some of which border active freshwater drainage discharge areas of varying importance. From a hydrochemical viewpoint, the important selection criteria are:

- A representative Baltic Sea end member for the Simpevarp area latitude which has not been influenced by freshwater discharge; and
- Representative compositions from coastal Baltic Sea localities which may be in hydraulic contact at depth with the mainland where deep boreholes are located.

Since presently there are inadequate data to assess the coastal locations, and more open Baltic Sea samples are being planned, it is not known which samples best represent the Baltic Sea end member. Consequently, the selection of waters at this juncture considered to be suitably close to a Baltic Sea end member for this latitude have been based on the charge balance (± 5%), chloride content within the range of 3,500–3,800 mg/L and complete environmental isotopes of tritium, ^{18}O, and deuterium. Samples restricted only to major ion analytical data have also been recommended for use.

2.5 Lake and stream water samples

Surface water samples have been evaluated based on charge balance (± 10%) and the presence of major ions and isotopic data. A ± 10% charge balance was chosen because of the analytical uncertainty at low ionic conentrations. In common with the soil pipe groundwaters, these surface waters have been subject to seasonal fluctuations, complex reaction processes in the biosphere and potential discharge influences. Consequently, in the absence of knowing what could be representative or not, all selected samples that conform to the above criteria are recommended at this juncture. Samples restricted only to major ion analytical data have also been recommended for use.

2.6 Precipitation

Thirty four samples are included collected during an approx. two year period. These waters have not undergone any representativeness check senso stricto. On the other hand, the main intention has been to monitor $\delta^{18}O$, δD and tritium, since these parameters are used to identify modern meteoric groundwater components at depth. Consequently, all the precipitation isotope data available are used for this purpose, namely from 10 samples. Disturbances, such as unpredictable annual and seasonal trends and possible evaporation, have not been evaluated in this present representativeness check.

2.7 Nordic sites

Hydrogeochemical evaluation of the Laxemar subarea entails comparison with other geographically located sites in its near-vicinity, i.e. Simpevarp, Äspö, Ävrö and Oskarshamn, and also other Fennoscandian sites such as Forsmark and Olkiluoto. Groundwater data from all these sites are compiled in the 'Nordic Table' and these data also have been evaluated with respect to their suitability. This was carried out in parallel to the evaluation of the Simpevarp v. 1.2 and Forsmark v. 1.2 data /Laaksoharju 2004, 2005/ and also involved earlier evaluations /e.g. Smellie and Laaksoharju 1992, Laaksoharju et al. 1995, Pitkänen et al. 1999, 2004/.

2.8 Organisation of evaluation

The Laxemar 1.2 data freeze has involved new groundwater data from the Laxemar, Ävrö and Simpevarp sites. These data and their judged quality are addressed separately in Chapters 3, 4 and 5 for each site and for each individual cored and percussion borehole. In addition, a brief summary of the groundwater quality and representativeness is given in Chapter 6.

3 The Laxemar site

Site characterisation at the Laxemar site has included the drilling of up to 24 percussion drillholes (HLX01–24) to depths varying from approx. 70–200 m, and six cored boreholes (KLX01–06) of which KLX01 extends to 1,078 m, KLX02 to 1,705 m, KLX03 and KLX04 to around 1,000 m, and KLX06 to 850 m vertical depth. Of these, percussion boreholes HLX01–08, 10, 14, 18, 20, 22 and 24, and cored boreholes KLX01, 02, 03, 04 and 06, are included in the Laxemar 1.2 data freeze database. Figures 1-1 and 1-4 show the locations of the boreholes at Laxemar, Simpevarp and Ävrö.

Representativeness checks had been carried out for the earlier drilled HLX01–08 percussion boreholes and the KLX01–02 cored boreholes; these are highlighted in the Nordic database Table described in Simpevarp 1.2 hydrogeochemical evaluation report (SKB R-04-74). For completeness the general geological and hydrological character of KLX01 and KLX02 are outlined below. The remainder of the groundwaters sampled are evaluated below and judged to be suitable, of limited suitability or unsuitable.

3.1 Cored Borehole KLX01

Borehole KLX01 (Figures 1-1, 1-4 and 3-1) was drilled to a near-vertical (85.3°) depth of 1,077.99 m; percussion drilling was initially carried out to 101 m followed by casing to this depth prior to the core drilling phase.

3.1.1 Geological and hydrogeological character

The composite log for borehole KLX01, integrating geology, fracture frequency and hydraulic conductivity, is presented in Figure 3-1.

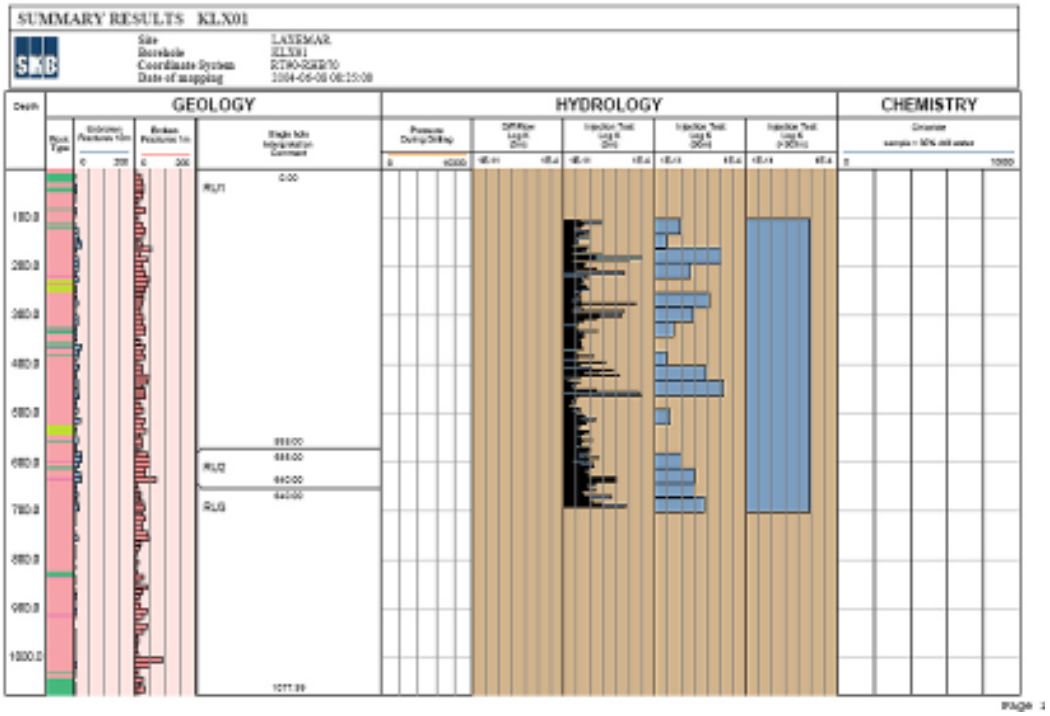

Figure 3-1. *Integrated geology, fracture frequency and hydraulic conductivity along borehole KLX01.*

The intercepted bedrock is dominated by Ävrö granite with sporadic thicknesses of fine-grained dioritoid (particularly close to the top and bottom of the borehole) and dioritoid at around 250 m and 550 m. In addition, small horizons of quartz monzodiorite and fine-grained granite (mixed with pegmatite) occur sporadically along the borehole.

Figure 3-2 indicates possible connections between fractured sections in the borehole and surface indicated discontinuities. These are believed to play an important role in facilitating deep groundwater recharge in this area.

The differential downhole flow measurement technique was not available following drilling in 1988, but injection tests to 700 m (Figure 3-1) reveal a range of hydraulic conductivity from 10^{-10}–10^{-5} ms^{-1} along the borehole length with the most transmissive section extending from 100 m (extent of the casing) to ~ 470 m. Groundwater samples from 272–277 m and 456–461 m are representive for this transmissive section. At greater depths to 700 m hydraulic conductivities are somewhat lower, averaging at around 10^{-9} ms^{-1} with the exception of 650–700 m where values of 10^{-7}–10^{-6} ms^{-1} were measured; this represents one of the groundwater sampling locations at 680–702.11 m. Groundwaters were taken also at greater depths, 910–921 m and 999–1,078 m respectively, with the latter corresponding to a significant fracture zone (Figures 3-1 and 3-2).

3.1.2 Groundwater quality and representativeness

Flushing water was obtained from percussion borehole HLX05 (0–150 m). The chemistry of this water shows it to be very dilute (< 10 mg/L Cl), Na-Ca-HCO_3 in type and typical stable isotope values of a modern meteoric recharge water.

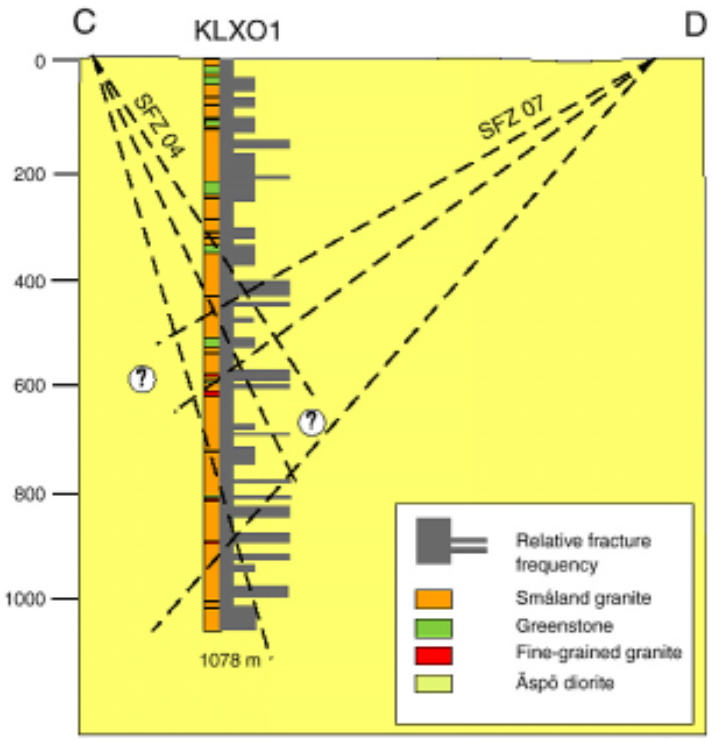

Figure 3-2. *Borehole KLX01: Interpretation of possible connections between fractured sections in the borehole and surface indicated discontinuities /Ekman 2001/. Section C–D is ~ 800 m long and oritented NW-SE, parallel to KLX02 (cf Figure 3-4). Note SFZ 04 and SFZ 07 refer to deformation zones interpreted prior to present site investigations initiated in 2002.*

Available data

Available data are mostly restricted to groundwater chemistry from isolated borehole sections.

Sampling from packed-off borehole sections

The following listed borehole sections were sampled. The groundwaters have been evaluated already for the Simpevarp 1.2 model description /Laaksoharju 2004/: see 'All Nordic Sites Table'. Indicated are those groundwaters deemed representative (highlighted in orange) and those considered of limited suitability and should be used with caution (highlighted in green).

- Section 272–277 m (1988-12-08): Less suitable; use with caution.
- Section 456–461 m (1988-11-23): Representative or suitable.
- Section 680–702.11 m (1988-11-03): Less suitable; use with caution.
- Section 680–702.11 m (1989-11-01): Less suitable; use with caution.
- Section 830–841 m (1990-10-09): Less suitable; use with caution.
- Section 910–921 m (1990-10-30/31): Less suitable; use with caution.
- Section 999–1,078 m (1990-11-19): Less suitable; use with caution.

3.2 Cored Borehole KLX02

Borehole KLX02 (Figures 1-1, 1-4 and 3-3) was drilled to a near-vertical (85°) depth of 1,700.50 m using flushing water from HLX10 (~ 110 m depth); percussion drilling was initially carried out to 200.80 m followed by casing to this depth prior to the core drilling phase. Drilling commenced on 1992-08-15 and was completed on 1992-11-29.

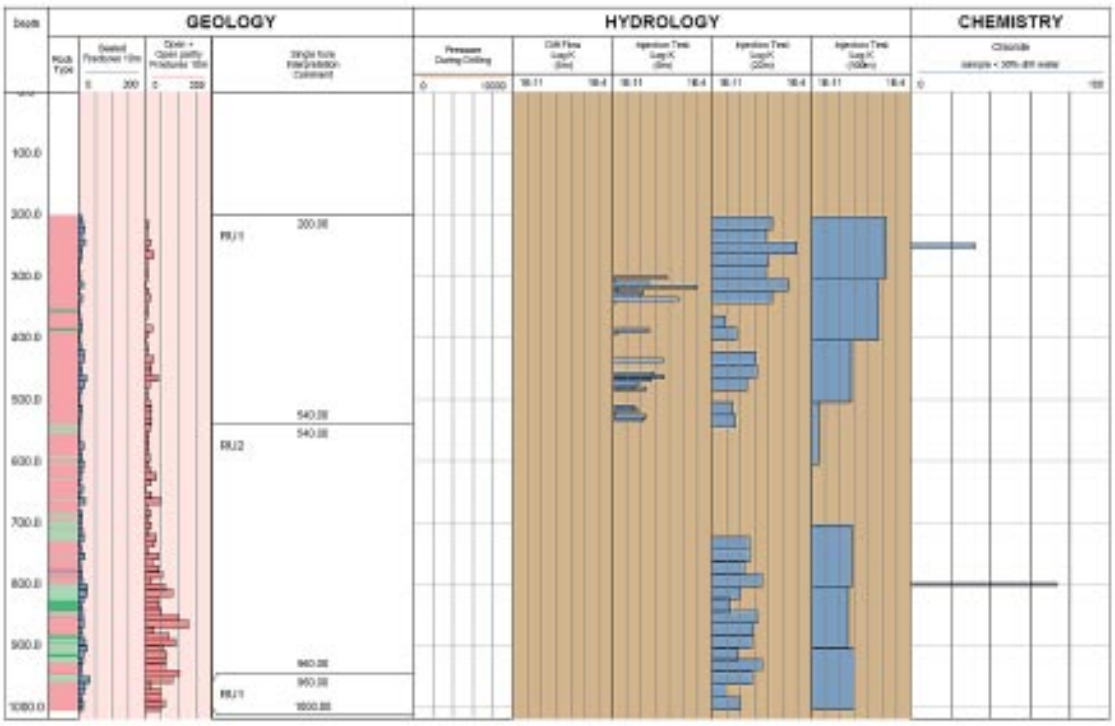

Figure 3-3. *Integrated geology, fracture frequency and hydraulic conductivity along borehole KLX02.*

3.2.1 Geological and hydrogeological character

The composite log to 1,000 m for borehole KLX02, integrating geology, fracture frequency and hydraulic conductivity, is presented in Figure 3-3, and another version to 1,700.50 m is shown in Figure 3-4.

The dominant rock type intercepted by KLX02 is the Ävrö granite (some 63% of the total borehole length); this is followed by 25% quartz monzodiorite. From 550–1,000 m fine-grained dioritoid (constituting some 10% of the core) becomes more frequent accompanied in cases by fine-grained diorite-gabbro. From approx. 950–1,450 m the Ävrö granite is dominant before changing to quartz monzodiorite below 1,450 m (Figure 3-4). Smaller horizons of fine-grained granite (approx. 2% of the core) occur sporadically along the borehole.

The mean fracturing is 2.36 fractures/m (crushed sections excluded), which is a lower frequency than for KLX01 (2.57 fractures/m). Open fractures characteristically increase with the increasing presence of fine-grained dioritoid, particularly from 730–1,100 m (Figure 3-3) with an average of 3.10 fractures/m frequent peaks exceeding 10 fractures/m. As indicated above, the overall lithology here is more heterogeneous with 50% Ävrö granite, nearly 30% dioritoids and 20% quartz monzodiorite. This fractured section therefore may represent the intersection of a major surface discontinuity (Figure 3-4). Between 730 m and 910 m oxidation occurs frequently; in minor parts of the core, mainly between 910 m and 1,068 m, also epidote and chlorite is found. Section 1,068–1,087 m is also strongly weathered. Finally, in section 1,105–1,111 m the core is again characterised by oxidation.

Below 1,120 m the fracture frequency decreases significantly, and section 1,120.1550 m displays the least fractured part of the borehole.

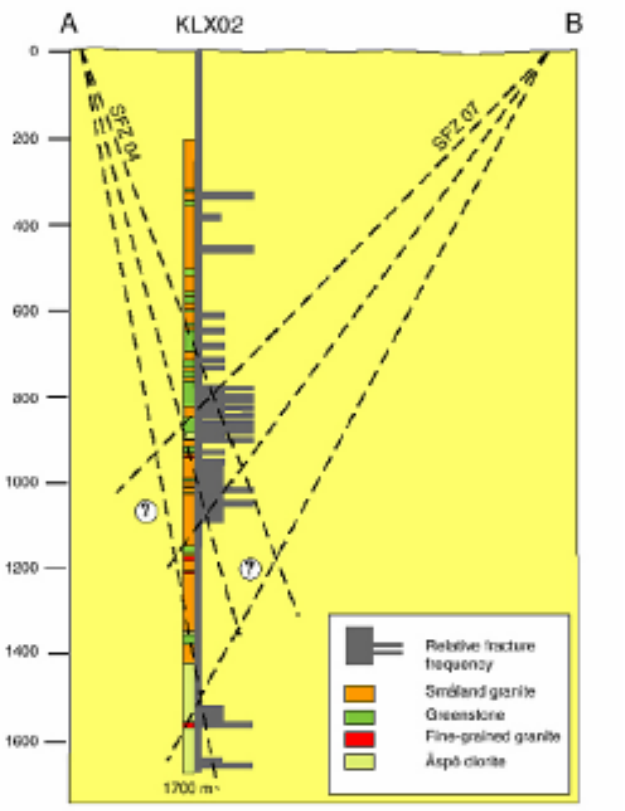

Figure 3-4. *Borehole KLX02: Interpretation of possible connections between fractured sections in the borehole and surface indicated discontinuities /Ekman 2001/. Section A–B is ~ 1,300 m long and oritented NW-SE, parallel to KLX01 (cf Figure 3-2).*

Differential downhole flow measurements were carried out in KLX02 from March–May, 1999 /Ekman 2001/. Injection tests to 1,000 m (Figure 3-3) reveal a range of hydraulic conductivity from 10^{-9}–10^{-5} ms^{-1} along the borehole length with the most transmissive section extending from 200 m (extent of the casing) to ~ 350 m. Groundwater samples from 315–321.5 m and 335–340.8 m are representive for this borehole section. From 350–1,000 m hydraulic conductivities fluctuate little, averaging around 10^{-9}–$10^{-7.5}$ ms^{-1}; 800–1,000 m depth is also characterised by an increased frequency of open fractures. At these depths groundwaters samples have been collected from 798–803.8 m and 1,090–1,096.2 m. Groundwaters were taken also at greater depths: 1,155–1,355 m and 1,420–1,705 m respectively.

Most of the accmulated data from KLX02 recognise the possibility of the following open borehole flow regime /Ekman 2001/:

- The upper part of the borehole, about 0–800 m, is more dynamic, i.e. the groundwater turnover time is shorter than in the bottom part of the borehole, section 800–1,700 m.
- Groundwater emerging from the shallow part of the bedrock recharges into the borehole above 200 m borehole length (i.e. between the casing and the borehole). This groundwater continues downward in the open borehole where portions discharge into fractures in the interval 200–800 m, except in a few sections, where flow recharges.
- At about 800 m, the downward moving groundwater encounters a minor, upwardly flowing groundwater flow from the deeper parts of the borehole, i.e. from the interval 800–1,700 m.
- The groundwater of shallow as well as of deep origin discharges into the highly fractured interval at 730–1,120 m.

The conclusion is that shallow groundwater is conducted via borehole KLX02 to larger depths, where mixing with deep groundwater occurs. With time, this process will affect increasingly large groundwater volumes around the borehole, whereby in situ conditions will be concealed. This fact stresses: 1) the need of early groundwater sampling, performed during drilling or shortly thereafter, and 2) if in situ conditions are to be preserved, installation of a straddle packer system in the borehole as soon as borehole investigation campaigns are concluded, in order to isolate fracture systems at different levels from each other. These open borehole conditions, lasting for months, has given rise to doubts surrounding the integrity of the KLX02 hydrochemistry, particularly resulting from the open borehole tube sampling campaigns.

3.2.2 Groundwater quality and representativeness

Flushing water was obtained from percussion borehole HLX10 (0–108 m. The groundwater is Na-HCO_3 in type, meteoric, dilute (6.3 mg/L Cl), recent (pmC = 55.73; 7.2 TU) and has a present-day recharge isotopic signature ($\delta^{18}O$ = –10.9‰ SMOW, δD = –78.8‰ SMOW).

Available data

Available data included groundwater chemistry from open hole tube sampling and groundwater chemistry from isolated borehole sections

Open hole tube sampling

As mentioned in section 2.2, open hole tube sampling must be treated with great caution. In borehole KLX02 open hole tube sampling was carried out on two occasions: 1993-08-03 and 1997-09-25. No representative groundwater samples have been selected but for the Simpevarp 1.2 model evaluation some samples of limited suitability were highlighted in green as long as they were used with caution. These were selected on the basis of more quantitative data from restricted borehole sections listed below in section 3.3.3.

Sampling from packed-off borehole sections

The following borehole sections were sampled and the groundwaters earlier evaluated (All Nordic Sites Table) for the Simpevarp 1.2 model description (SKB R-04-74). Indicated are those deemed representative (highlighted in orange in the 'All Nordic Sites Table').

- Section 315–321.5 m (1994-02-10): Representative.
- Section 335–340.8 m (1993-11-08): Representative.
- Section 798–800.9 m (1993-11-23): Representative.
- Section 1,090–1,096.2 m (1993-12-16): Representative.
- Section 1,155–1,165 m (1999-09-15): Representative.
- Section 1,345–1,355 m (1999-08-10): Representative.
- Section 1,385–1,392 m (1999-12-06): Representative.
- Section 1,420–1,705 m (1994-01-17): Representative.

3.3 Cored Borehole KLX03

Borehole KLX03 (Figures 1-1 and 1-4) was drilled to a depth of 1,000.42 m using flushing water from HLX14; percussion drilling was initially carried out to 100.35 m followed by casing to this depth prior to the core drilling phase. The sequence of borehole activities is presented in Appendix 1, Table 1-1.

3.3.1 Geological and hydrogeological character

The upper 600 m of borehole KLX03 penetrates a relatively homogeneous rock mass dominated by Ävrö granite; this is replaced to the bottom of the borehole by quartz monzodiorite (Figure 3-5). Close to this change in lithology, within the Ävrö granite between 605–620 m, there are several horizons of fine.grained dioritoid. Within the quartz monzodiorite between 720–760 m there are numerous horizons of fine-grained dioritoid and diorite-gabbro, accompanied by an increase in facture frequency (up to 15 fractures/m) and alteration. Increased fracture frequency (to 10 fractures/m) and some alteration also occurs within the quartz monzodiorite itself from 650–680 m.

The hydraulic character of borehole KLX03 is indicated in Figure 3-5 and in more detail in Figures 3-6 and 3-7. The differential downhole flow measurements /Rouhiainen et al. 2005, Figures 3-6 and 3-7/ reveal a general distribution of hydraulic transmissivity from 10^{-9} (lower detection limit) to 10^{-5} m^2s^{-1}; areas of greatest transmissivity are located between 100–300 m and 700–800 m, with slightly less (10^{-9}–$10^{-6.5}$ m^2s^{-1}) at around 400–450 m, 650 m and 975 m. Under 'natural conditions' (i.e. no pumping) the groundwater flow is from the borehole to the surrounding bedrock with a maximum measured flow rate of 10^{-4} mL min^{-1} at approx. 750 m. With pumping the groundwater flow is reversed towards the borehole, the variation in groundwater flow rates (10^{-2}–$10^{-5.5}$ mL min^{-1}) closely reflecting the variation of transmissivity in the surrounding bedrock. Between 950–1,000 m there is only a measureable flow rate (10^{4} mL min^{-1}) during pumping.

This suggests that during open borehole conditions, the upper approx. 500 m of the borehole and between 700–800 m, groundwater will preferentially move into the surrounding bedrock. With pumping, for example during sampling, this water will first have to be removed before 'representative' groundwater can be accessed. At the 950–1,000 m level, representative groundwater may be more immediately accessed.

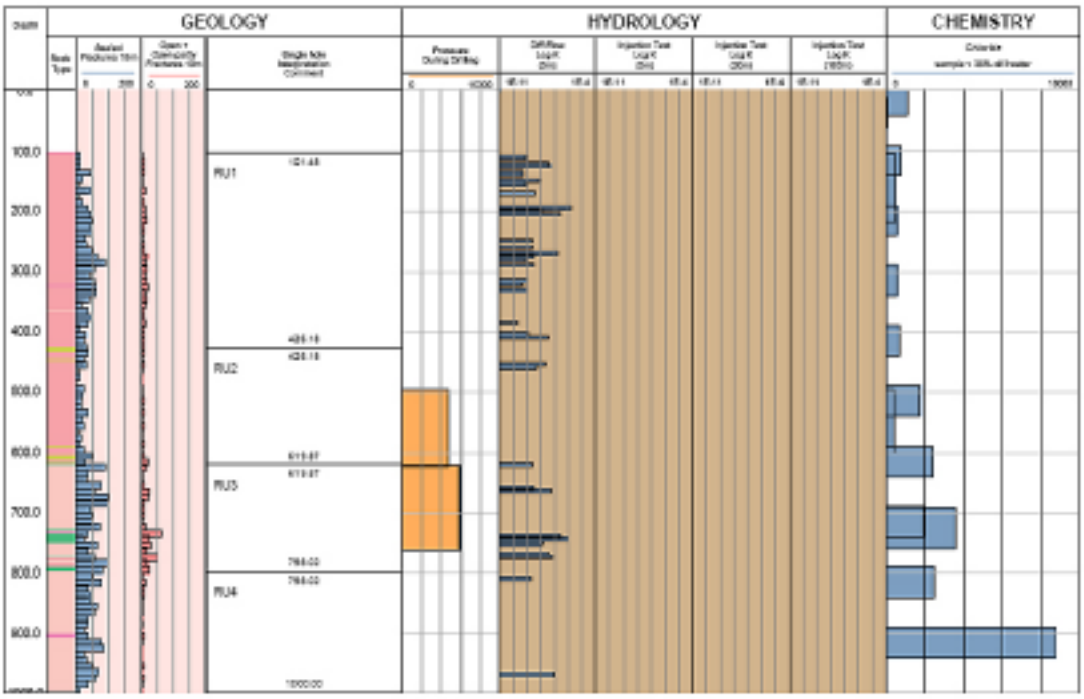

Figure 3-5. *Integrated geology, fracture frequency and hydraulic conductivity along borehole KLX03.*

The hydraulic complexity of the open borehole conditions is further supported by the electric conductivity log (Figure 3-8). During natural flow conditions (i.e. without pumping) a uniform dilute chemistry to around 750 m is shown, followed by a sharp increase in salinity which continues to the borehole bottom. This indicates three possibilities: a) input of dilute groundwater from the upper part of the borehole of greatest transmissivity (100–450 m) has penetrated to 750 m, b) the depth of the dilute water accurately reflects the extent of dilute formation groundwater, and c) the input of highly saline water from near the borehole bottom dominates to 750 m.

During pumping, however, there is a marked increase in salinity with the removal of dilute water from around 200 m to approx. 750 m (Figure 3-8). In contrast, there is no difference from 750 m to the borehole bottom. This indicates two conclusions: a) the chemistry of the highly saline groundwater at depth appears to be quite stable and thus probably representative, and b) the possibility that the dilute borehole waters reflect the chemistry of the formation groundwaters to 750 m depth is not correct. There is support therefore for the intrusion of dilute groundwater into the borehole from the upper, more transmissive, bedrock. Under open hole conditions this dilute water has moved into the surrounding bedrock where higher transmissivities allow, and subsequently removed during pumping to be replaced by more saline formation groundwaters. However, the highly saline groundwater to 750 m may also be an artefact of pumping and in reality the transition to highly saline groundwater may be much deeper, i.e. restricted to the 970 m level characterised by enhanced transmissivity (Figure 3-7).

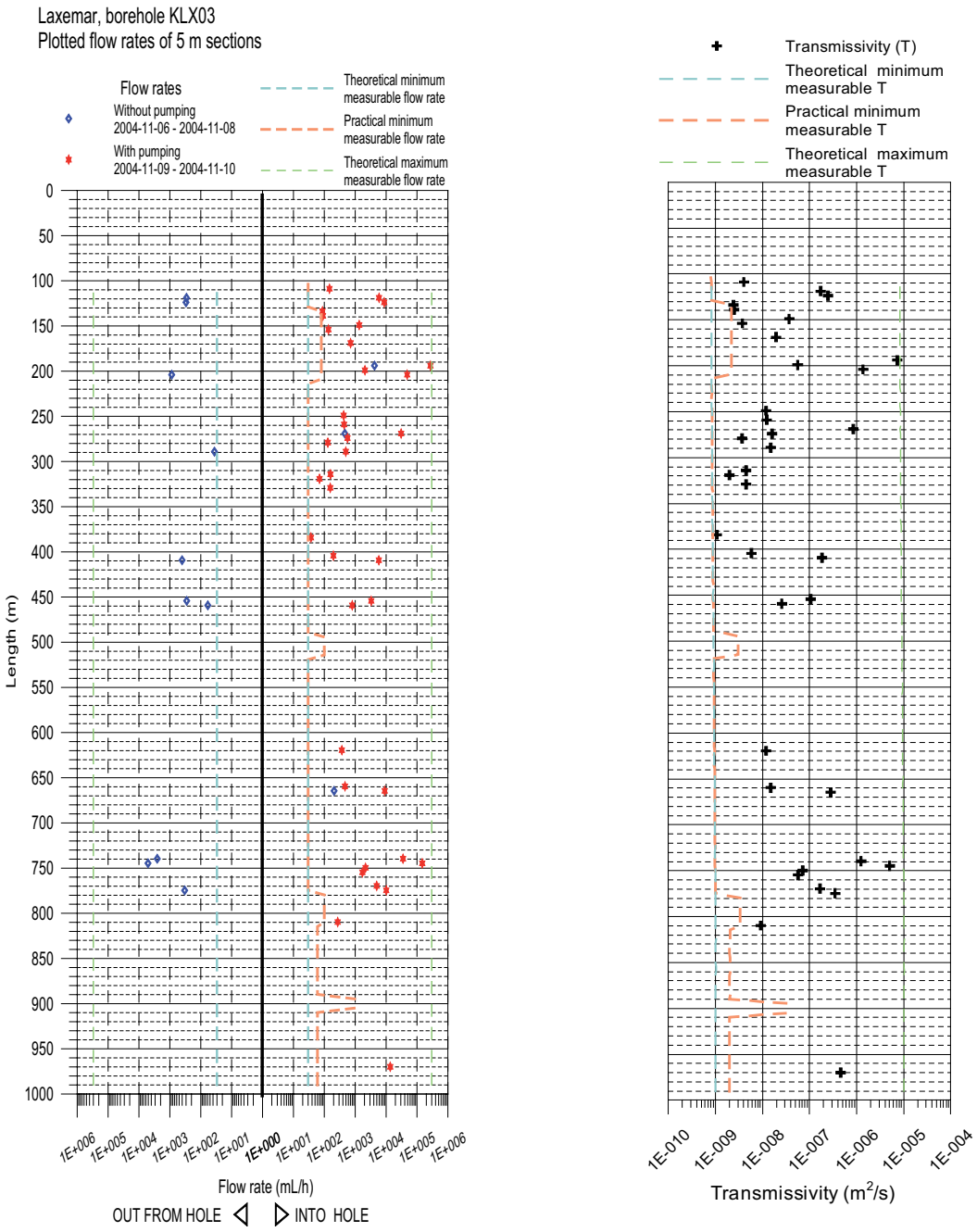

Figure 3-6. *Borehole KLX03: Groundwater flow rates and transmissivities based on differential flow measurements /Rouhianinen et al. 2005/.*

3.3.2 Groundwater quality and representativeness

Groundwater samples from borehole sections in KLX03 were taken on several occasions (Appendix 1):

- During drilling of the percussion borehole on two occasions using a simple packer system (2 samples, Class 3).
- During drilling of the cored borehole on four occasions using wire-line (4 samples, Class 3).
- Following borehole completion using the tube sampler (20 samples, Class 3).
- No samples were taken from packed-off borehole sections following borehole completion.

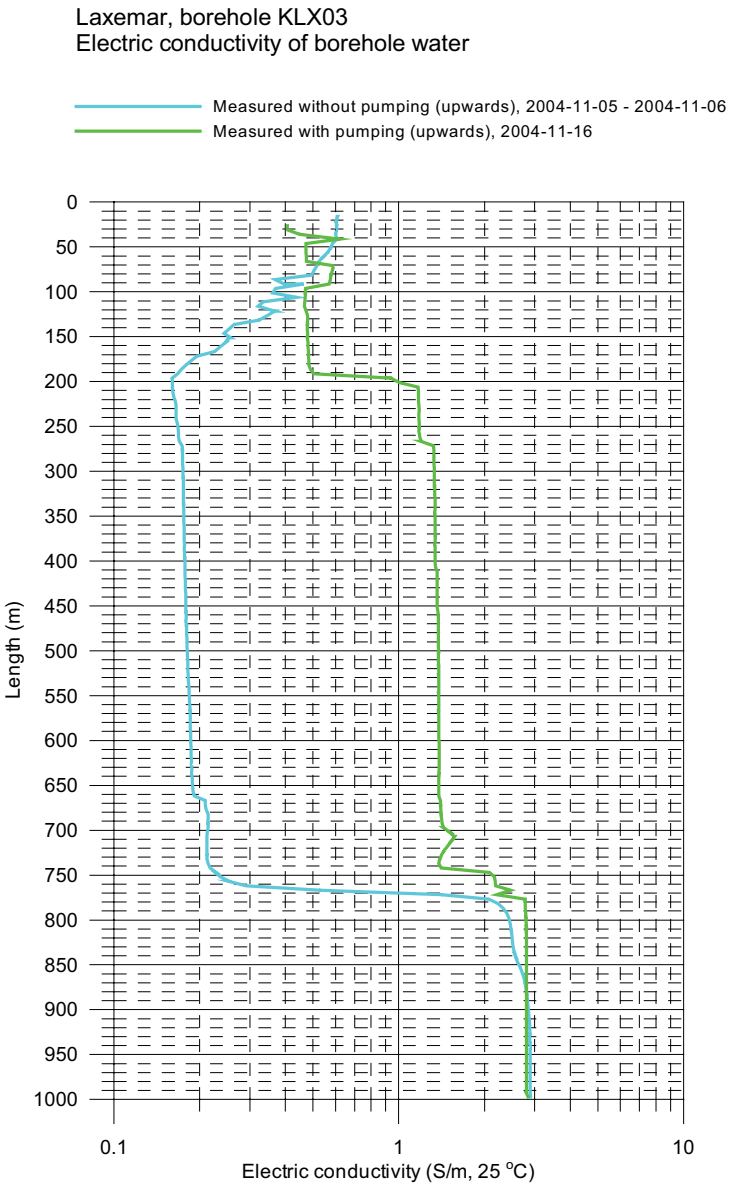

Figure 3-7. *Electric conductivity log for borehole KLX03 /Rouhianinen et al. 2005/.*

Percussion borehole samples – during drilling

Level 11.95–60.0 m

Analyses are incomplete and restricted mainly to the major ions HCO_3, Cl, SO_4, Br and F; no isotopic data are available. The shallow groundwater (probably Na-HCO_3 in type) is dilute (< 33.4 mg/L Cl) and assumed to be meteoric in origin.

Representativeness: Unsuitable because of incomplete analytical data. Limited qualitative use in establishing the presence of dilute, shallow derived groundwaters at this depth.

Level 11.95–100.30 m

Analyses are incomplete; those available reflect closely the groundwaters from the shallower borehole section described above.

Representativeness: Unsuitable because of incomplete analytical data. Limited qualitative use in establishing the presence of dilute, shallow derived groundwaters at this depth.

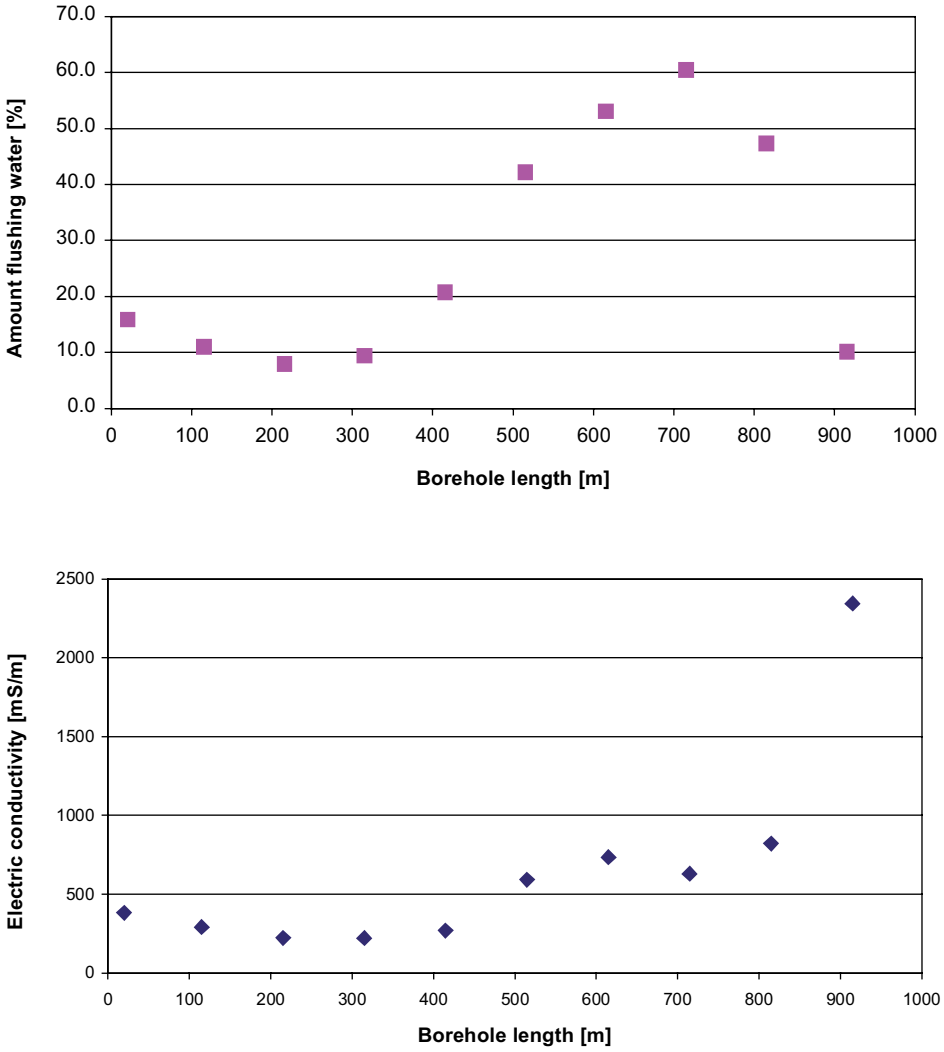

Figure 3-8. *Borehole KLX03: Distribution of residual drilling water (upper) and electric conductivity (lower) along the open borehole /Berg and Wacker, 2004/.*

Cored borehole samples – during drilling

Level 103.00–218.00 m

This groundwater has a fairly complete analysis. It is dilute but slightly more saline (507 mg/L Cl) than the shallower depths described above, and is therefore Na-Cl (HCO_3) in type. It is meteoric in origin, not recent (below detection tritium; 42.7 pmC) and has a cold recharge isotopic signature ($\delta^{18}O$ = –12.7‰ SMOW, δD = –89.7‰ SMOW). Furthermore it has little drilling water contamination (1.02%); the charge balance is slightly high (–5.898) but probably reflects the dilute character of the groundwater.

Representativeness: Suitable. (Highlighted in orange in the database).

Level 497.20–599.89 m

Analyses are incomplete and restricted mainly to the major ions HCO_3, Cl, SO_4, Br, F, Fe and Si; no isotopic data are available. The shallow groundwater (probably Na-Cl(HCO_3)in type) is dilute (381 mg/L Cl) and assumed to be meteoric in origin. Drilling water contamination is indicated (5.15 %).

Representativeness: Unsuitable because of incomplete analytical data and 5.15% drilling water. Limited qualitative use in establishing the presence of dilute, shallow derived groundwaters at this depth.

Level 600.00–695.24 m

Because of a recorded drilling water content of 102.00%, no analyses were carried out.

Representativeness: Unsuitable.

Level 692.86–761.11 m

Analyses are incomplete and restricted to the major ions HCO_3, Cl, SO_4, Br and F; no isotopic data are available. This groundwater is more brackish (3,550 mg/L Cl) with correspondingly low bicarbonate (41 mg/L) than the shallower horizons sampled. Drilling water contamination is high (30.3%).

Representativeness: Unsuitable because of incomplete analytical data and 30.3% drilling water. Limited qualitative use in establishing the presence of more brackish groundwaters at this depth.

Cored borehole samples – tube sampling

Following borehole completion, the borehole was flushed to remove excessive drilling debris (Appendix 1). The following day the connected tube array was lowered into the hole and during the same day raised, emptied and the samples sent for analysis. A total of 20 samples were collected, each representing 50 m borehole sections along the open borehole except for the uppermost borehole section which was 40 m (SKB P-04-299).

Analyses from each 50 m borehole section included electric conductivity, major ions but no trace element or isotopic data (Figure 3-8). The percentage of residual dilute drilling water is consistently high (range 8.0–60.5%) along the borehole with lower amounts at depths of 190–340 m (8.00–9.48 %) and at 890–940 m (10.20%); the highest contamination (60.50%) is at 690–740 m.

The electric conductivity measurements were carried out approx. two months before the measurements described above in Figure 3-7; the resulting trends show a close similarity which perhaps is not too surprising since both represent ‘natural flow’ open borehole conditions and reflect the dilute nature of the borehole waters. However greater salinities are present during the hydrochemical logging where values range from 224–382 mSm^{-1} (< 1,500 mg/L Cl) down to approx. 500 m depth, followed by a small increase to 592–822 mSm^{-1} (2,000–2,500 mg/L Cl) down to approx. 850 m. The final 850–1,000 m is characterised by a sharp increase in salinity to 2,340 mSm^{-1} (equiv. 8,720 mg/L Cl). Similar trends are shown by Na and Ca, with a reverse trend for HCO_3. Figure 3-7 shows generally lower salinities to around 750 m, with slightly higher salinity at greatest depths. The observed difference may be due to the inadequate flushing out of the borehole just prior to the hydrochemical logging causing some dispersion and mixing with the deeper saline waters at higher levels.

This suggests that in the upper 500 m of the borehole dilute, shallow-derived groundwaters are entering the borehole, largely replacing the drilling water removed during flushing of the borehole. At depths greater than 500 m flushing of the borehole has been less efficient and there remains a large drilling water component. Since the transmissivity is lower along this length, natural dilution and removal of the drilling water will be a long process and input of high saline groundwater into the borehole at around 850–1,000 m has resulted in some mixing.

Representativeness: Unsuitable because of excessive contamination by drilling water and mixing effects during open hole conditions.

3.4 Cored Borehole KLX04

Borehole KLX04 (Figures 1-1 and 1-4) was drilled to a depth of 993.49 m; percussion drilling was initially carried out to 100.40 m followed by casing prior to the core drilling phase. The sequence of borehole activities is presented in Appendix 1, Table 1-1.

3.4.1 Geological and hydrogeological character

Borehole KLX04 penetrates a relatively homogeneous rock mass dominated by Ävrö granite (Figure 3-9). Several sections of quartz monzodiorite occur between approx. 400–550 m and around 680–710 m. Granite (medium-grained) dominates below 900 m down to the bottom of the borehole. Thin intervals of gabbro and fine-grained dioritoid occur along the borehole.

Large lengths of the drillcore show fracture frequencies around 2–5 open fractures/m (200 to 450 m and 500 to 700 m). Lower fracture frequency is found in the upper 100–200 m and in the section between 700–860 m. The highest frequency of open fractures (5–10/m) is found at the bottom of the borehole between 870–980 m.

Based on the Laxemar 1.2 Geological Model two deformation zones are intersected by KLX04:

1) ZMNW929A at 873–973 m (and in KLX02 at 774–935 m).

2) ZSMEW007A at 346–355 m (and in KLX02 at 265–275 m and in KLX01 at 1,000–1,020 m).

The hydraulic character of borehole KLX04 is indicated in Figure 3-9 and in more detail in Figures 3-10 and 3-11.

The differential downhole flow measurements (Figure 3-10) reveal high transmissivities from 100–650 m depth ($10^{5.5}$–$10^{4.6}$ m^2s^{-1}) with the maximum at 200–300 m. From 650–880 m transmissivities are below detection (10^{9} m^2s^{-1}) and then increase to a maximum of around 10^{7} m^2s^{-1} at 880–980 m. Under ‘natural conditions’ (i.e. no pumping) the groundwater flow is from the borehole to the surrounding bedrock with a maximum measured flow rate of approx. 10^{5} mL min^{-1} at 300 m; at 880–980 m the flow rate is 10^{3} mL min^{-1} (Figure 3-10). With pumping the groundwater flow is reversed towards the borehole, the variation in groundwater flow rates (10^{2}–$10^{5.5}$ mL min^{-1}) closely reflecting the variation of transmissivity in the surrounding bedrock. Slightly higher hydraulic

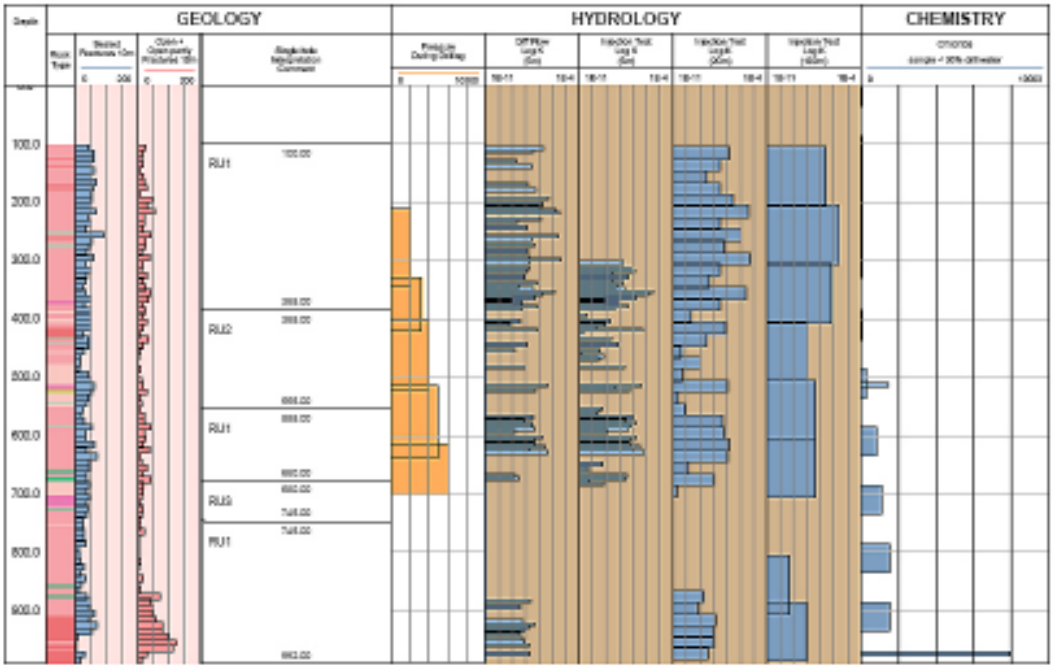

Figure 3-9. *Integrated geology, fracture frequency and hydraulic conductivity along borehole KLX04.*

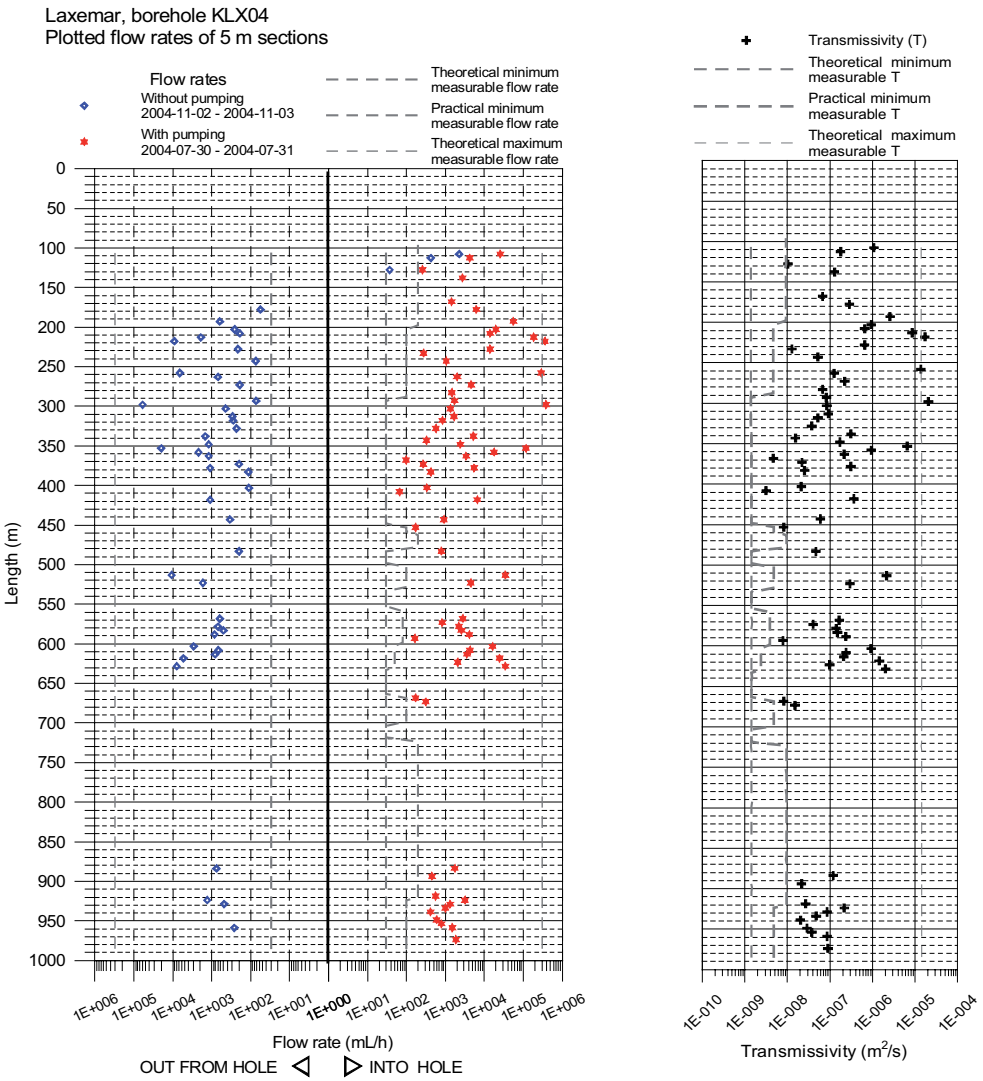

Figure 3-10. *Borehole KLX04: Groundwater flow rates and transmissivities based on differential flow measurements /Rouhiainen and Sokolnick 2005/.*

conductivity values are reported from the injection tests when compared to the differential flow measurements (Figures 3-9 and 3-10).

This suggests that during open borehole conditions, the upper approx. 650 m of the borehole in particular and to a lesser extent between 880–980 m, groundwater will preferentially move into the surrounding bedrock. With pumping, for example during sampling, this water will first have to be removed before 'representative' groundwater can be accessed.

The hydraulic complexity of the open borehole conditions is further supported by the electric conductivity log (Figure 3-11). This log was carried out following open hole air-lift pumping to clean the borehole and following subsequent tube sampling for hydrochemical logging (Appendix 2). During the initial pumping stage (red line) carried out at 5 m intervals (Figure 3-11), a constant salinity of 0.08 Sm^{-1} is indicated from 100–300 m. This followed by an increase to 0.15 Sm^{-1} until 350 m, and a further increase to 0.25 Sm^{-1} to 625 m. At this point there is a sharp decrease to around 0.07 sm^{-1} which stabilises to 800 m followed by a systematic increase to 0.16 Sm^{-1} at the borehole bottom. Further pumping at 1 m intervals (purple line) shows the same patterns but significantly the water being removed from the bedrock has a significantly higher salinity, especially with increasing depth. Comparison of these logs with the transmissivity distribution along the borehole (Figure 3-10) indicates the expected relationship down to 600–650 m: a) dilute groundwaters in the highest transmissive section, and b) more saline groundwaters in the less transmissive section

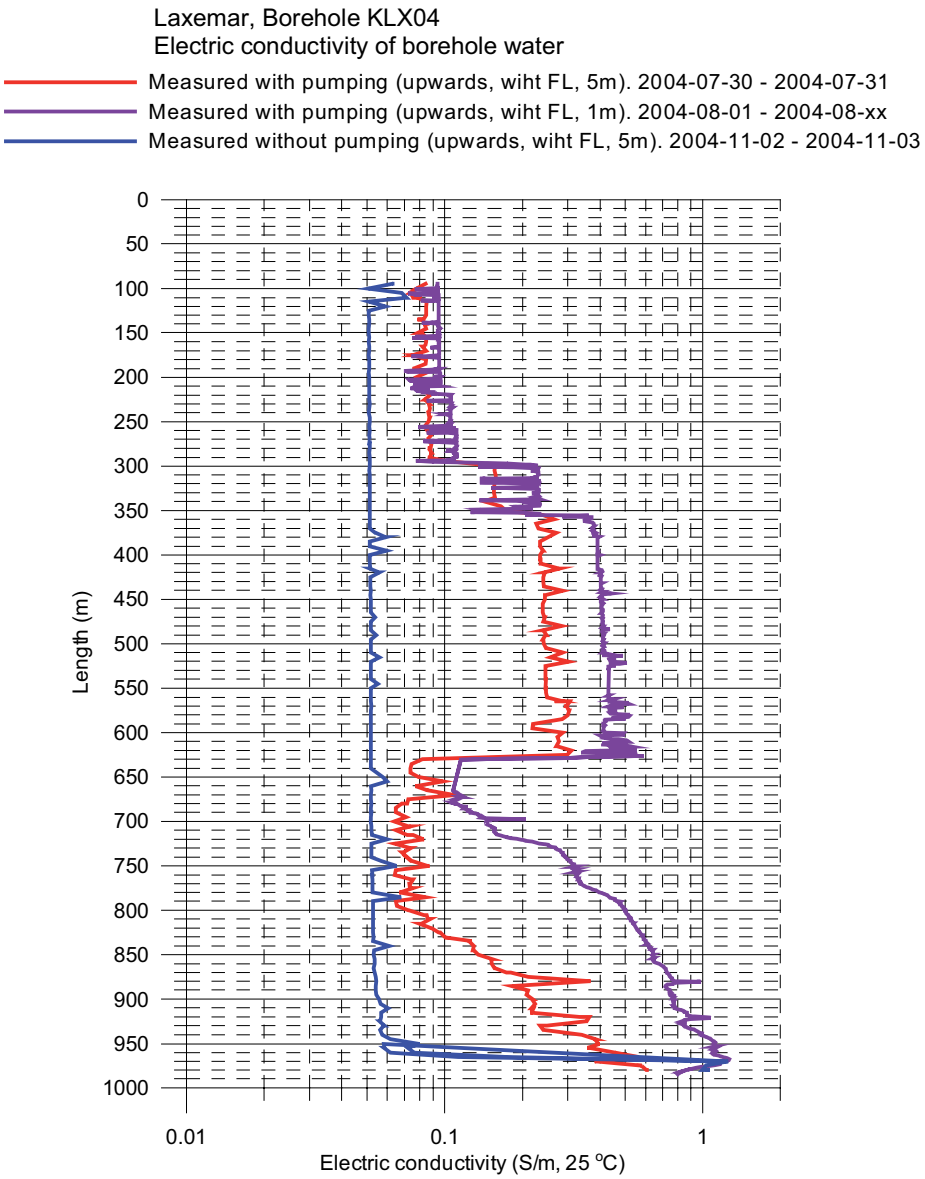

Figure 3-11. *Electric conductivity log for borehole KLX04 /Rouhiainen and Sokolnicki 2005/.*

to 600–650 m. What is surprising initially is the unexpected dilute water content at greater depths. As will be discussed below, this is due to large volumes of residual dilute drilling water in the borehole which have not been successfully removed by the air-lift pumping. However the increase in salinity close to the borehole bottom is due to the extraction of saline groundwaters from the transmissive section at 880–980 m.

Pumping was then carried out at 1 m intervals (purple line) resulting in an overall increase in salinity, particularly at depth (Figure 3-11). This indicates the removal of less saline contaminant waters from the surrounding bedrock, i.e. introduced during drilling and/or during open hole conditions. The very small changes from 100–300 m show that the contaminant water is of similar chemistry (i.e. dilute) to that of the formation groundwaters. From approx. 300–650 m the removal of the less saline contaminant water is more marked since the formation groundwaters accessed are more saline. At greater depths the accessing of saline formation groundwaters from the 880–980 m interval is dominating since the 650–850 m interval is hydraulically very tight.

After a lapse of 3 months the electric conductivity log was repeated under 'natural' no pumping conditions and indicated dilute water throughout the length of the borehole apart from the deepest part of the borehole (Figure 3-11). However during this lapse borehole KLX04 has been subjected to a comprehensive series of hydraulic injection tests and open hole geophysical logging etc. (Appendix 1). Since the fluid medium used in the hydraulic tests is a dilute water, coupled to the fact that the open borehole is dominated by dilute groundwaters (i.e. residual drilling water plus input of shallow dilute groundwater from the more highly hydraulic conductive sections in the upper part of the borehole), then perhaps it is not surprising that the electric conductivity measurements without pumping have resulted in a low salinity profile along the borehole. This underlines the necessity of prolonged pumping prior to groundwater sampling.

3.4.2 Groundwater quality and representativeness

Groundwater samples from KLX04 borehole sections were taken on several occasions (Appendix 1):

- During drilling of the cored borehole on 7 occasions using wire-line (2 samples, Class 3 and 5 samples, Class 1).
- Following borehole completion using the tube sampler (20 samples, Class 3).
- During PLU injection testing (36 samples, Class 1 and 2 samples, Class 5).
- From one predetermined packed-off borehole section (1 sample, Class 1, 2 samples, Class 4).
- Cored borehole samples – during drilling.

Cored borehole – during drilling

Level 103.00–213.14 m

This groundwater has a fairly complete analysis. It is dilute (28.6 mg/L Cl) and Na-HCO_3 in type, meteoric in origin, recent (4.1 TU; 61.3 pmC) and has a present-day recharge isotopic signature ($\delta^{18}O$ = –10.8‰ SMOW, δD = –76.8‰ SMOW). Furthermore the charge balance is acceptable (–1.026) but unfortunately the drilling water content is high (7.76%).

Representativeness: Limited suitability. (Highlighted in green in the database).

Level 210.00–329.14 m

Analyses are incomplete and restricted mainly to the major ions HCO_3, Cl, SO_4 and Br; no isotopic data are available. The shallow groundwater (probably Na-HCO_3 in type) is dilute (42.4 mg/L Cl), assumed to be meteoric in origin and appears similar to that described above. Drilling water contamination is excessive (40.70%).

Representativeness: Unsuitable because of incomplete analytical data and excessive contamination of drilling by water.

Level 329.00–403.82 m

No analytical data available because of excessive drilling water contamination (66.70%).

Representativeness: Unsuitable.

Level 401.00–515.10 m

No analytical data available because of excessive drilling water contamination (96.60%).

Representativeness: Unsuitable.

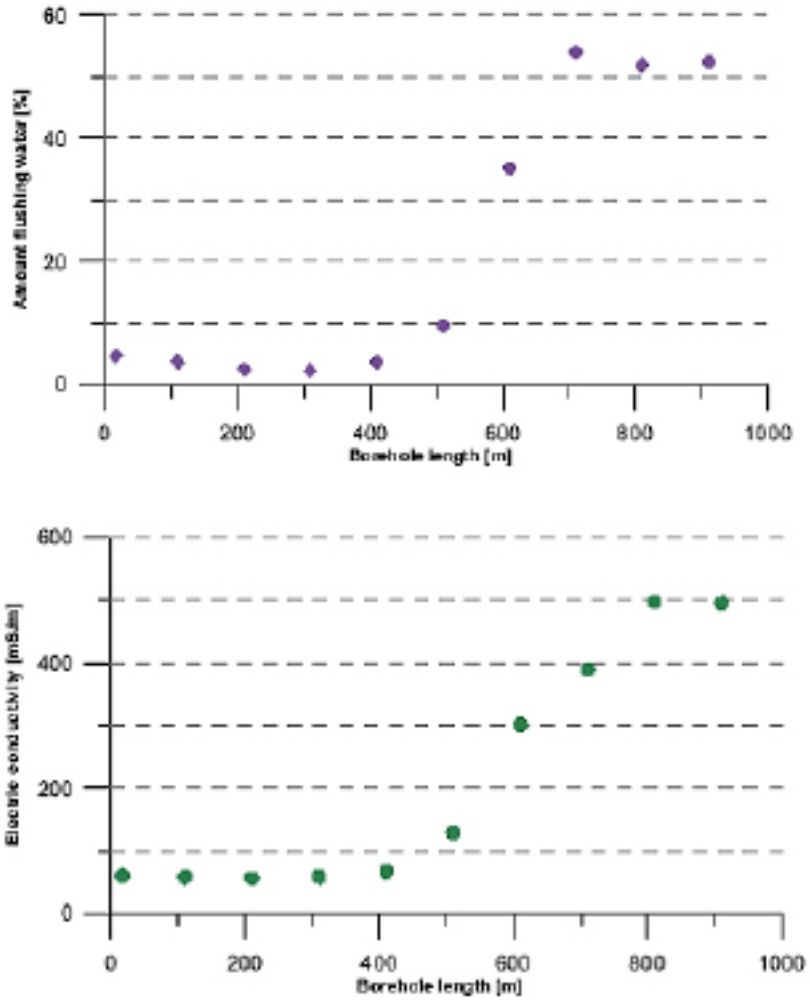

Figure 3-12. *Borehole KLX04: Distribution of residual drilling water (upper) and electric conductivity (lower) along the open borehole (SKB P-Report; submitted).*

Level 614.00–701.16 m

No analytical data available because of excessive drilling water contamination (97.60%).

Representativeness: Unsuitable.

Level 698.20–850.40 m

No analytical data available because of excessive drilling water contamination (91.10%).

Representativeness: Unsuitable.

Level 849.00–993.49 m

No analytical data available because of excessive drilling water contamination (105.00%).

Representativeness: Unsuitable.

Cored borehole samples – tube sampling

Tube sampling was carried out on completion of the PLU pumping tests followed by a series of rock stress and thermal property tests, and also just prior to the electric conductivity logs discussed above (Appendix 1). The connected tube array was lowered into the hole on 2004-07-08, raised, emptied and the samples sent for analysis. A total of 20 tubes/samples were collected, each representing 50 m sections along the open borehole except for the uppermost borehole section which was 35 m.

Figure 3-12 shows the distribution of residual drilling water and electric conductivity along borehole KLX04. To 500 m depth the drilling water contamination is consistently below 5% but always exceeds the 1% acceptance threshold. Below 600 m there is a steep rise in contamination to around 50% with a maximum of 54.10% at the 685–735 m level. Electric conductivity measurements (Figure 3-12) reflect this large residual component of dilute drilling water (see HLX10 description below), showing only a slight increase of salinity with increasing depth where a greater increase would have been expected. The maximum value is 500 mSm^{-1} (~ 1,500 mg/L Cl) from the deepest part of the borehole. Other plotted ions show a similar pattern, i.e. dilute HLX10 residual groundwater (combined with a greater percentage of similar shallow-derived groundwaters from KLX04) dominating the upper 500 m of the borehole, and mostly HLX10 combined with a smaller percentage of deep-derived highly saline groundwaters increasingly dominating the borehole at depths below 600 m.

These tube sample patterns, bearing in mind that these waters were collected prior to the electric conductivity logs discussed above (Figure 3-12) and immediately following inadequate air-lift pumping to clear the open borehole of residual dilute drilling water, underline their unsuitability for quantitative hydrochemical evaluation. The chemical patterns suggest that in the upper 500 m of the borehole dilute, shallow-derived formation groundwaters are entering the borehole, largely replacing the drilling water removed during flushing of the borehole. At depths greater than 500 m flushing of the borehole has been less efficient and there remains a large drilling water component. Since the transmissivity is lower along this length, especially from 700–850 m, natural dilution and removal of the drilling water will be a long process and input of high saline groundwater into the borehole at around 850–1,000 m has resulted in some mixing to higher levels

Representativeness: Unsuitable because of excessive contamination by drilling water and mixing effects during open hole conditions.

3.5 Borehole KLX06

Borehole KLX06 (Figures 1-1 and 1-4) is a 939.00 m long borehole inclined 60° to the surface and reaching a vertical depth of aprox. 800 m; percussion drilling was initially carried out to 100.30 m followed by casing prior to the core drilling phase. The sequence of borehole activities is presented in Appendix 1, Table 1-1. The aim of the borehole was to drill through the large Mederhult defomation zone (ZSMEW002A) which delineates the Simpevarp area to the north.

3.5.1 Geological and hydrogeological character

Borehole KLX06 penetrates a relatively homogeneous rock mass dominated between 100–417 m by Ävrö granite with subordinate fine-grained dioritoid (Figure 3-13). From 417–590 m the rock is more heterogeneous comprising fine-grained granite, pegmatite, granite, Ävrö granite, fine-grained dioritoid and fine-grained diorite/gabbro. From 590–843 m Ävrö granite dominates again with horizons of fine-grained diorite/gabbro, granite, fine-grained granite, quartz monzodiorite and pegmatite. From 843 m to the borehle bottom there is another heterogeneous length mainly of granite but also horizons of Ävrö granite, fine-grained granite, pegmatite, fine-grained dioritoid and fine-grained diorite/gabbro.

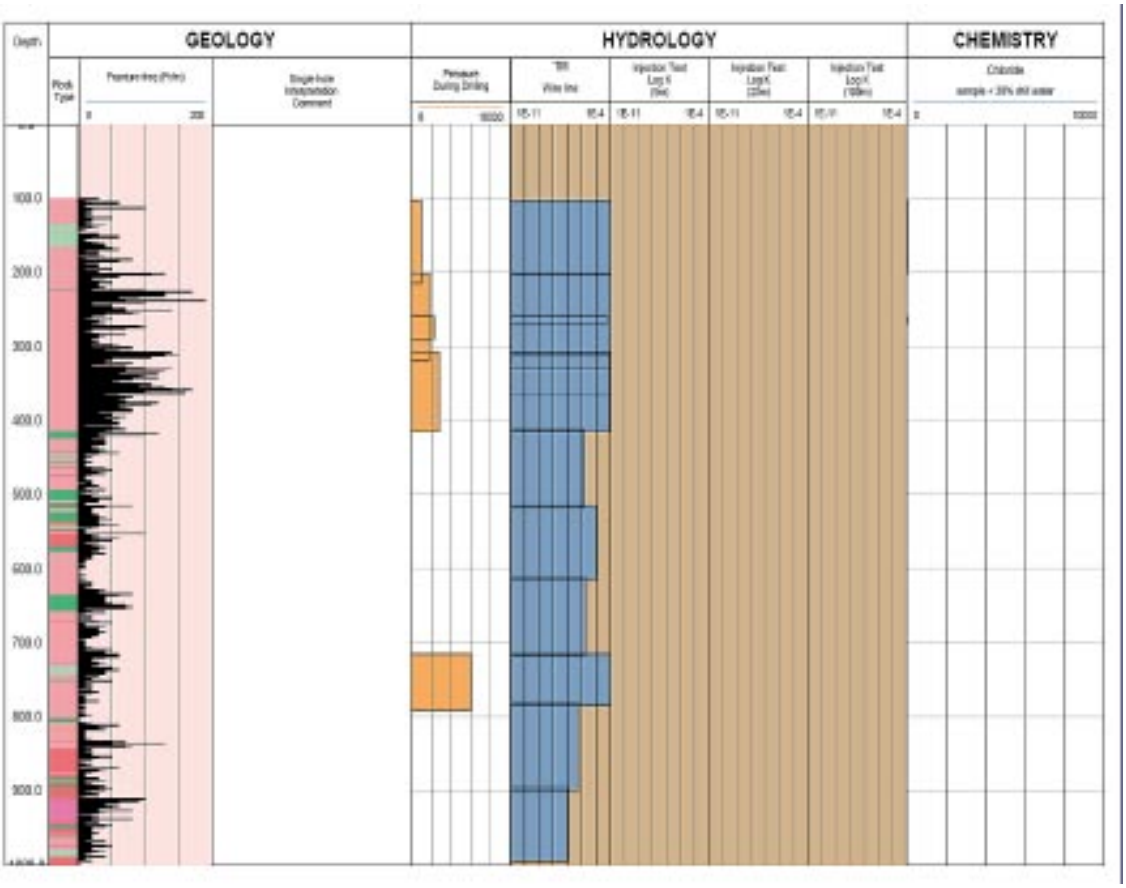

Figure 3-13. *Integrated geology, fracture frequency and hydraulic conductivity along borehole KLX06.*

The average fracture frequency for the borehole length is 0.5 fractures/m with increases between 200–260 m and 300–390 m characterised by intense alteration. This latter section, which shows a strong foliation in places and also some lamontite alteration, is interpreted to be the Mederhult deformation zone (ZSMEW002A). Around approx. 384 m a 5 cm clay horizon occurs. Beteen 629–658 m, 710–750 m and 919–940 m further increases in fracture frequency are observed.

Alteration sporadically occurs throughout the length of the borehole and sometimes these are associated with crush zones.

The hydraulic character of borehole KLX06 is indicated in Figure 3-13 and in more detail in Figure 3-14; no electric conductivity log is available for KLX06. The differential downhole flow measurements (Figure 3-14) reveal high transmissivities from 100–400 m depth (10^{6}–$10^{4.5}$ m^2s^{-1}) with the maximum at 200–300 m. From 400 m to the borehole bottom there is a sharp decrease in transmissivity to a average transmissivity of 10^{8}–10^{7} m^2s^{-1} with two maxima at 565 m ($10^{5.3}$ m^2s^{-1}) and 780 m (10^{6} m^2s^{-1}). Under 'natural conditions' (i.e. no pumping) the groundwater flow from 100–400 m is from the surrounding bedrock into the borehole with a maximum measured flow rate of 10^{5}–$10^{5.2}$ mL min^{-1}; from 400 m to the borehole bottom the natural flow is reversed with average rates of 10^{2}–10^{3} mL min^{-1} apart from the two high transmissive locations which record 10^{4} and 10^{5} mL min^{-1} respectively (Figure 3-14). With pumping the groundwater flow is reversed towards the borehole in the deeper borehole section. No hydraulic injection tests have been conducted.

These observations suggest that during open borehole conditions groundwater in the upper 400 m of the borehole in particular will preferentially flow into the borehole from the surrounding bedrock. With pumping, for example during sampling, formation groundwater samples may be expected quite rapidly. In contrast, along the rest of the borehole, groundwater will preferentially flow from the borehole to the surrounding bedrock; in this case this contaminant water will first have to be removed before 'representative' formation groundwaters can be accessed and sampled.

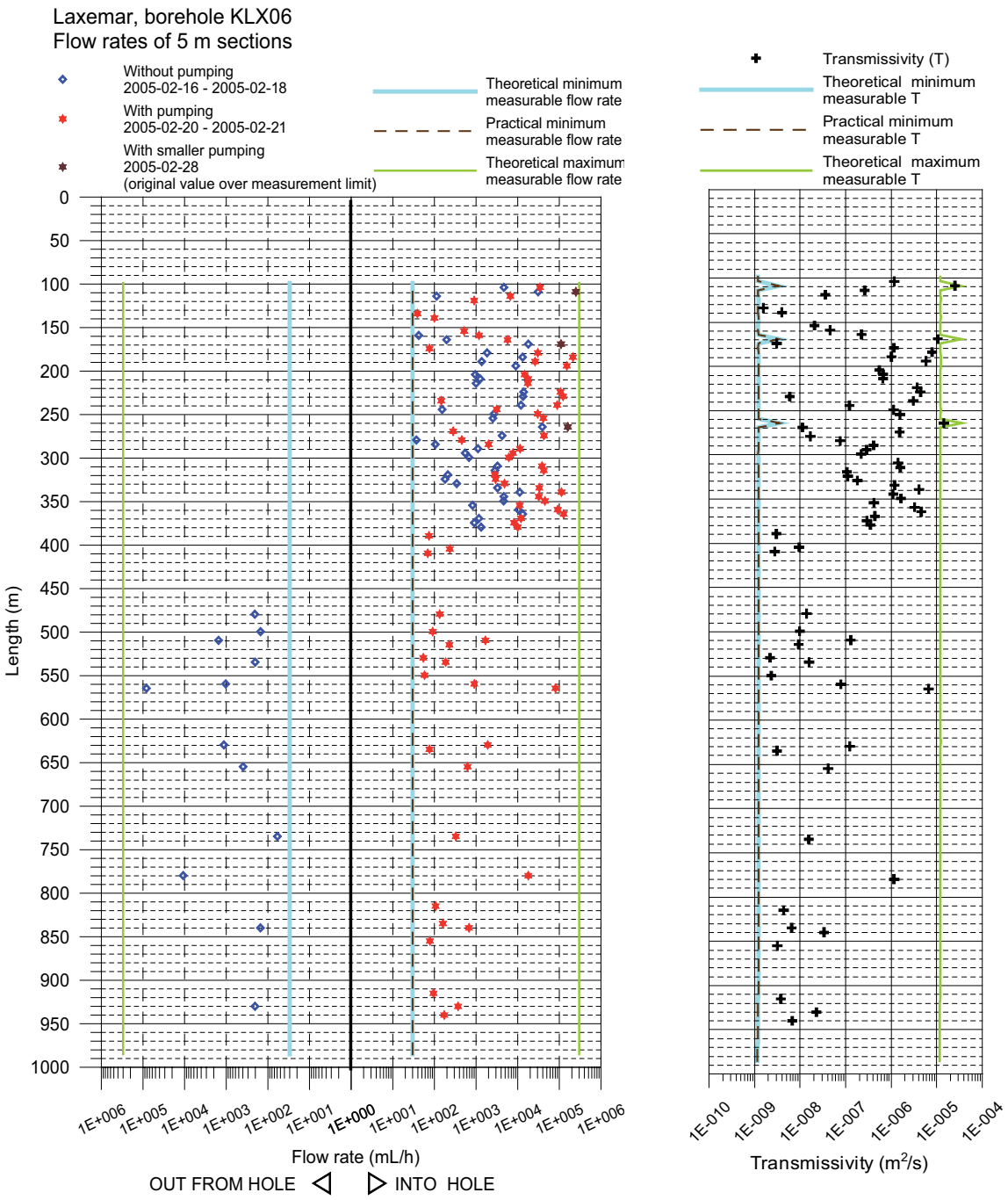

Figure 3-14. *Borehole KLX06: Groundwater flow rates and transmissivities based on differential flow measurements /Sokolnicki and Rouhiainen 2005/.*

3.5.2 Groundwater quality and representativeness

Groundwater samples were taken only from borehole sections during drilling of the cored borehole (Appendix 1). This was carried out on seven occasions using the wire-line method (8 samples, Class 3).

Cored borehole samples – during drilling

Level 102.00–202.26 m

Analyses are incomplete and restricted mainly to the major ions HCO_3, Cl, SO_4, Br and F; no isotopic data are available. The shallow groundwater (probably Na-HCO_3 in type) is dilute (25.4 mg/L Cl), assumed to be meteoric in origin and appears similar to other shallow groundwaters described above. High drilling water contamination is present (17.40%).

Representativeness: Unsuitable because of incomplete analytical data and > 1% drilling water. Limited qualitative use in supporting the presence of dilute groundwaters at this depth.

Level 265.50–268.50 m

Analyses are incomplete and restricted mainly to the major ions HCO_3, Cl, SO_4, Br and F; no isotopic data are available. The shallow groundwater (probably Na-HCO_3 in type) is dilute (15.70 mg/L Cl), assumed to be meteoric in origin and appears similar to other shallow groundwaters described above. Drilling water contamination is present (4.03%).

Representativeness: Unsuitable because of incomplete analytical data and > 1% drilling water. Limited qualitative use in supporting the presence of dilute groundwaters at this depth.

Level 200.50–310.20 m

No analytical data available; excessive contamination (47.50%).

Representativeness: Unsuitable.

Level 331.02–364.23 m

Analyses are incomplete and restricted mainly to the major ions HCO_3, Cl, SO_4, Br and F; no isotopic data are available. The shallow groundwater (probably Na-HCO_3 in type) is dilute (83.70 mg/L Cl), assumed to be meteoric in origin and appears similar to other shallow groundwaters described above. Excessive drilling water contamination is present (35.60%).

Representativeness: Unsuitable because of incomplete analytical data and > 1% drilling water. Limited qualitative use in supporting the presence of dilute groundwaters at this depth.

Level 307.50–415.49 m

No analytical data available; excessive contamination (66.50%).

Representativeness: Unsuitable.

Level 514.60–613.94 m

No analytical data available; excessive contamination (74.70%).

Representativeness: Unsuitable.

3.6 Percussion Borehole HLX10

Borehole HLX10 is drilled to a depth of 85 m and was used with the purpose of supplying flushing water to the drilling of cored borehole KLX04 (Figures 1-1 and 1.4). The sequence of borehole activities is presented in Appendix 1. Four groundwater samples (Class 3) were taken in sequence from the open borehole over a period of 1hr. 20 min. The groundwaters collected were at the initial pumping stage. Most data are restricted to the first sample described below.

Level 0–85.00 m

Analytical data are reasonably complete comprising stable isotopes and tritium and ^{14}C. The groundwater is Na-HCO_3 in type, meteoric, dilute (6.3 mg/L Cl), recent (pmC = 55.73; 7.2 TU) and has a present-day recharge isotopic signature ($\delta^{18}O$ = –10.9‰ SMOW, δD = –78.8‰ SMOW).

Representativitveness: Suitable but limited to Class 3 analysis. (Highlighted in orange in the database).

3.7 Percussion Borehole HLX14

Borehole HLX14 was drilled close to HLX13 to a depth of 115.90 m with the purpose of supplying flushing water to the drilling of cored boreholes KLX03 (Figures 1-1 and 1-4). The sequence of borehole activities is presented in Appendix 1. Four groundwater samples (Class 5) were taken, two in 2004-05-07 and a further two almost one month later in 2004-06-01. Most data are restricted to the first sample described below.

Level 0–115.90 m

Analytical are fairly complete. The groundwater is Na-HCO_3 in type, meteoric in origin, dilute (69.7 mg/L Cl), recent (pmC = 54.7; 3.8 TU) and has a present-day recharge isotopic signature ($\delta^{18}O$ = –11.2‰ SMOW, δD = –78.6‰ SMOW).

Representativeness: Suitable but lacks trace elements and special isotopes. (Highlighted in orange in the database).

3.8 Borehole HLX18

Borehole HLX18 was drilled close to HLX16, 17 and 19 to a depth of 181.20 m with the purpose of establishing the nature of the shallow groundwater in the area (Figures 1-1 and 1-4). The sequence of borehole activities is presented in Appendix 1. Sampling was restricted to two groundwaters (Class 1) taken in sequence directly following borehole completion.

Only electric conductivity values are available (127–821 mS/m).

Representativeness: Unsuitable because a lack of analytical data.

3.9 Borehole HLX20

Borehole HLX20 was drilled to a depth of 202.20 m with the purpose of supplying flushing water to the drilling of cored borehole KLX06 (Figures 1-1 and 1-4) and for establishing the nature of the shallow groundwater in the area. The sequence of borehole activities is presented in Appendix 1. Two groundwater samples (Class 5) were taken in sequence shortly following borehole completion. Most data are restricted to the first sample.

Level 0–202.20 m

Analytical data are fairly complete although isotope data are restricted to tritium and carbon; no stable isotope data are available. The analyses show the groundwater to be Na-HCO_3-(SO_4, Cl) in type, probably meteoric in origin, dilute (29.4 mg/L Cl) and not recent (pmC = 41.7; relative age ~ 7000 a; tritium at detection level = 0.8 TU).

Representativeness: Limited suitability because of the incomplete isotope analytical data; qualitative use in supporting the presence and nature of dilute, shallow derived groundwaters at Laxemar. (Highlighted in green in the database).

3.10 Borehole HLX22

Borehole HLX22 was drilled to a depth of 163.20 m with the purpose of establishing the nature of the shallow groundwater in the area (Figures 1-1 and 1-4). Grouting was necessary. The sequence of borehole activities is presented in Appendix 1. One groundwater sample (Class 3) was taken approx. 3 weeks following borehole completion and during the pumping flow rate measurements.

Analyses are incomplete and restricted mainly to the major ions HCO_3, Cl, SO_4, Br and F; no isotopic data are available. The groundwater is Na-HCO_3 in type, meteoric and dilute (< 30 mg/L Cl).

Representativeness: Unsuitable because of incomplete analytical data; potential qualitative use in supporting the presence and nature of dilute, shallow derived groundwaters at Laxemar.

3.11 Borehole HLX24

Borehole HLX24 was drilled to a depth of 175.20 m with the purpose of establishing the nature of the shallow groundwater in the area (Figures 1-1 and 1-4). Grouting was necessary. The sequence of borehole activities is presented in Appendix 1. One groundwater sample (Class 3) was taken one day following borehole completion and during pumping flow measurements.

Analyses are incomplete and restricted mainly to the major ions HCO_3, Cl, SO_4, Br and F; no isotopic data are available. The groundwater is Na-HCO_3 in type, meteoric and dilute (< 20 mg/L Cl).

Representativeness: Unsuitable because of incomplete analytical data; potential qualitative use in supporting the presence and nature of dilute, shallow derived groundwaters at Laxemar.

4 The Ävrö site

Prior to the Laxemar 1.2 data freeze, site characterisation at the Ävrö site has included the drilling of up to 8 percussion drillholes (HAV01–8) to depths of mostly 100 m, and two cored boreholes (KAV01 and KAV04A) of which KAV01 extends to 743.00 m and KAV04A to 1,004.00 m. Of these, percussion boreholes HAV09–14 (to depths of 142.20–220.5 m), together with cored boreholes KAV01 and KAV4A, are included in the Laxemar 1.2 data freeze. Figures 1-1 and 1-4 show the locations of the boreholes.

Representativeness checks have already been carried out for HAV01–08, KAV01 and KAV04A: these are highlighted in the Nordic Database Table described in the Simpevarp 1.2 hydrogeochemical evaluation report /Laaksoharju 2004, Appendix 1/. The remainder of sampling locations (some new, some resampled, some with additional measurements etc,) are evaluated below and judged to be suitable, of limited suitability or unsuitable.

4.1 Cored Borehole KAV01

Borehole KAV01 (Figures 1-1 and 1-4) was drilled at 89° (from the horizontal) to a depth of 743.6 m and cased to 11.74 m. The sequence of borehole activities is presented in Appendix 1, Table 1-2.

4.1.1 Geological and hydrogeological character

The geology of the KAV01 borehole is presented in Figure 4-1; only the interval 0–743 m was mapped. The lithology in KAV01 is dominated by the Ävrö granite cut by pegmatite, granite, fine-grained dioritoid and diorite-gabbro veins and dykes. The bedrock is almost devoid of structures except for a breccia at 450 m and very sparsely distributed thin sections with foliation. Generally, sealed fractures (interpreted) are not common but some sealed fracture networks and open fractures (interpreted) are more frequent at lower depths.

The 435–480 m interval might be regarded as a structurally weak section since a broad maximum in the frequency of open fractures (interpreted) coincide with peaks in crushed sections. These crushed sections contain sealed fracture networks and fractures, a breccia at 450 m, and also areas of strongest oxidation. Less significant weak sections may occur at approx. 660 m and 735 m in the borehole; these are also characterised by crushed sections, open fractures (interpreted), sealed fracture networks and oxidation.

With respect to fracture sets /Ehrenborg and Vladislav 2004/:

- In the 0–100 m interval two fracture sets can be observed: one SE-striking and moderately dipping (30° dip) and one SE-striking and strongly dipping set (75° dip).
- The 100–200 m interval contains a SSW-striking fracture set with moderate dip (50° dip). This fracture set is observed throughout the borehole to 700–742 m where it varies in strike from SSW in the 100–300 m interval to SW in the 300–700 m interval and then changes back somewhat to SW-WSW in the 700–742 m interval.
- An ENE striking fracture set with a steep dip (70° dip) occurs in the 200–400 m interval.
- At 400–500 m it is replaced with a similarly ENE striking but gently dipping (30° dip) fracture. This fracture set is not observed deeper down in KAV01.
- A WNW striking and gently dipping (35° dip) fracture set occurs in the 500–600 m interval.
- An almost vertical NW-striking fracture set (85° dip) occurs in the 500–600 m interval; this fracture set shows up as a weaker anomaly also at greater depth (600–700 m) in KAV01.

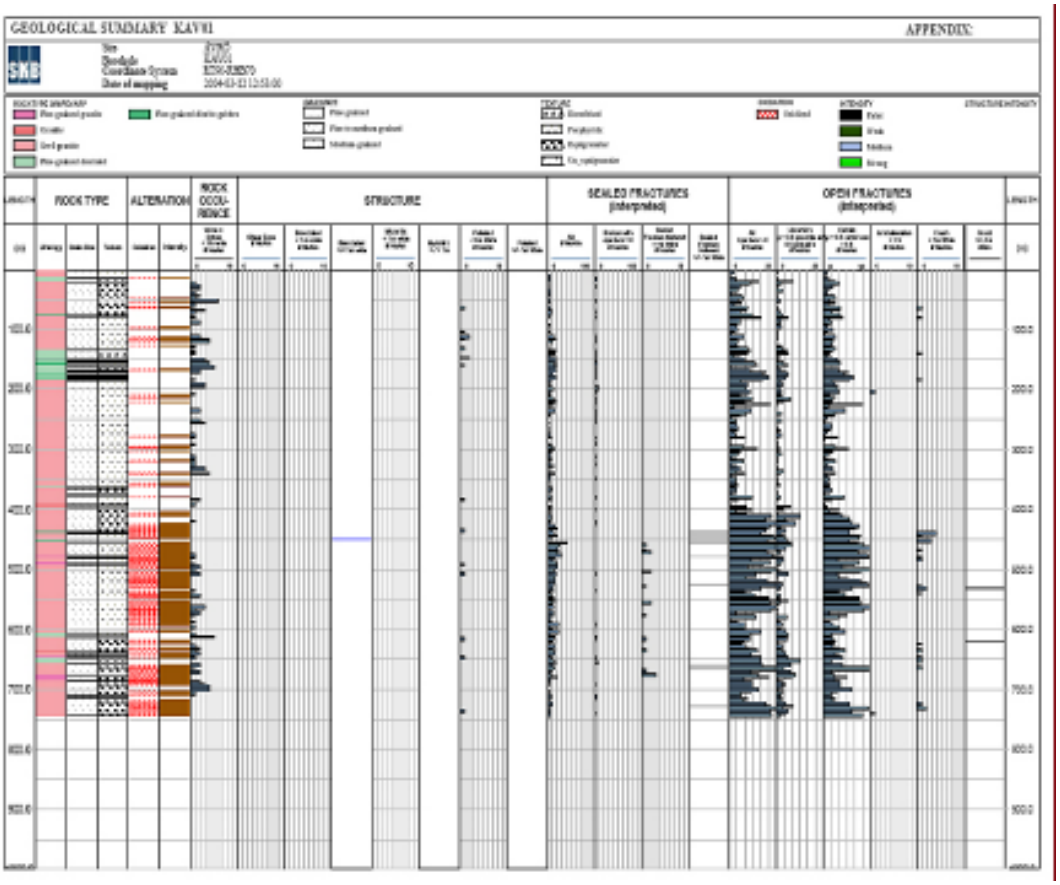

Figure 4-1. *Borehole KAV01: Lithology, structural interpretation and areas of alteration /Ehrenborg and Vladislav 2004/.*

The hydraulic character of borehole KAV01 is shown in Figures 4-2 and 4-3. The differential downhole flow measurements (Figure 4-2) indicate two borehole lengths of high transmissivity (10^{-9}–10^{-5} m^2s^{-1}) at approx. 70–250 m and 400–560 m with lower values (10^{-9}–10^{-7} m^2s^{-1}) at approx. 250–400 m and from 560–650 m; at greater depth no values are given but low transmissivities are expected (SKB P-04-213). Under 'natural' groundwater flow conditions (i.e. without pumping) flow into the borehole is expected in the upper 350 m and into the bedrock from the borehole in the lower 400–550 m. With pumping the groundwater flow is reversed towards the borehole in the deeper borehole section. No hydraulic injection tests have been conducted.

The downhole electric conductivity log (Figure 4-3) shows, during 'natural flow' conditions (i.e. without pumping), uniform and low electric conductivity values (0.03–0.04 Sm^{-1}) extending from 80 m to 550 m, whereupon a steady increase to 0.5 Sm^{-1} occurs at 650 m followed by a decrease to the borehole bottom (0.35 Sm^{-1}). With pumping the basic pattern is maintained although there is a consistent and significant increase in salinity along the borehole. This increase is more marked in the upper 400 m of the borehole.

These observations suggest that during open borehole conditions groundwater in the upper 400 m of the borehole will preferentially flow into the borehole from the surrounding bedrock. With pumping, for example during sampling, formation groundwater samples may be expected quite rapidly along this length. In contrast, along the deeper part of the borehole, groundwater will preferentially flow from the borehole to the surrounding bedrock; in this case this contaminant water will first have to be removed before 'representative' formation groundwaters can be accessed and sampled. This probably explains why pumping in Figure 4-3 shows a smaller increase in salinity at depth.

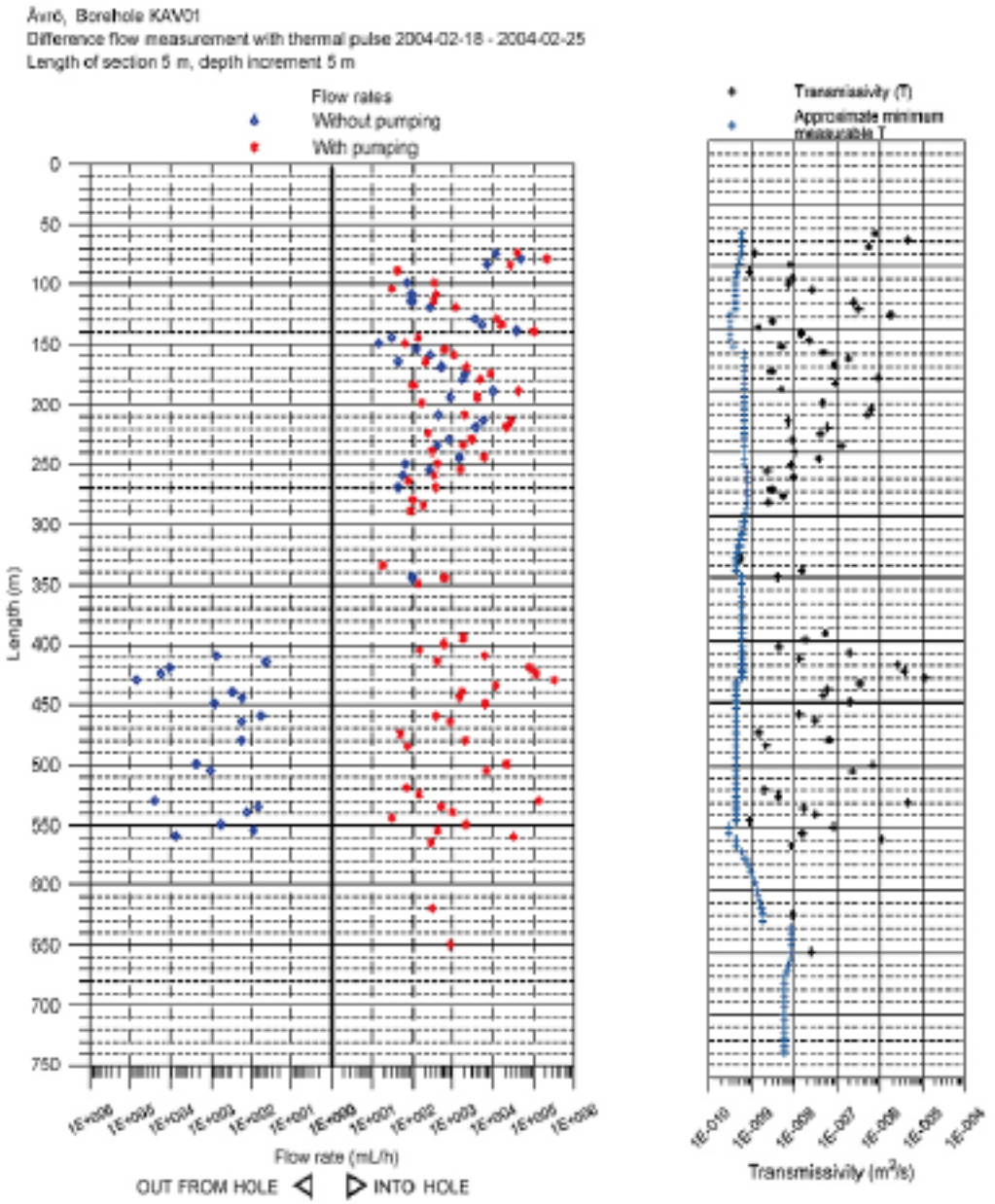

Figure 4-2. *Borehole KAV01: Induced and natural groundwater flow conditions (left) and transmissivity (right) measured during differential flow investigations /Rouhiainen and Pölännen 2004/.*

4.1.2 Groundwater quality and representativeness

Both cored and percussion boreholes were sampled. Following completion of KAV01 groundwater samples were only collected on one occasion, entailing open hole tube sampling (14 samples, Class 3).

Cored borehole samples – tube sampling

Tube sampling of KAV01 was carried out shortly after borehole completion and is documented in /Berg 2003/. It was noted that prior to sampling the borehole had been contaminated by a greasy substance. The tube array was lowered into the borehole on 2003-06-16 and retrieved the same day. A small leak developed at the bottom of the tube array (faulty valve) but the effect was minimised by speeding up the retrieval.

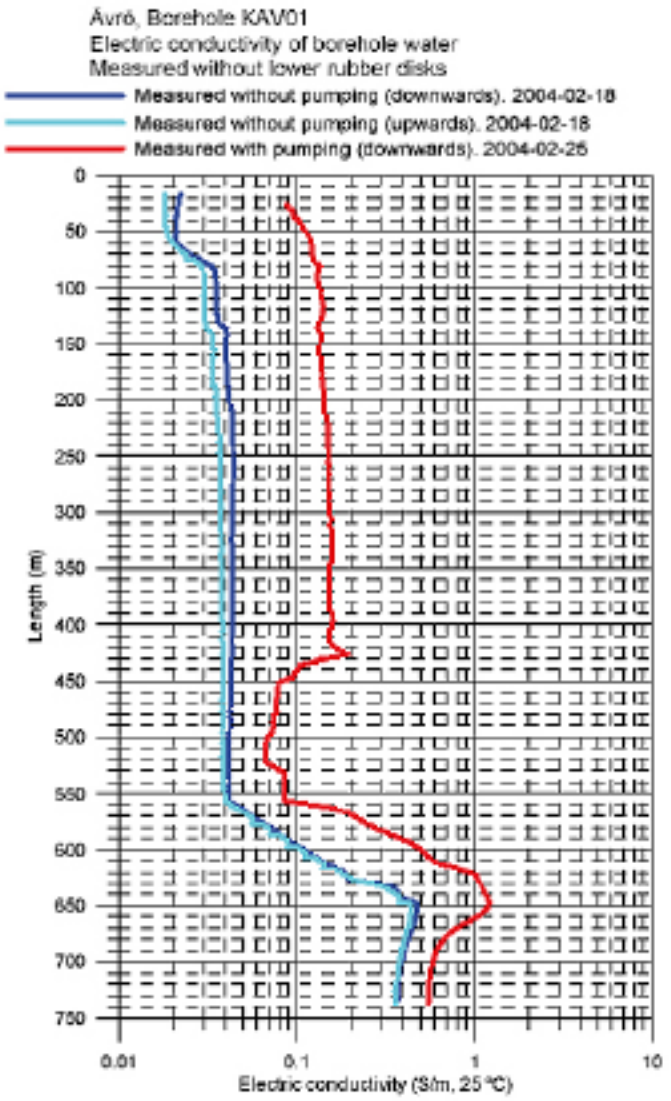

Figure 4-3. *Borehole KAV01: Electric conductivity log carried out during differential flow meter measurements /Rouhiainen and Pölännen 2004/.*

Figure 4-4 shows the distribution of residual drilling water and electric conductivity along borehole KAV01. The percentage of residual drilling water along the borehole was consistently below the 1 % acceptance threshold; somewhat higher values (~ 0.30–0.65%) occurred in the upper part of the borehole (150–350 m) and almost zero for the rest of the borehole. Towards depth there is a gradual increase in electric conductivity, i.e. ~ 35–60 mSm^{-1} to 650 m and then a sharper increase to around 75 mSm^{-1}. This hydrochemical sampling and measured electrical conductivity was carried out about 8 months before the downhole electrical log discussed above (Figure 4-3).

Comparing Figure 4-4 with the electric conductivity log described above (Figure 4-3) shows that the borehole is dominated by dilute groundwaters, probably originating from shallower depths in the borehole since there is no evidence of major drilling water contamination. The measured conductivity values are close on both occasions. However, measurements of electric conductivity with pumping do show that more saline water is present in the bedrock (up to 0.2 Sm^{-1} to 430 m) and this is supported by the lowering of electric conductivity at the high transmissive section from 400–560 m. This lowering indicates the removal of dilute water which has entered into the bedrock during open hole conditions, and the pumping has not been carried out long enough to remove this residual water and replace it by more representative saline formation groundwaters.

Representativeness: Unsuitable because of inadequate analytical data and also the sampled groundwaters are less saline than should be.

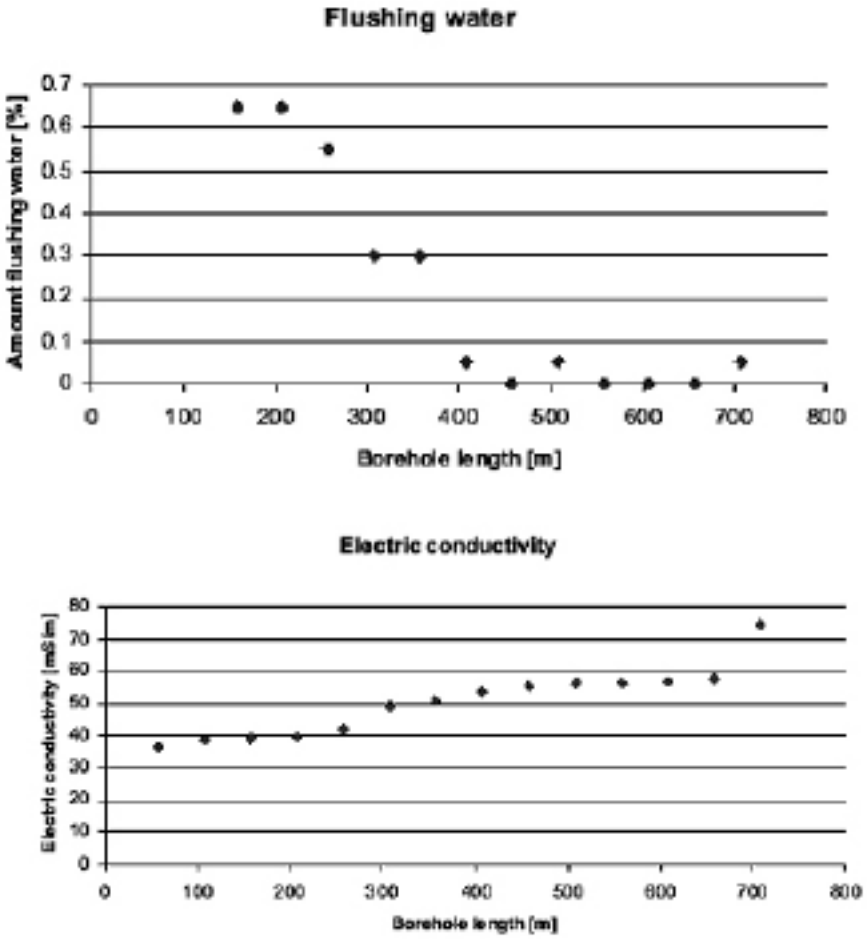

Figure 4-4. *Borehole KAV01: Distribution of residual drilling water (upper) and electric conductivity (lower) along the open borehole /Berg 2003/.*

4.2 Cored Borehole KAV04A

Borehole KAV04 (Figures 1-1 and 1-4) was drilled to a depth of 1,004.00 m; percussion drilling was initially carried out to 100.02 m followed by casing prior to the core drilling phase. The sequence of borehole activities is presented in Appendix 1, Table 1-2.

4.2.1 Geological and hydrogeological character

Figure 4-5 shows the main rock penetrated by drilling is the Ävrö granite. Fine-grained dioritoid, fine-grained granite and quartz monzodiorite also occur but less sytematically; fine-grained dioritoid is most prevailent at 400–430 m and at around 860–950 m. Fracture frequency increases markedly from 700 m to the borehole bottom (> 20 fractures/m) compared to shallower depths (< 15 fractures/m). This may indicate a major fracture zone between 700 m and the borehole bottom. The present understanding is that this fracture zone ZSMNE024A runs parallel with the Simpevarp-Ävrö shoreline (Figure 1-2). This zone is also documented in KAV01: 680–757 m, in KSH03A: 162–275 m and KSH01A: 540–631 m.

The hydraulic character of borehole KAV04A is shown in Figures 4-5 and 4-6. The differential downhole flow measurements (Figure 4-6) shows a relatively uniform range of high transmissivity ($10^{-8.5}$–10^{-6} m^2s^{-1}) extending for most of the borehole length down to 850 m, although less sporadic values are more characteristic from 450–850 m corresponding to the higher frequency of fractures (Figure 4-5). Two locations at approx. 260 m and 760 m show values up to 10^{-5} m^2s^{-1}, and two borehole sections appear to be fracture free and below detection (at 300–350 m and 410–480 m). From 900 m to the borehole bottom the rock fracture frequency is high (5–15 fractures/m) but the transmissivity is below detection (< 10^{-9} m^2s^{-1}).

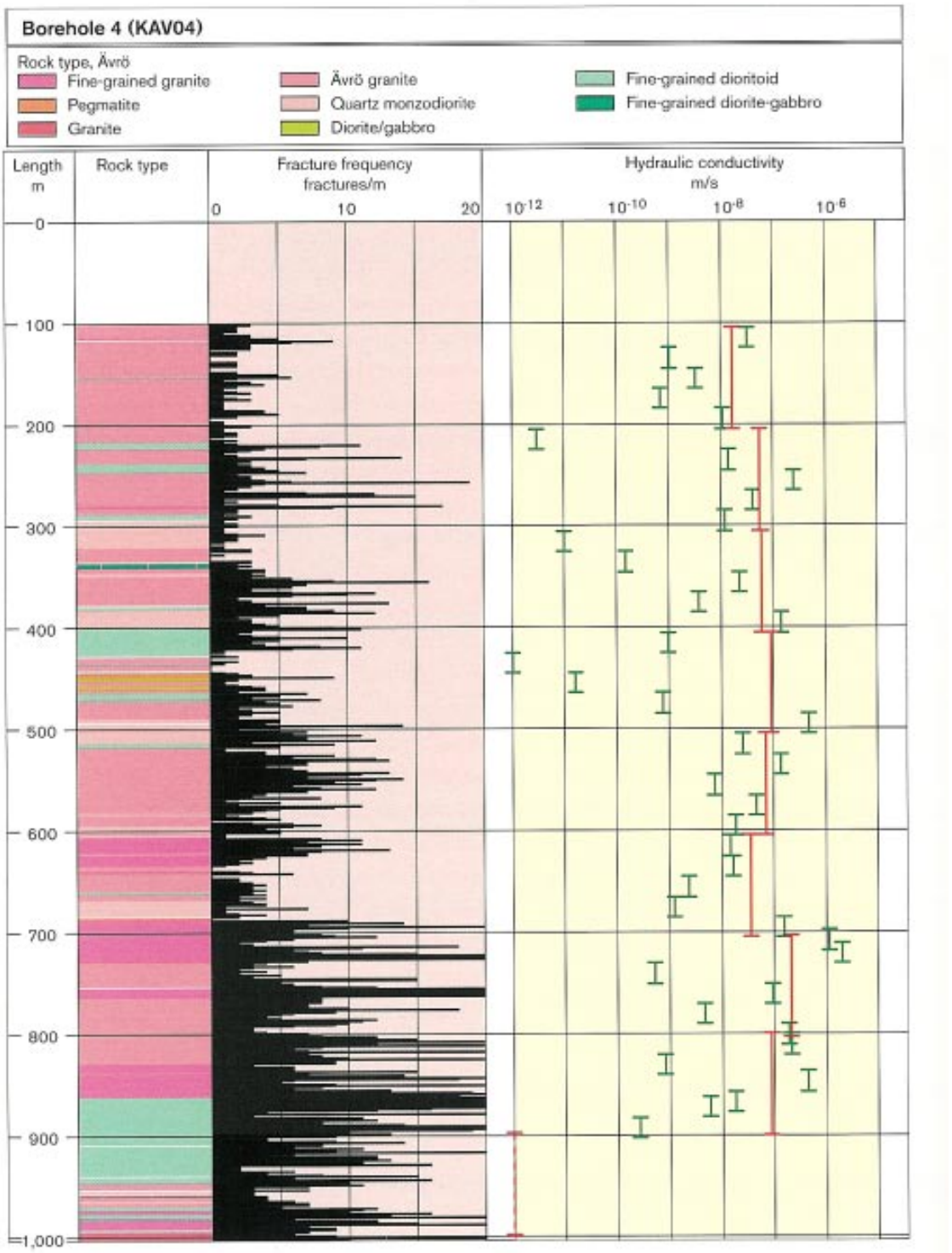

Figure 4-5. *Integrated geology, fracture frequency and hydraulic conductivity along borehole KAV04A.*

Unfortunately no 'undisturbed' groundwater flow conditions were measured in the borehole; as expected groundwater flow measured during pumping was from the bedrock into the borehole (Figure 4-6). Furthermore, no electric conductivity log was made during the differential flow measurements.

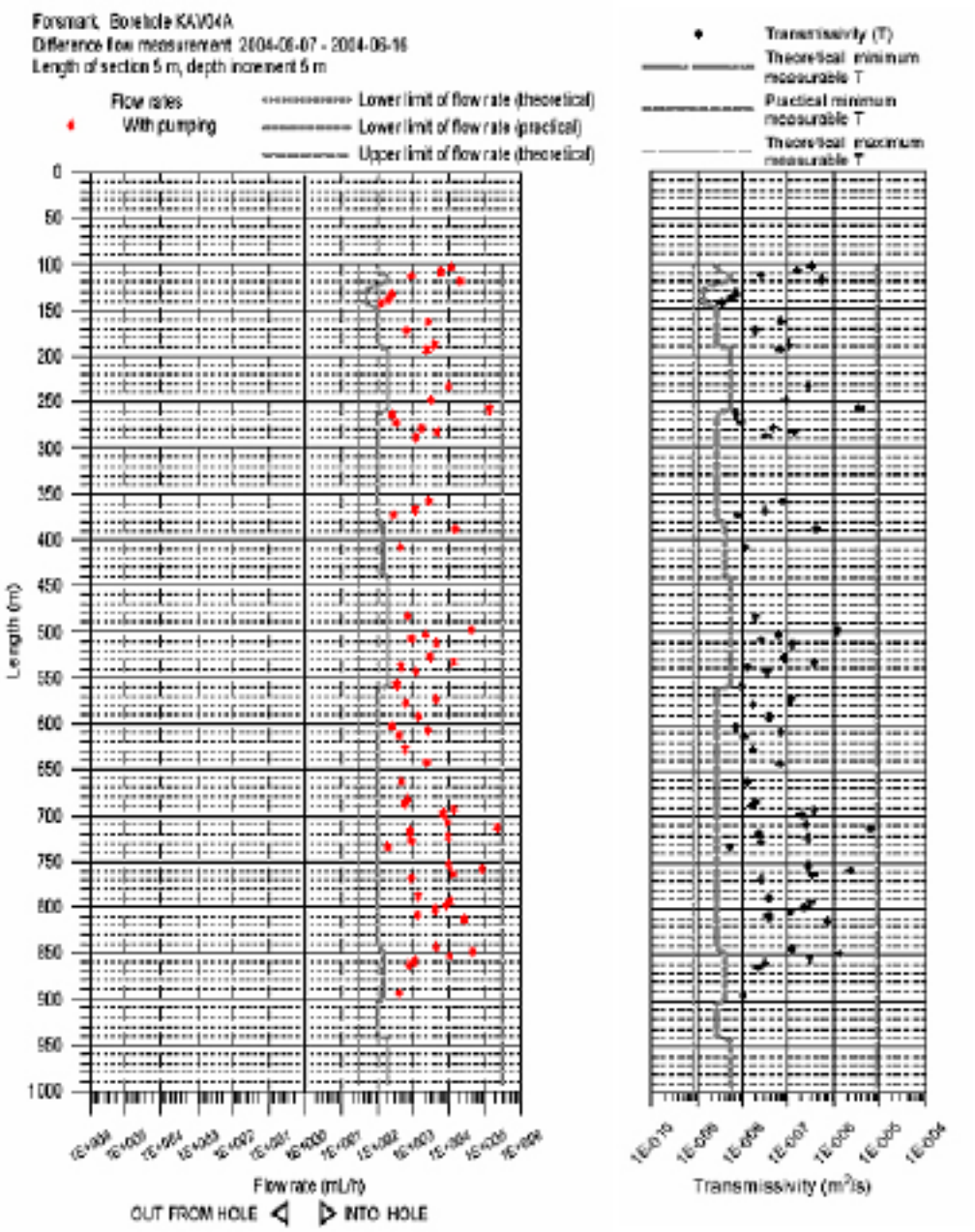

Figure 4-6. *BoreholeKAV04A: Induced groundwater flow conditions (left) and transmissivity (right) measured during differential flow investigations /Pölännen and Sokolnicki 2004/.*

4.2.2 Groundwater quality and representativeness

Groundwater samples from borehole sections were taken on several occasions (Appendix 2):

- During drilling of the percussion borehole on three occasions using a simple packer system (2 samples, Class 3; 1 sample, Class 5).
- During drilling of the cored borehole on 9 occasions using wire-line (4 samples, Class 3 and 5 samples, Class 1).
- Following borehole completion using the tube sampler (20 samples, Class 3).

Percussion borehole – during drilling

Level 47.60–50.60 m

Analyses are incomplete and restricted mainly to the major and minor ions; no isotopic data are available. The shallow groundwater is Na-HCO_3(SO_4 in type), dilute (< 33.4 mg/L Cl) and assumed to be meteoric in origin. The charge balance is > ± 5% (–10.95%) reflecting the dilute nature of the groundwater. There is no significant drilling water contamination (0.54%).

Representativeness: Unsuitable because of incomplete analytical data. Limited use in establishing the presence of dilute, shallow derived groundwaters at this depth.

Level 0–100.20 m

The first sample taken from this borehole length was unsuitable because of incomplete analyses (no isotopic data); it had also a slightly high charge balance (6.02%) but no evidence of drilling water contamination (0.13%). Because of these promising indications a decision was taken to resample the groundwater and upgrade to Class 5.

The resampled groundwater taken two days later has a fairly complete analysis and the charge balance is < ± 5%. It is similarly dilute as the previous groundwater (25.7 mg/L Cl) described above from level 47.50–50.60 m, and is clearly Na-HCO_3 in type with significant sulphate (76.03 mg/L). It is meteoric in origin, fairly recent or at least contains a modern component (2.8 TU; 46.25 pmC) and a stable isotopic signature suggesting relatively modern recharge ($\delta^{18}O$ = –10.9‰ SMOW, δD = –75.7‰ SMOW). Furthermore, there is no drilling water contamination (0.06%).

Representativeness: Suitable and useful in establishing the presence and nature of the dilute, shallow derived groundwaters at this depth. (Highlighted in orange in the database).

Cored borehole samples – during drilling

Level 245.85–293.05 m

Fairly complete analyses including isotopic data; charge balance < ± 5% but significant drilling water contamination (12.30%). The groundwater is Na-Ca-Cl(SO_4) in type, brackish (3,220 mg/L Cl), meteoric in origin, fairly old (1.10 TU; 29.7 pmC) and an isotopic signature indicating a cold recharge component ($\delta^{18}O$ = –13.1‰ SMOW, δD = –94.6‰ SMOW).

Representativeness: Limited suitability despite drilling water contamination (12.30%). Good qualitative use in establishing the presence and nature of brackish groundwaters at this depth. (Highlighted in green in the database).

Level 291.15–408.49 m

No analytical data; excessive drilling water content (85.20%).

Representativeness: Unsuitable.

Level 408.00–517.98 m

No analytical data apart from NO_2, N_2 and NH_4; excessive drilling water content (87.90%).

Representativeness: Unsuitable.

Level 516.15–603.42 m

Analyses are incomplete being restricted to some of the major ions HCO_3, Cl, SO_4, Br and F; no isotopic data are available. Groundwater is slightly brackish (1,750 mg/L Cl) with moderate HCO_3 (141 mg/L) and SO_4 (156 mg/L). Drilling water content is excessive (87.60%).

Representativeness: Unsuitable.

Level 513.15–602.90 m

No analytical data; excessive drilling water content (78.6%).

Representativeness: Unsuitable.

Level 710.90–730.08 m

Two samples were collected from this level one day apart. No analytical data; excessive drilling water content during the first sampling (94.2%) and also the second sampling (73.7%).

Representativeness: Unsuitable.

Level 729.00–805.52 m

No analytical data; excessive drilling water content (63.5%).

Representativeness: Unsuitable.

Level 729.00–819.01 m

Fairly complete analytical data but no carbon isotope data; considerable drilling water content (29.2 %). Water type is Na-Ca-Cl-SO_4, saline (8,240 mg/L Cl), old although a young component (1.8 TU) is present probably due to the drilling water contamination, and has a cold recharge signature ($\delta^{18}O$ = –12.3‰ SMOW, δD = –85.7‰ SMOW).

Representativeness: Unsuitable because of drilling water contamination (29.2%). Limited qualitative use in establishing the presence and nature of saline groundwaters at this depth.

Cored borehole samples – tube sampling

Tube sampling was carried out about one month after borehole completion and is documented by /Berg 2004/. The tube array was lowered into the borehole on 2004-06-08 and retrieved the same day. Complete water volumes were not obtained from the upper three tubes.

Figure 4-7 shows the distribution of residual drilling water and electric conductivity along borehole KAV04A. The percentage of residual drilling water along the borehole was consistently low but still above the 1% acceptance threshold level (1.45–5.04%) within the first 400 m. From 500 m to the borehole bottom, the residual drilling water component increased markedly from (9.52–28.10%), the highest value from around 600 m. This is reflected by the electric conductivity log which shows brackish groundwater values (500–750 mSm^{-1}) down to 400 m, followed by saline groundwaters (1,250–3,100 mSm^{-1}) with a maximum salinity (12,000 mg/L Cl) at approx. 850 m. Na, Ca and SO_4 also follow this general trend, whilst HCO_3, as expected, shows the reverse trend with depth. The deepest sample shows a slightly lower mineralisation (e.g. 10,000 mg/L Cl). The isotopic data show low tritium values with most < 2TU (one of 2.5 TU; detection limit of < 0.8 TU) and $\delta^{18}O$ indicates a significant cold recharge component (–13.0 to –11.7‰ SMOW). In all samples the relative charge balance is within the ± 5% acceptance threshold.

As indicated above, unfortunately no electric conductivity log was made during the differential flow measurements to compare with the hydrochemical logging shown in Figure 4-7. Nevertheless, the trends observed indicate that shallow-derived brackish groundwaters are entering into the upper 400 m of the borehole where the transmissivity is high and also at greater depth between 700–850 m. This is reflected by respective decreases in the residual drilling water contents and, as would be expected, the process of removing the drilling water is more efficient in the upper part of the borehole. The decrease or dilution of drilling water around 700–850 m may also reflect some input of saline groundwater at greater depth, which peaks at 12,000 mg/L Cl close to 900 m.

In conclusion, the borehole groundwaters represent a mixture of different origins; a) shallow-derived dilute to brackish groundwaters, b) deep saline groundwaters, and c) residual drilling water. Type (a) with subordinate amounts of Type (b) dominate the upper 400 m and Types (b) and (c) dominating from 400 m to the borehole bottom.

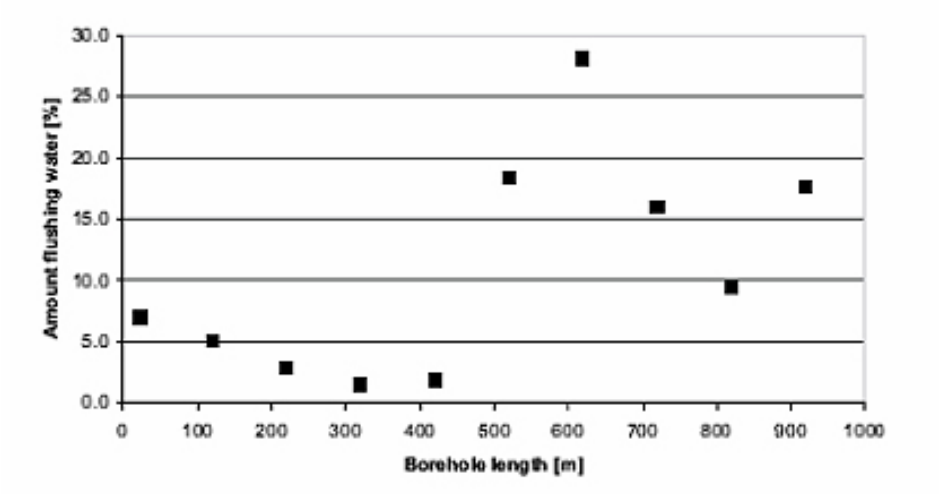

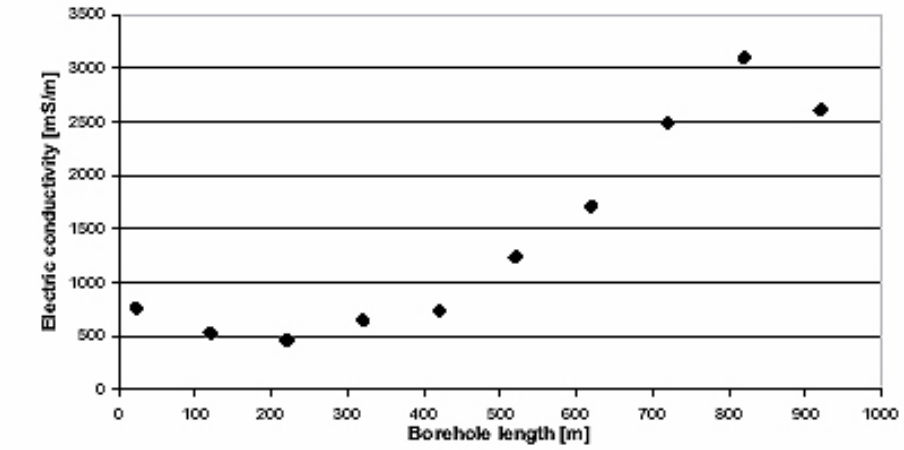

Figure 4-7. *Borehole KAV04A: Distribution of residual drilling water (upper) and electric conductivity (lower) along the open borehole /Berg 2004/.*

Representativeness: Unsuitable because of excess drilling water contamination (especially from 500 m to the borehole bottom) and the overall mixing of groundwaters from different origins.

4.3 Percussion Borehole HAV09

Borehole HAV09 was drilled at an angle of 68° (to the horizontal) to a depth of 200.20 m (cased to 14.9 m) with the purpose of supplying flushing water to the drilling of cored borehole KAV04 (Figure 1-4), and also for characterising the nature of the shallow groundwater in the area. The former purpose, however, was not successful because of an inadequate water yield. The sequence of borehole activities is presented in Table Appendix 1. One groundwater sample (Class 3) was taken from the open borehole directly after borehole completion; no more samples were collected.

Level 15.00–130.90 m

Analyses are incomplete being restricted to the major ions Na, Ca, K, Mg, HCO_3, Cl, SO_4, Br and F and the minor ions Fe, Mn, Li and Sr; no isotopic data are available. The groundwater is Na-Ca-Cl-(SO_4) in type and moderately brackish (2,561 mg/L Cl).

Representativeness: Unsuitable because of incomplete analytical data. Limited qualitative use in supporting the presence of brackish groundwaters at this depth.

4.4 Percussion Borehole HAV10

Borehole HAV10 was drilled at an angle of 68.5° (to the horizontal) to a depth of 100 m (cased to 11.9 m) with the purpose of supplying flushing water to the drilling of cored borehole KAV04 (Figure 1-4), and also for characterising the nature of the shallow groundwater in the area. The sequence of borehole activities is presented in Appendix 1. Two groundwater samples (Class 3) were taken from just below the casing to the borehole bottom directly after borehole completion; no more samples were collected.

Level 12.00–22.60 m

Analyses are incomplete being restricted to the major ions HCO_3, Cl, SO_4, Br and F; no isotopic data are available. The groundwater is Na- HCO_3-(SO_4), in type, dilute (19.1 mg/L Cl) and probably meteoric in origin.

Level 12.00–100.00 m

Analyses are incomplete being restricted to the major ions HCO_3, Cl, SO_4, Br and F; no isotopic data are available. The groundwater is Na- HCO_3-(SO_4) in type, dilute (23.4 mg/L Cl) and probably meteoric in origin.

Representativeness: Unsuitable because of incomplete analytical data. Limited qualitative use in supporting the presence of brackish groundwaters at this depth.

4.5 Borehole HAV11

Borehole HAV11 was drilled near the coast to a depth of 220.50 m (cased to 2.46 m) with the purpose of characterising the nature of the shallow groundwater in the area (Figure 1-4). The sequence of borehole activities is presented in Appendix 1. Two groundwater samples (Class 3) were taken on two occasions (1 day apart) from just below the casing to the borehole bottom, approx. one month after borehole completion; no more samples were collected.

Level 2.46–220.50 m (1st day)

Analyses are incomplete being restricted to some of the major ions Na, K, Ca and Mg (excluding HCO_3, Cl and SO_4) and minor ions Si, Fe, Mn, Li and Sr; no isotopic data are available. High Na (1,860 mg/L) and Ca (1,480 mg/L) suggests a brackish groundwater, possibly more saline than HAV09.

Representativeness: Unsuitable because of incomplete analytical data.

Level 2.46–220.50 m (2nd day)

The analytical data available are similar to the earlier sampled groundwater. However, there is a marked decrease in Na (to 525 mg/L) and Ca (to 270 mg/L) which suggests a change to a much more dilute groundwater type.

Representativeness: Unsuitable because of incomplete analytical data. Limited qualitative use in showing groundwater compositional changes over a short time period (1 day).

4.6 Borehole HAV12

Borehole HAV12 was drilled near the coast to a depth of 157.80 m (cased to 11.35 m) with the purpose of characterising the nature of the shallow groundwater in the area (Figure 1-4). The sequence of borehole activities is presented in Appendix 1. Two groundwater samples (Class 3) were taken on two occasions (2 days apart) from just below the casing to the borehole bottom, approx. six weeks after borehole completion; no more samples were collected.

Level 11.35–157.00 m

No analytical data available.

Representativeness: Unsuitable.

4.7 Borehole HAV13

Borehole HAV13 was drilled near the coast to a depth of 142.20 m (cased to 3.30 m) with the purpose of characterising the nature of the shallow groundwater in the area (Figure 1-4). The sequence of borehole activities is presented in Appendix 1. Two groundwater samples (Class 3) were taken on two occasions (1 day apart) from just below the casing to the borehole bottom, approx. nine weeks after borehole completion; no more samples were collected.

Level 3.31–142.20 m (1st day)

Analyses are incomplete being restricted to some of the major ions Na, K, Ca and Mg (excluding HCO_3, Cl and SO_4) and minor ions Si, Fe, Mn, Li and Sr; no isotopic data are available. Low Na (263 mg/L) and Ca (48.8 mg/L) suggest a dilute groundwater.

Representativeness: Unsuitable because of incomplete analytical data.

Level 3.31–142.20 m (2nd day)

Analyses are incomplete being restricted to some of the major ions Na, K, Ca and Mg (excluding HCO_3, Cl and SO_4) and minor ions Si, Fe, Mn, Li and Sr; no isotopic data are available. Higher Na (1,590 mg/L) and Ca (723 mg/L) suggests a more brackish groundwater.

Representativeness: Unsuitable because of incomplete analytical data. Limited qualitative use in showing groundwater compositional changes over a short time period (1 day).

4.8 Borehole HAV14

Borehole HAV14 was drilled inland to a depth of 182.40 m (cased to 12.85 m) with the purpose of characterising the nature of the shallow groundwater in the area (Figure 1-4). The sequence of borehole activities is presented in Appendix 1. Two groundwater samples (Class 3) were taken on two occasions (1 day apart) from just below the casing to the borehole bottom, approx. six weeks after borehole completion; no more samples were collected.

Level 12.85–182.20 m (1st day)

Analyses are incomplete being restricted to some of the major ions Na, K, Ca and Mg (excluding HCO_3, Cl and SO_4) and minor ions Si, Fe, Mn, Li and Sr; no isotopic data are available. Low Na (46.5 mg/L) and Ca (45.7 mg/L) suggests a dilute groundwater.

Representativeness: Unsuitable because of incomplete analytical data.

Level 12.85–182.20 m (2nd day)

Similar anaytical data and groundwater composition to the first sampling.

Representativeness: Unsuitable because of incomplete analytical data.

5 The Simpevarp Site

Since the Simpevarp 1.2 data freeze, the present Laxemar 1.2 data freeze includes data from four percussion drillholes (HSH02–05) to depths varying from 200–236.20 m, and additonal data from cored boreholes (KSH01A, KSH02A and KSH03A) of which KSH01A extends to 1,003.00 m, KSH02 to 1,001.11 m and KSH03A to 1,000.70 m. Figures 1-1 and 1-4 show the locations of the boreholes at the Simpevarp site.

The geological and hydrogeological setting and the representativeness checks for KSH01A, KSH02A and KSH03A carried out for the earlier Simpevarp 1.2 data freeze are presented in /Laaksoharju 2004/ and Appendix 1 to that report, and will not be repeated here. The present data (some new, some resampled, some with additional measurements etc) are evaluated below and judged to be suitable, of limited suitability or unsuitable.

5.1 Cored Borehole KSH01A

Borehole KSH01A (Figures 1-1 and 14) was drilled at an angle of 80.6° (to the horizontal) to a depth of 1,003.00 m; percussion drilling was initially carried out to 100.24 m followed by casing prior to the core drilling phase.

The data included in the Laxemar 1.2 data freeze have already been evaluated in /Laaksoharju 2004, Appendix 1/.

5.2 Cored Borehole KSH02A

Borehole KSH02A (Figures 1-1 and 1-4) was drilled at an angle of 85.4° (to the horizontal) to a depth of 1,000.70 m; percussion drilling was initially carried out to 65.85 m followed by casing to 80 m prior to the core drilling phase.

The data included in the Laxemar 1.2 data freeze have already been evaluated in /Laaksoharju 2004, Appendix 1/.

5.3 Cored Borehole KSH03A

Borehole KSH03A (Figures 1-1 and 1-4) was drilled at an angle of 57° (to the horizontal) to a depth of 1,001.11 m; percussion drilling was initially carried out to 100.60 m followed by casing at this depth prior to the core drilling phase.

The data included in the Laxemar 1.2 data freeze have already been evaluated in /Laaksoharju 2004, Appendix 1/.

5.4 Percussion Borehole HSH02

Borehole HSH02 was drilled at an angle of 80° (to the horizontal) to a depth of 200 m (cased to 12 m) with the purpose of supplying flushing water to the drilling of cored borehole KSH02 (Figures 1-1 and 1-4), and also for establishing the nature of the shallow groundwater in the area. The sequence of borehole activities is presented in Appendix 1. Five groundwater samples (4 of Class 3 and one unclassified) were taken from the open borehole some 6 months after borehole completion. An additional three samples (Class 3) were taken after a further 6 months.

Level 0–200.00 m

These samples have been evaluated earlier for the Simpevarp 1.2 data freeze. The analytical data are fairly complete and the final sampled groundwater has been selected as being representative; relative charge balance is within the ± 5% acceptance threshold. The groundwater is Na-HCO_3, dilute (22.6 mg/L Cl), meteoric in origin and recent (11 TU; 67.28 pmC) and has a modern recharge isotopic signature ($\delta^{18}O$ = –10.7‰ SMOW, δD = –76.3‰ SMOW).

Representativeness: Limited suitability because of Class 3 status; data are incomplete. (Highlighted in green in the database).

5.5 Percussion Borehole HSH03

Borehole HSH03 was drilled at an angle of 80° (to the horizontal) to a depth of 219 m (cased to 12 m) with the purpose of supplying flushing water to the drilling of cored borehole KHS01A (Figures 1-1 and 1-4) and also for establishing the nature of the shallow groundwater in the area. The sequence of borehole activities is presented in Appendix 1. Five groundwater samples (Class 2) and four samples (Class 3) were taken after borehole completion.

Level 0–201.00/0–200.00 m

Sampling at this level has been carried out on four different occasions (Appendix 1) over a period from 2002-08 -21 to 2004-02-03.

2002-08-21: The first groundwater section was sampled six weeks after borehole completion. The analytical data are fairly complete (absence of carbon isotopes) and the relative charge balance is within the ± 5% acceptance threshold. The groundwater is Na-HCO_3, dilute (53.1 mg/L Cl), meteoric in origin and recent (4.7 TU) and has a modern recharge isotopic signature ($\delta^{18}O$ = –10.6‰ SMOW, δD = –78.0‰ SMOW).

2002-09-05: The second groundwater, after a 15 day interval, shows a small increase in salinity; this leaves the uncertainty that further sampling/pumping may result in further increases.

2003-09-16: The third sampling (one Class 3), after about 6 months, shows a greater increase in salinity to 462.9 mg/L Cl.

2004-02-03: The fourth sampling (One Class 3), after a 4–5 months, shows an even greater salinity content (949 mg/L Cl).

Representativeness: Less suitable. Systematic increase in salinity with time, combined with a 200 m deep borehole representing mixed groundwaters of different origin, introduces uncertainty. However, the earliest most dilute samples are considered to represent the most transmissive borehole section, typifying near-surface groundwater types (Highlighted in green in the database).

Level 0–103.00 m

One Class 3 sample was collected. Fairly complete analytical data, no carbon isotopes. The groundwater is Na-HCO_3, dilute (55.1 mg/L Cl), meteoric in origin and recent (10 TU) and has a modern recharge isotopic signature ($\delta^{18}O$ = –10.7‰ SMOW, δD = –76.1‰ SMOW).

Representativeness: Limited suitability because of Class 3 status; data are incomplete. (Highlighted in green in the database).

Level 0–150.00 m

Four Class 2 samples were collected in sequence during one day (2003-03-04). Restricted to HCO_3 and Cl, the groundwaters show a fluctuation in salinity (721.6–1,018.6 mg/L Cl). No further data are available.

Representativeness: Unsuitable.

5.6 Percussion Borehole HSH04

Borehole HSH04 (Figures 1-1 and 1-4) was drilled at an angle of 80° (to the horizontal) to a depth of 236.20 m (cased to 12 m) with the purpose of establishing the nature of the shallow groundwater in the area. Two samples (Class 3) were taken from the same level some three months after borehole completion.

Level 3.01–236.00 m

2004-04-07: The analytical data are restricted to the major ions Na, K, Ca, Mg and SO_4 and major minor ions Mn. Li and Sr; no isotopic data are available.

2004-07-20: As the previous.

Representativeness: Unsuitable, incomplete data.

5.7 Percussion Borehole HSH05

Borehole HSH05 (Figure 1-2) was drilled at an angle of 80° (to the horizontal) to a depth of 200.20 m (cased to 12 m) with the purpose of establishing the nature of the shallow groundwater in the area. Two samples (Class 3) were taken from the same level some three months after borehole completion.

Level 3.34–200.20 m

2004-07-17: The analytical data are restricted to the major ions Na, K, Ca, Mg and SO_4 and major minor ions Mn. Li and Sr; no isotopic data are available.

2004-07-18: As the previous.

Representativeness: Unsuitable, incomplete data.

6 Summary of the evaluation

The representativeness check of the borehole groundwater samples from the Laxemar 1.2 data freeze revealed that there is only a very limited set of groundwater data suitable to be quality checked, and only very few of these available data are considered representative or suitable (highlighted in orange in SICADA), or of limited suitability but useable with caution (highlighted in green in SICADA). Most have been deemed as unsuitable. Of course data judged of limited suitability may still provide valuable information, for example: a) the use of some of the major ion analyses in hydrochemical plots, and b) observed compositional changes with time which may reflect groundwater mixing, either artificially induced by pumping and/or sampling or due to natural flow.

The absence of suitable data is attributed mainly to the very high portions of drilling fluid in many or the analysed groundwaters sampled during drilling, during pump and injection tests, and during subsequent tube sampling. Furthermore, there are few complete sets of data comprising major elements, stable deuterium and ^{18}O, and tritium, which are the minimum requirement to evaluate the representativeness of the groundwaters in terms of, for example, charge balance and the mixing of drilling water and near-surface groundwaters. However, groundwaters that have major ions, TOC, D and ^{18}O, tritium and ^{14}C are rated as suitable if the charge balances are < ± 5% and the drilling fluid < 1%. Table 6-1 refers to the Laxemar and Ävrö sites where the above criteria have been applied to establish the number of groundwater samples that fall into these categories.

In conclusion, only seven groundwater samples from the Laxemar and Ävrö sites are considered suitable or of limited suitability use, and six of these are all from the upper part of the bedrock (0–218 m) and of dilute groundwater character. These shallow groundwaters mainly represent a recent meteoric/older meteoric (tritium free) origin, except for KLX03: 103–218 m which is tritium free and shows mixing with a cold-climate recharge-water component. One sample included is from greater depth (KAV04A: 245–293 m) and is of brackish character although it contains a substantial drilling water component (12.3%). It is suitable for major ion chemistry use but, for example, is not recommended for tritium use since the sample has been influenced by the drilling water.

All tube samples from KLX03 and KLX04 are lacking stable isotope data and tritium which means that even those young dilute groundwaters with a relatively low percentage of drilling fluid (< 10 %), can consist of modern meteoric, older meteoric or glacial water of unknown proportions.

Groundwaters with higher chloride contents are detected at depth in all the boreholes but these samples are characterised by: a) excessive amounts of drilling water, or b) an incomplete set of analyses, or c) mixing of different groundwater types along the borehole lengths (e.g. KAV04A).

Table 6-1. Rated groundwater samples from the Laxemar and Ävrö sites.

Water sample (metres depth)	Suitable	Limited suitability	Comment
HLX10: 0–85	Yes		Class 3
HLX14: 0–115.90	Yes		Class 5
HLX20: 0–200.20		Yes	Class 5 No D and ^{18}O available
KLX03: 103–218	Yes		Class 3
KLX04: 103–213		Yes	Class 3 Drilling fluid 7.76%
KAV04: 0–100	Yes		Class 5
KAV04: 245.85–295.05		Yes	Class 3 Drilling fluid 12.37%

In conclusion the tube samples from all four sampled boreholes (KAV01, KAV04A, KLX03 and KLX04) are judged as unsuitable based on the above reasons. In addition, the KLX03 and KLX04 tube samples, based on information from the differential flow measurements, show significant differences in the behaviour of the electrical conductivity profiles versus depth. The difference in values resulting from pumping compared to without pumping indicate generally higher electrical conductivity during pumping. The tube samples, which are collected under natural flow conditions (i.e. equivalent to without pumping) in the open borehole, therefore do not reflect the maximum salinity recorded during pumping. Instead, the tube samples indicate mixing of groundwaters of different origin, especially mixing with near-surface groundwaters and, in many cases, extremely high portions of drilling water. It is therefore strongly recommended not to use the tube samples in the modelling exercises as they probably reflect a perturbed groundwater system and may give, for example, erroneous indications of near-surface groundwaters at great depth that do not reflect initial, undisturbed conditions.

The general uncertainty surrounding tube sampling has also been extended to borehole KLX02. Tube hydrochemical data from KLX02 have been consistently used over many years in several of the evaluation and modelling exercises. Even though there is a reasonably close correlation with some of the data from packed-off borehole sections, and a general absence of drilling water, there are discrepancies (e.g. tritium; sulphate) which can be attributed to open hole mixing. Consequently, selected tube hydrochemical data have been highlighted green in the Laxemar 1.2 data freeze table indicating limited suitability but to be used with caution. For example, in the majority of the ion-ion plots and for much of the water/rock geochemical equilibrium modelling these data have been excluded altogether.

7 Additional input

Included in the Laxemar v. 1.2 Hydrogeochemical Site Characterisation evaluation and already discussed in Chapter 2 are data representing surface and near-surface waters collected from the Baltic Sea, Lakes, Streams and also from shallow Soil Pipes installed the overburden. These data, because of the complex nature of the sampling locations (i.e. subject to annual and seasonal trends, potential recharge/discharge areas etc) have been evaluated based only on charge balance (Lake and Stream waters), charge balance and observed contamination during sampling (Soil Pipe waters) and charge balance and salinity (Baltic Sea waters). Some precipitation values are also included but have not undergone any representativeness check because of unpredictable annual and seasonal trends and possible evaporation.

In addition to the Ävrö and Simpevarp sites, evaluation of borehole groundwater data from the Laxemar subarea entails comparison with other geographically located sites in its near-vicinity, i.e. Äspö, Oskarshamn and also other Fennoscandian sites such as Forsmark and Olkiluoto. Some of these data have already undergone a quantitative representativeness judgement /e.g. Smellie and Laaksoharju 1992, Laaksoharju et al. 1995, Pitkänen et al. 1999, 2004, Laaksoharju 2004/ whilst the rest have been evaluated more qualitatively. Suggested groundwater values have been highlighted in the Nordic Groundwater Table available in ProjectPlace.

8 Hydrogeochemical evaluation

Since there are only few data available for the Laxemar 1.2 evaluation, updating of the Simpevarp 1.2 major ion and isotope plots which form the basis of interpretation will not be reproduced in full. Rather, selected plots which serve to best illustrate the evolutionary trends of the groundwaters have been selected, together with specific advances in interpretation of some of the isotope systematics. In addition, Chapter 9 deals with the issue of geosphere/biosphere interaction and Chapter 14 introduces some consequences of the presence of saline brines in the hydrochemical evaluation.

8.1 Updated major ion and isotope plots for the Simpevarp area

8.1.1 Chloride depth trends

The Laxemar subarea data show mostly dilute groundwaters (< 2,000 mg/L Cl) extending to at least 275 m in KLXO1 and to around 500–600 m for boreholes KLX03 and KLX04 situated in the inner part of the Laxemar subarea (Figures 1-1 and 1-4). In borehole KLX02 dilute groundwater was detected down to 800 m before a rapid increase in salinity to maximum values of around 47 g/L Cl at 1,700 m (Figure 8-1). The Simpevarp subarea data shows a higher level of salinity at shallow depths (brackish at around 5,000 mg/L Cl to approx. 300 m depth), more saline at intermediate depths (up to 10,000 mg/L Cl at 700 m) and also a more systematic increase to around 850 m (to a maximum of ~ 17,000 mg/L Cl) when compared to Laxemar.

8.1.2 Calcium versus chloride and sodium

Figure 8-2 shows calcium increasing steadily with chloride (at increasing depth) for both the Laxemar and Simpevarp subareas. Of note is the similarity in calcium content up to brackish levels (~ 5,000 mg/L Cl); here there commences a small decrease at the Simpevarp subarea which appears to be maintained to the deepest level sampled (~ 17,000 mg/L Cl). This difference is more acccentuated in Figure 8-3 where calcium is plotted against sodium.

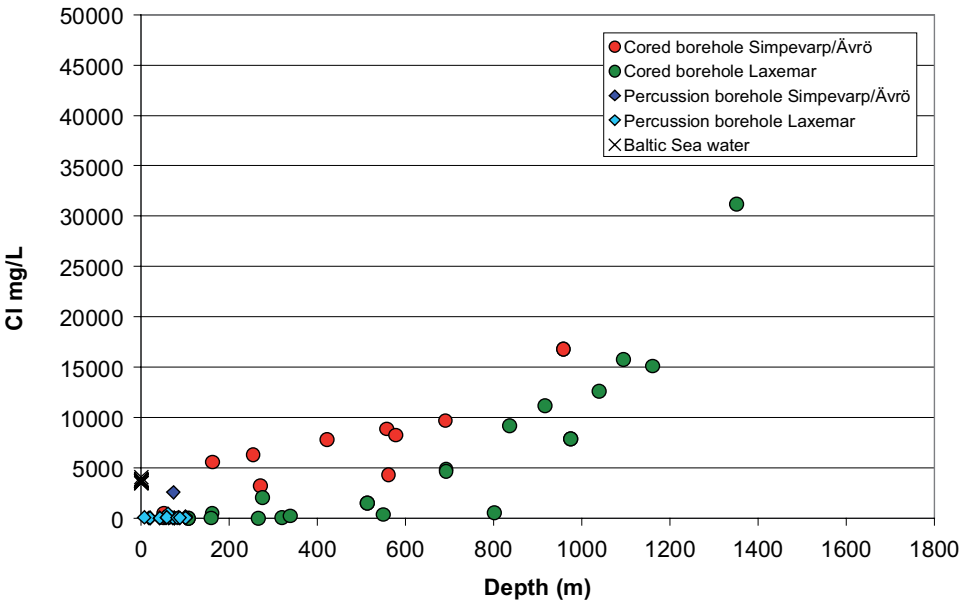

Figure 8-1. *Depth variation of chloride in the Simpevarp and Laxemar subareas.*

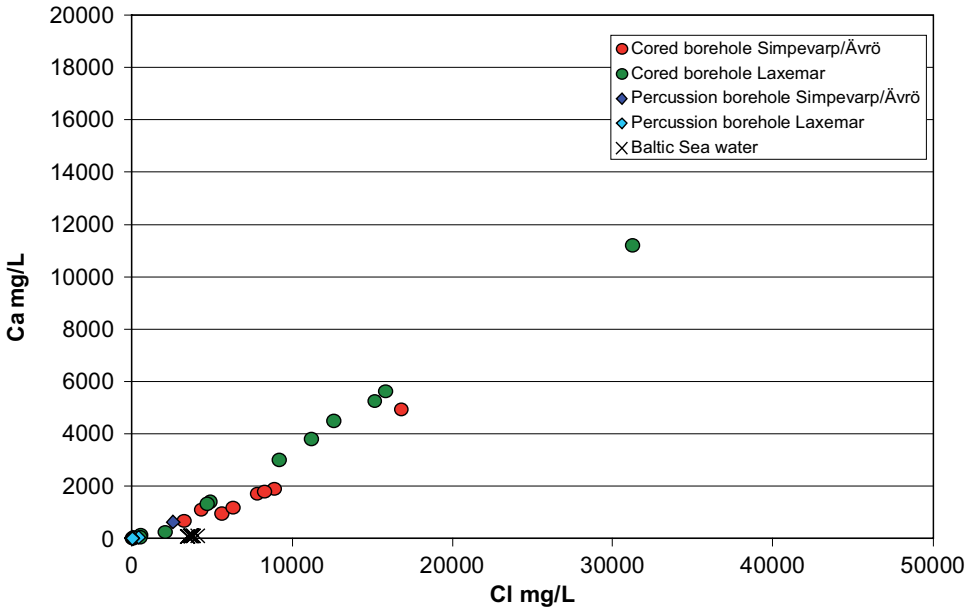

Figure 8-2. *Plot of Ca vs Cl for the Simpevarp and Laxemar subareas.*

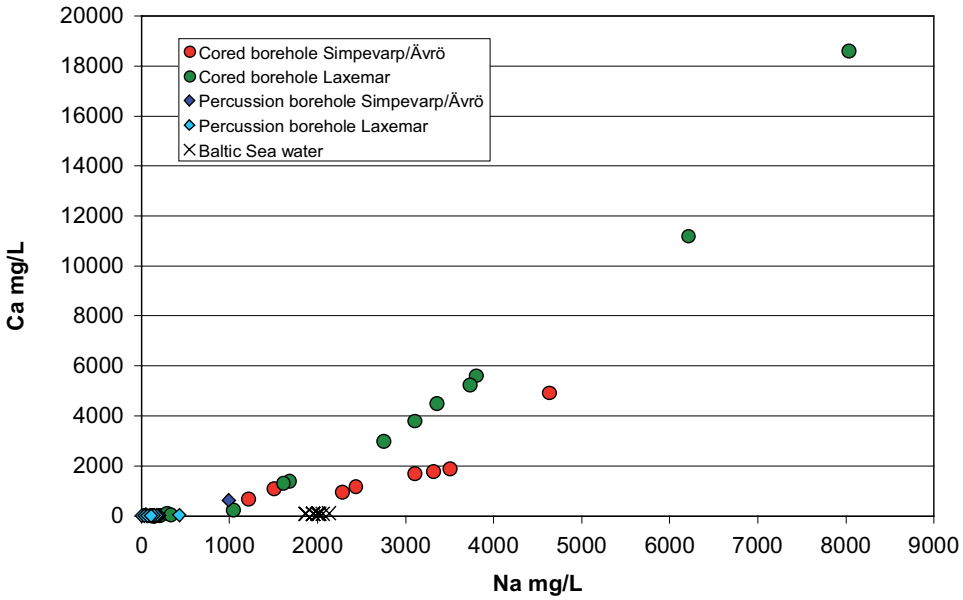

Figure 8-3. *Plot of Ca vs Na for the Simpevarp and Laxemar subareas.*

8.1.3 Magnesium versus chloride

Figure 8-4 shows the relationship of magnesium against chloride and underlines the generally higher magnesium contents in the Simpevarp samples (to ~ 70 mg/L) corresponding to more brackish conditions (3,000–7,000 mg/L Cl) and possibly suggesting a small Littorina or older seawater component. Over the same range of salinity the Laxemar groundwaters also show a small magnesium increase (to 30 mg/L Cl) before decreasing to near zero values at higher salinities (~ 15,000 mg/L Cl).

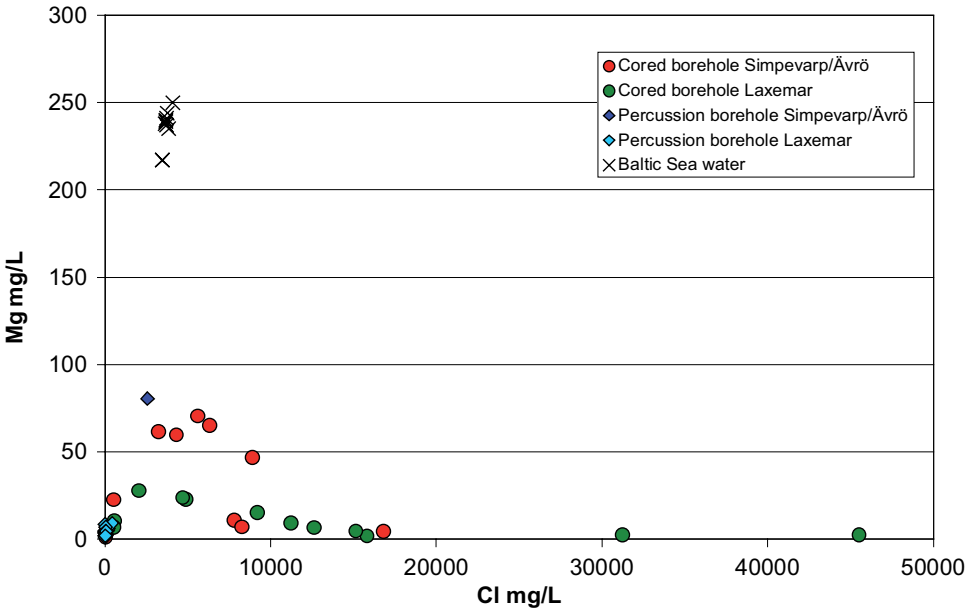

Figure 8-4. *Plot of Mg vs Cl for the Simpevarp and Laxemar subareas.*

8.1.4 Sulphate versus chloride and depth

Figure 8-5 shows a consistent increase in sulphate with increasing depth for both areas, with the main difference being, in common with chloride in Figure 8-1, that the increase at Simpevarp occurs at shallower levels in the bedrock (250 m at Simpevarp compared to around 600 m at Laxemar). In addition, there is a levelling off of sulphate at Laxemar at around 1,100 m which is not apparent so far at the maximum depth achieved at Simpevarp (900–1,000 m).

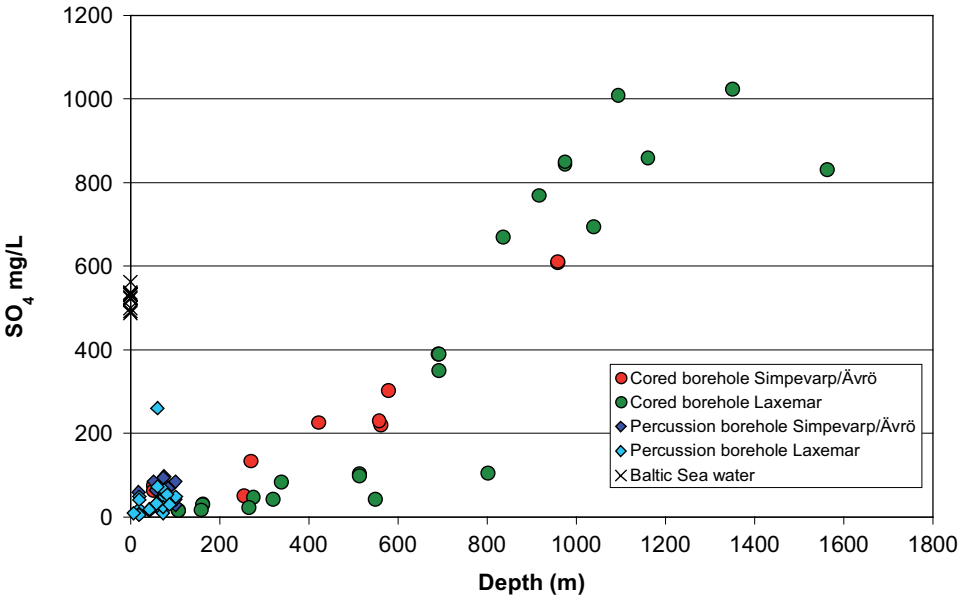

Figure 8-5. *Plot of SO_4 vs depth for the Simpevarp and Laxemar subareas.*

In Figure 8-6 sulphate is plotted against chloride and shows that the Laxemar subarea groundwaters indicate a levelling of sulphate at around 900–1,000 mg/L despite a significant increase in salinity from 15,000–50,000 mg/L Cl. This limitation of sulphate content in saline groundwaters was also noted by /Gascoyne 2004/ at the URL site in Canada; in this case it was attributed it to the solubility control exerted by gypsum which was close to saturation in the groundwaters. This is in accordance with geochemical modelling of the Simpevarp subarea groundwaters which identified the dissolution of gypsum as a possible source for sulphate in these groundwaters /Gimeno et al. in Laaksoharju 2004/.

The plot also reveals the generally higher chloride contents associated with the increase in sulphate in the Simpevarp subarea groundwaters; there doesn't appear to be any difference in the actual sulphate content to the depth so far sampled and analysed.

8.1.5 Bicarbonate versus depth and chloride

Figures 8-7 and 8-8 plot bicarbonate against depth and chloride respectively. Both plots show the expected rapid decrease in bicarbonate with increasing depth and correspondingly with increasing chloride. The small deviations or scatter in the depth trends caused by some of the Laxemar subarea cored boreholes reflect on one hand the differing hydrology at the borehole locations sampled and on the other hand possibly some open hole mixing effects.

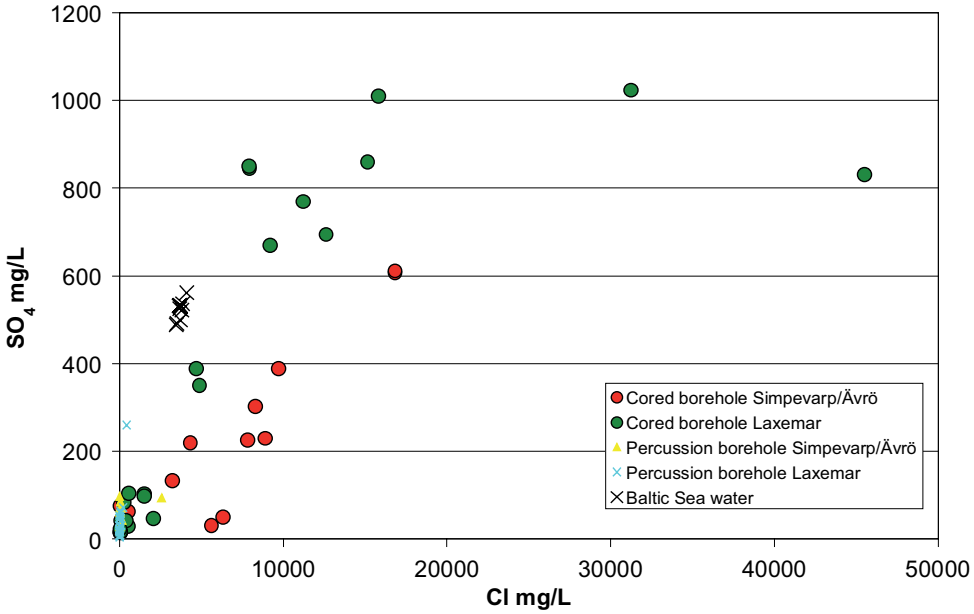

Figure 8-6. *Plot of SO_4 vs Cl for the Simpevarp and Laxemar subareas.*

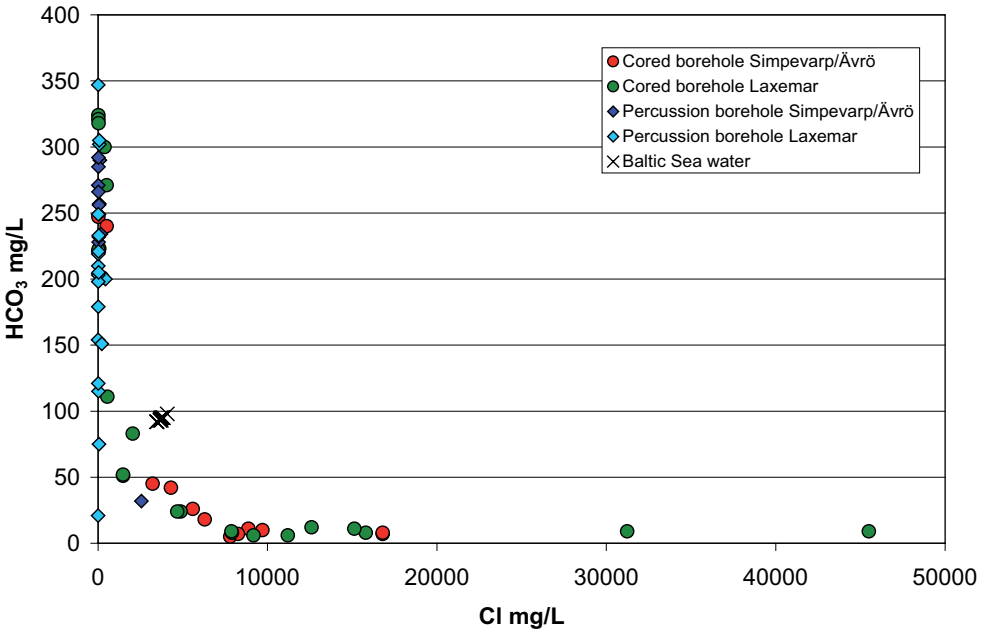

Figure 8-8. *Plot of HCO_3 vs Cl for the Simpevarp and Laxemar subareas.*

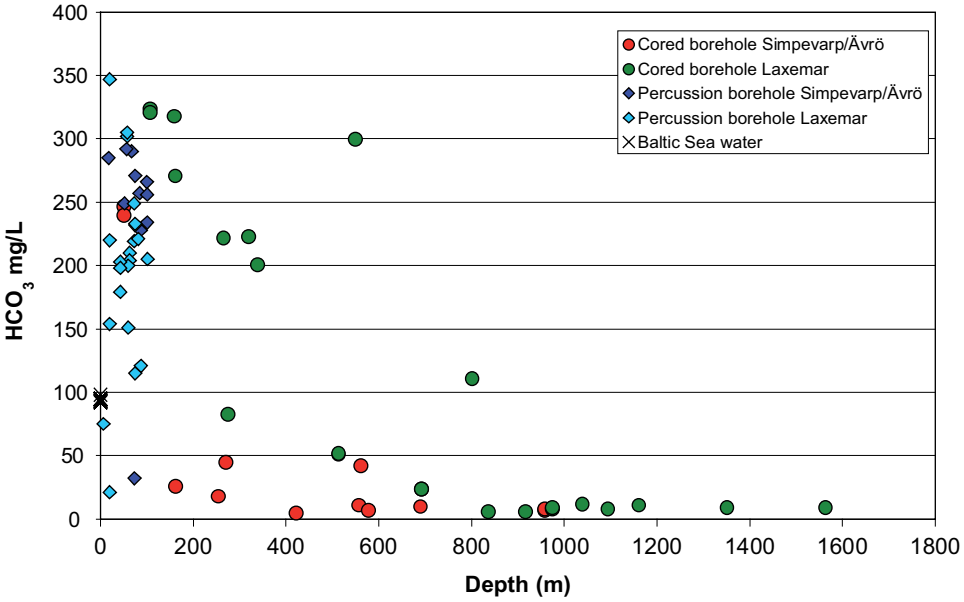

Figure 8-7. *Plot of HCO_3 vs depth for the Simpevarp and Laxemar subareas.*

8.1.6 Bromide/chloride versus chloride, magnesium and lithium

Figure 8-9 plots bomide/chloride ratio (wt.%) against chloride which helps to distinguish between groundwaters of a marine versus non-marine origin.

The figure shows shallow dilute groundwaters plotting at low chloride values and a broad range of bromide/chloride values. At higher salinities, close to the Baltic Sea end member, there is a distinct trend towards higher Br/Cl ratios with increasing salinity to around 10,000 mg/L Cl; this indicates a marine/non-marine mixing line where the non-marine component becomes increasingly important with increasing depth and salinity. At this point there is a levelling out of Br/Cl ratios which continues irrespective to the increasing salinity; this represents a dominance of the non-marine

component. It is interesting to note that most of the Simpevarp subarea samples lie along the marine/non-marine mixing line, supporting earlier indications that these groundwaters have a significant marine signature (possibly Littorina). In contrast, most of the Laxemar subarea samples indicate a non-marine origin, although there are three exceptions to this which suggest a marine signature; these are from two levels in KLX01 (labelled in Figure 8-9). However, since KLX01 is located in the vicinity of a Baltic Sea inlet to the north of the Laxemar subarea, a marine signature is not altogether unexpected. At the moment these data points should be considered anomalous. These characteristics are further illustrated by plotting Br/Cl against Mg (Figure 8-10) and Li (Figure 8-11), both sensitive in distinguishing between a marine and non-marine origin to the groundwaters.

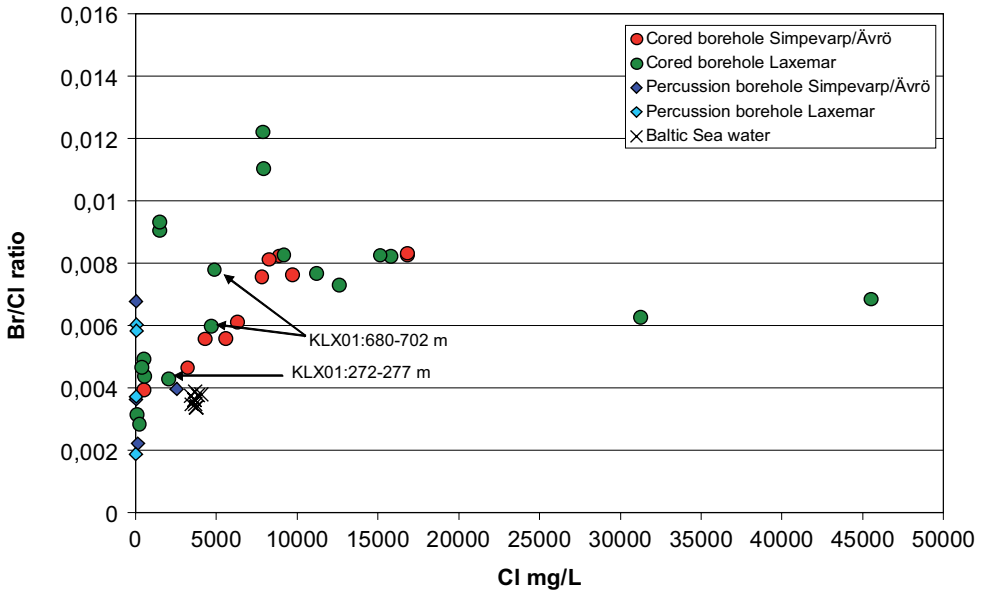

Figure 8-9. *Plot of Br/Cl vs Cl for the Simpevarp and Laxemar subareas.*

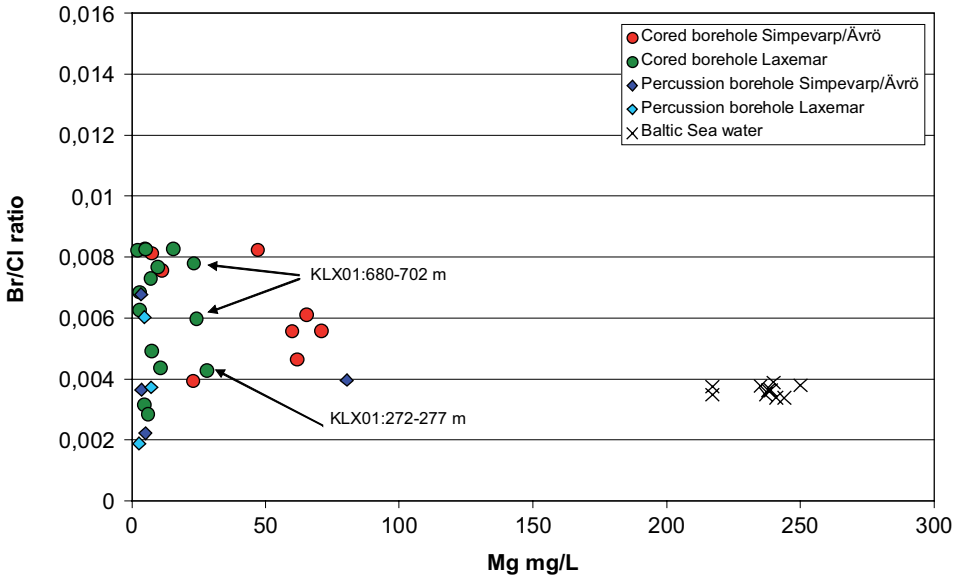

Figure 8-10. *Plot of Br/Cl vs Mg for the Simpevarp and Laxemar subareas.*

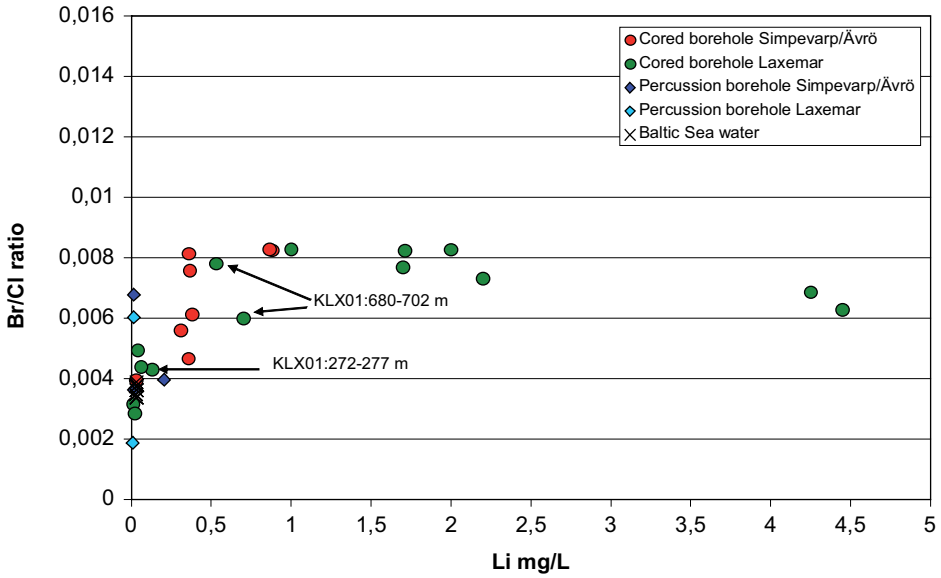

Figure 8-11. *Plot of Br/Cl vs Li for the Simpevarp and Laxemar subareas.*

8.1.7 Oxygen-18 versus deuterium

Figure 8-12 details the stable isotope data most of which plot on or close to the Global Meteoric Water Line indicating a meteoric origin. In accordance with much of the other hydrochemical data, three main groundwater groups are indicated: a) shallow dilute groundwaters ranging from $\delta^{18}O$ = –10.9 to –9.8‰ SMOW, δD = –78.7 to 67.1‰ SMOW, b) brackish to saline groundwaters ranging from $\delta^{18}O$ = –14.0 to –11.7‰ SMOW, δD = –100.0 to –86.2‰ SMOW, and c) highly saline from $\delta^{18}O$ = –11.7 to –8.9‰ SMOW, δD = –78.6 to –47.4‰ SMOW. The lighter isotopic values of the brackish groundwater group (b) indicate the presence of a cold recharge meteoric component (glacial melt water?). The limited data suggest there is no major Baltic Sea influence on the sampled groundwaters. One distinguishing feature is the characteristic deviation trend from the GMWL (i.e. the two highly saline groundwaters from –9.7 to –8.9‰ SMOW, δD = –61.7 to –47.4‰ SMOW)

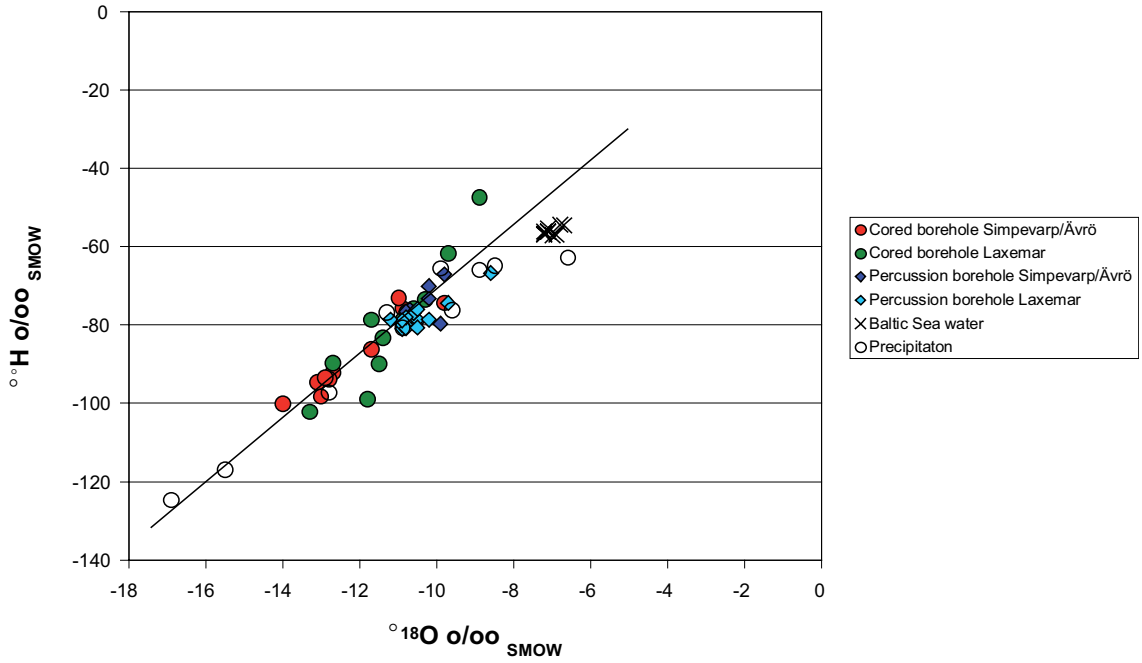

Figure 8-12. *Plot of $\delta^{18}O$ vs δD for the Simpevarp and Laxemar subareas (Global Meteoric Water Line (GMWL) is indicated).*

which appears to increase with increasing salinity. A similar deviation has been reported from the deep Canadian basement brines which has been discussed, among others, by /Frape and Fritz 1987/ who considered this an a indication of very intensive water/rock interactions under long residence times.

8.1.8 Oxygen-18 versus depth and chloride

Figure 8-13 shows the variation of $\delta^{18}O$ with depth underlining the shallow meteoric groundwaters (both Laxemar and Simpevarp) with an input recharge of around –11 to –12‰ SMOW, the brackish groundwaters (mainly Simpevarp) associated with light isotope cold climate $\delta^{18}O$ signatures to around 600–700 m and, finally, a gradual increase (mainly Laxemar) in $\delta^{18}O$ in groundwaters with increasing depth. This is further illustrated by Figure 8-14 by plotting $\delta^{18}O$ against chloride, especially the brackish nature of the groundwaters characterised by light isotope cold climate signatures.

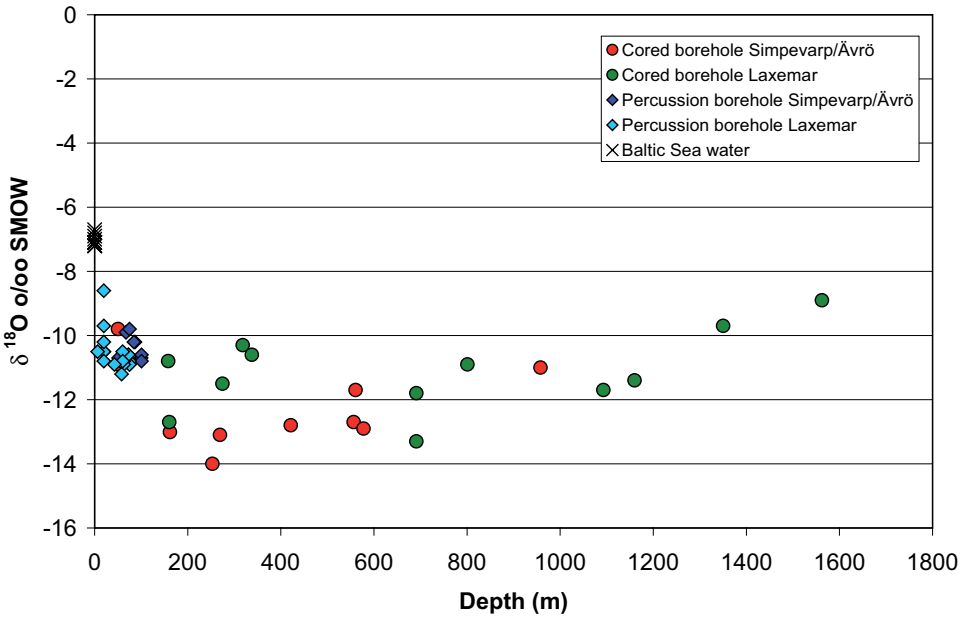

Figure 8-13. *Plot of $\delta^{18}O$ vs depth for the Simpevarp and Laxemar subareas.*

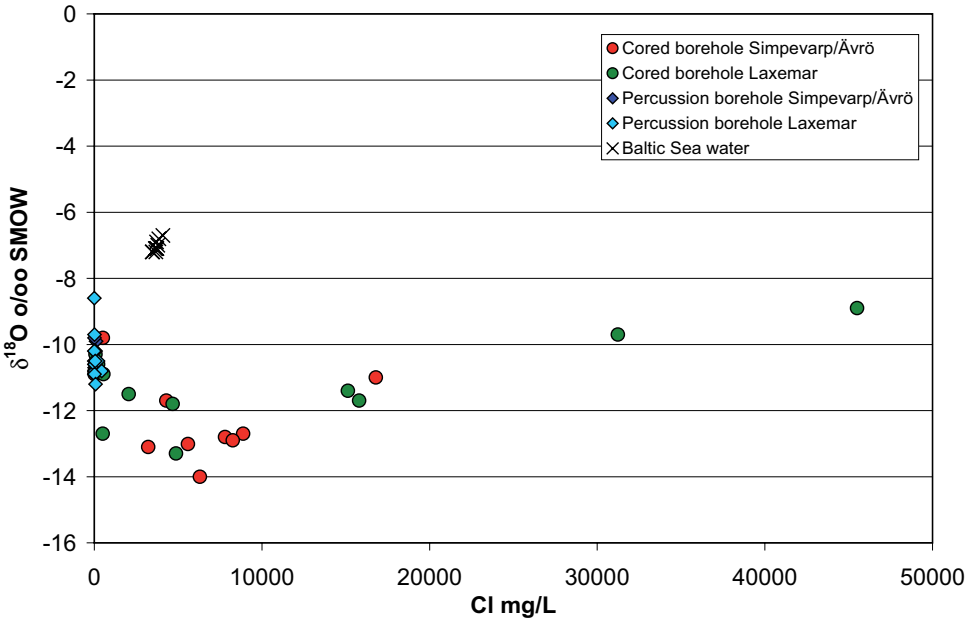

Figure 8-14. *Plot of $\delta^{18}O$ vs Cl for the Simpevarp and Laxemar subareas.*

8.2 Updating of specific isotope plots for the Simpevarp area

This section presents updated groundwater isotope data relating specifically to the interpretation and consequences of tritium, stable carbon and radiocarbon, stable sulphur ($\delta^{34}S$), stable and radiogenic strontium ($^{87/86}Sr$) and boron ($^{11/10}B$).

8.2.1 Tritium

Tritium produced by the bomb tests during the early 1960's is a good tracer for waters recharged within the past four decades. As part of an international monitoring campaign, peak values between 1,000 and 4,300 TU were recorded at Huddinge near Stockholm in the years 1963–1964 and values reaching almost 6,000 TU were recorded at Arjeplog and Kiruna in northern Sweden (IAEA database). Due to decay (half life of 12 years) and dispersion, in addition to a cessation of the nuclear bomb tests, precipitation tritium values decreased so that the measurements carried out at Huddinge during 1969 showed that values had dropped to between 74 and 240 TU.

Present day precipitation values at Simpevarp show a large spread in tritium (9 to19 TU) as well as in $\delta^{18}O$ (–6.6 to –16.9 $\delta^{18}O$ SMOW), the latter is due to seasonal variations. Generally, winter precipitation shows the lowest values and summer precipitation the highest values. There is no correlation between $\delta^{18}O$ and tritium values in the precipitation samples available so far (10 samples).

In Figure 8-15 tritium contents are plotted versus $\delta^{18}O$ for all surface water and precipitation samples from the Simpevarp area (sample site locations are shown in Figures 1-2 and 1-4). Surface lake and stream waters show values which range from 8–16 TU. The Baltic Sea samples show large variations in tritium (10–17.5 TU) but usually uniform $\delta^{18}O$ values of around –6 to –7‰ SMOW except for some samples from PSM002064 and PSM002064 situated north and south of Äspö, respectively (Figure 8-16). These have occasionally been influenced by surface water run off and thus show lower $\delta^{18}O$ values. The mean tritium values for the four Baltic Sea sampling points varies so that the highest mean value (15.1 TU) is found in the sampling point close to Kråkelund, whereas the others show mean values between 13.5 and 14 TU.

The lake and steam waters also show a relatively large spread in tritium values (from 8.5 to 15 TU). Concerning the lake samples most of these are sampled in Lake Frisksjön situated in the northern part of the Laxemar subarea, but two samples each from lake Götemaren (10.7 and 14.2 TU) and a small lake close to Jämserum west of the Laxemar subarea (11.3 and 10.0 TU) are also included. The stream waters (sampled from 10 different small streams) show tritium values between 8.5 and 15 TU (mean value of 12.0 TU). In more detail, the sampling points PSM002076, PSM002085 and PSM002086 situated in the eastern part of the Laxemar subarea show mean values in the interval of 12.3 to 12.9 TU, whereas the two sampling points (PSM002072 and PSM002083) showing the lowest mean values (11.4 and 11.5 TU) are situated in the northern and western part of the area. The $\delta^{18}O$ values in the stream waters are significantly lower than the values from the lakes (mean values of –11.1‰ SMOW compared with –8.3‰ SMOW). One explanation to this is that evaporation effects are much more evident from the open lake surfaces than from the small streams. Larger evaporation effects in the higher $\delta^{18}O$ waters are also supported by the change in slope (deviation from the Global Meteoric Water Line) for these samples (cf section 8.1.8; Figure 8-12)

Summarising the tritium information from the surface water samples it can be concluded that:

- Generally there is a spread in values between 8.5 to 19 TU which is almost equal to the variation in the precipitation (9–19 TU), i.e. the input term.
- The highest mean value is found in the Baltic Sea samples, with the highest contents (mean of 15.1 TU) in the samples east of Kråkelund, north of Simpevarp.
- The highest values for the lake and stream waters are found in the eastern part of the area even though mean values only deviate by 1–1.3 TU (11.4 compared with the highest value of 12.6 TU).

The question now to be addressed is how much of the tritium is due to fall-out contamination from the nuclear power plant? Present day contamination, although small, should be more apparent following the systematic decrease on global tritium values during the past five decades. Consequently,

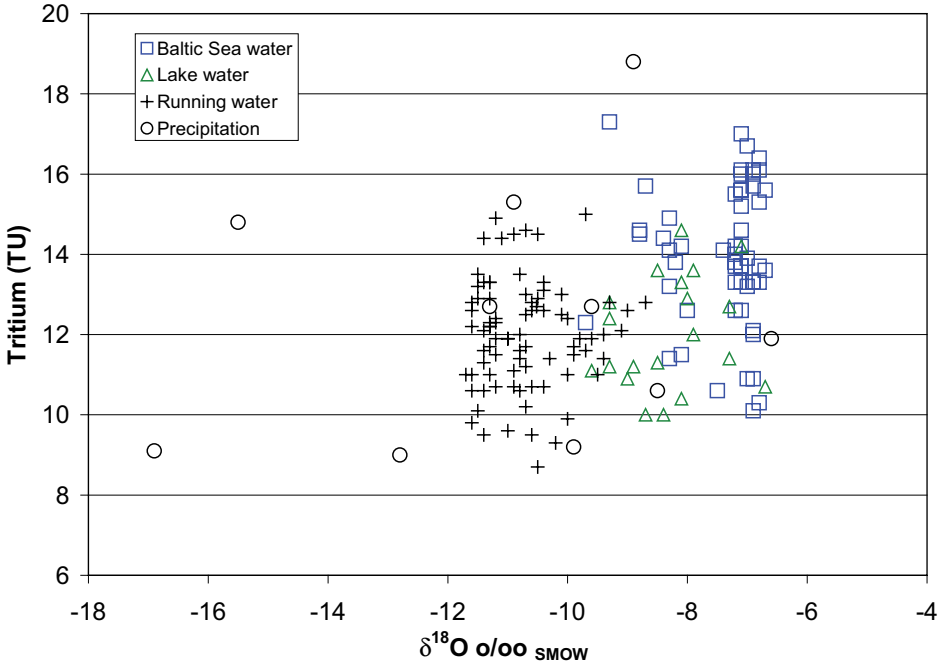

Figure 8-15. *Plot of $\delta^{18}O$ versus tritium in surface water samples from the Simpevarp area.*

Figure 8-16. *Surface sampling points. The Baltic Sea sample PSM002060 close to Kråkelund showed the highest mean value for tritium (15.1 TU).*

continued sampling of surface waters for tritium analyses is recommended with particular attention to surface waters samples taken: a) close to the cooling water outlet of the nuclear power plant, b) close to the power plant, and c) some 100 km away, preferably down-wind from the power plant.

One problem in using tritium for the interpretation of near-surface recharge/discharge is, as mentioned above, the variation in tritium content in precipitation over time, which implies that near-surface groundwaters with values around 15 TU can be 100% recent or a mixture of old meteoric (tritium free) and a small portion (10%) of water from the sixties at the height of the atmospheric nuclear bomb tests. In addition, although still not proven, small contributions of locally produced tritium from the nuclear plant may contribute an added uncertainty to the input data used in the modelling exercises.

Tritium in near surface and deep groundwaters

Taking into account the above discussion on tritium variability with time, together with: a) the much higher detection limit used for the analyses carried out prior to the start of the site investigations in 2002, and b) the less precise sampling techniques used for some of the older samples, it is suggested strongly that for detailed evaluation only the tritium values from the present site investigations should be used. This is illustrated in Figure 8-17 where only the 'representative' samples have been chosen; all tube samples and samples with drilling water contents above 10% have been excluded. This leaves only 12 samples from the percussion boreholes (2 from Laxemar subarea) and 12 samples from the cored borehole samples (of which 2 samples only are from the Laxemar subarea). In addition, 13 soil pipe samples have been analysed for tritium, all of which are situated on Ävrö or the Simpevarp peninsula.

The soil pipe samples, with one exception, show tritium and $\delta^{18}O$ values in accordance with the stream waters. The soil pipe SSM000022 situated on Ävrö deviates significantly in having tritium values close to the detection limit. The percussion boreholes show a larger spread in tritium values with some close to recent precipitation values and some close to the detection limit. The $\delta^{18}O$ values vary within a very small interval of –10.4 to –11.2‰ SMOW with the higher values originating from the Simpevarp (HSH) percussion boreholes and the lower values from the Laxemar (HLX) percussion boreholes.

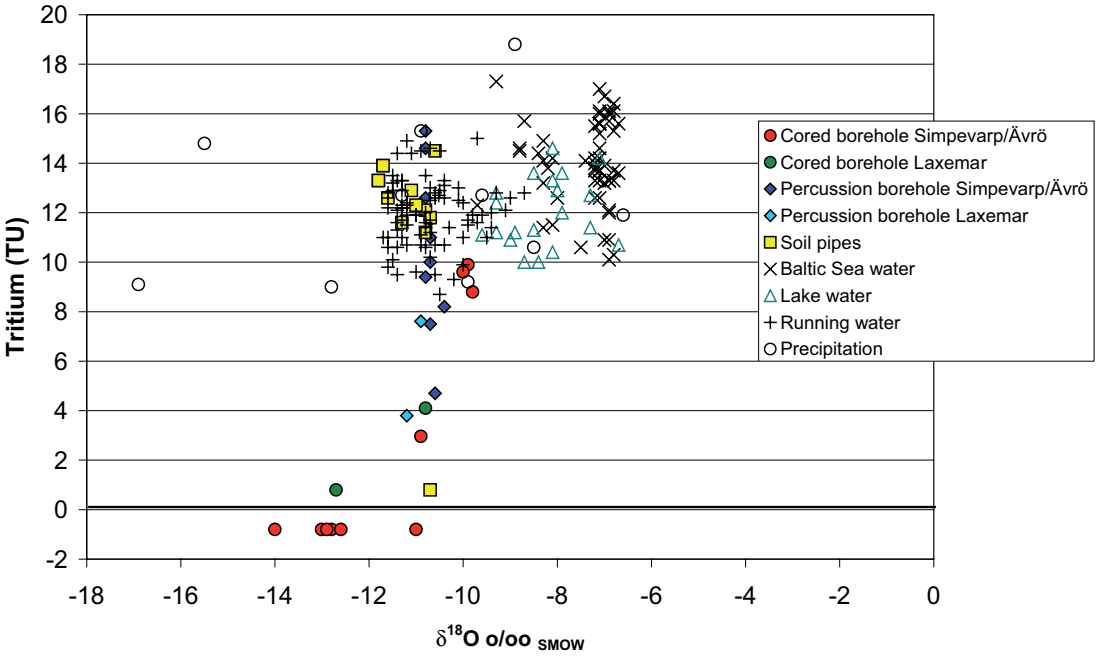

Figure 8-17. *Tritum versus $\delta^{18}O$ for surfacewaters and groundwaters from the Simpevarp and Laxemar subareas. Tritium values below detection limit (0.8 TU) are shown as negative values.*

The values from the cored boreholes are few and only two values from Laxemar are available representing relatively shallow sampling sections; KLX 03: 103–218 m and KLX04: 103–213 m. The KLX04 sample shows values similar to HLX 10; tritium close to 4 TU and $\delta^{18}O$ values around –11 ‰ SMOW. Both are dilute meteoric waters. The KLX03 sample, in contrast, shows tritium levels close to the detection limit and with a significantly lower $\delta^{18}O$ value (–12.7‰ SMOW) indicating a possible older cold climate meteoric water component. This water is less dilute, having Cl content of 507 mg/L.

All the samples analysed for tritium with chloride contents > 5,000 mg/L from the Simpevarp peninsula showed values below detection limit when tube samples and samples with high contents of drilling fluid are omitted (cf Figure 8-18). These samples are from depths of 150 m and deeper. Other analysed groundwaters (0–218 m) show low chloride contents and variable tritium contents.

It is obvious that the number of suitable groundwater samples analysed for tritium to date are very few and the possibility of evaluation is therefore restricted.

8.2.2 Carbon

^{14}C is produced in the atmosphere through the reaction $^{14}N+n \rightarrow {}^{14}C$ and decays with a half life of 5,730 years. However, reactions along the flow path, and especially in the soil and upper part of the bedrock, causes dilution of the signal so that still tritium-rich waters may show apparent ^{14}C ages of several thousand years. It is therefore recommended, as has been carried out at SKB for the past 10 years or so, that ^{14}C contents in groundwater samples should not be given as ages but instead be presented in units of pmC (percentage modern Carbon). One hundred percent modern carbon should be represented by the atmospheric value at 1950, i.e. prior to bomb test contamination of the atmosphere with ^{14}C (together with tritium). Figure 8-19 shows ^{14}C given as pmC plotted versus tritium in TU. The Baltic Sea samples show the highest ^{14}C values (around 105 to 110 pmC) which means that they have either some residual bomb test ^{14}C or, in common with the tritium values, contain a modern contribution from the nuclear power plant emissions resulting in higher than background

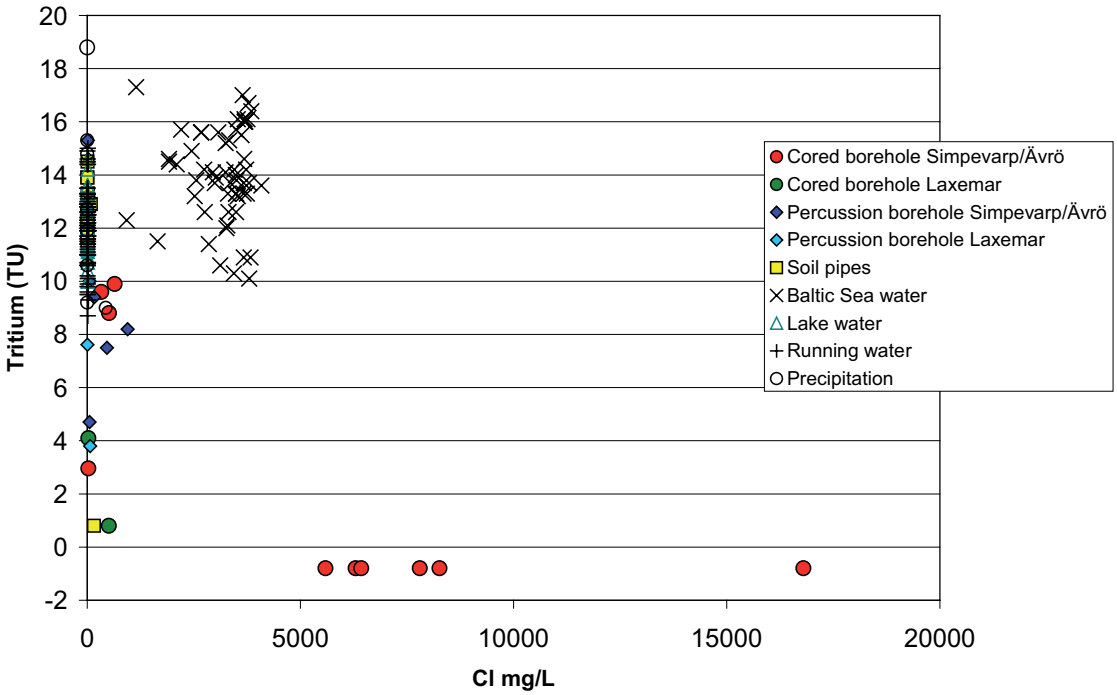

Figure 8-18. *Tritium (TU) versus Cl content (mg/L) for surface waters and groundwaters from the Simpevarp and Laxemar subareas. Tritium values below detection limit (0.8 TU) are shown as negative values.*

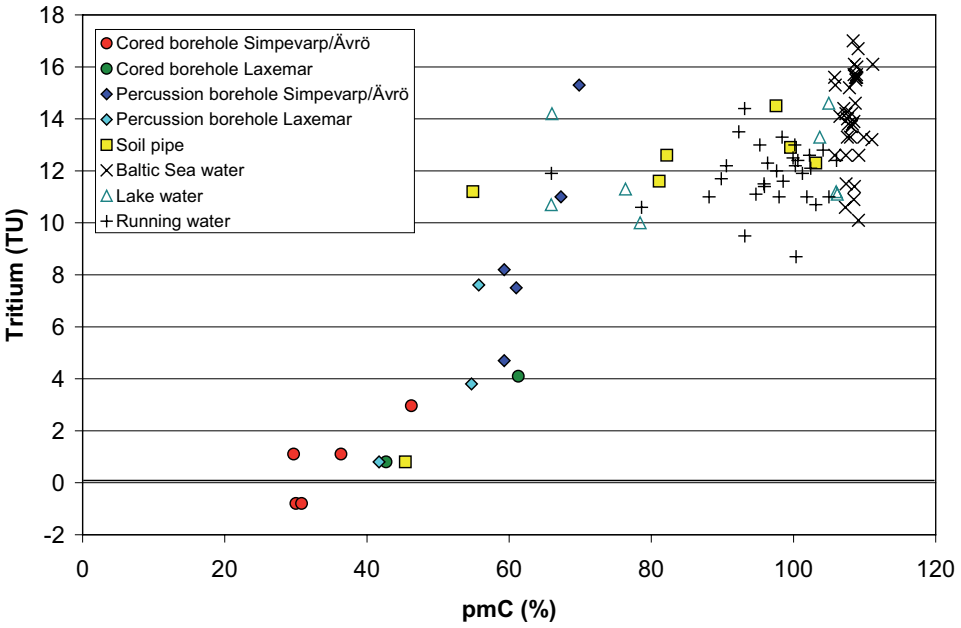

Figure 8-19. *Plot of ^{14}C (pmC) versus tritium (TU) for surface waters and groundwaters from the Simpevarp and Laxemar subareas. Tritium values below detection limit (0.8 TU) are shown as negative values.*

values. Most of the lake and stream waters show values ranging from 100 to 60 pmC, accompanied by high tritium values (~ 8–15 TU). With the exception of two samples (45 and 55 pmC) the soil pipes show values within the same interval as the surface waters. The percussion and cored boreholes show decreasing tritium contents with decreasing ^{14}C, so that the waters with very low tritium show the lowest ^{14}C values (around 30 pmC).

All samples analysed for ^{14}C are also analysed for stable carbon isotope ratios (given as $\delta^{13}C$ ‰ PDB). $\delta^{13}C$ together with HCO_3 contents are commonly used to evaluate possible processes that have taken place changing the ^{14}C contents in the groundwater.

Waters in equilibrium with atmospheric CO_2 show high $\delta^{13}C$ values (0 to –3‰ PDB). Incorporation of biogenic CO_2, produced by breakdown of organic material of variable age, lowers the $\delta^{13}C$ values significantly which is well illustrated in Figures 8-20 and 8-21 where the Baltic Sea samples show atmospheric values and the other surface waters show significantly lower $\delta^{13}C$. The ^{14}C values in most of these waters are relatively high (although somewhat lower than the Baltic Sea values) and it is probable that the organic source for the CO_2 is young, although some dilution with "dead carbon" (^{14}C free) has occurred. Some surface waters and most of the percussion and cored boreholes show similarly low $\delta^{13}C$ values but significantly lower ^{14}C values. In particular, the shallow groundwaters from the percussion boreholes and the two samples from KLX03: 103–218 m and KLX04 103–213 m show high HCO_3 contents (174 to 318 mg/L) indicating in situ production of CO_2. Several explanations for the decrease of ^{14}C are possible: 1) dissolution of calcite has contributed ^{14}C free carbon to the HCO_3, or 2) CO_2 has been produced from older organic material, or 3) these waters are old and very little ^{14}C has been contributed during a long period of time The combination of all these processes are possible for the groundwater samples. The fracture calcites show no homogeneous $\delta^{13}C$-values and it is therefore not possible to model calcite dissolution as a two end member mixing.

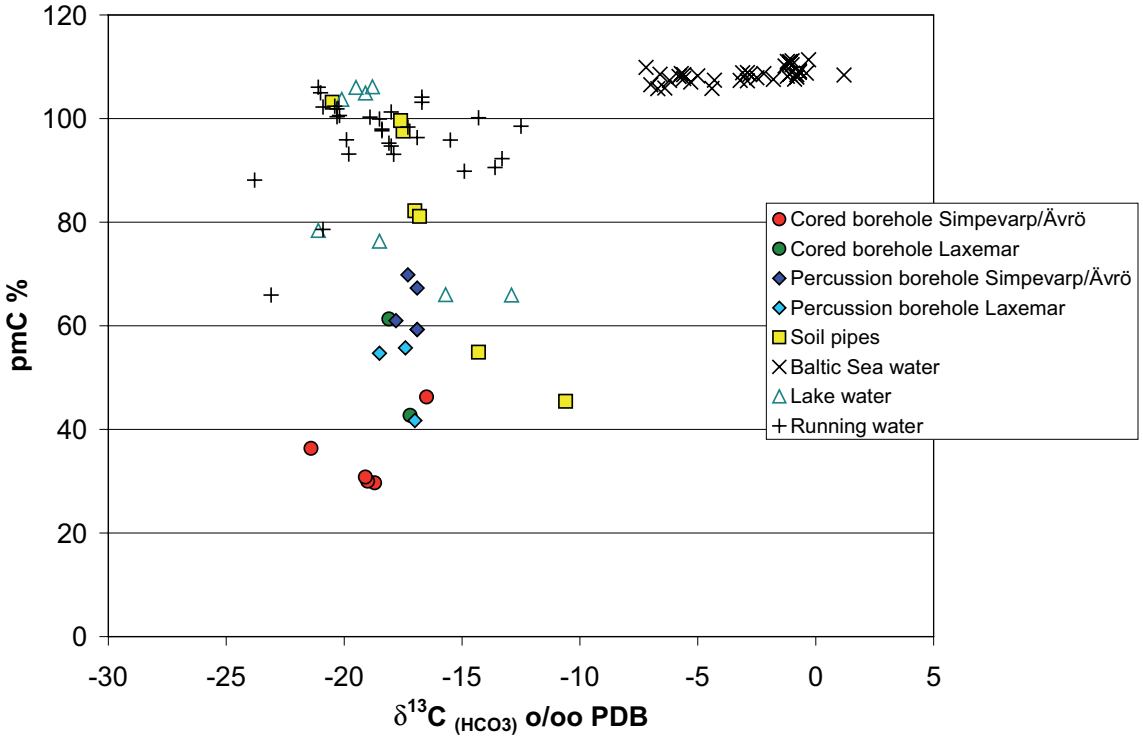

Figure 8-20. *Plot of ^{14}C (pmC) versus $\delta^{13}C$ (‰ PDB) for surface waters and groundwaters from the Simpevarp and Laxemar subareas.*

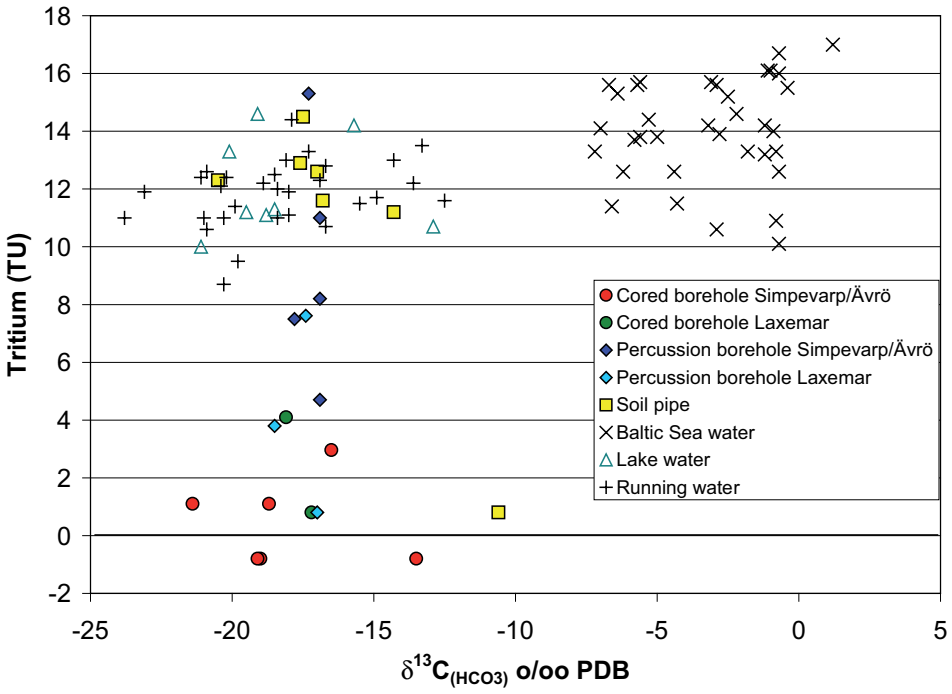

Figure 8-21. *Plot of tritium versus $\delta^{13}C$ in surface waters and groundwaters from the Simpevarp and Laxemar subareas.*

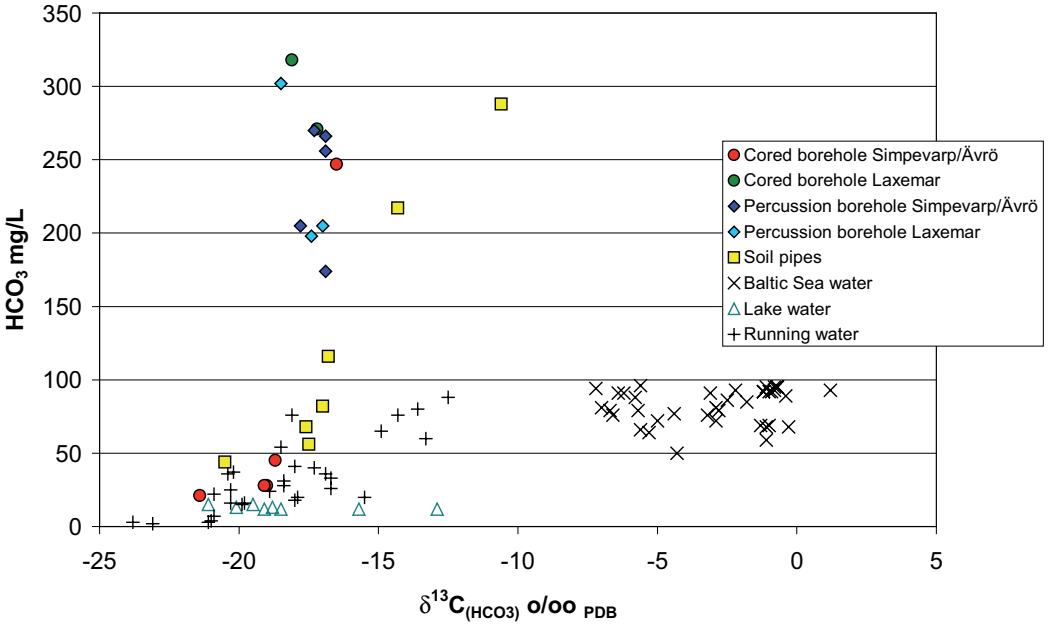

Figure 8-22. *$\delta^{13}C$ (HCO_3) versus HCO_3^- in surface waters and groundwaters from Simpevarp and Laxemar subareas.*

8.2.3 Sulphur

Sulphur isotope ratios, expressed as $\delta^{34}S$‰ CDT, have been measured in dissolved sulphate in Baltic Sea waters, surface waters and groundwaters from the Simpevarp and Laxemar subareas. Over 200 analyses have been performed of which the largest part involves surface and Baltic Sea waters. Of the cored and percussion borehole samples, only 21 remain when tube samples and samples with high drilling fluid contents are omitted. Three of these are from the Laxemar subarea. The isotope results are plotted versus $1/SO_4^{2-}$ (Figure 8-23) and versus Cl (Figure 8-24).

The recorded values vary within a wide range (–7 to +48‰ CDT) indicating different sulphur sources for the dissolved SO_4^{2-}. For the surface waters and most of the near-surface groundwaters (soil pipes) the SO_4^{2-} content is usually below 25 mg/L and the $\delta^{34}S$ relatively low but variable (–7 to +15‰ CDT) with most of the samples in the range 0–10‰ CDT. These relatively low values indicate that atmospheric deposition and oxidation of sulphides in the overburden is the origin for the SO_4^{2-}. There is a tendency towards lower $\delta^{34}S$‰ CDT with higher SO_4^{2-} contents in these waters but the variation is large. The Baltic Sea waters cluster around the +20‰ CDT marine line but show a relatively large spread (+16 to+23‰ CDT). The reason for this is not fully understood but suggestions include: a) contribution from land discharge sources (e.g. streams) to various degrees (low values), and b) potential bacterial modification creating high values in the remaining SO_4^{2-}.

The borehole groundwaters (Figure 8-23) show $\delta^{34}S$ values between +11.8 to +48.2‰ CDT with most of the samples in the range +15 to +25‰ CDT. Values higher than marine (< 20‰ CDT) are found in samples with Cl contents < 6,500 mg/L Cl (Figure 8-24). These latter values are interpreted as a product of sulphate reduction taking place in situ. The two highest values (+32 and +48‰ CDT) are detected in waters from HLX 14 and KLX03: 103–218 m. The SO_4^{2-} contents in these waters are low (around 30 mg/L) and the Cl content 70 and 503 mg/L, respectively. Such extreme $\delta^{34}S$ value as +48‰ CDT is a strong indicator of biological activity in closed conditions.

The groundwaters with higher salinities, all from the Simpevarp peninsula, share lower $\delta^{34}S$ but higher SO_4^{2-} contents. The $\delta^{34}S$ values of these groundwaters are, however, still within the range for the analysed Baltic Sea waters. Deep saline SO_4^{2-} sources may have resulted from the leaching of sediments and/or dissolution of gypsum previously present in fractures. Lowering of the $\delta^{34}S$ signature by oxidation of sulphides seems to be less probable for the groundwater samples and is not supported by fracture mineral investigations /Drake and Tullborg 2004/.

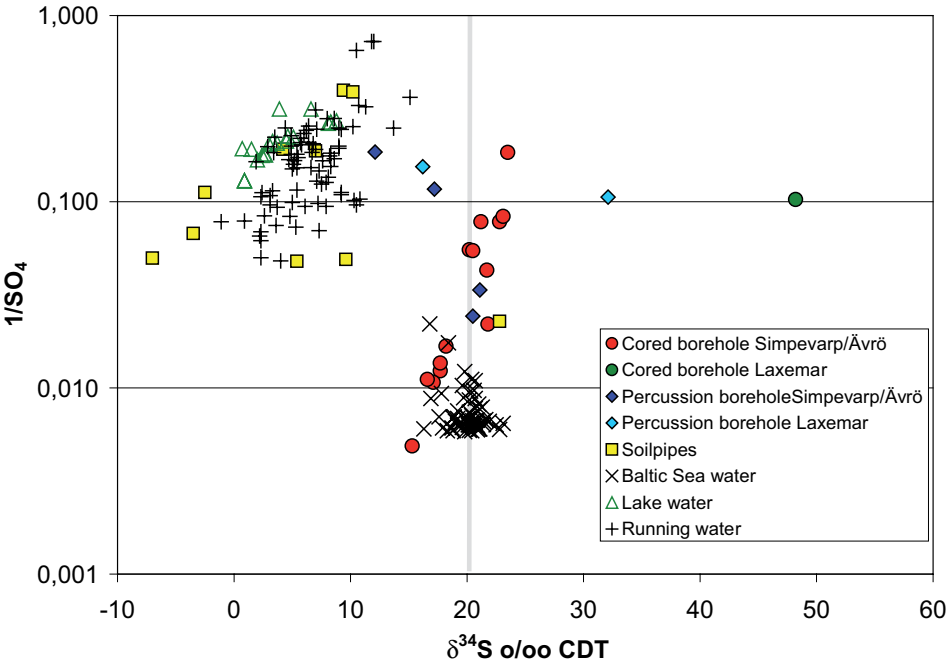

Figure 8-23. *Plot of $\delta^{34}S$ versus $1/SO_4^{2-}$ in surface waters and groundwaters. (The marine value is approx. +20‰ CDT).*

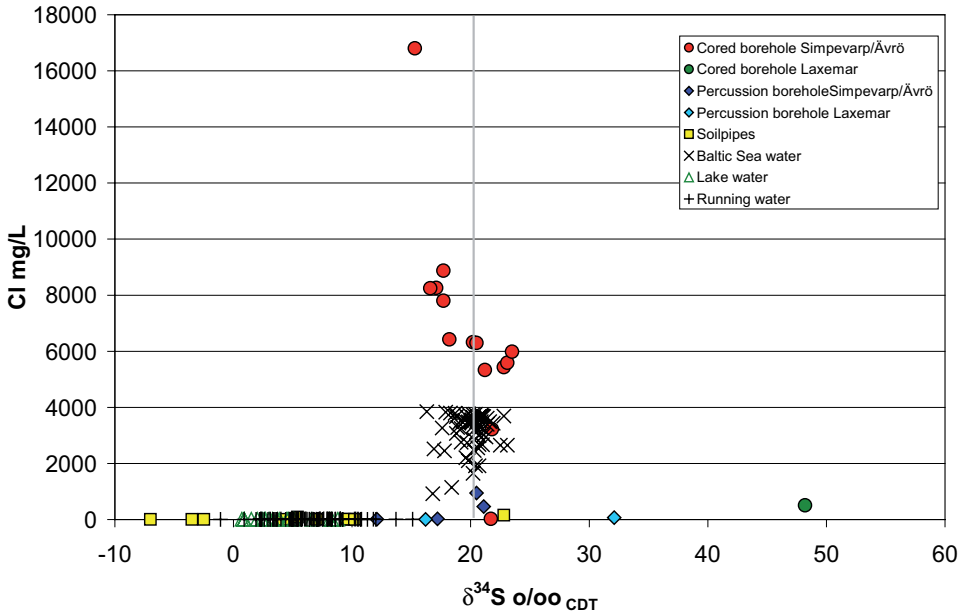

Figure 8-24. *Plot of $\delta^{34}S$ versus Cl in surface waters and groundwaters. The grey line indicates the marine value at around +20‰ CDT.*

As discussed in section 8.1.4, the SO_4^{2-} content in deep groundwaters from the Simpevarp area show different trends when plotted against the Cl content (Figure 8-6). The Laxemar subarea samples show relatively high SO_4 content in the saline waters, whereas two of the samples from the Simpevarp site and the KOV01 samples from the Oskarshamn site (close to the harbour) show extremely low values. The most saline groundwater at Simpevarp (16,800 mg/L Cl) has a SO_4 content of around 600 mg/L. Geochemical modelling /Gimeno et al. in Laaksoharju 2004/ indicates dissolution of gypsum as a possible source for SO_4 in the groundwaters. A few observations of fracture gypsum in the lower part of borehole KSH03A (the part that is located beneath the Baltic Sea east of Simpevarp; Figure 1-2) have been documented and also from KLX03 at a depth of 500–600 m. Unfortunately, no $\delta^{34}S$ measurements are so far available for this gypsum.

8.2.4 Strontium

^{87}Sr is a radiogenic isotope produced by the decay of ^{87}Rb (half-life $5x10^{10}$a). Strontium isotope ratios ($^{87}Sr/^{86}Sr$) in groundwater samples and Baltic Sea waters from the Simpevarp area are plotted against strontium content (1/Sr) in Figure 8-25.

Marine waters show a distinct Sr isotope signature (0.7092) which is very close to the measured values in the Baltic Sea waters. The near-surface groundwaters sampled in the soil pipes show low Sr content (< 0.3 mg/L) and a large variation in strontium isotope ratios from 0.712 to 0.733 indicating interaction (leaching) of minerals with different Rb/Sr ratio present in the overburden (Figure 1-1). The fresh groundwaters (< 1,000 mg/L Cl) sampled in the percussion boreholes and in the Laxemar cored boreholes KLX03: 103–218 m and KLX04: 103–213 m show a variation in the Sr content from 0.07 to 1.9 mg/L but contrastingly the Sr isotope ratio is very similar (0.7152 to 0.7158) and no trend related to Sr content can be observed. This is interpreted as a result of ion exchange homogenising the Sr isotope values along the flow paths. The only sample available from KAV01 shows a slightly higher Sr isotope ratio (0.7165). This is a sample from a shallow section (0–100 m) and it may well have a mixed origin; additional samples are needed for an interpretation.

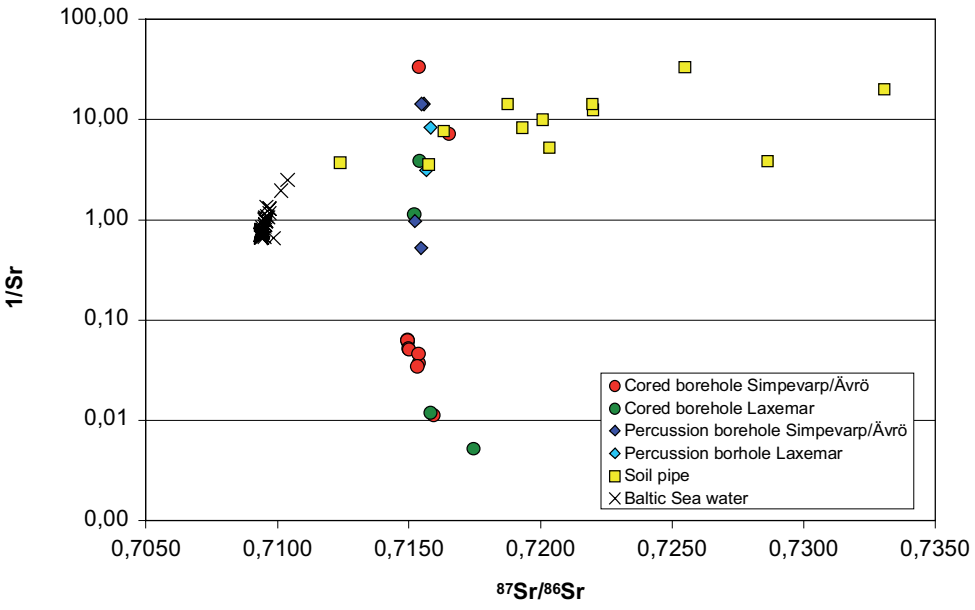

Figure 8-25. *Plot of $^{87}Sr/^{86}Sr$ ratios versus 1/Sr in Baltic Sea waters, near-surface waters and groundwaters from the Simpevarp and Laxemar subareas.*

For the more saline samples (Cl content < 5,000 mg/L) a trend towards somewhat higher Sr isotope ratios with depth (and increasing salinity) is indicated in Figure 8-26. Because of the limited data set (samples from 9 sections with salinities higher than 5,000 mg/L) it is not possible to explain this observation, but in the absence of any mineralogical reasons it is likely that greater residence times for these deep saline groundwaters result in more extensive mineral/water interactions. A trend with increasing Sr isotope ratios with increasing salinity for samples with salinities larger than 4,000 mg/L was identified by /Peterman and Wallin 1999/ based on a larger set of samples.

The possibility of tracing marine components by the use of Sr isotopes is often debated. Clay minerals in the fractures may, however, make such interpretations difficult. Examples from Forsmark show for example, that the strong present-day major ion Littorina Sea signature in the groundwaters is not reflected by any marine Sr isotope imprint. Instead, modification of the Sr isotope values is probably attributable to ion exchange processes.

In conclusion the available Sr isotope information from the Baltic sea waters, near surface waters and groundwaters show two or possibly three separate correlations between Sr isotopes and 1/Sr and Cl contents:

- Large variation in Sr ratios but relatively small variation in Sr content for the near-surface groundwaters indicating interaction (leaching) from overburden with different mineralogical compositions.
- Large variation in Sr content but small variation in Sr isotope ratios for the fresh groundwaters indicating homogenisation of the Sr isotope ratios due to mineral/water ineractions along the flow paths (mainly ion exchange).
- Tendency towards higher Sr isotope ratios with increasing Sr content for the saline samples possibly as a result of more stagnant conditions.

8.2.5 Uranium

Since Simpevarp 1.2, no additional useful data have been forthcoming from the Laxemar 1.2 data freeze. No updating has been carried out.

8.2.6 Boron

Due to the large relative mass difference between ^{10}B and ^{11}B and the high chemical reactivity of boron, significant isotope fractionation produces large variations in the $^{11}B/^{10}B$ ratios in natural samples from different geological environments. This results in high isotopic contrasts of potential mixing sources and also in process-specific changes in the isotope signature /Barth 1993/. Enhanced $\delta^{11}B$ has also been used as an indicator of permafrost conditions as it appears to become isotopically enriched in the fluid phase during freeze-out conditions /Casanova et al. 2005/. For example, deep saline groundwaters characterised by negative $\delta^{18}O$ values tend to correlate with high ^{11}B values.

The SICADA database values, previously reorted as ^{10}B (i.e. $^{10}B/^{11}B$) have now been recalculated to the more commonly used ^{11}B (i.e. $^{11}B/^{10}B$) from which $\delta^{11}B$ has been calculated. Boron analysis, not provided to date, has been implemented now into the analytical protocol and data will be forthcoming.

Boron isotope data are sporadic and initial scoping plots have been made using all data where both $\delta^{11}B$ and $\delta^{18}O$ have been analysed, i.e. including representative, limited suitability and unsuitable samples (SICADA Laxemar 1.2 Table). Figure 8-27 plots $\delta^{11}B$ against depth. This shows that almost all of the $\delta^{11}B$ data in the Simpevarp area plot between 20–60‰ which is in agreement with earlier published data from Fennoscandia and, in particular for this study, from Äspö (40–55‰) /Casanova et al. 2005/. Of interest are the three anomalously high $\delta^{11}B$ (80–110‰) cored borehole outliers from the Simpevarp site (KSH01A: 556 m, KSH02: 422 m and KSH02: 578 m). Otherwise the remaining borehole data fall within the same $\delta^{11}B$ range.

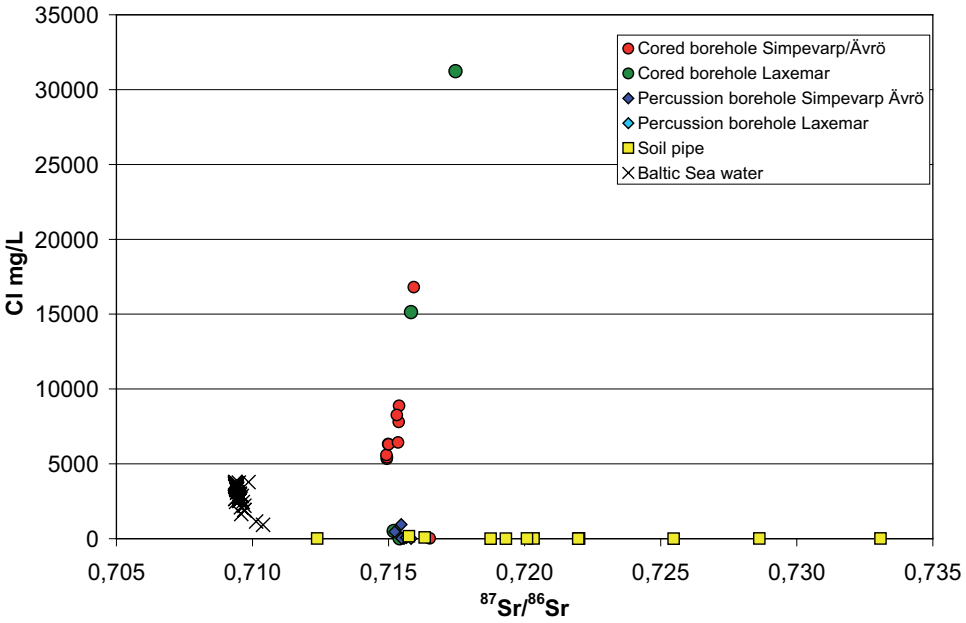

Figure 8-26. *Plot of $^{87}Sr/^{86}Sr$ ratios versus Cl in Baltic Sea waters, near-surface waters and groundwaters from the Simpevarp and Laxemar subareas.*

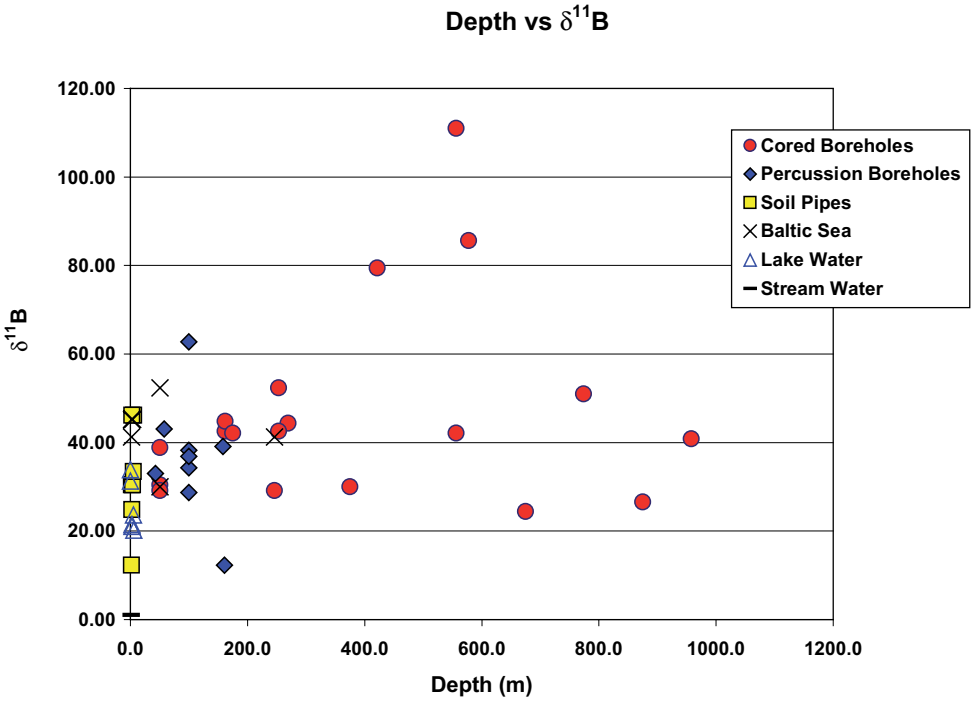

Figure 8-27. *Plot of $\delta^{11}B$ against depth for surface waters and groundwaters from the Simpevarp area.*

Figure 8-28 shows the relationship between $\delta^{11}B$ and $\delta^{18}O$. In this case the data have been presented showing the different degrees of suitability. Most of the unsuitability of these samples is due to excessive amounts of drilling water contamination (cf Chapter 3). The figure couples the three high $\delta^{11}B$ Simpevarp cored boreholes to somewhat lighter $\delta^{18}O$ values (–12.9 to –12.7‰ SMOW). According to the literature, this is consistent with the possibility that these three groundwaters might reflect freeze-out processes which occurred under permafrost conditions. The anomalous representative cored borehole sample with low $\delta^{11}B$ (and light $\delta^{18}O$ = –12.7‰ SMOW) represents a shallow groundwater environment (~ 160 m). There is no obvious explanation for the anomalously high $\delta^{11}B$ Stream water sample.

In addition, Figure 8-28 differentiates between Baltic Sea, Lake water and Stream water environments although, as might be expected, there is a degree of overlap with the lake and stream waters shown by both isotopic parameters. The soil pipe groundwaters show a close affinity with the shallow percussion boreholes and shallow depths sampled in the cored boreholes.

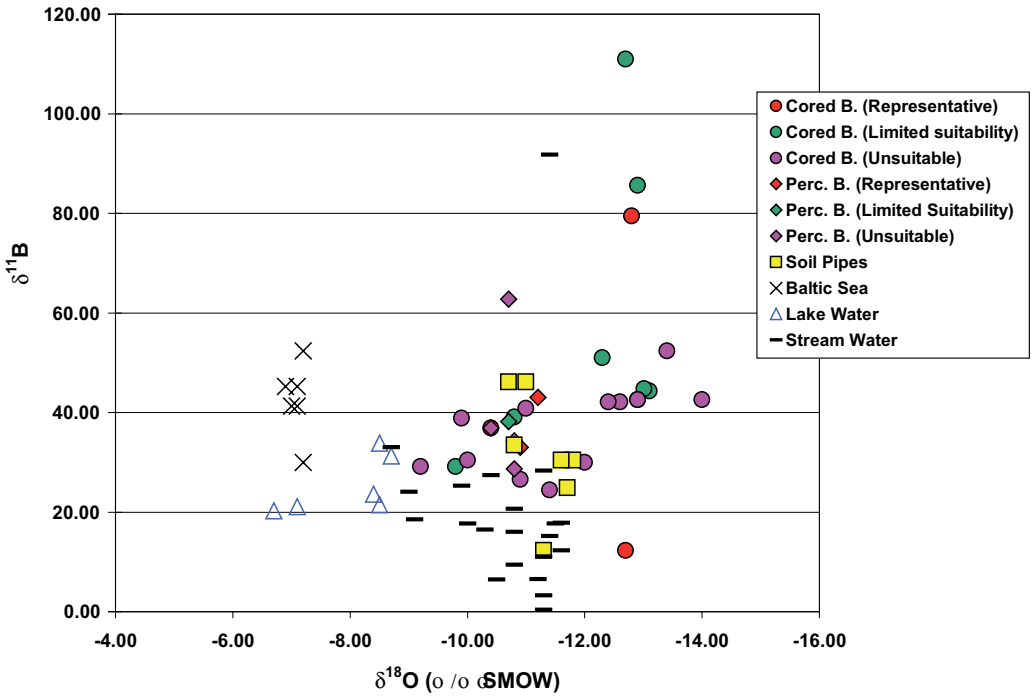

Figure 8-28. *Plot of $\delta^{11}B$ against $\delta^{18}O$ for surface waters and groundwaters from the Simpevarp area. Cored and percussion boreholes have been subdivided into degrees of suitability; Baltic Sea, Lake and Stream waters are generally catagorised as of 'Limited suitability' when used with caution.*

8.3 Evidence of redox indicators

Manganese (Mn^{2+}) was singled out as a potential redox indicator in the groundwater system and all available data from the Simpevarp and Laxemar subareas are plotted against depth in Figure 8-29. Mn^{2+} is produced by microbes during the oxidising of organic material under anaerobic conditions /Hallbeck in Laaksoharju 2004/. It should be emphasised that the presence of Mn^{2+} in groundwater is a strong indication of reducing conditions, but its absence (or very low content) in deep groundwaters can not be taken as an indication of oxidising conditions.

The relationshop of manganese with bicarbonate is shown in Figure 8-30. The three highest manganese values from the cored boreholes correlate with high bicarbonate in the 0–100 m interval. Even within the 100–600 m interval most of the cored borehole data show a weak relationship equating higher manganese with higher bicarbonate. The surface-derived waters show no significant trends. Figure 8-31 reflects largely Figure 8-29.

With the limited data available it is too early to draw any fast conclusions; on-going and future microbe studies /Hallbeck in Laaksoharju 2004/ should contribute significally to this discussion for the Laxemar Model v. 2.1 Stage.

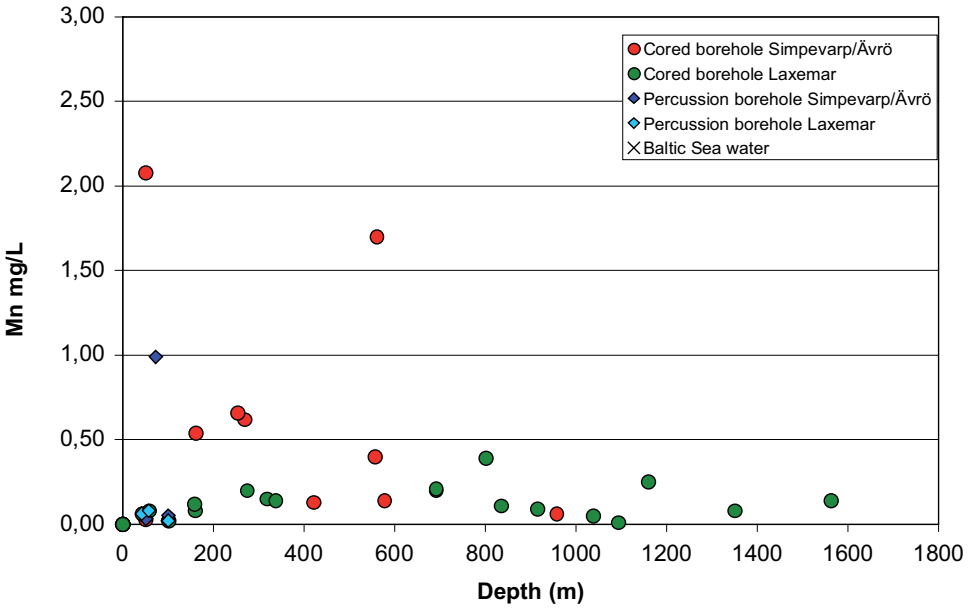

Figure 8-29. *Variation of Mn with depth for the Simpevarp and Laxemar subareas.*

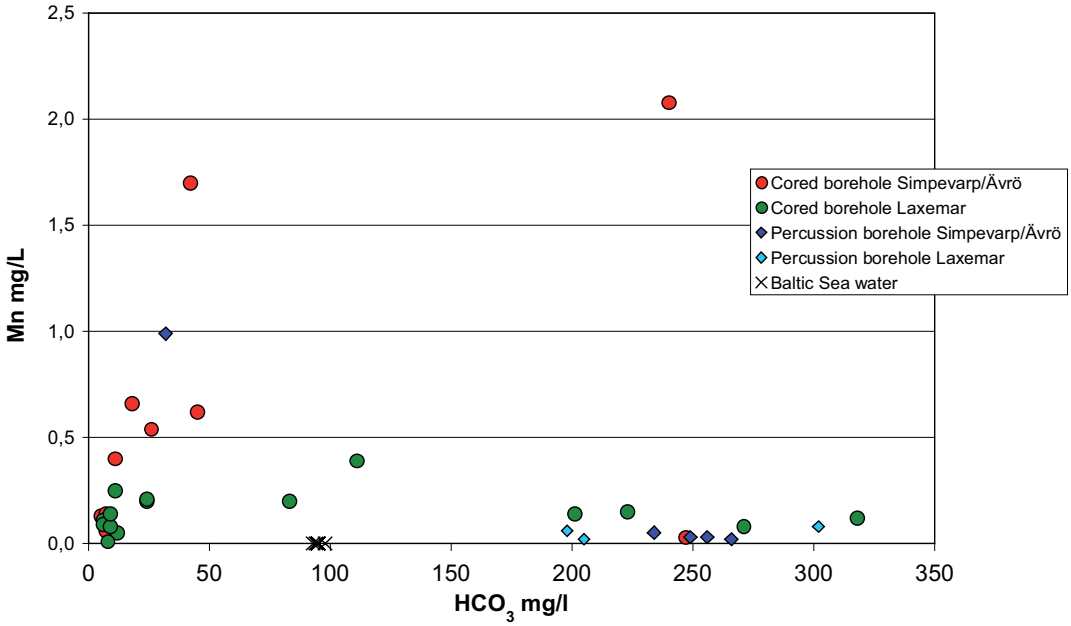

Figure 8-30. *Plot of Mn vs HCO_3 for the Simpevarp and Laxemar subareas.*

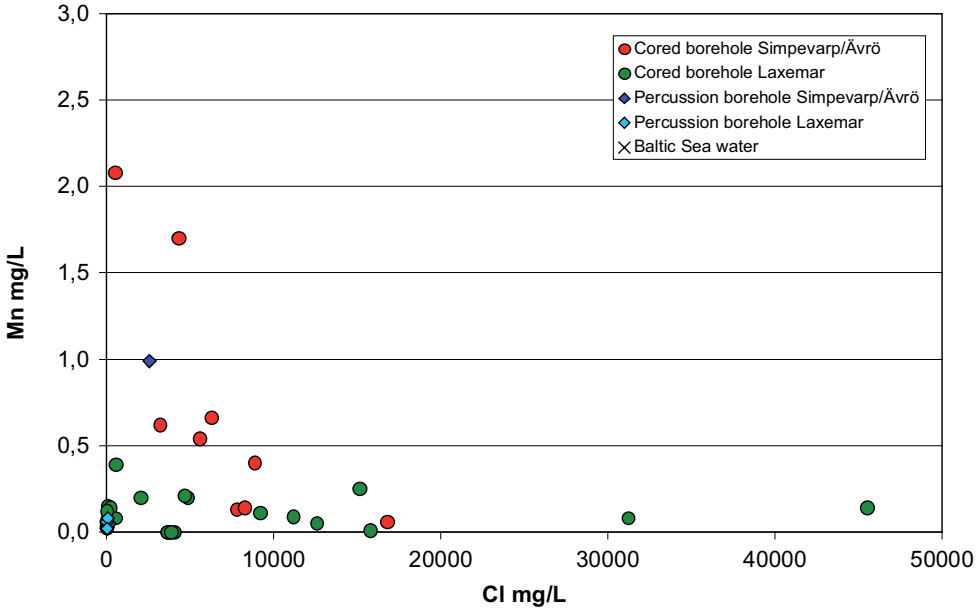

Figure 8-31. *Plot of Mn vs Cl for the Simpevarp and Laxemar subareas.*

9 Bedrock-overburden interface

9.1 Introduction and background

The bedrock-overburden interface is important in the present hydrogeochemical evaluation to: a) demarcate areas of recharge/discharge in the Simpevarp area, b) characterise the chemical and isotopic composition of the recharge water into the bedrock, and also of groundwaters at points of discharge from the bedrock, and c) establish the presence and understand the spatial extent of tritium and carbon isotope fallout from the nearby nuclear power facilities. Of major importance is to try and derive an input meteoric groundwater end member (at least a narrow range of values) that can be used in the evaluation and modelling excercises.

Due to limited data availability for this Laxemar 1.2 evaluation, only a brief general desription and preliminary conclusions can be drawn at this stage. Emphasis has been put on future data requirements in order to successfully address this complex interface problem in the next Laxemar 2.1 evaluation phase.

9.2 Factors affecting sub-surface groundwater quality

9.2.1 General

Depending of which surface and subsurface environments the waters and groundwaters are sampled from, the hydrological and hydrogeological setting will determine their composition due to transport and mixing between different reservoirs, i.e. atmospheric precipitation, soil pore space, lakes, streams and sea. Residence times will also vary influencing the reaction kinetic times for geochemical processes at the solid-solution interface in the subsurface environment. The time-scales for such solid-solution reactions to occur also may vary considerably (e.g. influence of seasonal fluctuations) although this factor may be addressed to a certain level by isotopic composition or tracer field experiments. No real attempt has been made here to include modelling calculations and transport mechanisms due to the lack of data and inadequate seasonal sampling. An attempt is made, however, to present an integrated approach towards the understanding of groundwater hydrogeochemical effects at the surface/sub-surface interface and to identify those areas of greatest concern where additional data are required.

9.2.2 Areas of recharge and discharge

Hydrological and hydrochemical issues

In terms of integration, a first attempt has been made to classify hydrogeological regimes as recharge areas and discharge areas. Recharge (or infiltation) areas may typically be expressed as the sum of precipitation, runnoff, evapotranspiration and moisture retention depending on topgraphy, i.e. whether runoff is positive (down to topographical depression points) or negative (away from slopes). The soil type and mineralogical composition of soils and their underlying bedrock is thus very important in determining the groundwater compostion. To what extent this will influence the present groundwater composition may be a factor of solubility of the rock-forming minerals present (and retention/reaction times). Moisture and porosity of soil and sediments is also important in retaining groundwaters (and their chemistries), for example accumulated salt due to evapotranspiration which, in turn, influences reaction times.

Even if the hydraulic conductivity (porosity) is regarded uniform with depth, the groundwater quality may change considerably from a topographically high area (i.e. recharge) to that of a low area (i.e. discharge) when taking into consideration overall physical factors such as high to low temperature and pressure, and chemical factors such as acid to basic conditions (acid exchange may change through equilibrium to basic exhange), suboxic to anoxic and even methanogenic conditions. For recharge the variation in chemistry is expected to be high (due to variable seasonal recharge rates and reaction times) than for discharge conditions where groundwater flow rates are generally slow and the hydrochemistry more uniform.

Chemical processes and reactions

Recharge and discharge conditions are compared in Figure 9-1 showing differences in groundwater level and in the nature of the overburden material close to the surface.

The processes indicated in Figure 9-1 include, in the soils of recharge areas and unsaturated zones, oxidation, precipitation and dissolution, cation exchange and organic reactions. Major constituents which result mainly from precipitation and sea spray are Ca^{2+}, Mg^{2+}, HCO^{-} and Cl^{-}, Na^{+} and SO_4^{2-}, although the latter two may also be weathering products. Depending on the soil composition and organic content, humic substances are also dissolved and organic decompostion consumes oxygen to produce CO_2. Both these consitutents are of great importance for redox conditions and thus bicarbonate content and proton availabity. The solubility of CO_2 increases the total carbonate concentration and results in a decrease in pH. The presence of humic substances also can affect weathering rates by increasing mineral dissolution.

Table 9-1 lists the major reactions which characterise the recharge area. In the database no dissolved organic carbon is reported although it can be noted that in many of the organic soils the debris may be a possible source of DOC. Also in these areas metals may in complex form be transported to deeper layers or sorbed. No mineral analyses have been done on the soil horizons to see if there are some sulphate-containing minerals that may possibly contribute to eventual sulphate anomalies, even in recharge areas where dry and low groundwater levels are present.

Table 9-1. Main reactions in the recharge area.

Decomposition/oxidation of organic matter:	$(CH_2O) + O_2 = CO_2 + H_2O$
Gas dissolution and redistribution:	$CO_2 + H_2O = H_2CO_3$ $H_2CO_3 = HCO_3 + H^+$ $H_2CO_3 = CO_3^{2-} + H^+$
Carbonate and silica dissolution (ex):	$CaCO_3 + H^+ = Ca^{2+} + HCO_3^-$ $CaAl_2Si_3O_8$ (s) + $^2H^+ + H_2O$ = kaolinite + Ca^{2+}
Sulphide mineral oxidation:	$4FeS_2 + 15O_2 + 14H_2O = 4Fe(OH)_3 + 16H^+ + SO_4^{2-}$ Sulphur components = SO_4^2– + $^2H^+$
Precipitation and dissolution of gypsum:	$CaSO_4 \times {}^2H_2O = Ca^{2+} + SO_4^{2-} + {}^2H_2O$
Cation exchange (ex):	Ca^{2+} + 2Na-X = 2Na+ + Ca-X Fe_2O_3 precipitates $NaCl = Na^+ + Cl^-$ $0.5Fe_2O_3 + 3^{H+} + e^- = > Fe_2^+ + 1.5H_2O$

If similar processes to those described for recharge are encountered in the discharge area (Table 9-2), they tend to be more continuous (if not, reaching near-equilibrium) and seasonally stable. The importance of redox reactions increases and thus also the buffering (i.e. stabilising) of the system. Base cation concentrations (due to ion exchange) may increase many times over as the groundwater moves towards the discharge zones. Furthermore an increase of dissolved organic carbon in soil solution due to increased groundwater levels (or rainfall) may be seen.

Table 9-2. Main processes influencing groundwater composition in the saturated zone and discharge areas.

Carbonate and silicate dissolution:	Carbonate minerals + H^+ = cations + HCO_3^- Silicate minerals + H^+ = Cations + H_2SO_3
Dissolutions of soluble salts (ex):	$NaCl = Na^+ + Cl^-$ $CaSO_4 \times {}^2H_2O = Ca^{2+} + SO_4^{2-} + {}^2H_2O$
Redox reactions (ex):	$0.5Fe_2O_3 + {}^3H^+ + e^- = > Fe_2^+ + 1.5H_2O$ $1/8SO_4^{2-} + 9/8H^+ + e^- = 1/8HS^- + 1/{}^2H_2O$
Cation exchange:	$Ca^{2+}/Mg^{2+}/Fe^{2+}$ + 2Na-Clay = $2Na^+ + Ca^{2+}/Mg^{2+}/Fe^{2+}$–Clay

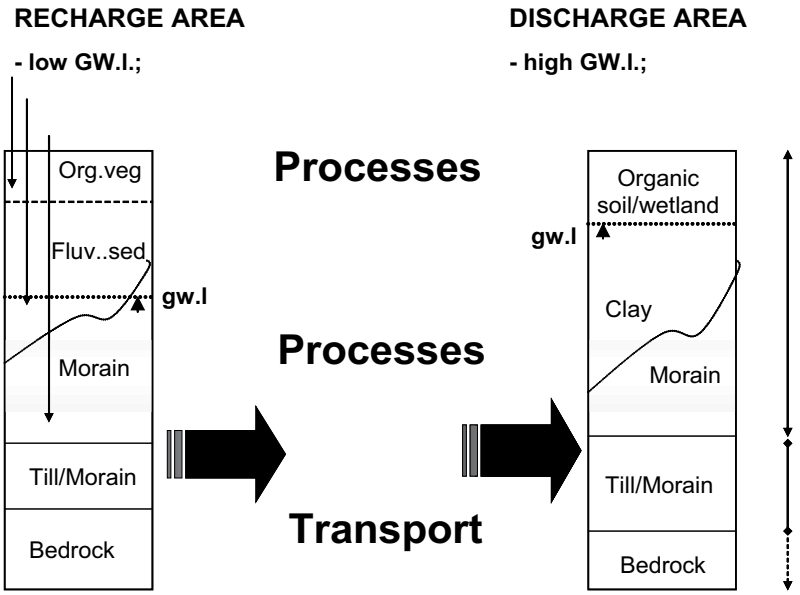

Figure 9-1. *Comparison of recharge/discharge in the overburden constituents.*

9.3 Geology and hydrology, and soil and vegetation cover

9.3.1 Elevation and topography

Considering the possible factors affecting groundwater composition and quality, all available data sources within the Simpevarp area should be addressed. The main initial consideration has been the elevation and topographical model of the whole area. This has served as the main basis for assessing a theoretical hydrological surface model indicating areas of low and high recharge respectively /Werner et al. 2005/.

9.3.2 Geology

The regional geological has been considered to identify which rock type is mainly underlying the surface and also which type characterises the location of the percussion boreholes. The regional geological setting has been described in Chapter 1 with the location of the boreholes shown in Figure 1-1. In general, the central Laxemar area is dominated by Ävrö granite with the subsidiary presence of quartz monzodiorite and granite and diorite/gabbro. Their mineralogical/geochemical composition are closely similar to that in the Simpevarp subarea described in /Laaksoharju 2004, Appendix 1/.

9.3.3 Soil type distribution

The general shallow soil overburden in the Laxemar area varies from 1–8 m and covers about half the modelling area; the rest consists mainly of exposed bedrock at higher elevations (Figure 9-2). The dominating soil types are sandy till, partly with peat underlain by clay or as a layer directly on coarse, boulder till or bedrock. What is not presently available is the mineralogical/geochemical composition of the various soil types, only the bulk chemistry of each soil type, and also there was no near-surface hydrological model available at the time (including the soil cover) with which to integrate the hydrochemistry. This is now available /Werner et al. 2005/.

9.3.4 Hydrology and hydrogeology

Even if the geochemical composition of rocks and their weathering products are important over long timescales, it is the deformation zones or where water-conductive zones are present at the local scale that is of more interest for understanding solute transport and the associated interactions with fracture minerals. In this respect special significance was given to the location of soil pipes and percussion boreholes at or close to potential water-conducting zones.

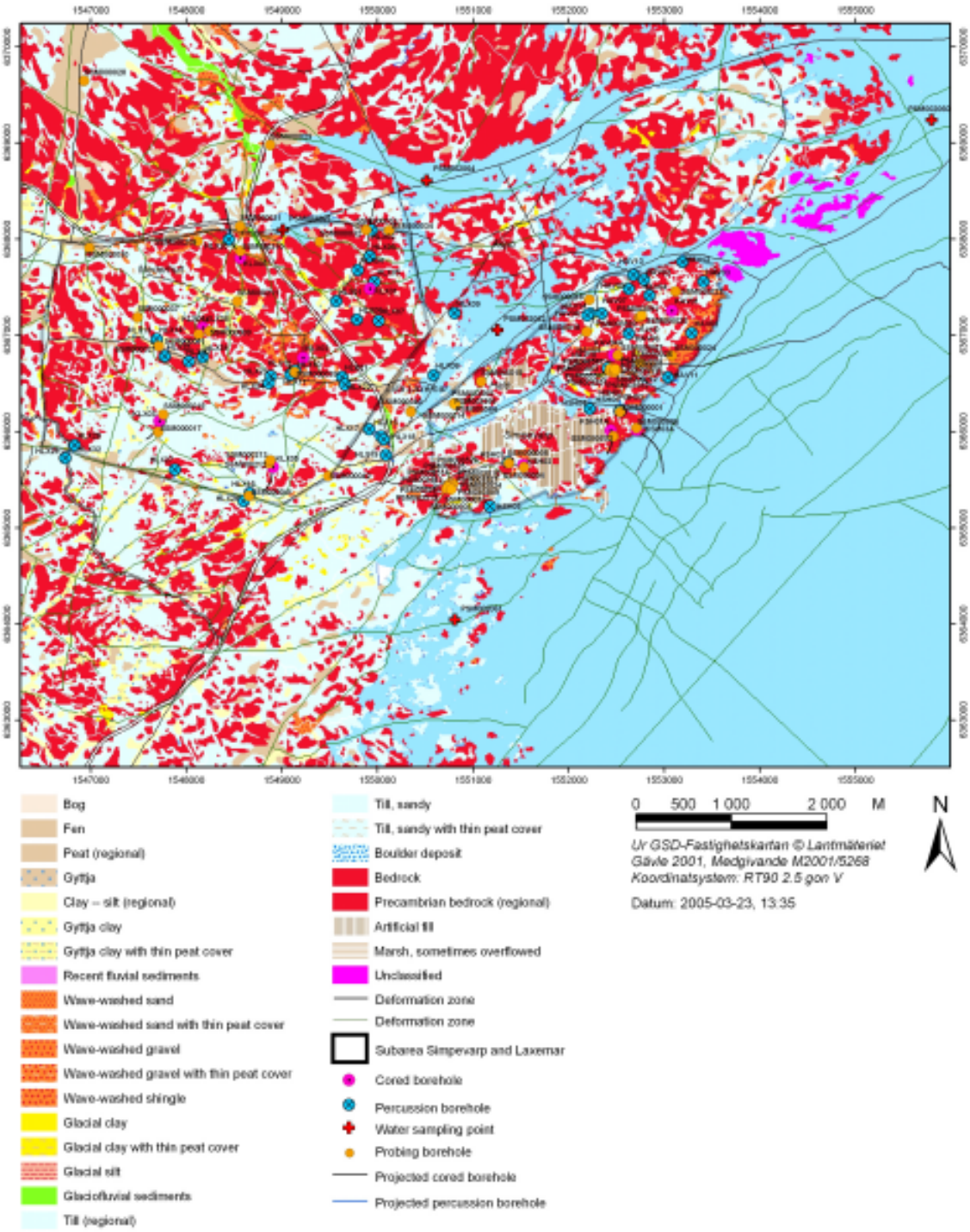

Figure 9-2. *Simpevarp area: Distribution of soil cover, bedrock exposure and the location of cored and percussion boreholes and soil pipes.*

In the surface modelling of the hydrology, surface deposits have been taken into consideration being assigned within different domains in terms of hydraulic properties taken from site data. This is important when considering residence and transport times in the hydrogeochemical regimes and for further modelling of such regimes. At this stage a preliminary GIS model (Bosson 2005, pers. comm.) was used to give an indication of the areas of discharge and recharge. The basis for this GIS model is the topographical information and the cell size used to compile an evaluation of resulting cells of zero integration of slopes and hights. These were then referred, depending on elevation (negative/low or high), to either recharge or discharge areas. The size of these modelled areas will depend on the usual parameters such as soil overburden, hydraulic conductivity, soil type, precipiation, evapotranspiration, runoff and infiltration etc. In addition, the size may vary according to: a) season, and b) the choice of cell size, and c) how many cells are chosen to demarcate a given a zero-derived cell.

9.4 Sampled surface water and near-surface groundwater locations and present status

Available water/groundwater data derive from four major sampled sources:

- Precipitation (rain and snow).
- Surface localities (lakes, streams and the Baltic Sea).
- Sub-surface localities in the overburden (soil pipes).
- Shallow bedrock localities (percussion boreholes).

An evaluation of all these water/groundwater types with respect to quality and representativeness has been discussed in Chapters 2 and 3. The main requirement for future precipitation and surface locality water sampling is tighter seasonal monitoring. This is crucial to help unravel much of the variability now observed, i.e. whether it is due to reactions and mixing and/or seasonal fluctuations? A further important point is to try and separate natural tritium and carbon isotope surface input from contamination from the nuclear power facilities.

9.4.1 Sub-surface groundwaters: Soil Pipes < 10 m depth

Figure 9-2 shows the locations of the soil pipes installed in the Simpevarp area. These are located in the overburden, some extending to the bedrock surface where the overburden is restricted, but most soil pipes are within the overburden (Figure 9-3). The objective of these soil pipes is three-fold: a) strategically selected locations to monitor the effects of nearby drilling of cored boreholes on the near-surface groundwater chemistry, b) locations (the majority) based on surface hydrology to monitor the seasonal variation of the groundwater chemistry to obtain a general overview of shallow water dynamics and chemistry, and c) localities suspected to represent recharge/discharge areas.

Groundwater composition in soil

Sampling of soil pipes has been performed since 2004 at the Simpevarp area (i.e. Simpevarp and Laxemar subareas where Ävrö and Hålö are both included). The sampling and analysis are performed four times per year to give some indication of the seasonal variation although such data are very limited. The analytical protocol is not the same for each of the different sampling occasions, and not all parameters therefore are sampled during the year.The main focus for this part of the site descriptive programme is not only to be descriptive, but: a) to provide a base for further understanding hydrogeochemical processes at the interface between the geosphere and biosphere, and b) to identify and characterise potential recharge/discharge areas by coupling hydrogeochemistry with hydrogeological parameters and geological features.

For this initial stage of the explorative evaluation of data there was only one sampling occasion of the four conducted that was adequately complete since it involved most of the sampling points. This was carried out during the autumn of 2004 (see SKB's internal controlling documents: AP PS 400-03-054, AP PS 400-05-024 and AP PS 400-04-077) and was chosen for this present

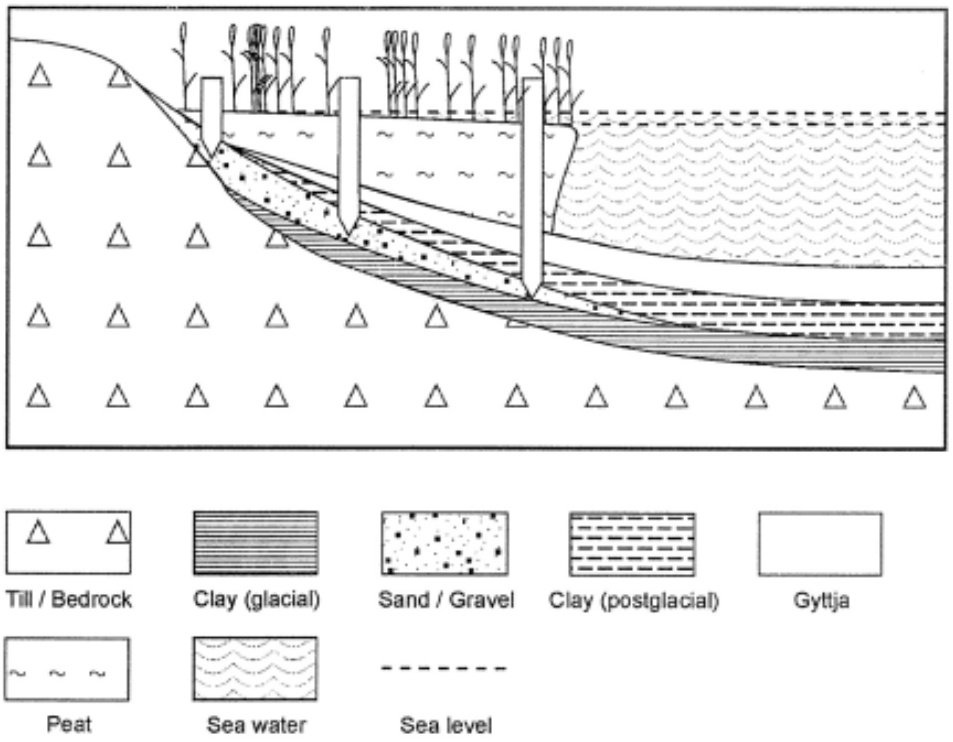

Figure 9-3. *Schematic profile showing the positioning of the soil pipes in the overburden (after Laaksoharju et al. XXXX).*

exercise to compare the different sampling points. Unfortunately there are only a limited amount of parameters and data available for evaluation, both from a hydrogeochemical and hydrological viewpoint, and most of these are located in the Simpevarp subarea whereas data from the Laxemar subarea are very limited.

Initial classification of surface waters and subsurface overburden groundwaters

This section describes the source and type data used and the evaluation approach employed.

Data used and evaluation approach

All original data used are stored in the primary databases (SICADA and/or GIS). The evaluation strategy was based on a large amount of background information which was systematically approached as follows:

a. Elevation maps showing the locations of the cored and percussion boreholes and soil pipes.

b. Regional hydrological identification of recharge/discharge areas and their relation to the locations of cored and percussion boreholes.

c. Hydrological characterisation of soil pipe locations in terms of potential recharge/discharge areas based on (b).

d. Correlation of soil pipe groundwater hydrochemistry with the hydraulically identified recharge/discharge areas; selection of areas showing a positive correlation.

e. The construction of anomalous (‘hot spot’) chemical distribution maps using the overburden soil pipe hydrochemical data.

Elevation map- sampling locations

Figure 9-4, based on topography, shows the locations of the boreholes and the soil pipes.

Regional hydrological identification of recharge/discharge areas

Figure 9-5, based on near-surface topography and hydrology, identifies which of the boreholes and soil pipes are associated with potential areas of recharge and discharge.

Hydrological and hydrochemical characterisation of soil pipe locations

Based on geological and hydrological information and the distribution of soil types in the overburden, a preliminary classification of the soil pipe data in terms of recharge/discharge could be carried out. Prior to this, however, an initial classification was conducted (data not shown) based on the hydrogeological modelling (in turn based on topography) /Werner et al. 2005/.

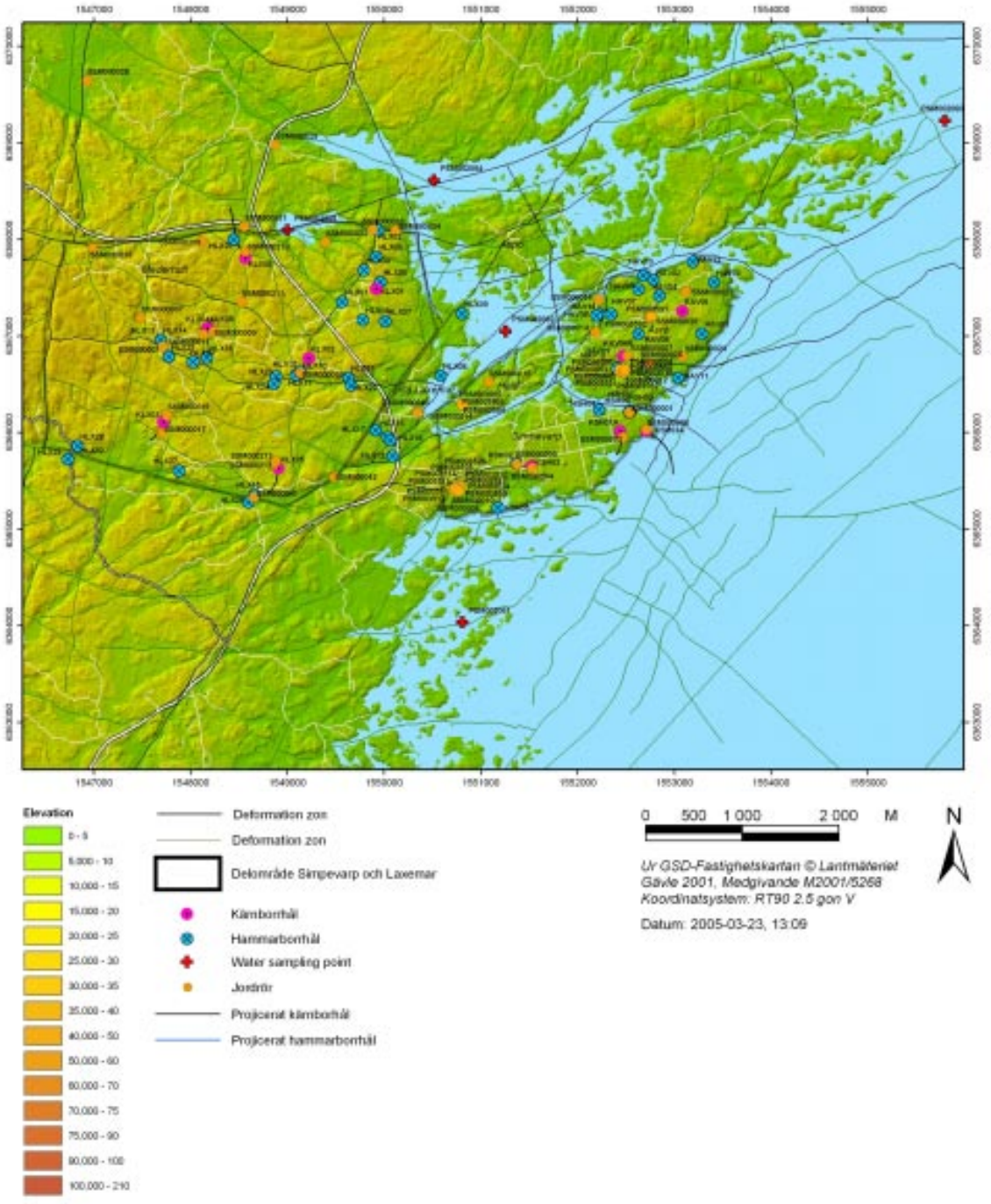

Figure 9-4. *Simpevarp area: Elevation map showing the locations of the cored and percussion boreholes and soil pipes.*

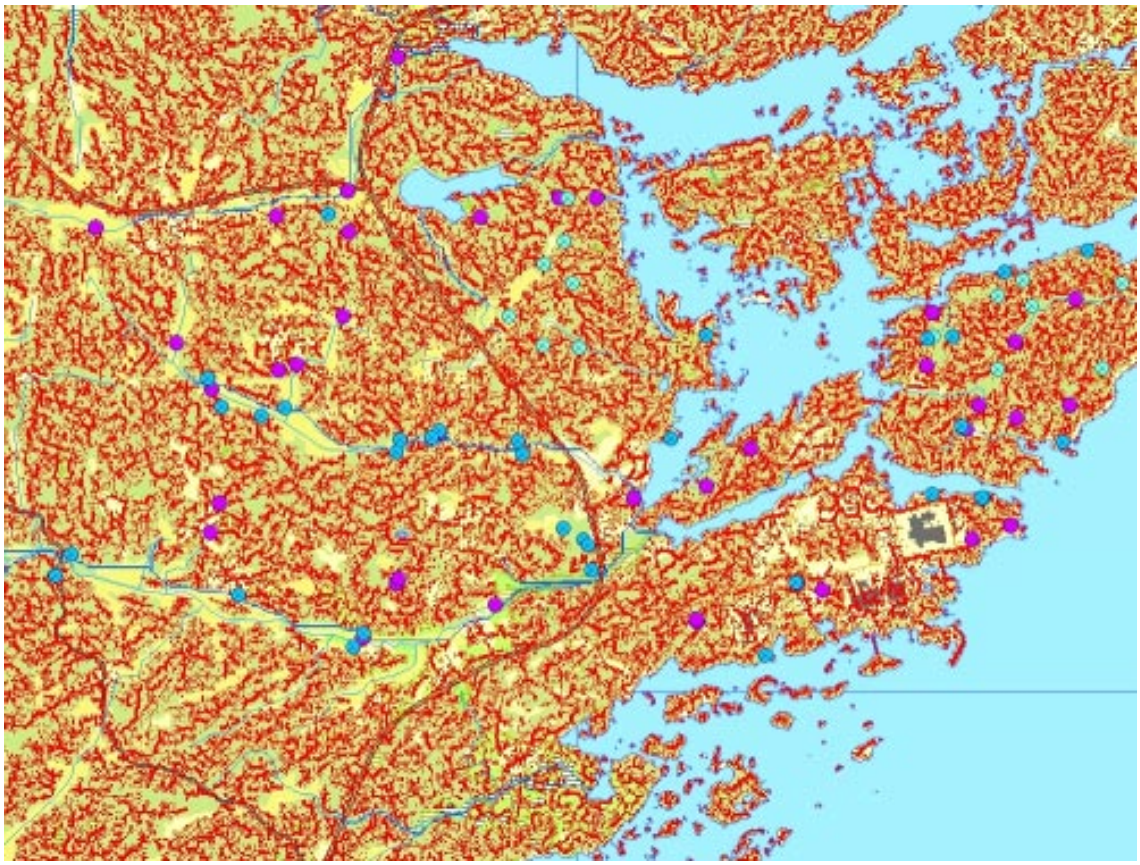

Figure 9-5. *Simpevarp area: Topographic/hydrologic-based map showing areas of potential discharge (in blue) and the location of soil pipes (purple infilled circles) and percussion boreholes (blue infilled circles). Green and yellow colouration represent intermediate areas where recharge and discharge can not be satisfactorily distinguished.*

Using the overburden soil pipe hydrochemical data a preliminary series of anomalous ('hot spot') chemical distribution maps was made (Figures 9-6 to 9-9). The available data (most of the data points) at this initial stage included only chloride (Figure 9-6), sulphate (Figure 9-7), pH (Figure 9-8) and alkalinity (Figure 9-9). In addition, some PSM pipes previously sampled during 1999 are illustrated in the figures, although only for comparison purposes. For the main Laxemar 1.2 data evaluation the chemical dataset used is that shown in Tables 9-3 and 9-4.

For the correlation of chemistry with areas of recharge and discharge, a sample series covering possible seasonal variations are required. Three samples taken during the spring, summer and autumn of 2004 were available for sampling locations SSM 08, 10, 12, 14, 18, 20, 22, 24 and 26. Of these, only SSM 12, 18 and 22 showed stable values for HCO_3 and Cl during the year. The highest levels of chloride and sulphate are found in the Simpevarp subarea in samples SSM 18 and SSM 22; alkalinity is generally high in samples SSM 22 and 12. SSM 18 in contrast shows a rather low but stable pH, which may be due to recharge but equally may also be a result of high microbial activity and organic decomposition. At local outflow and saturated conditions alkalinity is expected to be more stable over the years, which is the case, for example for SSM 22 (data not shown).

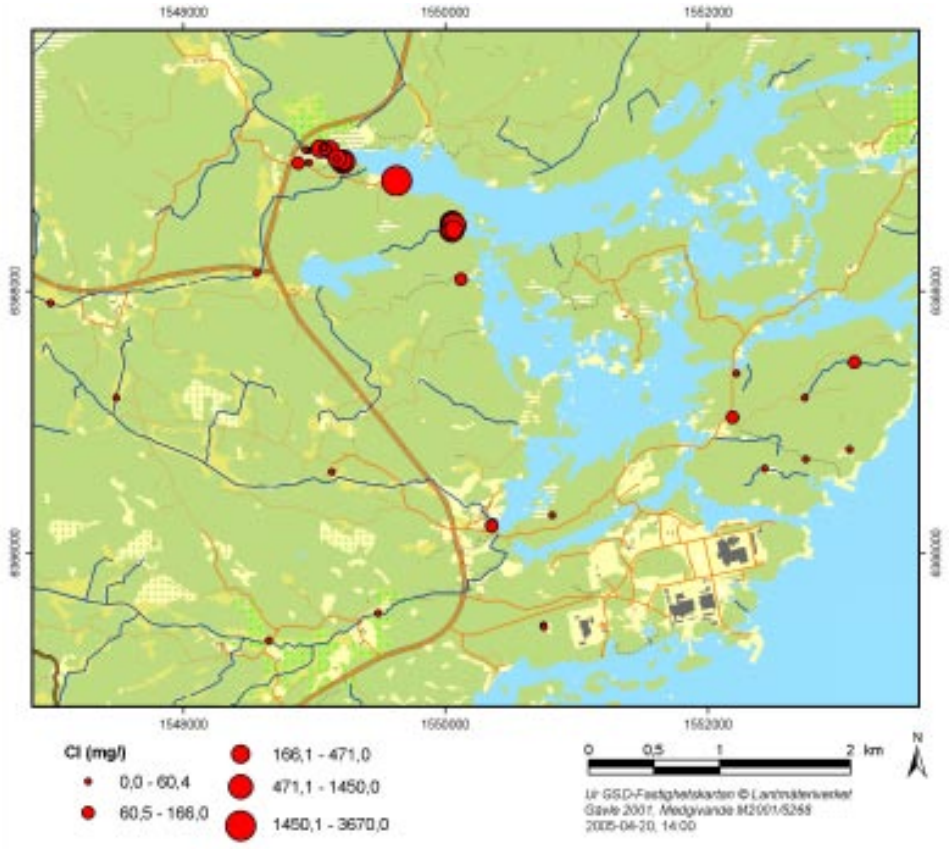

Figure 9-6. *Chloride concentration in soil pipes in the Simpevarp area.*

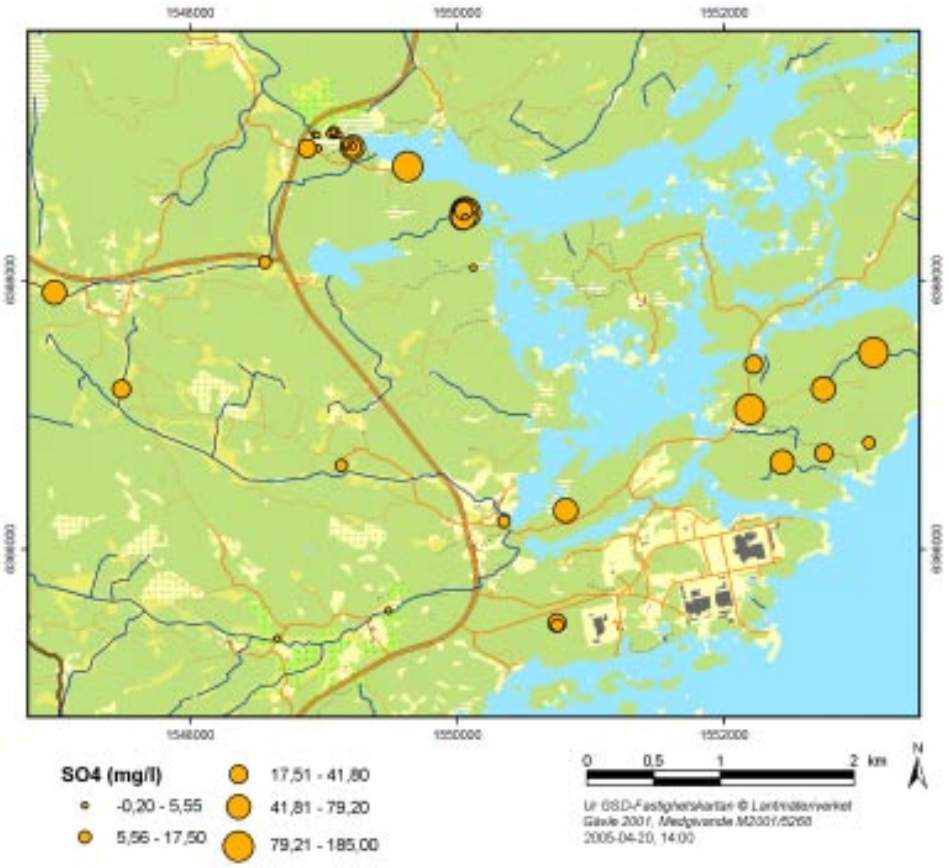

Figure 9-7. *Sulphate concentrations in soil pipes in the Simpevarp area.*

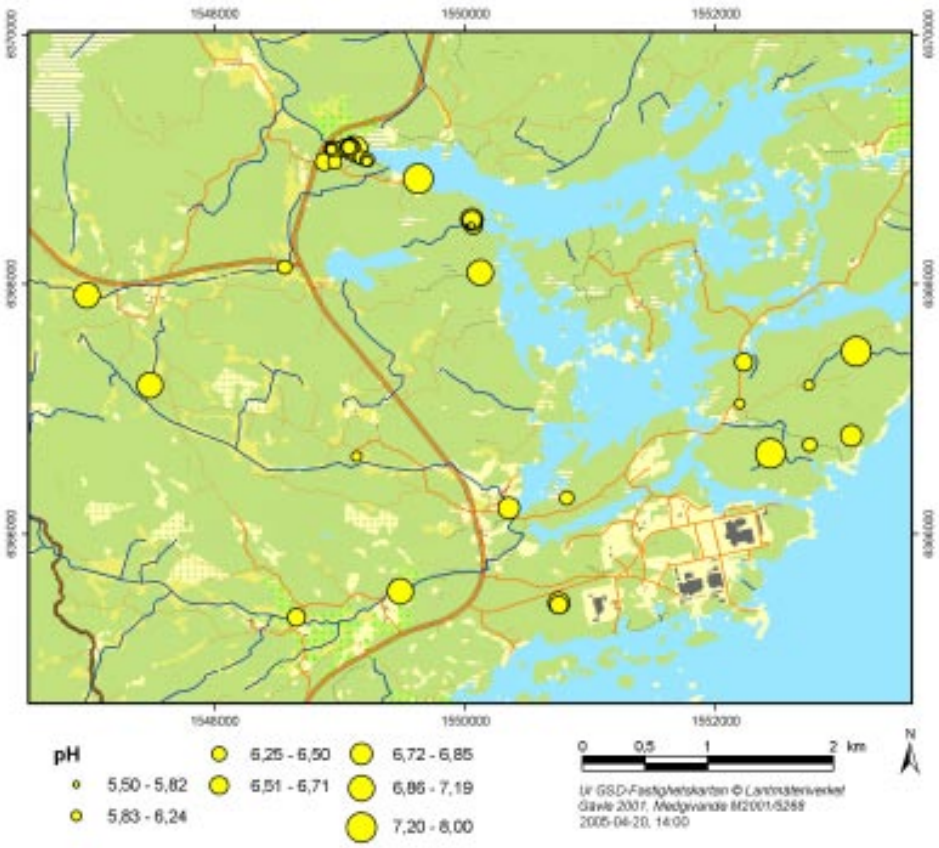

Figure 9-8. *pH in soil pipes in the Simpevarp area.*

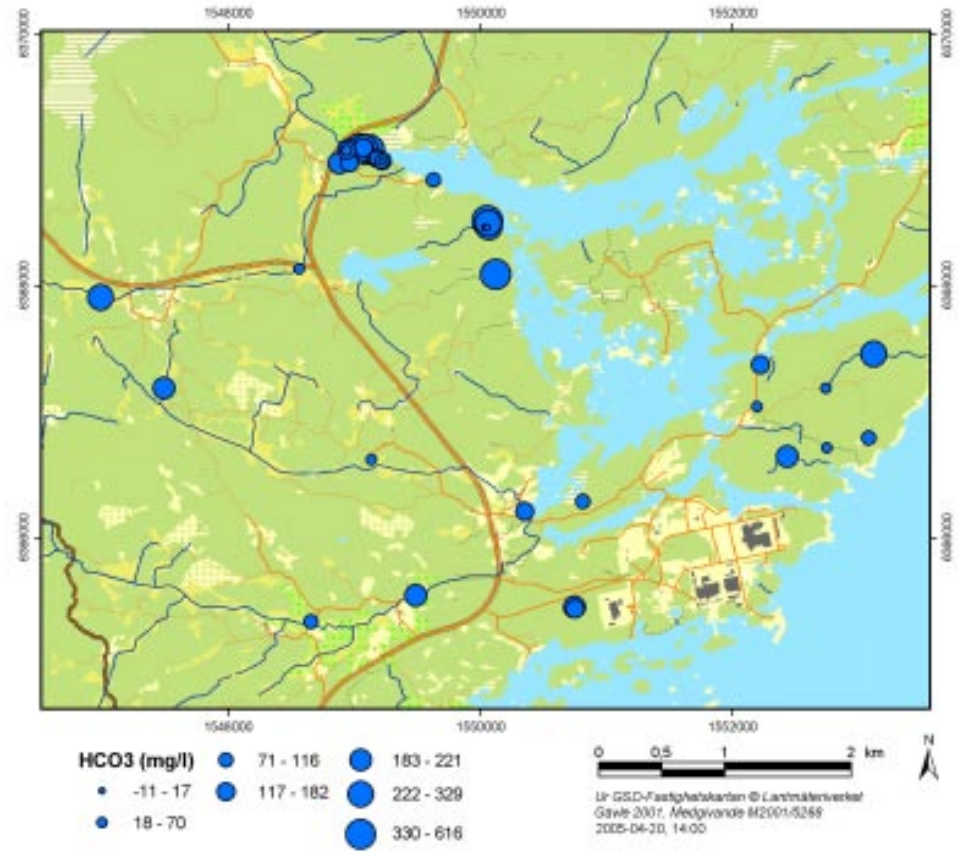

Figure 9-9. *Alkalinity in soil pipes in the Simpevarp area.*

Correlation of soil pipe groundwater hydrochemistry with the hydraulically identified recharge/discharge areas

Based on geological, hydrological and hydrochemical information and the distribution of soil types in the overburden, a preliminary classification of the soil pipe data in terms of recharge/discharge has been made (Tables 9-3 and 9-4).The localities of the different soil pipes in different zones based on the hydrogeological map (Figure 9-4) gave the first indication of the type of hydrological environment the soil pipe was located in. Combining this with the rest of the information, such as representative soil types in the overburden in conjuction with groundwater level (metre above sea level), a much improved estimate to the type of recharge/discharge environment was possible. However, when integrating the hydrochemistry, based only on the discharge/recharge map (in turn based on topography/modelling), some soil pipes were classified to the contrary. At a later stage structural information was used, for example, the distance to an identified fault zone which may influence the groundwater chemistry.

Table 9-3. Hydrological indications of groundwater recharge/discharge in the overburden hosting soil pipe monitoring instalations in the Simpevarp area.

SUBAREA	IDCODE	Topogr.In-/outflow	Environm. Setting	Deform. Zone	Geology	Soil strata dominating (in GW inlet)	Soil depth (tot)	GW inlet (screen) in soil tube	QW level in soil tube*
SIMPEVARP	**SSM000008**	**outflow**		**NE-SW**	**Fink.Dioritoid**	**boulder-rock**	**4.6**	**2.6-4.6**	**0.2**
SIMPEVARP	SSM000010	in-/outflow		NE-SW	Fink.Dioritoid	clayey gravel sand-boulders	2.0	1.4-2.4	0.3
SIMPEVARP	**SSM000012**	**outflow**		**E/SE-W**	**Ävrögranite**	**silty sandy till - boulders**	**6.1**	**4.7-5-7**	**0.6**
SIMPEVARP	SSM000014	inflow		w. NE-SW	Ävrögranite	sandy gravelly till	2.4	1.2-2.2	0.6
SIMPEVARP	SSM000016	in-/outflow		s. E-W	Ävrögranite	cobble bearing gravelly sand - boulders	2.6	1.5-2.5	1.3
SIMPEVARP	SSM000018	inflow		N/NE-SW	Ävrögranite	clayey till	3.2	1.8-2.8	0.25
SIMPEVARP	SSM000020	inflow		NE-SW	DZ*/Dioritoid	clay - gravilly sandy till	2.3	1.5-2.5	0.4
SIMPEVARP	**SSM000022**	**outflow**		**NE-SW**	**DZ-/Diorite/Gabbro**	**silty clay - silty sandy till - boulders**	**8.6**	**4.6-6.6**	**0.23**
SIMPEVARP	SSM000024	in-/outflow		n. E-W	Ävrögranite	sandy till (2.8m)	4.2	2.25-3.25	0.7
SIMPEVARP	SSM000026	in-/outflow		E-W	Ävrögranite	sandy till (2.3m)	4.2	1.8-3.8	0.2
LXM-Misterh	SSM000027	-	near village	-	Ävrögranite?	sand (1.2) - silty sand	5.0	2.8-4.8	1.4
LXM-Gäster*	**SSM000028**	**outflow**		**N-S**	**Ävrögranite**	**gyttja (1.0)**	**2.5**	**1.45-2.45**	**0.1**
LXM-Kärrsv.	**SSM000029**	**outflow**	**near seabay**	**s. WNW-ESE**	**Ävrögranite**	**silty fine sand (1.0) - ?**	**5.5**	**4.5-6.5?**	**0.6**
LAXEMAR	**SSM000030**	**outflow**	**inland stream**	**EW/Mederh**	**Ävrögranite**	**gyttja (1.2)- gravelly silty sand**	**3.8**	**2.8-3.8**	**0.4**
LAXEMAR	**SSM000031**	**outflow**	**inland stream**	**EW/Mederh**	**Qmonzodiorite**	**gravelly sandy till (0.9)**	**3.5**	**2.4-3.4**	**0.6**
LAXEMAR	SSM000032	in-/outflow	near lake	EW/Mederh	Qmonzodiorite	gyttja (0.7) - gyttja bearing clay with sand layers (0.3)	2.8	1.8-2.8	1.9
LAXEMAR	SSM000033	inflow	near sea	EW/Mederh	Ävrögranite	sandy clay (0.5) - clayey sandy till (0.3)	1.3	0.3-1.3	0.2
LAXEMAR	SSM000034	outflow?	seabed	EW/Mederh	Ävrögranite	fine sand (0.7)	4.0	2.5-3.5	0.5
LXM-Jämsen	**SSM000035**	**outflow**	**lakebed**	**?**	**?**	**sandy silty till (1.0)**	**3.5**	**2.5-3.5**	**0.5**
LAXEMAR	**SSM000037**	**outflow**	**inland stream**	**n. EW007**	**Ävrögranite**	**sandy gravelly till**	**3.8**	**2.65-3.65**	**1.3**
LAXEMAR	SSM000039	in-/outflow	inland	EW007	Ävrögranite	sandy till (1.8)	4.2	2.4-4.4	3.0
LAXEMAR	SSM000040	in-/outflow	seabed	s EW007 SW-NE	Ävrögranite	peat (1.5) - silty sandy till	2.3	1.1-2.1	0.2
LAXEMAR	**SSM000041**	**outflow**	**inland stream**	**EW/South**	**Qmonzodiorite/dioritoid**	**sandy clayey silt (1.8) - sandy silty till (1.2)**	**3.8**	**1.2-3.2**	**1.2**
LAXEMAR	**SSM000042**	**outflow**	**inland stream**	**EW/South**	**Ävrögranite**	**gravelly sand(0.8) - silty sandty till (1.5) - rock/boulders(0.7)**	**4.5**	**2.2-4.2**	**1.5**
DF ~deformation zone									
* ~ date differs from gw.sampling (see Johsson and Adestam, 2004)									

Table 9-4. Hydrochemical indications of groundwater recharge/discharge in the soil strata hosting soil pipe monitoring instalations in the Simpevarp area.

SUBAREA	IDCODE	Topogr.In-/outflow	Top soil <0.5 m - underlaying soil ¨<1m	nearby percussion bore hole	pH	HCO3 (mg/l)	Cl (mg/l)	SO4 (mg/l)	FeTOT (mg/l)	Fe2+ (mg/l)	Fe/S04	NH4_N (mg/l)
SIMPEVARP	**SSM000008**	**outflow**	**sandy clay**		**6,64**	**163**	**4,0**	**9,53**	**0,746**	**0,717**	**0,075**	**0,008**
SIMPEVARP	SSM000010	in-/outflow	silty clay		6,85	185	4,7	22,30	1,080	0,960	0,043	0,022
SIMPEVARP	**SSM000012**	**outflow**	**sand**		**7,63**	**204**	**16,5**	**71,30**	**2,840**	**2,740**	**0,038**	**0,169**
SIMPEVARP	SSM000014	inflow	gravelly sand		6,45	93	12,7	58,80	6,790	5,660	0,096	0,100
SIMPEVARP	SSM000016	in-/outflow	gravelly sand		6,55	137	3,5	21,00	4,160	2,930	0,140	0,003
SIMPEVARP	SSM000018	inflow	clay		5,98	46	112,0	185,00	0,552	0,357	0,002	0,051
SIMPEVARP	SSM000020	inflow	peat		6,22	64	3,7	56,50	1,870	1,660	0,029	0,018
SIMPEVARP	**SSM000022**	**outflow**	**peat**		**7,94**	**276**	**154,0**	**136,00**	**0,187**	**0,176**	**0,001**	**0,835**
SIMPEVARP	SSM000024	in-/outflow	boulder gravelly cobbly sand		6,79	93	7,1	14,50	2,000	1,810	0,125	0,033
SIMPEVARP	SSM000026	in-/outflow	gravelly sand		6,40	70	5,7	27,40	4,760	4,050	0,148	0,117
LXM-Misterh	SSM000027	-	top soil - peat (0.9)		5,82	17	7,4	21,40				
LXM-Gäster*	**SSM000028**	**outflow**	**gyttja bearing peat**									
LXM-Kärrsv.	**SSM000029**	**outflow**	**peat, gyttja**		**6,67**	**191**	**85,7**	**21,90**	**8,330**	**8,360**	**0,382**	**0,614**
LAXEMAR	**SSM000030**	**outflow**	**humus bearing peat (0.8)**	**-**	**7,19**	**257**	**15,9**	**45,80**	**1,790**	**1,770**	**0,039**	
LAXEMAR	**SSM000031**	**outflow**	**peat - gyttja bearing peat**	**HLX20**	**6,39**	**46**	**5,3**	**11,00**	**5,410**	**5,290**	**0,481**	**0,044**
LAXEMAR	SSM000032	in-/outflow	peat (0.4) - gyttja (0.7)	HLX04?								
LAXEMAR	SSM000033	inflow	peat	HLX02								
LAXEMAR	SSM000034	outflow?	peat - gyttj (0.6)	HLX02	6,92	546	136,0	-0,20	7,140	6,930		0,258
LXM-Jämsen	**SSM000035**	**outflow**	**top soil w. boulders (0.7)- silt (1.3)**	**-**	**6,71**	**87**						
LAXEMAR	**SSM000037**	**outflow**	**sandy topsoil - humus- cobble bearing gravelly sand**	**HLX13?, 14**	**6,94**	**221**	**15,9**	**24,30**	**5,810**	**4,920**	**0,202**	**0,221**
LAXEMAR	SSM000039	in-/outflow	sandy topsoil	HLX10-12;21-24	6,24	65	4,0	17,50	1,780	1,490	0,085	0,007
LAXEMAR	SSM000040	in-/outflow	peat w detritus - gyttja bearing peat w detritus	-	6,83	182	141,0	8,18				
LAXEMAR	**SSM000041**	**outflow**	**sandy ts - gravelly sand (0.8)**	**HLX15,26**	**6,60**	**116**						
LAXEMAR	**SSM000042**	**outflow**	**humus-boulder bearing gravelly sand**	**HLX16-19**	**6,97**	**200**						

Summary of the Soil Pipe data evaluation

The basic idea to evaluate the near-surface groundwater has been to identify the input chemistry of recharging water entering into the deep aquifer and also to increase understanding of the interaction between deep and shallow groundwaters during discharge. In order to accomplish this, the identification of discharge/recharge areas is vital.

A methodology has been outlined that involves two main steps:

- Provide a GIS model based on topography, together with additional information from the bedrock (including deformation zones) and soil types, to gain an overall understanding of the surface hydrogeology.
- Initial identification of recharge/discharge areas which are then compared (and revised) using groundwater chemical data from the soil pipes.

Unfortunately the available hydrochemical information from the soil pipes is largely restricted to the Simpevarp subarea with most of the samples from the Ävrö island. In addition, time series data of groundwater samples are only available for 10 sampling points, and most showed large variations in HCO_3, Cl and SO_4 during the sampling period. However, three soil pipes showed stable values (SSM 12, 18 and 22). A large annual variation may indicate a typical recharge setting but may also indicate changes from discharge to recharge.

In contrast stable conditions may indicate discharge, especially when combined with low tritium and ^{14}C contents, as is the case with SSM 22. In other cases when tritium indicated recent groundwater, it may be an indication of a more shallow discharge, alternatively slow recharge.

9.4.2 Shallow bedrock groundwater: Percussion boreholes (0–200 m)

The percussion boreholes are mostly sampled from the entire borehole and mixing of different groundwaters is therefore unavoidable. However, usually most of the groundwater emanates from only one or two specific fractures of higher transmissivity and such information (e.g. recorded measurements of hydraulic flow) was available for some of the boreholes. This contributed significantly to further understanding the shallow groundwater systems (0–200 m deep). Figure 9-4 shows the location of the percussion boreholes in the Simpevarp area. It should be noted that the percussion boreholes data also include the initial percussion drilled lengths of the major deep-cored boreholes which are now cased, normally to around 200 m.

Data used

When available, the following background data were used:

- Geophysical logs (BIPS, resistivity, fracturing).
- Recorded observations of hydraulic flow.
- Hydraulic tests and flow measurements.
- Hydraulic conductivity and transmissivity.

Using this information the hydrochemical data were, when possible, allocated to the following arbitrarily selected shallow depth intervals: 0–25 m, 25–50 m, 50–75 m, 75–100 m, 100–150 m, 150–200 m and 200–250 m. Selected ion and isotopic plots versus depth then were produced (see Appendix 2). The data were plotted (e.g. Figures 9-10 to 9-12) to identify any shallow groundwater trends that might, together with the Soil Pipe evaluation, give some indication of recharge/discharge features.

Data evaluation

From Figures 9-10 and 9-11 it was possible to detect hydrochemical trends when there were adequate data to cover the depth intervals. In most cases, however, there was only one data value which represented a borehole length 0–100 m or even 0–200 m. In these cases, all the values are the same for each depth interval since there was no indication of where the major groundwater source was located along the borehole.

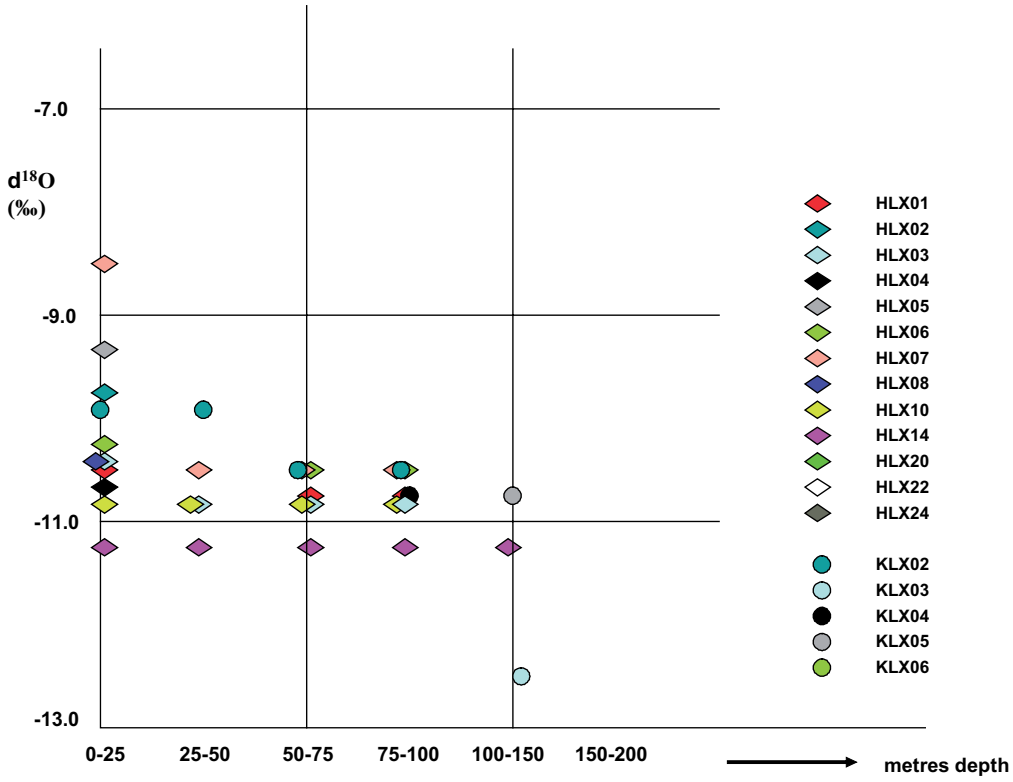

Figure 9-10. *Plot of $\delta^{18}O$ (‰ SMOW) versus depth for the Laxemar subarea.*

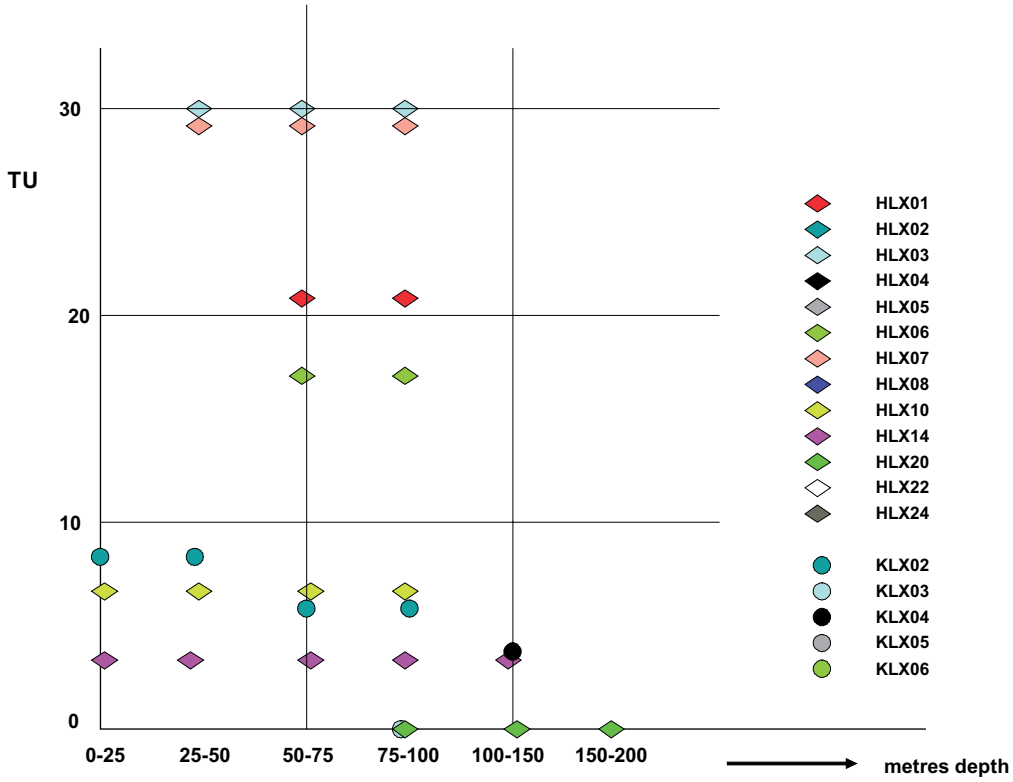

Figure 9-11. *Plot of tritium (TU) versus depth for the Laxemar subarea.*

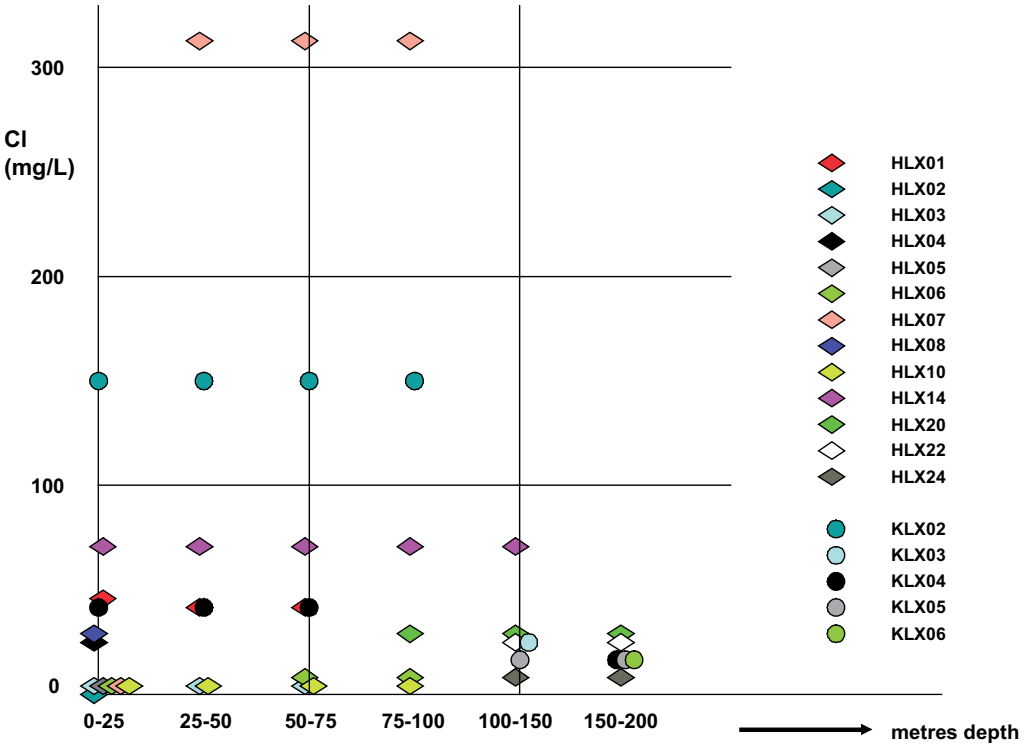

Figure 9-12. *Plot of chloride versus depth for the Laxemar subarea.*

Figure 9-10 shows the spread in $\delta^{18}O$ values in the most shallow groundwaters, but at 50 m there is a narrowing in range which persists to greater depths. This reduced range ($\delta^{18}O$ = –10.9 to –10.6‰ SMOW; HLX14 is excluded since the depth origin is unknown) is therefore most characteristic for the upper bedrock groundwaters and potentially may be useful as an input end member. Figure 9-11 shows the spread in tritium values with normal, recent input contents (around 7 TU) into the upper bedrock. The anomalously high tritium contents (15–30 TU) registered by boreholes HLX03, HLX07, HLX01 and HLX06 may indicate local discharge of groundwaters which date back to the 1950's and influenced by nuclear test fallout. Significantly borehole HLX07 also records higher than normal chloride values (Figure 9-12) which adds further support that this location may be a discharge locality in the Laxemar subarea. Alternatively and more probably for HLX01 and HLX06, showing lower tritium values, the recorded levels may be representative for rapid recharge precipitation at the time of collection and analysis in 1987. HLX03 with higher tritium is most probably the same.

Summary and integration of the soil pipe and percussion borehole data

Figure 9-13 underlines the areas where the percussion and soil pipe data can be used to support the recharge/discharge evaluations from the Soil Pipe data.

The data can be summarised as follows:

Laxemar site high tritium area

- Comprises HLX01, 03, 04, 05, 06 and 07
- HLX01, 03, 06 and 07 are high in tritium (HLX03/07 ~ 25–30 TU; HLX01/06 ~ 16–20 TU). Higher tritium in HLX01/06 (and HLX03) may simply reflect rapid recharge precipitation ranges when the groundwaters were collected and analysed in 1987.
- HLX07 is anomalous compared to the rest, showing:
  - Enhancement of Na, Ca, Mg, Cl, SO_4 (also HLX01).
  - Decrease in HCO_3.

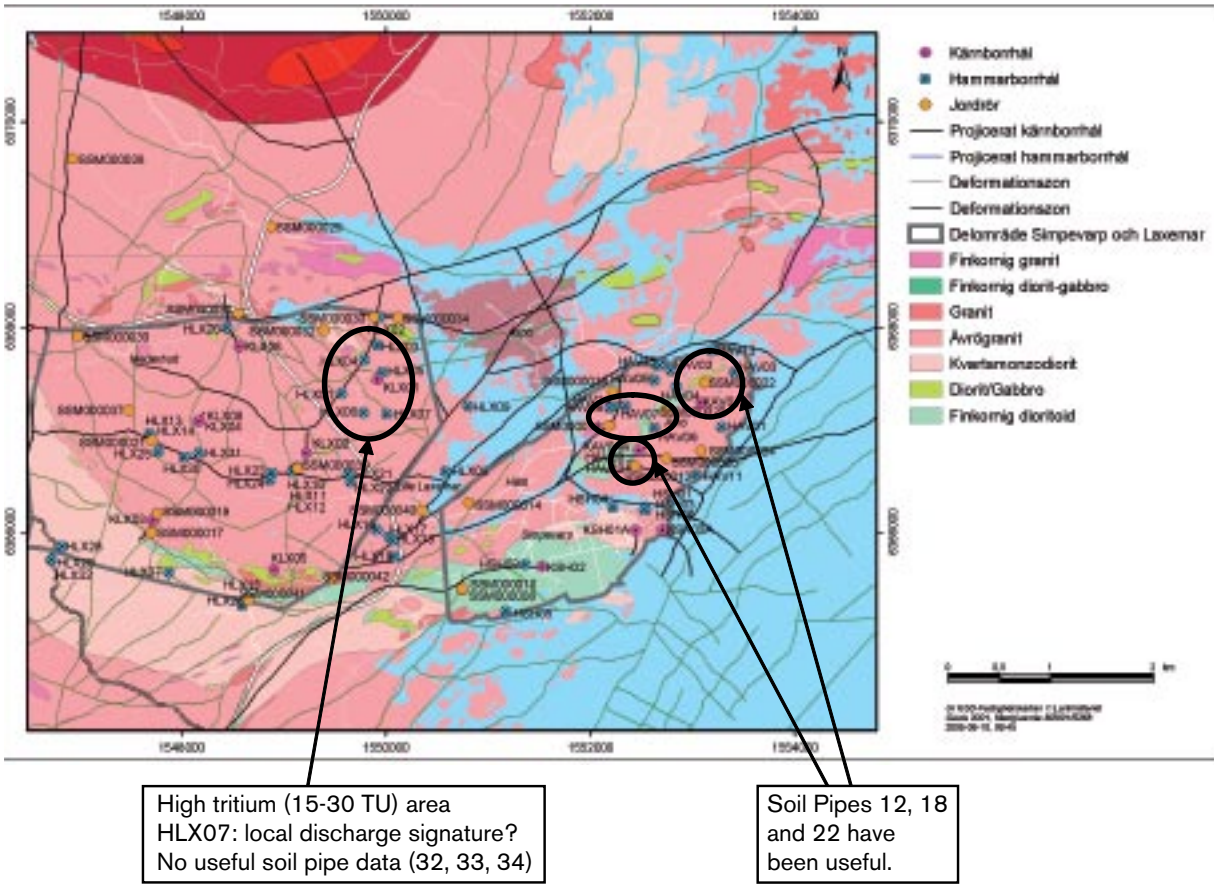

Figure 9-13. *Figure illustrating two important areas where the Soil Pipe and Percussion Borehole groundwater data have been useful.*

- Soil pipes 32, 33 and 34 are nearby but inadequate data for comparison.
- Possible indication of local recharge/discharge with residence times of ~ 50 years, i.e. since nuclear tests in the 1950's.

Ävrö site area

- Comprises boreholes HAV04, 05, 06, 07, 09, 10, 11, 12, 13, 14 and KAV 01, 04A.
- Soil Pipe 22 has been identified as a possible discharge location (e.g. low tritium and ^{14}C; 154 mg/L Cl; little seasonal variation in chemistry = deeper discharge?).
- HAV03 is located close by but there are a lack of data; the KAV01 data are not considered representative; HAV04 shows trends largely similar to Soil Pipe 22, thus supporting a deeper discharge location.
- Soil Pipe 18 may also be a possible discharge location (112 mg/L Cl; significant seasonal variation = shallow discharge?).
- HAV06, 07 are located close by Soil Pipe 18 and show similar shallow discharge trends; HAV14 lacks data.
- Soil Pipe 12 may be a possible recharge location (16.5 mg/L Cl; little seasonal variation = slow recharge from overburden?). This recharge is supported by nearby HAV10 and KAV04A.
- However HAV09 differs significantly, representing a more saline, deeper water? The resolution of the groundwater source is not known – anything from 0–150 m depth.

Simpevarp site area

- Comprises boreholes HSH02, 03, 04, 05, 06 and KSH01, 02, 03A.
- KSH02 and HSH02 are some distance from the Baltic Sea and show recharge features; the shallower HSH02 waters show higher tritium and lower SO_4.
- KSH01A and HSH03 close to the coast differ markedly due to KSH01A representing a much deeper groundwater source (150–200 m). HSH03 suggests recent recharge features.
- KSH03A at the coast shows generally local? recharge features.
- HSH05, also at the coast can not be assessed because of inadequate data.
- HSH04 and HSH05 record enhanced Mg (~ 180 and 115 mg/L respectively); this is considered to be due to the close proximity of the Baltic Sea.

9.5 Recommended issues for Laxemar 2.1

This preliminary evaluation has underlined the lack of suitable groundwater data from the Soil Pipe and percussion boreholes to make a thorough assessment of the surface/near-surface groundwater environment. Some of the most important issues requiring additional input are:

- Seasonal monitoring of strategically located soil pipes and percussion boreholes in conjunction with hydrogeological expertise.
- Future percussion boreholes should be initially sampled in greater detail (e.g. at 25 m intervals) and packer isolation installed for long-term monitoring.
- Improved groundwater analysis (e.g. class 4, including redox sensitive elements, organics and environmental isotopes).
- Tritium distribution – need for regional reference sampling points to assess potential surface extent of emissions from the nuclear facilities.
- Tritium distribution – need to resample existing percussion boreholes and soil pipes, at least those strategically located within or close to identified recharge/discharge areas.
- Mineralogical and geochemical studies of host overburden material.

10 Pore water studies of Borehole KLX03

In crystalline rocks the pore water resides in the low-permeability zones between the water-conducting zones related to regional or local fracture networks. Depending on the residence time of water in the water-conducting zones interaction with the water present in the pore space of the low-permeability zones might become significant. In addition, the pore water present in the low-permeability zones will be the first to interact with any artificial construction made in such zones (i.e. repository). For safety assessment considerations it is therefore important to know the composition of such pore water and its evolution over the last thousands to hundreds of thousands of years. The latter can be assessed by combining the information gained from pore water profiles through the a low-permeability zone with the chemical and isotopic data of water circulating in the fractures.

Pore water that resides in the pore space between minerals and along grain boundaries in crystalline rocks of low permeability cannot be sampled by conventional groundwater sampling techniques and therefore has to be characterised by applying indirect methods based on drillcore material. Such indirect methods only deliver parts of the pore water composition and several complementary methods have to be applied. In addition, indirect methods might get subjected to different types of processes such as water-rock interactions during the experiment, stress release of the rock occurring during drilling possibly leading to contamination by drilling fluid and also affecting the derivation rock porosity values. All such processes might cause the obtained results to deviate from in situ conditions. For the quantitative pore water characterisation such processes need to be evaluated and possibly corrected for. Great care was taken to avoid such problems or, at least further understand the repercussions.

Accessible, interconnected pore water has been extracted successfully by laboratory out-diffusion methods using drillcore samples from borehole KLX03 as part of the Laxemar hydrogeochemical site investigation programme. The objective was to characterise these waters chemically and isotopically and relate these data to the present and past groundwater evolution of the site. In addition, the method of extraction, together with interfaced measurements of interconnected porosity, provides the opportunity to derive diffusion coefficient values of potential use in predicting future rates of solute transport. All analytical data are tabulated in Appendix 3.

The samples from borehole KLX03 investigated for their pore water composition are listed in Table 10-1. Besides the sample depth the table also gives the major geological features such as rock type, and qualitative descriptions of the rock alteration and fracture frequency in the near-vicinity of the samples. Such information is required for the interpretation of the acquired data with respect to chemical reactions that occur during the experiments and the extent of in situ interaction between pore water and fracture groundwater. The complete analytical protocol was performed on 10 out of the 16 samples listed based on their occurrence with respect to lithology, rock alteration and fracture intensity.

Table 10-1. KLX03 borehole: list of samples used for pore-water studies and their major geological features.

Sample No	SKB Sample No	Average vertical depth (m)	Major lithology	Alteration/ tectonisation[1)]	Fracture intensity
KLX03-1	SKB 007250	159.22	Avrö granite	± 5 m	moderate
KLX03-2	SKB 007251	202.66	Avrö granite	± 5 m	moderate
KLX03-3	SKB 007252	253.72	Avrö granite	± 5 m	moderate
KLX03-4	SKB 007423	303.10	Avrö granite	± 10 m	moderate
KLX03-5	SKB 007424	355.66	Avrö granite	± 10 m	moderate
KLX03-6	SKB 007425	411.70	Avrö granite	± 10 m	moderate
KLX03-7	SKB 007426	462.76	Avrö granite	± 5 m	moderate
KLX03-8	SKB 007427	524.63	Avrö granite	± 20 m	weak
KLX03-9	SKB 007428	590.12	Avrö granite	± 20 m	weak
KLX03-10	SKB 007429	643.14	Avrö granite	± 10 m	moderate
KLX03-11	SKB 007430	695.95	Qtz-monzodiorite	± 1 m	high
KLX03-12	SKB 007431	803.21	Qtz-monzodiorite	± 1 m	very high
KLX03-13	SKB 007432	841.15	Qtz-monzodiorite	± 15 m	weak
KLX03-14	SKB 005349	894.53	Qtz-monzodiorite	± 5 m	weak
KLX03-15	SKB 005351	942.47	Qtz-monzodiorite	± 20 m	weak
KLX03-16	SKB 005352	979.78	Qtz-monzodiorite	± 15 m	weak

[1)] Approx. distance to next major alteration zone above or below the sample.

10.1 Rock Porosity

The characterisation of pore water in rocks of very low permeability requires knowledge of a porosity value. This is simply because the necessary indirect methods all include a dilution of the in situ pore water present. However, different porosity measurements deliver different types of porosity that are not all appropriate for pore water characterisation, but necessary to evaluate possible deviations of the porosity in the rock sample at the surface from that in situ. Thus, the definitions and nomenclature of the different types of porosity follows those given in /Smellie et al. 2003/ in that the *physical porosity* describes the ratio of total void volume to the total volume of rock (calculated from bulk and grain density), the *connected porosity* is described by the water-content porosity obtained from gravimetric water-loss measurements and the diffusion porosity is determined by diffusion experiments, in this case the isotope diffusive exchange method.

The difference between porosity values measured in the laboratory and those in situ aside from the analytical uncertainty, may be due to desaturation of the rock sample which might occur during sample recovery and handling. This was investigated by comparing the mass of the rock samples before and after the out-diffusion experiments (see below). In addition, the rock sample might suffer stress release due to retrieval from great depth. This was investigated by the isotope diffusive-exchange method which revealed a water-content porosity independent of stress release and, under favourable conditions, a diffusion porosity for water.

The results of the various porosity measurement are given in Tables A1, A2, and A3 (see Appendix 3). All samples were saturated upon their arrival in the laboratory. This was indicated by equal weights of the large-scale samples measured immediately after arrival at the laboratory and again after termination of the out-diffusion experiments (Figure 10-1).

The water content, WC, was obtained by gravimetric measurement of the weight loss, by drying the samples at 105°C to stable weight conditions. Where possible, the water content was determined for each sample on three subsamples to account for effects of the textural heterogeneity of the rocks. Drying time varied depending on the sample size and lasted as long as 170 days. The loss of weight with time of the non-fractured samples describes a diffusion-type curve suggesting that the loss of the pore water occurs mainly by diffusion as shown in Figure 10-2.

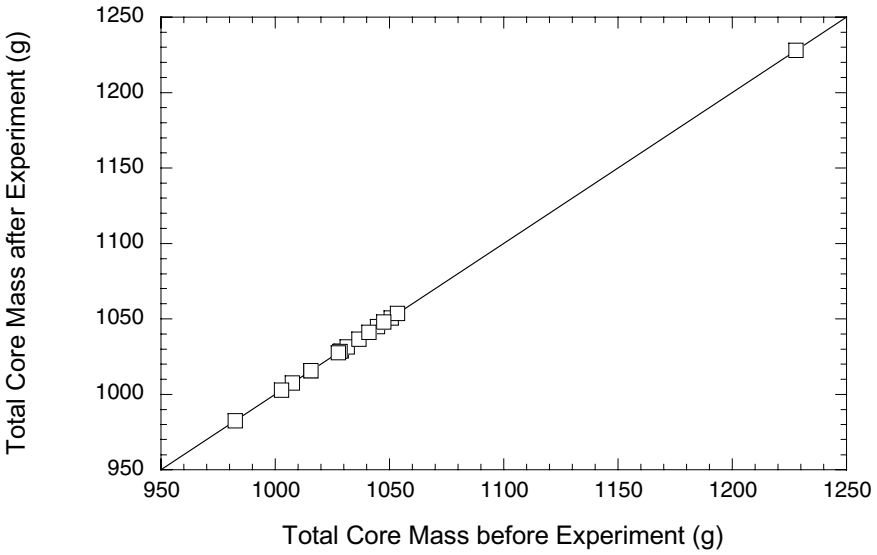

Figure 10-1. *Weight of samples used for out-diffusion experiments before and after the experiment. The identical weights indicate saturation of the sample at the time of arrival in the laboratory (error ± 0.002 g).*

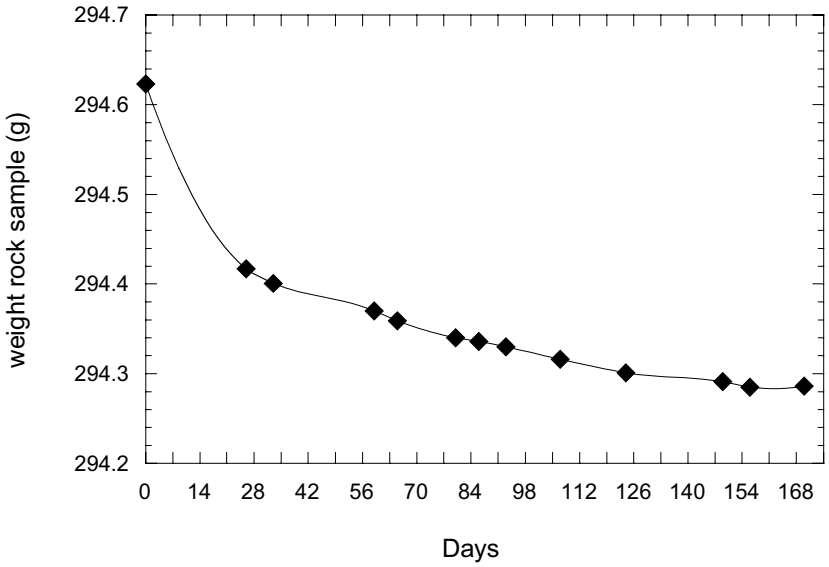

Figure 10-2. *Weight loss of sample KLX03-11 as a function of time. Initial saturated weight of the sample was 294.623 g; stable weight conditions were achieved after 170 days of drying at 105°C at 294.286 g (error ± 0.002 g).*

The most remarkable change in water content, and therefore in the water-content (or connected) porosity, occurs with the change in lithology from Avrö granite to quartz-monzodiorite (Figure 10-3). In the Avrö granite down to 620 m depth the water content and water-content porosity show a rather large variation with average values of 0.252 ± 0.074 wt.% and 0.71 ± 0.20 Vol.%, respectively. In the quartz-monzodiorite a more homogeneous distribution with depth is observed with the exception of one sample from a strongly tectonised interval (sample KLX03-12 at 803 m depth). Water content and water-content porosity are less than half of those of the Avrö granite with average values of 0.117 ± 0.065 wt.% and 0.32 ± 0.18 Vol.%, respectively.

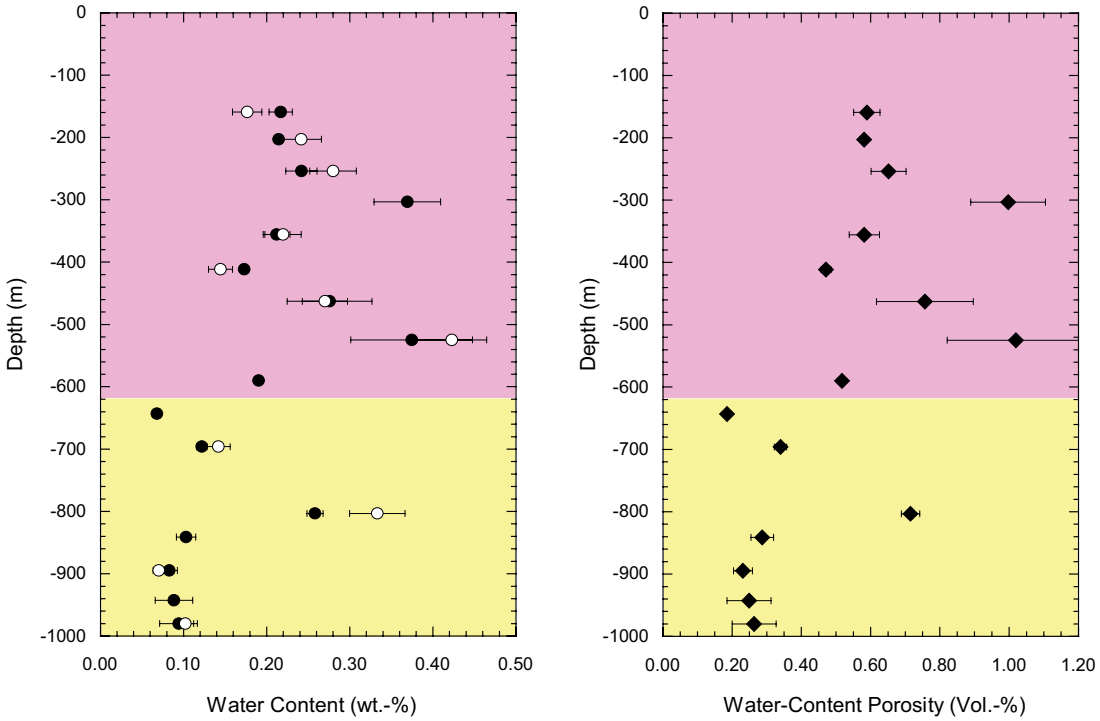

Figure 10-3. *Borehole KLX03: Water content (left) derived by drying (closed symbols) and by isotope diffusive exchange (open symbols) and water-content porosity (right) of drillcore samples as a function of depth. Note the change with changing lithology at about 620 m depth from Avrö granite (above; lilac colour) to quartz-monzodiorite (below; yellow colour).*

The water content of the rocks was also determined by the isotope diffusive-exchange method /Rübel et al. 2002/. In this method the oxygen and deuterium isotopes of the pore water are equilibrated over the vapour phase in a closed system with two test solutions of known isotopic composition. Using mass balance calculations the isotopic composition of the pore water (see below) and the water content can be calculated. The advantage of this method is that the rock sample does not have to be immersed into the test solution as with many other diffusive exchange experiments. As can be seen from Figure 10-3 the water contents derived by the isotope diffusive-exchange method agree well with those derived by drying and reflect the same differences between the different lithologies. The agreement between the two independent methods supports the fully saturated state of the sample upon arrival in the laboratory since desaturation would affect the two measurements in different ways.

10.2 General chemical characteristics of the pore water

The chemical composition of the pore water was determined by applying out-diffusion experiments. In these experiments a core sample of about 1 kg was placed in a vapour-tight PVC-cylinder and immersed in a test water of known composition. The pore water was allowed to exchange with the test water until steady state conditions between the two solutions were reached. This was tested by analysing the test water for chloride at regular time intervals. Steady state with respect to chloride was normally reached after about 90 days.

The low porosity and consequently low pore water content of the Avrö granite and quartz-monzodiorite requires the the use of relatively large rock samples for out-diffusion experiments in order to obtain: a) a reasonable amount of pore water and thus detectable chemical and isotopic signals, b) an optimised ratio of pore water to experiment solution in order to minimise the analytical uncertainties, and c) to account for the heterogeneity of the rock texture.

Strictly speaking, out-diffusion experiments only deliver direct information about chemically conservative elements of the pore water due to the inevitable interactions between rock and test water during the experiment. For the reactive components geochemical modelling strategies have to be applied to correct for the interaction. The more mineralised a pore water is, however, the more the observed elemental concentrations in the final experiment solution will be dominated by those prevailing in the pore water compared to the contributions of mineral dissolution reactions. Thus, the chemical composition of the experiment solution can also reveal certain indications about general chemical trends in the pore water before applying geochemical modelling.

In the Avrö granite the chemical type of experiment solutions changes from dilute Na-HCO_3 waters to more mineralised Na-Ca-SO_4-Cl waters towards the base of the granite at about 600 m depth (Figure 10-4). There are no indications that the mineral sulphide content in the granite varies strongly with depth and it appears that this trend reflects actual differences in the pore water. The chemical composition of the experiment solution from the quartz-monzodiorite displays a mineralisation intermediate between that of the Avrö granite and is generally of a Na-Ca-HCO_3-Cl type with chloride increasing with depth of sample. A high chloride concentration is obtained for one sample coming from a strongly tectonised interval at around 800 m depth (sample KlX03-12).

The chemistry of the experiment solutions in combination with the geological occurrence of the samples therefore suggest for the pore water: a) a possible stratification of the pore waters as a function of depth, and b) a dependence on rock type and fracture intensity.

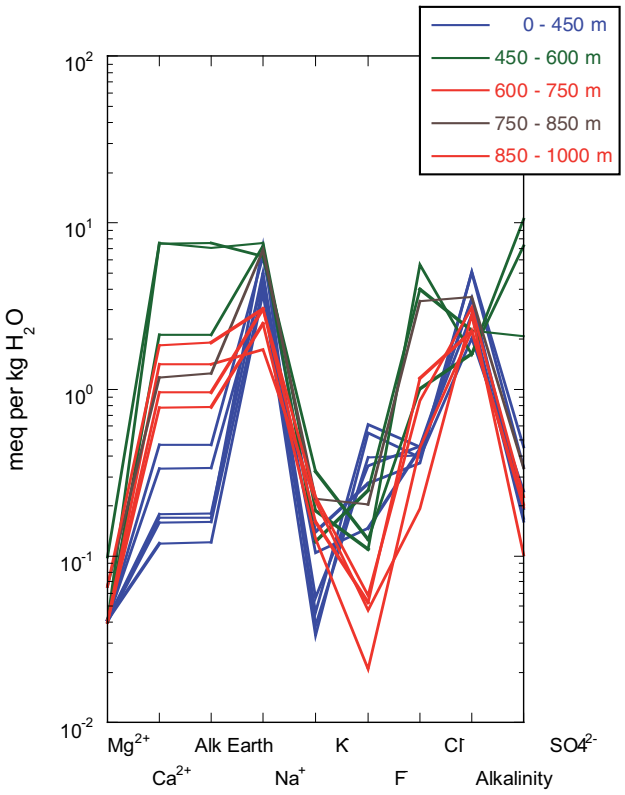

Figure 10-4. *Schoeller diagram of experiment solutions from the samples of drillcore KLX03 suggesting differences in chemical type and degree of mineralisation as a function of depth.*

10.3 Chloride concentration of the pore water

The non-reactive behaviour of chloride and the non-destructive nature of the out-diffusion experiments, for example which contrast with crush/leach aqueous extraction techniques, make the pore water the only source for dissolved chloride in the experiment solution. Therefore, the chloride concentration of the experiment solution can be converted to pore water concentrations using mass balance calculations given that steady state conditions in the out-diffusion experiment are achieved. Obviously, the analysed Cl concentrations have to be corrected for the volumes and concentrations of experiment solution that have been systematically removed during the experiment.

The derived chloride concentrations of the pore waters are shown in Figure 10-5 as a function of sample depth. The chloride concentration in the pore water of the Avrö granite is below 1,000 mg/kgH_2O down to about 450 m depth and increases then to about 9 g/kgH_2O towards the base of the granite. Chloride concentrations in the pore water of the quartz-monzodiorite are variable at the top and become rather constant between 4 to 5 g/kgH_2O at greatest depth. The concentration pattern of pore water chloride shown with depth generally correponds to the hydraulic transmissivity measured in the borehole (Figure 10-5). Low concentrations occur in the depth intervals with elevated transmissivity whereas high concentrations are observed in the intervals with very low transmissivty independent of rock type.

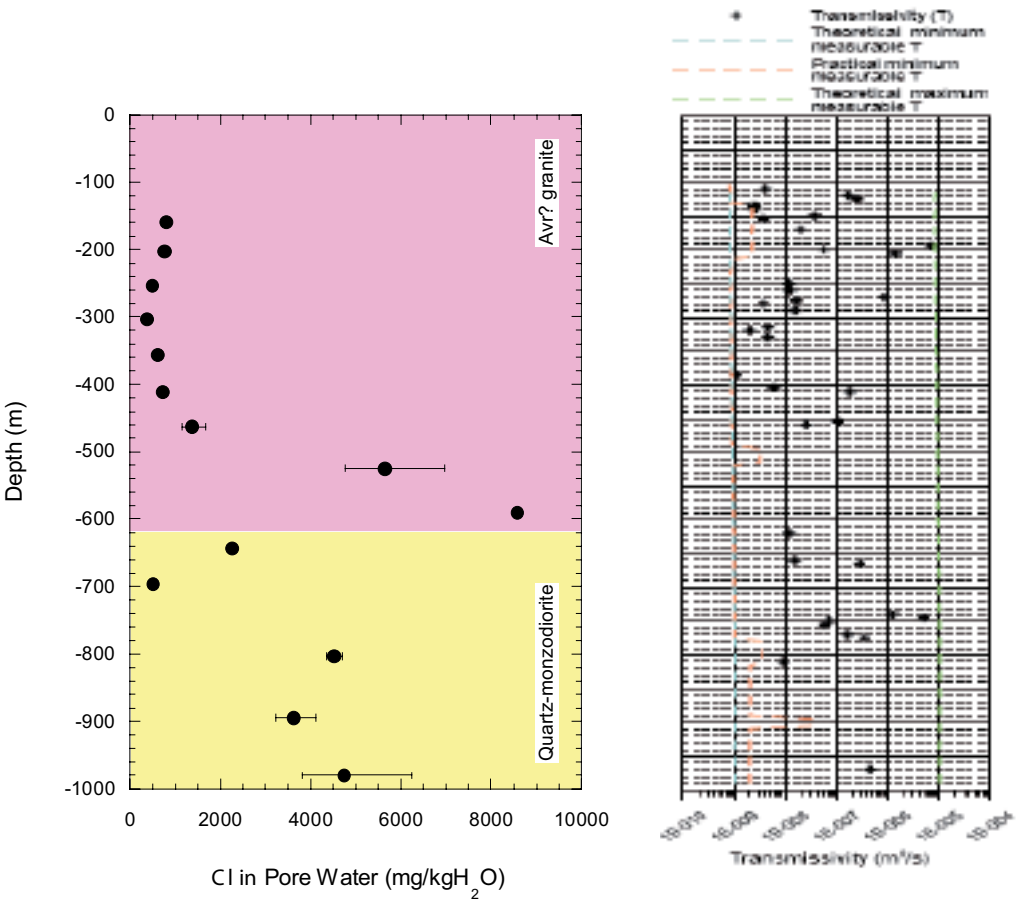

Figure 10-5. *Borehole KLX03: Chloride concentration in pore water as a function of sampling depth (left) and compared to the hydraulic transmissivity measured in the borehole (right).*

10.3.1 Sensitivity of derived chloride concentration

Every rock sample recovered from depth is potentially subjected to some stress release. Such release will result in an increase of the void volume of a rock sample and thus perturb bulk density measurements and, if drilled with a drilling fluid, also the water content because some drilling fluid might enter this newly created void volume. It is not well known if stress release in crystalline rocks occurs instantaneously (i.e. during drilling in the borehole) or more slowly over days, weeks, and/or even months. Also, in rocks with such low water content the measurements might simply not be accurate enough to resolve the effects of stress release. While a fully quantitative discussion is difficult with the data at hand, several semi-quantitative arguments can be considered.

From the mass balance equations used to calculate the pore water chloride concentration it follows that the concentration is inversely proportional to the mass of pore water, i.e. the water content of the rock sample. Measurements of the water content can be subjected to various perturbations that can deviate it from in situ conditions. One of them is desaturation of the samples, which would result in a too low water content and consequently in a too high calculated pore water concentration. Desaturation can be excluded as a perturbation based on the independent methods applied to determine the water content (cf section 10.1).

Stress release of the rocks is the second possibility to deviate the measured water contents from in situ conditions. Stress release could have occurred (or still can occur) continuously and slowly from the time of drillcore recovery to the end of the experiments in the laboratory and/or it could have occurred instantaneously during drilling in the borehole. In the first case this would result in a desaturation of the rock samples which, as mentioned above, is not observed. In the second case, the newly created pore space would, if connected with the core surface, become filled with the surrounding fluid used for drilling the borehole. This effect would not be detected by gravimetric water content measurements. However, if significant, it should have been detected in the water content determined by the isotope diffusive-exchange method, which seems not to be the case. Similarly, one would expect to see systematic perturbations in the chemical and isotopic composition of the out-diffusion experiments performed on the same rock type as a function of the sampling depth. This is because deep seated samples would suffer the strongest stress release and are also in contact with the drilling fluid for the longest duration of time (i.e. on average two hours at greatest depth and one hour at shallower depths). As will be shown below such indications appear to be absent for the investigated samples.

Another argument again significant stress release is given by the behaviour of the samples and experiment solutions during the out-diffusion experiments. Initial model calculations show that the out-diffusion of chloride from the pore water of the rock into the experiment solution can be described by diffusion as the dominant transport mechanism (cf section 10.3.2). Because the contact time between the drillcore and the drilling fluid was on average in the order of 1–2 hours, this suggests that the effect of possible dilution of the pore water by the less mineralised drilling fluid (i.e. from HLX14) is very limited and probably outside the resolution of applied methods.

From this combination of semi-quantitative arguments it appears that measurable effects of stress release are minimal. Nevertheless, possible effects of stress release shall be further explored. Instantaneous stress release in the borehole could result in; a) an increase of connected porosity resulting in a calculated dilution of the in situ pore water, b) an increase of connected porosity accompanied by dilution of the in situ pore water due to ingress of dilute drilling water, and c) an increase of connected porosity accompanied by an increase in salinity of the in situ pore water due to increased surface exposure resulting from cracking/fracturing. To date, in borehole KLX03, possibilities (a) and/or (b) are considered to be potentially the most feasible. Following the mass balance relationship, both (a) and (b) effects would result in an underestimation of the in situ pore water chloride concentration when determined with out-diffusion experiments and water content measurements. Possible dilution of the in situ pore water cannot be easily assessed in a quantitative way because of the unknown in situ chloride concentration. In contrast, estimates can be calculated for lower in situ water contents. From the inverse proportionality of the water content to the pore water chloride concentration it follows that an increase in the in situ water content due to stress release by 30% and 50% would result in an increase of the calculated pore water chloride concentration by a factor of about 1.3 and 2, respectively.

10.3.2 Preliminary modelling of chloride breakthrough

The monitoring of steady state conditions in the out-diffusion experiments was performed with small-sized samples (0.5 mL) that were taken at regular time intervals and analysed for chloride. Steady state conditions with respect to chloride diffusion is attained when the concentrations reach a plateau, i.e. when they remain constant. The chloride concentrations obtained describe a break-through curve, which can be modelled.

Figure 10-6 shows the preliminary modelling of the chloride breakthrough curve obtained for sample KLX03-7 (Avrö granite). The calculation was performed using an analytical solution of radial diffusion out of cylinder into a well-mixed solution reservoir /Crank 1975/. In this initial modelling the removal of small-sized samples of experiment solution was neglected in the transient phase, but incorporated in the mass balance for the steady state condition. In future calculations incorporation of this removal will lead to an improvement of the fit to the measured data.

For the Ävrö granite sample KLX03-7 the best fit of the measured data is obtained for a pore diffusion coefficient, D_P, for chloride of about 8.1×10^{-11} m²/s at a water-content porosity of 0.77 ± 0.14 Vol.% and at a temperature of 45°C. This converts to an effective diffusion coefficient, D_e, at 20°C of about 3.1×10^{-13} m²/s. This value is in excellent agreement with effective diffusion coefficients for dioritic rocks from the Laxemar area obtained from through-diffusion and through-electromigration experiments /$D_e = 3.9\times10^{-13}$ m²/s, Löfgren 2004/. It should be noted that these experiments have been performed on samples of 15 mm to 50 mm in thickness compared to the cylinders of about 50x190 m m used for the present out-diffusion experiments. Also, the samples used for through-diffusion and through-electromigration have been stored at the surface for variably long time periods (weeks to months) before the commencement of the experiments.

The agreement between diffusion coefficients derived by different techniques and on samples stored over different time periods argues against significant stress release after the retrieval of the drillcore from the borehole. Similarly, the different mass of the rock samples used in the different experiments also suggests that if significant instantaneous stress release had occurred in the borehole, the effect has been small to the extent that it has not been resolved by the presently applied techniques; more erratic results from the different methods applied would have been expected.

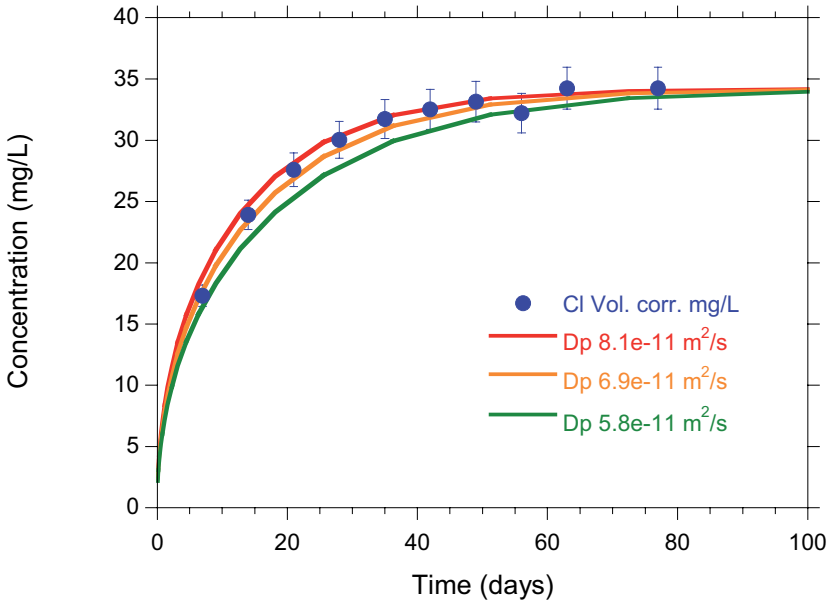

Figure 10-6. *Sample KLX03-7: Modelling of chloride out-diffusion at 45°C. The best fit is achieved for a diffusion coefficient D_P of 8.1×10^{-11} m²/s. The average porosity of the sample is 0.77 ± 0.14 Vol.%.*

10.4 Comparison of pore water and groundwater compositions

10.4.1 Chloride content

Chloride concentrations in pore water and formation groundwater of the Avrö granite are similar down to about 500 m depth suggesting steady state conditions between pore water and groundwater (Figure 10-7, left). This situation would slightly change at shallow levels when taking into account an assumed arbitrarily decreased water content due to stress release, in that the pore water at the most shallow levels would have higher chloride concentrations than the formation groundwater sampled at the same depth (Figure 10-7, right). Unfortunately, no formation groundwater could be sampled from the interval around 600 m where the pore water chloride concentrations are greatest in the entire profile. These might be expected to be greater than the formation groundwaters.

At increasing depth (i.e. near the top of the quartz monzodiorite) the pore water becomes more dilute than the formation groundwaters in the fractures suggesting that the pore water retains an older signature. Interestingly, this dilute pore water is not associated with a isotopic composition of glacial melt water, which might initially be expected (see below). Below about 800 m the chloride concentration of the pore water once again becomes similar to the fracture formation groundwaters (as does the overall chemical type), in common with the shallower levels described above and also in conjuction with an increase in transmissivity at around 750 m (Figure 10-5) . The pore water differs significantly, however, in chloride content and chemical type from the deepest formation groundwater sampled. Chloride concentrations similar to this deep formation groundwater could be roughly reached if the already very low measured water content of the samples is arbitrarily decreased by 50 % assuming stress release (Figure 10-7, right).

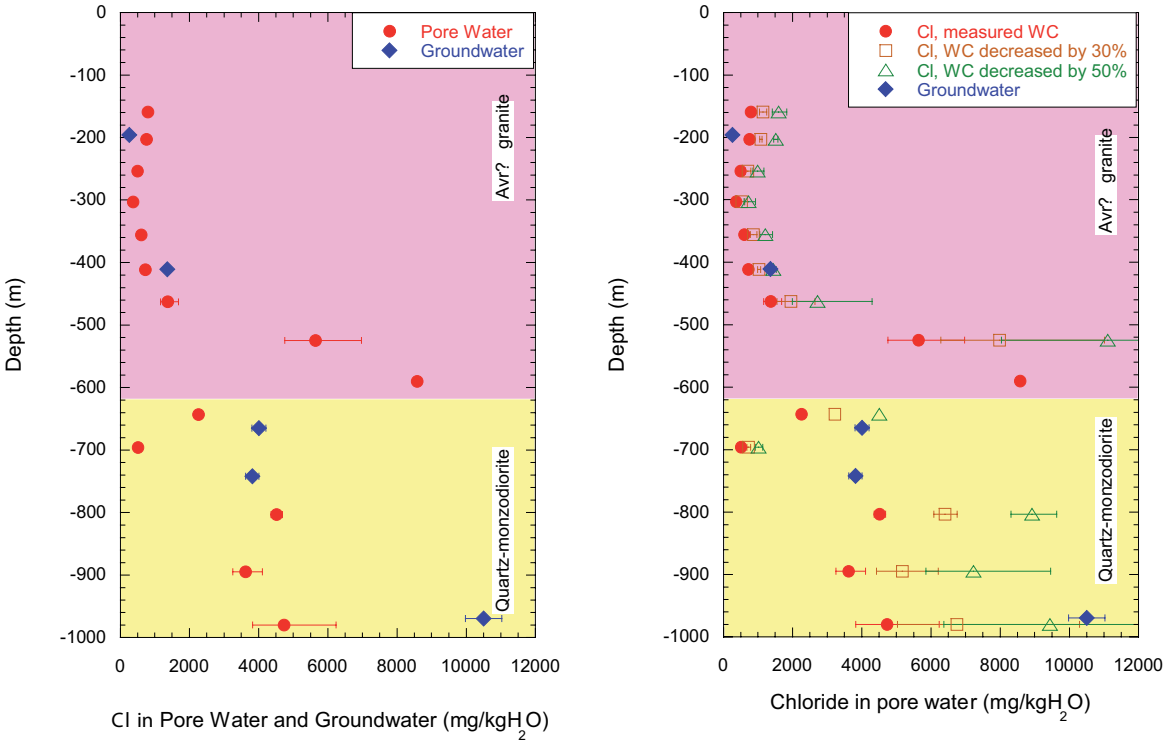

Figure 10-7. *Chloride concentrations of rock pore water from borehole KLX03 compared with groundwaters sampled from adjacent fractures as a function of sampling depth (left) and the same comparison with pore water chloride concentration calculated with arbitrarily decreased water contents to evaluate stress release effects (right; WC = water content).*

10.4.2 Isotope composition

The isotopic composition of the pore water derived by the isotope diffusive-exchange method developed by /Rogge 1997/ and /Rübel 2000/ is shown in Figure 10-8 in the conventional δ^2H– $\delta^{18}O$ diagram and compared to the Global Meteoric Water Line (GMWL) and proposed end-member compositions of various groundwater types /Laaksoharju et al. 1999/. The δ^2H and $\delta^{18}O$ values of the shallow samples plot on or close to the GMWL only slightly below the present-day precipitation end member. Except for the δ^2H signature of sample KLX03-6 there is no indication of a pronounced glacial component present in any sample. The $\delta^{18}O$ value of this sample is, however, too heavy for a glacial water and thus the derived composition is suspect. With increasing sample depth (and thus with increasing chloride concentration) the pore water isotope compositions plot to the left of the GMWL in the vicinity of the reference brine water. Such types of isotope compositions are known, for example, from very old, highly saline groundwaters in the Canadian Shield /Frape and Fritz 1987/.

The stable isotope composition of the pore water behaves differently to that of chloride in that no clear stratification with depth and/or with general water type is developed (Figure 10-9). At very shallow levels the pore waters and formation groundwaters have identical stable isotope compositions and thus support the steady state conditions between pore water and formation groundwater as already observed for chloride. At deep levels (i.e. within the quartz monzodiorite) the pore water is strongly enriched in the heavy isotopes compared to the fracture formation groundwater. Because of the higher diffusivity of water compared to that of solutes, steady state conditions would be achieved earlier for the water isotopes than for chloride. Therefore, this supports the differences observed for the chloride concentrations between pore water and formation groundwater when calculated using the measured water contents. The spatial distribution of the stable water isotopes is thus an additional argument against significantly higher chloride concentrations in the pore water due to stress release.

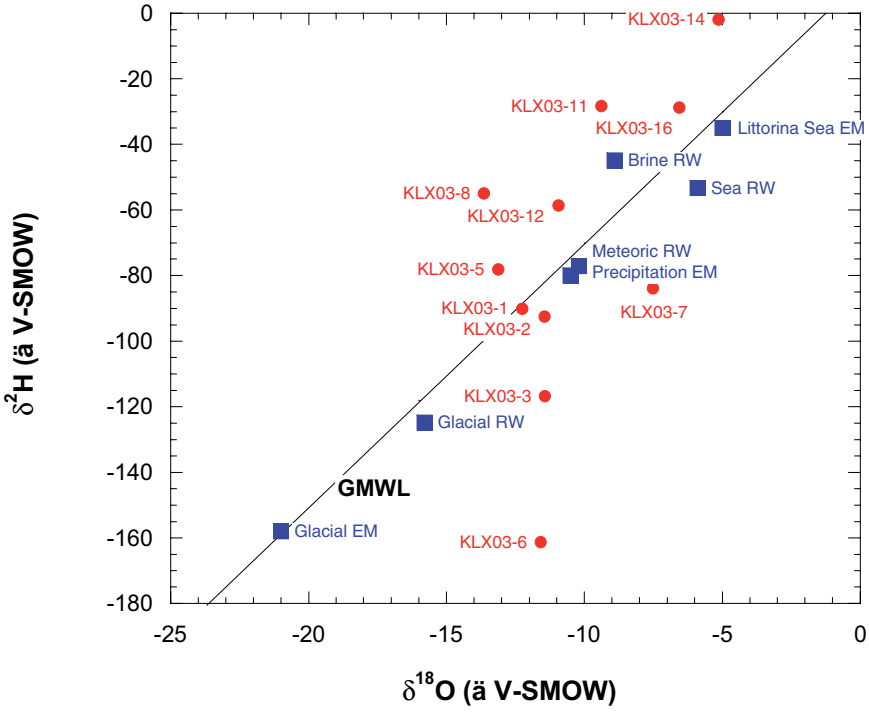

Figure 10-8. *Borehole KLX03: $\delta^{18}O$ and δ^2H values of pore water compared to the GWML and the isotopic compositions of proposed end-member (EM) and reference water (RW) compositions of various Swedish groundwaters /data from Laaksoharju et al. 1999/. Numbers refer to the laboratory samples.*

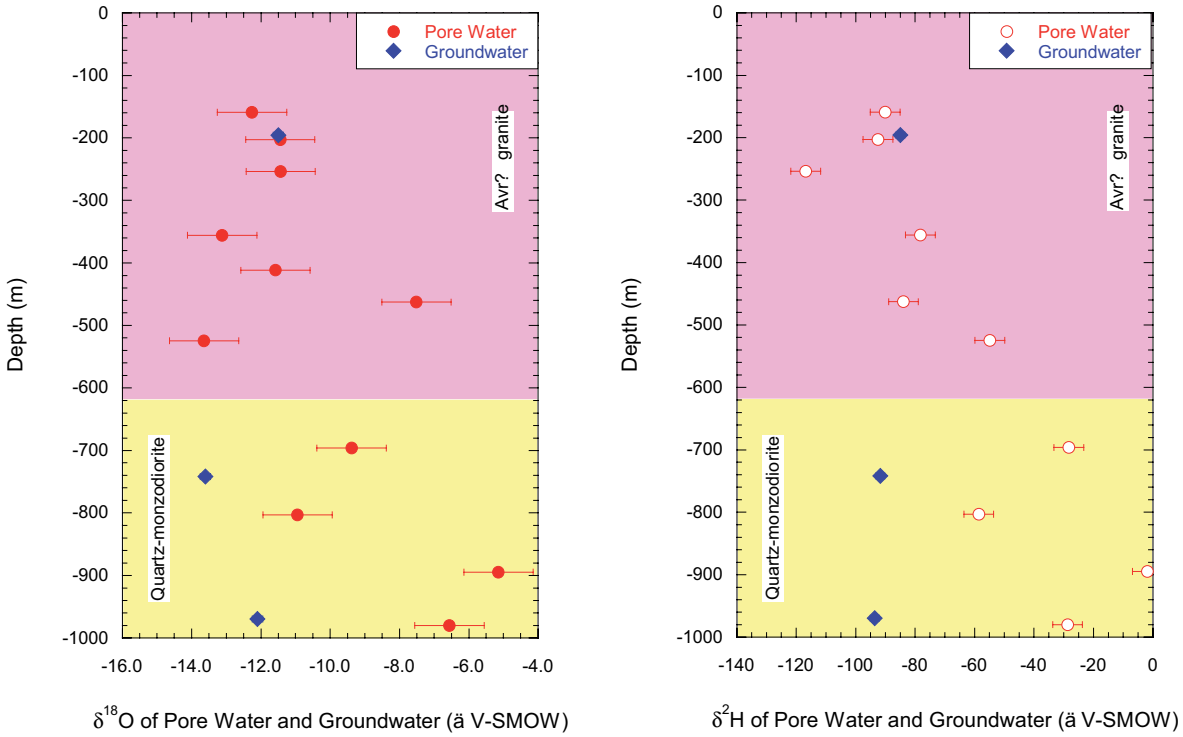

Figure 10-9. *Borehole KLX03: δ18O and δ2H values of pore water obtained from isotope diffusive exchange experiments as a function of sample depth in comparison to groundwater sampled from fractures (data from Table A4 with less reliable values not shown; error bars indicate the cumulative error).*

The chlorine isotopes, expressed as $\delta^{37}Cl$, differ from total chloride in their behaviour with depth when compared to the formation groundwater in fractures (Figure 10-10). In the Avrö granite the $\delta^{37}Cl$ values of the pore water are strongly enriched in ^{37}Cl and deviate significantly from those of the fracture groundwater. This is in contrast to the steady state conditions between pore and groundwater as indicated by total chloride. Exactly the contrary is observed at deeper levels in the quartz monzodiorite. Here the chlorine isotopes suggest steady state conditions while total chloride differs significantly in pore water and fracture groundwater (Figure 10-10). At present, these relationships are difficult to explain. In advection-dominated systems chlorine isotopes do not fractionate and a correlation with total chloride should be established. Chloride isotope fractionation, however, takes place during diffusion of chloride. To what degree the observed patterns can be related to such processes needs to be further investigated.

Total strontium concentrations in the experiment solutions are generally low and they are only weakly correlated with chloride indicating that strontium in the experiment solutions is mainly controlled by mineral dissolution reactions. This is reflected in the strontium isotope ratio, $^{87}Sr/^{86}Sr$, which is characteristic for the experiment solutions of Avrö granite and quartz-monzodiorite (Figure 10-11).

In the Avrö granite uniform $^{87}Sr/^{86}Sr$ ratios are obtained for the experiment solutions of pore water samples down to about 450 m depth. These experiment solutions also have identical $^{87}Sr/^{86}Sr$ ratios to that of the formation groundwater. This can be interpreted that weathering is the dominant process in the fracture formation groundwater and the experiment solution, consistent with the steady state between the fracture groundwater and the pore water as indicated by the chloride contents and the stable isotopes. Of interest are the two pore water samples from around 500–600 m in the Avrö granite. These samples have by far the highest total strontium concentrations associated with the lowest $^{87}Sr/^{86}Sr$ ratios in the experiment solution. This suggests a substantial contribution from the pore water to the experiment solution which is different from shallower levels. This is supported by differences in total chloride and the general chemical type observed for these pore waters (cf Figures 10-7 and 10-4).

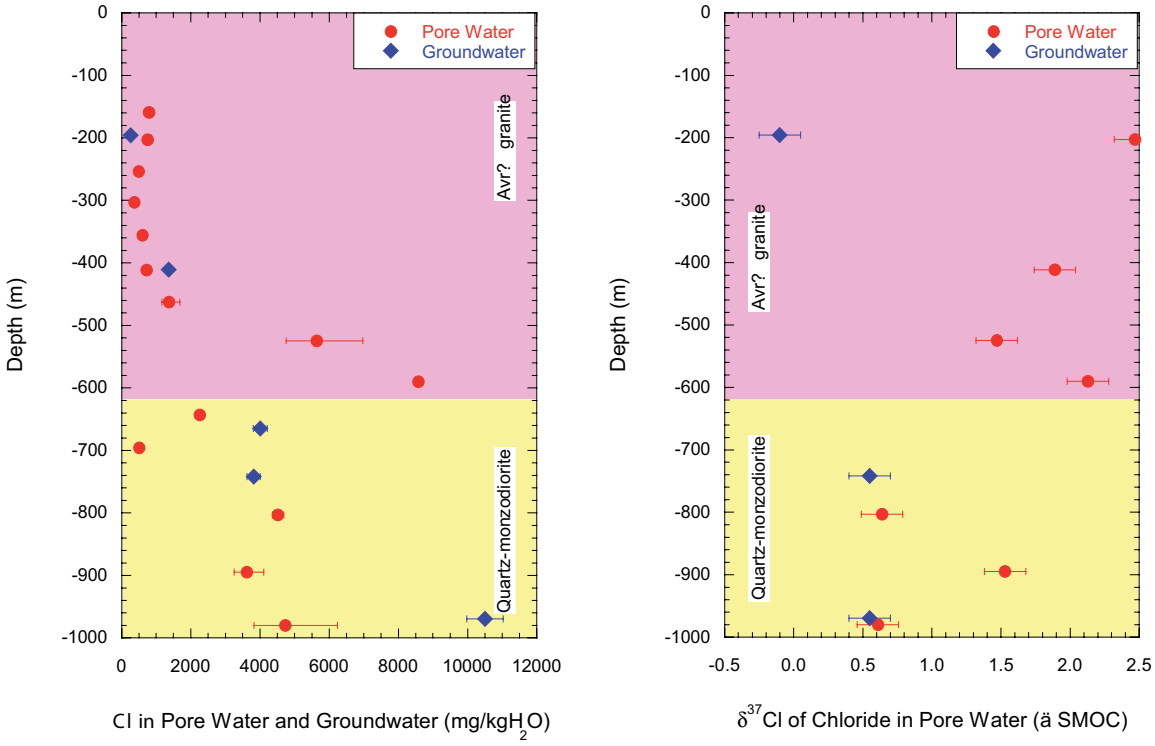

Figure 10-10. *Borehole KLX03: Chloride (left) and chlorine isotope ratio (right) of pore water compared with those of formationgroundwaters sampled from fractures as a function of sampling depth.*

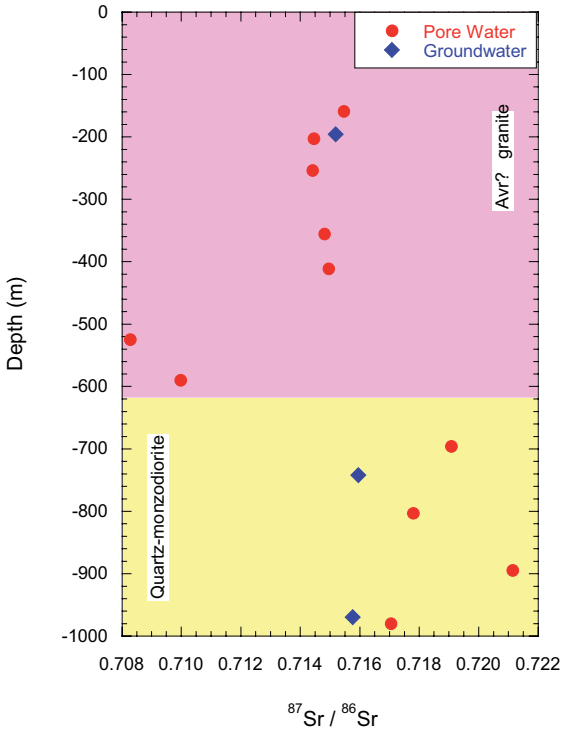

Figure 10-11. *Borehole KLX03: Strontium isotope ratio of pore water compared with those of fracture formation groundwaters as a function of sampling depth.*

In the quartz monzodiorite the $^{87}Sr/^{86}Sr$ ratio of the experiment solution are more radiogenic than those of the formation groundwaters. Since the time required for 'weathering' reactions to occur during the experiments is much shorter than the residence time of the formation groundwater in fractures at these depth levels, it appears that the more radiogenic $^{87}Sr/^{86}Sr$ ratio must be due to the contribution of the pore water. At these depths the difference between pore water and formation groundwater and the longer residence time of the pore water compared to the groundwater are consistent with the other parameters investigated.

10.5 Summary

Pore water that resides in the pore space between minerals and along grain boundaries in crystalline rocks of low permeability has been extracted successfully by laboratory out-diffusion methods using drillcore samples from borehole KLX03 from the Laxemar site. The obtained experiment solutions have been characterised chemically and isotopically and related to the in situ pore water composition of the rock, which in turn was related to the present and past formation groundwater evolution of the site. In addition, the method of extraction, together with interfaced measurements of interconnected porosity, provided the opportunity to derive diffusion coefficient values of potential use in predicting future rates of solute transport. Because of the very small volumes of pore water extracted, and the possibility of rock stress release occurring during drilling which might lead to contamination by drilling fluid and also affect the derivation rock porosity values, great care was taken to avoid such problems or, at least further understand the repercussions.

The characterisation of pore water in rocks from the Laxemar borehole KLX03 resulted in the following main conclusions:

- Independent derivation of water content (to calculate water content porosity) by drying and isotope diffusive exchange methods gave consistent results excluding artefacts such as desaturation of the samples.
- There is multiple evidence that no significant stress release and its potential effect on water content porosity values and related drilling water contamination has affected the rock samples; although quantitative proof cannot be given with the present data at hand, several qualitative arguments against such events happening have been discussed.
- The uncertainties surrounding the possibility of stress release effects were addressed by calculating the hypothetical variation in water content using a change of 50% by stress release; this would essentially increase the pore water chloride by a factor of 2. It is shown that such an increase would be inconsistent with determined parameters independent from water content measurements.
- Diffusion between rock pore water and adjacent formation groundwater-conducting fractures and fracture zones, and vice versa, is identified as the dominant transport process; calculated diffusion coefficients agree well with present-day knowledge from the Laxemar site.
- Chemical and isotopic pore water signatures are characteristic and show a variation of groundwater composition with rock type and depth. In the Avrö granite a shallow (< 450 m) and intermediate (450–600 m) zone can be distinguished. The pore water in the quartz monzodiorite indicates three zones (600–750 m, 750–850 m, and 850–1,000 m); this is in close agreement with the general trends in hydrochemistry of the adjacent formation groundwaters.
- There is little apparent evidence of a glacial melt signature in the pore waters; this could indicate that such waters had not diffused to the sampling location, or, they could have been subsequently removed, as suspected from the present steady state existing at shallower levels in the bedrock (to ~ 450 m).
- Pore waters at depth show an affinity with deep brine evolution.
- Steady state between pore water and formation groundwaters in the fractures is essentially only developed in the shallow zone of the Avrö granite, while at depths greater than 450 m the chemical and isotopic composition of the pore water differs markedly from those of the formation groundwaters in fractures.

11 Palaeohydrogeochemistry

Hydrogeological interpretations rely normally on borehole groundwater data and produce a picture of the present groundwater situation, which can also include the influence of perturbations such as groundwater short-circuiting in the surrounding bedrock and also along single boreholes under open hole conditions. Helping to unravel the influence of these perturbations (and other artefacts from borehole activities) to achieve an understanding of the 'undisturbed' formation groundwaters, and their palaeoevolution, is an integral part of the on-going hydrogeochemical evaluation process at the various candidate sites. To gain insight into palaeoevolution of the groundwater systems is greatly aided by the fracture mineralogy which, in the best of cases, can help to evaluate the hydrogeochemical stability over timescales of interest for repository safety and performance assessments. Calcite is the mineral most frequently used for palaeohydrogeological interpretations as it can form during different temperature and pressure conditions including present low temperature ambient groundwater environments. Stable isotope analyses (O, C and Sr) can provide information about the groundwater from which it precipitated and trace element compositions can add to this description. Under ideal conditions inclusion of formation groundwater is trapped within the developing calcite phases providing important information about the salinity and temperature of the in situ formation groundwaters. Many calcites show zonation and the character and succession of the different zones can give information about changes in the groundwater chemistry with time.

Within the EU project PADAMOT a number of samples from borehole KLX01 have been analysed in detail for the purpose of palaeohydrogeological interpretation. This work has now been compiled and the analyses will be made available for the Laxemar 2.1 modelling. Furthermore, stable isotope analyses (including not only O and C but also Sr) and chemical analyses of calcites from KLX03 and KLX04 have been carried out, which also will be included in the forthcoming model version Laxemar 2.1.

Uranium series analyses on fracture coatings from boreholes KSH01, KSH02 and KSH03 (in total 12 analyses) have been carried out and will be presented in the Laxemar 2.1 model version. Additional analyses from the Laxemar subarea are planned (samples are partly collected) and will be available for later model versions. The uranium series analyses provide very useful palaeohydrogeological information in that they not only provide information about redox conditions and uranium transport, but may also provide time constraints on these processes.

12 Conclusions

12.1 Major ions

- Overall depth trends show increasing TDS with increasing depth. There are significant differences in "depth trends" between the two subareas; in Simpevarp the upper fresh water regimes (mostly Na-HCO_3) reach only to approx. 150 m whereas in the central parts of the Laxemar subarea fresh water is found down to 500 m and in some cases as deep as 800 m.
- Ca/Na ratios increase markedly with depth and also illustrate differences between the two subareas down to around 1,000 m. The Simpevarp subarea saline groundwaters (~ 10,000–20,000 mg/L Cl) show a more Na-rich trend (Na-Ca-Cl dominant) compared with the Laxemar groundwaters which are more Ca-rich (Ca-Na-Cl dominant). At depths generally exceeding 1,000 m, higher saline Ca-Na-Cl groundwaters dominate in both areas.
- At a more regional scale, deep groundwaters at the Simpevarp subarea and Äspö (down to 1,000 m) are Na-Ca-Cl in type; deep groundwaters at Oskarshamn (KOV01; 1,000 m) and at Laxemar (1,300 to 17,000 m) are Ca-Na-Cl in type. Since Laxemar is inland and Oskarshamn is close to the coast, this should be an indication of discharging very deep groundwater at Oskarshamn. At greater depth below the Simpevarp subarea and Äspö than presently sampled, Ca-Na-Cl groundwaters are expected to dominate.
- Br/Cl ratios indicate an absence of marine signatures at Laxemar; all ratios are significantly higher than marine. Contrastingly at Simpevarp, lower ratios indicate a weak but significant marine signature.
- A clear marine signature in terms of high Mg values, marine Br/Cl ratios and relatively high $\delta^{18}O$ values is rare, but a small set of samples with a possible Littorina signature do exist from 150–300 m depth located in fracture zones close to the Baltic Sea. In addition, there also seems to be a small marine input (Littorina or older), distinguished by slightly higher Mg values and lower Ca/Na ratios, in the Simpevarp subarea waters which is absent in the Laxemar subarea (with the exception of the upper 700 m in KLX01 which shares similarities to the Simpevarp samples).
- $\delta^{18}O$ versus Cl indicates a contribution of cold climate or glacial melt waters to the brackish (i.e. 2,000–10,000 mg/L Cl) and deeper saline (i.e. 10,000–20,000 mg/L Cl) groundwater samples.
- The SO_4 contents vary considerably within the brackish and saline groundwaters. Microbially mediated sulphate reduction, traced as high $\delta^{34}S$ (> 20‰ CDT), is taking place not only in brackish waters but also in some fresh waters (i.e. KLX03 and HLX 14). The SO_4 contents in the more highly saline groundwaters indicate mixing of SO_4 from deep brine waters, which in turn may have reached their high SO_4 content through leaching of sediments and/or dissolution of gypsum previously present in fractures. The presence of gypsum in tight fractures in a few places within the site supports gypsum as a possible source for SO_4 in the deep groundwaters.
- Extracted pore waters from KLX03 in the Laxemar subarea show general agreement with the overall trends in hydrochemistry of the adjacent formation groundwaters. In bedrock horizons of low transmissivity (i.e. 500–600 m depth) the pore water salinity might be expected to exceed that of the groundwaters; unfortunately there are no such groundwater data from this level.
- Pore waters at depth show an affinity with deep brine evolution.
- There is little apparent evidence of a glacial melt signature in the pore waters, although some formation groundwaters near the surface do have a component. The absence of a glacial melt component in the pore waters studied could indicate that such melt waters had not diffused to the sampling location, or, they could have been subsequently removed, as might be suspected from the present steady state between the formation groundwaters and pore waters existing at shallower levels in the bedrock (to ~ 450 m).

- A preliminary evaluation of groundwater data representing the geosphere/biosphere interface has shown promising results. This has involved overburden data from Soil Pipes and upper bedrock (0–200 m) data from percussion boreholes. Integration of these data has identified areas of recharge/discharge which will be further investigated and quantified. This will help to characterise the chemical and isotopic composition of the recharge water end member into the bedrock, and also the evolution of groundwaters at points of discharge from the bedrock into the overburden.
- The overall picture from the evaluation is that discharge locations, at one location characterised by tritium free water, have been identified at the Simpevarp subarea (Ävrö), whereas near-surface groundwaters from Laxemar (only percussion borehole data available so far) are mainly characterised by recharge or shallow discharge (except for HLX20).

12.2 Isotope sytematics

Borehole isotope data are still relatively few and not very much new information has been forthcoming since the Simpevarp 1.2 version. However, tritium has been paid much attention together with ^{14}C since they represent isotopes of great interest for groundwater modelling. Furthermore they also provide the possibility to assess potential emissions from the nearby power plants.

12.2.1 Tritium

Tritium data from precipitation and surface stream, lake and sea water localities were studied with respect to its distribution, content and origin. It can be concluded that:

- Generally there is a spread in values between 8.5 to 19 TU for surface water localities which is almost equal to the variation in the precipitation (9–19 TU), i.e. the input term.
- The highest mean value is found in the Baltic Sea samples, with the highest contents (mean of 15.1 TU) in the samples east of Kråkelund, north of Simpevarp.
- The highest values for the lake and stream waters are found in the eastern part of the area even though mean values only deviate by 1–1.3 TU (11.4 compared with the highest value of 12.6 TU).

The question now to be addressed is how much of the tritium is due to emissions contamination from the nuclear power plant? Present day contamination, although small, should be more apparent following the systematic decrease in global tritium values during the past five decades. Consequently, continued sampling of surface waters for tritium analyses is recommended with particular attention to surface waters samples taken: a) close to the cooling water outlet of the nuclear power plant, b) close to the power plant, and c) some 100 km away, preferably down-wind from the power plant.

12.2.2 Tritium and carbon-14

Tritium is also related to the regional distribution of ^{14}C. This indicates that Baltic Sea samples show the highest ^{14}C values (about 105 to 110 pmC) which means that they have either some residual bomb test ^{14}C or, in common with the tritium values, contain a modern contribution from the nuclear power plant emissions resulting in higher than background values. Most of the lake and stream waters show values ranging from 100 to 60 pmC, accompanied by high tritium values (~ 8–15 TU). With the exception of two samples (45 and 55 pmC) the soil pipes show values within the same interval as the surface waters. The percussion and cored boreholes show decreasing tritium contents with decreasing ^{14}C, so that the waters with very low tritium show the lowest ^{14}C values (about 30 pmC).

12.2.3 Carbon

- All samples analysed for ^{14}C were also analysed for stable carbon isotope ratios (given as $\delta^{13}C$‰ PDB). These $\delta^{13}C$ ratios, together with HCO_3 contents, are commonly used to evaluate possible processes that have taken place resulting in ^{14}C changes in the groundwater.
- Waters in equilibrium with atmospheric CO_2 show high $\delta^{13}C$ values (0 to –3‰ PDB); this is exemplified by the Baltic Sea samples.
- Incorporation of biogenic CO_2, produced by breakdown of organic material of variable age, lowers the $\delta^{13}C$ values significantly; this is well illustrated by the surface waters showing significantly lower $\delta^{13}C$ values (–12 to –24‰).
- The ^{14}C values in most of these waters are relatively high (although somewhat lower than the Baltic Sea values) and it is probable that the organic source for the CO_2 is young, although some dilution with "dead carbon" (^{14}C free) has occurred. Some surface waters and most of the percussion and cored boreholes show similarly low $\delta^{13}C$ values but significantly lower ^{14}C values.
- In particular, the shallow groundwaters from the percussion boreholes and the two samples from KLX03: 103–218 m and KLX04 103–213 m show high HCO_3 contents (174 to 318 mg/L) and ^{14}C contents in the range of 70 to 40 pmC. Several explanations for the decrease of ^{14}C are possible: 1) dissolution of calcite has contributed ^{14}C free carbon to the HCO_3, or 2) CO_2 has been produced from older organic material, or 3) these waters are old and very little ^{14}C has been contributed during a long period of time. The combination of all these processes is possible for the groundwater samples. The fracture calcites show no homogeneous $\delta^{13}C$-values and it is therefore not possible to model calcite dissolution as a two end member mixing.

12.2.4 Sulphur

Sulphur isotope ratios, expressed as $\delta^{34}S$‰ CDT, have been measured in dissolved sulphate in Baltic Sea waters, surface waters and groundwaters from the Simpevarp and Laxemar subareas. The recorded values were found to vary within a wide range (–7 to +48‰ CDT) indicating different sulphur sources for the dissolved SO_4^{2-}, for example:

- For the surface waters and most of the near-surface groundwaters (soil pipes) the SO_4^{2-} content is usually below 25 mg/L and the $\delta^{34}S$ relatively low but variable (–7 to +15‰ CDT) with most of the samples in the range 0–10‰ CDT. These relatively low values indicate that atmospheric deposition and oxidation of sulphides in the overburden is the origin for the SO_4^{2-}. There is a tendency towards lower $\delta^{34}S$‰ CDT with higher SO_4^{2-} contents in these waters but the variation is large.
- The Baltic Sea waters cluster around the 20‰ CDT marine line but show a relatively large spread (+16 to +23‰ CDT). The reason for this is not fully understood but suggestions include: a) contribution from land discharge sources (e.g. streams) to various degrees (low values), and b) potential bacterial modification creating high values in the remaining SO_4^{2-}.
- The borehole groundwaters show $\delta^{34}S$ values between +11.8 to + 48.2‰ CDT with most of the samples in the range +15 to +25‰ CDT. Values higher than marine (< 20‰ CDT) are found in samples with Cl contents < 6,500 mg/L Cl. These latter values are interpreted as a product of sulphate reduction taking place in situ. The two highest values (+32 and +48‰ CDT) are detected in waters where SO_4^{2-} contents are low (around 30 mg/L) and the Cl contents 70 and 503 mg/L, respectively. Such extreme $\delta^{34}S$ values as +48‰ CDT is a strong indicator of closed, stagnant conditions with microbial activity.
- The groundwaters with higher salinities, all from the Simpevarp penninsula, share lower $\delta^{34}S$ but higher SO_4^{2-} contents. The reasons are uncertain and more information is needed. Possible explanations include dissolution of, for example gypsum, or inmixing of very deep saline water which in turn has received contributions of sulphate from leaching of sediments etc. The deep and intermediate groundwaters are very reducing and non-corroded pyrite is present in the fractures so that oxidation of sulphides in these groundwaters seems not to be a possibility.

12.2.5 Strontium

Available Sr isotope information from the Baltic Sea waters, near surface waters and groundwaters, show two or possibly three separate correlations between Sr isotopes and 1/Sr and Cl contents:

- Large variation in Sr ratios but relatively small variation in Sr content for the near-surface groundwaters indicating interaction (leaching) from overburden with different mineralogical compositions.
- Large variation in Sr content but small variation in Sr isotope ratios for the fresh groundwaters indicating homogenisation of the Sr isotope ratios due to mineral/water ineractions along the flow paths (mainly ion exchange).
- Tendency towards higher Sr isotope ratios with increasing Sr content for the saline samples possibly as a result of continued water/rock interactions.

12.2.6 Boron

Enhanced $\delta^{11}B$ has also been used as an indicator of permafrost conditions as it appears to become isotopically enriched in the fluid phase during freeze-out conditions. For example, deep saline groundwaters characterised by negative $\delta^{18}O$ values tend to correlate with high ^{11}B values.

Since the boron isotope data are sporadic, initial scoping plots have been made using all data where both $\delta^{11}B$ and $\delta^{18}O$ have been analysed. Almost all of the $\delta^{11}B$ data in the Simpevarp area plot between 20–60‰ which is in agreement with earlier published data from Fennoscandia including the Äspö HRL. Of interest are three anomalously high $\delta^{11}B$ (80–110‰) cored borehole outliers from the Simpevarp site (KSH01A: 556 m, KSH02: 422 m and KSH02: 578 m). Otherwise the remaining borehole data fall within the same $\delta^{11}B$ range.

Plotting $\delta^{11}B$ against $\delta^{18}O$ couples these three high $\delta^{11}B$ Simpevarp cored borehole groundwaters to somewhat lighter $\delta^{18}O$ values (–12.9 to –12.7‰ SMOW). According to the literature, this is consistent with the possibility that these groundwaters might reflect freeze-out processes which occurred under permafrost conditions.

13 Visualisation of the Simpevarp area data

13.1 Construction of 2-D models

Visualisation of the hydrogeochemical evaluation documented in this report is in the form of two vertical transects through the Laxemar and Simpevarp sites. The vertical extent of the transects is to 2,000 m depth to accommodate the deepest borehole (KLX02) in the Laxemar subarea. The approach to locate and construct the transects was carried out as follows.

The positions of the transects were chosen to intersect the Laxemar and Simpevarp subareas, approximately along the main regional groundwater flow direction (WNW-ESE transect) and perpendicular to this direction (SSW-NNE) as shown in Figures 13-1 and 13-2. In these figures the relationship of the groundwater flow direction with the distribution of the major structural features is also indicated.

Within the Simpevarp and Laxemar subareas the transects were adjusted to either intersect or pass in the close vicinity of the major boreholes of interest, i.e. KLX04, KLX08, KLX02, KSH02, KSH01A+B and KSH03A (transect WNW-ESE) and KLX03, KLX04, KLX08, and KLX06 (transect NNE-SSW).

Figure 13-1. *Structural map of the region including and surrounding the Laxemar and Simpevarp subareas (lighter boxed area). The black line represents the approx. main groundwater flow direction through the investigated sites. The major structural components intersected are also indicated.*

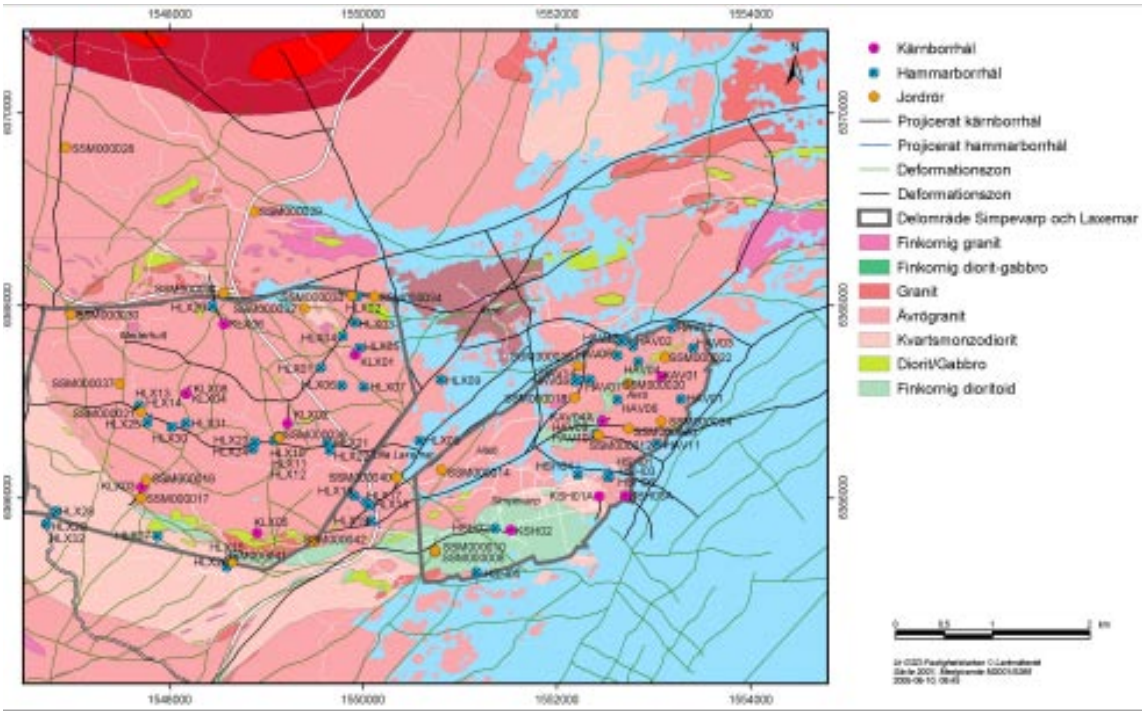

Figure 13-2. *Map showing the location of the sampling points and boreholes in the Simpevarp and Laxemar subareas. The positions of the WNW-ESE and NNE-SSW transect profiles are marked in black.*

Modelled 2-D versions of the vertical transects to 2,000 m depth were produced (Figure 13-3a, b) showing the position of the main structures, the location (actual or extrapolated) of the boreholes, and the known geology to 1,000–2,000 m. Using these modelled sections as a base, schematic manual versions then were produced to facilitate illustrating the most important structures/fault zones and their potential hydraulic impact on the groundwater flow. This hydraulic information was then integrated with the results of the hydrogeochemical evaluation results to visualise the vertical and lateral changes in the groundwater chemistry (Figures 13-4 and 13-5).

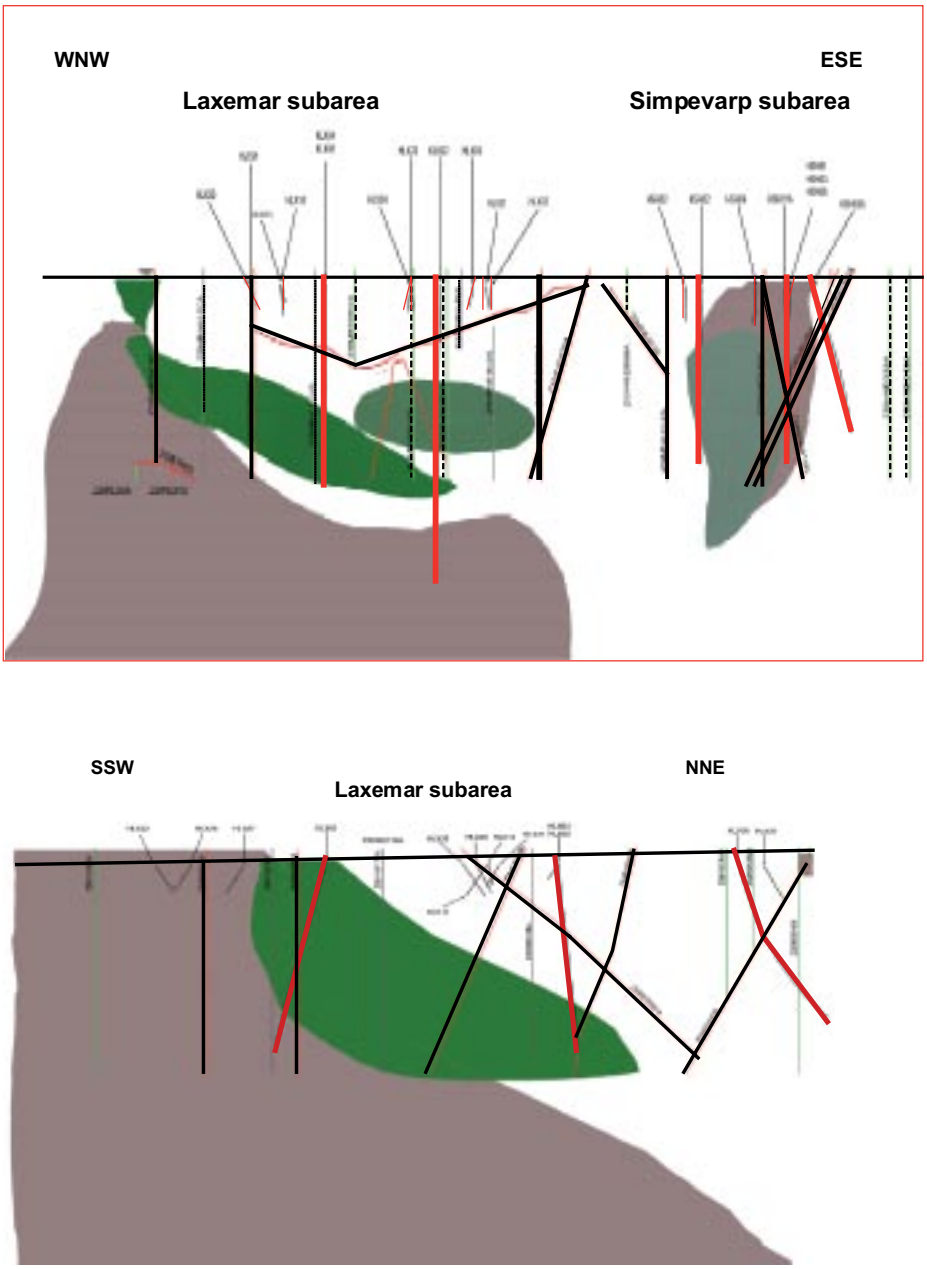

Figure 13-3a, b. *Modelled 2-D versions of the (a) WNW-ESE and (b) NNE-SSW vertical transects showing the many intersected structures, the known geology from drilling, and the location (actual or extrapolated) of the cored and percussion boreholes used in the hydrogeochemical characterisation. Accentuated are the cored boreholes (thick red lines) and most of the more important 'confident' structures (thick black lines). The major geological units (rock domains) present are the Ävrö granite (white), quartz monzodiorites (grey/pink colour), fine-grained dioritoids (grey-green colour) and a rock domain with a high frequency of diorite and gabbro with respect to proportions of Ävrö granite and quartz monzodiorite (dark green colour). Depth scale in both versions is 2,000 m; horizontal scale is ~7 km (a) and ~2.5 km (b).*

13.2 Hydrochemistry

The marked differences in the groundwater flow regimes between the Laxemar and Simpevarp areas are reflected in the groundwater chemistry.

Figure 13-4 shows along the main WNW-ESE transect the four major recognised groups of groundwaters and their interpreted spatial extent, denoted by A–D. The 'B' type groundwaters are subdivided into 'B_L' and 'B_S' types referring to Laxemar (L) and Simpevarp (S) respectively.

Figure 13-5 is oriented perpendicular to the main groundwater flow direction which is indicated by the encircled black dots. Only KLX03 has sufficient data (with some from KLX04) to give a good estimation of the depth extent of the various groundwater types A–D, and only B_L groundwaters are present as the transect is within the Laxemar subarea.

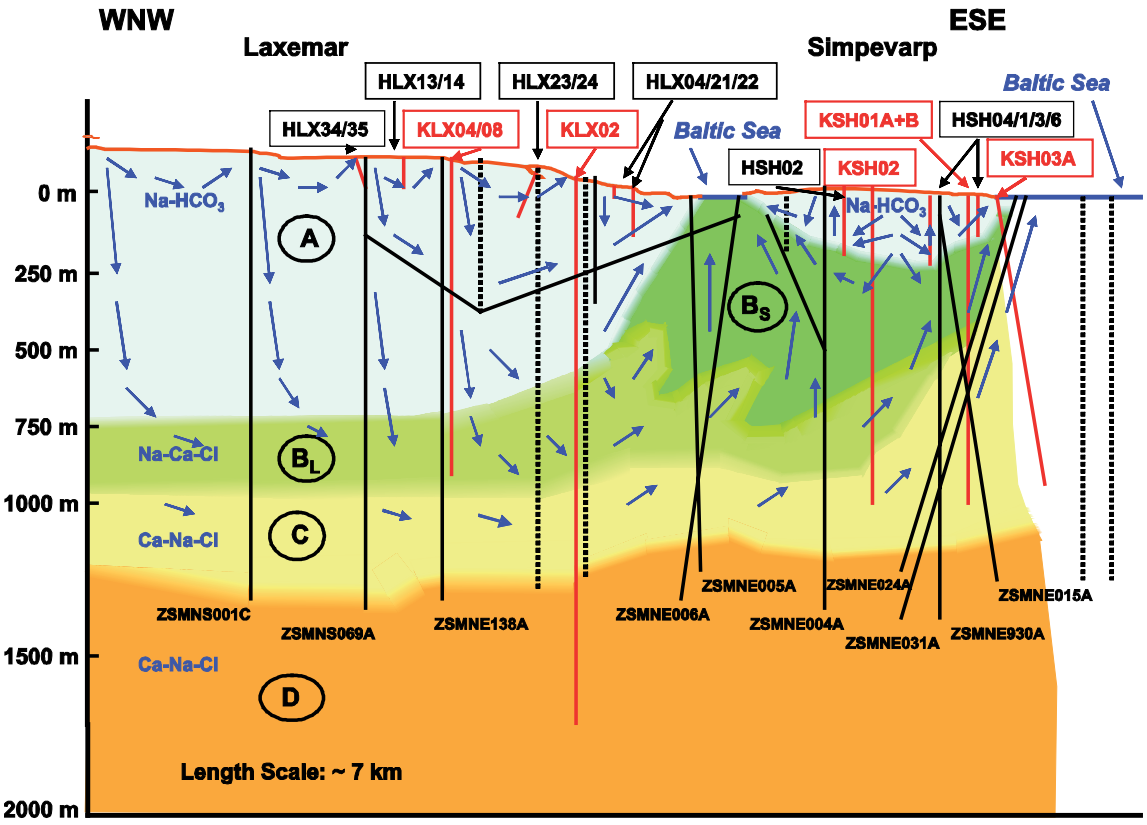

Figure 13-4. *Schematic 2-D visualisation along the WNW-ESE transect integrating the major structures, the major groundwater flow directions and the variation in groundwater chemistry from the sampled boreholes. Sampled borehole sections are indicated in red, major structures are indicated in black (full lines = confident; dashed lines = less confident), and the major grounwater types A–D are also indicated. The blue arrows are estimated groundwater flow directions; short arrows low flow rates, long arrows greater flow rates.*

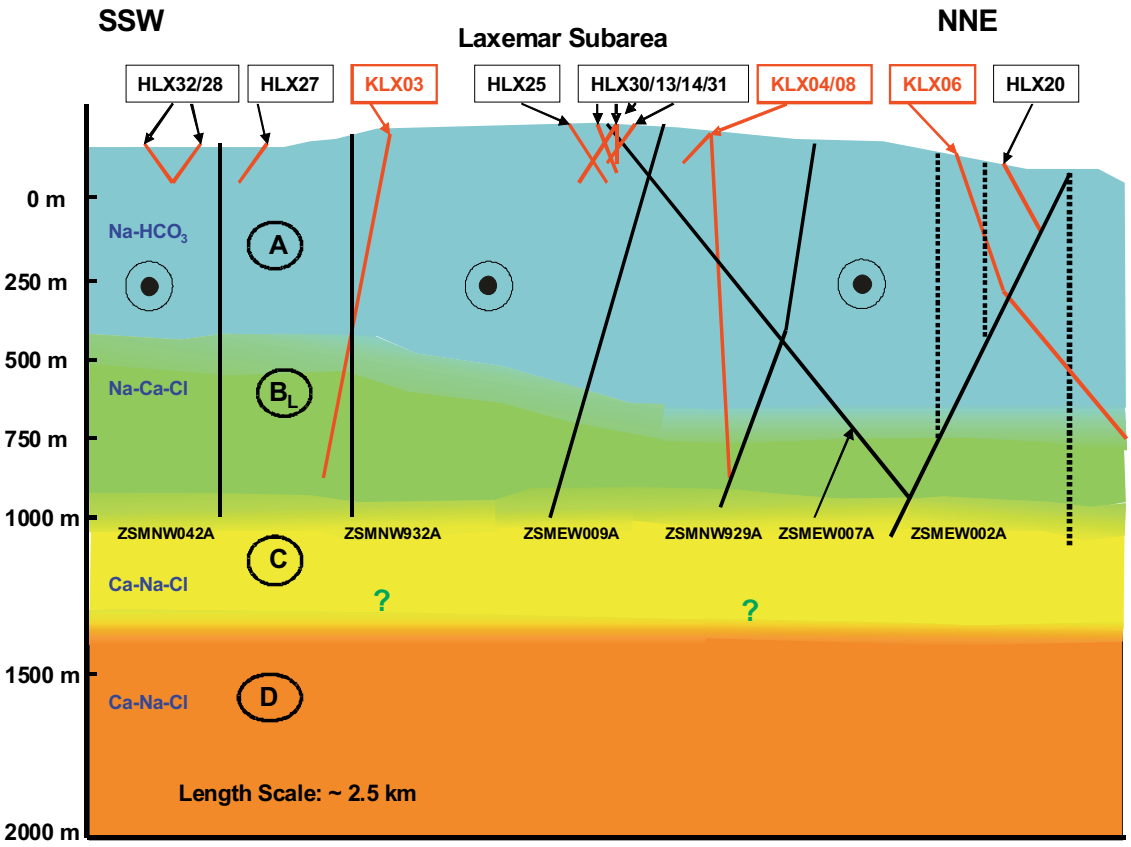

Figure 13-5. *Schematic 2-D model along the SSW-NNE transect integrating the major structures, the major groundwater flow directions and the variation in groundwater chemistry from the sampled boreholes. Sampled borehole sections are indicated in red, major structures are indicated in black (full lines = confident; dashed lines = less confident), and the major grounwater types A–D are also indicated. The encircled black dot symbol indicates the dominant horizontal/subhorizontal groundwater flow direction is out from the page.*

13.3 Summary of groundwater types

In terms of approx. depth, chemistry, major reactions and main mixing processes, the general features of these four groundwater types are summarised below.

13.3.1 Type A – Shallow (< 200 m) at Simpevarp but deeper (down to ~ 800 m) at Laxemar

'Dilute' groundwater (< 2,000 mg/L Cl; 0.5–3.5 g/L TDS); δ = –11 to –8‰ SMOW.

Mainly meteoric and Na-HCO_3 in type.

Redox: Marginally oxidising close to the surface, otherwise reducing.

Main reactions: Weathering; ion exchange (Ca, Mg); dissolution/precipitation of calcite; redox reactions (e.g. precipitation of Fe-oxyhydroxides); microbially-mediated reactions (SRB) which may lead to formation of pyrite.

Mixing processes: Mainly meteoric recharge water at Laxemar; potential mixing of recharge meteoric water and a modern sea component at Simpevarp; localised mixing of meteoric water with deeper saline groundwaters at Laxemar and Simpevarp.

13.3.2 Type B – Shallow to intermediate (150–600 m) at Simpevarp but deeper (down to ~ 500–950 m) at Laxemar

Brackish groundwater (2,000–10,000 mg/L Cl; 3.5–18.5 g/L TDS); δ = –14 to –11‰ SMOW.

B_L – Laxemar: Meteoric, mainly Na-Ca-Cl in type; Glacial/Deep saline components.

B_S – Simpevarp: Meteoric mainly Na-Ca-Cl in type but some Na-Ca(Mg)-Cl(Br) types (± marine, e.g. Littorina); Glacial/Deep saline components.

Redox: Reducing.

Main reactions: Ion exchange (Ca, Mg); precipitation of calcite; redox reactions (e.g. precipitation of pyrite).

Mixing processes: Potential residual Littorina Sea (old marine) component at Simpevarp, more evident in some fracture zones close to or under the Baltic Sea; potential glacial component at Simpevarp and Laxemar; potential deep saline (non-marine) component at Simpevarp and at Laxemar.

13.3.3 Type C – Intermediate to deep (~ 600–1,200 m) at Simpevarp but deeper (900–1,200 m) at Laxemar

Saline (10,000–20,000 mg/L Cl; 18.5–30 g/L TDS); δ = ~ –13‰ SMOW (? few data).

Dominantly Ca-Na-Cl in type at Laxemar but Na-Ca-Cl changing to Ca-Na-Cl only at the highest salinity levels at Simpevarp; increasingly enhanced Br/Cl ratio and SO_4 content with depth at both Simpevarp and Laxemar; Glacial/Deep saline mixtures.

Redox: Reducing.

Main reactions: Ion exchange (Ca).

Mixing processes: Potential glacial component at Simpevarp and Laxemar; potential deep saline (i.e. non-marine) and an old marine component (Littorina?) at shallower levels at Simpevarp; Deep saline (non-marine) component at Laxemar.

13.3.4 Type D – Deep (> 1,200 m) only identified at Laxemar

Highly saline (> 20,000 mg/L Cl; to a maximum of ~ 70 g/L TDS); δ = > –10‰ SMOW.

Dominantly Ca-Na-Cl with higher BrCl ratios and a stable isotope composition that deviates from the GMWL when compared to Type C groundwaters; Deep saline/brine mixture; Diffusion dominant transport processes.

Redox: Reducing.

Main reactions: Water/rock reactions under long residence times.

Mixing processes: Probably long term mixing of deeper, non-marine saline component driven by diffusion.

Compared to the Simpevarp 1.2 visualisation /Laaksoharju 2005/ one of the major differences is the extent of the brackish ‘B’ type groundwaters, especially in the Simpevarp subarea. This is in part due to the absence of borehole KLX01, omitted because: a) it is located too far from the transects to be satisfactorily projected, and b) it has a marine component which makes it more representative for the NE ‘close to the Baltic Sea’ part of the Laxemar subarea (see Figure 10-2) but anomalous in the ‘total’ Laxemar subarea context. The ‘B’ type groundwaters in the Laxemar subarea therefore become meteoric and brackish, containing a mixture of glacial/deep saline groundwaters but devoid of an old marine (i.e. Littorina) component. They are referred to as ‘B_L’ type groundwaters. In the Simpevarp subarea the ‘B’ type groundwaters differ in that there is a weak but significant component of Littorina present, and these are referred to as ‘B_S’ type groundwaters. As indicated in Figure 10-4 the B_L groundwaters are continuously moving into the Simpevarp subarea at depth, mixing with the B_S groundwaters and gradually discharging to shallower levels.

14 Note on the origin of brines and their relevance to site characterisation studies

14.1 Background

Groundwaters of high salinity are ubiquitous at depth in the Fennoscandian Shield and, as such, their origin and evolution form an integral part of the hydrogeochemical site characterisation investigations. Their influence to varying degrees is indicated close to repository depths under present-day undisturbed bedrock conditions through upward diffusion and mixing processes. Under disturbed conditions, for example during glacial events, the formation of near-surface 'freeze-out' brines in association with permafrost conditions may develop, possibly propagating down to repository depths. Permafrost may be accompanied also by an upward migration of old, deeper saline groundwaters to shallower levels. Furthermore, during the repository construction and operational phases, upconing of deep saline groundwaters is predicted to occur and on occasions this has been observed at the borehole scale at the Laxemar/Simpevarp and Fosmark sites. The main consequences of highly saline groundwater incursions at repository levels include: a) a potential source of sulphate which, through microbial activity (i.e. sulphate reducing bacteria), may produce sulphide; this, in turn, promotes canister corrosion, and b) the gradual deterioration of the bentonite buffer material.

To characterise these saline end members it is therefore important to understand fully the past and present (and potentially predict the future) hydrochemical evolution of the candidate site in question, and to use such information to help assess potential repercussions on long-term repository safety and performance.

14.2 Deep brines and origin of salts

14.2.1 The Swedish context

Based on available deep groundwater data from the Swedish Precambrian basement /Juhlin et al. 1998/, Figure 14-1 provides a schematic illustration of a vertical transect along the direction of the regional hydraulic gradient. Meteoric recharge is initiated in the central Palaeozoic Caledonides to the west and deep discharge is expected along the eastern coastline, in this case the coastal section has been constructed to include the Simpevarp area site investigation localites. The effect of the meteoric water recharge can be detected to depths approaching 5 km as indicated from the deep Gravberg borehole at Siljan, and to a lesser projected depth at the Sripa site (2–3 km) which lies within a major discharge area. From Zinkgruvan to the eastern coast, i.e. representing a distance of approx. 230 km., the generally low topography is characterised by more localised recharge/discharge systems extending to various depths but probably averaging out around 1,000 m; in this region deep, highly saline groundwaters and brines are correspondingly close to the the surface. At the site characterisation localities at Laxemar/Simpevarp and Forsmark it is therefore expected that these groundwaters and brines are present at relatively shallow depths (1,000–2,000 m).

14.2.2 Measured salinities

Brine is normally defined as a fluid comprising greater than 100 g/L TDS. In the Swedish basement at depths mostly around 1,000 m this compares with ~ 75 g/L TDS for the most saline groundwater at the Laxemar site (KLX02), ~ 40 g/L TDS at the Oskarshamn site (KOV01), ~ 30 g/L TDS at the Simpevarp site (KSH03A), ~ 20 g/L TDS at the Ävrö site (KAV04A), ~ 20 g/L TDS at the Äspö site (KAS03) and ~ 15 g/L TDS at the Forsmark site (KFM03A). With the exception of the Ävrö site (Ca/Na = 0.88), all these deep groundwaters are Ca-Na-Cl in type with the Ca/Na ratio ranging from 1.06 at the Simpevarp site to 2.34 at the Laxemar site. In the Finnish basement salinity levels around the 1,000 m depth are within a similar range, for example ~ 70 g/L TDS at Olkiluoto /KR4 861; Pitkänen et al. 1999/ and 44–48 g/L TDS at the Kotalahti Mine /1090; Blomqvist et al. 1989/.

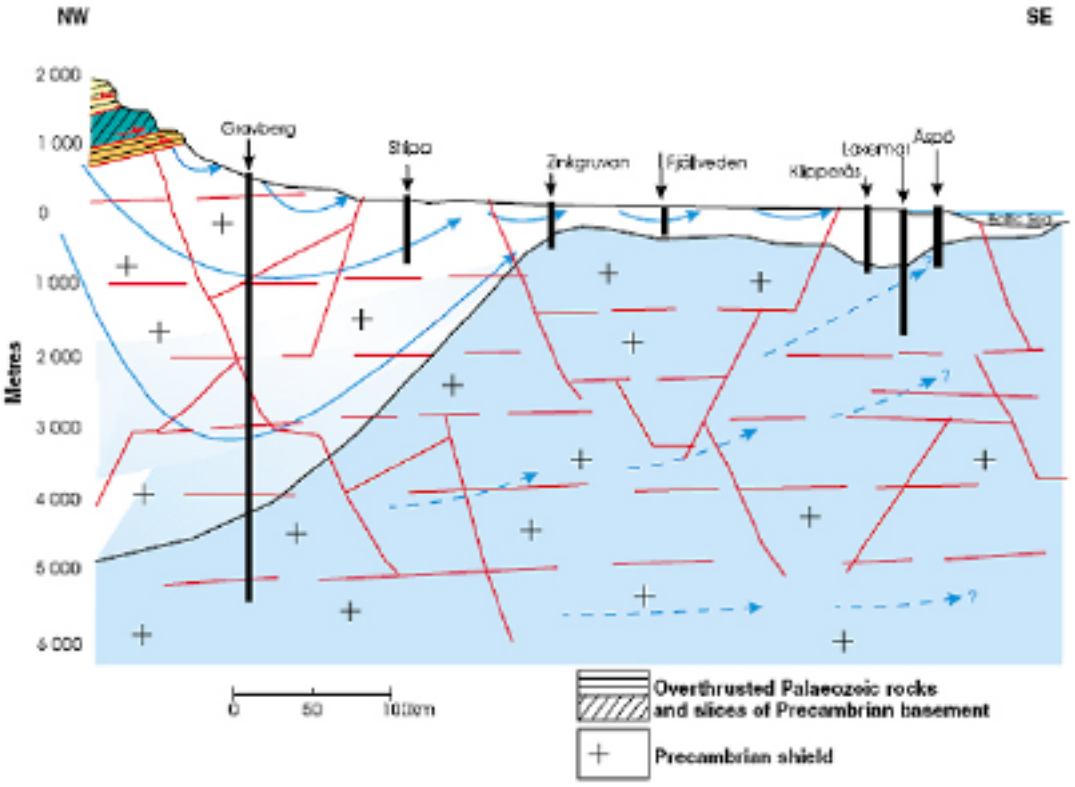

Figure 14-1. *Schematic NW-SE transect from the western Caledonoides to the SE coast showing the major regional recharge/discharge areas and the approx. depths of the highly saline groundwaters (light blue) and brines (darker blue colour) /after Juhlin et al. 1998/.*

For further illustration see Figure 14-2 which plots chloride with depth. Comparing Laxemar with Olkiluoto shows that the transition point to a highly saline environment is site dependent, ~ 800 m depth and ~ 1,200 m depth respectively, but probably averages out to around 1,000 m as suggested by the other plotted data.

In Canada reported salinities are considerably more concentrated than those so far measured in Sweden and Finland. Furthermore, in the Canadian Shield stagnant, diffusion dominated groundwater conditions are commonly established at depths greater than around 300 m irrespective of variations of local topography, distribution of recharge/discharge zones and rock types, and consequently salinities increase rapidly /Gascoyne et al. 1987/. Measured Ca-Na-Cl brine compositions from some deep mine sources at around 1,500–1,600 m (e.g. Sudbury, Ontario, Thompson, Manitoba and Yellowknife, North West Territories) range from 254–325 g/L TDS /Frape et al. 1984, Bottomley et al. 1999/ with high Ca/Na ratios of 37.6 and 42.7 respectively at Yellow Knife and Sudbury and a significantly lower ratio of 1.4 at Yellow Knife.

14.2.3 Sources of salinity

As summarised by /Lampén 1992/, there are several potential sources to the salinity measured in deep groundwaters:

Allochthonous sources such as: a) ancient Proterozoic (older than ~ 570 Ma) seawater or basinal brines, b) Palaeozoic (older than ~ 250 Ma) basinal brines, c) seawater and evaporites, and d) young Holocene (10-0 ka) brackish waters.

Autochthonous sources such as: a) residual metamorphic/igneous fluids, b) hydrolysis of silicate minerals, and c) dissolution/leaching of salts present interstitially in the rock matrix.

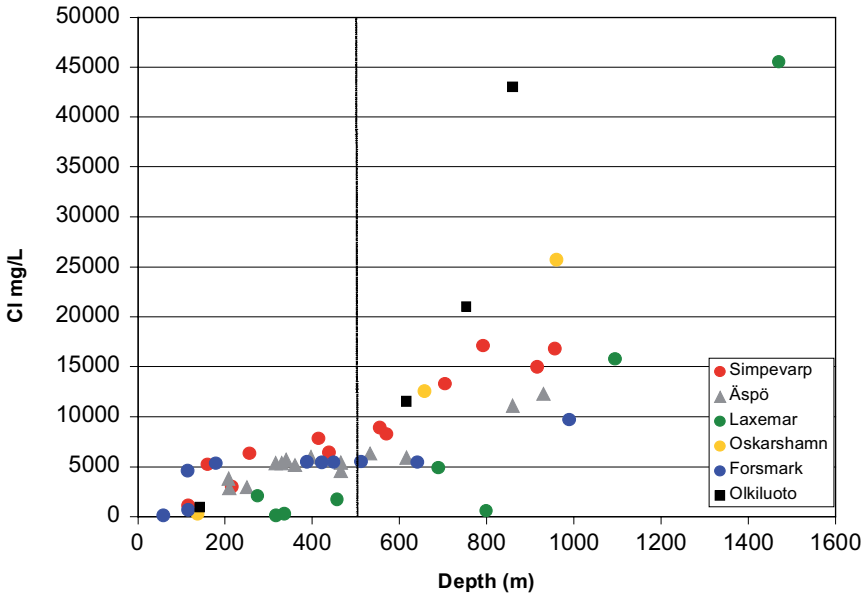

Figure 14-2. *Depth comparison of chloride between different Simpevarp area sites and other Fennoscandian sites.*

Under disturbed conditions, for example in the Fennoscandian Shield where crustal stress release is a on-going process responding to glacial isostatic recovery, an additional source may derive from the rupture and/or dissolution of fluid inclusions (which may be allochtonous or authochtonous in origin) located in and/or around some of the major rock-forming minerals (mostly quartz).

In conclusion, it is generally accepted that no one process or source can account for the observed salinities in the basement Shield areas of Canada and Fennoscandia and most reported occurrences seem to represent mixtures of meteoric water with a highly concentrated brine.

14.2.4 Origin of salinity: Chemical and isotopic indicators

To trace the origin and palaeoevolution of highly saline brines requires a coordinated and collective use of chemical and isotopic indicators. The following list of indicators reported in the literature has been used with varying success:

- ^{36}Cl age-dating (millions of years is characteristic).
- Ca/Na ratio > 1 (majority of Canadian basement brines and Fennoscandian highly saline groundwaters).
- High/low Br/Cl ratio (indicates a non-marine/marine origin respectively).
- High/low Li/Br ratio (indicates a non-marine/marine origin respectively).
- High radiogenic $^{87}Sr/^{86}Sr$ ratio (long residence time water/rock interaction processes).
- Positive $^{37}Cl/^{35}Cl$ ratios indicate a non-marine origin; negative ratios indicate a marine origin.
- High $\delta^{18}O$ and δD values (suggests long residence time water/rock interaction processes).
- High concentrations of dissolved gases of deep origin (N_2–$CH_4 \pm H_2 \pm {}^3He$) with high $\delta^{13}C$ values and the presence of ^3He indicating a deep mantle origin.
- Anomalous anaerobic microbial populations from depth.

14.2.5 Application to the Swedish basement groundwaters

To date no groundwaters of truely brine character have been sampled in the SKB site characterisation investigations. In all probability this is because of the limited depth of the drilling campaign as indicated by the greatest salinity associated with deepest drilled borehole at Laxemar

(KLX02: 1,705 m). A further 500–1,000 m of drilling most likely would have intercepted brine-type waters. The characterised deep groundwaters to around 1,000 m from the various sites are therefore mixtures of younger descending waters of different origin with variable amounts of deep, ancient brine waters. The antiquity of the brine component in the Simpevarp area is indicated from ^{36}Cl dating of groundwaters collected at different depths from the Äspö site /Louvat et al 1999/. The deepest level (~ 900 m), corresponding to the highest salinity, suggests a penetration of deep salinity into the host rock more than 1.5 Ma ago.

Major and trace ions

The enhanced mineralisation of the groundwaters at depth is considered to result from long residence times and intense water/rock reactions and this is reflected in both the major and trace ion contents in the groundwaters.

Figure 14-3 shows that with the notable exception of the Oskarshamn site (KOV01) and Olkiluoto, Finland (not shown), all sites generally show a consistent increase in sulphate with increasing salinity. However several of the deepest Laxemar groundwaters indicate a levelling of sulphate at around 900–1,000 mg/L despite a significant increase in salinity from 15,000–50,000 mg/L Cl. This limitation of sulphate content in deep saline groundwaters was also noted by /Gascoyne 2004/ at the URL site in Canada; in this case it was attributed it to the solubility control exerted by gypsum which was close to saturation in the groundwaters. This explanation is probably valid for the Swedish groundwaters.

Figures 14-4 and 14-5 exemplify the typical distribution of some trace elements with depth, in this case the distribution of Sr and Cs. The sharp increase at around 1,000 m is again noticeable, more accentuated by the Laxemar deep groundwaters at around 1,400–1,500 m which record 275 mg/L Sr and 15 μm/L Cs respectively.

The transition between a shallower, more dynamic hydraulic environment, influenced by by meteoric (and probably by marine-derived waters in the case of the Simpevarp subarea), to a deeper stagnant environment (> 1,000 m) increasingly dominated by a deep saline component, is reflected in several of the major ion-ion plots. For example, Figure 14-6 shows the gradual depth-related increase in bromide with increase in chloride. The shallow dilute groundwaters plot close to the modern sea dilution line whilst the deeper samples show an increasing deviation with depth; the highest salinity samples suggest a distinct non-marine or non- marine/old marine mixing origin.

By plotting Ca/Mg versus Br/Cl, Figure 14-7 provides a further opportunity to illustrate the complex mixed nature of Swedish basement groundwaters, particularly at depths < 1,000 m. The figure clearly shows the Baltic Sea group of modern marine waters and also the deepest and oldest non-marine (or non-marine/old marine mixing origin) highly saline groundwaters from the Laxemar and Oskarshamn (i.e. KOV01) sites. Between these two extreme end-members lie most of the groundwater data from the Simpevarp area sites. The red arrow shows the direction towards the deep, saline non-marine types, and much of the data along this pathway (i.e. to depths of around 1,000 m) represent groundwaters which contain an increasing component of the deep saline non-marine or non-marine/old marine mixing end member.

Stable isotopes

Stable chlorine isotopes may also be used as an indicator of marine vs non-marine derived groundwaters and therefore further support for detecting a transition towards non-marine deeper saline groundwaters. According to /Frape et al. 1996/ modern Baltic and possibly palaeo-Baltic waters may be recognised by negative $\delta^{37}Cl$ signatures related to salt leachates from Palaeozoic salt deposits south of the Baltic Sea. Influence by water-rock interaction (i.e. characteristic of deep, highly saline groundwaters and brines) tends to result in positive $\delta^{37}Cl$ signatures. /Clark and Fritz 1997/ also show a clear distinction between the Fennoscandian and Canadian Shield crystalline rock groundwaters and groundwaters from sedimentary aquifers.

Taking into consideration the analytical uncertainty of around ± 0.2‰ SMOC, Figure 14-8 shows that non-marine derived groundwaters significantly enriched in Br (i.e. Simpevarp and Laxemar), compared to low Br marine waters (i.e. Baltic Sea) and those groundwaters with a clear marine

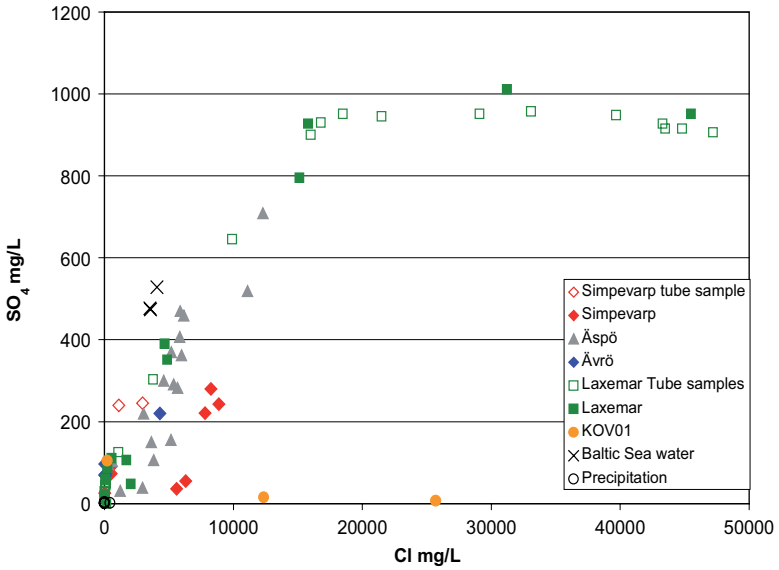

Figure 14-3. *Plot comparing Simpevarp subarea SO_4 vs Cl data.*

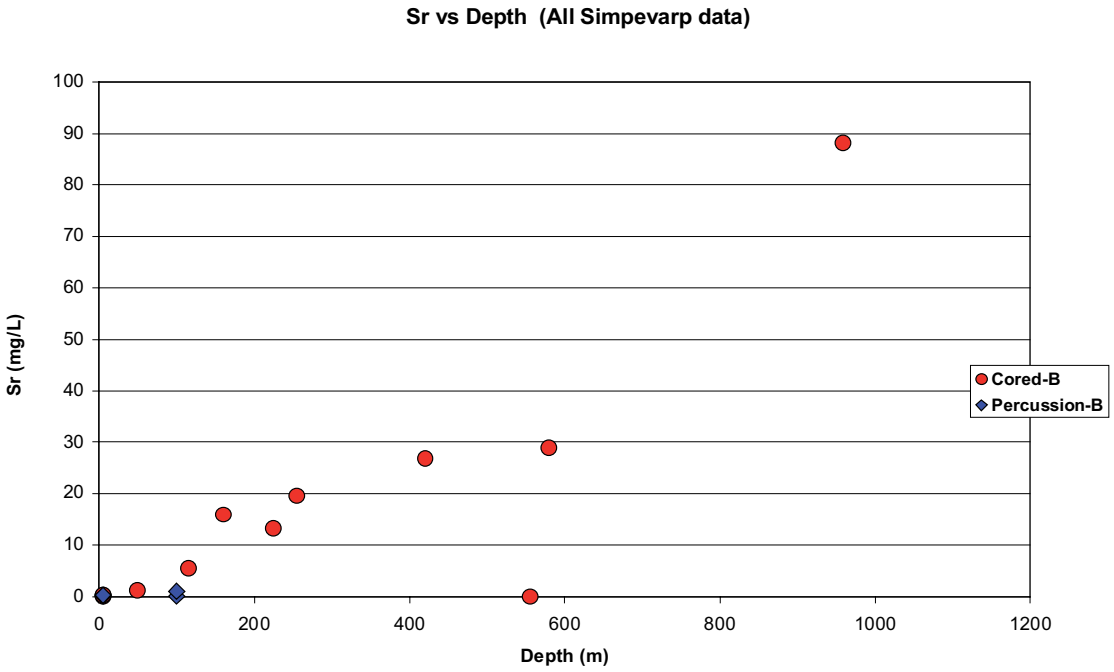

Figure 14-4. *Plot of strontium versus depth for the Simpevarp subarea (the deepest Laxemar groundwater recorded is 275 mg/L Sr – not shown).*

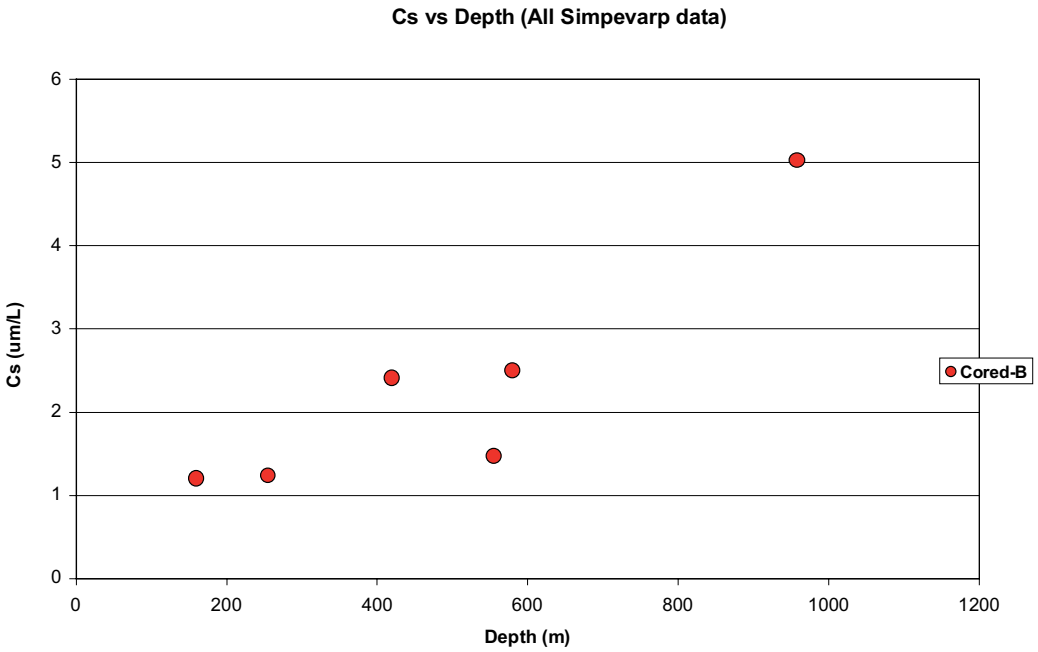

Figure 14-5. *Plot of ceasium versus depth for the Simpevarp subarea (the deepest Laxemar groundwater recorded is 15 µm/L Cs – not shown).*

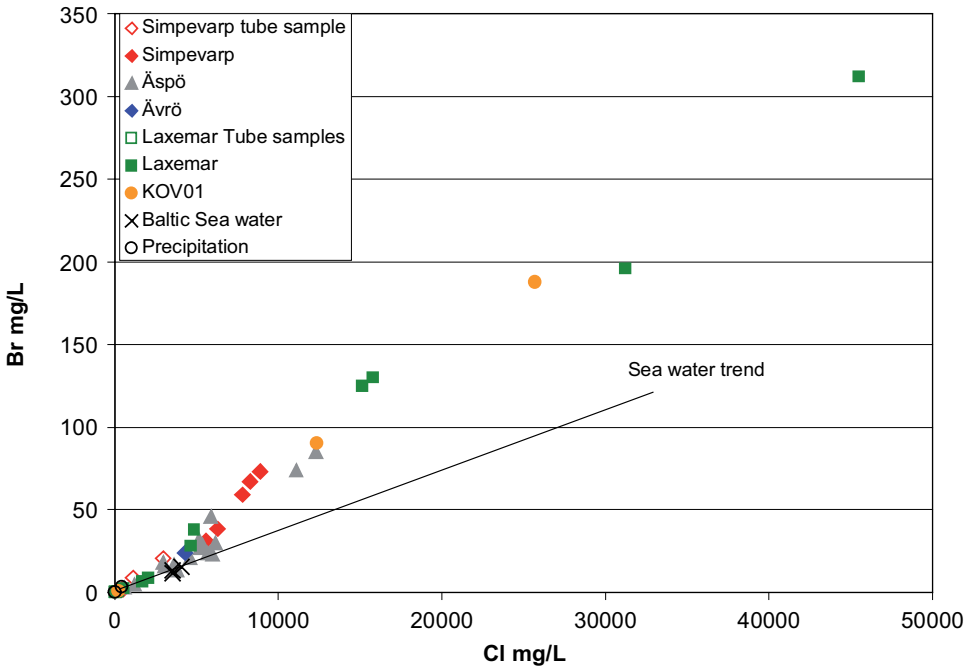

Figure 14-6. *Plot comparing Simpevarp area Br vs Cl data.*

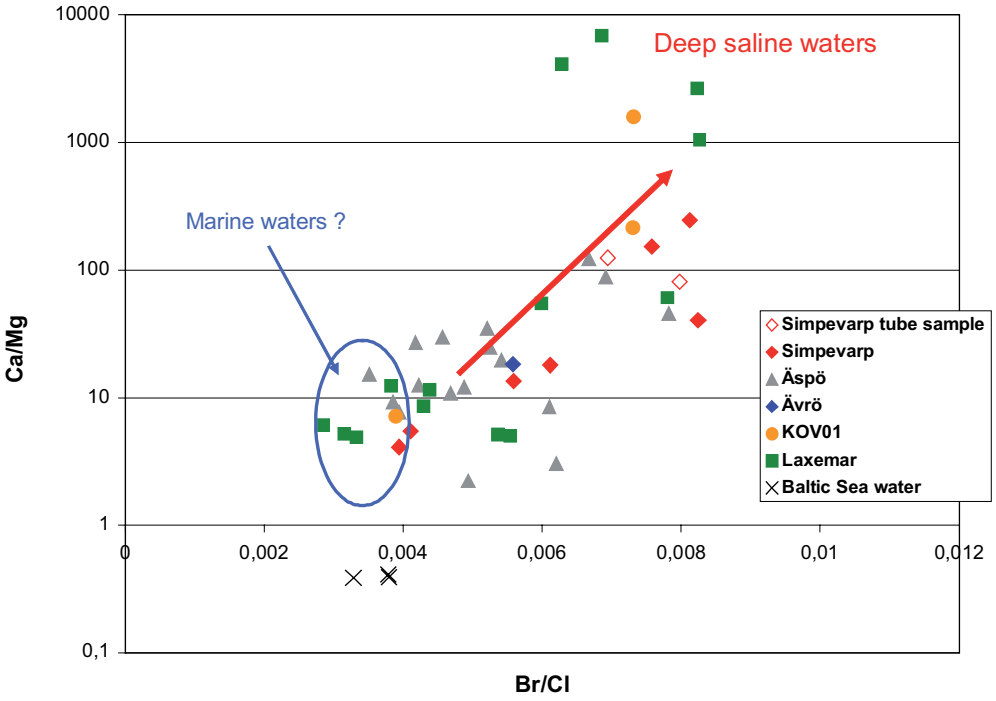

Figure 14-7. *Plot comparing Simpevarp area Ca/Mg vs Br/Cl data.*

signature (i.e. Forsmark), display positive $\delta^{37}Cl$ values. The Forsmark groundwaters characterised by more marine-derived Br/Cl ratios cluster closer to 0‰ SMOC with a similarily large spread of values as for the Baltic Sea samples. At Forsmark the more positive values (> 0.4‰ SMOC) reflect deeper groundwaters from the cored boreholes where mixing with marine waters is less marked. A dominant water/rock interaction interpretation from deep groundwaters essentially agrees with studies carried out in Finland /Frape et al. 1996/.

Stable $\delta^{18}O$ and δD data have been used in the Canadian Shield studies to differentiate deep brines from younger, shallow derived groundwaters. Figure 14-9 plots the Laxemar and Simpevarp subarea data and also compares these with the Äspö HRL groundwaters. The distinguishing feature, in common with the Canadian brine plots, is the characteristic deviation trend from the GMWL which increases with increasing salinity. This has been discussed, among others, by /Frape and Fritz 1987/ who considered this an a indication of very intensive water/rock interactions under long residence times.

The trend towards heavier $\delta^{18}O$ (and δD) values with increasing salinity is suggested in Figure 14-10 by the KOV01 and Laxemar groundwaters (deepest Laxemar value at $\delta^{18}O = -8.9$‰ SMOW is not shown); this follows the more negative values at lower salinities (i.e. depths) reflecting a younger, cold climate recharge component during previous glaciations.

A further isotopic approach has been the use of lithium and its isotopes ^{6}Li and ^{7}Li to differentiate between groundwater of marine or non-marine origin /Bottomley et al. 1999/. Such analyses are expensive and time-consuming and are presently not being considered for the Swedish programme.

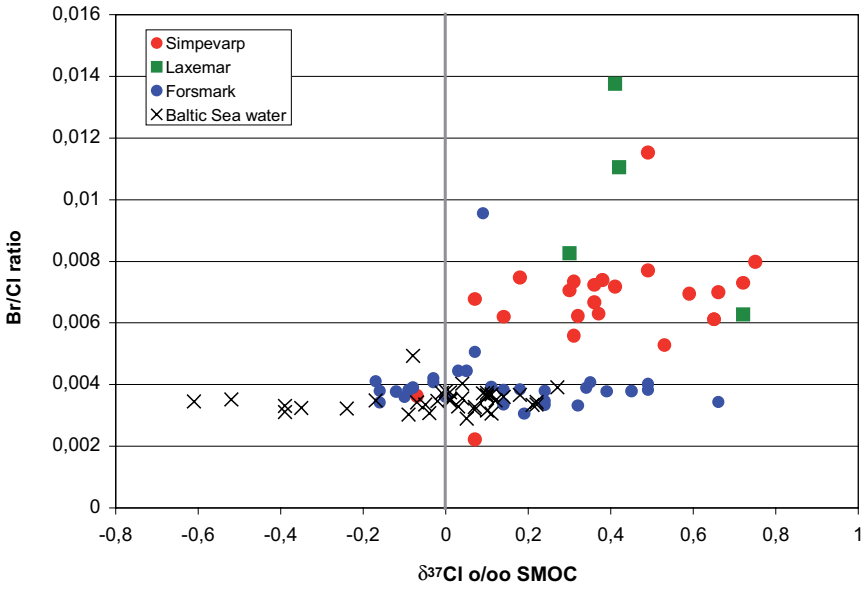

Figure 14-8. *Plot of $\delta^{37}Cl$ versus Br/Cl ratio in groundwaters from the Simpevarp area and Forsmark, and Baltic Sea waters from the Simpevarp and Forsmark areas.*

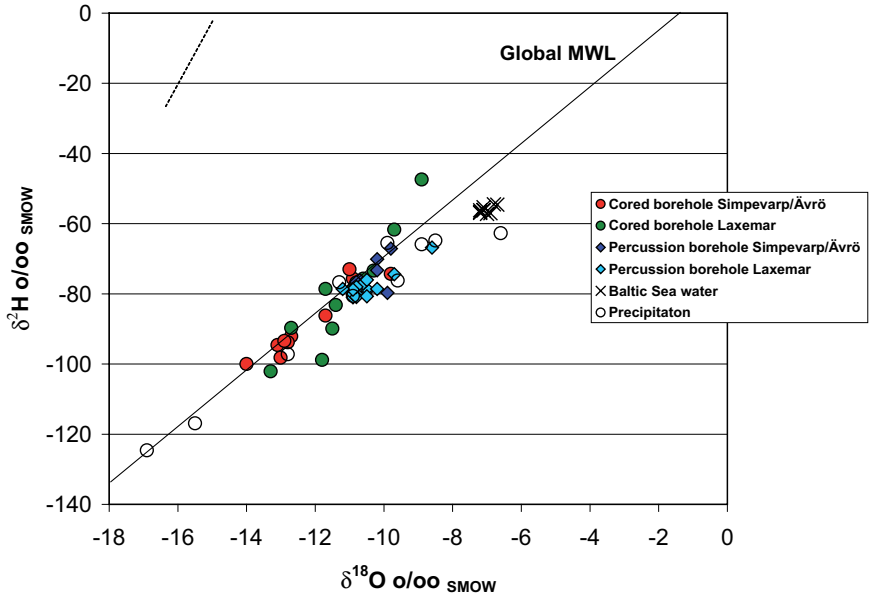

Figure 14-9. *$\delta^{18}O$ and δD trends in the Simpevarp and Laxemar subarea borehole groundwaters. (Baltic Sea waters and precipitation are added for reference).*

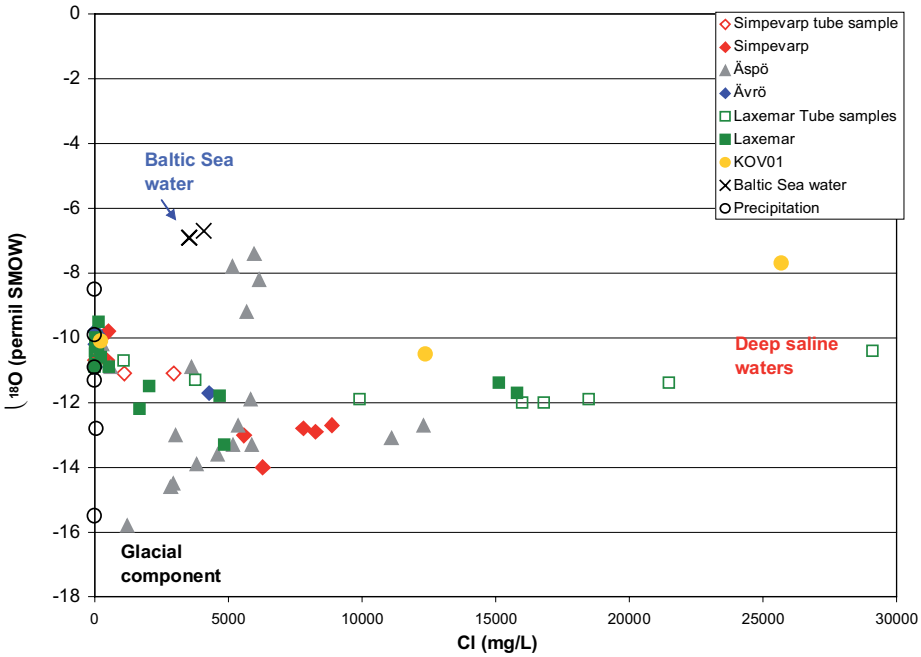

Figure 14-10. *Plot comparing Simpevarp area δ18O versus Cl data. (Baltic Sea waters and precipitation are added for reference).*

14.2.6 Summary and conclusions

Despite the overall lack of data at depths greater than 1,000 m from the Simpevarp area characterisation sites, with the exception of Laxemar KLX02, there are strong indications that:

- Ca(Na)-Cl groundwaters of deep origin are probably common throughout the Simpevarp area.
- True brines (> 100 g/L TDS) have not yet been sampled because of the restricted depth of the drilling campaigns.
- Under undisturbed conditions these deep saline waters have migrated upwards by diffusion processes and mixed with younger, downward moving groundwaters driven advectively by hydraulic gradients responding to surface topography. The degree of mixing is site specific, but is most prevalent from 500 m to around 1,000 m depth, although this could be extended to greater depths if more data were available.
- These mixing processes, and degrees of mixing, are clearly indicated from hydrochemical and isotopic considerations.
- At shallower depths (~ < 500 m) the hydraulic system is more dynamic and therefore dominated by younger groundwaters of different origin and age, although local discharge locations may have retained some evidence of groundwaters of deep origin.
- The deep saline groundwaters show most affinity to a non-marine origin although a non-marine/ old marine mixing origin cannot be excluded at this juncture.

14.3 Shallow freeze-out brines

14.3.1 Formation and evolution

In Fennoscandia when the continental ice sheet was formed at about 100,000 BP permafrost formation ahead of the advancing ice sheet probably extended to depths of several hundred metres. According to /Bein and Arad 1992/ the formation of permafrost in a brackish lake or a restricted coastal sea environment (e.g. similar to the Baltic Sea or Huson Bay in Canada) produced a layer of highly concentrated salinity ahead of the advancing freezing front. Since this saline water would be of high density, it subsequently would sink to lower depths, would avoid dilution by oceanic water, and potentially penetrate into the bedrock where it would eventually mix with formational groundwaters of similar density. However, whether the volume of high salinity water produced by this freeze-out process would be adequate to produce such widespread salinity effects deep in the bedrock as observed in the Fenoscandian basement is presently under debate.

Where the bedrock was not covered by brackish lake or restricted sea water, similar freeze-out processes would occur in the bedrock on a much smaller scale within the hydraulically active fractures and fracture zones, again resulting in formation of a higher density saline component which would gradually sink and eventually mix with existing saline groundwaters at depth.

With continued evolution and movement of the ice sheet, areas previously subject topermafrost would be eventually covered by ice accompanied by a rise in temperatureand slow decay of the underlying permafrost layer. This decay would melt the ice formed during the freeze-out processes introducing a dilute groundwater component into the groundwater system.

This freeze-out hypothesis is largely based on laboratory freezing experiments /e.g. Nelson and Thompson 1954/ which were able to distinguish between the products of evaporation and freezing (Figure 14-11). The solid products from evaporation consisted of halite with subsidiary gypsum, and from freezing, hydrahalite and mirabilite. The most important difference during freezing is the removal of the SO_4^{2-} ion in mirabilite ($Na_2SO_4 \times 10H_2O$). Present day evidence of freeze-out processes might therefore include the possible preservation of mirabilite or, most likely, a sulphate-rich lens or pocket of groundwater because of the highly metastable nature of mirabilite to temperature increase. To date no anomalous sulphate-rich groundwaters have been recognised from the Swedish investigated sites. One promising occurrence at the Palmottu natural analogue site in Finland subsequently has been interpreted as being hydrothermal in origin /Smellie et al. 2002a/.

14.3.2 Isotopic indicators

Suggested isotopic indicators of freeze-out processes have included $\delta^{37}Cl$, $\delta^{18}O$ and δD /Ruskeeniemi et al. 2004/ and $\delta^{11}B$ /Casanova et al. 2005/.

A $\delta^{37}Cl$, $\delta^{18}O$ and δD study was carried out as part of the Lupin Mine permafrost project in northern Canada. This study entailed the laboratory freezing of Canadian and Fennoscandian Shield groundwaters to assess the importance of geochemical and isotopic signatures in recognising and interpreting palaeogroundwaters /Ruskeeniemi et al. 2004/. Representing the Fennoscandian Shield were Na-SO_4 groundwaters from Palmottu and suspected to have been derived from freezing, referred to in section 1.3.1, and from the Canadian Shield a Ca-Cl brine from Sudbury which, according to /Herut et al. 1990/ may have been produced by freezing. Both column (for a slower rate of freezing) and batch (faster rate freezing) experiments were carried out at the University of Waterloo /Ruskeeniemi et al. 2004/.

Figure 14-12 shows that there was a successive enrichment of $\delta^{18}O$ and δD in the ice during the experiment, with that observed for Palmottu agreeing with predicted behaviour using fractionation factors reported from the literature. Groundwaters subjected to extended permafrost conditions might therefore be expected to be characterised by heavier $\delta^{18}O$ and δD values.

Figure 14-13 plotting $\delta^{37}Cl$ against Cl (above) and against $\delta^{18}O$ (below) shows a gradual depletion of $\delta^{37}Cl$ in the residual fluid during the freezing of the Palmottu $NaSO_4$ groundwater but on completion of the experiment there was little significant difference between the original groundwater and the

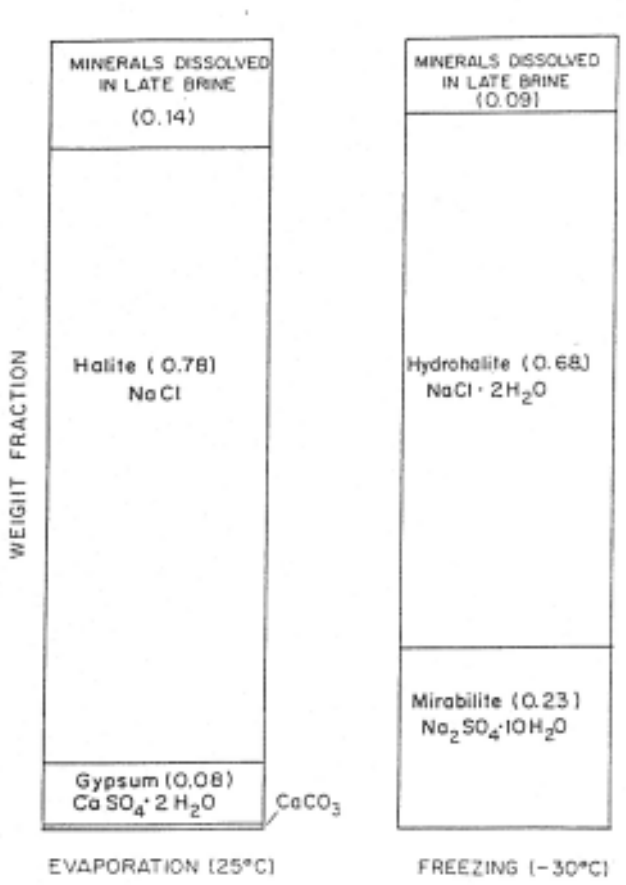

Figure 14-11. *A quantitative comparison between the products of seawater evaporation and freezing /Nelson and Thompson 1954, McCaffrey et al. 1987/.*

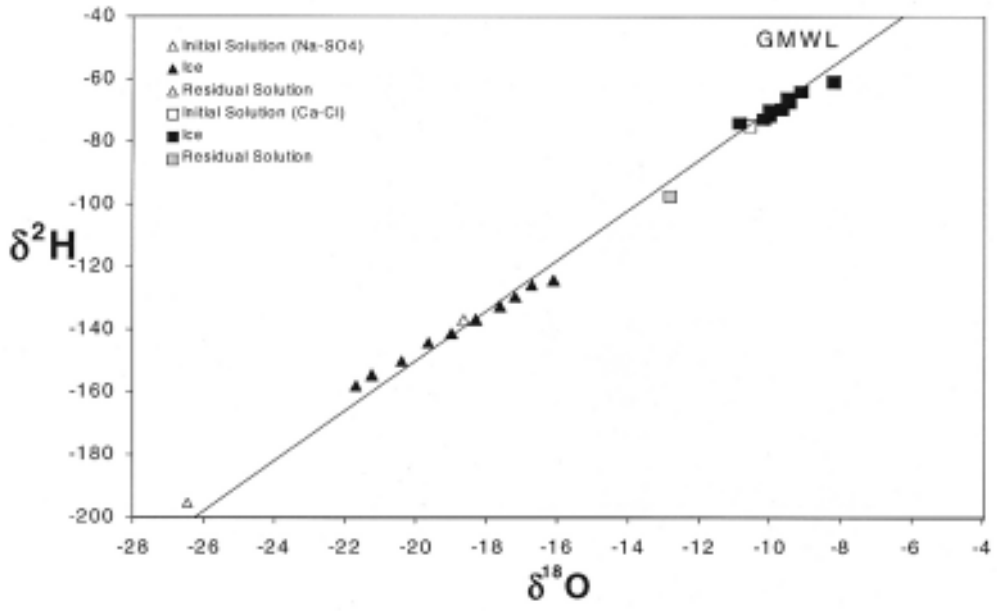

Figure 14-12. *$\delta^{18}O$ and δD for solutions from the column experiment using Palmottu ($NaSO_4$) and Sudbury (Ca-Cl) groundwaters /after Ruskeeniemi et al. 2004/.*

residual fluid. The Sudbury Ca-Cl groundwater shows even less effect with no evidence of depletion, except for one anomalous outlier which may be an experimental artefact, and ultimately no significant difference between the original groundwater and the residual fluid. Based on these results the use of $\delta^{37}Cl$ as a indicator of freeze-out processes appears to be unsuitable.

Another approach has been that of /Casanova et al. 2005/ who used boron and its isotopes to: a) establish the degree of water/rock interaction, b) assess groundwater mixing, and c) clarify freezing processes for groundwaters from the Äspö HRL in Sweden and several sites in Finland. This is made possible by the large relative mass difference between the isotopes ^{10}B and ^{11}B and the high chemical reactivity of boron; this causes significant isotope fractionation resulting in large variations in the $^{11}B/^{10}B$ ratios in natural samples.

With respect to freezing processes, /Casanova et al. 2005/ suggest that during permafrost development two components are produced; an ice component in the fracture stystems and a residual liquid component which is forced to greater depths ahead of the advancing freeze-out front. This process would be accompanied by the preferential fractionation of ^{10}B into the ice component and ^{11}B into the fluid phase. Although subsequent melting of the ice would mix with the residual fluid, and additional mixing with different groundwater incursions would also eventually occur with time, these modifications may be restricted to the more highly transmissive parts of the bedrock, whilst low transmissive parts (including dead-end pathways; microfractures; matrix pores etc) may have preserved fluids enriched in ^{11}B.

Figure 14-12 shows the relationship of $\delta^{11}B$ vs, depth and $\delta^{11}B$ vs $\delta^{18}O$ for Fenoscandian groundwaters, Baltic Sea waters and the Mean Sea Water field (MSW). The Äspö and Palmottu samples exhibit a similar pattern to that of Olkiluoto and Hästholmen, i.e. a tendency for $\delta^{11}B$ enrichment with depth and $\delta^{11}B$ enrichment correlated with depleted $\delta^{18}O$. These trends may suggest the general presence of a freeze-out signature at depths greater than 400–500 m. Mixing processes since the last glaciation have, however, diluted to varying degrees any signature that may have existed and present data are therefore ambiguous. In fact, water/rock interaction processes at increasing depth might also explain the observed data distribution. Quantitative sampling from matrix pore space water, microfractures and other low hydraulically conductive fractures close to a major transmissive fracture zone would be a minimum requirement to be addressed in future studies.

14.3.3 Summary and conclusions

- Laboratory studies show that surface to near-surface freezing of groundwater can produce a residual fluid of high salinity and, because of its high density, may migrate along hydraulically active fractures and settle at great depth in the bedrock.
- Freezing during permafrost conditions has occurred in the Fennoscandian Shield and may have penetrated to depths of 480 m /Boulton et al. 2001/ or more, i.e. at least to repository levels.
- Propagation of a freezing front down into the bedrock may force the residual fluid into low transmissive areas adjacent to the main transmissive pathways, i.e. dead-end pathways; microfractures; matrix pores etc.
- These low transmissive ‘traps’ are the most promising source of undiluted residual fluids and therefore may provide the best evidence of freeze-out processes.
- The residual fluids should not only be characterised by high salinities, but may also have enriched signatures of $\delta^{11}B$ and depletions of $\delta^{18}O$ and δD; $\delta^{37}Cl$ does not appear to be a sensitive indicator.

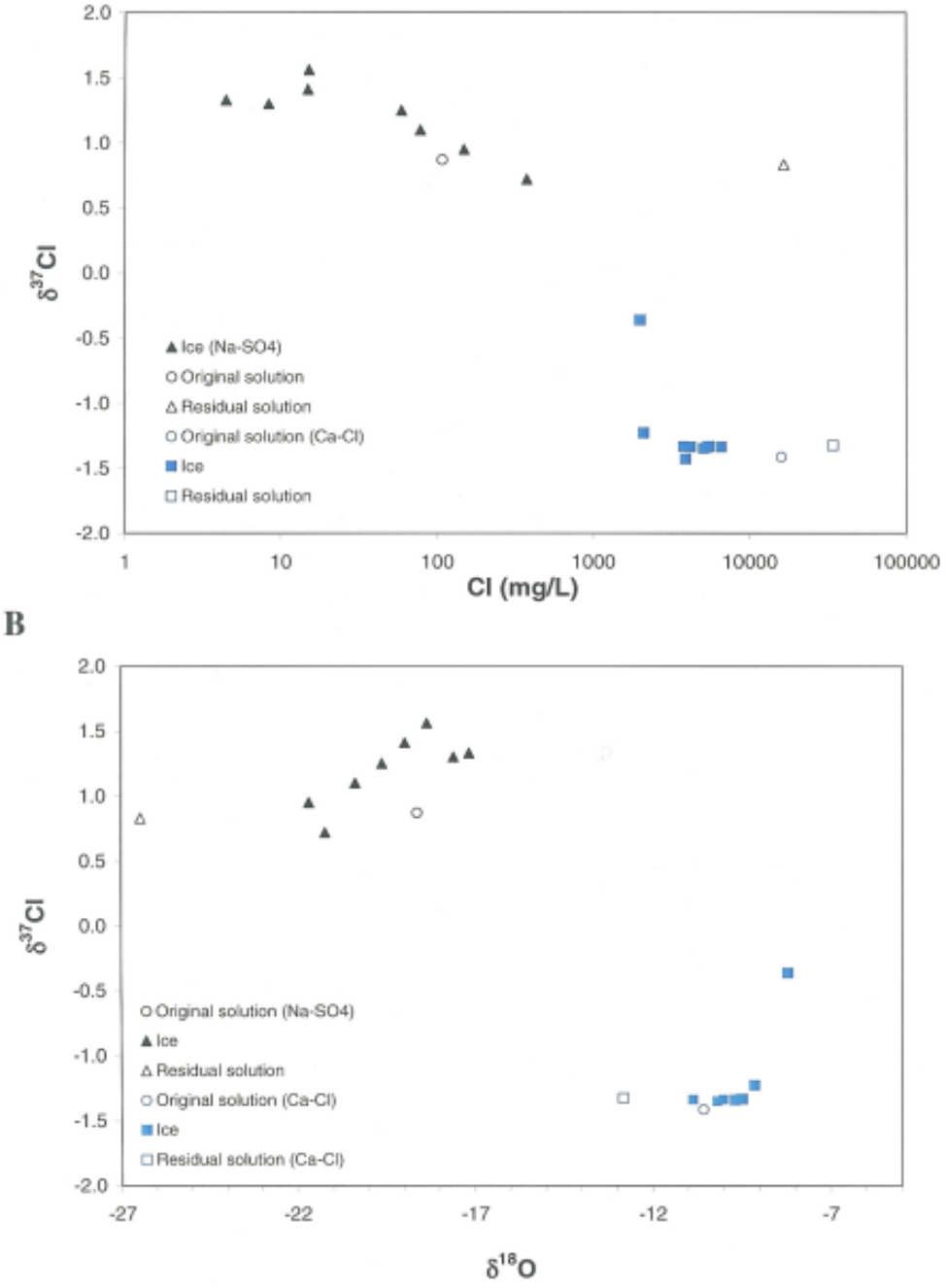

Figure 14-13. *Chlorine isotopic composition versus chloride concentration (above) and oxygen isotopic composition (below) for groundwaters from Palmottu and Sudbury /after Ruskeeniemi et al. 2004/.*

14.4 Origin of the brine end member

As outlined in section 1.2.3, there are several sources of salts that may combine to form highly saline groundwaters and ultimately hypersaline brines at great depth. However the fact that these deep saline groundwaters and brines are extremely old, have been subject to mixing, exist under near-stagnant hydraulic conditions and therefore long residence times, they have undergone intensive water/rock interactions which have served to mask any evidence of their original source and origin. Several hydrochemical and isotopic indicators are available to help unravel their hydrogeochemical evolution, but these have had only limited success and there is still much debate.

Considerable literature has been produced from the Canadian Shield brine occurrences /e.g. Fritz and Frape 1982, Gascoyne et al. 1989, Herut et al. 1990, Bottomley et al. 1999 and references within/ and although there is no dispute that the brine salinity is of marine basin origin, there is on-going debate as to the main mechanism responsible for concentrating the the hypersaline brine; evidence exists for both evaporative and cyrogenic processes.

In the Fennoscandian Shield the origin of the salinity is less clear; much evidence points to non-marine sources such as residual metamorphic/igneous fluids and fluid inclusions /Nordstrom et al. 1989/ accompanied by intensive meteoric water/rock interactions. The problem with these interactions is that they may mask any evidence of addressing the possibility of whether non-marine/old marine mixing has occurred at some period of time in the distant past. A marine origin for the brine salinity has been invoked by /Fontes et al. 1989/ and suggested also by /Louvat et al. 1999/ and /Casanova et al. 2005/. Therefore it is still an open question.

15 References

Andersson P, Byegård J, Dershowitz B, Doe T, Hermanson J, Meier P, Tullborg E L, Winberg A, 2002. Final report of the TRUE Block Scale. 1. Characterisation and model development SKB TR-02-13, Svensk Kärnbränslehantering AB.

Bath A, Milodowski A, Ruotsalainen P, Tullborg E-L, Cortés Ruiz A, Aranyossy J-F, 2000. Evidences from mineralogy and geochemistry for the evolution of groundwater systems during the quaternary for use in radioactive waste repository safety assessment (EQUIP project). EUR 19613 EN, Luxembourg.

Barth S, 1993. Boron isotope variations in nature: A synthesis. Geol. Rundsch, 82, 640–641.

Bein A, Arad A, 1992. Formation of saline groundwaters in the Baltic region through freezing of seawater during glacial periods. J. Hydrol., 140, 75–87.

Berg C, 2003. Hydrochemical logging in KAV01, Oskarshamn site investigation. SKB P-03-89, Svensk Kärnbränslehantering AB.

Berg C, 2004. Hydrochemical logging in KAV04A, Oskarshamn site investigation. SKB P-04-304, Svensk Kärnbränslehantering AB.

Bottomley D J, Katz A, Chan L H, Starinsky A, Douglas M, Clark I D, Raven K G, 1999. The origin and evolution of Canadian Shield brines: evaporation or freezing of seawater? New lithium isotope and geochemical evidence from the Slave craton. Chem. Geol., 155, 295–320.

Boulton G, Gustafson M, Schelkes K, Casanova J, Moren L, 2001. Palaeohydrology and geoforcasting for performance assessment in geosphere repositories for radioactive waste disposal (PAGEPA). EUR 19784 EN, Luxembourg.

Blomqvist R, Lahermo P, Lahtingen R, Halonen S, 1989. Geochemical profiles of deep groundwater in Precambrian bedrock in Finland.Proc. Explor. ’87: Third Decennial Int. Conf. on Geophys. and Geochem. Explor. for Min. and Groundwater (ed. G.D. Garland), Ontario Geol. Surv., Spec. Vol. 3.

Casanova J, Négrel P, Blomqvist R, 2005. Boron isotope fractionation in groundwaters as an indicator of past permafrost conditions in the fractured crystalline bedrock of the fennoscandian shield. Water Res., 39, 362–370.

Clark I, Fritz P, 1997. Environmental isotopes in hydrogeology. Lewis Publishers, New York.

Crank J, 1975. The mathematics of diffusion. Oxford University Press, 2nd edition.

Drake H, Tullborg E-L, 2004. Fracture mineralogy – results from XRD, microscopy, SEM/EDS and stable isotopes analyses. SKB P-04-250, Svensk Kärnbränslehantering AB.

Ekman L, 2001. Project Deep Drilling KLX02, Phase 2.Methods, scope, summary and results. Summary Report. SKB TR-01-11, Svensk Kärnbränslehantering AB.

Ehrenborg J, Vladislav S, 2004. Borehole mapping of core drilled borehole KAV01. Oskarshamn site investigation. SKB P-04-130, Svensk Kärnbränslehantering AB.

Fontes J-C, Fritz P, Louvat D, Michelot J-L, 1989. Aqueous sulphates from the Stripa ground-water system. Geochim. et Cosmochim. Acta, 53, 1783–1789.

Frape S K, Fritz P, 1982. The chemistry and isotopic composition of saline groundwaters from the Sudbury Basin, Ontario. Canad. J. Earth Sci., 19, 645–661.

Frape S K, Fritz P, McNutt R H, 1984. Water-rock interaction and chemistry of groundwaters from the Canadian Shield. Geochim. Cosmochim. Acta, 48, 1617–1627.

Frape S K, Fritz P, 1987. Geochemical trends from groundwaters from the Canadian Shield. In: (eds.) P. Fritz and S.K. Frape. Saline waters and gases in crystalline rocks. Geol. Assoc. Canada Spec. Paper 33, 19–38.

Frape S K, Byrant G, Blomqvist R, Ruskeeniemi T, 1996. Evidence from stable chlorine isotopes for multiple sources of chloride in groundwaters from crystalline shield environments. In: Isotopes in Water Resources Management, 1966. IAEA-SM-336/24, Vol. 1, 19–30.

Gascoyne M, Davidson C C, Ross J D, Pearson R, 1987. Saline groundwaters and brines in plutons in the Canadian Shield. In: (eds.) P. Fritz and S.K. Frape. Saline waters and gases in crystalline rocks. Geol. Assoc. Canada Spec. Paper 33, 53–68.

Gascoyne M, Ross J D, Purdy A, Frape S K, Drimmie R J, Fritz P, Betcher R N, 1989. Evidence for penetration of sedimentary basin brines into an Archean granite of the canadian Shield. WRI, (ed.) Miles. Balkema, Rotterdam.

Gascoyne M, 2004. Hydrogeochemistry, groundwater ages and sources of salts in a granitic batholith on the Canadian Shield, southeastern Manitoba. Appl. Geochem., 19, 4, 519–560.

Gimeno J, Auqué L F, Gómez J B, 2004. Mass balance modelling. In M. Laaksoharju (ed.), Hydrogeochemical evaluation of the Simpevarp area, version 1.2. SKB R-04-74, Svensk Kärnbränslehantering AB.

Hallbeck L, 2004. Explorative analyses of microbes, colloids and gases. In: M. Laaksoharju (ed.), Hydrogeochemical evaluation of the Simpevarp area, version 1.2. SKB R-04-74, Svensk Kärnbränslehantering AB.

Herut B, Starinsky A, Katz A, Bein A, 1990. The role of seawater freezing in the formation of subsurface brines. Geochim. et Cosmochim Acta, 33, 1321–1349.

Juhlin C, Wallroth T, Smellie J, Eliasson T, Ljunggren C, Leijon B, Beswick J, 1998. The Very Deep Hole Concept – Geoscientific appraisal of conditions at great depth. SKB TR-98-05, Svensk Kärnbränslehantering AB.

Lampén P, 1992. Saline groundwater in crystalline bedrock – a literature study. Nucl. Waste Comm. Finnish Power Comp., Tech. Rep. (YJT-92-23), Helsinki, Finland.

Laaksoharju M, Smellie J, Nilsson, A-C, Skårman C, 1995. Groundwater sampling and chemical characterisation of the Laxemar deep borehole KLX02. SKB TR-95-05, Svensk Kärnbränslehantering AB.

Laaksoharju M, Tullborg E-L, Wikberg P, Wallin B, Smellie J A T, 1999. Hydrogeochemical conditions and evolution of the Äspö HRL, Sweden. Appl. Geochem., 14, 819–834.

Laaksoharju M (ed.), 2004. Hydrogeochemical evaluation of the Simpevarp area, version 1.2. SKB R-04-74, Svensk Kärnbränslehantering AB.

Laaksoharju M (ed.), 2005. Hydrogeochemical evaluation of the Forsmark area, version 1.2. SKB R-05-17, Svensk Kärnbränslehantering AB.

Landström O, Tullborg E-L, 1995. Interactions of trace elements with fracture filling minerals from the Äspö Hard Rock Laboratory. SKB TR-95-13, Svensk Kärnbränslehantering AB.

Löfgren M, 2004. Diffusive properties of granitic rocks as measured by in situ electrical methods. PhD Thesis, KTH Royal Insititute of Technology, Department of Chemical Engineering and Technology, Stockholm, Sweden,115p.

Louvat D, Michelot J L, Aranyossy J-F, 1999. Origin and residence time of salinity in the Äspö groundwater system. Appl. Geochem., 14, 917–925.

Mazurek M , Bossart P, Eliasson T, 1997. Classification and characterisation of water-conducting features at Äspö: Results of investigations on the outcrop scale. SKB ICP-97-01, Svensk Kärnbränslehantering AB. (ISSN 1104-3210).

Munier R, 1993. Segmentation, fragmentation and jostling of the Baltic shield with time. Thesis, Acta Universitatus Upsalienses 37. Uppsala, Sweden.

Nelson K H, Thompson T G, 1954. Deposition of salts from sea water by frigid concentration. J. Mar. Res., 13, 166–182.

Nordstrom D K, Lindblom S, Donahoe R J, Barton C C, 1989. Fluid inclusions in the Stripa granite and their possible influence on the groundwater chemistry. Geochimica Cosmochimica Acta, 53, 1741–1755.

Peterman Z E, Wallin B, 1999. Synopsis of strontium isotope variations in groundwater at Äspö, southern Sweden. Appl. Geochem., 14, 939–951.

Pitkänen P, Luukkonen A, Ruotsalainen P, Leino-Forsman H, Vuorinen U, 1999. Geochemical modelling of groundwater evolution and residence time at the Olkiluoto site. Posiva Tech Rep. (98-10), Posiva, Helsinki, Finland.

Pitkänen P, Partamies S, Luukkonen A, 2004. Hydrogeochemical interpretation of baseline groundwater conditions at the Olkiluoto site. Posiva Tech. Rep. (2003-07), Posiva, Helsinki, Sweden.

Puigdomenech I, Ambrosi J-P, Eisenlohr L, Lartigue J-E, Banwart S, Bateman K, Milodowski A E, West J M, Griffault L, Gustafsson E, Hama K, Yoshida H, Kotelnikova S, Pedersen K, Michaud V, Trotignon L, Morosini M, Rivas Perez J, Tullborg E-L, 2001. O_2 depletion in granitic media. SKB TR-01-05, Svensk Kärnbränslehantering AB.

Rogge T, 1997. Eine molekular-diffusive Methode zur Bestimmung des Porenwassergehaltes und der Zusammensetzung von stabilen Isotopen im Porenwasser von Gestein. Unpubl. Diploma Thesis, Institut für Umweltphysik, University of Heidelberg, 76p.

Rouhiainen P, Pöllanen J, Sokolnicki M, 2005. Oskarshamn site investigation. Difference flow logging of borehole KLX03 Subarea Laxemar. SKB P-05-67, Svensk Kärnbränslehantering AB.

Ruskeeniemi T, Ahonen L, Paananen M, Frape S, Stotler R, Hobbs M, Kaija J, Degnan P, Blomqvist R, Jensen M, Lehto K, Moren L, Puigdomench I, Snellman M, 2004. Permafrost at Lupin. Report of Phase II. GTK Tech. Rep. (YST-119), GTK, Helsinki, Finland.

Rübel A P, 2000. Stofftransport in undruchlässigen Gesteinsschichten – Isotopenuntersuchungen im Grund- und Porenwasser. PhD Thesis, Institut für Umweltphysik, University of Heidelberg, Der Andere Verlag, Osnabrück, Germany, 184p.

Rübel A P, Sonntag Ch, Lippmann J, Pearson F J, Gautschi A, 2002. Solute transport in formations of very low permeability: Profiles of stable isotope and dissolved noble gas contents of pore water in the Opalinus Clay, Mont Terri, Switzerland. Geochim. Cosmochim. Acta, 1311–1321.

SKB, 2005. Preliminary site description. Simpevarp subarea version 1.2. SKB R-05-08, Svensk Kärnbränslehantering AB.

Smellie J, Laaksoharju M, 1992. The Äspö Hard Rock Laboratory: Final evaluation of the hydrogeochemical pre-investigations in relation to existing geological and hydraulic conditions. SKB TR-92-31, Svensk Kärnbränslehantering AB.

Smellie J A T, Blomqvist R, Frape S K, Pitkänen P, Ruskeeniemi T, Suksi J, Casanova J, Gimeno M J, Kaija J, 2002a. Palaeohydrogeological implications for long-term hydrochemical stability at Palmottu. EUR 19118 EN, Luxembourg.

Smellie J, Laaksoharju M, Tullborg E-L, 2002b. Hydrogeochemical site descriptive model – a strategy for the model development during site investigations. SKB R-02-49, Svensk Kärnbränslehantering AB.

Smellie J A T, Waber H N, Frape S K, 2003. Matrix fluid chemistry experiment, Final Report. SKB TR-03-18, Svensk Kärnbränslehantering AB.

Werner K, Bosson E, Berglund S, 2005. Description of climate, surface hydrology and near-surface hydrogeology. Simpevarp 1.2. SKB R-05-04, Svensk Kärnbränslehantering AB.

Appendix 1

Borehole activities prior to, during, and subsequent to groundwater sampling

Samples collected for groundwater analysis are highlighted in light green.
Samples collected by tube sampling are highlighted in dark green.

Table 1-1. Laxemar borehole activity log.

Activity	Start date	Stop date	Idcode	Secup	Seclow
Pumping, start	2003-03-12 13:35:00	2003-03-12 13:35:00	HLX10		
Water sampling, class 3	2003-03-12 13:40:00	2003-03-12 13:40:00	HLX10	0.00	85.00
Water sampling, class 3	2003-03-12 14:05:00	2003-03-12 14:05:00	HLX10	0.00	85.00
Water sampling, class 3	2003-03-12 14:30:00	2003-03-12 14:30:00	HLX10	0.00	85.00
Water sampling, class 3	2003-03-12 15:00:00	2003-03-12 15:00:00	HLX10	0.00	85.00
Pumping, stop	2003-03-12 15:05:00	2003-03-12 15:05:00	HLX10		
BIPS-logging	2004-10-20 16:00:00	2004-10-20 17:15:00	HLX10	4.00	27.10
Radar logging	2004-10-20 17:45:00	2004-10-20 18:20:00	HLX10	0.00	81.80
Percussion drilling	2004-03-08 10:00:00	2004-03-11 10:00:00	HLX14	0.00	115.90
PLU Pumping test	2004-03-11 00:00:00	2004-03-11 00:00:00	HLX14	11.90	115.90
Water sampling, class 5	2004-05-07 00:00:00	2004-05-07 00:00:00	HLX14	0.00	115.90
Water sampling, class 5	2004-05-07 00:05:00	2004-05-07 00:05:00	HLX14	0.00	115.90
Water sampling, class 5	2004-06-01 18:08:00	2004-06-01 18:08:00	HLX14	0.00	115.90
Water sampling, class 5	2004-06-01 18:08:00	2004-06-01 18:08:00	HLX14	1.00	115.90
Percussion drilling	2004-07-01 12:00:00	2004-07-06 17:30:00	HLX18	0.00	181.20
Borehole preparation	2004-07-05 12:35:00	2004-07-06 13:45:00	HLX18	15.12	181.20
Water sampling, class 1	2004-07-05 15:15:00	2004-07-05 15:20:00	HLX18	15.10	66.90
Water sampling, class 1	2004-07-06 13:55:00	2004-07-06 14:00:00	HLX18	15.10	181.20
BIPS-logging	2004-07-14 12:15:00	2004-07-14 14:30:00	HLX18	0.00	180.30
Radar logging	2004-07-14 14:30:00	2004-07-14 15:10:00	HLX18	0.00	168.50
Geophysical logging	2004-08-25 16:09:00	2004-08-25 16:54:00	HLX18	0.24	181.49
Percussion drilling	2004-06-15 09:30:00	2004-06-21 12:00:00	HLX20	0.00	202.20
Borehole preparation	2004-06-16 00:00:00	2004-06-17 18:00:00	HLX20	9.10	202.20
Water sampling, class 5	2004-06-24 07:50:00	2004-06-24 07:50:00	HLX20	0.00	202.20
Water sampling, class 5	2004-06-24 07:55:00	2004-06-24 07:55:00	HLX20	0.00	202.20
Borehole preparation	2004-09-16 08:32:00	2004-09-16 08:32:00	HLX22		
Water sampling, class 3	2004-09-17 08:40:00	2004-09-17 08:40:00	HLX22	0.00	163.20
BIPS-logging	2004-09-26 09:50:00	2004-09-26 11:37:00	HLX22	9.00	162.30
Radar logging	2004-09-29 12:15:00	2004-09-29 13:15:00	HLX22	0.00	159.80
Geophysical logging	2004-10-02 09:03:00	2004-10-02 09:23:00	HLX22	8.10	161.10
Percussion drilling	2004-09-06 13:00:00	2004-09-09 10:00:00	HLX24	0.00	175.20
Borehole preparation	2004-09-07 00:00:00	2004-09-07 00:00:00	HLX24	120.90	120.90
Water sampling, class 3	2004-09-10 10:33:00	2004-09-10 10:33:00	HLX24	0.00	175.20
BIPS-logging	2004-09-29 09:50:00	2004-09-29 11:48:00	HLX24	9.00	174.30
Radar logging	2004-09-30 12:00:00	2004-09-30 13:00:00	HLX24	0.00	171.90

Activity	Start date	Stop date	Idcode	Secup	Seclow
Geophysical logging	2004-10-03 09:06:00	2004-10-03 09:26:00	HLX24	8.20	174.40
Percussion drilling	2004-05-03 14:30:00	2004-05-13 11:00:00	KLX03	0.00	100.35
Water sampling, class 3	2004-05-04 21:00:00	2004-05-04 21:00:00	KLX03	11.95	60.00
Water sampling, class 3	2004-05-04 22:45:00	2004-05-04 22:45:00	KLX03	11.95	100.30
Core drilling	2004-05-28 18:00:00	2004-09-07 09:00:00	KLX03	100.35	1000.42
PLU Pumping test – air lift	2004-05-30 21:00:00	2004-05-30 21:30:00	KLX03		
Flush water out	2004-05-31 01:56:00		KLX03	101.96	
PLU Pumping test – air lift	2004-05-31 18:03:00	2004-06-01 06:00:00	KLX03		
Microbiology	2004-06-03 16:07:00	2004-06-03 16:08:00	KLX03		
PLU Pumping test – air lift	2004-06-03 18:14:00	2004-06-04 00:20:00	KLX03		
PLU Pumping test – wire line	2004-06-04 01:15:00	2004-08-14 00:00:00	KLX03	103.00	218.02
Water sampling, class 3	2004-06-04 12:55:00	2004-06-04 12:55:00	KLX03	103.00	218.02
PLU Pumping test – air lift	2004-06-04 18:27:00	2004-06-05 08:52:00	KLX03		
Water sampling, class 3	2004-08-14 09:45:00	2004-08-14 09:45:00	KLX03	497.02	599.89
PLU Pumping test – air lift	2004-08-14 10:58:00	2004-08-17 00:00:00	KLX03		
Water sampling, class 3	2004-08-17 16:15:00	2004-08-17 16:15:00	KLX03	600.00	695.24
PLU Pumping test – air lift	2004-08-18 14:11:00	2004-08-23 00:00:00	KLX03		
Water sampling, class 3	2004-08-23 11:20:00	2004-08-23 11:20:00	KLX03	692.86	761.11
PLU Pumping test – air lift	2004-08-23 13:01:00	2004-09-20 00:00:00	KLX03		
Water sampling, class 3	2004-09-21 15:31:00	2004-09-21 15:34:00	KLX03	0.00	40.00
Water sampling, class 3	2004-09-21 15:35:00	2004-09-21 15:38:00	KLX03	40.00	90.00
Water sampling, class 3	2004-09-21 15:40:00	2004-09-21 15:43:00	KLX03	90.00	140.00
Water sampling, class 3	2004-09-21 15:45:00	2004-09-21 15:48:00	KLX03	140.00	190.00
Water sampling, class 3	2004-09-21 15:49:00	2004-09-21 15:52:00	KLX03	190.00	240.00
Water sampling, class 3	2004-09-21 15:54:00	2004-09-21 15:57:00	KLX03	240.00	290.00
Water sampling, class 3	2004-09-21 15:59:00	2004-09-21 16:02:00	KLX03	290.00	340.00
Water sampling, class 3	2004-09-21 16:04:00	2004-09-21 16:07:00	KLX03	340.00	390.00
Water sampling, class 3	2004-09-21 16:08:00	2004-09-21 16:11:00	KLX03	390.00	440.00
Water sampling, class 3	2004-09-21 16:12:00	2004-09-21 16:15:00	KLX03	440.00	490.00
Water sampling, class 3	2004-09-21 16:17:00	2004-09-21 16:20:00	KLX03	490.00	540.00
Water sampling, class 3	2004-09-21 16:22:00	2004-09-21 16:25:00	KLX03	540.00	590.00
Water sampling, class 3	2004-09-21 16:26:00	2004-09-21 16:26:00	KLX03	590.00	640.00
Water sampling, class 3	2004-09-21 16:30:00	2004-09-21 16:33:00	KLX03	640.00	690.00
Water sampling, class 3	2004-09-21 16:34:00	2004-09-21 16:37:00	KLX03	690.00	740.00
Water sampling, class 3	2004-09-21 16:40:00	2004-09-21 16:43:00	KLX03	740.00	790.00
Water sampling, class 3	2004-09-21 16:45:00	2004-09-21 16:48:00	KLX03	790.00	840.00
Water sampling, class 3	2004-09-21 16:49:00	2004-09-21 16:52:00	KLX03	840.00	890.00
Water sampling, class 3	2004-09-21 16:53:00	2004-09-21 16:56:00	KLX03	890.00	940.00
Water sampling, class 3	2004-09-21 16:57:00	2004-09-21 17:00:00	KLX03	940.00	990.00
Radar logging	2004-09-25 10:05:00	2004-10-06 13:00:00	KLX03	100.00	995.00
BIPS-logging	2004-09-26 08:00:00	2004-09-26 20:30:00	KLX03	100.00	994.20
Geophysical logging	2004-09-27 00:08:00	2004-09-28 00:08:00	KLX03	100.00	988.00
Percussion drilling	2004-02-11 11:30:00	2004-02-18 14:00:00	KLX04	0.00	100.40
PLU Pumping test – air lift	2004-02-19 16:23:00	2004-03-19 20:20:00	KLX04		
Core drilling	2004-03-13 11:00:00	2004-06-28 10:12:00	KLX04	0.00	993.49
PLU Pumping test – air lift	2004-03-18 13:26:00	2005-03-25 00:00:00	KLX04		
Water sampling, class 3	2004-03-25 00:00:00	2004-03-25 00:00:00	KLX04	103.00	213.14

Activity	Start date	Stop date	Idcode	Secup	Seclow
PLU Pumping test – air lift	2004-03-25 10:13:00	2004-04-18 00:00:00	KLX04		
Water sampling, class 3	2004-04-18 04:00:00	2004-04-18 04:00:00	KLX04	210.00	329.14
PLU Pumping test – air lift	2004-04-18 09:01:00	2004-05-07 00:00:00	KLX04		
Water sampling, class 1	2004-05-07 14:56:00	2004-05-07 14:56:00	KLX04	329.00	403.82
PLU Pumping test – air lift	2004-05-07 19:23:00	2004-05-25 00:00:00	KLX04		
Water sampling, class 1	2004-05-24 23:50:00	2004-05-24 23:50:00	KLX04	401.00	515.10
PLU Pumping test – air lift	2004-05-25 08:18:00	2004-06-11 00:00:00	KLX04		
Water sampling, class 1	2004-06-11 11:00:00	2004-06-11 11:00:00	KLX04	614.00	701.16
PLU Pumping test – air lift	2004-06-12 08:05:00	2004-06-20 00:00:00	KLX04		
Water sampling, class 1	2004-06-20 03:00:00	2004-06-20 03:00:00	KLX04	698.20	850.40
PLU Pumping test – air lift	2004-06-22 12:58:00	2004-06-29 00:00:00	KLX04		
Water sampling, class 1	2004-06-29 08:40:00	2004-06-29 08:40:00	KLX04	849.00	993.49
Water sampling, class 1	2004-07-06 14:55:00	2004-07-06 14:55:00	KLX04		
Water sampling, class 1	2004-07-06 15:15:00	2004-07-06 15:15:00	KLX04		
Water sampling, class 1	2004-07-06 16:50:00	2004-07-06 16:50:00	KLX04		
Water sampling, class 1	2004-07-07 07:45:00	2004-07-07 07:45:00	KLX04		
Water sampling, class 1	2004-07-07 08:05:00	2004-07-07 08:05:00	KLX04		
Water sampling, class 1	2004-07-07 13:25:00	2004-07-07 13:25:00	KLX04		
Water sampling, class 3	2004-07-08 19:25:00	2004-07-08 19:27:00	KLX04	0.00	35.00
Water sampling, class 3	2004-07-08 19:28:00	2004-07-08 19:31:00	KLX04	35.00	85.00
Water sampling, class 3	2004-07-08 19:33:00	2004-07-08 19:36:00	KLX04	85.00	135.00
Water sampling, class 3	2004-07-08 19:37:00	2004-07-08 19:40:00	KLX04	135.00	185.00
Water sampling, class 3	2004-07-08 19:41:00	2004-07-08 19:44:00	KLX04	185.00	235.00
Water sampling, class 3	2004-07-08 19:45:00	2004-07-08 19:48:00	KLX04	235.00	285.00
Water sampling, class 3	2004-07-08 19:50:00	2004-07-08 19:53:00	KLX04	285.00	335.00
Water sampling, class 3	2004-07-08 19:54:00	2004-07-08 19:57:00	KLX04	335.00	385.00
Water sampling, class 3	2004-07-08 19:57:00	2004-07-08 20:00:00	KLX04	385.00	435.00
Water sampling, class 3	2004-07-08 20:01:00	2004-07-08 20:04:00	KLX04	435.00	485.00
Water sampling, class 3	2004-07-08 20:05:00	2004-07-08 20:08:00	KLX04	485.00	535.00
Water sampling, class 3	2004-07-08 20:10:00	2004-07-08 20:13:00	KLX04	535.00	585.00
Water sampling, class 3	2004-07-08 20:15:00	2004-07-08 20:17:00	KLX04	585.00	635.00
Water sampling, class 3	2004-07-08 20:20:00	2004-07-08 20:23:00	KLX04	635.00	685.00
Water sampling, class 3	2004-07-08 20:25:00	2004-07-08 20:28:00	KLX04	685.00	735.00
Water sampling, class 3	2004-07-08 20:29:00	2004-07-08 20:32:00	KLX04	735.00	785.00
Water sampling, class 3	2004-07-08 20:33:00	2004-07-08 20:36:00	KLX04	785.00	835.00
Water sampling, class 3	2004-07-08 20:38:00	2004-07-08 20:41:00	KLX04	835.00	885.00
Water sampling, class 3	2004-07-08 20:42:00	2004-07-08 20:45:00	KLX04	885.00	935.00
Water sampling, class 3	2004-07-08 20:47:00	2004-07-08 20:50:00	KLX04	935.00	985.00
BIPS-logging	2004-07-12 15:00:00	2004-07-14 00:00:00	KLX04	12.00	573.00
BOREMAP/BIPS	2004-07-22 00:00:00	2004-10-18 16:59:00	KLX04	0.00	991.22
BOREMAP/BIPS	2004-07-22 10:03:00	2004-11-01 14:49:00	KLX04	100.30	991.22
PLU Differential Flow logging	2004-07-30 11:24:00	2004-07-31 11:36:00	KLX04	95.20	988.23
PLU Differential Flow logging	2004-08-01 11:25:00	2004-08-04 06:32:00	KLX04	94.68	986.76
PLU Differential Flow logging	2004-08-06 08:42:00	2004-08-06 12:08:00	KLX04	219.00	305.00
PLU Injection test	2004-08-20 10:27:00	2004-08-26 00:00:00	KLX04	105.11	205.11
Water sampling, class 1	2004-08-26 11:47:00	2004-08-26 11:47:00	KLX04		
Water sampling, class 1	2004-08-26 11:49:00	2004-08-26 11:49:00	KLX04		
PLU Injection test	2004-08-26 14:00:00	2004-09-08 00:00:00	KLX04	385.47	405.47

Activity	Start date	Stop date	Idcode	Secup	Seclow
Water sampling, class 1	2004-09-08 21:30:00	2004-09-08 21:30:00	KLX04	971.21	976.21
PLU Injection test	2004-09-09 20:00:00	2004-09-17 08:08:00	KLX04	971.21	976.21
Water sampling, class 1	2004-09-10 00:00:00	2004-09-10 00:00:00	KLX04	0.00	976.21
Water sampling, class 1	2004-09-10 09:00:00	2004-09-10 09:00:00	KLX04	971.21	976.21
Water sampling, class 1	2004-09-11 06:10:00	2004-09-11 06:10:00	KLX04	971.21	976.21
Water sampling, class 1	2004-09-12 18:00:00	2004-09-12 18:00:00	KLX04	971.21	976.21
Water sampling, class 1	2004-09-13 14:00:00	2004-09-13 14:00:00	KLX04	971.21	976.21
Water sampling, class 1	2004-09-14 08:45:00	2004-09-14 08:45:00	KLX04	971.21	976.21
Water sampling, class 1	2004-09-14 16:00:00	2004-09-14 16:00:00	KLX04	971.21	976.21
Water sampling, class 1	2004-09-15 09:45:00	2004-09-15 09:45:00	KLX04	971.21	976.21
Water sampling, class 1	2004-09-15 16:00:00	2004-09-15 16:00:00	KLX04	971.21	976.21
Water sampling, class 1	2004-09-16 07:50:00	2004-09-16 07:50:00	KLX04	971.26	976.21
Water sampling, class 5	2004-09-16 11:00:00	2004-09-16 12:30:00	KLX04	971.21	976.21
Water sampling, class 5	2004-09-16 12:30:00	2004-09-16 14:00:00	KLX04	971.21	976.21
Water sampling, class 1	2004-09-16 12:30:00	2004-09-16 12:30:00	KLX04	971.26	976.21
Water sampling, class 1	2004-09-17 00:00:00	2004-09-17 00:00:00	KLX04	510.00	515.00
PLU Injection test	2004-09-17 17:30:00	2004-09-29 09:07:00	KLX04	510.56	515.56
Water sampling, class 1	2004-09-18 07:55:00	2004-09-18 07:55:00	KLX04	510.00	515.00
Water sampling, class 1	2004-09-18 17:40:00	2004-09-18 17:40:00	KLX04	510.00	515.00
Water sampling, class 1	2004-09-19 07:50:00	2004-09-19 07:50:00	KLX04	510.00	515.00
Water sampling, class 1	2004-09-19 18:20:00	2004-09-19 18:20:00	KLX04	510.00	515.00
Water sampling, class 1	2004-09-20 07:55:00	2004-09-20 07:55:00	KLX04	510.00	515.00
Water sampling, class 1	2004-09-20 19:00:00	2004-09-20 19:00:00	KLX04	510.00	515.00
Water sampling, class 1	2004-09-21 08:10:00	2004-09-21 08:10:00	KLX04	510.00	515.00
Water sampling, class 5	2004-09-21 10:00:00	2004-09-21 17:45:00	KLX04	510.00	515.00
Water sampling, class 1	2004-09-21 17:45:00	2004-09-21 17:45:00	KLX04	510.00	515.00
Water sampling, class 1	2004-09-22 08:00:00	2004-09-22 08:00:00	KLX04	510.00	515.00
Water sampling, class 1	2004-09-22 17:35:00	2004-09-22 17:35:00	KLX04	510.00	515.00
Water sampling, class 1	2004-09-23 08:00:00	2004-09-23 08:00:00	KLX04	510.00	515.00
Water sampling, class 1	2004-09-23 17:30:00	2004-09-23 17:30:00	KLX04	510.00	515.00
Water sampling, class 1	2004-09-24 08:10:00	2004-09-24 08:10:00	KLX04	510.00	515.00
Water sampling, class 1	2004-09-24 18:20:00	2004-09-24 18:20:00	KLX04	510.00	515.00
Water sampling, class 1	2004-09-25 08:20:00	2004-09-25 08:20:00	KLX04	510.00	515.00
Water sampling, class 1	2004-09-25 17:20:00	2004-09-25 17:20:00	KLX04	510.00	515.00
Water sampling, class 1	2004-09-26 08:10:00	2004-09-26 08:10:00	KLX04	510.00	515.00
Water sampling, class 1	2004-09-26 17:30:00	2004-09-26 17:30:00	KLX04	510.00	515.00
Water sampling, class 1	2004-09-27 08:15:00	2004-09-27 08:15:00	KLX04	510.00	515.00
Water sampling, class 1	2004-09-27 18:00:00	2004-09-27 18:00:00	KLX04	510.00	515.00
Water sampling, class 1	2004-09-28 08:05:00	2004-09-28 08:05:00	KLX04	510.00	515.00
Water sampling, class 1	2004-09-28 17:55:00	2004-09-28 17:55:00	KLX04	510.00	515.00
Water sampling, class 5	2004-09-29 08:30:00	2004-09-29 08:30:00	KLX04	510.00	515.00
PLU Injection test	2004-09-29 16:45:00	2004-09-30 13:47:00	KLX04	104.00	109.00
Water sampling, class 1	2004-09-30 08:00:00	2004-09-30 08:00:00	KLX04	104.00	109.00
Water sampling, class 4	2004-09-30 10:10:00	2004-09-30 10:10:00	KLX04	104.00	109.00
Water sampling, class 4	2004-09-30 10:12:00	2004-09-30 10:12:00	KLX04	104.00	109.00
Geophysical logging	2004-10-20 13:19:00	2004-11-17 00:00:00	KLX04	17.20	1001.30
Percussion drilling	2004-08-03 10:30:00	2004-08-10 11:30:00	KLX06	0.00	100.30
Core drilling	2004-08-13 10:00:00	2004-08-13 10:00:00	KLX06		
PLU Pumping test – air lift	2004-08-31 08:05:00	2004-09-05 00:00:00	KLX06		

Activity	Start date	Stop date	Idcode	Secup	Seclow
Water sampling, class 3	2004-09-05 06:17:00	2004-09-05 06:17:00	KLX06	103.00	202.26
PLU Pumping test – air lift	2004-09-05 07:52:00	2004-09-11 00:00:00	KLX06		
Water sampling, class 3	2004-09-10 10:22:00	2004-09-10 10:22:00	KLX06	265.50	268.50
Water sampling, class 3	2004-09-11 09:09:00	2004-09-11 09:09:00	KLX06	260.50	268.70
PLU Pumping test – air lift	2004-09-11 10:09:00	2004-09-13 00:00:00	KLX06		
Water sampling, class 3	2004-09-13 08:41:00	2004-09-13 08:41:00	KLX06	200.50	310.20
PLU Pumping test – air lift	2004-09-13 09:56:00	2004-09-19 00:00:00	KLX06		
Water sampling, class 3	2004-09-19 09:56:00	2004-09-19 09:56:00	KLX06	331.02	364.23
PLU Pumping test – air lift	2004-09-19 11:23:00	2004-09-23 00:00:00	KLX06		
Water sampling, class 3	2004-09-23 09:26:00	2004-09-23 09:26:00	KLX06	307.50	415.49
PLU pressure measurement – wire line	2004-09-23 16:30:00	2004-10-09 00:00:00	KLX06	307.50	415.49
Water sampling, class 3	2004-10-09 06:32:00	2004-10-09 06:32:00	KLX06	514.60	613.94
PLU Pumping test – air lift	2004-10-10 06:28:00	2005-10-29 00:00:00	KLX06		
Water sampling, class 3	2004-10-29 06:40:00	2004-10-29 06:40:00	KLX06	715.14	784.94
PLU Pumping test – air lift	2004-10-29 09:17:00	2004-11-11 00:00:00	KLX06		

Tube samples are shown in dark green.

Table 1-2. Ävrö borehole activity log

Activity	Start date	Stop date	Idcode	Secup	Seclow
Percussion drilling	2003-10-13 08:00:00	2003-10-16 18:30:00	HAV09	0.00	200.20
Water sampling, class 3	2003-10-16 07:35:00	2003-10-16 07:35:00	HAV09	15.00	130.90
Water sampling, unclassified	2003-10-16 14:50:00	2003-10-16 14:50:00	HAV09	15.00	200.20
Geophysical logging	2003-12-04 10:10:00	2003-12-04 10:41:00	HAV09	0.00	200.00
BIPS-logging in borehole	2003-12-13 15:15:00	2003-12-13 17:45:00	HAV09	14.00	199.00
Radar logging	2003-12-14 09:00:00	2003-12-14 09:50:00	HAV09	0.00	186.00
Percussion drilling	2003-10-20 10:00:00	2003-10-22 15:00:00	HAV10	0.00	100.00
PLU Pumping test – air lift	2003-10-22 00:00:00	2003-10-22 00:00:00	HAV10	11.90	100.00
Water sampling, class 3	2003-10-22 08:50:00	2003-10-22 08:50:00	HAV10	12.00	22.60
Water sampling, class 3	2003-10-22 14:00:00	2003-10-22 14:00:00	HAV10	12.00	100.00
Geophysical logging	2003-12-04 19:15:00	2003-12-04 19:32:00	HAV10	0.00	100.00
BIPS-logging	2003-12-13 17:45:00	2003-12-13 19:30:00	HAV10	0.00	99.00
Radar logging	2003-12-14 07:30:00	2003-12-14 09:00:00	HAV10	0.00	87.00
Percussion drilling	2004-06-07 14:50:00	2004-06-14 09:00:00	HAV11	0.00	220.50
Water sampling, class 3	2004-07-12 13:32:00	2004-07-12 13:42:00	HAV11	2.46	220.50
Water sampling, class 3	2004-07-13 08:27:00	2004-07-13 19:04:00	HAV11	2.46	220.50
BIPS-logging	2004-09-22 15:15:00	2004-09-22 18:20:00	HAV11	5.00	219.35
Radar logging	2004-09-23 08:20:00	2004-09-23 09:18:00	HAV11	0.00	215.34
Percussion drilling	2004-05-12 06:00:00	2004-05-19 08:00:00	HAV12	0.00	157.80
Water sampling, class 3	2004-06-30 18:30:00	2004-06-30 18:40:00	HAV12	11.35	157.00
Water sampling, class 3	2004-07-02 11:48:00	2004-07-02 11:48:00	HAV12	11.35	157.00
BIPS-logging	2004-09-23 14:10:00	2004-09-23 16:40:00	HAV12	5.00	156.75
Radar logging	2004-09-23 17:20:00	2004-09-23 20:00:00	HAV12	0.00	154.00

Activity	Start date	Stop date	Idcode	Secup	Seclow
Percussion drilling	2004-05-24 08:00:00	2004-05-27 13:00:00	HAV13	0.00	142.20
Water sampling, class 3	2004-07-20 10:55:00	2004-07-20 11:15:00	HAV13	3.31	142.20
Water sampling, class 3	2004-07-21 08:44:00	2004-07-21 18:45:00	HAV13	3.31	142.20
BIPS-logging	2004-09-24 11:15:00	2004-09-24 14:15:00	HAV13	8.00	140.22
Radar logging	2004-09-24 14:30:00	2004-09-24 15:15:00	HAV13	0.00	127.72
Percussion drilling	2004-06-01 11:50:00	2004-06-04 10:00:00	HAV14	0.00	182.40
Water sampling, class 3	2004-07-07 13:02:00	2004-07-07 13:13:00	HAV14	12.85	182.00
Water sampling, class 3	2004-07-08 08:50:00	2004-07-08 19:40:00	HAV14	12.85	182.00
Core drilling	2003-06-11 15:10:00	2004-01-10 10:00:00	KAV01	0.00	757.31
Water sampling, class 3	2003-06-16 19:22:00	2003-06-16 19:38:00	KAV01	33.00	83.00
Water sampling, class 3	2003-06-16 19:35:00	2003-06-16 19:40:00	KAV01	83.00	133.00
Water sampling, class 3	2003-06-16 19:41:00	2003-06-16 19:44:00	KAV01	133.00	183.00
Water sampling, class 3	2003-06-16 19:45:00	2003-06-16 19:48:00	KAV01	183.00	233.00
Water sampling, class 3	2003-06-16 19:49:00	2003-06-16 19:51:00	KAV01	233.00	283.00
Water sampling, class 3	2003-06-16 19:54:00	2003-06-16 19:56:00	KAV01	283.00	333.00
Water sampling, class 3	2003-06-16 19:57:00	2003-06-16 20:00:00	KAV01	333.00	383.00
Water sampling, class 3	2003-06-16 20:02:00	2003-06-16 20:05:00	KAV01	383.00	433.00
Water sampling, class 3	2003-06-16 20:07:00	2003-06-16 20:10:00	KAV01	433.00	483.00
Water sampling, class 3	2003-06-16 20:12:00	2003-06-16 20:15:00	KAV01	483.00	533.00
Water sampling, class 3	2003-06-16 20:17:00	2003-06-16 20:20:00	KAV01	533.00	583.00
Water sampling, class 3	2003-06-16 20:22:00	2003-06-16 20:25:00	KAV01	583.00	633.00
Water sampling, class 3	2003-06-16 20:26:00	2003-06-16 20:28:00	KAV01	633.00	683.00
Water sampling, class 3	2003-06-16 20:30:00	2003-06-16 20:32:00	KAV01	683.00	733.00
Geophysical logging	2003-10-01 14:00:00	2003-10-02 00:00:00	KAV01	0.00	742.00
Radar logging	2003-10-07 08:00:00	2003-10-07 18:00:00	KAV01	72.00	734.00
BIPS-logging	2003-12-14 17:30:00	2003-12-15 12:00:00	KAV01	69.00	742.00
Differential Flow logging	2004-02-18 16:25:00	2004-02-27 00:00:00	KAV01	56.35	793.25
Percussion drilling	2003-10-06 09:00:00	2003-11-01 10:00:00	KAV04A	0.00	100.02
Water sampling, class 3	2003-10-09 10:10:00	2003-10-09 10:15:00	KAV04A	47.60	50.60
Water sampling, class 3	2003-10-09 13:00:00	2003-10-09 13:15:00	KAV04A	0.00	100.20
Water sampling, class 5	2003-10-21 12:30:00	2003-10-21 12:30:00	KAV04A	0.00	100.20
Core drilling	2003-12-10 13:55:00	2004-05-03 14:53:00	KAV04A	99.55	1004.00
PLU Pumping test – air lift	2003-12-11 07:12:00	2003-12-11 20:00:00	KAV04A		
Sampling of drilling water	2003-12-11 09:30:00	2004-04-29 14:30:00	KAV04A	106.29	1000.40
Flush water out	2003-12-11 09:30:00		KAV04A	106.29	
Sampling of returned water	2003-12-11 09:30:00		KAV04A	106.29	249.48
PLU Pumping test – air lift	2003-12-12 06:25:00	2004-01-25 00:00:00	KAV04A		
Water sampling, class 1	2004-02-04 08:05:00	2004-02-04 08:05:00	KAV04A	291.15	408.49
PLU Pumping test – air lift	2004-02-04 08:25:00	2004-02-20 00:00:00	KAV04A		
Water sampling. class 3	2004-02-21 08:00:00	2004-02-21 08:00:00	KAV04A	408.00	517.98
PLU Pumping test – air lift	2004-02-21 08:20:00	2004-02-26 00:00:00	KAV04A		
Water sampling, class 1	2004-02-26 08:35:00	2004-02-26 08:35:00	KAV04A	516.15	603.42
PLU Pumping test – air lift	2004-02-26 11:45:00	2004-03-15 00:00:00	KAV04A		
Microbiology	2004-03-15 14:07:00	2004-03-16 00:00:00	KAV04A		
PLU Pumping test – air lift	2004-03-17 07:06:00	2004-03-26 00:00:00	KAV04A		
Water sampling, class 1	2004-03-30 08:25:00	2004-03-30 08:25:00	KAV04A	710.90	730.08
PLU Pumping test – air lift	2004-03-30 08:30:00	2004-03-31 00:00:00	KAV04A		

Activity	Start date	Stop date	Idcode	Secup	Seclow
Water sampling, class 1	2004-03-31 07:40:00	2004-03-31 07:40:00	KAV04A	710.90	730.08
PLU Pumping test – air lift	2004-03-31 08:50:00	2004-04-13 00:00:00	KAV04A		
Water sampling, class 1	2004-04-14 08:50:00	2004-04-14 08:50:00	KAV04A	729.00	805.52
PLU Pumping test – air lift	2004-04-14 08:50:00	2004-04-15 00:00:00	KAV04A		
Water sampling, class 3	2004-04-16 07:30:00	2004-04-16 07:30:00	KAV04A	729.00	819.01
PLU Pumping test – air lift	2004-04-17 08:37:00	2004-05-06 00:00:00	KAV04A		
BIPS-logging	2004-05-24 13:00:00	2004-05-25 14:30:00	KAV04A	100.00	998.00
Radar logging	2004-05-25 14:30:00	2004-05-27 00:00:00	KAV04A	100.00	990.00
Geophysical logging	2004-06-01 08:26:00	2004-06-08 00:00:00	KAV04A	0.30	778.00
Water sampling, class 3	2004-06-08 12:59:00	2004-06-08 13:01:00	KAV04A	0.00	45.00
Water sampling, class 3	2004-06-08 13:02:00	2004-06-08 13:04:00	KAV04A	45.00	95.00
Water sampling, class 3	2004-06-08 13:05:00	2004-06-08 13:08:00	KAV04A	95.00	145.00
Water sampling, class 3	2004-06-08 13:09:00	2004-06-08 13:12:00	KAV04A	145.00	195.00
Water sampling, class 3	2004-06-08 13:13:00	2004-06-08 13:15:00	KAV04A	195.00	245.00
Water sampling, class 3	2004-06-08 13:18:00	2004-06-08 13:21:00	KAV04A	245.00	295.00
Water sampling, class 3	2004-06-08 13:22:00	2004-06-08 13:25:00	KAV04A	295.00	345.00
Water sampling, class 3	2004-06-08 13:26:00	2004-06-08 13:29:00	KAV04A	345.00	395.00
Water sampling, class 3	2004-06-08 13:30:00	2004-06-08 13:36:00	KAV04A	395.00	445.00
Water sampling, class 3	2004-06-08 13:37:00	2004-06-08 13:40:00	KAV04A	445.00	495.00
Water sampling, class 3	2004-06-08 13:41:00	2004-06-08 13:43:00	KAV04A	495.00	545.00
Water sampling, class 3	2004-06-08 13:44:00	2004-06-08 13:47:00	KAV04A	545.00	595.00
Water sampling, class 3	2004-06-08 13:48:00	2004-06-08 13:51:00	KAV04A	595.00	645.00
Water sampling, class 3	2004-06-08 13:52:00	2004-06-08 13:54:00	KAV04A	645.00	695.00
Water sampling, class 3	2004-06-08 13:55:00	2004-06-08 13:58:00	KAV04A	695.00	745.00
Water sampling, class 3	2004-06-08 13:59:00	2004-06-08 14:02:00	KAV04A	745.00	795.00
Water sampling, class 3	2004-06-08 14:03:00	2004-06-08 14:06:00	KAV04A	795.00	845.00
Water sampling, class 3	2004-06-08 14:07:00	2004-06-08 14:09:00	KAV04A	845.00	895.00
Water sampling, class 3	2004-06-08 14:10:00	2004-06-08 14:13:00	KAV04A	895.00	945.00
Water sampling, class 3	2004-06-08 14:14:00	2004-06-08 14:17:00	KAV04A	945.00	995.00
PLU Differential Flow logging	2004-06-11 12:23:00	2004-06-13 01:27:00	KAV04A	95.16	999.17
PLU Differential Flow logging	2004-06-11 12:23:00	2004-06-13 01:23:00	KAV04A	100.16	994.17
PLU Differential Flow logging	2004-06-13 14:28:00	2004-06-15 22:40:00	KAV04A	95.14	901.84
PLU Injection test	2004-07-26 13:46:00	2004-08-13 00:00:00	KAV04A	105.17	205.17

Tube samples are shown in dark green.

Table 1-3. Simpevarp borehole activity log

Activity	Start date	Stop date	Idcode	Secup	Seclow
Percussion drilling	2002-06-27 07:00:00	2002-07-08 19:00:00	HSH02	0.00	200.00
Borehole preparation	2002-06-27 11:31:00	2002-09-16 00:00:00	HSH02	3.40	200.00
BIPS-logging	2002-09-16 19:24:00	2002-09-16 21:25:00	HSH02	11.00	180.00
Radar logging	2002-09-17 10:45:00	2002-09-17 13:10:00	HSH02	2.00	195.32
Geophysical logging	2002-09-17 15:50:00	2002-12-14 00:00:00	HSH02	0.00	195.66
Water sampling, class 3	2003-01-31 10:09:00	2003-01-31 10:09:00	HSH02	0.00	200.00
Water sampling, class 3	2003-01-31 10:17:00	2003-01-31 10:17:00	HSH02	0.00	200.00
Water sampling, class 3	2003-01-31 10:50:00	2003-01-31 10:50:00	HSH02	0.00	200.00
Water sampling, class 3	2003-02-03 13:00:00	2003-02-03 13:00:00	HSH02	0.00	200.00

Activity	Start date	Stop date	Idcode	Secup	Seclow
Water sampling, unclassified	2003-02-03 13:00:00	2003-02-03 13:00:00	HSH02	0.00	200.00
Instrument testing	2003-04-09 00:00:00	2003-08-27 00:00:00	HSH02	1.00	200.00
Water sampling, class 3	2003-08-27 10:30:00	2003-08-27 10:30:00	HSH02	0.00	200.00
Water sampling, class 3	2003-08-27 15:20:00	2003-08-27 15:20:00	HSH02	0.00	200.00
Water sampling, class 3	2003-08-27 19:30:00	2003-08-27 19:30:00	HSH02	0.00	200.00
Percussion drilling	2002-07-02 17:30:00	2002-07-09 19:00:00	HSH03	0.00	201.00
Borehole preparation	2002-07-03 00:00:00	2002-08-21 00:00:00	HSH03		
Water sampling, class 3	2002-08-21 16:30:00	2002-08-21 16:30:00	HSH03	0.00	201.00
Water sampling, class 3	2002-08-22 18:00:00	2002-08-22 18:00:00	HSH03	0.00	103.00
Water sampling, class 3	2002-09-05 15:55:00	2002-09-05 15:55:00	HSH03	0.00	201.00
BIPS-logging	2002-09-16 10:35:00	2002-09-16 12:48:00	HSH03	11.00	196.11
Radar logging	2002-09-18 12:45:00	2002-09-18 13:50:00	HSH03	0.00	194.84
Geophysical logging	2002-09-18 13:29:00	2003-01-25 00:00:00	HSH03	0.00	194.84
Water sampling, class 2	2003-03-04 13:46:00	2003-03-04 13:46:00	HSH03	0.00	150.00
Water sampling, class 2	2003-03-04 14:20:00	2003-03-04 14:20:00	HSH03	0.00	150.00
Water sampling, class 2	2003-03-04 14:30:00	2003-03-04 14:30:00	HSH03	0.00	150.00
Water sampling, class 2	2003-03-04 15:40:00	2003-03-04 15:40:00	HSH03	0.00	150.00
Water sampling, class 2	2003-03-04 15:50:00	2003-03-04 15:50:00	HSH03	0.00	150.00
Water sampling, class 3	2003-09-16 08:00:00	2003-09-16 08:05:00	HSH03	0.00	200.00
Water sampling, class 3	2004-02-03 13:15:00	2004-02-03 13:15:00	HSH03	0.00	200.00
Percussion drilling	2004-04-05 09:00:00	2004-04-13 19:30:00	HSH04	0.00	236.20
Borehole preparation	2004-04-05 13:30:00	2004-04-05 14:00:00	HSH04	0.00	12.20
Water sampling, class 3	2004-07-15 10:20:00	2004-07-15 10:50:00	HSH04	3.01	236.00
Water sampling, class 3	2004-07-20 10:55:00	2004-07-20 11:15:00	HSH04	3.01	236.00
Percussion drilling	2004-04-14 07:00:00	2004-04-19 20:00:00	HSH05	0.00	200.20
Borehole preparation	2004-04-14 13:15:00	2004-04-14 13:30:00	HSH05	0.00	6.20
Water sampling, class 3	2004-07-17 13:31:00	2004-07-17 13:41:00	HSH05	3.34	200.20
Water sampling, class 3	2004-07-18 08:18:00	2004-07-18 18:19:00	HSH05	3.34	200.20
Water sampling, unclassified	2002-11-06 11:00:00	2002-11-06 11:00:00	SSM000001	2.00	2.20
Water sampling, class 3	2003-04-22 09:45:00	2003-04-22 09:55:00	SSM000001	2.00	2.20
Water sampling, unclassified	2002-11-06 11:15:00	2002-11-06 11:15:00	SSM000002	2.00	2.10
Water sampling, class 3	2003-04-22 09:58:00	2003-04-22 10:05:00	SSM000002	2.00	2.10

Laxemar subarea: Upper bedrock hydrochemistry

Water-conducting sections																				
Borehole (HLX-)	**01**	**02**	**03**	**04**	**05**	**06**	**07**	**08**	**09**	**10**	**11**	**12**	**13**	**14**	**15**	**16**	**17**	**18**	**19**	**20**
0–25 m	X?	X?	X?	X?	X?	X?	X?	X?		X?				X?	NW	NW	NW			
25–50 m			X							X?				X?	NW	NW	NW			
50–75 m	X		X			X				X?				X?	NW	NW	NW			
75–100 m	X		X			X				X?			X?	X?	NW	NW	NW			X
100–150 m														X?	NW	NW	X?	X	X	X
150–200 m															NW	NW	NW	X	X	X

Borehole (HLX-)	**01**	**02**	**03**	**04**	**05**	**06**	**07**	**08**
0–25 m			NW				NW	NW
25–50 m			NW				NW	NW
50–75 m			X				NW	NW
75–100 m			X				X	NW
100–150 m								

Water-conducting sections																				
Borehole (HLX-)	**21**	**22**	**23**	**24**	**25**	**26**	**27**	**28**	**29**	**30**	**31**	**32**	**33**	**34**	**35**	**36**	**37**	**38**	**39**	**40**
0–25 m			X	X		NW			NW		X	X	X							
25–50 m			X			NW														
50–75 m	X	X	X		X	NW				X										
75–100 m	X					NW		X		X		X								
100–150 m	X	X	X	X	X	NW	X	X		X	X		X							
150–200 m		X	X	X	X	NW	X	X				X	X							

X = Indicates section(s) with greatest recorded groundwater flow into the borehole.
‘NW = Iindicates no water flow recorded.
X? = Unknown groundwater flow source.

Chloride

Borehole (HLX-)	01	02	03	04	05	06	07	08	09	10	11	12	13	14	15	16	17	18	19	20
0–25 m	46.6	1.0	5.2	32	5.4	4.2	3	56.4	–	6	–	–	–	70	–	–	–	–	–	–
25–50 m	–	–	8.4	–	–	–	318	–	–	6	–	–	–	70	–	–	–	–	–	–
50–75 m	41.6	–	8.4	–	–	8.9	318	–	–	6	–	–	–	70	–	–	–	–	–	–
75–100 m	41.6	–	8.4	–	–	8.9	318	–	–	6	–	–	–	70	–	–	–	–	–	29.5
100–150 m	–	–	–	–	–	–	–	–	–	–	–	–	–	70	–	–	–	–	–	29.5
150–200 m	–	–	–	–	–	–	–	–	–	–	–	–	–	–	–	–	–	–	–	29.5

Borehole (KLX-s)	01	02	03	04	05	06
0–25 m	–	149	–	43.6	–	
25–50 m	–	149	–	43.6	–	
50–75 m	–	146	–	–	–	
75–100 m	–	146	27.2	–	–	
100–150 m	–	–	–	23.4	28.6	25.4

Chloride

Borehole (HLX-)	21	22	23	24	25	26	27	28	29	30	31	32	33	34	35	36	37	38	39	40
0–25 m	–	–	–	–	–	–	–	–												
25–50 m	–	–	–	–	–	–	–	–												
50–75 m	–	–	–	–	–	–	–	–												
75–100 m	–	–	–	–	–	–	–	–												
100–150 m	–	23	–	15.1	–	–	–	–												
150–200 m	–	23	–	15.1	–	–	–	–												

Bicarbonate																				
Borehole (HLX-)	**01**	**02**	**03**	**04**	**05**	**06**	**07**	**08**	**09**	**10**	**11**	**12**	**13**	**14**	**15**	**16**	**17**	**18**	**19**	**20**
0–25 m	–	31	–	220	347	154	21	75	–	193	–	–	–	304	–	–	–	–	–	–
25–50 m	–	–	207	–	–	–	176	–	–	193	–	–	–	304	–	–	–	–	–	–
50–75 m	233	–	207	–	–	234	176	–	–	193	–	–	–	304	–	–	–	–	–	–
75–100 m	233	–	207	–	–	234	176	–	–	193	–	–	–	304	–	–	–	–	–	205
100–150 m	–	–	–	–	–	–	–	–	–	–	–	–	–	304	–	–	–	–	–	205
150–200 m	–	–	–	–	–	–	–	–	–	–	–	–	–	–	–	–	–	–	–	205

Borehole (KLX-)	01	02	03	04	05	06
0–25 m	–	220	–	268	–	–
25–50 m	–	220	–	268	–	–
50–75 m	–	202	–	–	–	–
75–100 m	–	202	347	–	–	–
100–150 m	–	–	–	323	–	216

Bicarbonate																				
Borehole (HLX-series)	**21**	**22**	**23**	**24**	**25**	**26**	**27**	**28**	**29**	**30**	**31**	**32**	**33**	**34**	**35**	**36**	**37**	**38**	**39**	**40**
0–25 m	–	–	–	–	–	–	–	–												
25–50 m	–	–	–	–	–	–	–	–												
50–75 m	–	–	–	–	–	–	–	–												
75–100 m	–	–	–	–	–	–	–	–												
100–150 m	–	221	–	121	–	–	–	–												
150–200 m	–	221	–	121	–	–	–	–												

Sulphate																				
Borehole (HLX-series)	**01**	**02**	**03**	**04**	**05**	**06**	**07**	**08**	**09**	**10**	**11**	**12**	**13**	**14**	**15**	**16**	**17**	**18**	**19**	**20**
0–25 m	48.7	4.5	–	41.1	6.9	7.4	4.4	9.0	–	6.5	–	–	–	31.4	–	–	–	–	–	–
25–50 m	–	–	20.4	–	–	–	72.0	–	–	6.5	–	–	–	31.4	–	–	–	–	–	–
50–75 m	61.5	–	20.4	–	–	16.1	72.0	–	–	6.5	–	–	–	31.4	–	–	–	–	–	–
75–100 m	61.5	–	20.4	–	–	16.1	72.0	–	–	6.5	–	–	–	31.4	–	–	–	–	–	47.9
100–150 m	–	–	–	–	–	–	–	–	–	–	–	–	–	31.4	–	–	–	–	–	47.9
150–200 m	–	–	–	–	–	–	–	–	–	–	–	–	–	–	–	–	–	–	–	47.9

Borehole (KLX-series)	**01**	**02**	**03**	**04**	**05**	**06**
0–25 m	–	20.4	–	19.7	–	–
25–50 m	–	20.4	–	19.7	–	–
50–75 m	–	19.4	–	–	–	–
75–100 m	–	19.4	11.6	–	–	–
100–150 m	–	–	–	15.8	–	24.3

Sulphate																				
Borehole (HLX-series)	**21**	**22**	**23**	**24**	**25**	**26**	**27**	**28**	**29**	**30**	**31**	**32**	**33**	**34**	**35**	**36**	**37**	**38**	**39**	**40**
0–25 m	–	–	–	–	–	–	–	–												
25–50 m	–	–	–	–	–	–	–	–												
50–75 m	–	–	–	–	–	–	–	–												
75–100 m	–	–	–	–	–	–	–	–												
100–150 m	–	53.1	–	29.6	–	–	–	–												
150–200 m	–	53.1	–	29.6	–	–	–	–												

Bromide																				
Borehole (HLX-series)	**01**	**02**	**03**	**04**	**05**	**06**	**07**	**08**	**09**	**10**	**11**	**12**	**13**	**14**	**15**	**16**	**17**	**18**	**19**	**20**
0–25 m	0.15	4.5	–	0.06	5.2	–	–	0.21	–	0.21	–	–	–	0.41	–	–	–	–	–	–
25–50 m	–	–	–	–	–	–	–	–	–	0.21	–	–	–	0.41	–	–	–	–	–	–
50–75 m	–	–	–	–	–	–	–	–	–	0.21	–	–	–	0.41	–	–	–	–	–	–
75–100 m	–	–	–	–	–	–	–	–	–	0.21	–	–	–	0.41	–	–	–	–	–	–
100–150 m	–	–	–	–	–	–	–	–	–	–	–	–	–	0.41	–	–	–	–	–	–
150–200 m	–	–	–	–	–	–	–	–	–	–	–	–	–	–	–	–	–	–	–	–

Borehole (KLX-series)	**01**	**02**	**03**	**04**	**05**	**06**
0–25 m	–	–	–	0.26	–	–
25–50 m	–	–	–	0.26	–	–
50–75 m	–	–	–	–	–	–
75–100 m	–	–	–	–	–	–
100–150 m	–	–	–	–	–	–

Bromide																				
Borehole (HLX-series)	**21**	**22**	**23**	**24**	**25**	**26**	**27**	**28**	**29**	**30**	**31**	**32**	**33**	**34**	**35**	**36**	**37**	**38**	**39**	**40**
0–25 m	–	–	–	–	–	–	–	–												
25–50 m	–	–	–	–	–	–	–	–												
50–75 m	–	–	–	–	–	–	–	–												
75–100 m	–	–	–	–	–	–	–	–												
100–150 m	–	–	–	–	–	–	–	–												
150–200 m	–	–	–	–	–	–	–	–												

Sodium																				
Borehole (HLX-series)	**01**	**02**	**03**	**04**	**05**	**06**	**07**	**08**	**09**	**10**	**11**	**12**	**13**	**14**	**15**	**16**	**17**	**18**	**19**	**20**
0–25 m	108	4.3	60	102	50	17	3	36	–	68	–	–	–	138	–	–	–	–	–	–
25–50 m	–	–	71	–	–	–	300	–	–	68	–	–	–	138	–	–	–	–	–	–
50–75 m	138	–	71	–	–	74	300	–	–	68	–	–	–	138	–	–	–	–	–	–
75–100 m	138	–	71	–	–	74	300	–	–	68	–	–	–	138	–	–	–	–	–	107
100–150 m	–	–	–	–	–	–	–	–	–	–	–	–	–	138	–	–	–	–	–	107
150–200 m	–	–	–	–	–	–	–	–	–	–	–	–	–	–	–	–	–	–	–	107

Borehole (KLX-series)	**01**	**02**	**03**	**04**	**05**	**06**
0–25 m	–	137	–	94	–	–
25–50 m	–	137	–	94	–	–
50–75 m	–	134	–	–	–	–
75–100 m	–	134	330	–	–	–
100–150 m	–	–	–	118	–	–

Sodium																				
Borehole (HLX-series)	**21**	**22**	**23**	**24**	**25**	**26**	**27**	**28**	**29**	**30**	**31**	**32**	**33**	**34**	**35**	**36**	**37**	**38**	**39**	**40**
0–25 m	–	–	–	–	–	–	–	–												
25–50 m	–	–	–	–	–	–	–	–												
50–75 m	–	–	–	–	–	–	–	–												
75–100 m	–	–	–	–	–	–	–	–												
100–150 m	–	–	–	–	–	–	–	–												
150–200 m	–	–	–	–	–	–	–	–												

Calcium																				
Borehole (HLX-series)	**01**	**02**	**03**	**04**	**05**	**06**	**07**	**08**	**09**	**10**	**11**	**12**	**13**	**14**	**15**	**16**	**17**	**18**	**19**	**20**
0–25 m	16.8	7.4	16.1	11.9	45.4	24.7	4.4	9.8	–	12.9	–	–	–	18.8	–	–	–	–	–	–
25–50 m	–	–	16	–	–	–	34.8	–	–	12.9	–	–	–	18.8	–	–	–	–	–	–
50–75 m	11.1	–	16	–	–	18.4	34.8	–	–	12.9	–	–	–	18.8	–	–	–	–	–	–
75–100 m	11.1	–	16	–	–	18.4	34.8	–	–	12.9	–	–	–	18.8	–	–	–	–	–	7.5
100–150 m	–	–	–	–	–	–	–	–	–	–	–	–	–	18.8	–	–	–	–	–	7.5
150–200 m	–	–	–	–	–	–	–	–	–	–	–	–	–	–	–	–	–	–	–	7.5

Borehole (KLX-series)	**01**	**02**	**03**	**04**	**05**	**06**
0–25 m	–	54.1	–	41.1	–	–
25–50 m	–	54.1	–	41.1	–	–
50–75 m	–	45.7	–	–	–	–
75–100 m	–	45,7	46.8	–	–	–
100–150 m	–	–	–	17.2	–	–

Calcium																				
Borehole (HLX-series)	**21**	**22**	**23**	**24**	**25**	**26**	**27**	**28**	**29**	**30**	**31**	**32**	**33**	**34**	**35**	**36**	**37**	**38**	**39**	**40**
0–25 m	–	–	–	–	–	–	–	–												
25–50 m	–	–	–	–	–	–	–	–												
50–75 m	–	–	–	–	–	–	–	–												
75–100 m	–	–	–	–	–	–	–	–												
100–150 m	–	–	–	–	–	–	–	–												
150–200 m	–	–	–	–	–	–	–	–												

Potassium																				
Borehole (HLX-series)	**01**	**02**	**03**	**04**	**05**	**06**	**07**	**08**	**09**	**10**	**11**	**12**	**13**	**14**	**15**	**16**	**17**	**18**	**19**	**20**
0-25 m	3.8	0.7	3.1	3.0	3.8	1.5	0.5	2.6	-	2.8	-	-	-	3.1	-	-	-	-	-	-
25-50 m	-	-	5.0	-	-	-	5.4	-	-	2.8	-	-	-	3.1	-	-	-	-	-	-
50-75 m	3.0	-	5.0	-	-	2.4	5.4	-	-	2.8	-	-	-	3.1	-	-	-	-	-	-
75-100 m	3.0	-	5.0	-	-	2.4	5.4	-	-	2.8	-	-	-	3.1	-	-	-	-	-	1.3
100-150 m	-	-	-	-	-	-	-	-	-	-	-	-	-	3.1	-	-	-	-	-	1.3
150-200 m	-	-	-	-	-	-	-	-	-	-	-	-	-	-	-	-	-	-	-	1.3

Borehole (KLX-series)	**01**	**02**	**03**	**04**	**05**	**06**
0-25 m	-	3.9	-	3.1	-	-
25-50 m	-	3.9	-	3.1	-	-
50-75 m	-	3.9	-	-	-	-
75-100 m	-	3.9	3.3	-	-	-
100-150 m	-	-	-	2.4	-	-

Potassium																				
Borehole (HLX-series)	**21**	**22**	**23**	**24**	**25**	**26**	**27**	**28**	**29**	**30**	**31**	**32**	**33**	**34**	**35**	**36**	**37**	**38**	**39**	**40**
0-25 m	-	-	-	-	-	-	-	-												
25-50 m	-	-	-	-	-	-	-	-												
50-75 m	-	-	-	-	-	-	-	-												
75-100 m	-	-	-	-	-	-	-	-												
100-150 m	-	-	-	-	-	-	-	-												
150-200 m	-	-	-	-	-	-	-	-												

Magnesium																				
Borehole (HLX-series)	**01**	**02**	**03**	**04**	**05**	**06**	**07**	**08**	**09**	**10**	**11**	**12**	**13**	**14**	**15**	**16**	**17**	**18**	**19**	**20**
0–25 m	3.9	1.0	4.1	2.7	8.7	3.4	1.2	7.2	–	4.4	–	–	–	4.7	–	–	–	–	–	–
25–50 m	–	–	4.1	–	–	–	7.6	–	–	4.4	–	–	–	4.7	–	–	–	–	–	–
50–75 m	2.0	–	4.1	–	–	3.6	7.6	–	–	4.4	–	–	–	4.7	–	–	–	–	–	–
75–100 m	2.0	–	4.1	–	–	3.6	7.6	–	–	4.4	–	–	–	4.7	–	–	–	–	–	2.1
100–150 m	–	–	–	–	–	–	–	–	–	–	–	–	–	4.7	–	–	–	–	–	2.1
150–200 m	–	–	–	–	–	–	–	–	–	–	–	–	–	–	–	–	–	–	–	2.1

Borehole (KLX-series)	**01**	**02**	**03**	**04**	**05**	**06**
0–25 m	–	4.4	–	8.3	–	–
25–50 m	–	4.4	–	8.3	–	–
50–75 m	–	4.3	–	–	–	–
75–100 m	–	4.3	7.2	–	–	–
100–150 m	–	–	–	4.1	–	–

Magnesium																				
Borehole (HLX-series)	**21**	**22**	**23**	**24**	**25**	**26**	**27**	**28**	**29**	**30**	**31**	**32**	**33**	**34**	**35**	**36**	**37**	**38**	**39**	**40**
0–25 m	–	–	–	–	–	–	–	–												
25–50 m	–	–	–	–	–	–	–	–												
50–75 m	–	–	–	–	–	–	–	–												
75–100 m	–	–	–	–	–	–	–	–												
100–150 m	–	–	–	–	–	–	–	–												
150–200 m	–	–	–	–	–	–	–	–												

Tritium*

Borehole (HLX-series)	01	02	03	04	05	06	07	08	09	10	11	12	13	14	15	16	17	18	19	20
0–25 m	–	–	–	–	–		–	–	–	7.2	–	–	–	3.8	–	–	–	–	–	–
25–50 m	–	–	30	–	–	–	25	–	–	7.2	–	–	–	3.8	–	–	–	–	–	–
50–75 m	21	–	30	–	–	17	25	–	–	7.2	–	–	–	3.8	–	–	–	–	–	–
75–100 m	21	–	30	–	–	17	25	–	–	7.2	–	–	–	3.8	–	–	–	–	–	0.8
100–150 m	–	–	–	–	–	–	–	–	–	–	–	–	–	3.8	–	–	–	–	–	0.8
150–200 m	–	–	–	–	–	–	–	–	–	–	–	–	–	–	–	–	–	–	–	0.8

Borehole (KLX-series)	01	02	03	04	05	06
0–25 m	–	8.4	–	–	–	–
25–50 m	–	8.4	–	–	–	–
50–75 m	–	5.9	–	–	–	–
75–100 m	–	5.9	0.2	–	–	–
100–150 m	–	–	–	4	–	–

Tritium*

Borehole (HLX-series)	21	22	23	24	25	26	27	28	29	30	31	32	33	34	35	36	37	38	39	40
0–25 m	–	–	–	–	–	–	–	–												
25–50 m	–	–	–	–	–	–	–	–												
50–75 m	–	–	–	–	–	–	–	–												
75–100 m	–	–	–	–	–	–	–	–												
100–150 m	–	–	–	–	–	–	–	–												
150–200 m	–	–	–	–	–	–	–	–												

Oxygen-18																				
Borehole (HLX-series)	**01**	**02**	**03**	**04**	**05**	**06**	**07**	**08**	**09**	**10**	**11**	**12**	**13**	**14**	**15**	**16**	**17**	**18**	**19**	**20**
0–25 m	–10.5	–9.8	–10.5	–10.8	–9.7	–10.2	–8.6	–10.5	–	–10.9	–	–	–	–11.2	–	–	–	–	–	–
25–50 m	–	–	–10.9	–	–	–	–10.7	–	–	–10.9	–	–	–	–11.2	–	–	–	–	–	–
50–75 m	–10.8	–	–10.9	–	–	–10.6	–10.7	–	–	–10.9	–	–	–	–11.2	–	–	–	–	–	–
75–100 m	–10.8	–	–10.9	–	–	–10.6	–10.7	–	–	–10.9	–	–	–	–11.2	–	–	–	–	–	–
100–150 m	–	–	–	–	–	–	–	–	–	–	–	–	–	–11.2	–	–	–	–	–	–
150–200 m	–	–	–	–	–	–	–	–	–	–	–	–	–	–	–	–	–	–	–	–

Borehole (KLX-series)	**01**	**02**	**03**	**04**	**05**	**06**
0–25 m	–	–9.9	–	–	–	–
25–50 m	–	–9.9	–	–	–	–
50–75 m	–	–10.5	–	–	–	–
75–100 m	–	–10.5	–12.7	–	–	–
100–150 m	–	–	–	–10.8	–	–

Oxygen-18																				
Borehole (HLX-series)	**21**	**22**	**23**	**24**	**25**	**26**	**27**	**28**	**29**	**30**	**31**	**32**	**33**	**34**	**35**	**36**	**37**	**38**	**39**	**40**
0–25 m	–	–	–	–	–	–	–	–												
25–50 m	–	–	–	–	–	–	–	–												
50–75 m	–	–	–	–	–	–	–	–												
75–100 m	–	–	–	–	–	–	–	–												
100–150 m	–	–	–	–	–	–	–	–												
150–200 m	–	–	–	–	–	–	–	–												

Deuterium																				
Borehole (HLX-)	**01**	**02**	**03**	**04**	**05**	**06**	**07**	**08**	**09**	**10**	**11**	**12**	**13**	**14**	**15**	**16**	**17**	**18**	**19**	**20**
0–25 m	–79.2	–75.9	–78.6	–80.9	–74.4	–78.6	–66.8	–80.7	–	–78.8	–	–	–	–78.6	–	–	–	–	–	–
25–50 m	–	–	–80.0	–	–	–	–77.0	–	–	–78.8	–	–	–	–78.6	–	–	–	–	–	–
50–75 m	–79.0	–	–80.0	–	–	–77.0	–77.0	–	–	–78.8	–	–	–	–78.6	–	–	–	–	–	–
75–100 m	–79.0	–	–80.0	–	–	–77.0	–77.0	–	–	–78.8	–	–	–	–78.6	–	–	–	–	–	–
100–150 m	–	–	–	–	–	–	–	–	–	–	–	–	–	–78.6	–	–	–	–	–	–
150–200 m	–	–	–	–	–	–	–	–	–	–	–	–	–	–	–	–	–	–	–	–

Borehole (KLX-)	**01**	**02**	**03**	**04**	**05**	**06**
0–25 m	–	–77.4	–	–	–	–
25–50 m	–	–77.4	–	–	–	–
50–75 m	–	–75.1	–	–	–	–
75–100 m	–	–75.1	–89.7	–	–	–
100–150 m	–	–	–	–76.8	–	–

Deuterium								
Borehole (HLX-series)	**21**	**22**	**23**	**24**	**25**	**26**	**27**	**28**	**29**	**30**	**31**	**32**	**33**	**34**	**35**	**36**	**37**	**38**	**39**	**40**
0–25 m	–	–	–	–	–	–	–	–												
25–50 m	–	–	–	–	–	–	–	–												
50–75 m	–	–	–	–	–	–	–	–												
75–100 m	–	–	–	–	–	–	–	–												
100–150 m	–	–	–	–	–	–	–	–												
150–200 m	–	–	–	–	–	–	–	–												

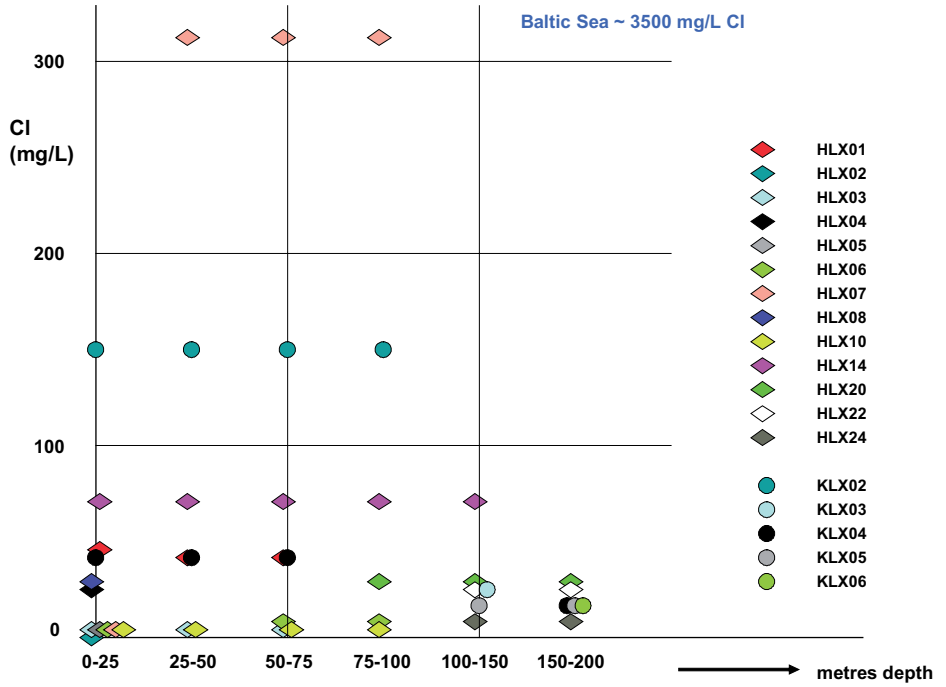
Baltic Sea ~ 3500 mg/L Cl
300
Cl
(mg/L)
200
100
0
0-25
25-50
50-75
75-100
100-150
150-200
metres depth
HLX01
HLX02
HLX03
HLX04
HLX05
HLX06
HLX07
HLX08
HLX10
HLX14
HLX20
HLX22
HLX24
KLX02
KLX03
KLX04
KLX05
KLX06

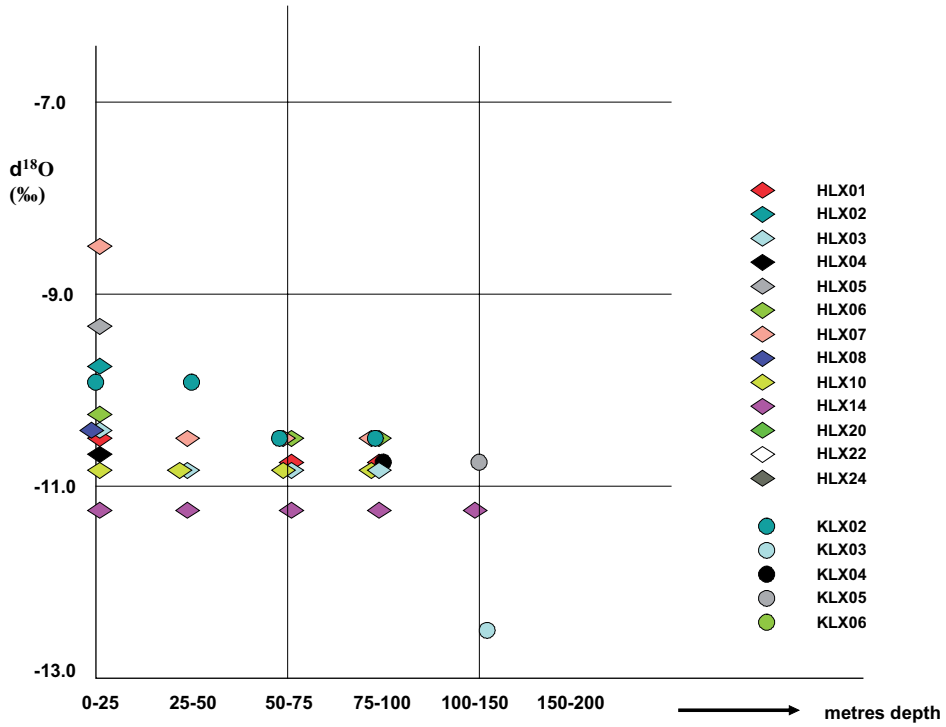
-7.0
d18O
(‰)
-9.0
-11.0
-13.0
0-25
25-50
50-75
75-100
100-150
150-200
metres depth
HLX01
HLX02
HLX03
HLX04
HLX05
HLX06
HLX07
HLX08
HLX10
HLX14
HLX20
HLX22
HLX24
KLX02
KLX03
KLX04
KLX05
KLX06

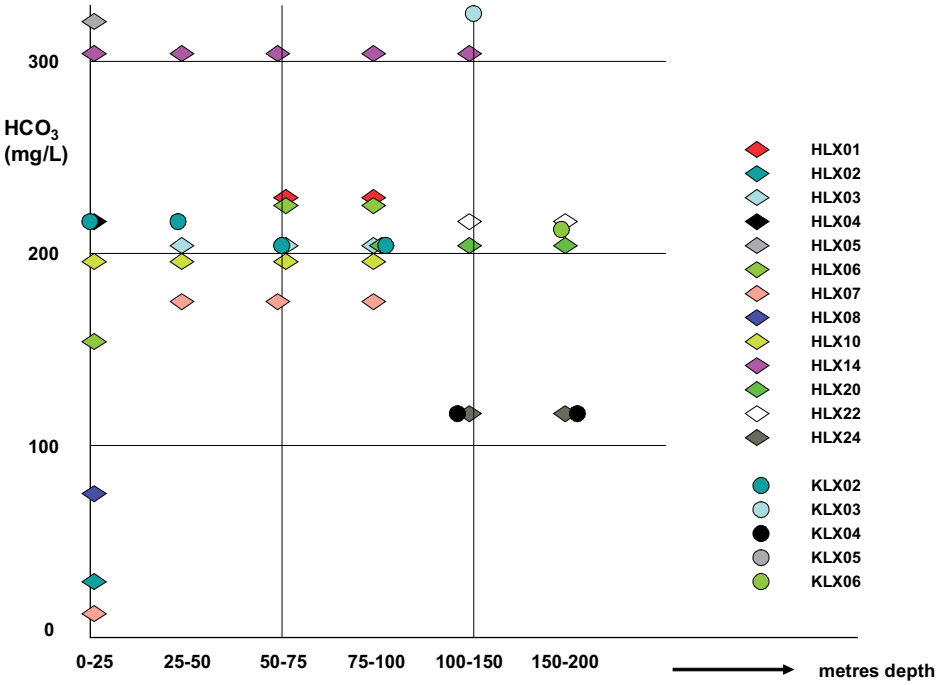
300
200
100
0
HCO3
(mg/L)
0-25
25-50
50-75
75-100
100-150
150-200
metres depth
HLX01
HLX02
HLX03
HLX04
HLX05
HLX06
HLX07
HLX08
HLX10
HLX14
HLX20
HLX22
HLX24
KLX02
KLX03
KLX04
KLX05
KLX06

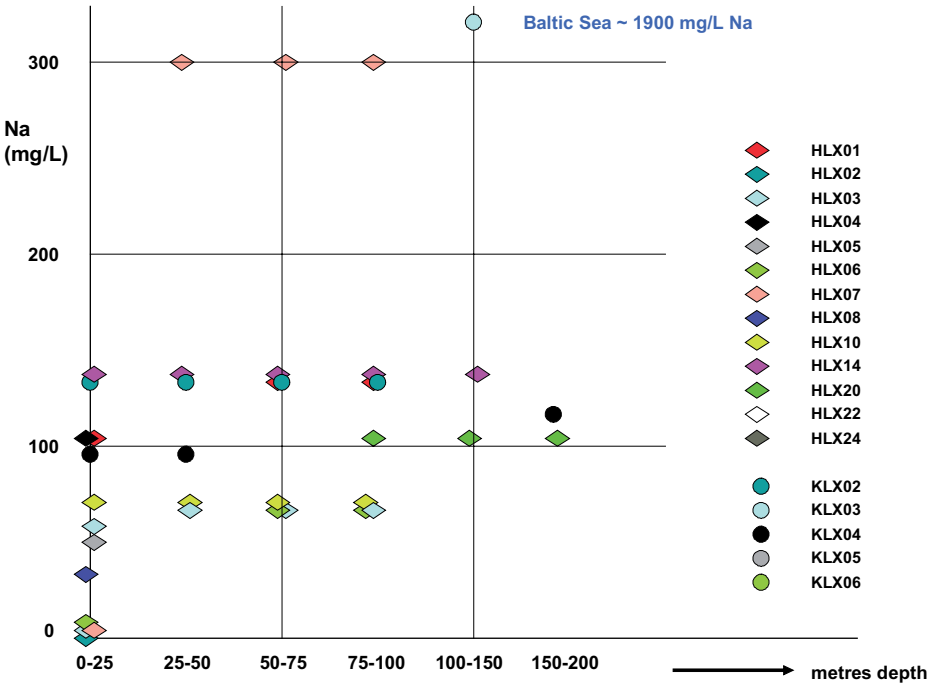
Baltic Sea ~ 1900 mg/L Na
300
200
100
0
Na
(mg/L)
0-25
25-50
50-75
75-100
100-150
150-200
metres depth
HLX01
HLX02
HLX03
HLX04
HLX05
HLX06
HLX07
HLX08
HLX10
HLX14
HLX20
HLX22
HLX24
KLX02
KLX03
KLX04
KLX05
KLX06

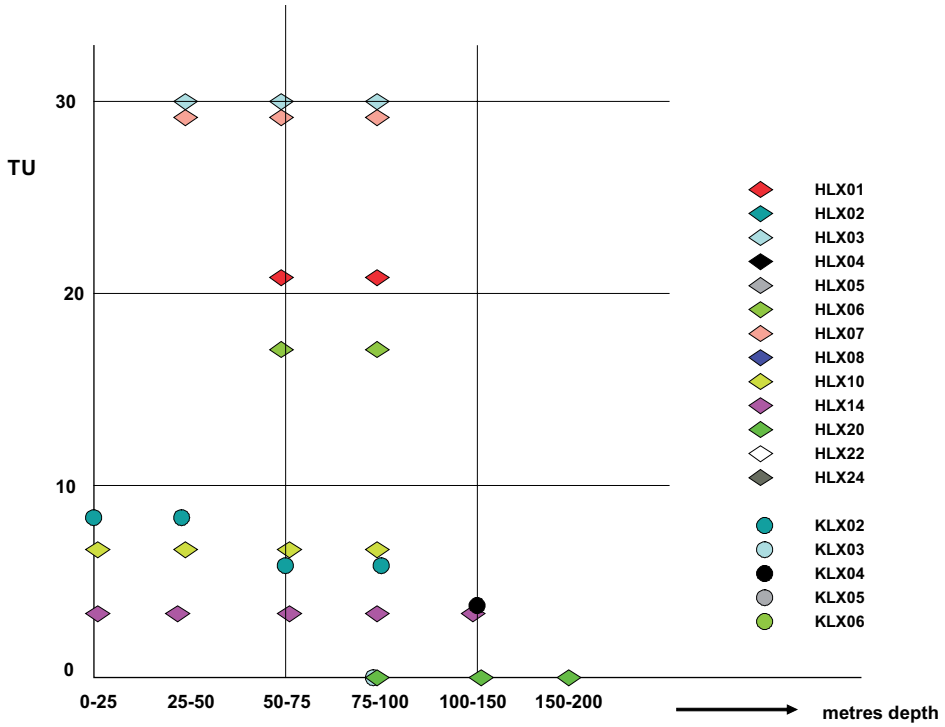
TU
30
20
10
0
0-25
25-50
50-75
75-100
100-150
150-200
metres depth
HLX01
HLX02
HLX03
HLX04
HLX05
HLX06
HLX07
HLX08
HLX10
HLX14
HLX20
HLX22
HLX24
KLX02
KLX03
KLX04
KLX05
KLX06

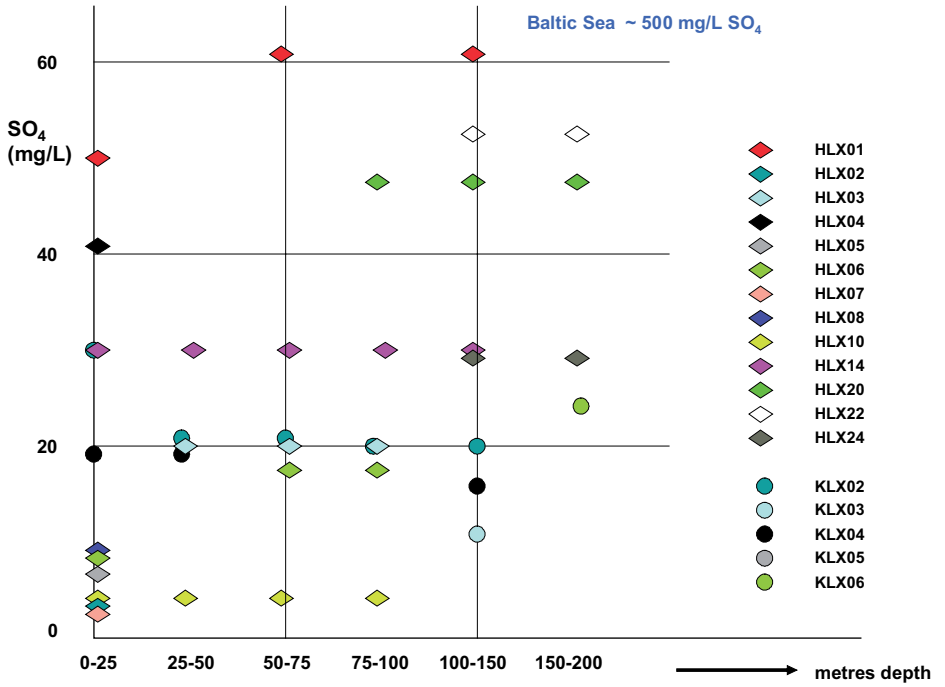
Baltic Sea ~ 500 mg/L SO4
SO4 (mg/L)
60
40
20
0
0-25
25-50
50-75
75-100
100-150
150-200
metres depth
HLX01
HLX02
HLX03
HLX04
HLX05
HLX06
HLX07
HLX08
HLX10
HLX14
HLX20
HLX22
HLX24
KLX02
KLX03
KLX04
KLX05
KLX06

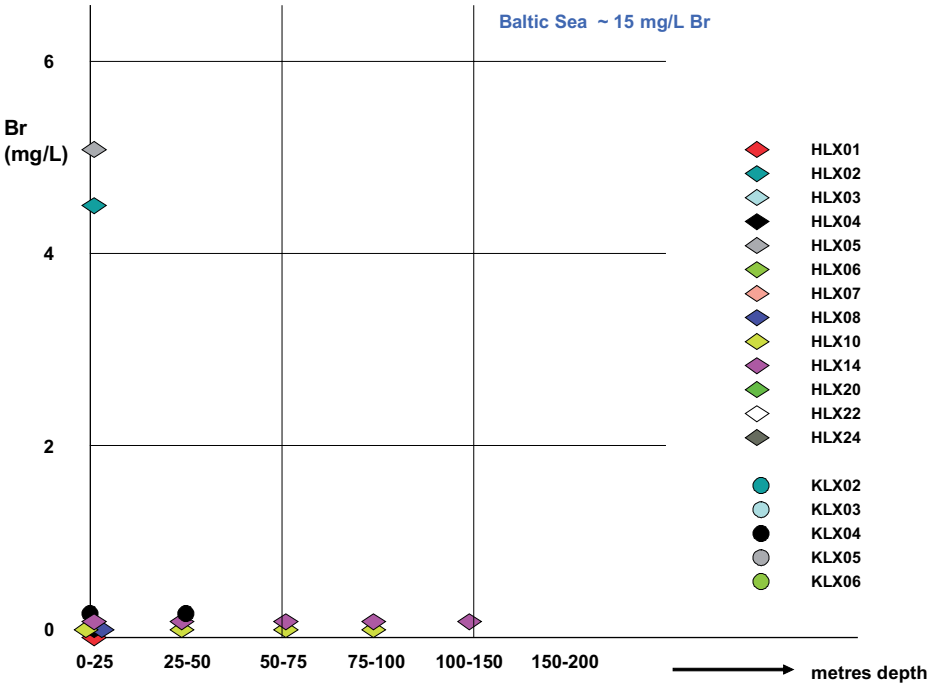
Baltic Sea ~ 15 mg/L Br
Br
(mg/L)
6
4
2
0
0-25
25-50
50-75
75-100
100-150
150-200
metres depth
HLX01
HLX02
HLX03
HLX04
HLX05
HLX06
HLX07
HLX08
HLX10
HLX14
HLX20
HLX22
HLX24
KLX02
KLX03
KLX04
KLX05
KLX06

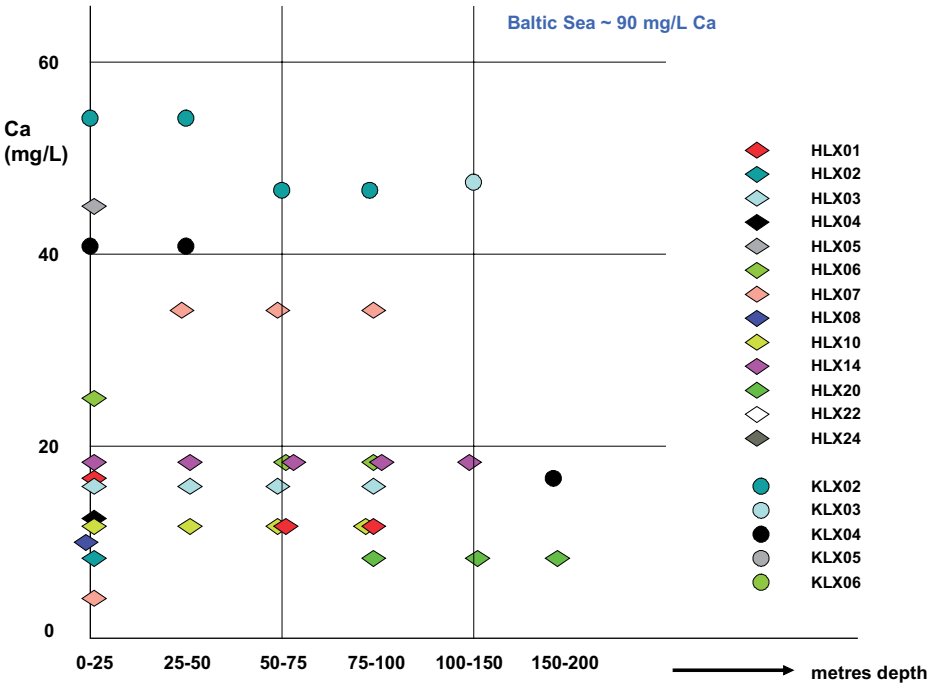
Baltic Sea ~ 90 mg/L Ca
Ca
(mg/L)
60
40
20
0
0-25
25-50
50-75
75-100
100-150
150-200
metres depth
HLX01
HLX02
HLX03
HLX04
HLX05
HLX06
HLX07
HLX08
HLX10
HLX14
HLX20
HLX22
HLX24
KLX02
KLX03
KLX04
KLX05
KLX06

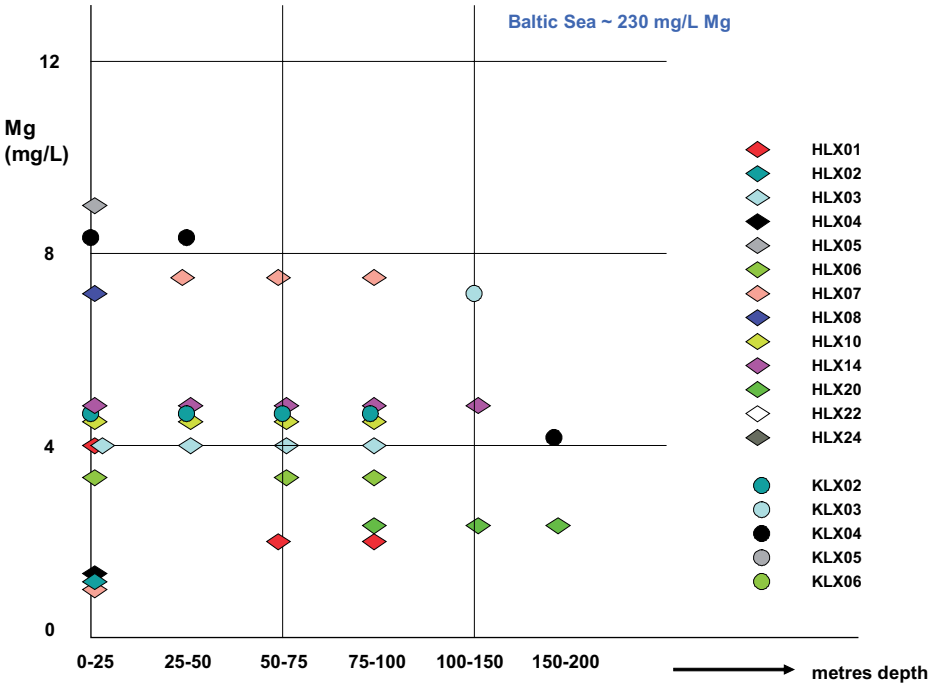
Baltic Sea ~ 230 mg/L Mg
12
8
4
0
Mg
(mg/L)
0-25
25-50
50-75
75-100
100-150
150-200
metres depth
HLX01
HLX02
HLX03
HLX04
HLX05
HLX06
HLX07
HLX08
HLX10
HLX14
HLX20
HLX22
HLX24
KLX02
KLX03
KLX04
KLX05
KLX06

Simpevarp subarea: Upper bedrock hydrochemistry

Simpevarp Site Boreholes

Water-conducting sections

Borehole (HSH-series)	01	02	03	04	05	06
0–25 m	X?	X?		X?	X?	X?
25–50 m	X?	X?		X?	X?	X?
50–75 m	X?		X	X?	X?	X?
75–100 m	X?	X?		X?	X?	X?
100–150 m	X?			X?	X?	X?
150–200 m	X?			X?	X?	X?

Borehole (KSH-series)	01A	01B	02	03A	03B
0–25 m		NW	X?	X?	X?
25–50 m		NW	X?	X?	X?
50–75 m		NW	X?	X?	X?
75–100 m		NW	X?	X?	X?
100–150 m	X	NW	X?	X?	X?

X = Indicates section(s) with greatest recorded groundwater flow into the borehole.
NW = Indicates no water flow recorded.
X? = Unknown groundwater flow source.

Chloride

Borehole (HSH-series)	01	02	03	04	05	06
0–25 m	–	22.6	–	–	–	–
25–50 m	–	22.6	–	–	–	–
50–75 m	–	–	55.1	–	–	–
75–100 m	–	22.6	–	–	–	–
100–150 m	–	–	–	–	–	–
150–200 m	–	–	–	–	–	–

Borehole (KSH-series)	01A	01B	02	03A	03B
0–25 m	–	–	–	–	–
25–50 m	–	–	–	510	–
50–75 m	–	–	24.7	510	–
75–100 m	–	–	–	–	–
150–200 m	5590	–	–	–	–

Bicarbonate

Borehole (HSH-series)	01	02	03	04	05	06
0–25 m	–	266	–	–	–	–
25–50 m	–	266	–	–	–	–
50–75 m	–	–	249	–	–	–
75–100 m	–	266	–	–	–	–
100–150 m	–	–	–	–	–	–
150–200 m	–	–	–	–	–	–

Borehole (KSH-series)	01A	01B	02	03A	03B
0–25 m	–	–	–	–	–
25–50 m	–	–	–	240	–
50–75 m	–	–	245	240	–
75–100 m	–	–	–	–	–
150–200 m	26	–	–	–	–

Sulphate

Borehole (HSH-series)	01	02	03	04	05	06
0–25 m	–	28.7	–	–	–	–
25–50 m	–	28.7	–	–	–	–
50–75 m	–	–	85	–	–	–
75–100 m	–	28.7	–	–	–	–
100–150 m	–	–	–	–	–	–
150–200 m	–	–	–	–	–	–

Borehole (KSH-series)	01A	01B	02	03A	03B
0–25 m	–	–	–	–	–
25–50 m	–	–	–	63.7	–
50–75 m	–	–	75.8	63.7	–
75–100 m	–	–	–	–	–
150–200 m	31.7	–	–	–	–

Bromide

Borehole (HSH-series)	01	02	03	04	05	06
0–25 m	–	–	–	–	–	–
25–50 m	–	–	–	–	–	–
50–75 m	–	–	0.20	–	–	–
75–100 m	–	–	–	–	–	–
100–150 m	–	–	–	–	–	–
150–200 m	–	–	–	–	–	–

Borehole (KSH-series)	01A	01B	02	03A	03B
0–25 m	–	–	–	–	–
25–50 m	–	–	–	2.01	–
50–75 m	–	–	0.58	2.01	–
75–100 m	–	–	–	–	–
150–200 m	31.24	–	–	–	–

Sodium

Borehole (HSH-series)	01	02	03	04	05	06
0–25 m	–	122	–	1685	485	–
25–50 m	–	122	–	1685	485	–
50–75 m	–	–	154	1685	485	–
75–100 m	–	122	–	1685	485	–
100–150 m	–	–	–	1685	485	–
150–200 m	–	–	–	1685	485	–

Borehole (KSH-series)	01A	01B	02	03A	03B
0–25 m	–	–	–	–	–
25–50 m	–	–	–	292	–
50–75 m	–	–	112	292	–
75–100 m	–	–	–	–	–
150–200 m	2280	–	–	–	–

Calcium

Borehole (HSH-series)	01	02	03	04	05	06
0–25 m	–	5.1	–	142	107	–
25–50 m	–	5.1	–	142	107	–
50–75 m	–	–	13.2	142	107	–
75–100 m	–	5.1	–	142	107	–
100–150 m	–	–	–	142	107	–
150–200 m	–	–	–	142	107	–

Borehole (KSH-series)	01A	01B	02	03A	03B
0–25 m	–	–	–	–	–
25–50 m	–	–	–	93.8	–
50–75 m	–	–	18.7	93.8	–
75–100 m	–	–	–	–	–
150–200 m	960	–	–	–	–

Potassium

Borehole (HSH-series)	01	02	03	04	05	06
0–25 m	–	2.15	–	56.9	17.5	–
25–50 m	–	2.15	–	56.9	17.5	–
50–75 m	–	–	3.37	56.9	17.5	–
75–100 m	–	2.15	–	56.9	17.5	–
100–150 m	–	–	–	56.9	17.5	–
150–200 m	–	–	–	56.9	17.5	–

Borehole (KSH-series)	01A	01B	02	03A	03B
0–25 m	–	–	–	–	–
25–50 m	–	–	–	6.94	–
50–75 m	–	–	3.58	6.94	–
75–100 m	–	–	–	–	–
150–200 m	14.7	–	–	–	–

Magnesium

Borehole (HSH-series)	01	02	03	04	05	06
0–25 m	–	1.4	–	180	56.9	–
25–50 m	–	1.4	–	180	56.9	–
50–75 m	–	–	3.5	180	56.9	–
75–100 m	–	1.4	–	180	56.9	–
100–150 m	–	–	–	180	56.9	–
150–200 m	–	–	–	180	56.9	–

Borehole (KSH-series)	01A	01B	02	03A	03B
0–25 m	–	–	–	–	–
25–50 m	–	–	–	6.94	–
50–75 m	–	–	4.2	6.94	–
75–100 m	–	–	–	–	–
150–200 m	70.8	–	–	–	–

Tritium*

Borehole (HSH-series)	01	02	03	04	05	06
0–25 m	–	11	–	–	–	–
25–50 m	–	11	–	–	–	–
50–75 m	–	–	10	–	–	–
75–100 m	–	11	–	–	–	–
100–150 m	–	–	–	–	–	–
150–200 m	–	–	–	–	–	–

Borehole (KSH-series)	01A	01B	02	03A	03B
0–25 m	–	–	–	–	–
25–50 m	–	–	–	8.8	–
50–75 m	–	–	4.2	8.8	–
75–100 m	–	–	–	–	–
150–200 m	–	–	–	–	–

* Non-standardised values recorded.

Oxygen-18

Borehole (HSH-series)	01	02	03	04	05	06
0–25 m	–	–10.7	–	–	–	–
25–50 m	–	–10.7	–	–	–	–
50–75 m	–	–	–10.7	–	–	–
75–100 m	–	–10.7	–	–	–	–
100–150 m	–	–	–	–	–	–
150–200 m	–	–	–	–	–	–

Borehole (KSH-series)	01A	01B	02	03A	03B
0–25 m	–	–	–	–	–
25–50 m	–	–	–	–9.8	–
50–75 m	–	–	–	–9.8	–
75–100 m	–	–	–	–	–
150–200 m	–13.1	–	–	–	–

Deuterium

Borehole (HSH-series)	01	02	03	04	05	06
0–25 m	–	–76.3	–	–	–	–
25–50 m	–	–76.3	–	–	–	–
50–75 m	–	–	–76.1	–	–	–
75–100 m	–	–76.3	–	–	–	–
100–150 m	–	–	–	–	–	–
150–200 m	–	–	–	–	–	–

Borehole (KSH-series)	01A	01B	02	03A	03B
0–25 m	–	–	–	–	–
25–50 m	–	–	–	–74.3	–
50–75 m	–	–	–	–74.3	–
75–100 m	–	–	–	–	–
150–200 m	–98.2	–	–	–	–

Ävrö Site

Water-conducting sections

Borehole (HAV-series)	01	02	03	04	05	06	07	08	09	10	11	12	13	14
0–25 m									X?	X				
25–50 m				X?					X?					
50–75 m				X?	X?				X?					
75–100 m				X?	X?	X?	X?		X?				X	
100–150 m									X?		X		X	X
150–200 m											X	X		X

Borehole (KAV-series)	01	04A
0–25 m		
25–50 m		
50–75 m		X
75–100 m	X	
100–150 m	X	X
150–200 m		
200–250 m	X	X?

X = Indicates section(s) with greatest recorded groundwater flow into the borehole.
NW = Indicates no water flow recorded.
X? = Unknown groundwater flow source.

Chloride

Borehole (HAV-series)	01	02	03	04	05	06	07	08	09	10	11	12	13	14
0–25 m									2561	19.1				
25–50 m				106					2561					
50–75 m				106	15				2561					
75–100 m				106	15	36	73		2561				X	
100–150 m									2561		X		X	X
150–200 m											X	X		X

Borehole (KAV-series)	01	04A
0–25 m		
25–50 m	15.5	
50–75 m	15.5	22.6
75–100 m	15.5	
100–150 m		
150–200 m		
200–250 m		

Bicarbonate

Borehole (HAV-series)	01	02	03	04	05	06	07	08	09	10	11	12	13	14
0–25 m									32	285				
25–50 m				290					32					
50–75 m				290	271				32					
75–100 m				290	271	228	257		32					
100–150 m									32					
150–200 m														

Borehole (KAV-series)	01	04A
0–25 m		
25–50 m	167	
50–75 m	167	261
75–100 m	167	
100–150 m		
150–200 m		
200–250 m		

Sulphate

Borehole (HAV-series)	01	02	03	04	05	06	07	08	09	10	11	12	13	14
0–25 m									94	60				
25–50 m				71					94					
50–75 m				71	97				94					
75–100 m				71	97	71	69		94					
100–150 m									94					
150–200 m														

Borehole (KAV-series)	01	04A
0–25 m		
25–50 m	28	
50–75 m	28	71
75–100 m	28	
100–150 m		
150–200 m		
200–250 m		

Bromide

Borehole (HAV-series)	01	02	03	04	05	06	07	08	09	10	11	12	13	14
0–25 m									10.5	0				
25–50 m									10.5					
50–75 m									10.5					
75–100 m									10.5					
100–150 m									10.5					
150–200 m														

Borehole (KAV-series)	01	04A
0–25 m		
25–50 m	0	
50–75 m	0	0
75–100 m	0	
100–150 m		
150–200 m		
200–250 m		

Sodium

Borehole (HAV-series)	01	02	03	04	05	06	07	08	09	10	11	12	13	14
0–25 m									992					
25–50 m				202					992					
50–75 m				202	144				992					
75–100 m				202	144	127	139		992				263	
100–150 m									992		525		263	46.5
150–200 m											525			46.5

Borehole (KAV-series)	01	04A
0–25 m		
25–50 m		
50–75 m		112
75–100 m		
100–150 m		
150–200 m		
200–250 m		

Calcium

Borehole (HAV-series)	01	02	03	04	05	06	07	08	09	10	11	12	13	14
0–25 m									626					
25–50 m				13					626					
50–75 m				13	12				626					
75–100 m				13	12	11	21		626				48.8	
100–150 m									626		270		48.8	45.7
150–200 m											270			45.7

Borehole (KAV-series)	01	04A
0–25 m		
25–50 m		
50–75 m		6.8
75–100 m		
100–150 m		
150–200 m		
200–250 m		

Potassium

Borehole (HAV-series)	01	02	03	04	05	06	07	08	09	10	11	12	13	14
0–25 m									10.8					
25–50 m				4					10.8					
50–75 m				4	3				10.8					
75–100 m				4	3	1.6	2		10.8				4.2	
100–150 m									10.8		9.6		4.2	2.7
150–200 m											9.6			2.7

Borehole (KAV-series)	01	04A
0–25 m		
25–50 m		
50–75 m		1.9
75–100 m		
100–150 m		
150–200 m		
200–250 m		

Magnesium

Borehole (HAV-series)	01	02	03	04	05	06	07	08	09	10	11	12	13	14
0–25 m									80.5					
25–50 m				3					80.5					
50–75 m				3	3				80.5					
75–100 m				3	3	14	2		80.5				11.7	
100–150 m									80.5		29.2		11.7	5.4
150–200 m											29.2			5.4

Borehole (KAV-series)	01	04A
0–25 m		
25–50 m		
50–75 m		11
75–100 m		
100–150 m		
150–200 m		
200–250 m		

Tritium*

Borehole (HAV-series)	01	02	03	04	05	06	07	08	09	10	11	12	13	14
0–25 m														
25–50 m				0										
50–75 m				0	0									
75–100 m				0	0	0	2							
100–150 m														
150–200 m														

Borehole (KAV-series)	01	04A
0–25 m		
25–50 m		
50–75 m		
75–100 m		
100–150 m		
150–200 m		
200–250 m		

* Non-standardised values recorded.

Oxygen-18

Borehole (HAV-series)	01	02	03	04	05	06	07	08	09	10	11	12	13	14
0–25 m														
25–50 m				–9.9										
50–75 m				–9.9	–9.8									
75–100 m				–9.9	–9.8	–10.2	–10.2							
100–150 m														
150–200 m														

Borehole (KAV-series)	01	04A
0–25 m		
25–50 m		
50–75 m		
75–100 m		
100–150 m		
150–200 m		
200–250 m		

Deuterium

Borehole (HAV-series)	01	02	03	04	05	06	07	08	09	10	11	12	13	14
0–25 m														
25–50 m				–79.7										
50–75 m				–79.7	–67.1									
75–100 m				–79.7	–67.1	–70.1	–73.3							
100–150 m														
150–200 m														

Borehole (KAV-series)	01	04A
0–25 m		
25–50 m		
50–75 m		
75–100 m		
100–150 m		
150–200 m		
200–250 m		

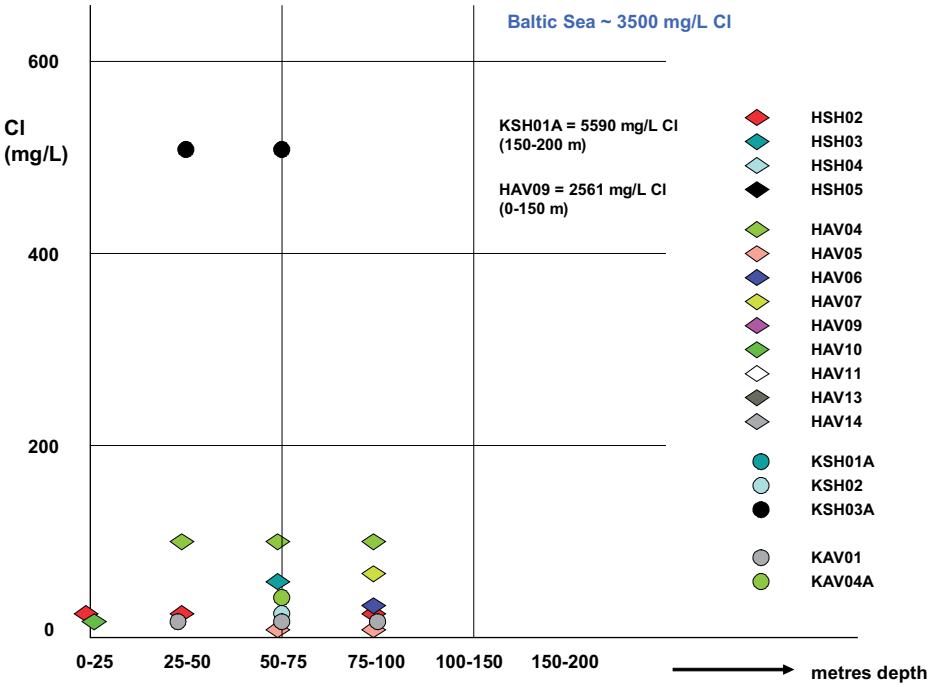
Baltic Sea ~ 3500 mg/L Cl
600
400
200
0
Cl
(mg/L)
KSH01A = 5590 mg/L Cl
(150-200 m)
HAV09 = 2561 mg/L Cl
(0-150 m)
HSH02
HSH03
HSH04
HSH05
HAV04
HAV05
HAV06
HAV07
HAV09
HAV10
HAV11
HAV13
HAV14
KSH01A
KSH02
KSH03A
KAV01
KAV04A
0-25
25-50
50-75
75-100
100-150
150-200
metres depth

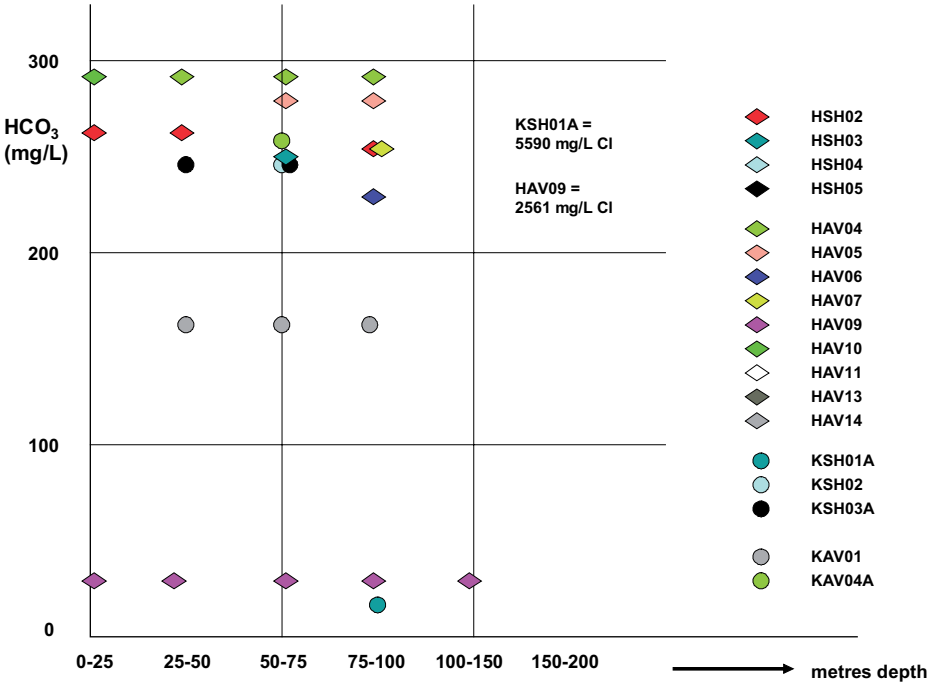
300
200
100
0
HCO3
(mg/L)
KSH01A =
5590 mg/L Cl
HAV09 =
2561 mg/L Cl
HSH02
HSH03
HSH04
HSH05
HAV04
HAV05
HAV06
HAV07
HAV09
HAV10
HAV11
HAV13
HAV14
KSH01A
KSH02
KSH03A
KAV01
KAV04A
0-25
25-50
50-75
75-100
100-150
150-200
metres depth

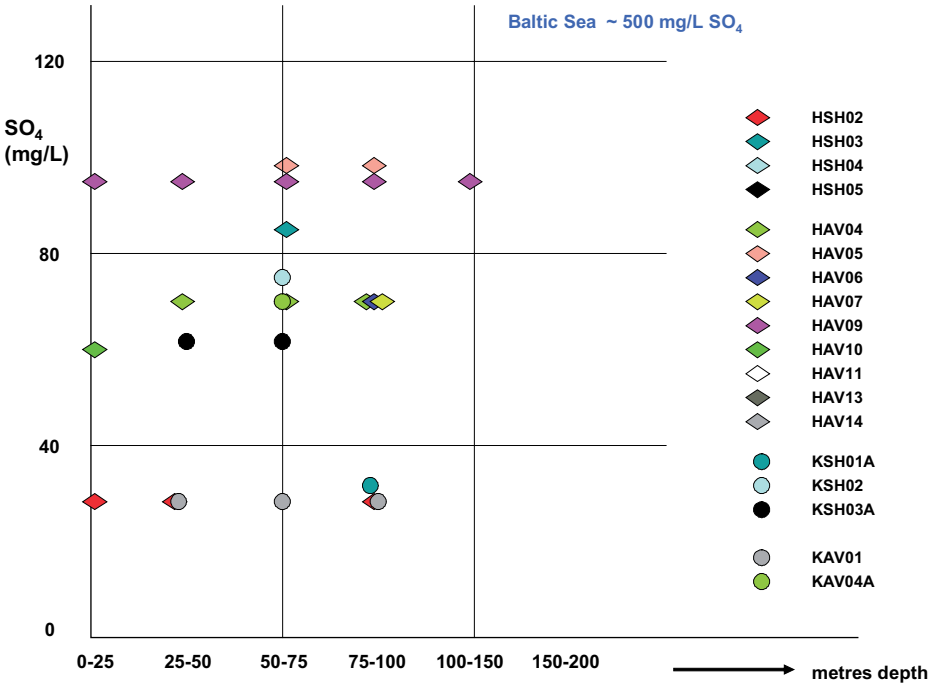
Baltic Sea ~ 500 mg/L SO4
SO4 (mg/L)
120
80
40
0
0-25
25-50
50-75
75-100
100-150
150-200
metres depth
HSH02
HSH03
HSH04
HSH05
HAV04
HAV05
HAV06
HAV07
HAV09
HAV10
HAV11
HAV13
HAV14
KSH01A
KSH02
KSH03A
KAV01
KAV04A

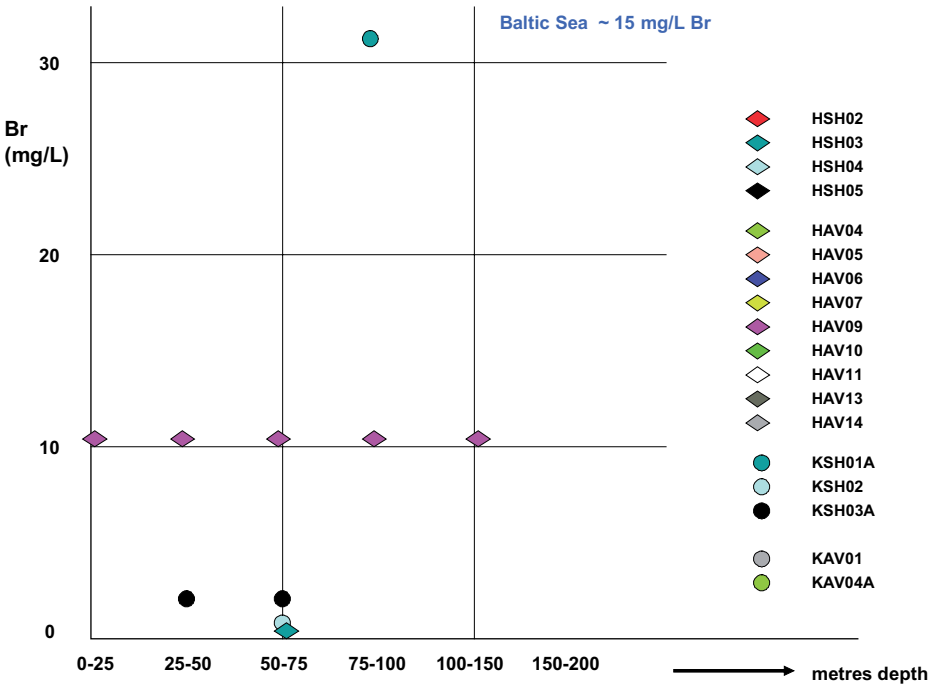
Baltic Sea ~ 15 mg/L Br
Br (mg/L)
30
20
10
0
0-25
25-50
50-75
75-100
100-150
150-200
metres depth
HSH02
HSH03
HSH04
HSH05
HAV04
HAV05
HAV06
HAV07
HAV09
HAV10
HAV11
HAV13
HAV14
KSH01A
KSH02
KSH03A
KAV01
KAV04A

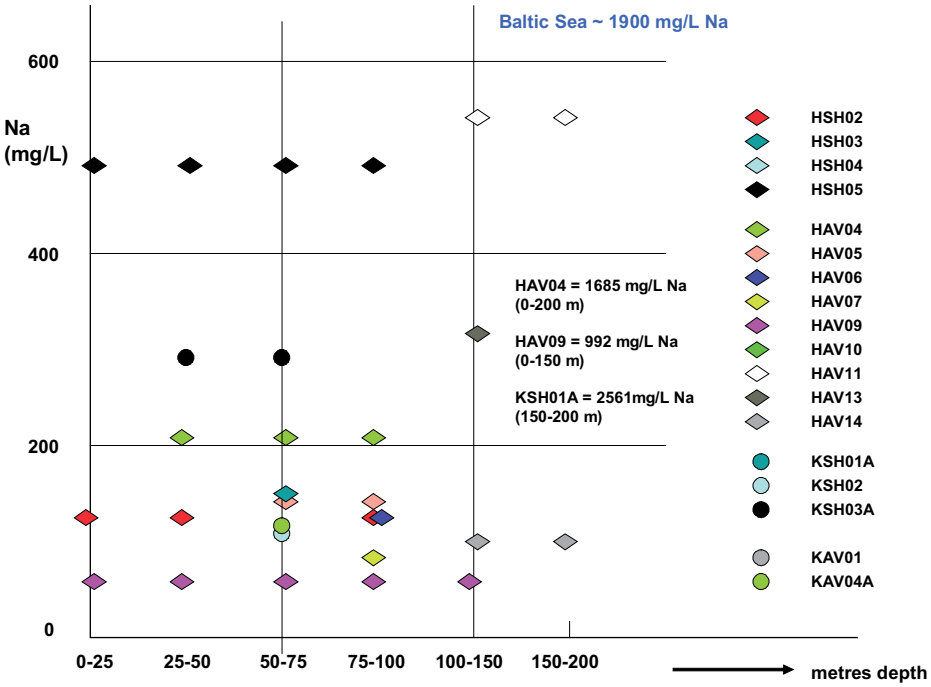
Baltic Sea ~ 1900 mg/L Na
Na
(mg/L)
600
400
200
0
HAV04 = 1685 mg/L Na
(0-200 m)
HAV09 = 992 mg/L Na
(0-150 m)
KSH01A = 2561mg/L Na
(150-200 m)
HSH02
HSH03
HSH04
HSH05
HAV04
HAV05
HAV06
HAV07
HAV09
HAV10
HAV11
HAV13
HAV14
KSH01A
KSH02
KSH03A
KAV01
KAV04A
0-25
25-50
50-75
75-100
100-150
150-200
metres depth

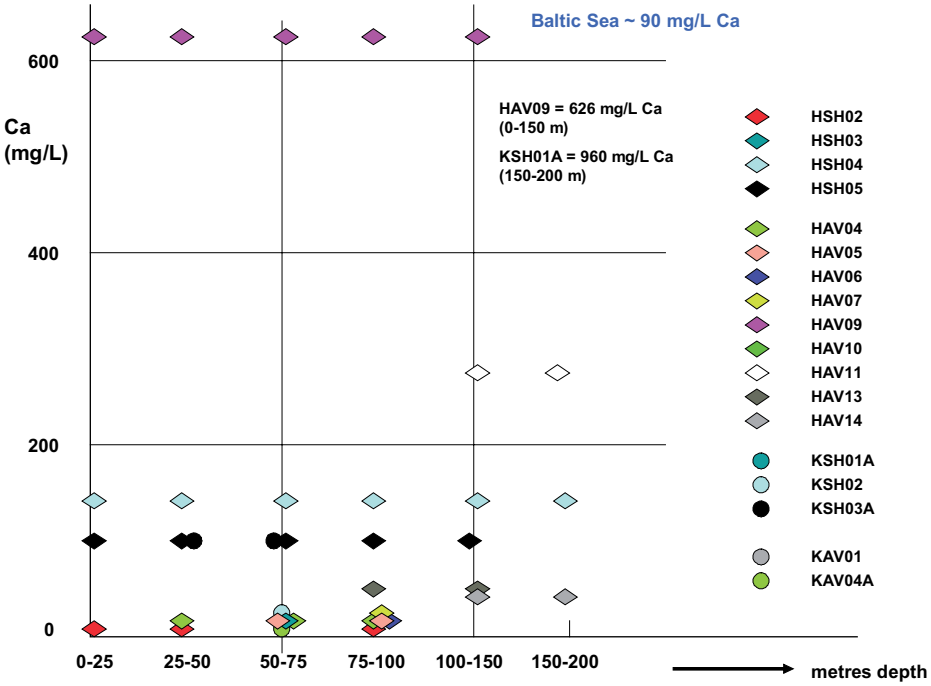
Baltic Sea ~ 90 mg/L Ca
Ca
(mg/L)
600
400
200
0
HAV09 = 626 mg/L Ca
(0-150 m)
KSH01A = 960 mg/L Ca
(150-200 m)
HSH02
HSH03
HSH04
HSH05
HAV04
HAV05
HAV06
HAV07
HAV09
HAV10
HAV11
HAV13
HAV14
KSH01A
KSH02
KSH03A
KAV01
KAV04A
0-25
25-50
50-75
75-100
100-150
150-200
metres depth

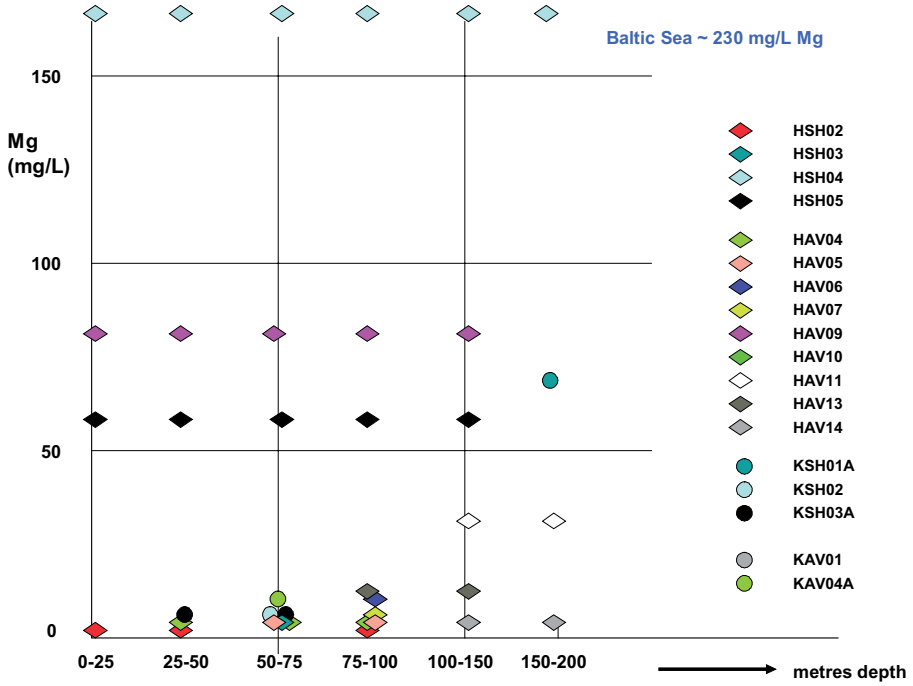
Baltic Sea ~ 230 mg/L Mg
Mg
(mg/L)
150
100
50
0
0-25
25-50
50-75
75-100
100-150
150-200
metres depth
HSH02
HSH03
HSH04
HSH05
HAV04
HAV05
HAV06
HAV07
HAV09
HAV10
HAV11
HAV13
HAV14
KSH01A
KSH02
KSH03A
KAV01
KAV04A

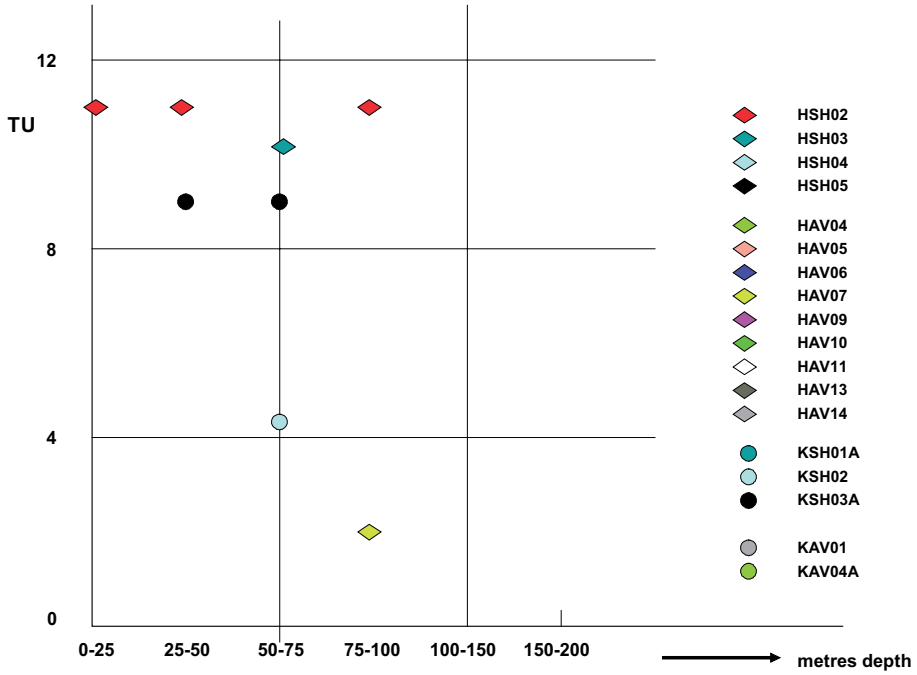
TU
12
8
4
0
0-25
25-50
50-75
75-100
100-150
150-200
metres depth
HSH02
HSH03
HSH04
HSH05
HAV04
HAV05
HAV06
HAV07
HAV09
HAV10
HAV11
HAV13
HAV14
KSH01A
KSH02
KSH03A
KAV01
KAV04A

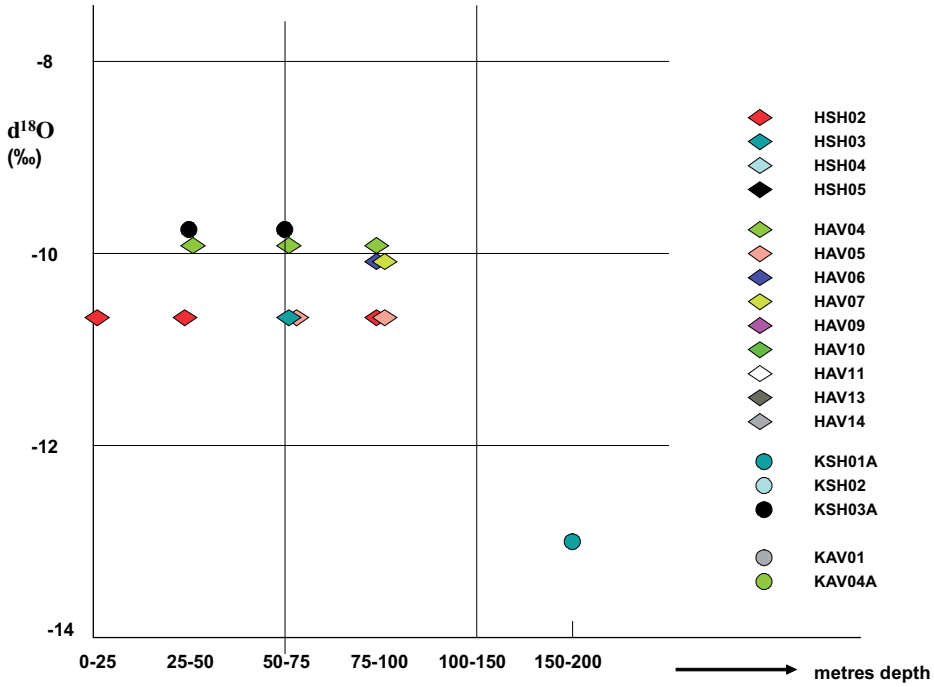
-8
-10
-12
-14
d18O
(‰)
0-25
25-50
50-75
75-100
100-150
150-200
metres depth
HSH02
HSH03
HSH04
HSH05
HAV04
HAV05
HAV06
HAV07
HAV09
HAV10
HAV11
HAV13
HAV14
KSH01A
KSH02
KSH03A
KAV01
KAV04A

Appendix 3

Laxemar: Pore water data from borehole KLX03

Table A1. Bulk and grain density and physical porosity of samples from borehole KLX03.

Laboratory Sample No	Bulk density dry[1] (g/cm3)	Grain Density[2] (g/cm3)	Physical Porosity (Vol.-%)	Mass of sample (g)	Bulk Density wet[3] (g/cm3)
KLX03-1				1,015.640	2.72
KLX03-2				1,028.960	2.72
KLX03-3				1,227.891	2.71
KLX03-4				1,031.454	2.72
KLX03-5				1,028.396	2.75
KLX03-6				1,007.473	2.74
KLX03-7				1,027.610	2.76
KLX03-8				1,015.631	2.74
KLX03-9				1,002.790	2.73
KLX03-10				982.509	2.73
KLX03-11	2.800	2.825	0.93	1,036.704	2.79
KLX03-12				1,050.850	2.78
KLX03-13				1,053.568	2.80
KLX03-14				1,044.860	2.80
KLX03-15				1,041.053	2.81
KLX03-16				1,047.565	2.80

[1] Determined by Hg-displacement on dry rock sample.
[2] Determined by He-pycnometry on dry rock sample.
[3] Determined from mass and volume of saturated (wet) drillcore sample used for out-diffusion experiment.

Table A2. Average water content by drying at 105°C and water-content porosity of rock samples from borehole KLX03.

Laboratory Sample No	Number of samples	Water Content average (wt.-%)	Water Content 1 σ (wt.-%)	WC-Porosity average (Vol.-%)	WC-Porosity 1 σ (Vol.-%)
KLX03-1	3	0.217	0.014	0.588	0.038
KLX03-2	3	0.214	0.004	0.581	0.012
KLX03-3	3	0.242	0.019	0.661	0.051
KLX03-4	3	0.369	0.040	0.997	0.108
KLX03-5	3	0.212	0.016	0.582	0.044
KLX03-6	3	0.173	0.005	0.471	0.014
KLX03-7	3	0.276	0.051	0.757	0.139
KLX03-8	3	0.375	0.073	1.019	0.198
KLX03-9	1	0.190		0.51	
KLX03-10	1	0.068		0.186	
KLX03-11	3	0.122	0.006	0.339	0.018
KLX03-12	3	0.258	0.010	0.715	0.027
KLX03-13	3	0.103	0.012	0.287	0.032
KLX03-14	3	0.083	0.010	0.232	0.027
KLX03-15	3	0.089	0.022	0.249	0.063
KLX03-16	3	0.094	0.023	0.263	0.064

Table A3. $\delta^{18}O$ and $\delta^{2}H$ of pore water and water content derived from isotope diffusive exchange method.

Laboratory Sample No	Average Vertical Depth (m)	$\delta^{18}O$[1)] pore water (‰ V-SMOW)	$\delta^{2}H$[1)] pore water (‰ V-SMOW)	Water Content[1)] (wt.-%)
KLX03-1	159.22	–12.26	–90.1	0.1767
KLX03-2	202.66	–11.44	–92.5	0.2417
KLX03-3	253.72	–11.43	–116.8	0.2799
KLX03-4	303.10			
KLX03-5	355.66	–13.12	–78.2	0.2197
KLX03-6	411.70	–11.58	*–161.2*	*0.1445*
KLX03-7	462.76	–7.51	–83.9	0.2702
KLX03-8	524.63	–13.64	–54.9	0.4226
KLX03-9	590.12			
KLX03-10	643.14			
KLX03-11	695.95	–9.38	–28.3	0.1420
KLX03-12	803.21	–10.94	–58.6	0.3333
KLX03-13	841.15			
KLX03-14	894.53	–5.14	*–1.9*	*0.0704*
KLX03-15	942.47			
KLX03-16	979.78	–6.56	–28.7	0.1020

[1)] Light shaded areas: indications for slight evaporation during experiment, true calculated $\delta^{18}O$ and $\delta^{2}H$ values might be more negative.

Dark shaded areas: analysis of traced test water with larger than standard error (possibly memory effect during ^{2}H mass spectrometric measurement) and calculated values are less reliable.

Data in italics: not used for further interpretation.

Table A4. Chemical composition of solutions from out-diffusion experiments at steady state conditions.

Out-Diffusion Experiment Solution	Units	KLX03-1	KLX03-2	KLX03-3	KLX03-4	KLX03-5	KLX03-6	KLX03-7	KLX03-8	KLX03-9
Sample Description										
Vertical Depth	m	159.22	202.66	253.72	303.10	355.66	411.70	462.76	524.63	590.12
Rock Type										
Water-Rock Ratio		0.118	0.106	0.091	0.105	0.111	0.086	0.108	0.110	0.116
Experiment Temperature	ºC	20	45	45	45	45	45	45	45	45
Experiment Time	days	190	100	100	100	100	100	99	90	90
Misc. Properties										
Chemical Type	Na-HCO_3^- (F)-(Cl)	Na-HCO_3^- (Cl)	Na-HCO_3	Na-HCO_3^- (F)-(Cl)	Na-HCO_3	Na-HCO_3^- (Cl)	Ca-Na-SO_4^- (HCO_3)	Na-Ca-Cl-HCO_3^- SO_4	Na-Ca-Cl-HCO_3^- SO_4	Na-HCO_3^- (F)-(Cl)
pH (lab)	-log(H+)	8.02	7.89	8.15	7.55	7.85	7.88	7.27	7.34	7.36
Electrical Conductivity	µS/cm	390	475	637	353	625	446	1303		983
Sample Temperature	ºC	20	20	20	20	20	20	20	20	20
Cations										
Sodium (Na+)	mg/L	93.3	116	166	87.2	145	101	145	173	167
Potassium (K^+)	mg/L	1.8	2.2	1.5	1.3	5.5	4.1	12.6	7.3	4.8
Magnesium (Mg^+2)	mg/L	< 0.5	< 0.5	< 0.5	< 0.5	< 0.5	< 0.5	1.2	0.8	< 0.5
Calcium (Ca^+2)	mg/L	3.2	3.6	3.4	2.4	9.3	6.7	149	140	42.5
Strontium (Sr^{+2})	mg/L	0.012	0.053	0.047	0.097	0.13	0.1	1.7	1.8	0.68
Anions										
Fluoride (F^-)	mg/L	11.7	6.6	7.4	10.4	5.2	2.8	2.4	2.1	4.7
Chloride (Cl^-)	mg/L	16	16.2	14.3	13.8	12.9	15.5	35.8	198	142
Bromide (Br^-)	mg/L	< 0.1	< 0.1	< 0.1	< 0.1	< 0.1	< 0.1	< 0.1	1.3	0.58
Sulfate (SO_4^{-2})	mg/L	7.8	8.1	16.4	11.8	21.7	9.3	506	347	100
Nitrate (NO_3^-)	mg/L	< 0.5	< 0.5	< 0.5	< 0.5	< 0.5	< 0.5	< 0.5	1.4	< 0.5
Total Alkalinity as HCO_3^-	mg/L	171.5	213.6	307.5	123.9	309.4	211.7	100.1	98.8	137.3
Calc. Parameters										
Total dissolved solids	mg/L	305	366	517	251	509	351	954	969	599
Charge Balance	%	2.71	8.30	9.23	10.28	5.78	6.46	3.24	3.32	5.14

Out-Diffusion Experiment Solution	Units	KLX03-10	KLX03-11	KLX03-12	KLX03-13	KLX03-14	KLX03-15	KLX03-16	Standard Solution
Sample Description									
Vertical Depth	m	643.14	695.95	803.21	841.15	894.53	942.47	979.78	
Rock Type									
Water-Rock Ratio		0.109	0.109	0.101	0.106	0.107	0.110	0.111	
Experiment Temperature	ºC	45	45	45	20	45	45	45	
Experiment Time	days	90	90	90	149	89	89	89	
Misc. Properties									
Chemical Type		Na-Ca-HCO_3-Cl	Na-Ca-HCO_3	Na-(Ca)-HCO_3-Cl		Na-Ca-HCO_3-Cl		Na-Ca-HCO_3-Cl	
pH (lab)	-log(H+)	7.43	7.4	7.32	7.45	7.26	7.32	7.27	
Electrical Conductivity	µS/cm		328	830		486		400	14
Sample Temperature	ºC	20	20	20		20		20	20
Cations									
Sodium (Na^+)	mg/L	57.3	40.1	158		70.3		69.9	0.2
Potassium (K^+)	mg/L	5	8.4	8.6		8.9		6.3	< 0.1
Magnesium (Mg^{+2})	mg/L	0.5	< 0.5	0.8		0.8		< 0.5	0.3
Calcium (Ca^{+2})	mg/L	15.6	28.3	23.6		37		19.2	0.1
Strontium (Sr^{+2})	mg/L	0.081	0.16	0.19		0.25		0.12	
Anions									
Fluoride (F^-)	mg/L	0.4	0.9	3.9		1.1		1	< 0.1
Chloride (Cl^-)	mg/L	15.9	6.8	120		30.3		41.4	1.1
Bromide (Br^-)	mg/L	0.23	< 0.1	0.59		< 0.1		0.18	< 0.1
Sulfate (SO_4^{-2})	mg/L	9.8	4.9	16.2		10.9		9.5	< 0.1
Nitrate (NO_3^-)	mg/L	0.7	4	6.3		< 0.5		< 0.5	
Total Alkalinity as HCO_3^-	mg/L	138.5	172.7	220.3	159.9	189.2	160.5	136.7	< 0.1
Calc. Parameters									
Total dissolved solids	mg/L	243	262	552		349		284	< 2
Charge Balance	%	7.16	2.11	3.95		10.21		6.42	2.57

Table A5. Isotopic composition of solutions from out-diffusion experiments at steady state conditions.

Laboratory Sample No	Average Vertical Depth (m)	$\delta^{18}O$[1] ‰ V-SMOW	$\delta^{2}H$[1] ‰ V-SMOW	$\delta^{37}Cl$ ‰ V-SMOC	Sr ppm	$^{87}Sr/^{86}Sr$	$^{87}Sr/^{86}Sr$ 1 σ
KLX03-1	159.22			b.d.[2]	0.024	0.715469	0.000029
KLX03-2	202.66	*69*	*–205*	2.47[3]	0.034	0.714463	0.00002
KLX03-3	253.72	*157*	*–858*	b.d.[2]	0.034	0.714416	0.000024
KLX03-4	303.10	*–12*	*60*				
KLX03-5	355.66	*–589*	*87*	b.d.[2]	0.068	0.714817	0.000032
KLX03-6	411.70			1.89	0.088	0.714955	0.000021
KLX03-7	462.76						
KLX03-8	524.63			1.47	1.851	0.708281	0.00002
KLX03-9	590.12			2.13	0.74	0.709984	0.000027
KLX03-10	643.14						
KLX03-11	695.95			b.d.[2]	0.139	0.71908	0.000027
KLX03-12	803.21			0.64	0.272	0.717795	0.000037
KLX03-13	841.15			b.d.[2]			
KLX03-14	894.53			1.53[3]	0.203	0.721149	0.000023
KLX03-15	942.47						
KLX03-16	979.78			0.61	0.166	0.717054	0.000034

[1] Calculated data in italics are meaningless and not used for further interpretation (see text for explanation).
[2] b.d. = Below detection due to low Cl content.
[3] Very small signal, not used for further interpretation.

Table A6. Chloride concentration of pore water calculated from out-diffusion solutions and the water content of the samples.

Laboratory Sample No	Average Vertical Depth (m)	Pore Water Cl mg/kg H_2O	Pore Water Cl + error mg/kg H_2O	Pore Water Cl – error mg/kg H_2O
KLX03-1	159.22	806	55	48
KLX03-2	202.66	765	16	15
KLX03-3	253.72	503	41	35
KLX03-4	303.10	374	44	35
KLX03-5	355.66	613	49	42
KLX03-6	411.70	730	22	21
KLX03-7	462.76	1,377	305	210
KLX03-8	524.63	5,647	1,327	893
KLX03-9	590.12	8,578		
KLX03-10	643.14	2,260		
KLX03-11	695.95	513	28	25
KLX03-12	803.21	4,519	171	159
KLX03-13	841.15			
KLX03-14	894.53	3,629	483	381
KLX03-15	942.47			
KLX03-16	979.78	4,739	1,498	915

Shaded area: Pore-water Cl concentrations of these samples are preliminary and will change to slightly higher values (~ 5%) because Cl time series samples not yet analysed; therefore, values are only corrected for mass removed by Cl time series samples, but not for the Cl removed by these samples.

Appendix 2

Explorative analyses of microbes, colloids and gases

Contribution to the model version 1.2

Lotta Hallbeck

Vita vegrandis

September 2005

Contents

1 Microbiology and microbial model 275
1.1 Introduction 275
1.2 The subsurface microbial model 275
1.2.1 The surface biosphere 275
1.2.2 The oxygen gradient zone 276
1.2.3 The anaerobic subsurface zone 276
1.2.4 The deep sulphate-reducing zone 277
1.2.5 The deep autotrophic zone 277
1.2.6 The deep chemosphere 277
1.3 Data available 278
1.4 Evaluation of the microbial and chemical data 279
1.4.1 Total number of microorganisms and organic carbon, total (TOC) or dissolved (DOC) 279
1.4.2 Fractionation filtration for humic and fulvic acids 280
1.4.3 The isotopic composition of organic carbon and carbon-14 dating 281
1.5 Redox potential in groundwater 281
1.6 Manganese-reducing bacteria and manganese 283
1.7 Ferrous iron and iron-reducing bacteria 284
1.8 Sulphate-reducing bacteria, sulphate and sulphide 284
1.9 Methanogens 286
1.10 Acetogens 286
1.11 The microbial model 286
1.11.1 Classification of most probable number (MPN) numbers into *-signs to be used in "The microbial subsurface model" 286
1.11.2 Characterisation of the influence by different metabolic groups of microorganisms 288
1.11.3 The microbial model in the Simpevarp regional area 288
1.12 Significance of attached microorganisms in the subsurface model 290
1.13 Metabolic rates in the subsurface model 291
1.14 Conclusions 292

2 Colloids 293
2.1 Introduction 293
2.2 Methods 293
2.2.1 Databases 293
2.2.2 Evaluation of the colloid data 293
2.3 Colloids versus depth 294
2.4 Colloids versus chloride 294
2.6 Composition of the colloids 295
2.7 Conclusion 297

3 References 299

Appendix 1 The microbial data available from the regional Simpevarp area 301

1 Microbiology and microbial model

1.1 Introduction

Microorganisms are abundant in Fennoscandian Shield ground water from surface down to at least 1,500 m /Pedersen 1993, Haveman et al. 1999/. To understand the present undisturbed hydro-biogeochemical conditions at a site the following parameters are of interest: pH, E_h, S^{2-}, S^0, SO_4^{2-}, HCO_3^-, HPO_4^{2-}, nitrogen species and TDS together with colloids, fulvic and humic acids, dissolved organic compounds and microorganisms. In addition, the concentrations of dissolved gasses are of importance to explore for a complete model since many microorganisms consume and/or produce different gasses. Further, for a full understanding it is necessary to be able to predict how changing conditions during the construction of a repository and during the following phases of the repository will influence microbes in the ground water and vice versa.

Microbial parameters of interest are the total number and the presence of different metabolic groups of microorganisms /Pedersen 2001/. These data will indicate activity of specific microbial populations at a certain site and how they interact with the geochemistry. The groups cultured for in the microbial part of the site investigation were iron-reducing bacteria (IRB), manganese-reducing bacteria (MRB), sulphate-reducing bacteria (SRB), auto- and heterotrophic methanogens and auto- and heterotrophic acetogens.

'Most probable number of microorganisms' (MPN), is a statistical cultivation method for numbering the most probable number of different cultivable metabolic groups of microorganisms /Anonymous 1992/.

This part of the report will deal with the microbial data available so far from the site investigation in the Laxemar subarea but also in the regional Simpevarp area.

1.2 The subsurface microbial model

Investigations of the microorganisms in ground water in the Fennoscandian Shield have been ongoing since the middle of the 80th /Pedersen 2002/. Comparisons of compiled data from the different sites investigated have made it possible to create a conceptual model of the biogeochemical system consisting of surface and subsurface ground water in the Fennoscandian Shield (Figure 1-1).

The model includes 5 different biospheres or zones and one abiotic chemosphere in a layered structure. The depths where the described biospheres can be found may differ between sites. All groups of microorganisms will not be present at all sites. This is because the geochemical environment may be such that one or several groups cannot be active there. The presence of iron-reducing bacteria can be used as an example. This group depends on the presence of bio-available ferric iron compounds. If there are no such compounds, the iron-reducers will be absent. Despite of this, the relative positions of the different zones and microbial groups will always be the same. Below follows a description of the zones in the biogeochemical subsurface system:

1.2.1 The surface biosphere

The surface biosphere is where plants, animals, microbes and man interact. With energy from the sun photosynthetic organisms convert carbon dioxide to organic material. In this process oxygen is produced. The organic material is used in biosynthesis and transformed to heat and kinetic energy by organisms in their heterotrophic metabolism.

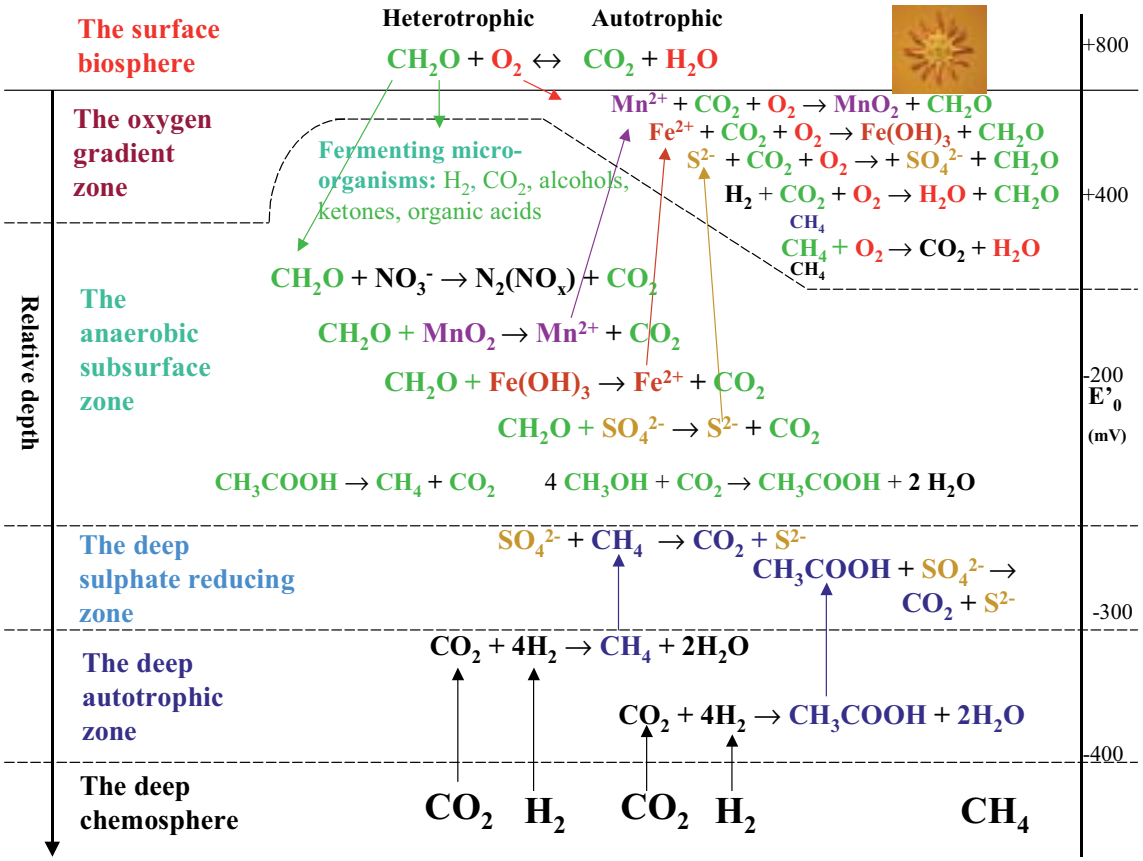

Figure 1-1. *Conceptual model for microbial processes in Fennoscandian Shield groundwater.*

1.2.2 The oxygen gradient zone

The most common organisms in this zone oxidise organic carbon with oxygen reduction. There are also microbes that utilize reduced inorganic compounds such as hydrogen gas, ferrous iron, manganese (II), and sulphide as energy and electron donors. The reduced species are produced in the underlying anaerobic subsurface zone, see section 1.2.3. The electron acceptor in the metabolisms of these organisms is mostly oxygen but anaerobic electron acceptors have been identified i.e. nitrate /Straub et al. 1996/. The organisms are often autotrophic and use carbon dioxide as carbon source. The organisms are gradient organisms and live in environments not fully oxygen saturated. This is because they compete with the chemical oxidation of the reduced species but also because they are to some extent sensitive to high oxygen concentrations since they lack enzyme systems that deactivate toxic oxygen species.

In this zone also methane-oxidizing bacteria live, the so-called methylotrophs. This group oxidise methane with oxygen and gain energy from the oxidation.

1.2.3 The anaerobic subsurface zone

In the anaerobic subsurface zone three groups of anaerobic microorganisms live, the fermenting microorganisms, the anaerobic respiring microorganisms and methane and acetate-producing microorganisms.

1.2.3.1 Fermenting microorganism

This group does not use an external electron acceptor in their metabolism. Instead they split organic molecules into two or more compounds of which one will become more oxidised and one becomes more reduced than the metabolised compound. As example the common organism “Baker’s yeast” can be used. This yeast ferment glucose to ethanol and carbon dioxide.

Fermenting organisms are found mostly in environments with high input of organic material but low concentrations of compounds that can serve as anaerobic electron acceptors. Typical examples of such environments are composts and bogs. The products from fermentations are short fatty acids such as butyric acid, acetic acid, lactic acid, alcohols, ketones, aldehydes and the gasses carbon dioxide and hydrogen.

1.2.3.2 Anaerobic respiring microorganisms

This group of microorganisms use oxidized inorganic compounds as electron acceptors in the same manner as aerobic organisms use oxygen gas. Anaerobic respiring organisms most commonly found in granitic groundwater are nitrate-, iron-, manganese- and sulphate reducing microorganisms. The reduced electron acceptors are nitrogen gas or other reduced nitrous gasses, ferrous iron, manganese (II) and hydrogen sulphide. Their energy and carbon sources are often sugars and organic acids. The succession of organisms in this zone depends on the energy they gain from the different redox reactions.

The reduced electron acceptors from this zone, are the ones that are used by the organisms in the oxygen gradient zone, see 1.2.2.

1.2.3.3 Methanogens and acetogens

In the most reduced niches in the *Anaerobic subsurface* zone methanogens and acetogens live. The methanogens are microorganisms that belong to the domain *Archaea.* In their metabolism they produce methane from either C1-compounds or acetate, so-called heterotrophic methanogens (HA) or from hydrogen gas and carbon dioxide, so-called autotrophic methanogen (AM). In connection with the *Anaerobic subsurface zone*, mostly heterotrophic methanogens flourish.

Acetogens, on the other hand, are acetate-producing microorganisms that belong to the domain *Bacteria*. Also among the acetogens there are heterotrophs and autotrophs. The heterotrophic acetogens (HA) produce acetate from C1-compounds and the autotrophic acetogens use hydrogen gas and carbon dioxide to produce acetate. Most of the acetogens present in the *Anaerobic subsurface zone* seem to be facultative autotrophic and can use both inorganic and organic carbon sources.

The acetogens and methanogens in the *Anaerobic subsurface zone* are the organisms at the end of the degradation chain of the organic carbon coming from photosynthetically fixed carbon dioxide.

1.2.4 The deep sulphate-reducing zone

In this zone sulphate-reducers thrive but the carbon and energy sources they utilise do not originate from photosynthesis on the ground surface. The sources of organic carbon are instead acetate and methane produced in the deep autotrophic zone, see 1.2.5, with hydrogen gas produced deeper down in the chemosphere, see 1.2.6. So far anaerobic sulphate reduction with sulphate has only been reported from measurements in situ. This process is probably a two-step reaction with both methane oxidizing *Archaea* and hydrogen oxidizing sulphate reducers involved /Valentine 2002/.

1.2.5 The deep autotrophic zone

The methanogens and acetogens in this zone utilise hydrogen gas as energy source originating from inorganic hydrogen producing processes /Apps and van de Kamp 1993/ further down in the subsurface. They produce methane and acetate that will be used in *The deep sulphate-reducing zone*. Some methane diffuses up to shallower depth and will be oxidised by methylotrophic microorganism in *The oxygen gradient zone*, 1.2.2. Acetate is one of the most central metabolites in all metabolisms know and will be consumed more or less instantly.

1.2.6 The deep chemosphere

The deep chemosphere starts where the condition in the environment no longer is suitable for life. It is probably the high temperature that set the limit for life. The highest of temperatures in which microorganisms can live, as we know today, is 113°C /Stetter 1996/.

1.3 Data available

At the time for the data freeze for the Laxemar model version 1.2, 30 November 2004, no new microbial data were available. In this report data from the data file compiled by Maria Gimeno, U. of Zaragosa, together with microbial data from the sites earlier reported in SKB Reports and scientific papers are used. Information of available data is compiled in Table 1-1. In addition to the microbial data, chemical information from the boreholes in the Laxemar subarea but also the regional Simpevarp is investigated.

Table 1-1. Compilation of the available microbial and geochemical data from the Laxemar and Simpevarp subareas.

Bore hole	Depth	Total no of microorganisms	Groups determined by MPN	Chemistry data	Reference
KSH01A	161.75	yes	IRB, MRB, SRB	yes	SICADA /Wacker et al. 2004/
	253.25	yes	IRB, MRB, SRB, HM, AM, HA	yes	SICADA /Wacker et al. 2004/
	556.5	yes	IRB, MRB, SRB, HM, AM, HA, AA	yes	SICADA /Wacker et al. 2004/
KLX01	274.5	yes	n.d.	yes	SICADA /Pedersen and Ekendahl 1990/
	466	yes	n.d.	yes	SICADA /Pedersen and Ekendahl 1990/
	691.06	yes	SRB	yes	SICADA /Pedersen and Ekendahl 1990/
	835.5	yes	n.d.	yes	SICADA /Pedersen and Ekendahl 1992/
	915.5	yes	n.d.	yes	“
	1038.5	yes	n.d.	yes	“
KLX02	1160.0	yes	JRB, SRB, HA, AA	yes	SICADA /Mäntynen 2000/
	1350	yes	JRB, SRB, HA, AA	yes	SICADA SKB report
	1388.5	yes	JRB, SRB, HA, AA	no	report Posiva
KAV01	420	Yes	n.d.	Yes	SICADA
	522	Yes	n.d.	Yes	SICADA
	558	yes	n.d.	Yes	SICADA
	635	yes	n.d.	yes	SICADA
KAS02	208.5	yes	n.d	yes	SICADA
	316.5	yes	n.d.	yes	SICADA
	326.0	no	n.d.	yes	SICADA
	465.5	yes	n.d.	yes	SICADA
	532.5	no	n.d.	yes	SICADA
	863.02	no	n.d.	yes	SICADA
	892.02	no	n.d.	yes	SICADA
KAS03	131.5	yes	n.d.	yes	SICADA
	249.5	No	n.d.	yes	SICADA
	466.5	No	n.d.	yes	SICADA
	616.0	No	n.d.	yes	SICADA
	846.0	Yes	n.d.	yes	SICADA
	931.03	no	n.d.	yes	SICADA
KAS04	230.5	yes	SRB	yes	SICADA
	338.5	yes	n.d.	yes	SICADA
	460.49	yes	SRB	yes	SICADA

n.d. not determined

1.4 Evaluation of the microbial and chemical data

1.4.1 Total number of microorganisms and organic carbon, total (TOC) or dissolved (DOC)

There is a positive correlation between total numbers of microorganisms and the amount of carbon in the subsurface system. Figure 1-2 shows the total number of microorganisms and TOC or DOC values in ground water at different depth in boreholes in the Laxemar subarea. An interesting finding is that the total number of microorganism and organic carbon decrease down to a depth of about 800 m. Further down the number of microorganisms starts to increase. The TOC and DOC also follow this trend. The organic carbon values for borehole KLX02 at the depths of 1,160 m and especially 1,350 m are very high with 10 and 98 mg l^{-1}, respectively. We need more data from these depths to be able to evaluate the correctness in these measurements. One plausible explanation for the increased cell numbers is the increase in temperature at such depth. Higher temperature will enhance the number of microorganisms by increased growth rate. In Figure 1-3 data from the Simpevarp regional area are compiled and the data from the other subareas show the same trend as the local data for Laxemar.

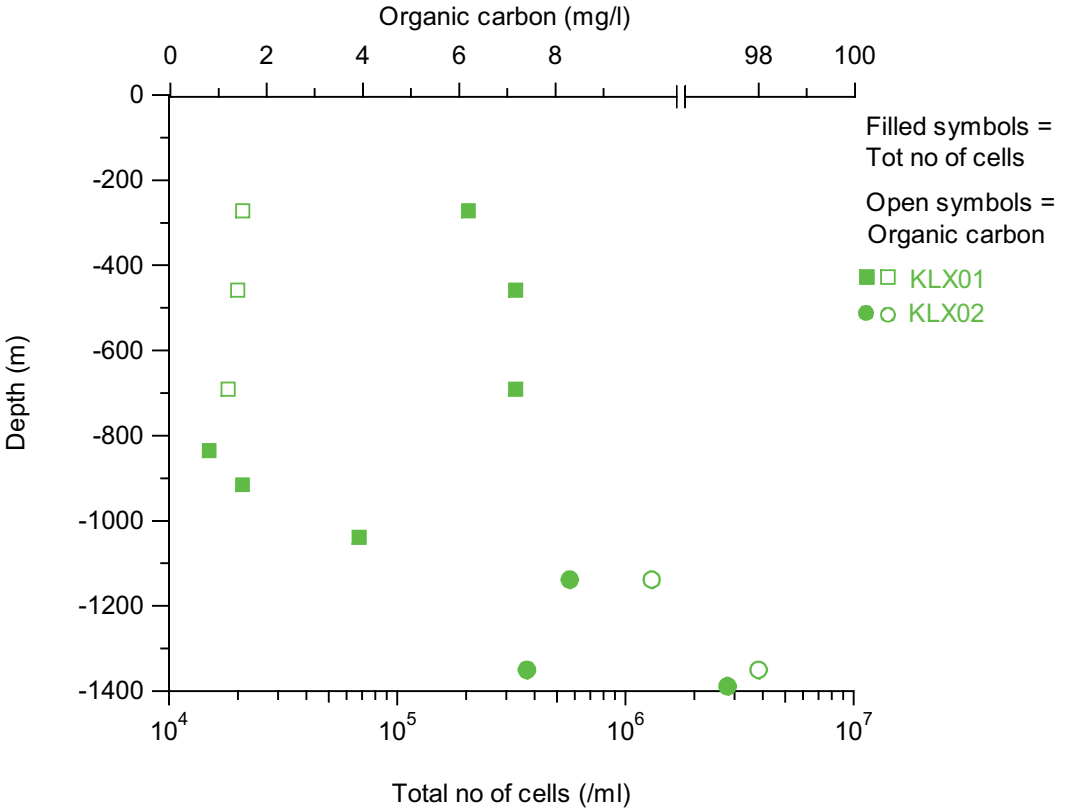

Figure 1-2. *Total number of microorganisms and organic carbon vs. depth in the Laxemar subarea.*

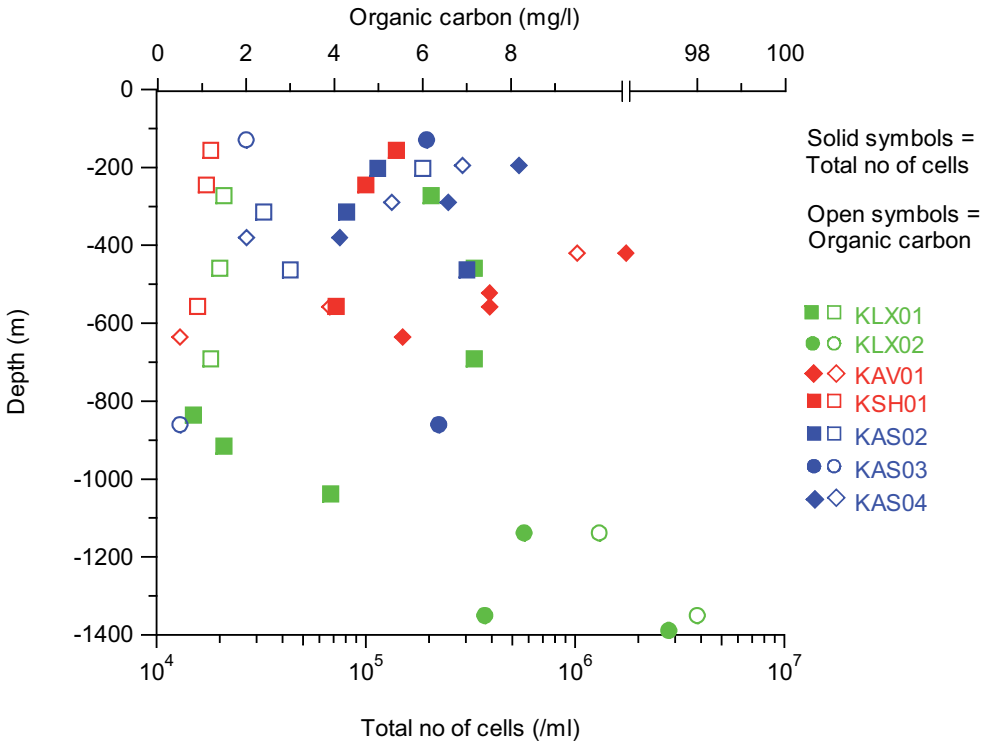

Figure1-3. *Total number of microorganisms and organic carbon vs. depth in the regional Simpevarp area.*

1.4.2 Fractionation filtration for humic and fulvic acids

To understand the size distribution the organic material in ground water, fractionation filtrations were done with ground water from the sections 161.8 m and 556.5 m in borehole KSH01A. Defined cut off filters (pore size), 1,000 D and 5,000 D, were used, see also 2.6. This filtration showed that the main part of the organic material was smaller than 1,000 D but some also was larger than 5,000 D. In the fraction > 1,000 D but < 5,000 D no organic material was found. The results are compiled in Table 1-2. In this table also the DOC value from the ordinary analyses are included.

Table 1-2. Organic material in ground water in borehole KSH01A, Simpevarp subarea.

Fraction DOC (mg l–1)	KSH01A 161,8 m	KSH01A 556.5 m
< 1,000 D	1.0 ± 0.1	1.0 ± 0.1
> 1,000 D but < 5,000 D	n.d.	n.d.
DOC > 5,000 D	0.06 ± 0.04	0.04 ± 0.03
DOC (in SICADA)	0.9–1.5	< 1–1.1

1.4.3 The isotopic composition of organic carbon and carbon-14 dating

The isotopic composition and carbon-14 dating of the organic material in ground water from section 253.3 in borehole KSH01A was done. The analysis showed that the $\delta^{13}C$ (dev PDB) was –27.0. The pmC dating gave an age of 85.2 years.

1.5 Redox potential in groundwater

Measurement of the redox potential in ground water gives an understanding if the ground water chemistry system has a reducing or oxidising capacity. Further, all by microorganisms catalysed metabolic reactions are oxidation-reduction reactions and by that influence the measured redox potential in the system, see discussion about the microbial model, see 1.11.

The available redox data for ground water in the Laxemar subarea are plotted versus depth in Figure 1-4. In this figure all data available in the data file extracted from SICADA are used. As can be seen, some data in the depth region from 800 to 1,100 m, group together with redox values around –150 mV. These values are probably to high and in Figure 1-5 these values were removed. By that redox values describe a decreasing trend with depths. In Figure 1-6, data from Äspö and Ävrö subareas are included in the scatter plot. These data strengthen the decreasing trend.

To understand this system there is also a need for measurements done in the surface water – subsurface water interface, which is in depths of 0–200 m. This will give an understanding how input of organic matter and oxygen from the surface system affect the redox buffer capacity of the microbial ground water ecosystem.

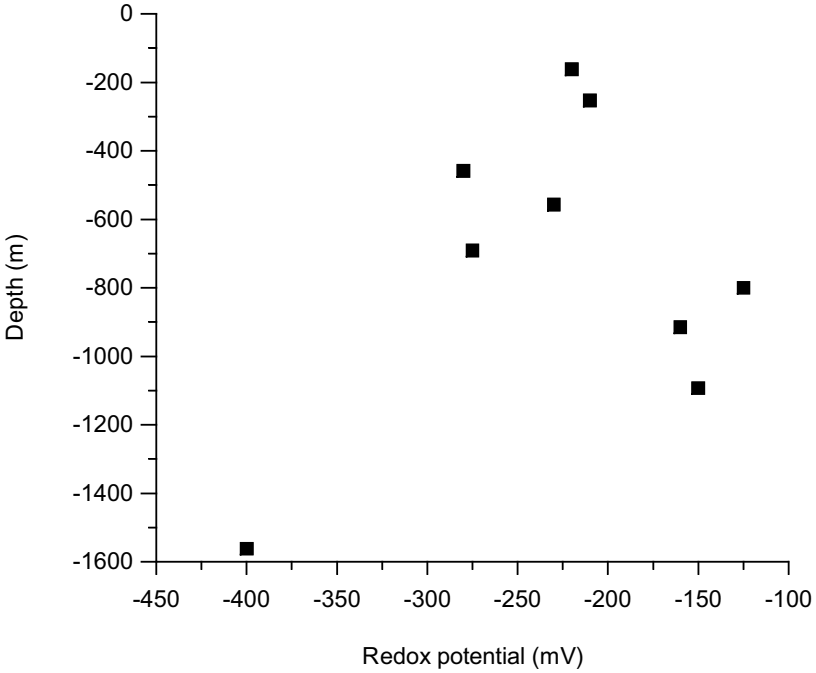

Figure 1-4. *Redox values measure in ground water from the Laxemar subarea. All data available in SICADA are included.*

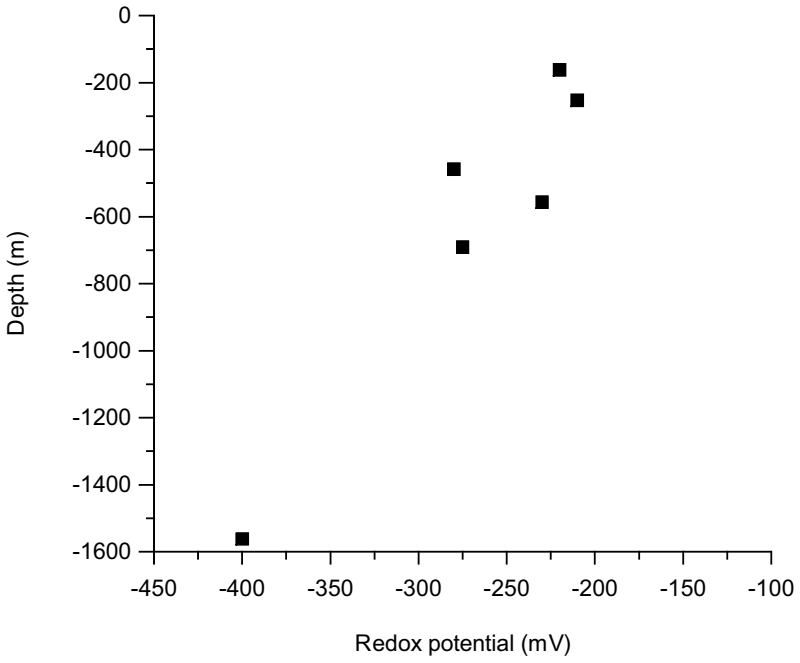

Figure 1-5. *Redox values measure in ground water from the Laxemar subarea. Some data regarded as wrong were excluded. Compare Figure 1-4.*

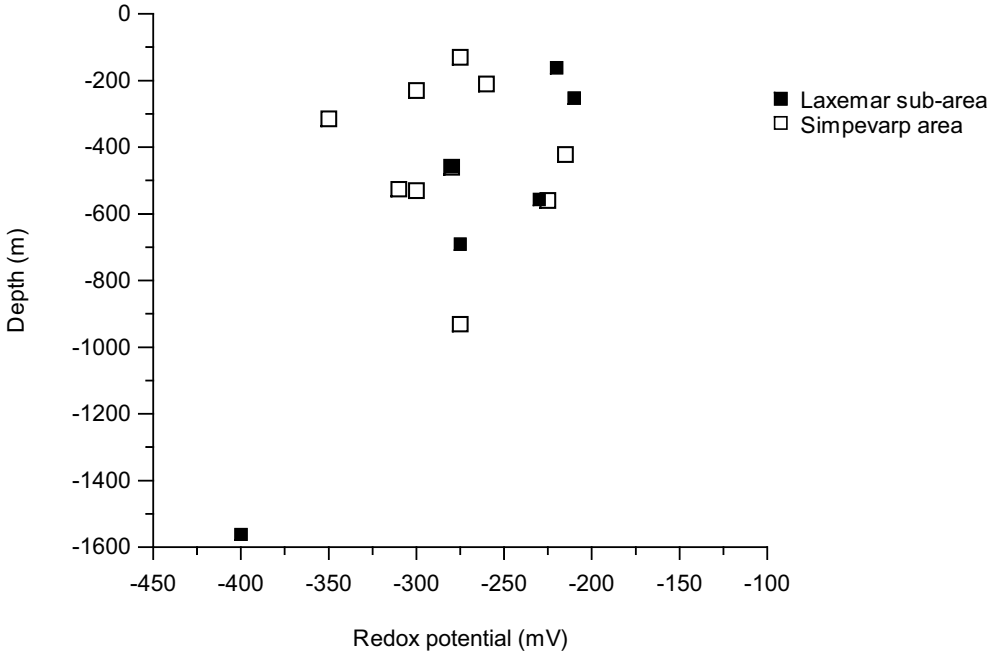

Figure 1-6. *Redox values available in SICADA from the regional Simpevarp area. Some data regarded as wrong were excluded. Compare Figure 1-4 and 1-5.*

1.6 Manganese-reducing bacteria and manganese

Manganese in solution is in the manganese (II) state. Due to the insolubility of MnO2, that form of manganese (IV) will be solid in natural water within pH range 5–8. Figure 1-7 shows the amount of manganese (II) in ground water in the regional Simpevarp area. The data show that it is in borehole KAV01, between 400 and 600 m, at Ävrö that had manganese amounts higher than 1.5 mg l^{-1}. Amounts around 1 mg l^{-1} were found at depth from 100 m down to 600 m with the highest amounts in the Äspö subarea.

High manganese (II) values can be a result of manganese reducing bacteria oxidizing organic matter in an anaerobic environment. MPN values of manganese-reducing bacteria in three sections in the borehole KSH01A showed trace amounts or no such organisms. The relative high manganese values in KAV01 can be a result of manganese-reduction.

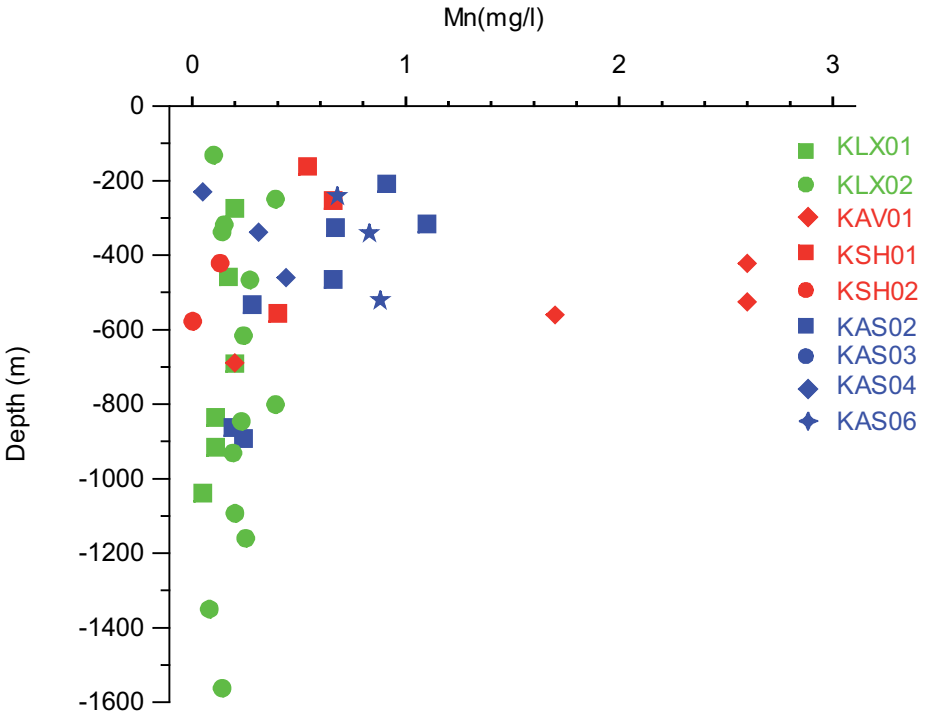

Figure 1-7. *Amounts of manganese plotted versus depth in ground water in the regional Simpevarp area. The Laxemar subarea is represented by boreholes KLX01 and KLX02.*

1.7 Ferrous iron and iron-reducing bacteria

In Figure 1-8 it can be seen that the highest amounts of ferrous iron were found in borehole KAV01, at the depths 422,5 m, 526,5 m and 560,5 m. These three depths coincide with where the highest manganese values were found, see section 1.6. This is in agreement with a common observation of concomitant high amounts of iron and manganese. In borehole KLX02 the ferrous iron amounts were high at relative deep depths with 1 to 1.5 mg l^{-1}.

The only MPN data for iron-reducing bacteria that are available are from KSH01A, where only trace amounts of them were found and from 1,160 m depth in KLX02. In this section 3.3 × 102 iron reducers were found. This is in agreement with the amount of ferrous iron found at the same depth.

1.8 Sulphate-reducing bacteria, sulphate and sulphide

The sulphate amounts increase with depth as can be seen in Figure 1-9 with a maximum of 1,000 mg l^{-1} in the deepest ground water sampled in KLX02. There is a different trend in KLX02, which gives an exponential decreasing trend for some of the deeper samples.

In Figure 1-10 the sulphide values can be coupled to MPN number for SRB at three depths. The highest MPN number, 5.6 × 104 ml^{-1} was found in KLX01 at 680 m. In this section also the highest amount of sulphide was found with 2.5 mg l^{-1}. The second highest sulphide value, 1.5 mg l^{-1} in KAS04 at 195 m, has a corresponding MPN value of 1,600 SRB per ml. At 380 m in KAS04 the sulphide value was below 0.5 mg l^{-1} and less than 100 SRB per ml.

In a more or less closed system with high sulphate-reducing activity a decrease in sulphate should be seen. In ground water systems with high amounts of and a supply of sulphate by the inflow of ground water such decrease will less pronounced.

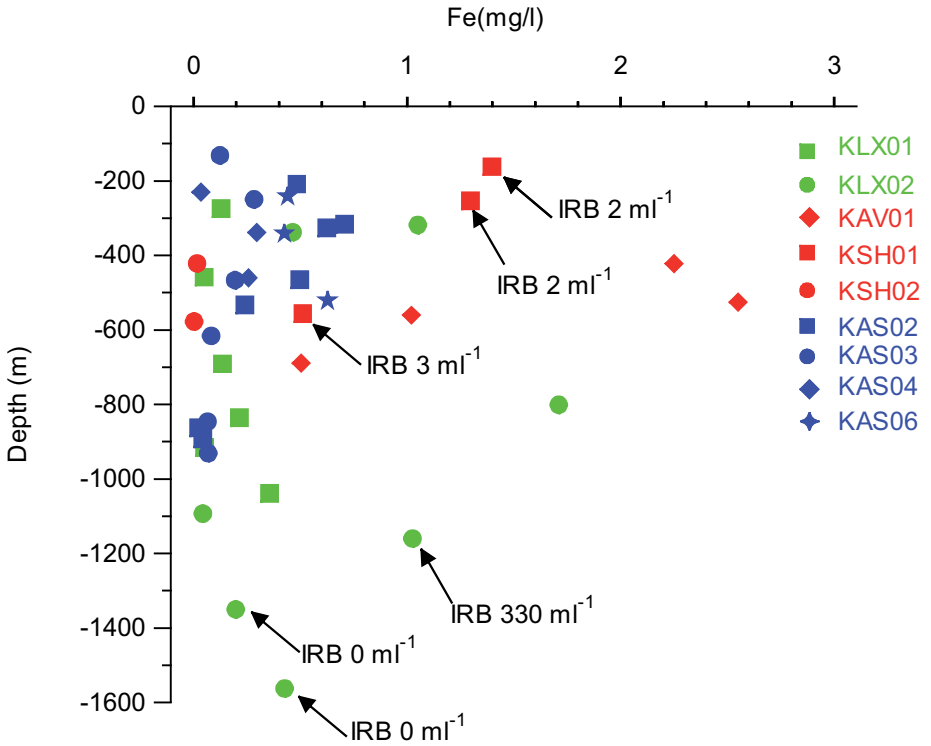

Figure 1-8. *Amounts of ferrous iron versus depth in the regional Simpevarp area. The local subarea of Laxemar is represented by boreholes KLX01 and KLX02.*

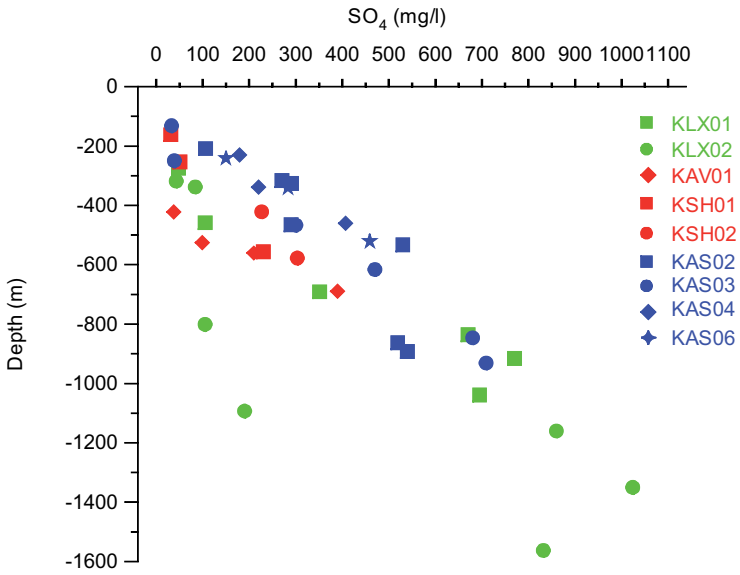

Figure 1-9. *The amount of sulphate versus depth in the regional Simpevarp area. The local subarea Laxemar is represented by the boreholes KLX01 and KLX02.*

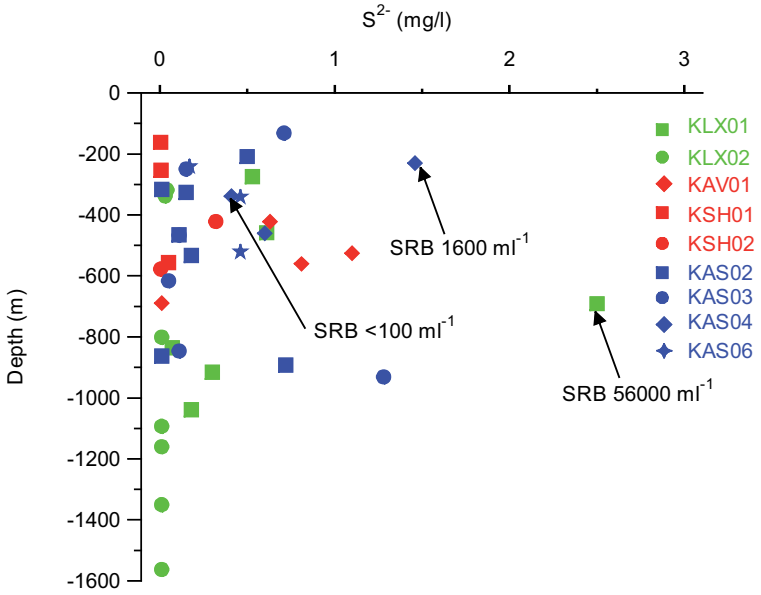

Figure 1-10. *The amount of sulphide versus depth in the regional Simpevarp area. The local subarea Laxemar is represented by the boreholes KLX01 and KLX02. The arrows show the MPN numbers for sulphate-reducing bacteria.*

1.9 Methanogens

Figure 1-11 shows the methane concentration versus depth in the regional Simpevarp area. The Laxemar subarea is represented by measurements in borehole KLX01. There is still no MPN data for methanogens from boreholes in this area. Data for heterotrophic methanogens are available from 3 depths in the borehole KSH01A. They were available and treated also in the Simpevarp 1.2 report. Conclusions drawn from Figure 1-11 are that the methane concentrations are highest at depths between 250 m down to 700 m. Still, no high MPN numbers of methanogens has been found neither in the Laxemar subarea nor in the regional Simpevarp area. However, methanogens have been found in high numbers in boreholes along the Äspö tunnel /Kotelnikova and Pedersen 1998/ and in the boreholes at the Microbe site in the tunnel /Pedersen 2005/.

1.10 Acetogens

The highest amount of acetogens found so far in the Simpevarp area is 900 per ml in borehole KSH01A at 253.5 m depth. Also at 1,160 m depth in KLX02 numbers of 100–200 acetogens per ml were found. At the other depths there were only traces of acetogens. The heterotrophic acetogens produce acetate from C1-compounds. Heterotrophic acetogens have been found at shallower depths than autotrophic acetogens but the autotrophs might be facultative autotrophs and by that be able to use both carbon dioxide and organic carbon /Kotelnikova and Pedersen 1998, Haveman and Pedersen 2002/. So far, there are no acetate data available; however, acetate would be an important parameter to measure in the future.

1.11 The microbial model

In this section the available microbiology and chemistry data will be merged in the microbial model for the regional Simpevarp area.

1.11.1 Classification of most probable number (MPN) numbers into *-signs to be used in “The microbial subsurface model”

A classification has been done in order to rank the measured MPN values in relation to their relative influence on the geochemical situation in the analysed groundwater (Table 1-3).

Table 1-3. Classification and interpretation of measured MPN values in ground water.

Measured number	Classification	Interpretation
Below detection limit	–	Not present
1–10	(*)	Present without influence[1]
11–50	*	Present with putative influence[1] if growth promoting changes occur
51–1,000	**	Present with influence[1]
> 1,000	***	Dominating with high influence[1]

[1] Influence here means that the organism group has an effect on the geochemistry of the ground water.

Recall that sampling of ground water from one section isolated with packers always include all ground water surrounding the section that is extracted by pumping from the aquifers. Because of this, two or more microorganisms groups can look abundant in one section but their habitats could be separate due to different fractures under natural circumstances.

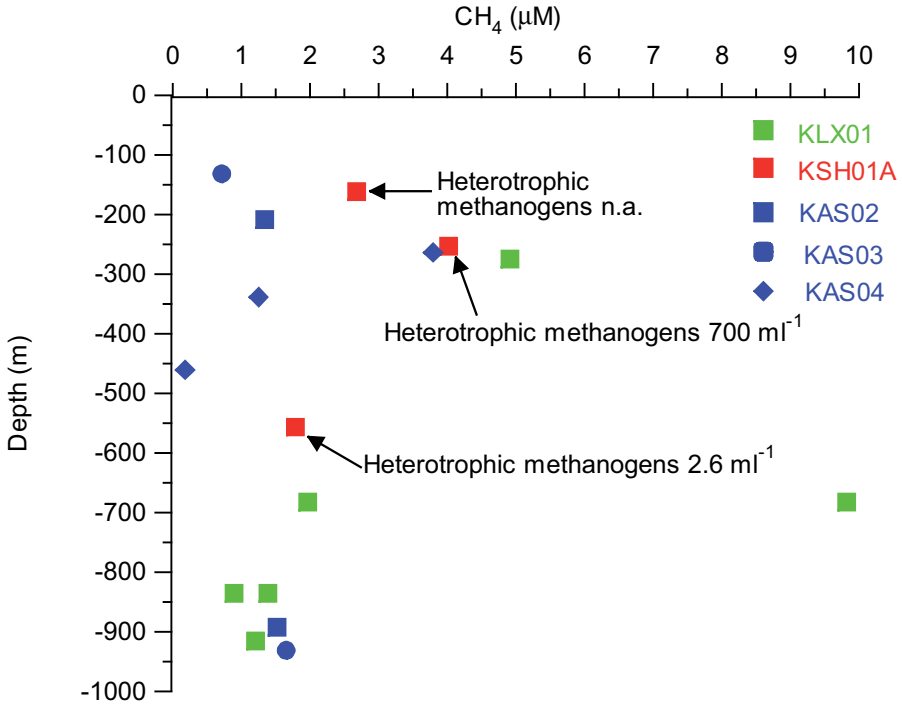

Figure 1-11. *Methane concentration versus depths in boreholes in the regional Simpevarp area. Most probable numbers of microorganisms (MPN) for heterotrophic methanogens in the borehole KSH01A are depicted in the figure.*

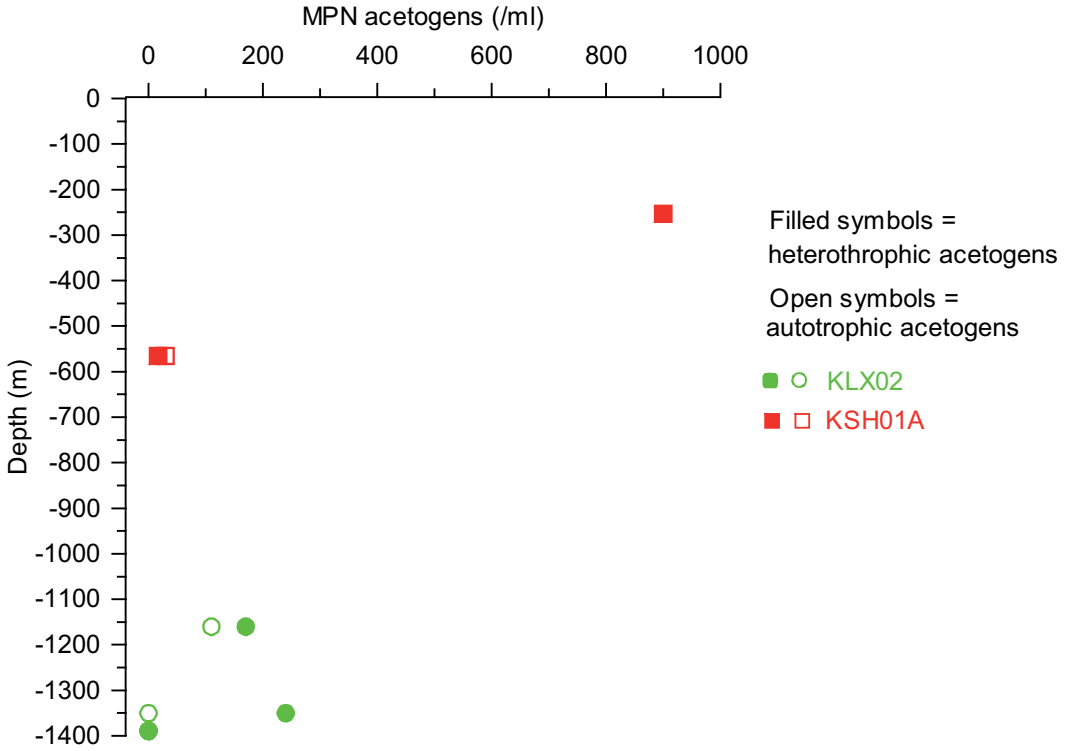

Figure 1-12. *Most probable numbers of cells (MPN) for auto- and heterotrophic acetogens versus depths in two boreholes in the Simpevarp area.*

The MPN measurements used in this report have been performed the last 14 years. During this time span, the analyse sensitivity have been increased especially during the last three years. Because of this some of the older data can be misleading. For positive results this means that the physiological group is present but the actual number could have been higher. Negative results should not be seen as absolute because the actual detection limit may have been much higher compared to the results obtained during the site investigations. The next data freeze will include new microbial data and they generally are equal to, or higher than older results.

1.11.2 Characterisation of the influence by different metabolic groups of microorganisms

Different microbial groups will influence the surrounding environment in specific ways depending on the metabolic group that is dominating. In Table 1-4, these activities are listed together with possible effects on the surroundings.

Table 1-4. Activity and effects of the different physiological groups of microorganisms found in deep ground water.

Metabolic groups of microorganisms	Activity	Effect
Aerobic respiration	Oxidation of organic material with oxygen reduction.	Depletion of oxygen and organic material. Increase in alkalinity. Lowering the redox potential.
Anaerobic respiration	Oxidation of organic material with reduction of compounds other than oxygen.	
Iron reducing bacteria	Oxidation of organic material with ferric iron reduction.	Depletion of organic material and ferric iron. Increase in ferrous iron and alkalinity. Lowering the redox potential.
Manganese reducing bacteria	Oxidation of organic material with manganese(IV) ion reduction.	Depletion of organic matter and manganese (IV) ions. Increase of manganese (II) ions and alkalinity. Lowering the redox potential.
Sulphate reducing bacteria	Oxidation of organic material with sulphate reduction.	Depletion of organic matter and sulphate. Increase of sulphide and in alkalinity. Lowering the redox potential.
Methanogens		
Heterotrophic methanogens	Convert organic material to methane and carbon dioxide.	Decrease of organic material. Increase of methane gas and carbon dioxide (alkalinity). Redox not influenced.
Autotrophic methanogens	Oxidation of hydrogen gas and reduction of carbon dioxide to methane gas.	Depletion of hydrogen gas and alkalinity. Increase of methane. Redox lowered.
Acetogens		
Heterotrophic acetogens	Convert organic material to acetate	Decrease of organic material other than acetate. Increase in the concentration of acetate. Redox not influenced.
Autotrophic acetogens	Oxidation of hydrogen gas with reduction of carbon dioxide to acetate.	Depletion of hydrogen gas and alkalinity. Increase of acetate. Redox lowered.

1.11.3 The microbial model in the Simpevarp regional area

Since there is rather few data microbial data from the local Laxemar area the microbial model will be presented in regional scale only.

The colours in the model are used as listed below:

- light grey: The process is not yet studied.
- dark grey: The process is present but without influence.
- green: The carbon compounds originates from the surface biosphere.
- blue: The carbon compounds originate from the deep autotrophic zone.
- black: Compounds from the deep chemosphere.
- turquoise: Processes found but not anticipated and not yet confirmed.

The model shows, so far, that the dominating microbial process in The anaerobic subsurface zone is heterotrophic sulphate reduction. This zone is found at depths from 100 to 500 m. The deep sulphate reducing zone is found at about 600 to 900 m. In the depth region 1,000 to 1,400 m The deep autotrophic zone is found. Here we also have indications that there are iron reduction and

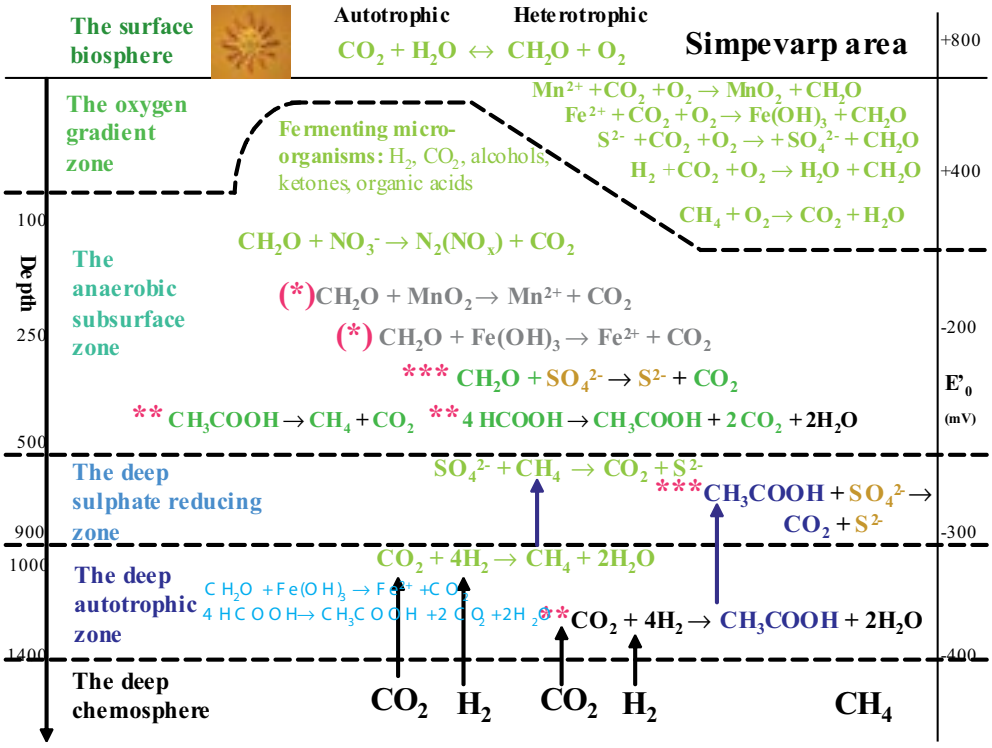

Figure 1-13. *The microbial model of the regional Simpevarp area based on data available at the time for data freeze Laxemar 1.2. The star signs before the reactions depict the significance of the reaction according to the classification in Table 1-2, see 1.11.1.*

heterotrophic acetogenesis ongoing but this must be verified by thorough MPN studies. The origin of carbon dioxide and hydrogen gas in this zone from The deep chemosphere need also to be verified with stable isotope studies of the gas in the ground water.

1.12 Significance of attached microorganisms in the subsurface model

In all aquatic systems where microorganisms are present cells will attach to surfaces, in a so-called biofilm. Also in the subsurface environment such biofilms will be formed. The presence of attached microorganisms on fracture surfaces in the subsurface environment is of course of great importance. To be able to calculate the capacity of the microbial community to cope with changes in the ground water system the attached cells must be included.

/Pedersen and Ekendahl 1992/ compared the amount of attached microorganisms with the amount of free-living microorganisms in groundwater in the borehole KLX01 in the Laxemar subarea. This was done by introduction of glass surfaces into flowing ground water during 19 days. They found that 0.94×10^5 to 1.2×10^5 cells cm^{-2}, were attached to the glass surfaces. The amounts of free-living cells in the groundwater were 0.15×10^5 to 0.68×10^5 ml^{-1}. Studies of the assimilation of different nutrients showed that the microorganisms were alive both in the biofilm and in the water phase. Generally, the attached microbes were significantly more active than the unattached microbes.

Scoping calculations of the number of attached cells that should be added to the unattached cells to give a correct number of cells present in the groundwater system i.e. water and surfaces are found in Table 1-5. The calculations are made with a fracture that is one m2 having a width of 1 mm. The volume of water in the fracture is then 1×10^{-3} m^3. The total surface area is 2×1 $m^2 = 2$ m^2.

Table 1-5. Number of unattached and attached microorganisms in ground water from the borehole KLX01. Calculation of the surface to volume ratio of microorganisms.

Borehole	Depth (m)	Unattached cells × 10^{10} (m^{-3})	Unattached cells in the water volume in the fracture × 10^7	Attached cells × 10^{10} (m^{-2})	Attached cells to the fracture surfaces × 10^9	Surface to volume ratio
KLX01	836	1.5	1.5	0.09	1.88	125
KLX01	915.5	2.1	2.1	1.1	2.4	114
KLX01	1,038.5	6.8	6.8	1.5	2	29

These calculations show that the number of unattached microorganisms (AODC) in a fracture should be multiplied with about 100 to get a correct value of the total amount of microbes present in the model fracture.

There are no studies done on the distribution of the different metabolic groups in biofilm population from ground water. Therefore it is assumed, until more data are available, that the distribution is the same as in the free-living phase.

1.13 Metabolic rates in the subsurface model

To be able to calculate rates and estimation of time scales for the microbial processes in the ground water environment knowledge of metabolic rates for the different metabolic groups are needed. So far very few studies have been done on this issue. One study was done by /Pedersen and Ekendahl 1992/ in which they measured lactate consumption by microorganisms in anaerobic cultures with microorganisms from the borehole KLX01 at three depths, 836.0 m, 915.5 m, and 1,038,5 m. These experiments were done under optimal conditions at 20°C and the rates measured are probably much higher than under natural conditions. If it is assumed that all lactate consumed was oxidised by sulphate reduction the following reaction took place (Equation 1):

$$2CH_3CHOHCOO^- + 3SO_4^{2-} \rightarrow 6HCO_3^- + {}^3HS^- + H^+ \qquad \text{(Equation 1)}$$

In Table 1-6 and 1-7 the rates of lactate consumption and sulphide production at the different depths are presented. The experiments were done both with ground water, unattached microorganisms and with glass surfaces with biofilms of attached microorganisms.

As can be seen in Table 1-6 the production of hydrogen sulphide increased with depth and the maximum production was very high with almost 4 mg HS^{-1} m^{-3} day^{-1}.

If these values of rate are used in the theoretical fracture from section 1.12 the following amounts of sulphide will be produced per day at the different depths, see Table 1-8.

Table 1-6. Rates of lactate uptake and hydrogen sulphide production in in vitro experiments with unattached microorganisms from borehole KLX01 in Laxemar subarea.

Depth (m)	µmol lactate m^{-3} day^{-1}	µmol HS m^{-3} day^{-1}	µg HS m^{-3} day^{-1}
836	5.6	8.4	278
915.5	17	25.5	844.25
1,038.5	76	114	3,774.3

Table 1-7. Rates of lactate uptake and hydrogen sulphide production in in vitro experiments with attached microorganisms from borehole KLX01 in Laxemar subarea.

Depth (m)	µmol lactate m^{-2} day^{-1}	µmol HS m^{-2} day^{-1}	µg HS m^{-2} day^{-1}
836	2.6	3.9	129
915.5	6.0	9.0	297
1,038.5	0.14	0.21	6.9

Table 1-8. Calculated amounts of hydrogen sulphide produced in a theoretical fracture with an area of 1 m^2 and a width of 1 mm under optimal conditions. The microorganisms are from KLX01 in Laxemar subarea.

Depth (m)	Attached microorganisms (µg day^{-1})	Unattached microorganisms (µg day^{-1})
836	258	0.278
915.5	294	0.844
1,038.5	13.8	3.77

The calculations above once again show the importance of the attached microorganisms in the subsurface system.

1.14 Conclusions

From the data used in this report the following conclusions can be drawn:

- In the regional Simpevarp area three of the proposed zones in the subsurface microbial model has been identified: the anaerobic subsurface zone at least from 100 to 500 m, the deep sulphate reducing zone between 600 and 900 m and the deep autotrophic zone from 1,000 m to at least 1,400 m. The depths have to be seen as preliminary.
- In the anaerobic subsurface zone sulphate reducing bacteria, heterotrophic methanogens and heterotrophic acetogens are the dominating microorganisms.
- In the deep sulphate reducing zone acetate oxidation has been observed but no methane oxidation.
- In the deep autotrophic zone autotrophic acetogens have been observed.
- The very few available data on attached microorganisms and production of hydrogen sulphide under optimal conditions indicate that the attached microorganisms in a 1 mm wide fracture produce up to 1,000 times more hydrogen sulphide per day than unattached microorganisms do.

2 Colloids

2.1 Introduction

Particles in the size range 10^{-3} to 10^{-6} mm are regarded as colloids. Their small size prohibits them to settle which render them a potential to transport radionuclides in groundwater. The aim of the study of colloids in the site investigation of Laxemar 1.2, was to quantify and determine the composition of colloids in groundwater from boreholes. The results will be included in the modelling of the hydrochemistry at the site.

In the hydrogeochemical model report Simpevarp 1.2 /Laaksoharju 2004/ colloid data from one borehole in the Simpevarp subarea, KAV01 at Ävrö and one from the Laxemar subarea KLX01 were analysed. These data were from 1987–1989. In this report a new set of data is included. These are from borehole KSH01A in the Simpevarp subarea and 3 sections in this borehole were sampled, 161.75 m, 253.3 m and 556.5 m. The samplings were made the 23 April, 2003, 19 May, 2003 and 15 September, 2003, respectively.

2.2 Methods

The method used was filtering the groundwater through a series of connected filters in a closed system under the pressure of argon. The filters had 0.2 and 0.05 µm pore size. Before the filters a pre-filter with a pore-size of 0.4 µm was placed. The mineral composition of the colloids on the filters was determined with ICP and the quantities of the analysed elements were recalculated in µg l^{-1} (ppb) considering the water flow (ml h^{-1}) registered through the filters. The elements analysed were calcium (Ca), iron (Fe), sulphur (S), manganese (Mn), aluminium (Al) and silicon (Si). Also the precipitations on the pre-filters were analysed.

The composition of inorganic colloids were also determined concomitant with fractionation of humic and fulvic acids from two sections in KSH01A, 161.8 m and 556.5 m. The equipment for this consisted of membrane filters with defined cut off (pore size), a peristaltic pump, flexible tubing and vessels. The equipment and performance is described in SKB MD 431.043. (SKB internal controlling document). Samples were analysed by ICP-AES. The determined elements were Ca, Fe, K Na S, Si, Al, Ba, Cd, Co, Cr. Cu, Hg, Li, Mn, Mo, Ni, P, Pb, Sr, V and Zn. Of these elements data for Fe, Si, Al and Mn were reported /Wacker et al. 2004/.

For the organic colloids see Microbiologic report section 1.4.2.

2.2.1 Databases

The data used were extracted from the file Laxemar_1_2_All_data_2005_def.xls provided by Maria Gimeno at the Project Place and from the SKB P-report P-04-12 /Wacker et al. 2004/. The data from the colloid filtration used here are compiled in Table 2-1.

2.2.2 Evaluation of the colloid data

The 0.2 µm filter from section 253,3 m was broken and because of this no total amount of colloid data are available from this section. All other data available were used in the evaluation.

In a report by /Laaksoharju et al. 1995/, calcium values calculated as calcite and sulphur values calculated as pyrite were both withdrawn from the total amount of colloids. In this presentation the same approach was used with the exception that the sulphur values are not recalculated as pyrite but are shown as sulphur.

2.3 Colloids versus depth

In a valuation of the background values for colloids in groundwater, the amount of colloids versus depth is studied. It can be seen in Figure 2-1 that the amount of colloids was highest in borehole KLX01. 458.5 m with 92.03 µg l–1. This is because of a high amount of aluminium colloids in this sample, see 2.6. The explanation is a probable contamination from drilling. The other data are from around 13 to 33 µg l^{-1}. The more recent data from borehole KSH01A are the lowest. Since there is only two samples from this study it is difficult to speculate in the explanation for this but an improved sampling technique is a plausible suggestion.

The average amount of colloids in this study was 23.1 SD ± 7.14 if the value from KLX01, 458.5 m is omitted. These values agree very well with data reported from colloid studies in Switzerland (30 SD ± 10 and 10 SD ± 5 µg l^{-1}) /Degueldre 1994/ but about ten times lower than reported from Canada (300 SD ± 300 µg l^{-1}) /Vilks et al. 1991, Laaksoharju et al. 1995/.

2.4 Colloids versus chloride

Figure 2-2 shows the amount of colloids versus chloride. In groundwater with a high chloride concentration the amount of colloids usually decreases because higher ion strength increases the precipitation of different solid particles. The chloride concentrations in this data set vary from 500 to almost 8,900 mg l–1. The only sample with high amounts of colloids is the KLX01, 458.5 m with 92.03 µg l–1 and this is probably a contamination from drilling as discussed above, see 2.3. All the other data are low and do not vary much even if the chloride concentrations of the samples have large span.

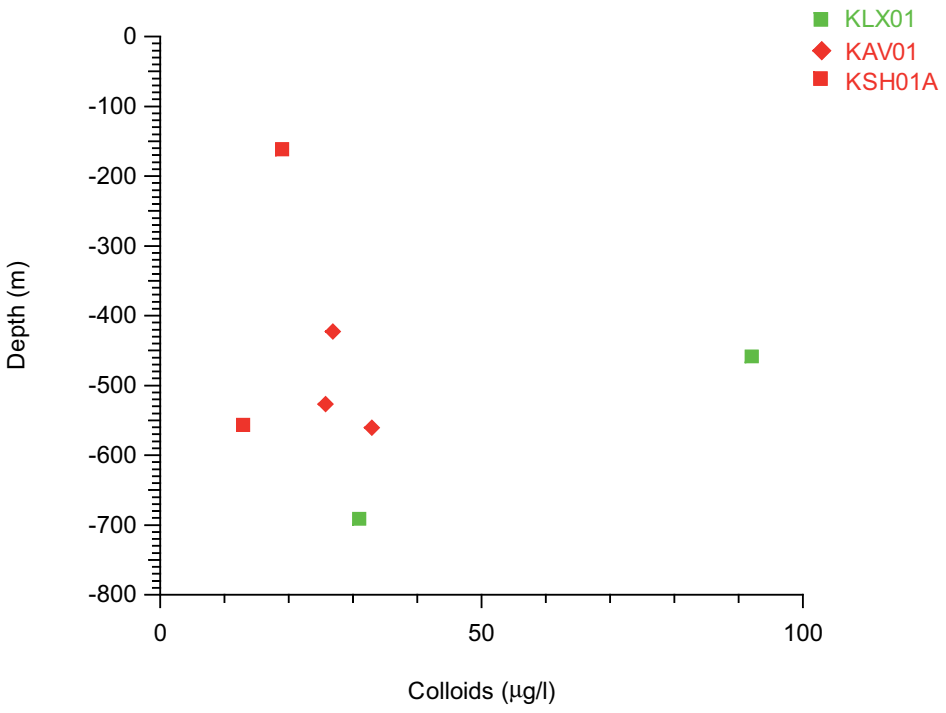

Figure 2-1. *Colloids (µg l^{-1}) plotted versus depth in samples from the boreholes KLX01, KAV01 and KSH01A in the regional Simpevarp area.*

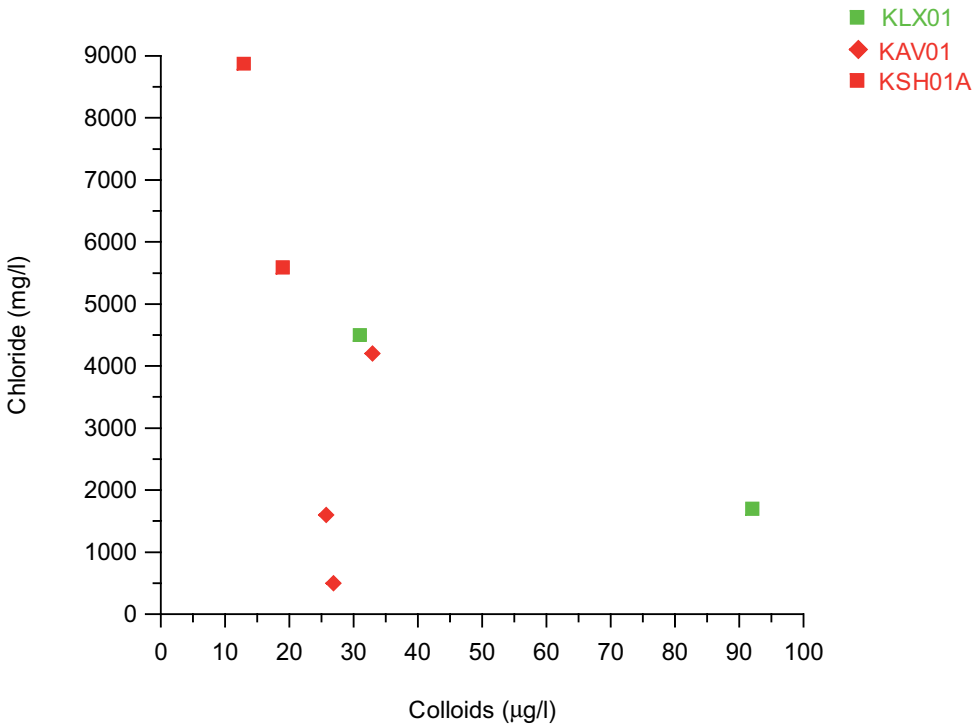

Figure 2-2. *Colloids (µg l^{-1}) plotted versus amount of chloride in the groundwater in samples from the boreholes KLX01, KAV01 and KSH01A in the regional Simpevarp area.*

2.5 Colloids versus iron

High iron concentrations in groundwater force the precipitation of other compounds by its ability for co-precipitation, which produces larger particles. Thus the amount of colloids will decrease with increasing iron concentration. Figure 2-3 shows the colloids versus the iron content in groundwater from the regional Simpevarp area. The data show no clear trend. The only data that is much higher than the others is the KLX01, 458.5 m with 92.03 µg l^{-1}, as discussed above, see 2.3 and 2.4, even though this sample has the lowest iron value.

2.6 Composition of the colloids

The composition of the colloids has also been studied. Table 1 shows the values for the elements analysed, calcium (Ca), iron (Fe), sulphur (S), manganese (Mn), Aluminium (Al) and silica (Si), recalculated as colloid phases calcite, iron hydroxide, manganese dioxide, K-Mg-Illite clay and silica oxide. Sulphur was not recalculated to any other colloid phase.

Figure 2-4 shows the composition of the colloids sampled from different depths in the three bore-holes. In this figure sulphur is shown. In Figure 2-5 on the other hand these values are removed. In both figures the calcite is omitted since it might be considered as an artefact due to pressure changes during sampling.

In Figures 2-4 and 2-5 it can be seen that manganese oxides were found in borehole KAV01 at to depths, 422.5 and 526.5 m. This is in agreement with the relative high manganese values found in this borehole, see section 1.6. It is also in this borehole where the highest iron values are found together with the 691 m section in KLX01.

The Figures 2-4 and 2-5 also illustrate the high aluminium value at 458.5 m in KLX01. Some aluminium, here represented as K-Mg-Illite, was also found in KAV01, 560,5 m and in the KSH01A borehole, but in low amounts, see 2.3, 2.4 and 2.5. There were high amounts of sulphur in KLX01 and KAV01. If this is an artefact or not still has to be evaluated. If sulphate-reduction is ongoing and

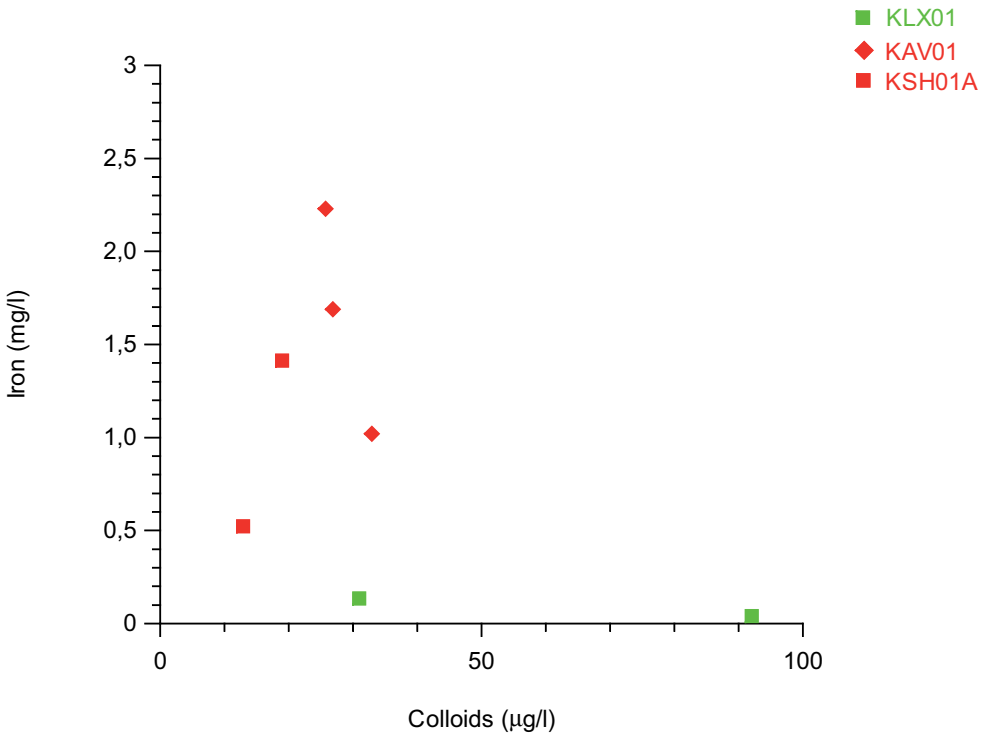

Figure 2-3. *Colloids (µg l^{-1}) plotted versus iron in groundwater in samples from the boreholes KLX01, KAV01 and KSH01A in the regional Simpevarp area.*

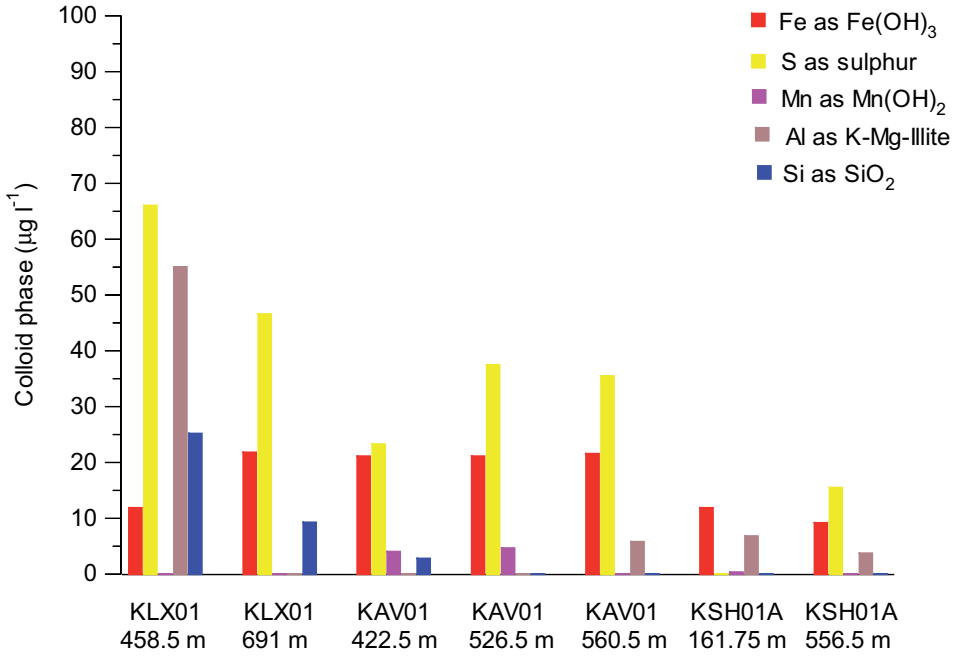

Figure 2-4. *The composition of colloids sampled from the boreholes KLX01, KAV01 and KSH01A in the regional Simpevarp area Calcite is omitted in this figure.*

thus sulphide is produced the colloid sulphur might be iron sulphide (Figure 2-4 and 2-5). Some of the iron will the also be iron sulphide and not iron hydroxide as used in the figures here.

In the colloid fraction which was obtained in the fractionation filtration, > 1,000 D but < 5,000 D, no amounts of iron, silicon or manganese could be determined in neither of the sections analysed, 161.8 m and 556.5 m in KSH01A. All measured amounts were < 1,000 D. An adsorption of iron to the filter equipment was observed.

2.7 Conclusion

The amount of colloids as reported here seems to agree with the amount of colloids earlier reported from Switzerland, Äspö and Bangombe /Laaksoharju et al. 1995/. The possibility that some of the iron and sulphur colloids might be iron sulphides has to be further studied.

Data for the numbers of particles could increase the value of colloid analyse by making it possible to calculations of amounts binding sites for radionuclides in the different colloid fractions.

Table 1. Element analyses of colloid fractions 0.05 µm and 0.2 µm and 0.4 µm precipitation from borehole KSH01A, Simpevarp subarea.

Borehole	KSH01A 161.75 m			KSH01A 253.3 m			KSH01A 556.5 m		
Pore Size (µm)	0.05	0.2	0.4	0.05	0.2	0.4	0.05	0.2	0.4
Chloride (mg l^{-1})	5,590	5,590	5,590	6,298	6,298	6,298	8,876	8,876	88.76
Iron (mg l^{-1})	1.413	1.413	1.413	1.318	1.318	1.318	0.523	0.523	0.523
Colloid phase (µg l^{-1})									
Ca as Calcite $CaCO_3$	267.2	199.2	244.75	385.2	d.m.	262.6	448.5	436.2	703
Fe as $Fe(OH)_3$	3.82	8.02	389.5	0.764	d.m.	150.2	3.44	5.73	10.7
S as sulphur	b.d.	b.d.	1.4	16.4	d.m.	5.2	7.8	7.7	15.6
Mn as $Mn(OH)_2$	0.168	0.162	1.70	0.162	d.m.	1.05	0	0	0.162
Al as K-Mg-Illite clay: $K_{0.6}Mg_{0.25}Al_{2.3}Si_{3.5}O_{10}(OH)_2$	3.09	3.71	92.7	2.47	d.m.	82.2	1.236	2.47	4.9
Si as SiO_2	b.d.	b.d.	b.d.	b.d.	d.m.	26.6	b.d.	b.d.	18.08
Sum (ppb, µg l^{-1})	274.3	211.1	730.0	405.0	–	527.8	461.0	452.1	752.4
Sum omitting calcite	7.08	11.9	485.3	19.8	–	265.25	12.5	15.9	49.4
Sum omitting calcite and sulphur	7.08	11.9	483.9	3.4	–	260.0	4.7	8.2	33.8

b.d. below detection limit
d.m. data missing due to broken filter.

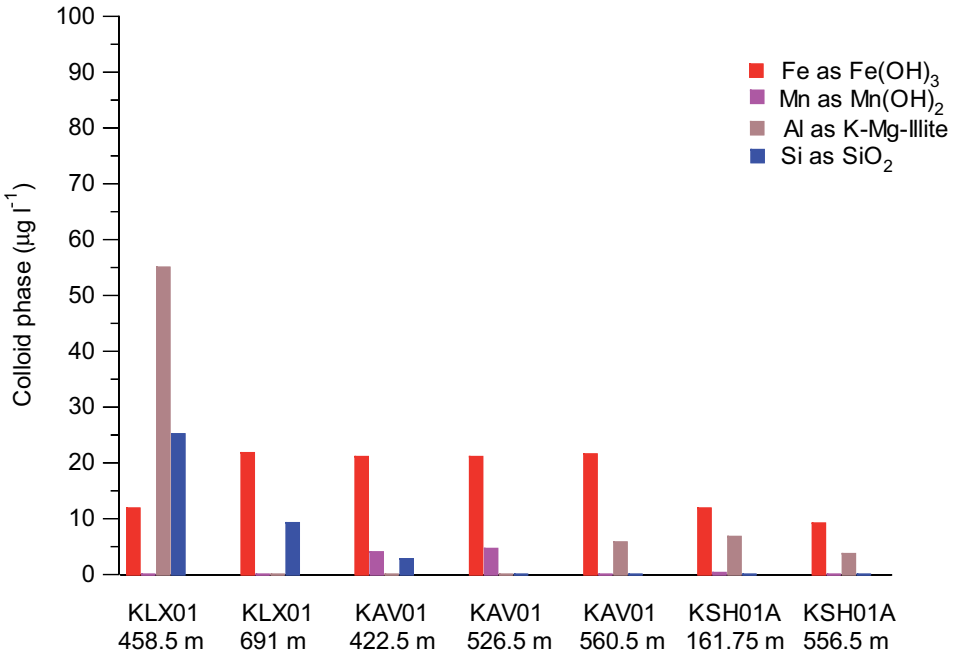

Figure 2-5. *The composition of colloids sampled from the boreholes KLX01, KAV01 and KSH01A in the regional Simpevarp area. Calcite and sulphur values are omitted in this figure.*

3 References

Anomymous, 1992. Estimation of bacterial density, pp 977–980 Standard methods for the examination of water and wastewater, 18th ed. American Public Health Association, Washington, D.C.

Apps J A, van de Kamp P C, 1993. Energy gases of abiogenic origin in the Earth's crust. The future of Energy gases. U.S. Geological Survey Professional Papers. United States Government Printing Office, Washington., pp 81–132.

Degueldre C, 1994. Colloid properties in groundwater from crystalline formation. Paul Scherrer Institute, Villigen, Switzerland.

Haveman S A, Pedersen K, Ruotsalainen P, 1999. Distribution and Metabolic Diversity of Microorganisms in Deep Igneous Rock Auifers of Finland. Geomicrobiology Journal 16, 277–294.

Haveman S A, Pedersen K, 2002. Distribution of culturable microorganisms in Fennoscandian Shield groundwater. FEMS Microbiology Ecology 39, 129–137.

Kotelnikova S, Pedersen K, 1998. Distribution and activity of methanogens and homoacetogens in deep granitic aquifers at Äspö Hard Rock Laboratory, Sweden. FEMS Microbiology Ecology 26, 121–134.

Laaksoharju M, Degueldre C, Skårman C, 1995. Studies of colloids and their importance for repository performance assessment. Stockholm, Sweden.

Laaksoharju M, 2004. Hydrogeological evaluation for Simpevarp model version 1.2. Prelimanry description of the Simpevarp area. Swedish Nuclear Fuel and Waste Management Co, Stockholm, Sweden.

Mäntynen M, 2000. Field measuring results from the microbe and gas analysis for the PAVE ground water samples from borehole KLX02 in Laxemar. Posiva Working Report 2000-42. Helsiniki, Finland.

Pedersen K, Ekendahl S, 1990. Distribution and Activity of Bacteria in Deep Granitic Groundwater of Southeastern Sweden. Microbial Ecology 20, 37–52.

Pedersen K, Ekendahl S, 1992. Assimilation of CO2 and Introduced Organic Compounds by Bacterial Communities in Graoundwater from Southeastern Sweden Deep Crystalline Bedrock. Microbial Ecology 23, 1–14.

Pedersen K, 1993. The deep subterranean biosphere. Earth-Science Reviews 34, 243–260.

Pedersen K, 2001. Diversity and activity of microorganisms i deep igneous rock aquifers of the Baltic shield, pp 97–139 In J.K. Fredrickson and M. Fletcher (eds.), Subsurface microbiology and biogeochemistry. Wiley-Liss Inc., New York.

Pedersen K, 2002. Microbial processes in the disposal of high level radioactive waste 500 m underground in Fennoscandian shield rocks, pp 279–311 In M.J. Keith-Roach and F.R. Livens (eds.), Interactions of microorganisms with radionuclides. Elsevier, Amsterdam.

Pedersen K, 2005. Äspö Hard Rock Laboratory. The MICROBE framework. Site descriptions, instrumentation, and characterisation. Swedish Nuclear Fuel and Waste Management Co, Stockholm, Sweden.

Stetter K O, 1996. Hyperthermophilic procaryotes. FEMS Microbiol. Rev. 18, 145–148.

Straub K L, Benz M, Schink B, Widdel F, 1996. Anaerobic, nitrate-dependent microbial oxidation of ferrous iron. Appl. Environ. Microbiol. 62, 1458–1460.

Valentine D L, 2002. Biogeochemistry and microbial ecology of methane oxidation in anoxic environments: a review. Antonie Van Leeuwenhoek 81, 271–282.

Vilks P, Miller H, Doern D, 1991. Natural colloids and suspended praticles in Whiteshell Research area, Manitoba, Canada, and their potential effect on radiocolloid formation. Applied Geochemistry 8, 565–574.

Wacker P, Berg C, Bergelin A, 2004. Complete hydrochemical characterisation in KSH01A. Results from four investigated sections, 156.5–167.0, 245.0–261.6, 586.0–596.7 and 548.0–565.4 m. Oskarshamn site investigation. Swedish Nuclear Fuel and Waste Management Co, Stockholm.

Appendix 1

The microbial data available from the regional Simpevarp area

Borehole	Depth (m)	Total no. of cells (x 10^5 ml^{-1})	JRB (ml^{-1})	MRB (ml^{-1})	SRB (ml^{-1})	HM (ml^{-1})	AM (ml^{-1})	HA (ml^{-1})	AA (ml^{-1})
KLX01	195	2.0	–	–	–	–	–	–	–
	290	1.1	–	–	–	–	–	–	–
	680	3.3	–	–	5.6 × 104	–	–	–	–
	835.5	0.15	–	–	–	–	–	–	–
	915.5	0.21	–	–	–	–	–	–	–
	1,038.5	0.68	–	–	–	–	–	–	–
KLX02	1,160	5.7	3.3 × 102	–	nd.	nd.	nd.	1.7 × 102	1.1 × 102
	1,350	3.7	nd.	nd.	nd.	nd.	nd.	2.4 × 102	nd.
	1,389	28	nd.	nd.	nd.	nd.	nd.	nd.	nd.
KSH01A	161.75	1.4	2.1	3.3	1.6 × 102	–	–	–	–
	253.3	1.0	2.1	nd.	22	700	nd.	9 × 102	–
	565.5	0.72???	3.3	nd.	35	2.6	nd.	17	30
KAS04	195	5.4	–	–	1.6 × 103	–	–	–	–
	290	2.5	–	–	–	–	–	–	–
	380	0.75	–	–	< 102	–	–	–	–

– not analysed
nd. not detected.

Appendix 3

PHREEQC modelling

Contribution to the model version 1.2

María J Gimeno, Luis F Auqué, Javier B Gómez
Department of Earth Science, University of Zaragoza

September 2005

Contents

Introduction 307
1 State of knowledge at previous model version 309

2 Evaluation of primary data 311
2.1 Representativity of the data 312
2.2 Explorative analysis 312
2.2.1 Summary of the evaluation of scatter plots 312

3 Geochemical Modelling 315

4 Sensitivity and uncertainty analysis 319
4.1 PHREEQC and mass balance calculations 319
4.1.1 Forward modelling 319
4.1.2 Inverse modelling with PHREEQC 321
4.1.3 Discussion and conclusions 325
4.2 M4: Mixing proportion sensitivity to end-member composition variability 325
4.2.1 Motivation 325
4.3 M4 verification: chemical reactions effects on the calculated mixing proportions. 333
4.3.1 Samples representative of pure mixing 333
4.3.2 Samples with mixing and ionic exchange 334
4.3.3 Samples with mixing and sulphate reduction 335
4.3.4 Calculations only with conservative elements 335
4.3.5 Discussion and conclusions 336

5 References 339

1 Introduction 345

2 Water type classification 345

3 Descriptive and quantitative modelling using the M3 modelling code 347
3.1 M3 modelling 347
3.2 The reference waters used 348
3.3 Test of models 349
3.4 Mixing proportions along KLX02 calculated with five different models 353
3.5 Additional tests of models 353
3.6 Comparison between M3 and M4 codes 359

4 Site specific hydrogeochemical uncertainties 363
4.1 Model uncertainties 363

5 The use of DIFF measurements 365

6 Visualisation of the sampling locations 367

7 Concluding remarks 369

8 References 371

Appendix 1 Water type classification of the Simpevarp samples by using AquaChem 373

Appendix 2 Measured data and M3 mixing calculations for Laxemar 1.2, bedrock data, model 5 375

Appendix 3 EC from DIFF measurements, measured Cl and calculated mixing proportions with model 5 along KLX02 377

Introduction

For the Site Descriptive Modelling phase in Laxemar (Laxemar 1.2), the selected format has been to include all relevant data in the Simpevarp and Laxemar subareas together with the available information from Äspö (before the tunnel construction) and Ävrö.

Most analyses of groundwaters have been already used in the Simpevarp 1.2 phase /Laaksoharju et al. 2004a/, and therefore, this work has focused more on the improvement of the methodology and tools used for this kind of study, and the sensitivity and uncertainty analysis of them.

This contribution is now focussed on the following main points:

- Tabular compilations of the chemical and isotopic data from SICADA to create the final tables for modellers.
- Evaluation of the quality and representativity of the hydrogeochemical data.
- Reevaluation of previous models in the light of new available geological and hydrogeological information.
- New mass balance and mixing calculations using PHREEQC and M4 along the main flow lines in the area.
- Sensitivity analysis of the mixing and mass balance calculations and the establishment of a general procedure for this type of analysis.
- Uncertainty analysis.

This report is organized in five parts, of which Chapters 2 to 4 contains the main results and develoments. The contents are organized as follows:

- Chapter 1: state of knowledge at previous model versions.
- Chapter 2: evaluation of the data, where the newly delivered dataset is presented and described.
- Chapter 3: new modelling calculations performed with PHREEQC using the mass balance approach.
- Chapter 4: sensitivity and uncertainty analysis of the modelling results and of the procedures and tools ; (this is the core chapter in the report).
- Chapter 5: discussion and main conclusions.

1 State of knowledge at previous model version

The main findings from the Simpevarp 1.2 phase can be summarised as follows.

Groundwaters in the Laxemar area can be divided into three groups based on their salinity:

(1) **Saline groundwaters.** Mixing with a brine end member is responsible, directly or indirectly, for most of their chemical content, especially for waters with Cl > 10,000 mg/L. Their alkalinity is low, and is controlled by equilibrium with calcite. The pH is also controlled by calcite equilibrium and, possibly, aluminosilicate reactions. In contrast to other Fennoscandian sites, sulphate is controlled by gypsum (gypsum has been identified in fracture filling minerals) in high saline groundwaters. The old mixed waters tend, with time, to re-equilibrate with a relatively constant mineral assemblage, irrespective of their initial elemental contents. These reactions are slow and can be approached by equilibrium modelling (with aluminosilicates), although other alternatives can be explored (clay minerals).

(2) **Brackish groundwaters.** They have been submitted to more complex mixing processes, with participation of all possible end-members. A combination of slow and fast chemical reactions (eg. Na-K-Ca ion exchange, calcite precipitation, etc) have operated on the mixed waters.

(3) **Non saline groundwaters.** These waters are the result of "pure" water-rock interaction or mixing of the previous types with recent waters. They lack a clear thermodynamic control; if there is any, it is by fast chemical reactions (ionic exchange, surface complexation reactions, calcite dissolution-precipitation, etc) coupled with the more important irreversible processes (RFM dissolution, decomposition of organic matter, etc).

The redox state of groundwaters in the Laxemar area appears to be well described by sulphur redox pairs in agreement with some previous studies in this area and in other sites from the Fennoscandian Shield. From the analysis performed in the POM area it can be concluded that CH4/CO2 might be another important redox pair in determining the redox state /Laaksoharju 2004a/. Therefore, although the sulphur system can be considered the best suited to characterise the redox state of the groundwaters, a better understanding of the iron system is needed to assess its particular contribution to the redox state or to the reductive capacity of the groundwater system.

2 Evaluation of primary data

The dataset used in this phase was supplied by SICADA as Laxemar 1.2 Data Freeze, and includes old (Simpevarp 1.2 Data Freeze) and new (post-Simpevarp 1.2 Data Freeze) samples. Therefore, part of the samples included in this data freeze coincide with those shown in Appendix A in /Laaksoharju 2004a/ (SKB R 04-74). The new samples are shown in this report's Appendix A.

The new samples (all collected in 2004) include:

30 samples from the Ävrö subarea:

- 8 samples from percussion boreholes (two samples from each of the following boreholes: HAV11, HAV12, HAV13 and HAV14).
- 22 samples from the cored borehole KAV04: 20 tube samples (from 0 to 1,000 m depth) and 2 packered samples (729–805 m and 729–819 m).

112 samples from Laxemar:

- 10 samples from percussion boreholes: 4 samples from borehole HLX14 (one of them selected as representative sample for modelling purposes), two samples from HLX18, two from HLX20 (one of them selected as representative), one from HLX22 and one from HLX24.
- 102 sample from cored boreholes:
  - 26 samples from KLX03: 20 tube samples (from 0 to 990 m depth) and 6 packered samples (12–60 m, 12–100 m, 103–218 m [1 representative sample], 497–600 m, 600–695 m and 693–761 m).
  - 69 samples from KLX04: 21 tube samples (from 0 to 985 m depth) and 48 packered samples (104–109 [3], 103–213 [1 representative sample], 210–329 [1], 329–404 [1], 401–515 [1], 510–515 [25], 614–701 [1], 698–850 [1], 849–993 [1], 971–976 [13]).
  - 7 packered samples from KLX06 (103–202 [1], 200–310 [1], 260–268 [2], 307–415 [1], 331–364 [1], 514–613 [1]).

360 from Simpevarp:

- 44 groundwater samples:
  - 4 samples from percussion boreholes: 2 samples from each of the following boreholes, HSH04 and HSH05.
  - One sample from KSH02 cored borehole (422.3–423.3 m).
  - 39 shallow groundwater (0–10 m depth) samples from soil pipes (one of them selected as representative sample for modelling).
- 296 surface water samples:
  - 92 sea water samples.
  - 64 lake water samples (48 selected as representative samples).
  - 140 running water samples (65 selected as representative samples).
- 20 samples of precipitation (13 selected as representative samples).

Altogether, there are 502 new water samples, but not all of them with a complete chemical analysis at the time of the data freeze. Some of them have been considered representative for modelling purposes (as indicated above; see orange, green and pink rows in Table A-1 in Appendix A, this report).

Analysed data include the same parameters chosen as in the previous stage (see Table A1). The pH and conductivity values used in this report are those determined in the laboratory (except for surface waters where pH was determined in the field). There are no data for Eh and temperature neither for the surface waters nor for the new sampled groundwaters.

2.1 Representativity of the data

This analysis is presented in Smellie and Tullborg (this issue).

2.2 Explorative analysis

Following the same approach used in previous stages for geochemical groundwater modelling /Simpevarp 1.1 and 1.2, Laaksoharju et el. 2004ab/, the evaluation of this new set of data started with the explorative analysis of different groundwater variables. The evaluation already reported in version 1.2 (mainly for Simpevarp subarea) will not be repeated here .

Here the main hydrogeochemical characters of all the studied subareas are analysed as a whole. The analysis was performed following the same methodology (ion-ion plots) used in the previous Simpevarp 1.1 and 1.2 reports, but, as in this case the whole set of new samples follows exactly the same trends as the previous set, we will only state the main conclusions without including the plots with the new samples .

2.2.1 Summary of the evaluation of scatter plots

Hydrochemical data were graphically presented in previous reports using X-Y plots to derive trends that may facilitate interpretation. Since chloride is generally conservative in normal groundwaters, its use is appropriate to study hydrochemical evolution trends when coupled to ions, ranging from conservative to non-conservative, to provide information on mixing, dilution, sources and sinks. Moreover, here chloride acts as a tracer of the main irreversible process operating in the system mixing, which has been demonstrated in previous work /Laaksoharju 2004a/. Here follows a summary of the diverse geochemical trends apparent in Simpevarp area groundwaters, including the new samples from the Laxemar 1.2 data freeze.

As an example of the behaviour of the new samples, we present here the evolution of chloride with depth. Figure 2-1a shows the results already presented in the Simpevarp 1.2 phase. Figure 2-1b shows all new samples from Laxemar 1.2 data freeze. These new samples closely follow the trends described in previous reports. The most important new information refers to the deepest waters in the Ävrö subarea (compare Figures 2-1a and b, diamonds) which clearly follow the expected trend.

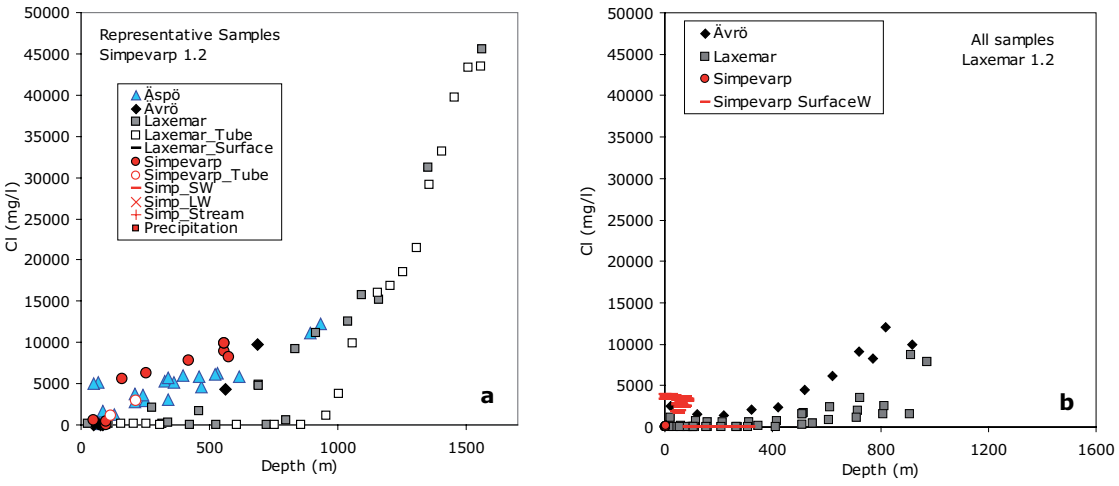

Figure 2 1. *Evolution of chloride with depth in the Simpevarp area. (a) Representative samples delivered in the Simpevarp 1.2 data freeze; (b) All samples from Laxemar 1.2 data freeze; samples with the symbol of Simpevarp Surface waters (red horizontal bar) include: seawater, lakes, streams and precipitation; all other samples in plot (b) are groundwaters.*

As a general rule chloride increases with depth but it shows a different trend in Laxemar than in the other three subareas (Simpevarp, Äspö and Ävrö; Figure 2-1a). Considering only representative samples from the Simpevarp subarea (there are no representative samples deeper than 580 m), chloride gradually increases with depth up to 10 g/L. Äspö and Ävrö samples (up to 1,000 m depth) show the same progressive increase, but reach chloride contents up to 14 g/L (Figure 2-1b). Laxemar, although close by, is representative of a more mainland environment and involves greater depths. As we already pointed out in the previous reports /Laaksoharju 2004a, Laaksoharju et al. 2004b/, the Laxemar data show dilute groundwaters extending to approx. 600 m and for KLX02 to around 1,000 m before a rapid increase in salinity to maximum values of around 47 g/L Cl at 1,700 m. There are still not enough data from Simpevarp (nor from Äspö or Ävrö) to check whether groundwaters there will follow the same rapid increase in salinity with depth as in Laxemar.

Sodium shows a positive linear correlation with chloride concentration (Figure 2-2), which suggests that mixing is the main process controlling Na content. The deviation of representative groundwater samples from the sea water dilution line can be interpreted as mixing with a saline end member (green triangle labelled “Brine” in Figure 2-2a). This is clearly seen in Laxemar samples (Cl> 10,000 mg/L), which show a near conservative behaviour for this element. Simpevarp samples show sodium contents following a line with a slope between SWDL and the line followed by Laxemar samples.

As for the other chemical variables, their behaviour in the new samples with respect to chloride falls on the same trends as before (Simpevarp 1.2 phase; Laaksoharju 2004a) and, therefore, the description and conclusion presented for Simpevarp 1.2 phase, are still valid for Laxemar 1.2.

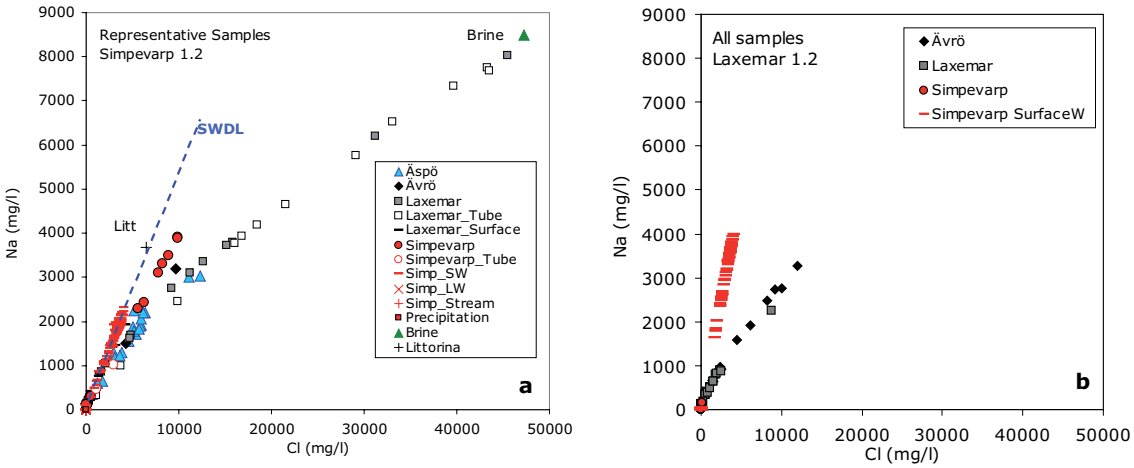

Figure 2 2. *Evolution of sodium with respect to chloride in Simpevarp area. (a) Representative samples delivered in the Simpevarp 1.2 data freeze; (b) All the samples from Laxemar 1.2 data freeze; samples with the symbol of Simpevarp Surface waters (red horizontal bar) include: seawater, lakes, streams and precipitation; all other samples in plot (b) are groundwaters.*

3 Geochemical Modelling

Mass balance and reaction-path modelling (presented in this chapter and in the next) have been carried out with PHREEQC /Parkhurst and Appelo 1999/ using the WATEQ4F thermodynamic database. The principles behind these calculations were described in previous reports /Laaksoharju et al. 2004a/. Speciation-solubility calculations, the study of the aluminosilicate minerals and the redox state of the system were thoroughly analysed in /Laaksoharju 2004a/ and, as is the case for the ion-ion plots, the inclusion of the new data freeze samples does not alter previously drawn conclusions .

Therefore, the main goal of this chapter is to investigate the processes that control water composition at the Simpevarp area based on a small subset of selected samples from the two main subareas (Laxemar and Simpevarp). These samples have a wide depth distribution and are representative of the depth evolution of the system. They are shown in Table 3-1.

Modelling was carried out using the mass balance and mixing approach implemented in PHREEQC. The calculation procedure consists of assuming that each selected water is the result of (a) mixing with the water immediately above it and with several end members (old waters already present in the rock system), and (b) reaction according to a preselected set of chemical reactions (only the simplest ones).

Once the samples have been selected (Table 3-1), the next step involves the selection of the end members to be used in the calculations. The end members available for the modelling are the same as in previous studies, namely Brine, Glacial, Littorina and Precipitation. However, as in this specific modelling we are only dealing with groundwaters, we decided to add a new end member representative of a “Dilute Granitic Groundwater (DGW)” instead of a precipitation end member. This end member was chosen among several representative samples in the Simpevarp Area (Table 3-2).

Table 3-1. Samples selected for modelling.

Subarea	Borehole	Sample	Depth
Laxemar	KLX02	2738	318
		2712	801
		2934	1,093
		2722	1,160
		2931	1,350
		2731	1,562
Simpevarp	KSH01A	5263	161.8
		5268	253.3
		5288	556.6

Table 3-2. Samples in Laxemar 1.2 data set representative of a dilute granitic groundwater (the selection was made by expert judgment, Smellie and Tullborg, pers. comm.). The sample highlighted in blue has been finally used as the DGW end member.

Subarea Borehole	Sample number	Na (mg/l)	K (mg/l)	Ca (mg/l)	Mg (mg/l)	HCO_3 (mg/l)	Cl (mg/l)	SO_4 (mg/l)	D (dev)	Tritium corrected	O18 (dev)
Laxemar HLX10	3904	68	2.81	12.9	4.4	198	6.3	17.84	–78.8	6.8094886	–10.9
Bockholmen HBH05	2112	19.2	3	38.5	3.8	162	12	21.5	–68.4	11.913098	–9.9
Simpevarp SSM000012	7245	38.7	6.64	56.7	9.2	217	12.6	63.90	–74.9	11.2	–10.8
Laxemar KLX04	7253	118	2.44	17.2	4.1	318	28.6	17.40	–76.8	4.1	–10.8
Laxemar HLX14	7345	138	3.08	18.8	4.7	302	69.7	31.30	–78.6	3.8	–11.2
Äspö HAS05	2	237	4	25	6	370	119	118	–73.8	0.7750399	–9.9

In order to check the “quality” of each dilute granitic water as an end member, several test were made with M4 /Laaksoharju 2005, Appendix C in Appendix 3/. The samples in Table 3-3 were included as end members together with the previous four ones, and a PCA analysis was carried out with different subsets of samples: (a) all samples from Laxemar 1.2, (b) only ground-waters, including soil pipes, and (c) only groundwaters, excluding soilpipes. For each combination of end members, M4 gives the percentage of samples that can be explained by mixing alone (i.e. those samples that fall inside the hyper-tetrahedron that have the end members as vertices). The assumption is made that the combination of end members which gives the highest percentage is the optimal one.

The result of these tests indicate that, independently of the set of samples included in the PCA analysis (all waters, groundwater and soilpipes, or only groundwaters), the optimal combination of end members is Brine + Glacial + Littorina + DGW, with sample HBH05 as the DGW end member (highlighted in blue in Table 3-2).

After the samples and the end members have been selected, we started the mass balance calculations following two evolutionary trends with depth (Table 3-3), one in Laxemar subarea (borehole KLX02) and the other in Simpevarp subarea (borehole KSH01A). In both cases, the trend starts by “evolving” a precipitation water into a diluted granitic groundwater. In this case the final solution is explained only by chemical reactions (no mixing) representative of the intense weathering in the overburden. The next step in both trends is the evolution from the representative diluted groundwater to the first real sample in the depth line. Now, apart from pure water-rock interaction, the potential mixing with “old” waters (Br, Gl, Lit and DGW) is also taken into consideration in the balance. From that point on, all the subsequent steps include mixing of five end members (Previous Sample + DGW + Gl + Lit + Br, as initial solution) and reactions involving calcite, silica, CO2(g), organic matter, cation-exchange (+ eq. gypsum in Laxemar) to reproduce the chemical and isotopic composition of the new sample. Results are shown in Figures 3-1 and 3-2.

In both depth lines mixing proportions evolve from dominant DGW proportions towards a more saline signature (Brine end member), more obvious in the Laxemar trend as the depth interval is three times longer than in the Simpevarp example.

Table 3-3. The two depth evolution trends modelled by mass balance and reaction-path.

KLX02 (Laxemar)	KSH01A (Simpevarp)
Precipitation	Precipitation
Dilute Granitic GW (HBH05)	Dilute Granitic GW (HBH05)
2738 (318 m) (73 mg/l Cl)	5263 (162 m) (5,590 mg/l Cl)
2712 (800 m) (548 mg/l Cl)	5268 (253 m) (6,298 mg/l Cl)
2934 (1,160 m) (15,000 mg/l Cl)	5288 (556 m) (8,876 mg/l Cl)
2931 (1,350 m) (31,230 mg/l Cl)	
2731 (1,562 m) (45,500 mg/l Cl)	

Reactions are also similar although the amount of mass transfer is different. In general there is a clear dissolution process of the rock forming minerals (except for iron oxyhydroxides precipitation and CO2 ingassing in the overburden) in the shallow part of the system, and a trend towards equilibrium with the selected minerals as depth increases (precipitation with progressively lower mass transfers). Cation exchange can play an important role in the balance including Ca, Na, Mg and K (Figures 3-1 and 3-2).

For this exercise, the considered reactions are the simplest ones. A better understanding of the actual chemical processes operating in the system could be obtained when more data about the minerals dominating at each depth and about the real hydrogeological flow lines in the system become available.

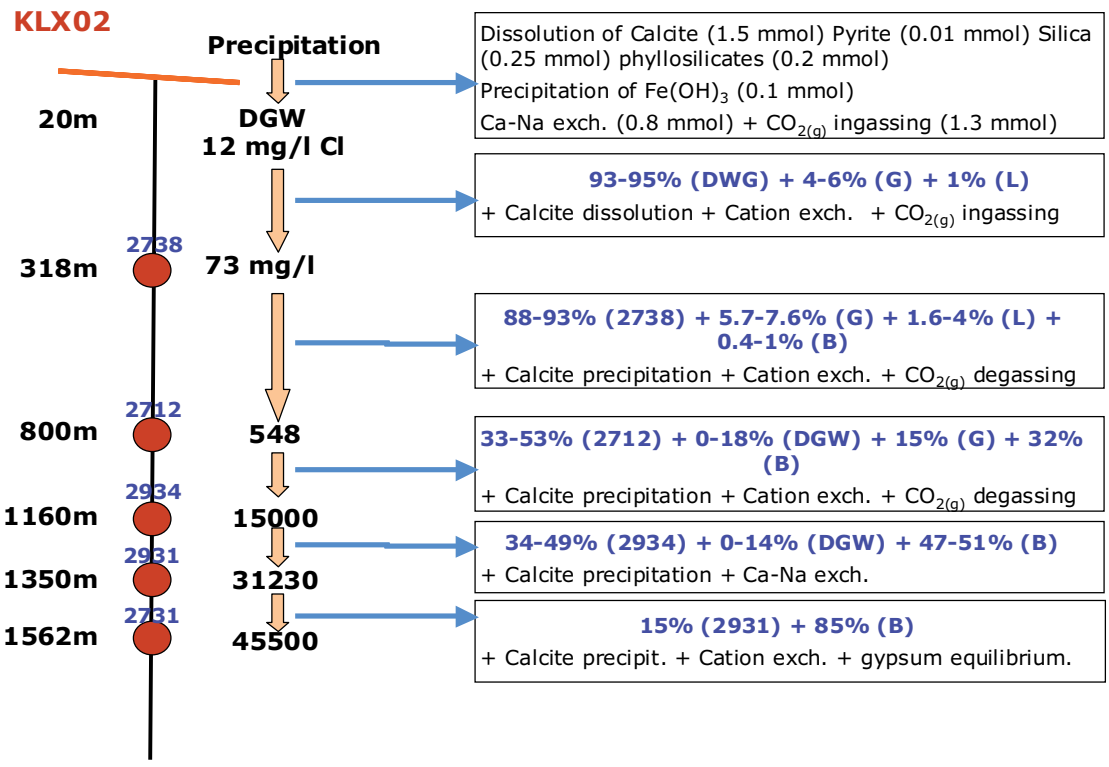

Figure 3-1. *Mixing and mass balance calculations obtained in the depth evolution trend represented by KLX02.*

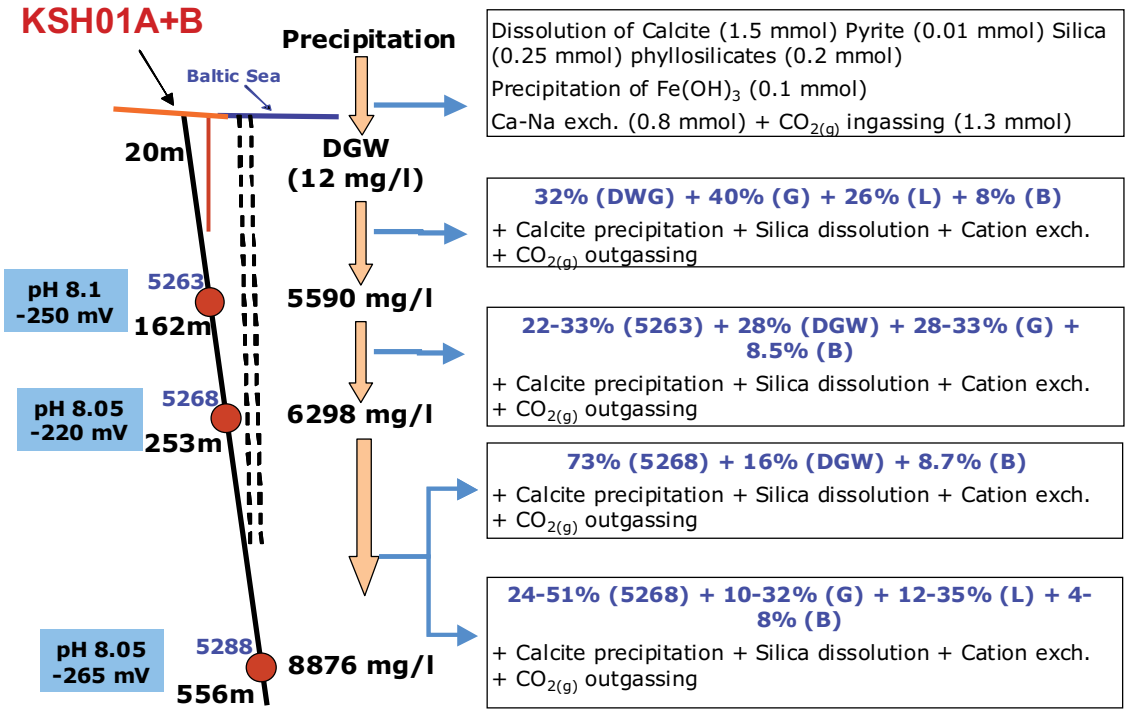

Figure 3-2. *Mixing and mass balance calculations obtained in the depth evolution trend represented by KSH01A.*

4 Sensitivity and uncertainty analysis

As it has been already presented in the introduction of this report, this work focuses on both the study and improvement of the methodology and tools used for modelling by the UZ group, and the sensitivity and uncertainty analysis of them.

The two main modelling tools used by this group are PHREEQC, a geochemical code, and M4, a PCA-based mixing code. The analysis has three parts:

1. Checking the inverse approach methodology (mass balance calculations) implemented in PHREEQC by means of synthetic waters created with PHREEQC built-in direct-approach capabilities.
2. Checking the effects of the compositional variability of the end members on the mixing proportions calculated with M4.
3. Using the synthetic samples created in part 1 with PHREEQC, to check the effects of chemical reactions on the mixing proportions calculated by M4.

4.1 PHREEQC and mass balance calculations

In order to check the inverse approach implemented in PHREEQC (and to cross-check M4) we have created several synthetic waters representative of groundwaters affected by two broad geochemical processes: mixing with old waters and reaction with the rock forming and fracture filling minerals. This procedure was carried out with the direct approach implemented in PHREEQC. With the knowledge of the processes responsible for the chemical composition of these waters, we have then used the inverse approach in order to recover those processes using selected chemical data of the waters (the principle of the inverse method).

4.1.1 Forward modelling

To create the synthetic waters with PHREEQC, four end members have been used: Brine (Br), Littorina (Lit), Glacial (Gl) and Precipitation (P). The following two mixing proportions have been used:

Water 1: 60% Br + 10% Lit + 30% Gl + 0% P

Water 2: 1.6% Br + 50.8% Lit + 24.4% Gl + 23.2% P

The chemical composition obtained with these mixing proportions is shown in Tables 4-1 and 4-2. Chemical characters of Water 1 are similar to the deepest and more saline groundwaters found in the Laxemar subarea. The chemical composition of Water 2 is similar to many brackish groundwaters in different places of the Scandinavian Shield with a Littorina imprint.

The chemical composition of these waters (obtained from a conservative mixing of the four mentioned end members), has been modified by imposing different reactions (at 25°C and with WATEQ4F thermodynamic database):

(a) equilibrium reactions with different mineral phases (samples 1a and 2a);

(b) ionic exchange (involving Na, Ca, K and Mg) and calcite equilibrium (samples 1b, 1b' and 2b, 2b');

(c) coupling of type (b) and sulphate reduction (samples 1c and 2c);

(d) sulphate-reduction ONLY (samples 1d and 2d).

Type-a waters. The effects of equilibrium with calcite, albite, adularia and kaolinite on the groundwaters composition have been already evaluated /Laaksoharju 2004a, 2005/. In most cases the amount of mass transfer and the corresponding chemical changes are very low.

Together with calcite, two of the most common phyllosicates found in fracture fillings, illite and chlorite, were selected for the equilibrium calculations. The chemical composition of Type (a) waters, obtained as a result of these reactions over the mixed waters (sample 1 and 2) are shown in Tables 4-1 and 4-2 under the columns labelled Sample 1a (Table 4-1) and Sample 1b (Table 4-2). Compared with the original mixed waters, the chemical composition in these reequilibrated waters barely changes.

Type-b waters. As far as we know, no measurements of the cation exchange capacity (CEC) of fracture filling materials have been made. Therefore, some indirect estimations /Viani and Bruton 1997/ have been used for the calculations with PHREEQC. The final chemical composition of the waters affected by cation exchange (samples type b) is shown in Tables 4-1 and 4-2. Under the headings Sample 1b (Table 4-1) and Sample 2b (Table 4-2) are two columns (b and b'), which show the resultant composition considering different exchange capacity values, 0.1 (1b, 2b) and 0.2 (1b', 2b') mol/kg H_2O. In contrast with type-a waters, the chemical variation introduced by cation exchange (Na, K, Ca and Mg) is bigger.

Type-c and d waters. The sulphate-reduction process has been defined by the reaction

$$SO_4^{2-} + 2\ CH_2O + OH^- \rightarrow HS^- + 2HCO_3^- + H_2O$$

using a reaction progress of 1 mmol. The effect of this simple progress on the sulphate and carbonate concentrations in waters (Tables 4-1 and 4-2, columns "Samples 1d" and "Sample 2d") are consistent with the ranges found in groundwaters affected by sulphate reduction /Laaksoharju and Wallin 1997/. This sulphate reduction reaction has been combined with the cation exchange reactions (CEC= 0.2 mol/kg H_2O) in order to create samples type-c.

Table 4-1. Chemical and isotopic composition of the synthetic waters generated with the first mixing proportions (60% Br + 10% Lit + 30% Gl + 0% P) and different sets of reactions (waters type (a), (b), (c) and (d)). Concentrations in mg/l.

Mixing proportions 1: 60% Br + 10% Lit + 30% Gl + 0% P						
	Sample 1	Sample 1a	Sample 1b		Sample 1c	Sample 1d
	Only Mixing	Mixing + equilibrium (calcite, illite, chlorite)	Mixing + cation exchange (CE) + calcite eq. b: CEC = 0.1	b': CEC = 0.2	Mixing + CE + calcite eq. + SR	Mixing + sulphate reduction (SR)
pH	7.16	7.99	6.97	6.97	6.28	7.25
Na	5,894.58	5,894.58	5,991.13	6,073.90	6,476.21	5,894.58
K	43.24	42.62	40.70	25.25	40.11	43.24
Ca	12,557.06	12,545.04	12,488.90	12,440.80	12,064.08	12,557.06
Mg	46.74	50.48	42.78	39.57	39.93	46.74
HCO_3^-	18.61	2.92	18.01	17.49	85.66	122.03
Cl	31,326.30	31,326.30	31,326.30	31,326.30	31,326.30	31,326.30
SO_4^{2-}	678.84	678.84	678.84	678.84	582.78	582.78
Br	212.56	212.56	212.56	212.56	212.56	212.56
d^2H (per mil)	–78.14	–78.14	–78.14	–78.14	–78.14	–78.14
$d^{18}O$ (per mil)	–12.11	–12.11	–12.11	–12.11	–12.11	–12.11
Tritium (^3H)	0	0	0	0	0	0

Table 4-2. Chemical and isotopic composition of the synthetic waters generated with the second mixing proportions (1.6% Br + 50.8% Lit + 24.4% Gl + 23.2% P) and different sets of reactions. Concentrations in mg/l.

Mixing proportions 2: 1.6% Br + 50.8% Lit + 24.4% Gl + 23.2% P						
	Sample 1	Sample 1a	Sample 1b		Sample 1c	Sample 1d
	Only Mixing	Mixing + equilibrium (calcite, illite, chlorite)	Mixing + cation exchange (CE) + calcite eq. b: CEC = 0.1	b': CEC = 0.2	Mixing + CE + calcite eq. + Sulphate reduction (SR)	Mixing + SR
pH	7.41	7.63	7.38	7.34	7.14	7.65
Na	2,036.20	2,036.20	1,853.43	1,769.06	2,236.20	2,036.20
K	69.83	68.97	53.99	51.61	50.79	69.83
Ca	412.02	408.82	658.51	742.68	369.46	412.02
Mg	230.34	231.53	183.74	178.32	152.85	230.34
HCO_3^-	50.92	46.13	50.64	50.03	147.05	168.16
Cl	4,158.60	4,158.60	4,158.60	4,158.60	4,158.60	4,158.60
SO_4^{2-}	473.66	473.66	473.66	473.66	377.60	377.60
Br	17.02	17.02	17.02	17.02	17.02	17.02
d^2H (per mil)	–77.13	–77.13	–77.13	–77.13	–77.13	–77.13
$d^{18}O$ (per mil)	–10.09	–10.09	–10.09	–10.09	–10.09	–10.09
Tritium (^3H)	39	39	39	39	39	39

Therefore, for each selected mixing proportion (1 and 2) there are six synthetic samples with which we have checked the inverse approach implemented in PHREEQC and in M4.

4.1.2 Inverse modelling with PHREEQC

This approach allows us to calculate all the possible mixing proportions (with respect to several selected end members) and mass transfers (with respect to a set of selected chemical reactions) able to justify the chemistry of a specific water sample.

In this case, the waters to justify (called "final waters" in the calculation procedure) are the synthetic waters presented above (except type-d samples, which are only used in M4 sensitivity analysis, section 4.3), and the end members (called "initial waters" in PHREEQC terminology): Brine, Littorina, Glacial and Precipitation, the same used in the direct modelling to create the synthetic waters (section 4.1.1). Some additional calculations were performed including more end members (Sea Sediment and Baltic) in order to check the effects of the end member selection in the final results.

Several sets of mineral phases (reactions) have been considered in the mass balance calculations (the same reactions used for the creation of synthetic waters):

- Set a: calcite, illite and chlorite (used in the synthetic waters) and also plagioclase, CH_2O, K-mica, and CO2.
- Set b: calcite, CaX2, NaX, MgX2 and KX.
- Set c: Set b plus the sulphate-reduction reaction.
- Set c': Set a plus the sulphate-reduction reaction.

In the following analysis, we use two or more of these sets in the mass balance calculations of the synthetic samples (1, 1a, 1b, 1c, 2, 2a, 2b, 2c) in order to assess the effect of the selection on the final results.

The chemical parameters used in the calculations (termed "constraints" in the terminology of the approach) are: pH, Na, K, Ca, Mg, HCO_3, SO_4, Cl, Br, δ^2H and $\delta^{18}O$. Except for Br, these elements have been already used in previous calculations (Forsmark 1.1, 1.2 and Simpevarp 1.1). Bromide has been included together with Cl, δ^2H, $\delta^{18}O$ and sulphate, as conservative elements during mixing. These elements are essential parameters in determining the mixing proportions because their concentration in the final water only depends on the end members mixing proportions. Calculations were repeated by deleting some of these conservative elements (Br or sulphate) and the results did not change very much in most cases. All other chemical parameters used in the calculations are subject to mole transfers and they are dissolved/precipitated from/to reacting phases to satisfy the calculation constrains (chemical concentrations of the elements).

Inverse modelling in PHREEQC also allows the treatment of analytical uncertainties, including both chemical and isotopic uncertainties. The value used for pH uncertainty is 0.05 pH units, 0.1 per mil for $\delta^{18}O$ uncertainty, 1 per mil for δ^2H uncertainty and 5% for the rest of the elements considered in the calculations.

In what follows, we present the mass balance results for the different types of samples under different headings: samples 1 and 2 (only mixing) and Type-a, b and c samples (mixing and reaction).

Results for Samples 1 and 2 (only mixing)

These synthetic samples are the result of conservative mixing between end members in the proportions indicated in section 4.1.1. Therefore, in principle, the inverse method of PHREEQC should only need the end members as initial waters to obtain these final waters (no mineral phases needed). However, in order to avoid errors in the resolution algorithm the definition of a feasible set of phases (reactions) is required. When doing this, and independently of the phases, PHREEQC obtains a set of possible models. The first one is always the pure mixing model which consistently reproduces (Table 4-3) the original mixing proportions of the synthetic samples. For these models, propagating the assumed uncertainties in order to maximize their effect in the mixing proportions, an uncertainty of 5% in the calculated mixing proportions is obtained.

The other models found by PHREEQC have certain amounts of mass transfers with respect to the set of selected samples. These transfers are insignificant and only produce variations of several tenths of percent in the mixing proportions (well inside the assumed uncertainties).

These results indicate that PHREEQC is able to detect with high precision the existence of a conservative mixing process. This seems obvious, as the synthetic waters have been created with the same code. However, the mathematical algorithm used for the inverse modelling is completely different to the one used in the direct method and, up to now, it has not been used in the way it is used in the study of this kind of systems.

Table 4-3. Mixing proportions obtained by inverse modelling with PHREEQC for Samples 1 and 2 (created by pure mixing with the direct approach).

		Sample 1		Sample 2	
		Synthetic data (PHREEQC direct approach)	Inverse approach Results without mass transfer	Synthetic data (PHREEQC direct approach)	Inverse approach Results without mass transfer
% Mixing	Brine	60	59.41	1.6	1.61
	Littorina	10	10.55	50.8	51.18
	Glacial	30	30.03	24.4	24.60
	Precipitation	0	0.00	23.2	24.61

Results for Samples 1a and 2a

Type-a samples were created assuming mixing (with mixing proportions 1 and 2) and equilibrium with calcite, illite and chlorite. As we showed in Tables 4-1 and 4-2, the effect of these reactions on the dissolved concentration of the selected elements is very small, indeed smaller in most cases than the analytical uncertainty considered in the calculations.

When including the first set of phases (Set a column in Table 4-4, the same set of reactions used for the creation of these waters), the obtained models reproduce almost perfectly the mixing proportions of the samples and the very low mass transfers (Table 4-4). Even in some models there are not mass transfers needed to justify the final waters. This means that waters type (a) could be explained only by conservative mixing, which is reasonable considering that the chemical changes produced by the reactions are inside the preset uncertainty limits. Taking into account these input uncertainties, maximum variations in the mixing proportions are of the order of ± 2%.

When including the second set of phases (Set b column in Table 4-4, ionic exchange), PHREEQC obtains again some models with only mixing which reproduce almost perfectly the mixing proportions of the samples (Table 4-4). The rest of the models with higher mass transfers produce more variable mixing proportions, although always close to the theoretical ones. Mass transfers associated to the exchange reactions are reasonable and they represent a minor percent of the dissolved concentrations.

These results show the variations associated to the uncertainty ranges assigned to the calculations. The variations related to uncertainties in the set of phases, can increase that variation up to a maximum of 9%.

Table 4-4. Mixing proportions obtained by inverse modelling with PHREEQC to reproduce the chemical contents in Samples 1a and 2a created by mixing and reaction with the direct approach. The influence of changing the set of phases in the mass balance calculations is also evaluated and shown under columns labelled "Set a" and "Set b".

	Sample 1a				Sample 2a			
		Inverse approach				Inverse approach		
	Synthetic data (Direct approach)	Set a	Set b No mass transfer	Set b With mass transfer (range)	Synthetic data (Direct approach)	Set a	Set b No mass transfer	Set b With mass transfer (range)
% Brine	60	59.02	59.07	63–65	1.6	1.65	1.60	1.6–1.9
% Littorina	10	10.9	10.88	7.4–10.9	50.8	50.48	50.55	47.6–50.9
% Glacial	30	30.07	30.05	25.4–31.1	24.4	24.23	24.27	22.7–24.5
% Precipitation	0	0.0	0.0	0.0–8.7	23.2	23.64	23.53	22.9–27.8

Results for samples 1b and 2b

In samples type (b) ionic exchange processes and calcite equilibrium introduce chemical changes in the waters more important than the insignificant changes produced by the mineral equilibrium (type a; Tables 4-1 and 4-2).

When including the second set of phases (column "Set b"in Table 4-5), which is the same set of reactions used to generate the waters , different models are obtained. Some of them reproduce exactly the original mixing proportions and mass transfers used for the creation of these waters. Table 4-5 gives the range of variation in mixing proportions taking into account the whole set of models found by PHREEQC. These variations are most important in the Precipitation end member, although always lower than 10%.

When considering the first set of phases (column "Set a"in Table 4-5; mineral equilibrium) the number of models found by PHREEQC and the variation in mixing proportions are lower. Mixing proportions for Sample 1b agree very well with the original proportions. As for Sample 2b, differences between original and calculated proportions are lower than 8%, being the highest for the Precipitation end member. Both mass transfers (of the order of tenths of millimoles) and the direction of reactions (dissolution-precipitation) are reasonable in the light of this methodology.

These results indicate that mixing proportions can be well reproduced with no important effects from reactions. However, as different sets of reactions are able to justify the chemistry of the final waters, it means the need of delimitating the effective reactions that are taking place in the system, using additional approaches

Although this fact could support the use of the methodology to obtain the mixing proportions, it involves an important uncertainty in itself. As mixing is the dominant process in determining the water composition, the effects of reactions (basic processes controlling other parameters not implicitly considered in the mass balance calculations, eg. Eh) are, in most cases, hidden in the uncertainty ranges used in the calculations.

Table 4-5. Mixing proportions results obtained by inverse modelling with PHREEQC to reproduce the chemical contents in Samples 1b and 2b created by mixing and reaction (ionic exchange) with the direct approach. The influence of changing the set of phases in the mass balance calculations is also evaluated and shown under columns labelled "Set a" and "Set b".

	Sample 1b			Sample 2b		
	Synthetic data (Direct approach)	Inverse approach		Synthetic data (Direct approach)	Inverse approach	
		Set b (low mass transfer)	Set a		Set b (low mass transfer)	Set a
% Brine	60	57.6–63.3	59.50	1.6	0.0–3.0	3.0
% Littorina	10	8.5–12.5	10.45	50.8	44.0–58.0	44.6
% Glacial	30	28.1–30.1	30.03	24.4	20.9–28.3	31.2
% Precipitation	0	0.5–7.5	0.0	23.2	13.0–31.0	21.2

Results for Samples 1c and 2c

These samples represent the effects of ionic exchange, calcite equilibrium and sulphate-reduction. However, when including the third set of phases (column "Set c" in Table 4-6; the same set of reactions used to create these waters) the models obtained show the highest variation in mixing proportions.

Sulphate-reduction affects dissolved sulphate content. This element is in very high concentration in the two sets of synthetic waters and it can be explained by mixing of the two end members with the highest sulphate content: Littorina and Brine. This is the reason for finding mixing proportion variations of up to 8% for these end members depending on whether sulphate is treated as a conservative or a non conservative element.

Although these variations could be considered acceptable in most cases, it casts a shadow of doubt on the results, indicating the need of independently checking the presence of sulphate-reduction process, or of delimitating its extension with additional data (iron and sulphide concentrations, sulphur isotopes data, etc), most of them not available up to now.

When using the fourth set of phases (column "Set c'" in Table 4-6), the models found predict mixing proportions closer to the original ones and with a smaller variability. These results indicate, again, that similar mixing proportions can be obtained using very different sets of reactions.

Table 4-6. Mixing proportions results obtained by inverse modelling with PHREEQC to reproduce the chemical contents in Samples 1c and 2c created by mixing and reaction (ionic exchange and sulphate reduction) with the direct approach. The influence of changing the set of phases in the mass balance calculations is also evaluated and shown under columns labelled "Set c" and "Set c'".

	Sample 1c			Sample 2c		
	Synthetic data (Direct approach)	Inverse approach		Synthetic data (Direct approach)	Inverse approach	
		Set c (range)	Set c' (range)		Set c (range)	Set c' (range)
% Brine	60	62.6–68.4	64.0–64.5	1.6	0.8–2.1	1.1–1.2
% Littorina	10	0.0–8.0	6.0–8.0	50.8	45.6–58.6	50.6–56.5
% Glacial	30	25.0–29.5	28.2–28.9	24.4	21.6–33.1	24.3–27.4
% Precipitation	0	0.0–11.3	0.0	23.2	12.0–30.7	15.0–23.9

4.1.3 Discussion and conclusions

Mixing and mass balance calculations performed with PHREEQC, give a reasonable estimate of the considered end members mixing proportions. The use of, at least, three conservative elements (Cl, δ^2H, $\delta^{18}O$) seems to provide extra robustness to the calculated proportions independently of the reactions (phases) included in the calculations. This statement must be conveniently explained.

First, all these results start with a selection of the end members to be used in the calculations. The effects of a different selection were already checked elsewhere /Laaksoharju 1999, Luukonen 2001/ and can dramatically modify the obtained mixing proportions and mass transfers. Several calculations were made in the present work with two additional end members (Sea Sediment and Baltic) in the inverse modelling not used in the direct calculations. The results indicate that Littorina proportions were the most affected, either lowering its proportions or producing the transfer of its proportion to one of the two new end members, Baltic or Sea Sediment. Therefore, the end members selection is a fundamental point in this methodology and it requires a very careful hydrogeological and geochemical study of the system.

Second, sulphate-reduction in waters with high sulphate contents (similar to the ones used in this work) produces additional variations, mainly in the mixing proportions of the end members which supply this component to the waters (Brine and Littorina). Therefore, the real presence of this process must be clearly established before the mass balance calculations are performed. Alternatively, the inclusion of a higher number of parameters in the model should be taken into account.

Finally, with the analytical data used in the mass balance calculations, the chemistry of groundwaters can be explained by invoking the actuation of different reactions, mainly ionic exchange and equilibrium with different mineral phases (mainly aluminosilicates and calcite). However, the lack of aluminium data in the studied groundwaters and exchange capacity constants in the fracture filling minerals, are two important limitations, both in assessing the feasibility and extent of these processes before the balance calculation are carried out, and in the overall performance of the approach.

4.2 M4: Mixing proportion sensitivity to end-member composition variability

A procedure has been developed to assess the impact of the compositional variability of water end members on the calculated mixing proportions. This scheme is based on a PCA analysis performed with a modified version of M3 code /Laaksoharju et al 1995, Laaksoharju and Wallin 1997, Laaksoharju et al. 1999ab, Laaksoharju et al. 2000/. This section describes the procedure and the results obtained using Laxemar 1.2 data set (Local Model, 356 superficial and groundwaters).

4.2.1 Motivation

The calculation of water mixing proportions by means of a PCA analysis is a well established and useful practice when dealing with a large number of samples /Laaksoharju and Skårman 1995ab, Smellie and Karlsson 1996, Gurban et al. 1998, Laaksoharju et al. 1999ab, Laaksoharju 2004a/. However, this type of analysis has the drawback of a priori selecting a set of end members, whose number and compositions are fixed in advance. A preliminary exploratory analysis can, in principle, identify the end members to be used, but this selection, mainly based on expert judgment, is always tricky and, in many cases, difficult to justify /Bath and Jackson 2002, Svensson et al. 2002/.

The selection is even more critical when the mixing proportions coming out of the PCA analysis are to be used by hydrogeologists to “transport” them spatially through the system (using flow lines) or temporally through time (to predict future changes in water composition).

In order to overcome these difficulties, here we propose a modification of the standard PCA procedure (as implemented in M3 code) that takes into account the intrinsic compositional variability of the end members. The procedure starts from a pre-selected number of end members, i.e. no attempt is made here of defining which end members to use in the analysis (the selection could be made by expert judgment or using the procedure explained in Appendix C of the Appendix 3 in /Laaksoharju 2005/, and has the following steps (Figure 4-1):

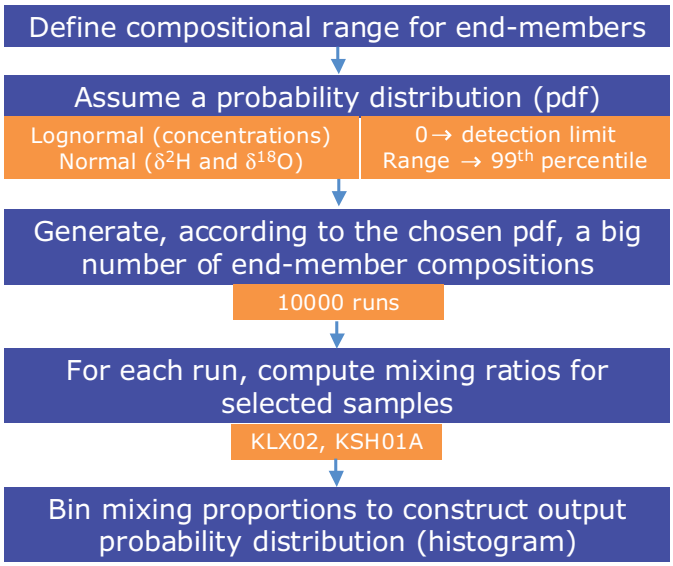

Figure 4-1. *Flowchart of the procedure implemented to assess the impact that the compositional variability of end members has on mixing proportions.*

1. Define the compositional variability of the end-members.
2. Construct a probability density function (input probability) from the compositional ranges.
3. Generate, according to the chosen input probabilities, a large number of end member compositions.
4. For each run, compute the mixing proportions of selected samples.
5. Bin mixing proportions to construct the output probability.

What follows is a brief summary of each step.

Definition of the compositional range for the selected end-members. Each end member is characterized by two samples (real or synthetic) that represent the maximum variability expected for that end member. The selection is made by expert judgment, taking into account all the geochemical and hydrological knowledge of the system. Note that this is not the same as selecting, by expert judgment, a fixed composition for the end member, as the standard PCA analysis does. Here expert judgment selects a range of compositions, relaxing in this way the requirement of knowing the exact composition of each end member to be used in the mixing calculation. Table 4-7 summarises the ranges that have been defined for the end members in the modelling of Laxemar 1.2 data set (Local Model). The extreme values for each end member have been selected in the following way:

Table 4-7. Compositional ranges of the end members used in Laxemar 1.2 PCA mixing modelling.

End member	Na (mg/l)	K (mg/l)	Ca (mg/l)	Mg (mg/l)	HCO_3 (mg/l)	Cl (mg/l)	SO_4 (mg/l)	δ^3H (‰)	^3H (TU)	$\delta^{18}O$ (‰)
Brine 1	8,500.00	45.5	19,300.00	2.12	14.10	47,200.0	906.0	–44.9	0.00	–8.9
Brine 2	9,540.00	28.0	18,000.00	130.00	8.20	45,200.0	8.4	–49.5	0.00	–9.3
Glacial 1	0.17	0.4	0.18	0.10	0.12	0.5	0.5	–158.0	0.00	–21.0
Glacial 2	0.17	0.4	0.18	0.10	0.12	0.5	0.5	–125.0	0.00	–17.0
Littorina 1	3,674.00	134.0	151.00	448.00	93.00	6,500.0	890.0	–38.0	0.00	–4.7
Littorina 2	1,960.00	95.0	93.70	234.00	90.00	3,760.0	325.0	–53.3	0.00	–5.9
Rain 1	0.00	0.0	0.00	0.00	0.00	0.0	0.0	–125.0	0.00	–17.0
Rain 2	0.00	0.0	0.00	0.00	0.00	0.0	0.0	–44.0	168.00	–6.9
DGW 1	19.20	3.0	38.50	3.80	162.00	12.0	21.5	–68.4	11.91	–9.9
DGW 2	237.00	4.0	25.00	6.00	370.00	119.0	118.0	–73.8	0.78	–9.9

- **Brine 1** corresponds to the most saline sample found in Laxemar and it is characterised by a very high sulphate content. This is the sample that has been used as the Brine end member in the previous works at Simpevarp and Forsmark areas.
- **Brine 2** corresponds to the sample KRA/860/2 (from Finland) which is considered the most saline sample in Finland and is characterised by a low sulphate content. This is the sample that has been used as the Brine end member in the site characterisation studies in Finland.
- **Glacial 1** corresponds to a glacial melt water present in the system several thousand years ago, and it is the Glacial end member used in the previous works at Simpevarp and Forsmark areas.
- **Glacial 2** corresponds to a modern glacial melt water (different values for stable isotopes).
- **Littorina 1** corresponds to the theoretical composition of the Littorina Sea, so it represents an old Baltic sea water. It has been used by the Finnish in their site characterisation studies and it has also been used as the Littorina end member in the previous works in Simpevarp and Forsmark areas.
- **Littorina 2** corresponds to the present Baltic waters. It is the sample used as the Baltic end member in the previous works at Simpevarp and Forsmark areas.
- **Rain 1** corresponds to an old winter rain with no tritium and very low values for the stable isotopes.
- **Rain 2** corresponds to the summer rain in the sixties with the maximum tritium and the highest values for the stable isotopes.
- **DGW 1** corresponds to a sample from the Bockholmen subarea (borehole HBH05) which is representative of a diluted granitic groundwater.
- **DGW 2** corresponds to a sample from the Äspö subarea (borehole HAS05) which is representative of a diluted granitic groundwater. Together with the DGW 1 cover the whole range of chemical and isotopic compositions of very shallow granitic groundwaters, below the overburden.

Mixing calculations have been carried out in Laxemar 1.2 with four end members: Brine + Glacial + Littorina + Rain when dealing with the whole data set (superficial and groundwaters, 356 samples), and Brine + Glacial + Littorina + Dilute Groundwater when dealing only with the groundwaters (158 samples).

Construction of the input probabilities. For the definition of the probability density functions (pdfs) that characterize the compositional variation of each end member we have adopted the following two assumptions: (1) all compositional variables follow a *log-normal distribution;* and (2) the ranges listed on Table 4-7 have been equated to the *95th percentile* of the chosen probability function, which means that we allow for end member compositions outside the reported range.

Once a probability function has been chosen and the statistical meaning of the empirical compositional range defined, the input probability functions are completely characterized (Figure 4-2).

Figure 4-3 plots the pdfs for all ten compositional variables used in the PCA mixing analysis: seven chemical species (Na, K, Ca, Mg, HCO_3, Cl, and SO_4), two stable isotopes (^2H and ^{18}O), and 3H. The pdfs have been constructed binning 10,000 values for each compositional variable and normalizing to ensure that the area under the curve is one.

The concentrations of Na, K, Ca, Mg, HCO_3, Cl, SO_4 and ^3H have been approximated by a pdf as explained above. However, ^2H and ^{18}O pose an special problem because they are delta-values, calculated as the ratio of two concentrations and then normalized with respect to a reference concentration, what means that they can have both positive and negative values. This is incompatible with a lognormal distribution, which is only defined for positive real numbers. To overcome this difficulty, we use the fact that a lognormal distribution can be approximated by a Gaussian distribution when the coefficient of variation α, the standard deviation divided by the mean, is very low (less than one), as is the case for deuterium and ^{18}O values in Laxemar 1.2 data set. The coefficient of variation of deuterium is $\alpha = 0.173$ and that of ^{18}O is $\alpha = 0.176$. Using a Gaussian distribution for deuterium and ^{18}O simplifies the procedure and does not introduce a measurable error.

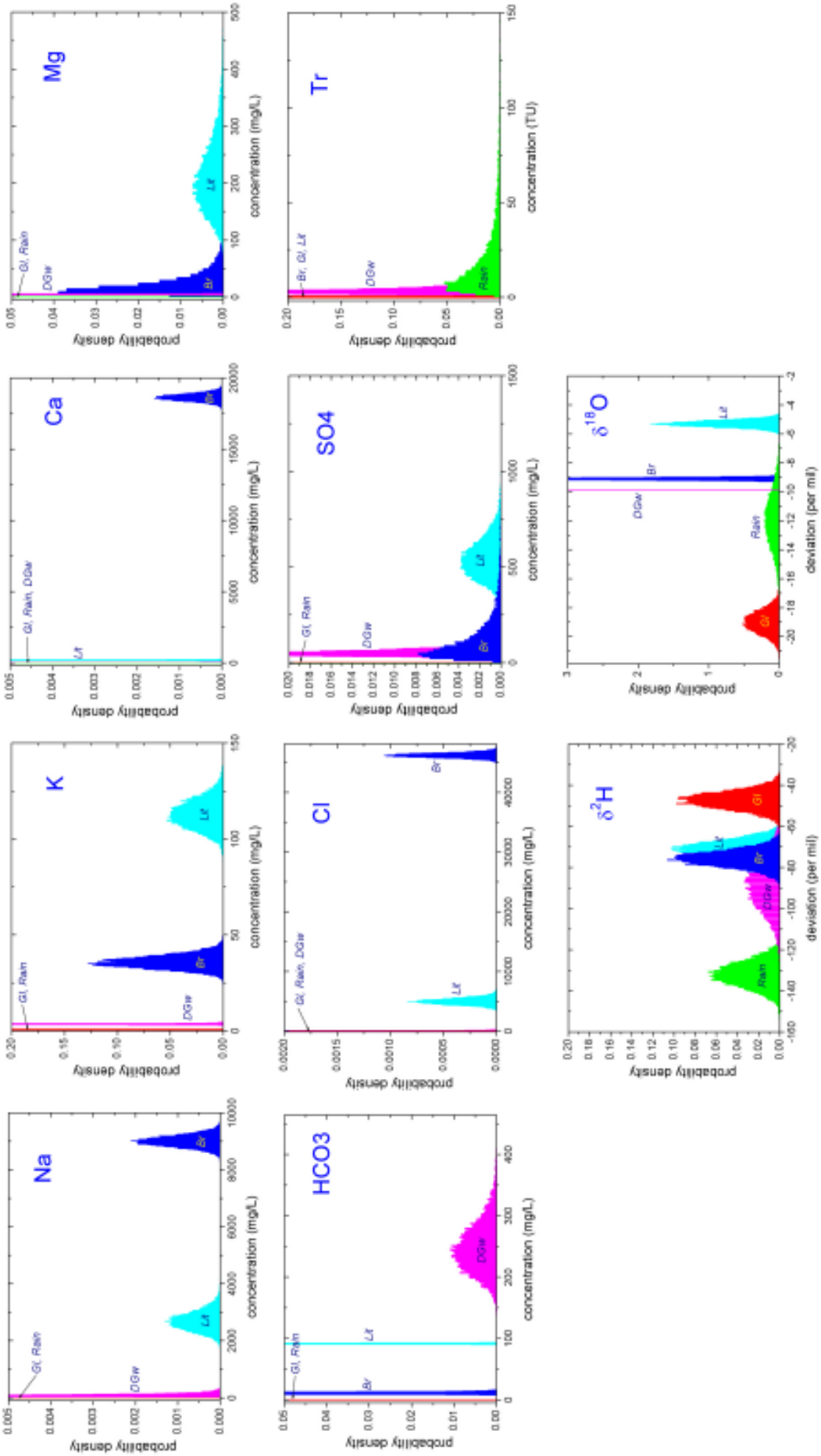

Figure 4-2. *Input probability density functions for all the chemical and isotopic variables considered in the PCA, as constructed from the compositional ranges of the end-members Brine (blue), Glacial (red), Littorina (cyan), Rain (green) and Dilute Groundwater (magenta).*

Generation of end member compositions. Once the input probability density functions are defined, the procedure generates a large number of compositions for each end member. These compositions are randomly sampled from the corresponding pdf and fed into the PCA analysis. The upper graph in Figure 4-3 is a PC1-PC2 plot of the Laxemar 1.2 groundwater data set (158 samples), where 10,000 compositions have been generated using end members Brine + Glacial + Littorina + Dilute Groundwater. The end member compositions are plotted in different colours while the position of the samples are in black. The lower graph in Figure 4-3 is the corresponding plot for the whole Laxemar 1.2 data set (357 samples) and using Brine + Glacial + Littorina + Rain as end members.

To generate the end member compositions we have taken into account the correlation between ^{2}H and ^{18}O delta-values (Figure 4-4). In practice this means that we give a random value to ^{18}O according to its input pdf and then compute the ^{2}H delta-value using the regression quoted in Figure 4-4. This regression is a weighted least-squared fit to 1,660 superficial and groundwater samples from the Baltic Shield. To the predicted deuterium value we add a random Gaussian deviate of ± 3.5 per mil, which is the dispersion of deuterium values around the best-fit line (inset in Figure 4-4). We use this method for fresh and brackish waters, but not for brines (Cl > 25,000 mg/L), as they do not follow the regression line but plot above it, inside the blue ellipse in Figure 4-4.

Computation of mixing proportions. Once the PCA coordinates of each sample are known, we compute their mixing proportions by means of a hyperspace version of M3 code which uses the information stored in all principal components. The procedure has been described in /Laaksoharju 2005/, and we refer the reader to the literature.

Construction of the output probability densities. Each run gives, for each sample, a set of mixing proportions. For example, run #234 gives, say, the following mixing proportions for Sample #5268: Brine = 11.3%, Glacial = 58.6%, Littorina = 12.1%, and Dilute Groundwater = 18.0%. Then the 10,000 runs, each with a different composition for the end members, give 10,000 different mixing proportions for sample #5268 (and for any other selected sample, of course). In that way we can assess how the variability in the composition of the end members is propagated to the calculated mixing proportions. If the computed mixing proportions for a particular sample have a very broad variability (let's say, from 10% to 80% of the glacial end member), it would mean that mixing proportions are very sensitive to changes in the composition of the end members, casting serious doubts on the mixing results. If, on the other hand, mixing proportions for a sample concentrate around particular values, it would mean that they are not too sensitive to changes in end member composition, strengthening the case for a robust result.

Figure 4-5 shows the output pdfs for 3 selected groundwater samples from borehole KSH01A (Simpevarp area) and Figure 4-6 the output pdfs for six samples from borehole KLX02 (Laxemar area). As can immediately be appreciated, the range of mixing proportions for each of the selected samples is quite narrow, considering the a priori compositional variability of the end members. This is a strong indication that the computed mixing proportions are indeed a robust estimator of the mixing behaviour of the waters.

Table 4-8 shows the mean and standard deviation of the mixing proportions for the 9 analysed samples. The maximum deviation is ± 5.2% (i.e. approx. 68% of the calculated mixing proportions are inside a bracket of width 10.4%) and the average deviation 2% (i.e. the average of 36 standard deviations: nine samples times four end members each).

The important conclusion that can be drawn from the above results is that, once the number and type of end members are known, the inclusion of the compositional variability of the end members in the PCA analysis gives a robust estimation of the mixing proportions, in the sense that the output probability functions are narrow, predicting mixing proportions tightly concentrated around a mean value. The bonus of this analysis, apart from the robustness itself, resides in the statistical bracketing of the variability of the mixing proportions, which is a fundamental issue when "exporting" these results for hydrogeological modelling.

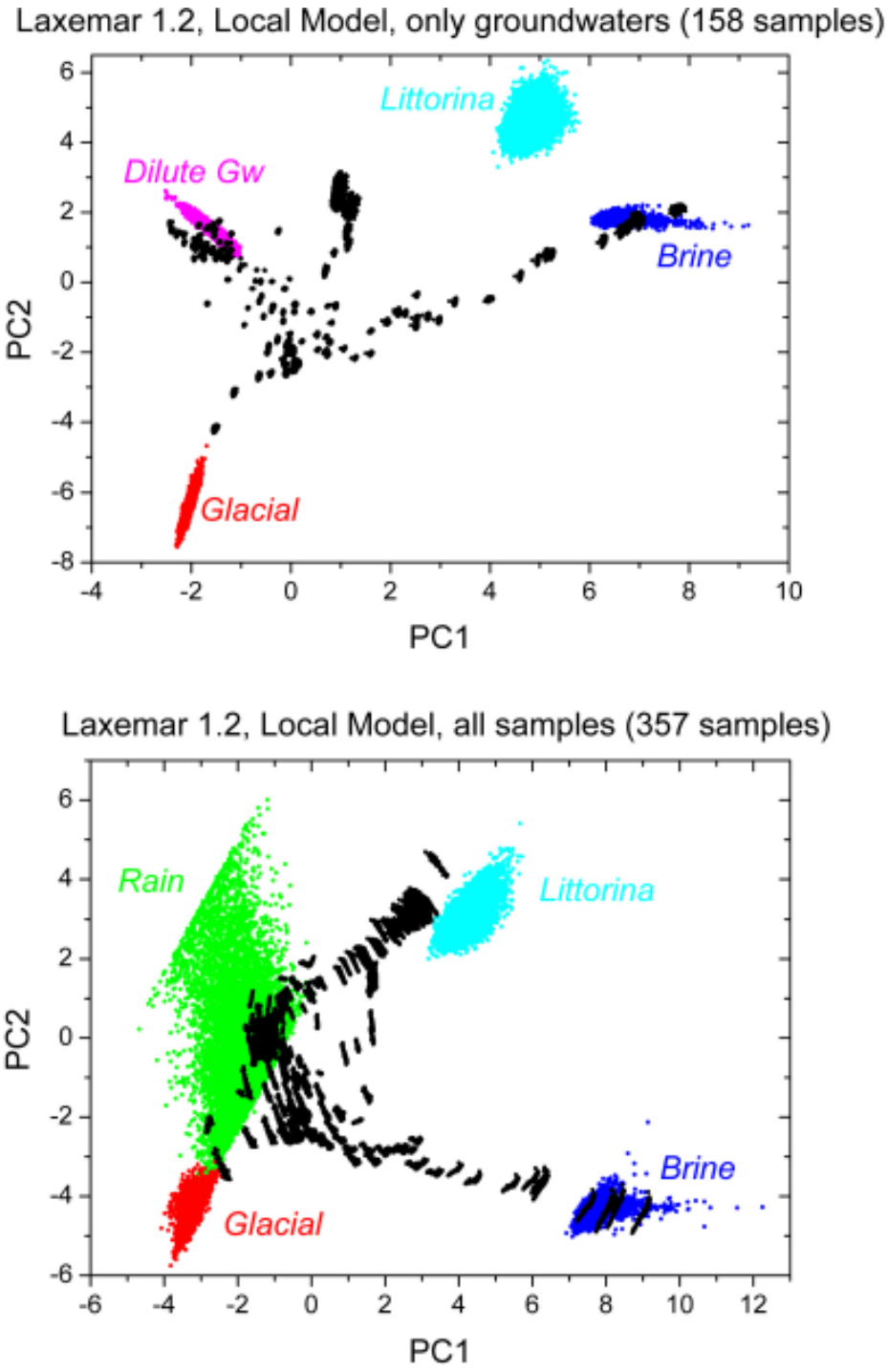

Figure 4-3. *PCA plot for Laxemar 1.2 Local Model data set. Upper graph: Only groundwaters (158 samples). Lower graph: Superficial and groundwaters (357 samples). Each end member is represented by 10,000 compositions (coloured dots) taken from a pdf defined by a predefined compositional range. Black dots correspond to the samples. These plots are like the superposition of 10,000 individual PCA plots, each computed with a different set of compositions for the end-members.*

Table 4-8. Mean and standard deviation for the mixing proportions of the selected samples from boreholes KLX02 and KSH01A.

		Brine (%)		Glacial (%)		Littorina (%)		Dilute Gw (%)	
	Sample	Mean	Std	Mean	Std	Mean	Std	Mean	Std
Laxemar KLX02	2738	1.8	1.3	9.1	3.0	2.4	1.3	86.7	5.2
	2712	6.4	1.1	22.1	2.5	4.6	1.1	66.8	4.2
	2934	50.4	1.5	29.9	1.8	0.0	0.0	19.7	2.3
	2722	56.1	1.6	31.2	1.8	0.0	0.0	12.7	2.4
	2931	81.7	3.0	11.6	0.9	0.0	0.0	6.7	3.4
	2731	98.3	3.6	0.0	0.1	0.0	0.1	1.7	3.6
Simpevarp KSH01A	5263	9.1	1.2	51.2	2.8	17.2	1.6	22.5	2.9
	5268	11.5	1.2	57.0	3.0	14.7	1.4	16.8	2.9
	5288	24.2	1.2	45.4	2.5	9.2	1.4	21.2	2.6

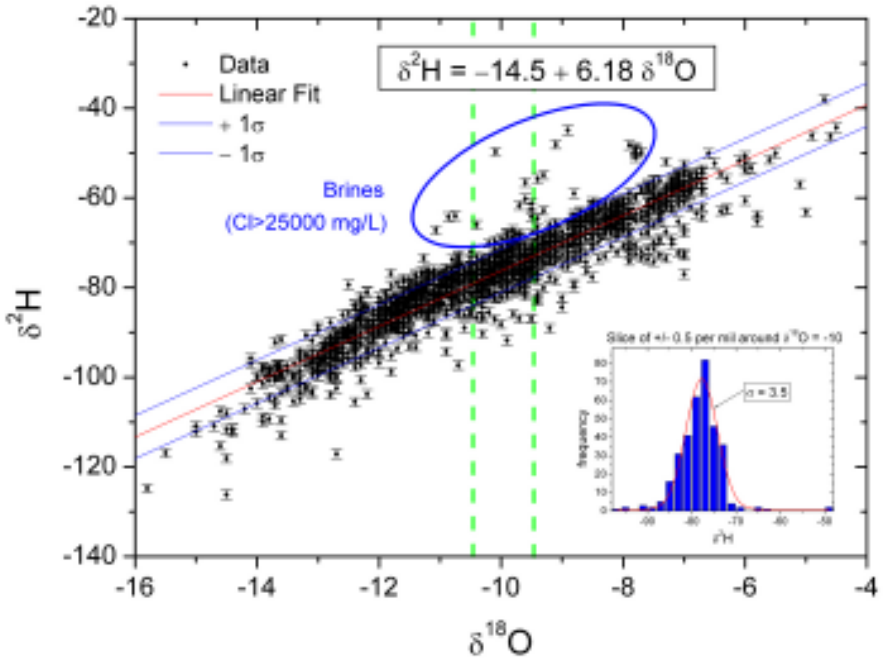

Figure 4-4. *δ^2H-$\delta^{18}O$ plot for 1,660 groundwater and superficial samples of the Baltic Shield. The red line is a weighted least square fit to the data assuming a δ^2H error equal to the detection limit (2‰). The blue lines are the ± 1σ bounds (68.3 % of the data point fall between the blue lines). The inset shows, for a slice centred around $\delta^{18}O$ = –10 (green vertical dashed lines), the dispersion of the data points, which is ± 3.5‰ in terms of the standard deviation. We are assuming that $\delta^{18}O$ values are exact (no error in the horizontal axis). This correlation has been applied to all samples with a Cl content less than 25,000 mg/L.*

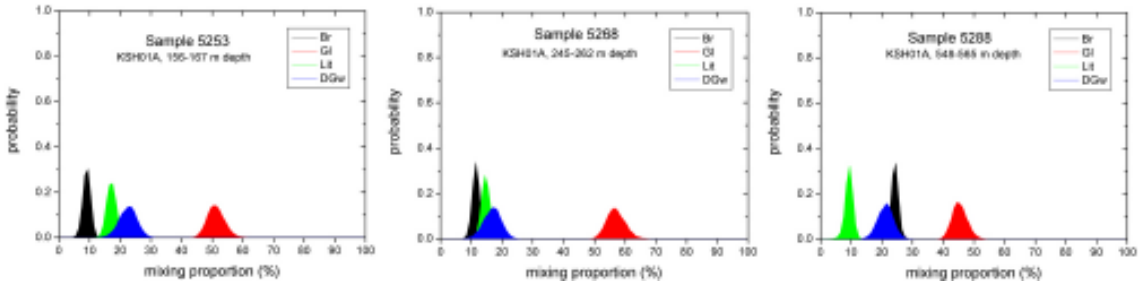

Figure 4-5. *Mixing proportions for three samples from borehole KSH01A (Simpevarp area). End members used for the calculations are Brine + Glacial + Littorina + Dilute Groundwater. For the PCA analysis only groundwater samples from Laxemar 1.2 iteration were used (158 samples).*

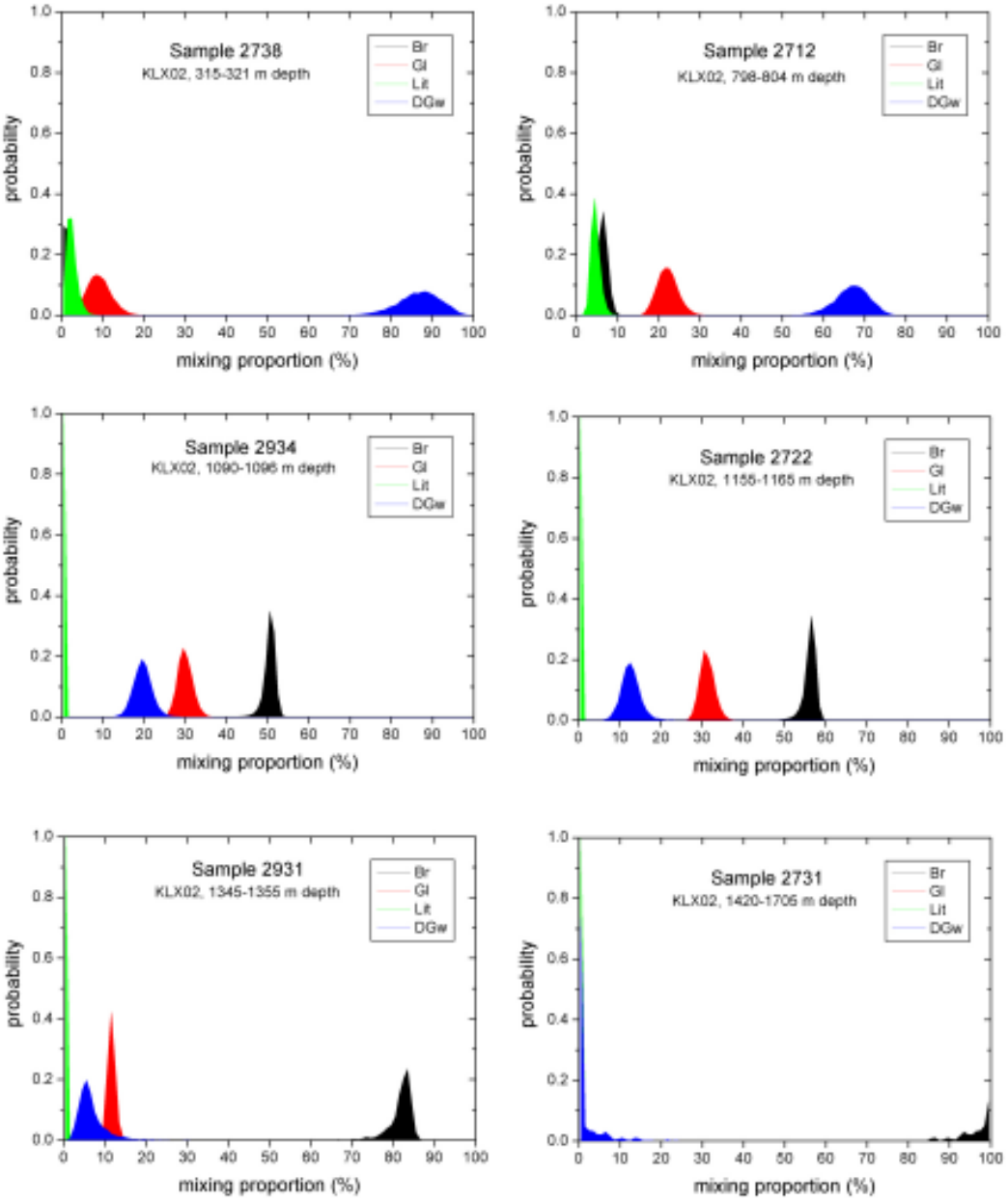

Figure 4-6. *Mixing proportions for selected samples of KLX02 borehole (Laxemar area). End members used for the calculations are Brine + Glacial + Littorina + Dilute Groundwater. For the PCA analysis only groundwater samples from Laxemar 1.2 iteration were used (158 samples).*

4.3 M4 verification: chemical reactions effects on the calculated mixing proportions.

Synthetic waters created by PHREEQC in section 4.1.1 with known mixing proportions and reaction processes, have been used for verifying M4 performance. These samples (Tables 4-1 and 4-2) group into two sets defined by two different mixing proportions. The compositional variability inside each set is related to the addition of reactions to the basic mixing.

Ideally, for each set, M4 should provide mixing proportions as close as possible to the original ones, independently to the variability introduced by the reactions. Then, the chemical differences between the synthetic water and the water obtained from the M4-calculated mixing proportions, could be used, via a mass balance step, for checking the existing reactions (method traditionally used in M3 calculations).

In order to verify this assumptions, the synthetic waters shown in Tables 4-1 and 4-2 have been included in Laxemar 1.2 dataset (Local Model, groundwaters only). Mixing proportions have been calculated considering Brine, Glacial, Littorina and Precipitation (= Rain) as end members. The variables used for these calculations are: Na, K, Ca, Mg, HCO_3. SO_4, Cl, δ^2H, $\delta^{18}O$, 3H. The results obtained for the different synthetic samples are shown below.

4.3.1 Samples representative of pure mixing

Here, the synthetic waters created by conservative mixing (samples 1 and 2) and by mixing and equilibrium (samples 1a and 2a) are included (Table 4-9).

As Table 4-9 shows, M4 reproduces very well the mixing proportions for all samples. This result is important in itself, as it demonstrates that the hyperspace generalization of the PCA analysis implemented in M4 is able to correctly evaluate the "simple" mixing processes in waters. M4 uses the information stored in all principal components for calculating the mixing proportions, improving in that way the procedure implemented in M3, which uses only the information stored in the first two principal components. As M3 results for samples 1 and 2 noticeably deviate from the original proportions, this code will not be used in the following discussion.

Table 4-9. M4 results for the synthetic waters created by conservative mixing (Samples 1 and 2) and for those in which chemical reactions produce only minimal deviations from pure mixing (Samples 1a and 2a). The upper part of the table (% Mixing) contains the calculated mixing proportions. The lower part (% mass balance) shows the mass balance calculated by M4 for the three conservative elements (Cl, δ^2H and $\delta^{18}O$). Results of mass balance for conservative elements are calculated as (concentrations in sample – predicted concentrations)/concentrations in sample.

		Water samples 1			Water samples 2		
		Synthetic data (PHREEQC)	M4 results Sample 1 Pure mixing	Sample 2 Mixing + mineral eq.	Synthetic data (PHREEQC)	M4 results Sample 1 Pure mixing	Sample 2 Mixing + mineral eq.
% Mixing	Brine	60	60.0	58.2	1.6	1.4	1.3
	Littorina	10	11.5	12.4	50.8	51.7	51.8
	Glacial	30	28.5	29.4	24.4	24.4	24.9
	Precipitation	0	0.0	0.0	23.2	22.5	21.9
% Mass Balance	Cl		7.2	9.7		3.1	4.02
	δ^2H		2.3	3.0		0.4	0.01
	$\delta^{18}O$		1.7	3.0		0.0	0.00

The ability to identify pure mixing processes (in which all the elements behave as conservative) allows us to check, for the first time, the actual non conservative behaviour of the chemical elements included in the PCA analysis. In this methodology, similar to the one implemented in M3, reacting constituents were treated on exactly the same footing as the non-reactive ones and therefore the reacting constituents also influence the computed mixing fractions of every water sample. This problem is explored in the following sections.

4.3.2 Samples with mixing and ionic exchange

M4 results for those synthetic samples created by mixing and ionic exchange (samples 1b, 1b', 2b and 2b') show different mixing proportions with respect to the ones used to create the samples. These differences depend on the type of sample (Table 4-10).

For samples 1b and 1b', with Brine as the major end member, M4 mixing proportions have an uncertainty of 7% for Littorina and lower for the rest of the end members (specially for Glacial). The predicted concentration of the conservative elements (Cl, δ^2H, $\delta^{18}O$) is in very good agreement with the original ones, and always with uncertainties below 6%.

For samples with Littorina as the main end member (samples 2b and 2b') M4 results are far away from the original mixing proportions, specially for Brine and Littorina (Table 4-10). Mass balances show differences of around 50% (for Cl) with respect to the synthetic sample.

These results are particularly important when checking the reliability of the mixing proportions provided by M4. In fact, they indicate that the effects of the chemical reactions propagate into the calculated mixing proportions and, therefore, M4 mixing proportions can not be used to calculate the mass balance of the non conservative elements. This is obvious looking at mass balances, in Table 4-10, for chloride, conservative element whose calculated concentration should be in a perfect agreement with the value in the synthetic water.

The noise produced by a set of chemical reactions in the analysis performed by M4 is not homogeneous and depends on the chemical characteristics of the sample. While in some cases (1b and 1b') the variation in the mixing proportions can be acceptable, in others (2b and 2b') they are really far from the synthetic ones.

Table 4-10. M4 results for the synthetic waters created by mixing and ionic exchange plus calcite equilibrium (Samples 1b, 1b', 2b and 2b'). The difference between b and b' samples is the amount of the cation exchange: samples 1b and 2b are obtained with a value of 0.1 mol/kg H_2O, and samples 1b' and 2b' with a value of 0.2 mol/kg H_2O. The upper part of the table (% Mixing) contains the calculated mixing proportion. The lower part (% mass balance) shows the mass balance calculated by M4 for the three conservative elements (Cl, δ^2H and $\delta^{18}O$. Results of mass balance for conservative elements are calculated as (concentrations in sample – predicted concentrations)/concentrations in sample.

		Water samples 1			Water samples 2		
		Synthetic data (PHREEQC)	M4 results CEC increase →		Synthetic data (PHREEQC)	M4 results CEC increase →	
			Sample 1b	Sample 1b'		Sample 2b	Sample 2b'
% Mixing	Brine	60	61.24	65.89	1.6	8.1	8.5
	Littorina	10	9.94	2.94	50.8	36.6	35.3
	Glacial	30	28.82	31.17	24.4	23.8	24.1
	Precipitation	0	0.00	0.00	23.2	31.4	32.1
% Mass Balance	Cl		5.7	0.1		49.9	55.9
	δ^2H		1.7	2.2		4.2	4.8
	$\delta^{18}O$		0.8	3.3		6.0	6.9

4.3.3 Samples with mixing and sulphate reduction

The effects of the sulphate-reduction processes on the chemical variables included in this kind of statistical analysis are only visible in sulphate and bicarbonate concentrations. Sulphate reduction is a reaction with relatively simple effects on two parameters, as it can be clearly seen in Tables 4-1 and 4-2 comparing the concentrations in the column for samples 1d and 2d, with those under the column for samples 1 and 2: only sulphate and bicarbonate change.

M4 results depends on the sample (Table 4-11). For the saline water the calculated mixing proportions are close to the original ones; however, for the brackish water the values are really far. Mass balance calculations for the conservative elements are very useful (again) to detect this problem: while in sample 1d the deviation in chloride is under 5%, in sample 2d, it is around 80%.

Table 4-11. M4 results for the synthetic waters created by mixing and sulphate-reduction (Samples 1d and 2d). The upper part of the table (% Mixing) contains the calculated mixing proportions. The lower part (% mass balance) shows the mass balance calculated by M4 for the three conservative elements (Cl, δ^2H and $\delta^{18}O$). Results of mass balance for conservative elements are calculated as (concentrations in sample – predicted concentrations)/concentrations in sample.

		Water samples 1		Water samples 2	
		Synthetic data (PHREEQC)	M4 results	Synthetic data (PHREEQC)	M4 results
			Sample 1d Sulphate-reduction		Sample 2d Sulphate-reduction
% Mixing	Brine	60	64.4	1.6	12.6
	Littorina	10	4.5	50.8	22.7
	Glacial	30	23.6	24.4	13.7
	Precipitation	0	7.5	23.2	51.0
% Mass Balance	Cl		2.0		78.5
	δ^2H		5.4		0.5
	$\delta^{18}O$		3.3		3.0

4.3.4 Calculations only with conservative elements

From all the previous results, it can be said that the modifications introduced by the chemical reactions on some elements give rise to deviations in the mixing proportions calculated by M4. These deviations can be more or less important depending on the type of reaction, its extent and the type of water involved, all unknowns in a study with real water samples.

A possible solution to this problem could be to limit the mixing PCA analysis to elements behaving conservatively in the system. Among all the elements considered in the calculations (Na, K, Ca, Mg, HCO_3, SO_4, Cl, Br, δ^2H and $\delta^{18}O$) only three of them (Cl, δ^2H and $\delta^{18}O$) have an a priori conservative behaviour. The trouble is that the mathematical method implemented in M4 needs a number of compositional variables equal or higher than the number of end members. Therefore, as in this analysis we are working with four end members, an additional conservative element is needed. For this purpose, bromide has been selected as the fourth conservative element.

In order to verify this approach, the same M4 calculations were performed on the same set of Laxemar and synthetic waters as above, but only with 4 input variables, Cl, Br, δ^2H and $\delta^{18}O$ (in this case only two synthetic samples are used, sample 1 and 2, as the procedure only considers elements not modified by reaction).

M4 results (Table 4-12) reproduce the mixing proportions and the mass balances for the conservative elements very well. Mixing proportions are similar to the values obtained with M4 using all the chemical variables as conservative elements. That is, the decrease in the number of input parameters does not reduce the precision in the mixing proportions estimation.

Table 4-12. M4 results for the synthetic waters created by conservative mixing (Samples 1 and 2) using both, the total set of elements (as conservative elements; results already shown in Table 4-9) and only the conservative elements (Cl, Br, δ^2H and $\delta^{18}O$). The upper part of the table (% Mixing) contains the predicted mixing proportions. The lower part (% mass balance) shows the mass balance calculated by M4 for the three conservative elements (Cl, δ^2H and $\delta^{18}O$). Results of mass balance for conservative elements are calculated as (concentrations in sample – predicted concentrations)/concentrations in sample.

		Sample 1			Sample 2		
		Synthetic data (PHREEQC)	M4 results		Synthetic data (PHREEQC)	M4 results	
			All elements (considered conservative)	Only conservative elements		All elements (considered conservative)	Only conservative elements
% Mixing	Brine	60	60.0	59.3	1.6	1.4	1.9
	Littorina	10	11.5	10.6	50.8	51.7	49.5
	Glacial	30	28.5	30.0	24.4	24.4	23.9
	Precipitation	0	0.0	0.0	23.2	22.5	24.7
% Mass Balance	Cl		7.2	0.9		3.1	0.07
	δ^2H		2.3	0.001		0.4	0.001
	$\delta^{18}O$		1.7	0.008		0.0	0.0

A more comprehensive verification of these results is needed (with a wider range of synthetic samples), but nevertheless the use of conservative elements in M4 for the mixing proportion calculations can be an important methodological improvement as it seems to be able to avoid the noise produced by the conservative elements and therefore extending the qualitative interpretation of the mass balances to a more quantitative one.

4.3.5 Discussion and conclusions

The uncertainty and sensitivity analysis performed in this section has demonstrated that the PCA analysis implemented in M4 is able to reproduce, with high accuracy, the mixing proportions of synthetic waters (brackish and saline waters) created only by conservative mixing of several end members (i.e. all the elements behave conservatively)

This capability, not shared by M3, has allowed us to assess, for the first time the errors produced by this methodology on real samples in which the elements can behave as non conservative (affected by chemical reactions). When chemical reactions only produce slight variations with respect to the chemical composition of the conservative mixing (lower than 2%), M4 gives values in very good agreement with the real ones for the mixing proportions.

When chemical reactions produce an important compositional change (higher than 10% for the studied samples) M4 mixing proportions do not reproduce the original values, and the departure depends on the chemical reaction and/or the type of water. For example, the effect of a simple reaction like sulphate-reduction (only affecting two of the elements included as variables in the calculations, sulphate and bicarbonate, can be responsible of important deviations in the calculated mixing proportions. The noise produced by the non conservative elements in this kind of statistical analysis propagates straightforwardly to the mixing proportions calculated by the code.

These results have important consequences on the methodology of M4 use when conservative and non conservative elements are included. The noise introduced by the reactions in the studied set of waters may be unknown a priori and therefore, its effects on the calculated mixing proportions would also be unknown. Therefore, M4 mixing proportions should not be used without first checking its reliability looking at the mass balance of the conservative elements.

Nevertheless, once the mixing proportions are calculated, mass balances, also provided by the code (with respect to the conservative elements, especially chloride), can easily detect those samples in which reactions have produced a distortion of the calculated mixing proportions. An analysis of this sort (Figure 4.7) should be considered a basic tool when assessing the reliability of the calculated mixing proportions.

A very promising alternative could be the use of M4 only with really conservative elements in each system. The scoping calculations performed with this methodology indicate that the calculated mixing proportions agree very well with the synthetic ones and are not affected by the reduction in the number of compositional variables used as input data. This approach can be inadequate depending on the number of end members to be considered and the availability of conservative elements in each studied case. Nevertheless, it offers the possibility of obtaining quantitative and reliable mixing proportions and its use, combined with additional methodologies (eg. classical mass balance or the methodology presented in section 4.2), should be explored.

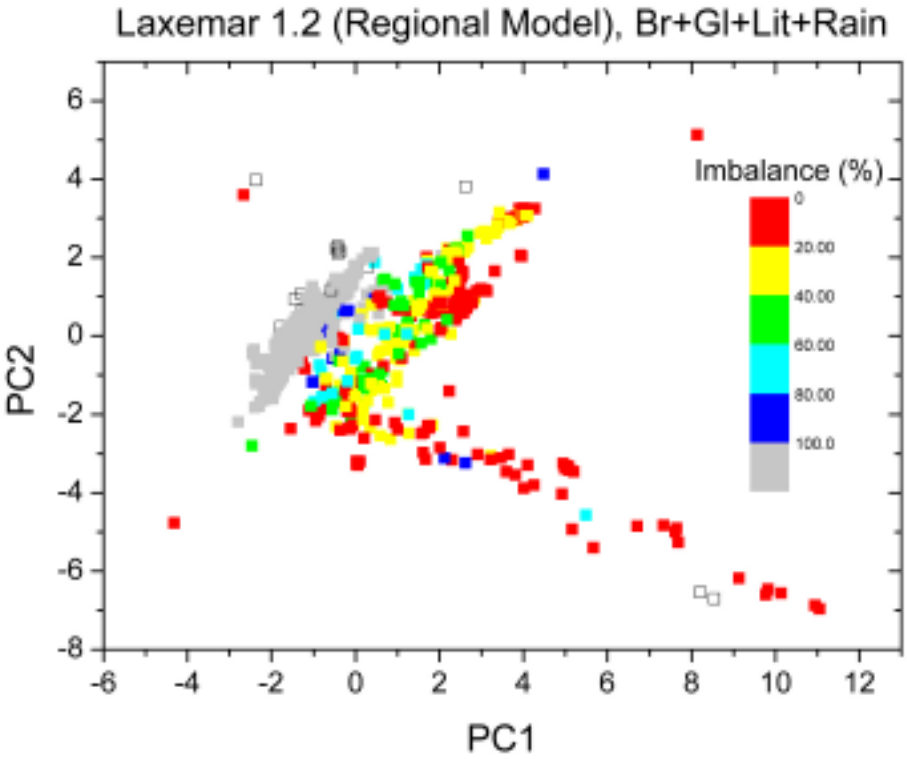

Figure 4-7. *Chlorine imbalance (measured as an absolute percent deviation from the real Cl content) in Laxemar 1.2 Regional Model consisting of 1,088 samples. Grey samples have Cl imbalance greater than 100% and mainly correspond to superficial waters with very low Cl content. Open squares are samples not explained by mixing (outside M4 hyper-tetrahedron). Only those waters with an imbalance smaller than 20% should be considered for modelling purposes.*

5 References

Bath A H, Jackson C P, 2002. Äspö Hard Rock Laboratory: Task Force on modelling of ground-water flow and transport of solutes. Review of Task 5. SKB IPR-03-10, Svensk Kärnbränslehantering AB.

Gurban I, Laaksoharju M, Ledoux E, Madé B, Salignac A L, 1998. Indications of uranium transport around the reactor zone at Bangombé (Oklo). SKB TR-98-06, Svensk Kärnbränslehantering AB.

Laaksoharju M, Skarman C, 1995a. Groundwater sampling and chemical characterization of the HRL tunnel at Äspö, Sweden. PR 25-95-29, Svensk Kärnbränslehantering AB.

Laaksoharju M, Skarman C, 1995b. Multivariate mixing and mass balance calculations of the Cigar Lake groundwaters. (Internal Report), Svensk Kärnbränslehantering AB.

Laaksoharju M, Smellie J A T, Nilsson A-C, Skarman C, 1995. Groundwater sampling and chemical characterisation of the Laxemar deep borehole KLX02. SKB TR-95-05, Svensk Kärnbränslehantering AB.

Laaksoharju M, Wallin B (ed.), 1997. Evolution of the groundwater chemistry at the Äspö Hard Rock Laboratory. Proceedings of the second Äspö International Geochemistry Workshop, Äspö, Sweden, June 6–7, 1995. Svensk Kärnbränslehantering AB.

Laaksoharju M, 1999. Groundwater characterisation and modelling: problems, facts and possibilities. Ph. D. Dissertation, Royal Institute of Technology, Stockholm, 144 p.

Laaksoharju M, Gurban I, Andersson C, 1999a. Indications of the origin and evolution of the groundwater at Palmottu. The Palmottu Analogue Project. (Technical Report 99-03), EC-NST, Luxembourg, Luxembourg.

Laaksoharju M, Tullborg E L, Wikberg P, Wallin B, Smellie J, 1999b. Hydrogeochemical conditions and evolution at the Äspö HRL, Sweden. Appl. Geochem., 14, 835–860.

Laaksoharju M, Andersson C, Gurban I, Gascoyne M, 2000. Demonstration of M3 modelling of the Canadian Whiteshell Research Area (WRA) hydrogeochemical data. SKB TR-01-37, Svensk Kärnbränslehantering AB.

Laaksoharju M (ed.), 2004a. Hydrogeochemical evaluation of the Simpevarp area, model version 1.2. Preliminary site description of the Simpevarp area SKB R 04-74, Svensk Kärnbränslehantering AB, 463 p.

Laaksoharju M (ed.), Smellie J, Gimeno M, Auqué L, Gomez, Tullborg E-L, Gurban I, 2004a. Hydrochemical evaluation of the Simpevarp area, model version 1.1. SKB R 04-16, Svensk Kärnbränslehantering AB.

Laaksoharju M, Smellie J, Gimeno M, Auqué L, Gómez J, Tullborg E-L, Gurban I, 2004b. Hydrogeochemical evaluation of the Simpevarp area, model version 1.1. SKB R 04-16, Svensk Kärnbränslehantering AB, 398 p.

Laaksoharju M (ed.), 2005. Hydrogeochemical evaluation of the Forsmark site, model version 1.2. Preliminary site description of the Forsmark area SKB R 05-17, Svensk Kärnbränslehantering AB.

Luukkonen, 2001. Groundwater mixing and geochemical reactions. An inverse-modelling approach. In: Luukkonen, A. and Kattilakoski, E. (eds.) Äspö Hard Rock Laboratory. Groundwater flow, mixing and geochemical reactions at Äspö HRL. Task 5. Äspö Task Force on groundwater flow and transport of solutes. SKB IPR-02-41, Svensk Kärnbränslehantering AB.

Parkhurst D L, Appelo C A J, 1999. User's guide to PHREEQC (Version 2) , a computer program for speciation, batch reaction, one dimensional transport, and inverse geochemical calculations.

(Science Report WRRIR 99-4259), USGS, 312 p.

Smellie J A T, Karlsson F, 1996. A reappraisal of some Cigar Lake issues of importance to performance assessment. SKB TR-96-08, Svensk Kärnbränslehantering AB, 93 p.

Svensson U, Laaksoharju M, Gurban I, 2002. Äspö Hard Rock Laboratory: Impact of the tunnel construction on the groundwater system at Äspö. Task 5. ÄspöTask Force on groundwater flow and transport of solutes. SKB IPR-02-45, Svensk Kärnbränslehantering AB.

Viani B E, Bruton C J, 1997. In assessing the role of cation exchange in controlling groundwater chemistry during fluid mixing in fractured granite at Äspö, Sweden. In: Laaksoharju, M. and Wallin, B. (eds.) Evolution of the groundwater chemistry at the Äspö Hard Rock Laboratory. SKB R-97-04, Svensk Kärnbränslehantering AB.

Appendix 4

M3 calculations

Contribution to the model version 1.2

Gurban I, 3D-Terra, Montreal

Laaksoharju M, Geopoint AB, Stockholm

September 2005

Contents

1 Introduction 383

2 Visualization and spatial analysis of the hydrochemical database 385
2.1 Description of the hydrochemical visualization tool 385
2.2 Visualization of near-suface hydrochemical database 388
2.3 Visualization of bedrock hydrochemical database 392

3 Numerical modelling of groundwater flow, salinity and tritium transport 411
3.1 Introduction 411
3.2 Model description 411
3.2.1 Model domain 411
3.2.2 Mathematical model 414
3.2.3 Numerical discretization 415
3.3 Groundwater flow model 416
3.4 Decaying tritium transport model 423

4 Conclusions 429

5 References 431

Appendix 6 Groundwater data for Laxemar 1.2 433

Appendix 7 Groundwater data from Nordic sites 435

1 Introduction

This report presents the results of the water classification, mixing modeling and 3D visualization of Laxemar 1.2 data obtained by sampling and analyzing groundwaters obtained from packer-isolated boreholes in the Laxemar area, south-eastern Sweden. This work is being done as part of SKB's site characterization studies of selected areas in Sweden, for disposal of spent nuclear fuel. The focus of this report is on updating the hydrochemical model of the area, to make uncertainty tests and to present models that can be better integrated with the hydrodynamic models. The need for additional uncertainty tests was identified during the Simpevarp 1.2 modelling phase. Issues such as the use of normalised tritium values, the use of tritium as a variable in Principal Coponent Analysis (PCA) and the use of different end members are addressed. The computer code, Tecplot, is used for visualisation of measured Cl data. The Drilling Impact Study (DIS) evaluation could not be performed because of lack of new borehole data. A first attempt to use electrical conductivity values of groundwater, gathered during the Differential Flow measurements (DIFF), as a hydrochemical variability indicator, was made for borehole KLX02.

2 Water type classification

A classical geochemical evaluation and modelling tool, AquaChem, was used for water type classification of Laxemar 1.2 samples. The aim of water classification is to simplify the groundwater information. Most surface waters are of Ca-HCO_3 or Na-Ca-HCO_3 type and the sea water is of Na-Cl type. The deeper groundwaters are mainly of Na-Ca-Cl or Ca-Na-Cl type. These water classes are illustrated by using different standard plots in Figure 1 and the results are listed for all samples in Appendix 1.

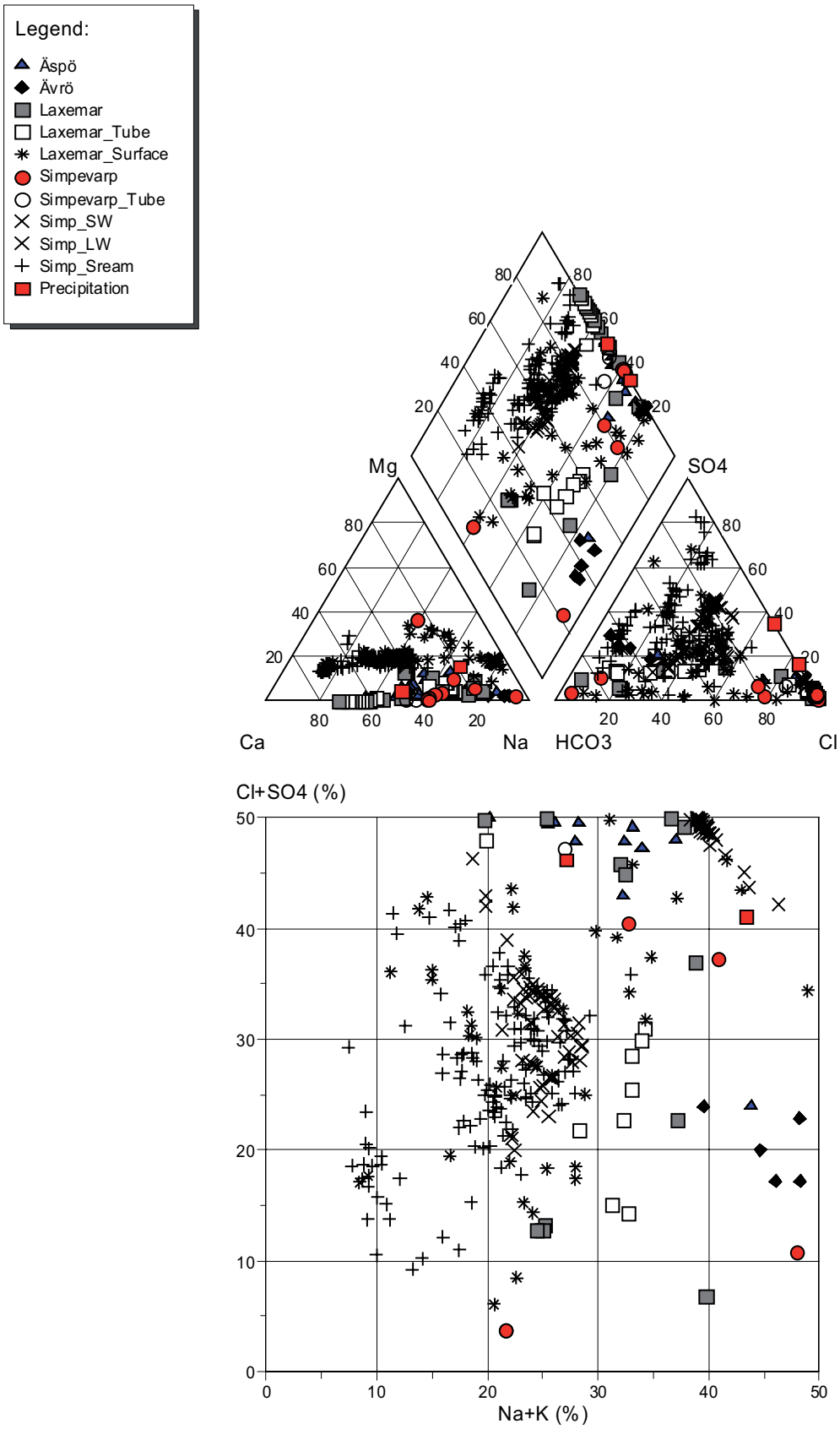

Figure 1. *Multicomponent plots used for classification of thehydrogeochemical data. From top to bottom: Piper plot and Ludwig-Langelier plot applied on all Simpevarp data using AquaChem.*

3 Descriptive and quantitative modelling using the M3 modelling code

3.1 M3 modelling

A challenge in groundwater modelling is to reveal the origin, mixing and reactions altering the composition of groundwater samples. The groundwater modelling concept M3 (Multivariate Mixing and Mass-balance calculations, /Laaksoharju et al. 1995, Laaksoharju et al. 1999b/ can be used for determining this.

In M3 modelling the assumption is that the groundwater composition is always a result of mixing and reactions. M3 modelling uses a statistical method to analyse variations in groundwater compositions so that the mixing components, their proportions, and chemical reactions are revealed. The method quantifies the contribution to hydrochemical variations caused by mixing of groundwater masses in a flow system, by comparing groundwater compositions to identified reference waters. Subsequently, contributions to variations in non-conservative solutes from reactions are calculated.

The M3 method has been tested, evaluated, compared with standard methods and modified over several years within domestic and international research programmes supported by SKB. The main test and application site for the model has been the Äspö Hard Rock Laboratory (HRL) /Laaksoharju and Wallin (eds.) 1997, Laaksoharju et al. 1999a/. Mixing seems to play an important role at many crystalline and sedimentary rock sites where M3 calculations have been applied in different sites in Sweden /Laaksoharju et al. 1998/, Canada /Smellie and Karlsson 1996/, Oklo in Gabon /Gurban et al. 1998/ and Palmottu in Finland /Laaksoharju et al. 1999c/.

The features of the M3 method are:

- It is a mathematical tool which can be used to evaluate groundwater compositional field data, to help construct a conceptual model for the site and to support expert judgement for site characterisation.
- It uses the entire hydrochemical data set to construct a model of geochemical evolution, in contrast to a thermodynamic model that simulates reactions or predicts the reaction potential for a single water composition.
- The results of mixing calculations can be integrated with hydrodynamic models, either as a calibration tool or to define boundary conditions.
- Experience has shown that to construct a mixing model based on physical understanding can be complicated especially at site scale. M3 results can provide additional information of the major flow paths, flow directions and residence times of the different groundwater types which can be valuable in transport modelling.
- The numerical results of the modelling can be visualised and presented for non-expert use.

The M3 method consists of four steps in which the first step is a standard principal component analysis (PCA), then selection of reference waters, followed by calculations of mixing proportions, and finally mass balance calculations /for more details see Laaksoharju et al. 1999b, Laaksoharju 1999d/.

For the Simpevarp 1.1 phase /Laaksoharju et al. 2004/, 2 models were built: at regional scale and at local scale. 113 samples from Simpevarp met the M3 criteria (data available for major elements and isotopes) and were used in the M3 modelling. These samples were from boreholes (core and percussion), soil pipes, lake water, stream water and precipitation. In the Simpevarp 1.2 phase (applied on data from the Simpevarp area) the version 1.1 was up-dated with the new data. For this phase, 2 models were built at a regional scale and at a local scale. 326 samples from Simpevarp met the M3 criteria and were used in the M3 modelling. These samples were again from boreholes (core and percussion), soil pipes, lake water, stream water and precipitation. From the 326 samples available, 180 were considered representative from a hydrochemical point of view and 146 non representative. The present Laxemar 1.2 phase employs the data from Simpevarp 1.2 model and new data available at Laxemar site. From the 355 samples available, 175 are considered representative from hydrochemical point of view.

3.2 The reference waters used

The following reference waters were used in the M3 modelling (for analytical data see Table 3-1):

- Brine type of reference water: Represents the sampled deep brine type (Cl = 47,000 mg/L) of water found in KLX02: 1,631–1,681 m /Laaksoharju et al. 1995a/. An old age for the Brine is suggested by the measured 36Cl values indicating a minimum residence time of 1.5 Ma for the Cl component /Laaksoharju and Wallin 1997/.
- Glacial reference water: Represents a possible melt-water composition from the last glaciation > 13,000 BP. Modern sampled glacial melt water from Norway was used for the major elements and the $\delta^{18}O$ isotope value (21‰ SMOW) was based on measured values of $\delta^{18}O$ in calcite surface deposits. The $\delta^{2}H$ value (158‰ SMOW) is a modelled value based on the equation ($\delta H = 8 \times \delta^{18}O + 10$) for the meteoric water line.
- **Littorina Water:** Represents modelled Littorina water (see Table 3-1).
- **Modified Sea water (Sea sediment):** Represents Baltic Sea affected by microbial sulphate reduction.
- **Baltic:** Corresponds to modern Baltic sea water.
- **Rain 1960:** Corresponds to infiltration of meteoric water (the origin can be rain or snow) from 1960. Sampled modern meteoric water with a modelled high tritium (2,000 TU) content was used to represent precipitation from that period.
- **Age corrected Rain 1960:** Corresponds to infiltration of meteoric water (the origin can be rain or snow) from 1960. Sampled modern meteoric water with a modelled high tritium content was used to represent precipitation from that period. The age corrected value for the tritium was 168 TU.
- **Modern Rain:** Corresponds to modern precipitation.
- **Synthetic meteoric:** Corresponds to modern precipitation, with value 0 for the major components and -80, -10 and 100 for H2, O18 and H3 respectively.
- **Dilute Groundwater:** corresponds to a shallow groundwater (–56.35 m depth) representing the shallow end member for the local model in Laxemar and Simpervarp area.
- Different possible recharge water compositions have to be tested in order to find the optimum one to describe the data.

Table 3-1. Groundwater analytical or modelled data* used as reference waters in the M3 modelling for Laxemar 1.2.

	Cl (mg/l)	Na (mg/l)	K (mg/l)	Ca (mg/l)	Mg (mg/l)	HCO_3 (mg/l)	SO_4 (mg/l)	^{3}H (TU)	$\delta^{2}H$ ‰	$\delta^{18}O$ ‰
Brine	47,200	8,500	45.5	19,300	2.12	14.1	906	0	–44.9	–8.9
Glacial	0.5	0.17	0.4	0.18	0.1	0.12	0.5	0	–158*	–21*
Littorina sea*	6,500	3,674	134	151	448	93	890	0	–38	–4.7
Sea Sediment	3,383	2,144	91.8	103	258	793	53.1	0	–61	–7
Baltic	3,760	1,960	95	234	93.7	90	325	20	–53.3	–5.9
Rain 1960	0.23	0.4	0.29	0.24	0.1	12.2	1.4	2000	–80	–10.5
Age corrected Rain 1960	0.23	0.4	0.29	0.24	0.1	12.2	1.4	168	–80	–10.5
Modern Rain	0.23	0.4	0.29	0.24	0.1	12.2	1.4	20	–80	–10.5
Synthetic meteoric*	0	0	0	0	0	0	0	100	–80	–10.5
Dilute GW	119	237	4	25	6	370	118		–73.8	–9.9

3.3 Test of models

Several M3 modelling concerns were identified during the phases 1.1 and 1.2 of the site modeling project. In this exercise the following concerns were addressed:

- *Can a better resolution be obtained by using only site specific data in the modeling?* In order to optimize the statistical modeling used in the M3 calculations, as many observations as possible are required. Therefore, data from as many Nordic sites as possible are analysed and the information compiled together. The dataset is called "All Nordic Sites" containing data from the sites: Finnsjön, Fjällveden, Forsmark, Gideå, Karlshamn, Klipperäs, Kråkemåla, Oskarshamn, Svartboberget, Taavinunnanen, Olkiluoto, Kivetty and Romuvaara. All Nordis sites data are used in the PCA modeling for comparison purposes despite different geographical locations.
- *Are all variables useful in the PCA?* As many meaningful variables as possible are used in the M3 modelling. A fixed set of variables will, for instance, allow comparisons between the groundwater features of the Laxemar and Forsmark sites. The variables used are the major components (Na, K, Ca, Mg, Cl, HCO_3 and SO_4) and the isotopes H2, O18 and H3. An important concern was the use of tritium. Samples collected at different years are difficult to compare directly because of radioactive decay. The tritium values can also be affected by discharges from the nearby nuclear plants in both areas. The tritium values were time corrected and included in the test runs.
- *Should samples from the surface and bedrock be analysed together in the same PCA?* There are no clear indications of direct flow connections between surface and bedrock systems. Global models included all types of data and were analyzed separately from data containing only results from bedrock (bedrock models).

Five tests runs were performed on the Laxemar data in order to test the optimum end member for shallow water input into the groundwater system. The following models were tested:

1) Laxemar 1.2 data and all Nordic site data.
2) Laxemar 1.2 data and all Nordic site data with age corrected tritium.
3) Laxemar 1.2 data and all Nordic site data with age corrected tritium and a synthetic meteoric end-member.
4) Only bedrock Laxemar 1.2 data and all Nordic site data with age corrected tritium.
5) Only bedrock Laxemar 1.2 data, no tritium and a local dilute shallow groundwater as an end-member.

The 5 models from above are presented in Figures 2 to 6. The reference waters and end members used are listed in Table 3-1. End member is a extreme water that may have affected the water composition on a site. Reference water is a selected water composition used for modeling purposes.

To illustrate the impact of the changes on each model, the mixing proportions along the borehole KLX02 calculated for the models are presented in Figures 7 to 11.

Model 1: The PCA applied on Laxemar 1.2 data and all Nordic site data is illustrated in Figure 2. A total of 355 samples from Simpevarp area were used for this plot. The PCA in Figure 2 shows surface water affected by seasonal variation (winter – summer precipitation), a marine trend showing Baltic Sea water influence and for some Äspö samples a possible Littorina sea water influence. A glacial and finally a deep groundwater trend are also shown.

Model 2: The PCA applied on Laxemar 1.2 data and all Nordic Sites data is illustrated in Figure 3. The tritium values were age corrected with the following formula: Tn = Tsample*exp (-0.055764*(2004-Year)). The year 2004 is used as reference for the calculations.

Model 3: The PCA applied on Laxemar 1.2 data and all Nordic Sites data is illustrated in Figure 4. The tritium values were age corrected. A synthetic meteoric end member was used as an end-member in this calculation (see Table 3-1).

Model 4: The PCA applied on Laxemar 1.2 data and all Nordic Sites data is illustrated in Figure 5. The tritium values were age corrected. A synthetic meteoric end member was used for the calculations (see Table 3-1).

Model 5: The PCA applied only on Laxemar 1.2 data is illustrated in Figure 6. Due to uncertainties in the tritium values (decay, nuclear plant activity etc) the tritium was not included in this model. Local shallow reference water (dilute groundwater see Table 3-1) was selected as an end-member for this model to represent shallow water sampled from the bedrock. Numerical values are listed in Appendix 2.

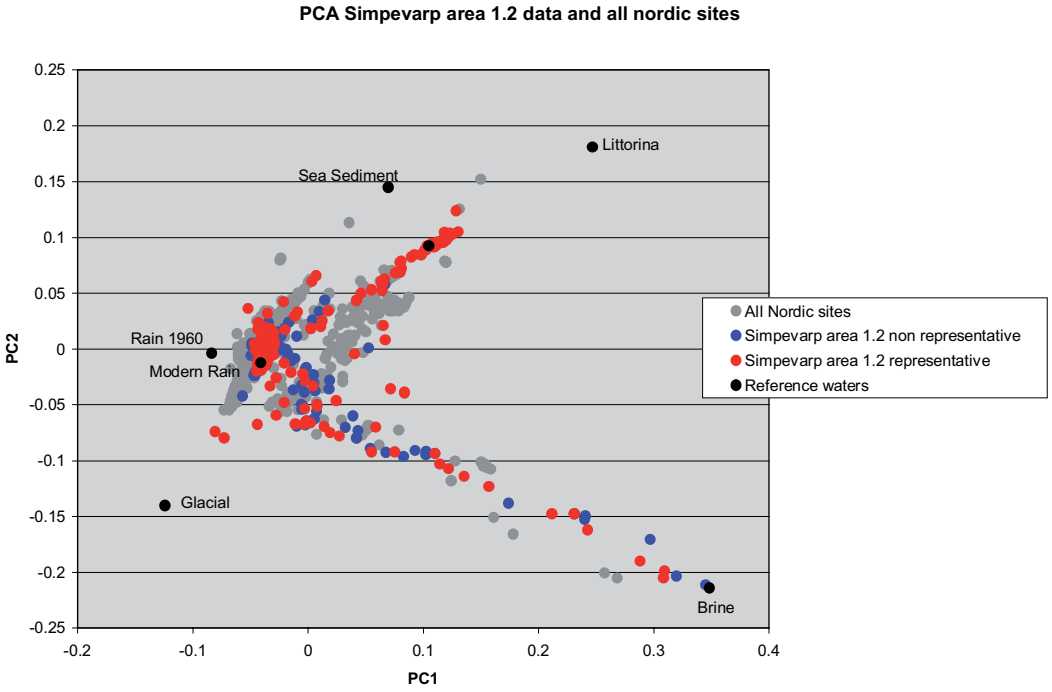

Figure 2. *The figure shows the results of principal component analysis and identification of the reference waters. (Variance: First principal component: 0.40824, First and second principal components: 0.63596, First, second and third principal components: 0.74703). The Sea sediment, Littorina, Brine, Glacial and Rain 1960 reference waters are used as end members for the modelling. The model uncertainty of ± 10 % is shown as an error bar; the analytical uncertainty is ± 5 % and represents therefore half of the error bar.*

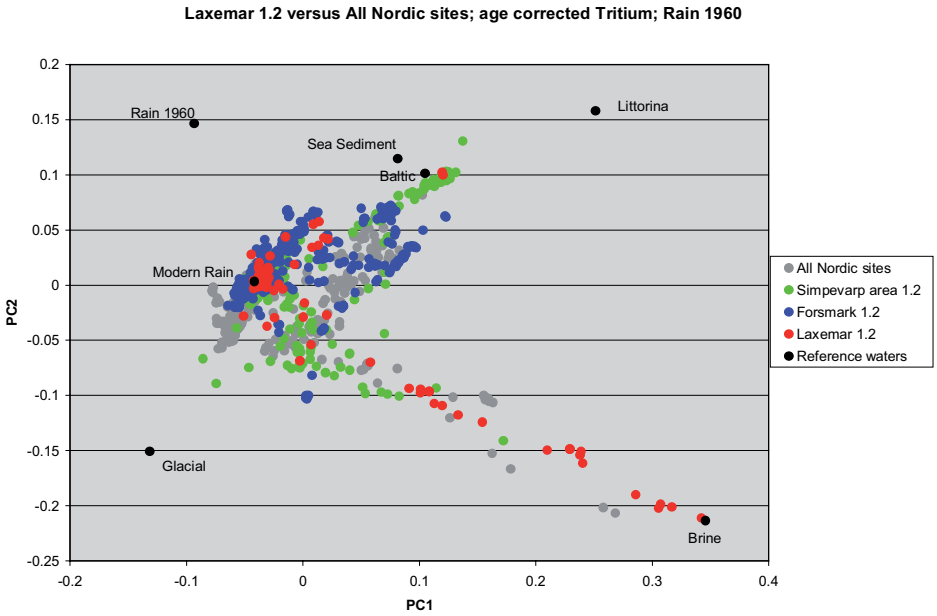

Figure 3. *The figure shows the results of principal components analysis and the identification of the reference waters. (Variance: First principal component: 0.42143, First and second principal components: 0.66282, First, second and third principal components: 0.77478). The tritium values were age corrected, based on the year 2004 as reference age The Littorina, Brine, Glacial and Rain 1960 reference waters are used as end members for the modelling.*

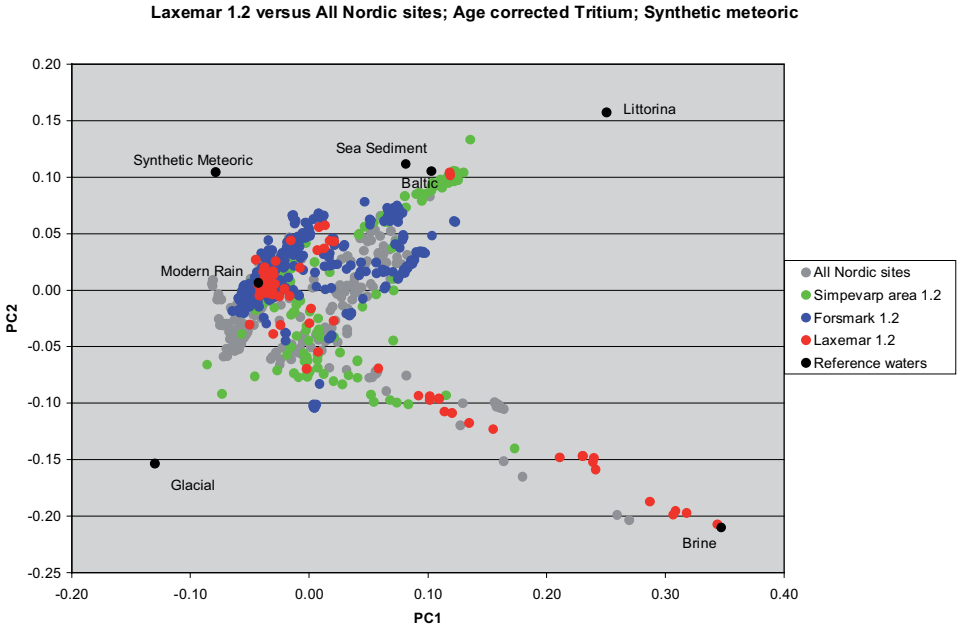

Figure 4. *The figure shows the results of principal components analysis and the identification of the reference waters. (Variance: First principal component: 0.42136, First and second principal components: 0.66156, First, second and third principal components: 0.77381). The tritium values were age corrected by using the year 2004 as the reference year. The Littorina, Brine, Glacial and Synthetic meteoric reference waters are used as end members for the modelling.*

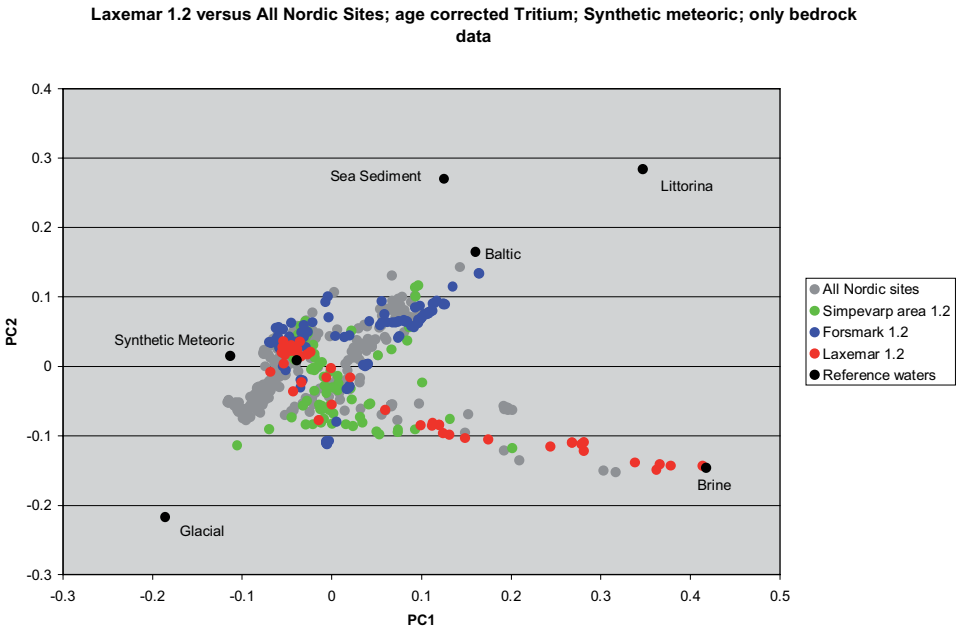

Figure 5. *The figure shows the results of principal components analysis and the identification of the reference waters. (Variance: First principal component: 0.4425, First and second principal components: 0.66068, First, second and third principal components: 0.7826). The tritium values were age corrected using the year 2004 as the reference year. The figure shows only the bedrock data; all the surface waters (sea water, running water, lake water, soil pipes were removed in order to obtain a bedrock model). The Littorina, Brine, Glacial and Synthetic meteoric reference waters are used as end members for the modelling.*

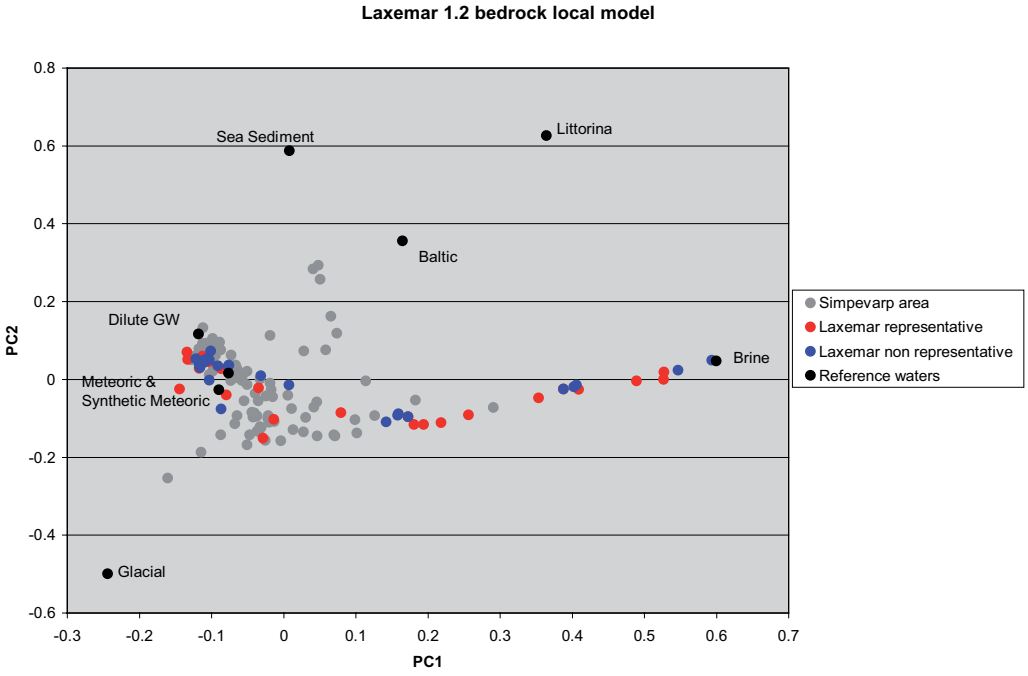

Figure 6. *The figure shows the results of principal components analysis and the identification of the reference waters. (Variance: First principal component: 0.48803, First and second principal components: 0.75323, First, second and third principal components: 0.90506). The tritium variable was not included in the modeling. The figure shows only the bedrock data for Simpevarp area; all the surface waters (sea water, running water, lake water, soil pipes were excluded from this bedrock model). The Littorina, Brine, Glacial and Dilute Groundwater reference waters are used as end members for the modeling.*

3.4 Mixing proportions along KLX02 calculated with five different models

The M3 mixing modeling results for KLX02 are shown in Figures 7–11. They are based on the five models presented in section 3.2.

The models 1, 4 and 5 give very similar and feasible mixing proportions along KLX02. The results did not change from the original model where all available data and non corrected tritium values were used (Model 1, used for Simpevarp 1.2). The use of the synthetic end member for the bedrock data or the use of a dilute groundwater for the local bedrock model, gives similar values as well. The local bedrock model with the dilute GW end-member seems to be the most suitable. When comparing Laxemar and Forsmark sites a common dilute groundwater with high HCO_3 is required. The dilute groundwater used as end member in Laxemar can not describe all the samples in Forsmark.

3.5 Additional tests of models

Different additional tests were performed such as including/excluding soil pipe data using age-corrected tritium or excluding tritium. The following tests were performed:

1) All bedrock samples + soil pipes, all major components, H2, O18 and normalized tritium.
2) All bedrock samples, no soil pipes, all major components, H2 O18 and normalized tritium.
3) All bedrock samples + the soil pipes, all major components, H2, O18 but without the tritium variable.
4) All bedrock samples, no soil pipes, all major components, H2, O18 but without the tritium variable.

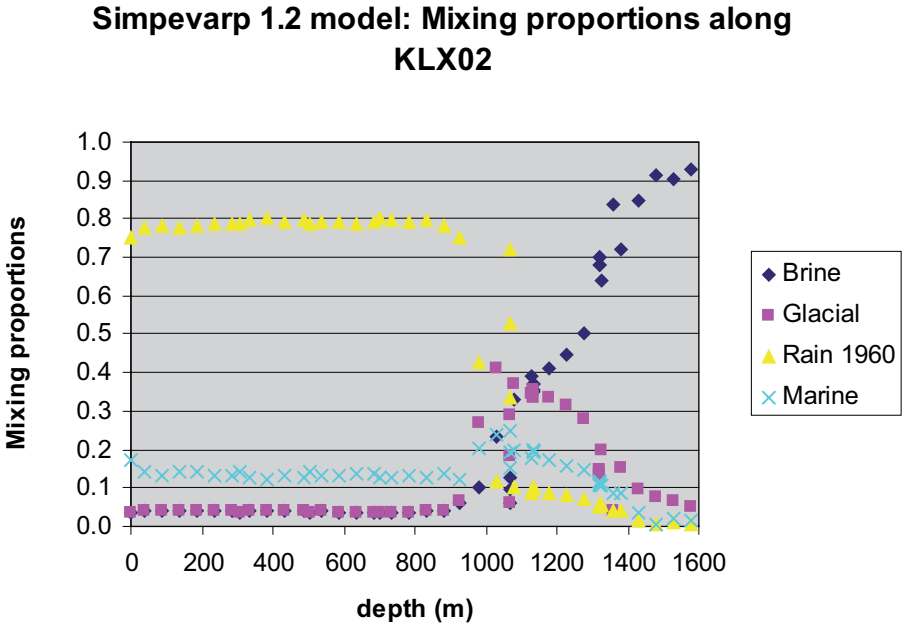

Figure 7. Mixing proportions along KLX02 calculated for Model 1.

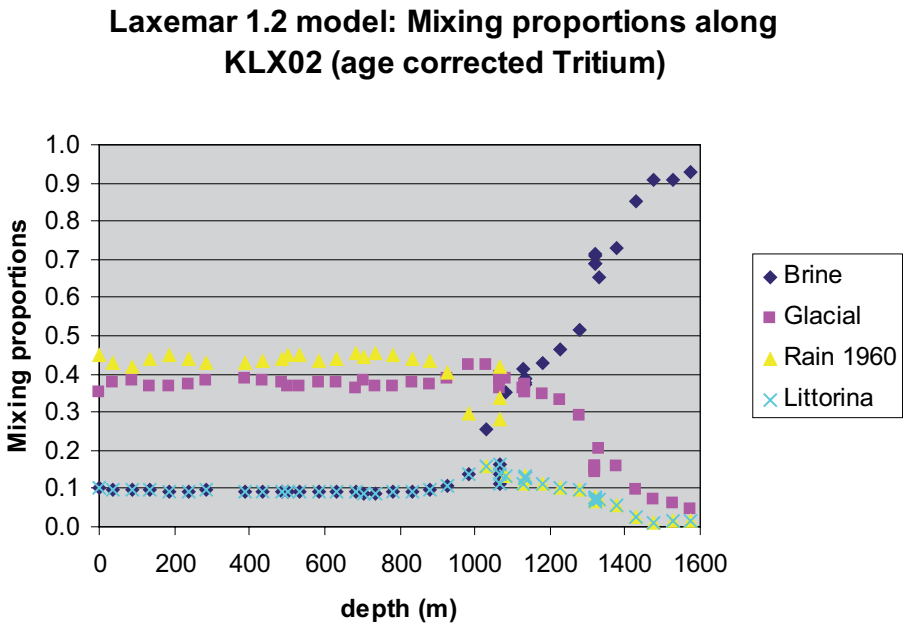

Figure 8. *Mixing proportions along KLX02 calculated for Model 2.*

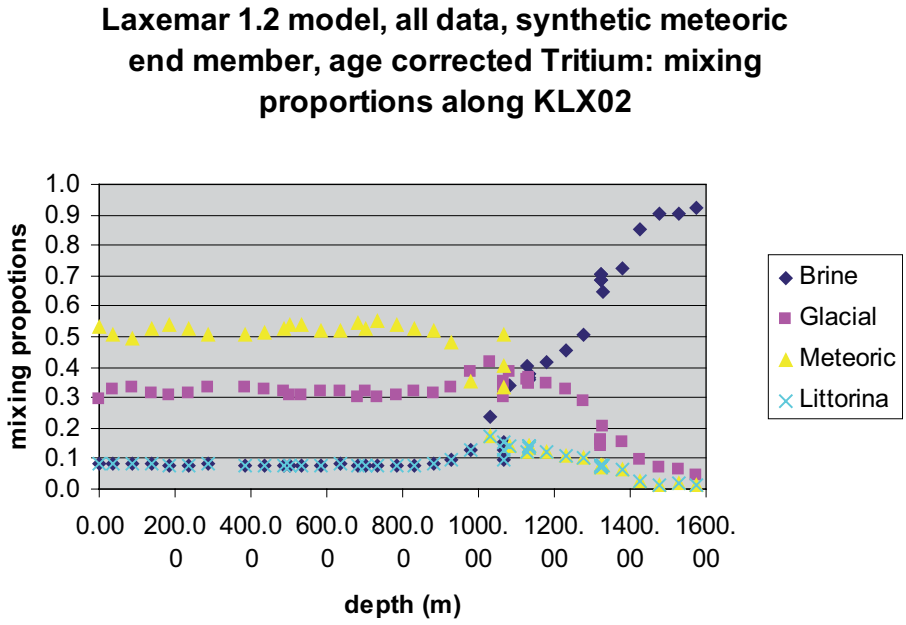

Figure 9. *Mixing proportions along KLX02 calculated for Model 3.*

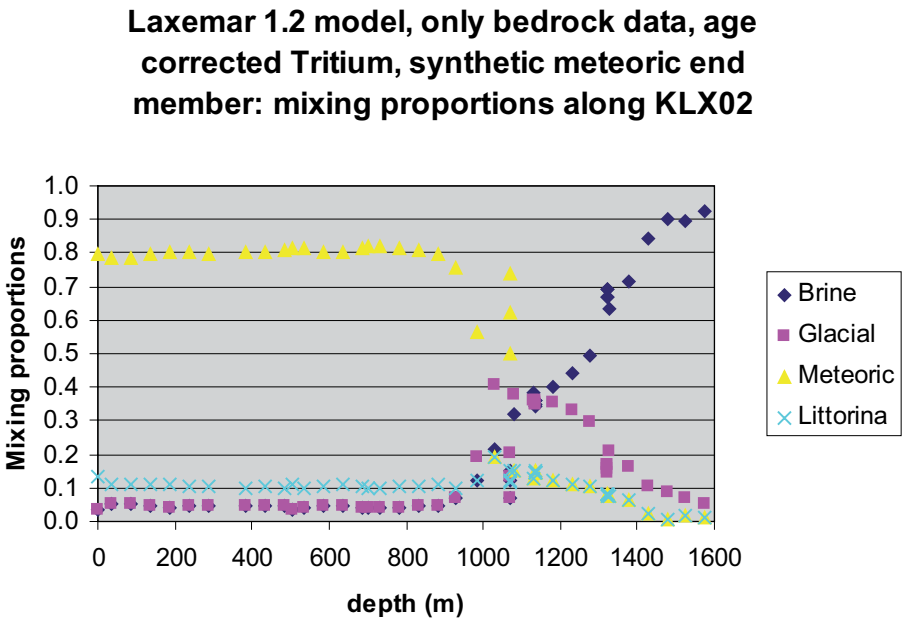

Figure 10. *Mixing proportions along KLX02 calculated for Model 4.*

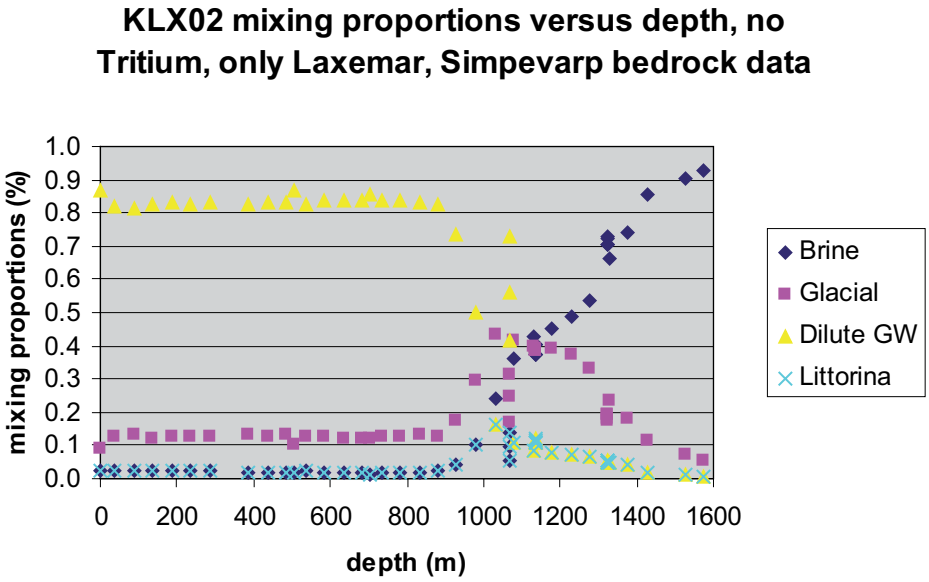

Figure 11. *Mixing proportions along KLX02 for Model 5.*

The PCA's for the above models are shown in Figures 12–16.

In the PCA analysis above as many samples from Laxemar/Simpevarp and Forsmark were included since this gives:

a) More robust calculations.

b) The possibility to compare both sites.

c) Returns mixing proportions based on same end-members used by the hydrogeologists.

The tests show that there are two possible models:

1. one case reflecting the overburden (including the soil pipes), then the surface end member would be PLX53 (sample 3021) and SFM0017 (sample 4515);
2. the second option would be to exclude the information from the overburden and to model only samples from the bedrock. The end member from the bedrock reflecting the upper bedrock part would be i.e. HFM04 (sample 4399).

In the Table 3-2 the compositions of tested shallow/surface end members are listed.

Table 3-2. Possible shallow M3 end-members.

ID Code	Sample ID	Na (mg/l)	K (mg/l)	Ca (mg/l)	Mg (mg/l)	HCO_3 (mg/l)	Cl (mg/l)	SO_4 (mg/l)	D(‰)	O^{18} (‰)	Tr(TU)	Tr Age correct
Modern rain		0.4	0.29	0.24	0.1	12.2	0.23	1.4	–70	–10		15.00
HBH05	2112	19.2	3	38.5	3.8	162	12	21.5	–68.4	–9.9	11.91	11.91
Soil pipe SSM000012	7245	38.7	6.64	56.7	9.2	217	12.6	63.90	–74.9	–10.80	11.20	11.20
PLX53	3021	176	7.96	51.4	52	616	166	9.09	–80.4	–10.3	12.8	9.69
SFM0017	4515	153	8.55	44.3	11.3	535	17.7	7.42	–84.9	–11.5	7.8	7.38
HFM09	8335	274	5.6	41.1	7.5	465	181	85.1	–80.6	–11.1	12.1	12.10
KFI01	Midsec 208.50	45	2.5	61	7	320	11	1	–88	–11.6	40	10.49
KFI01	Midsec 295.5	56	2.9	59	7.5	325	18	1	–88	–11.6	46	12.06
KFI01	Midsec 295.5	88	2.8	50	6.5	350	37	1	–87	–11.6	40	10.49
BFI01	Midsec 77.5 ID1207	24	3.2	76	6.3	220	61	8.3	–88.2	–11.97	36	13.19
HFM04 midsec 125.85	4399	169	6.68	27.6	6.9	390	72	44.65	–84.5	–11.7	14.4	12.88
HFM04 midsec 125.85	4400	167	6.57	28.3	7	390	71.4	43.7	–83.9	–11.7	13.2	11.81

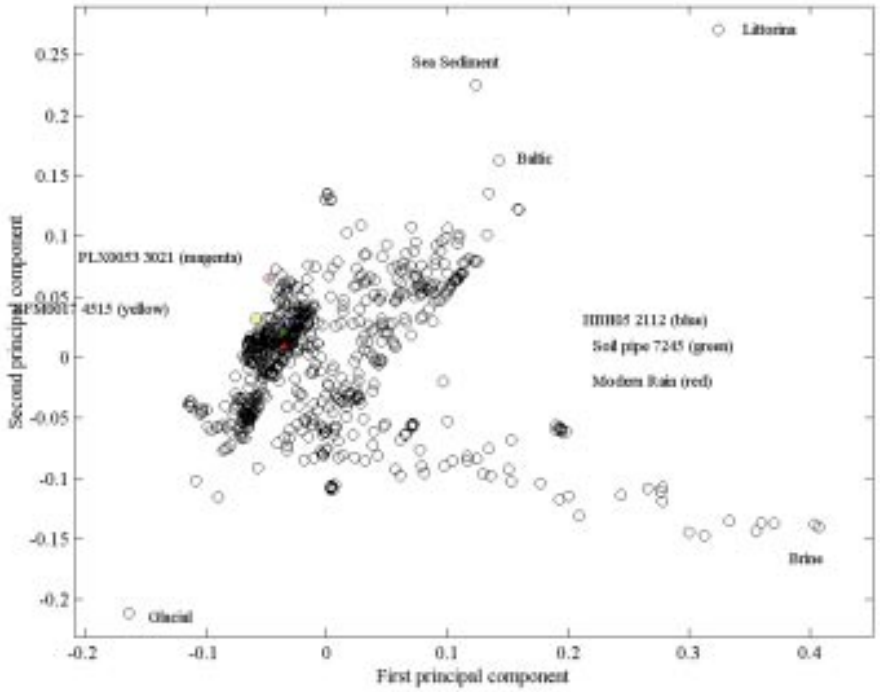

Figure 12. *Ground water data and soil pipes for Laxemar, Simpevarp, Forsmark and all Nordic sites; major elements and ^{2}H, ^{18}O and 3H; Variance: 0.43968, 0.65791, 0.77858.*

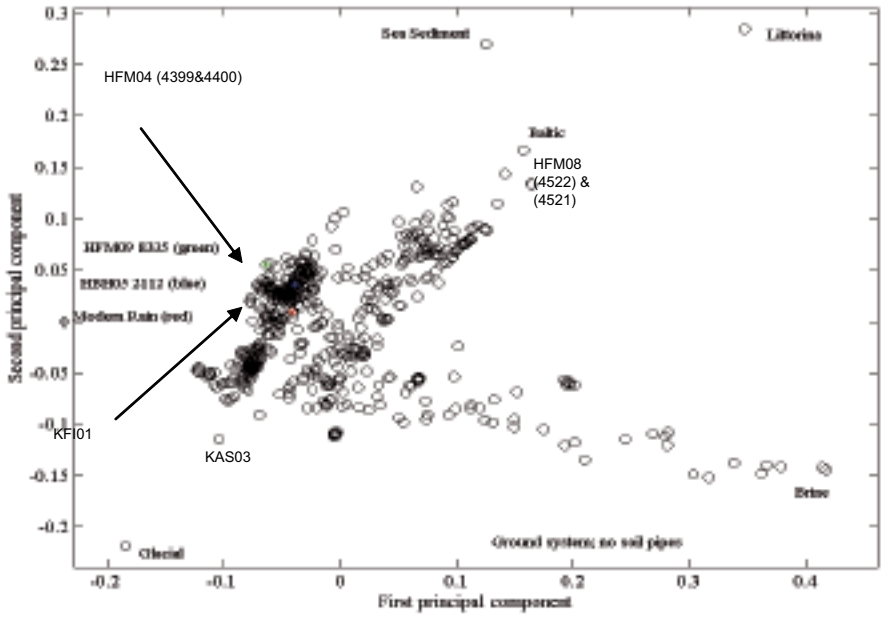

Figure 13. *Ground water data (no soil pipes) for the Laxemar, Simpevarp, Forsmark areas and all Nordic sites; major elements and ^{2}H, ^{18}O and ^{3}H ; Variance: 0.4439, 0.66233, 0.78432.*

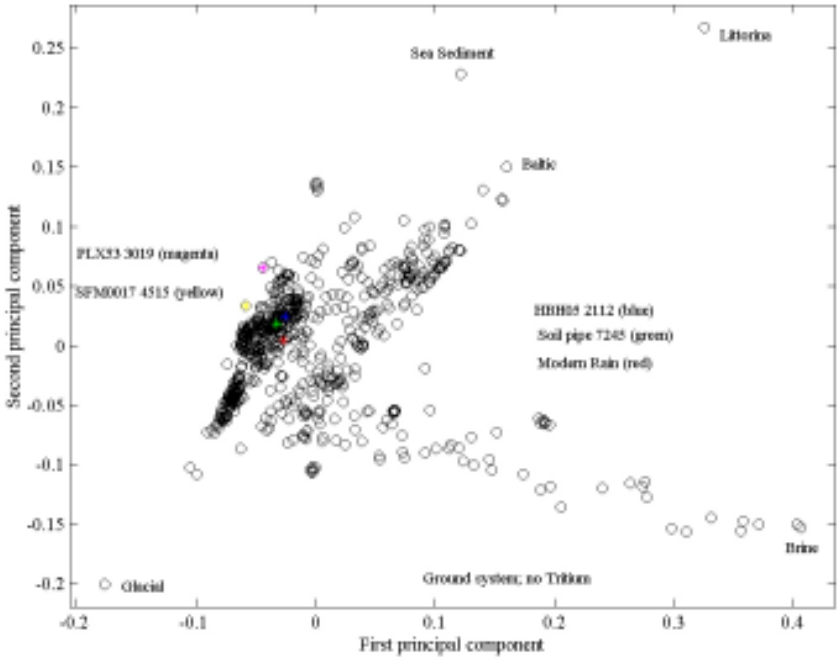

Figure 14. *Ground water data and soil pipes for the Laxemar, Simpevarp, Forsmark areas and all Nordic sites; major elements and ^{2}H and ^{18}O (no Tritium); Variance: 0.47564, 0.71616, 0.84636.*

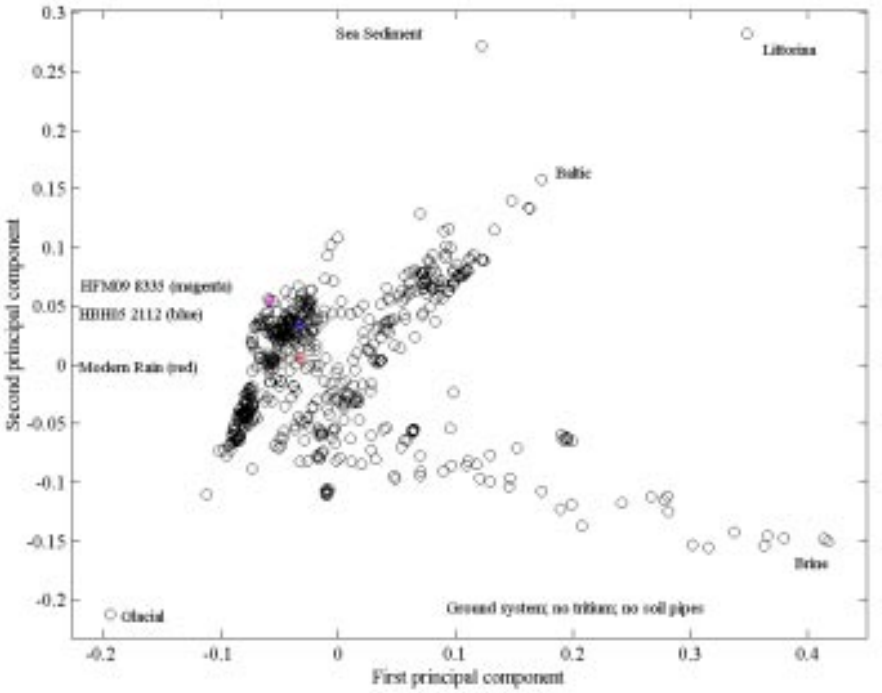

Figure 15. *Ground water data (no soil pipes) for the Laxemar, Simpevarp, Forsmark areas and all Nordic sites; major elements and ^{2}H and ^{18}O; (no Tritium); Variance: 0.48332, 0.7253, 0.85971.*

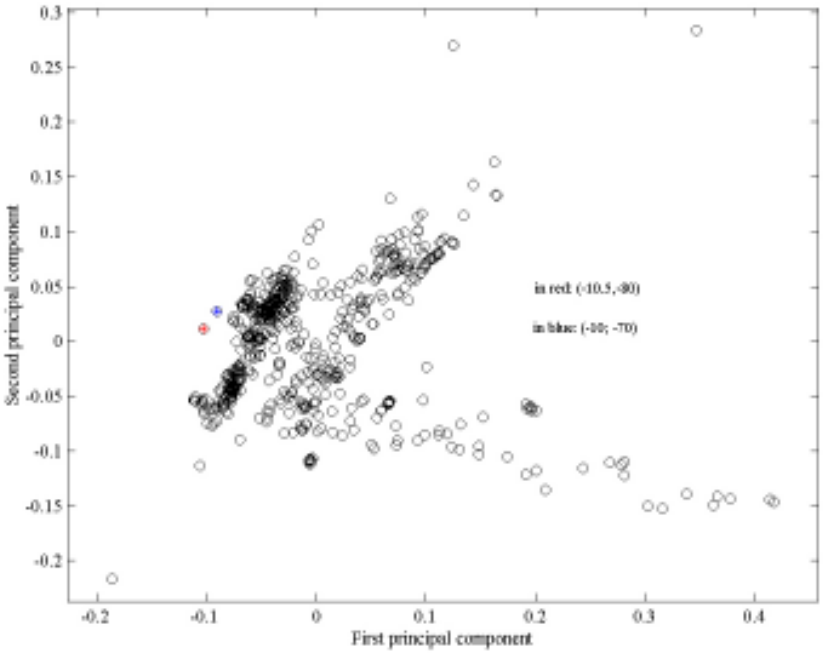

Figure 16. *Test of two synthetic meteoric end members (blue and red dots). This test is an example of how the PCA can be used to select an optimum end-member. The sample representing the blue dot plots closer to the observations and is therefore more suitable than the sample represented by the red dots.*

3.6 Comparison between M3 and M4 codes

The Figures 17 to 19 show the comparison between the different mixing proportions calculated with the M3 and M4 codes. M4 is an option in the new version of M3 program where the mixing proportions are calculated in a multivariate space rather than 2D. See Appendix 3. The M3 code is described at the Chapter 3 of this report. The M4 code (M3 modified) is described in the report provided by the University of Zaragoza team (Appendix 3). The trend of the M3 and M4 mixing proportions is similar. M3 and M4 calculate similar amount of Brine mixing proportions. M4 calculates slightly higher values for the Glacial and Littorina mixing proportions. M3 calculates higher Meteoric mixing proportions.

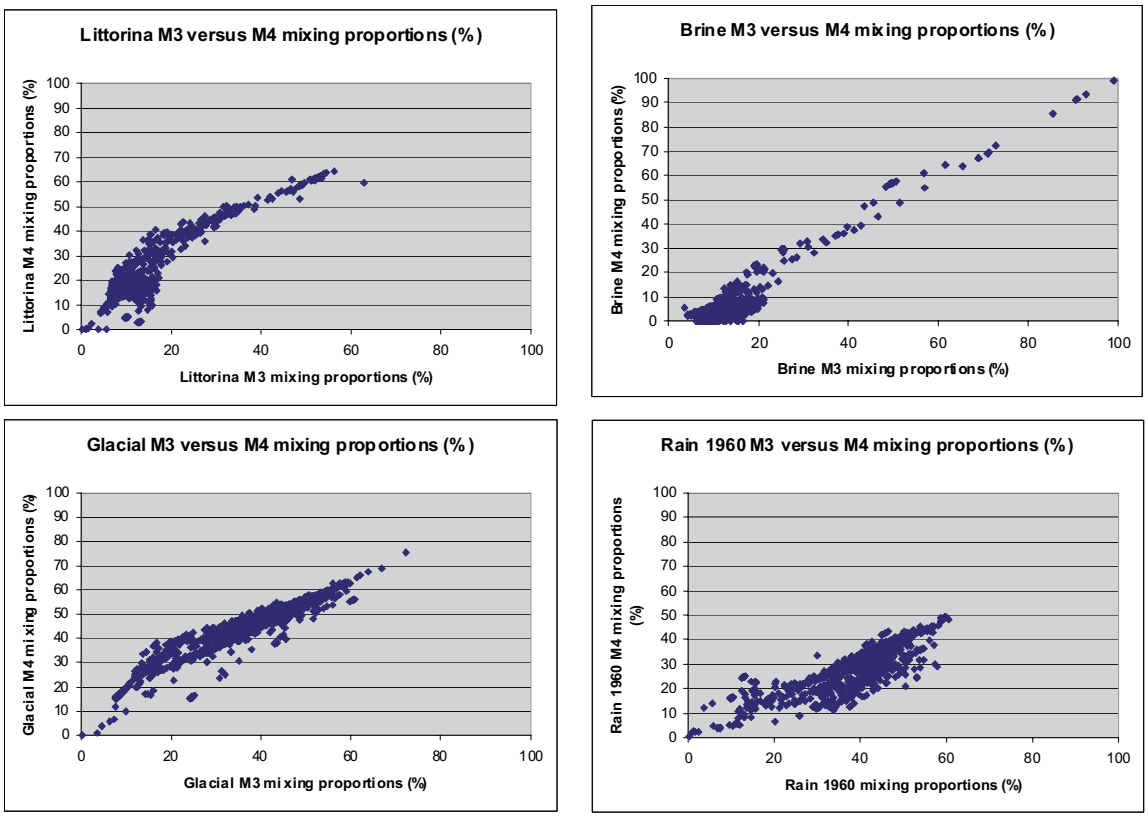

Figure 17. *M3/M4 comparison for model 2: age-corrected Tritium, Rain 1960 as Meteoric end member applied on all data available.*

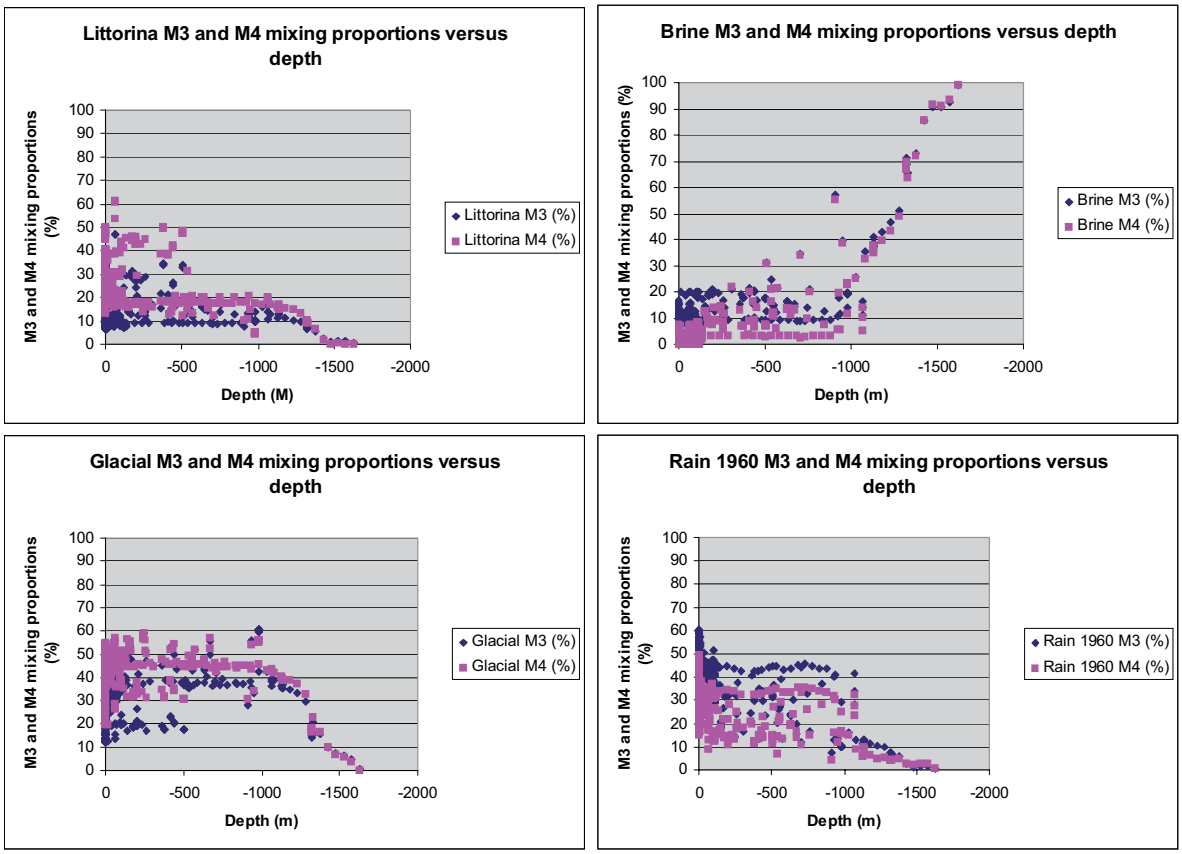

Figure 18. *M3/M4 comparison for model 2 plotted with sampling depth. Model 2 contains age-corrected Tritium, Rain 1960 as meteoric end member.*

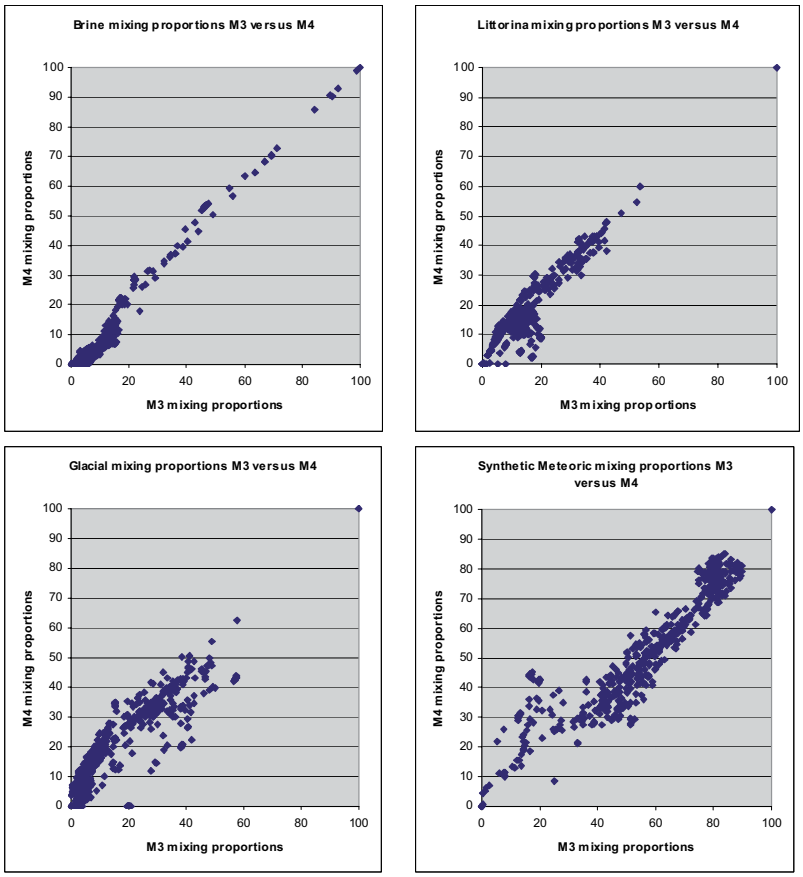

Figure 19. *M3/M4 mixing proportion comparison for model 4 with age corrected tritium, Synthetic Meteoric end member and with only bedrock data.*

4 Site specific hydrogeochemical uncertainties

At every phase of the hydrogeochemical investigation programme – drilling, sampling, analysis, evaluation, modelling – uncertainties are introduced which have to be accounted for, addressed fully and clearly documented to provide confidence in the end result, whether it will be the site descriptive model or repository safety analysis and design /Smellie et al. 2002/. Handling the uncertainties involved in constructing a site descriptive model has been documented in detail by /Andersson et al. 2001/. The uncertainties can be conceptual uncertainties, data uncertainty, spatial variability of data, chosen scale, degree of confidence in the selected model, and error, precision, accuracy and bias in the predictions. Some of the identified uncertainties recognized during the Simpevarp modelling exercise and during the DIS exercise are discussed below.

The following data uncertainties have been estimated, calculated or modelled

- Drilling; may be ± 10–70%.
- Effects from drilling during sampling; is < 5%.
- Sampling; may be ± 10%.
- Influence associated with the uplifting of water; may be ± 10%.
- Sample handling and preparation; may be ± 5%.
- Analytical error associated with laboratory measurements; is ± 5%.
- Mean groundwater variability at Simpevarp during groundwater sampling (first/last sample); is about 25%.
- The M3 model uncertainty; is ± 0.1units within 90% confidence interval.

Conceptual errors can occur from e.g. the paleohydrogeological conceptual model. The influences and occurrences of old water end-members in the bedrock can only be indicated by using certain element or isotopic signatures. The uncertainty is therefore generally increasing with the age of the end-member. The relevance of an end-member participating in the groundwater formation can be tested by introducing alternative end-member compositions or by using hydrodynamic modelling to test if old water types can resign in the bedrock during prevailing hydrogeological conditions.

4.1 Model uncertainties

The following factors can cause uncertainties in M3 calculations:

1. Input hydrochemical data errors originating from sampling errors caused by the effects from drilling, borehole activities, extensive pumping, hydraulic short-circuiting of the borehole and uplifting of water which changes the in-situ pH and Eh conditions of the sample, or as analytical errors.
2. Conceptual errors such as incorrect general assumptions, selecting inorrect type/number of end-members and mixing samples that are not mixed.
3. Methodological errors such as oversimplification, bias or non-linearity in the model, and the systematic uncertainty, which is attributable to use of the centre point to create a solution for the mixing model.

An example of a conceptual error is assuming that the groundwater composition is a good tracer for the flow system. The water composition is not necessarily a tracer of mixing directly related to flow since there is not a point source as there is when labelled water is used in a tracer test.

Another source of uncertainty in the mixing model is the loss of information in using only the first two principal components. The third principal component gathers generally around 10% of the groundwater information compared with the first and second principal components, which contain

around 70% of the information. A sample could appear to be closer to a reference water in the 2D surface than in a 3D volume involving the third principal component. In the latest version of M3 the calculations can also be performed in 3D.

Uncertainty in mixing calculations is smaller near the boundary of the PCA polygon and larger near the center. The uncertainties have been handled in M3 by calculating an uncertainty of 0.1 mixing units (with a confidence interval of 90%) and stating that a mixing portion < 10% is under the detection limit of the method /Laaksoharju et al. 1999b/.

5 The use of DIFF measurements

The electrical conductivity (EC) measurements performed during the DIFF measurements (differential flow measurements) could give valuable information about not only the inflow/outflow from the borehole but also disturbances of and changes in chemistry. These measurements are the first measurements conducted after drilling and it is therefore of special interest to follow these changes in comparison with chemistry (e.g. Cl obtained from the borehole during sampling campaigns). The variability can indicate disturbances and can hence be used for confidence building.

The EC was measured along KLX02 without and during pumping. The EC and the measured Cl during sampling along the borehole are compared in Figure 20. The measured Cl sampled in open borehole seems to resemble the EC measured without pumping. The EC measured during pumping show a much higher salinity than samples taken in open borehole conditions. This indicates again that samples in open borehole reflect mixing processes in the open borehole rather than undisturbed bedrock conditions. For modeling and model calibrations with hydrogeology only samples from sealed-off bedrock sections should be used. The EC distribution and the comparison with measured Cl should be investigated in all boreholes. The EC from the DIFF measurements, the measured Cl and the calculated mixing proportions are listed in Appendix 3.

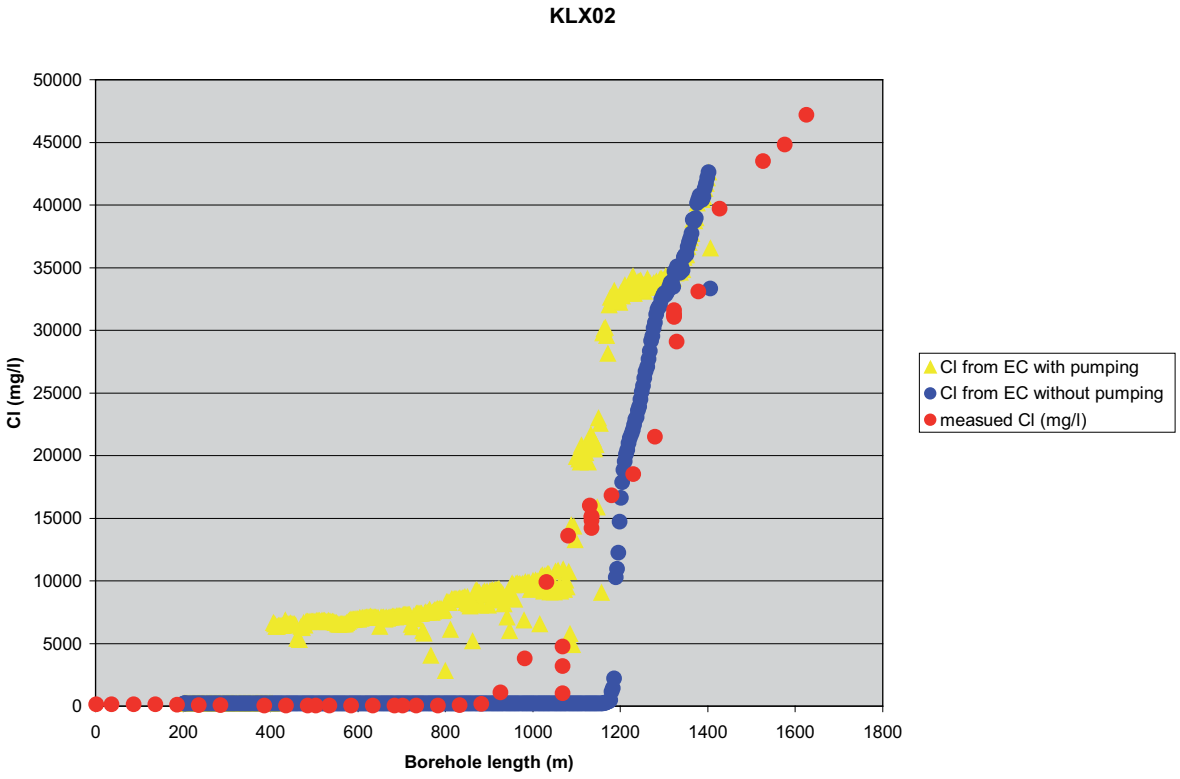

Figure 20. *Comparison of electrical conductivity and Cl measured along KLX02.*

6 Visualisation of the sampling locations

The 3D visualization of the Cl distribution in Laxemar 1.2 was performed by using the computer code Tecplot. The purpose of the visualization is to show, the distribution of the borehole data included in the Laxemar 1.2 dataset. Both 2D and a 3D visualizations of Cl are shown in Figures 21 and 22.

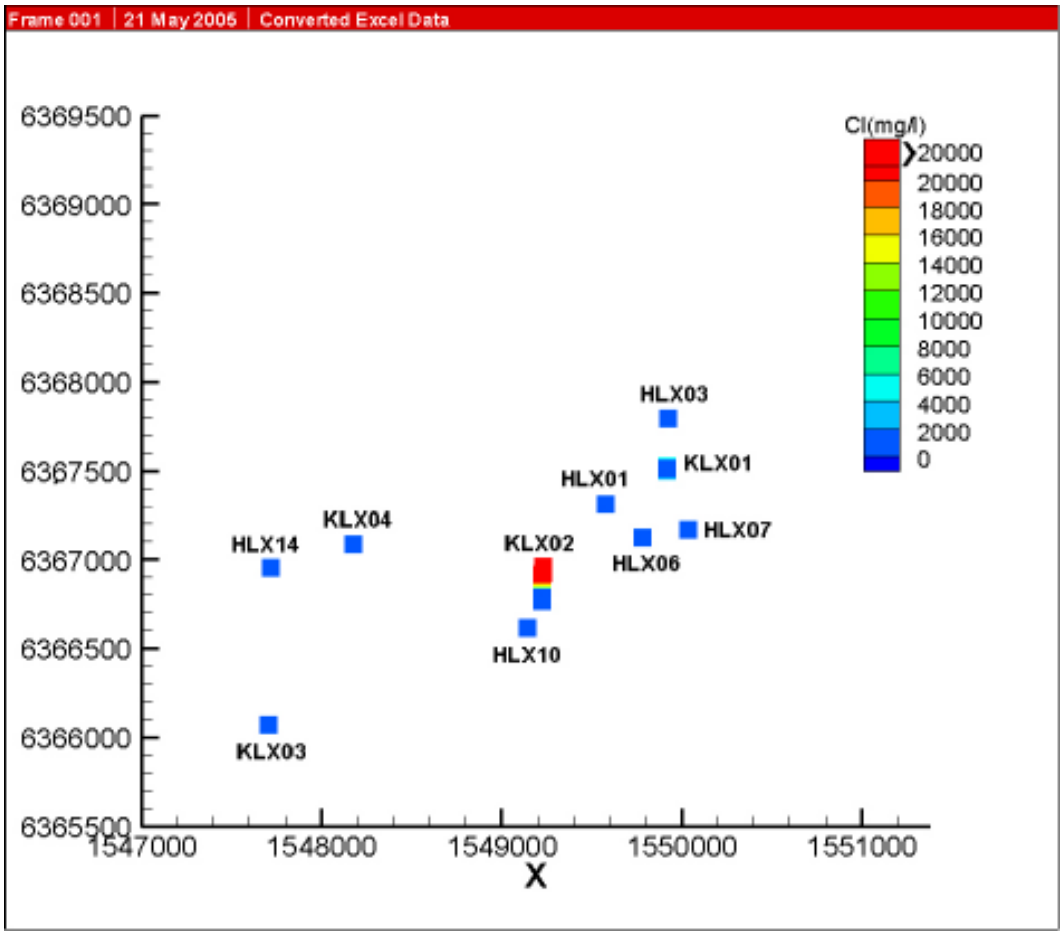

Figure 21. *2D visualization of the Cl data measured in boreholes in Laxemar 1.2, Simpevarp area.*

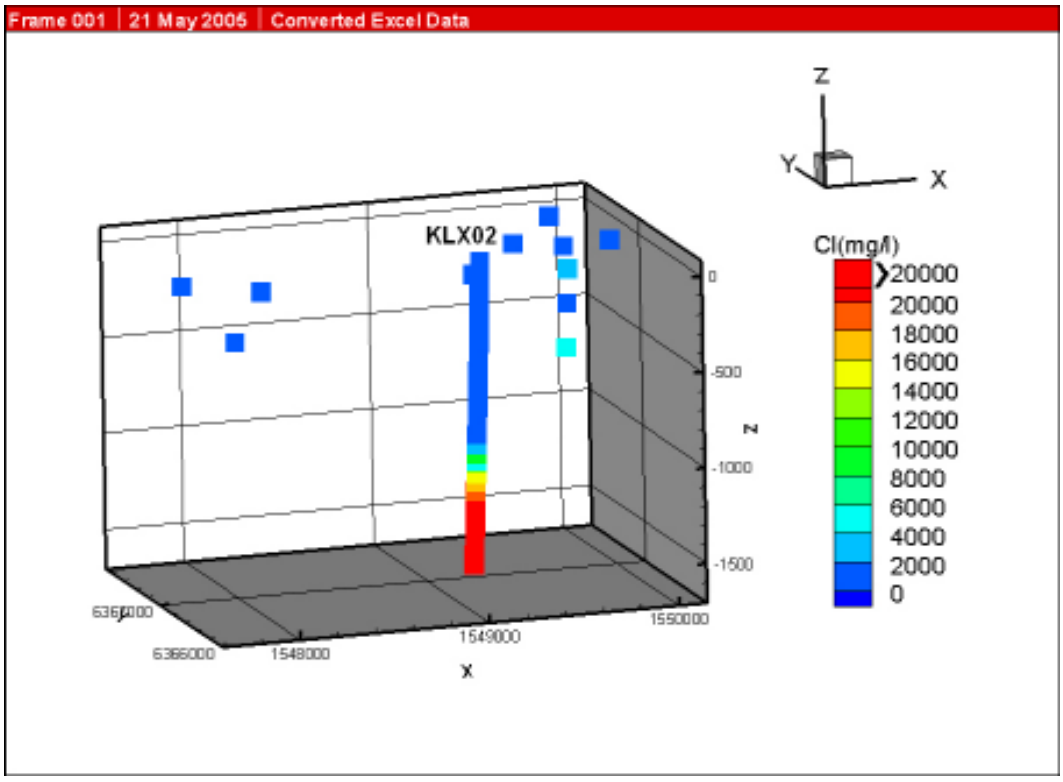

Figure 22. *3D visualization of the Cl data measured in boreholes in Laxemar 1.2, Simpevarp area.*

7 Concluding remarks

This work represents the phase 1.2 of the hydrochemical evaluation and modelling of the Laxemar data. This comprises the explorative analyses (AquaChem), M3 modelling, alternative models, explorative data tests and 3D/2D visualisation of the data. The following conclusions are drawn:

- M3 modelling helped to summarize and understand the data.
- The alternative models helped to address different previously unsolved issues such as: the age-corrected tritium, the use of tritium as a variable, tests with different end members, the use of the whole data set in order to build a surface-bedrock model and the use of local bedrock model.
- In order to try to test alternative models, the Tritium values were normalised to present date (reference year 2004). Since the normalised tritium is described by a mathematical formula, the normalised tritium data do not give any new information and did not change the appearance of the PCA. In M3 calculations only, independent elements could bring new information.
- The visualisation helps to understand the distribution of the data at the site. The visualisation helps to better understand the distribution of the data in the domain.
- The DIFF and Cl measurements along a borehole can be used to validate the variance in mixing proportions along the borehole. This information can be used for confidence building.
- The different M3 modelling tests resulted in the following conclusions: a) When calculating mixing proportions only samples from the boreholes will be used, b) A synthetic non-site specific end-member will be used, which reflects a general composition that may have affected the groundwater samples. For instance, the new synthetic end-member for meteoric water has the composition: 0 for Na, K, Mg, Ca, SO_4, HCO_3, Cl and D = –80, O18 = –10.5 and Tritium = 100. For the other end-members such as Littorina and Glacial we use the existing modelled compositions. Due to the fact that tritium values could be affected by discharges from the nuclear plant, models without tritium will be used. In case only bedrock data is used, a site specific dilute groundwater end member will be selected. If different sites such as Laxemar and Forsmark are compared, a new synthetic dilute groundwater end member should be identified.

8 References

Andersson J, Christiansson R, Munier R, 2001. Djupförvarsteknik: Hantering av osäkerheter vid platsbeskrivande modeller. SKB TD-01-40, Svensk Kärnbränslehantering AB.

Gurban I, Laaksoharju M, Ledoux E, Made B, Salignac AL, 1998. Indications of uranium transport around the reactor zone at Bagombé (Oklo). SKB TR-98-06, Svensk Kärnbränslehantering AB.

Laaksoharju M, Smellie J, Nilsson A-C, Skårman C, 1995. Groundwater sampling and chemical characterisation of the Laxemar deep borehole KLX02. SKB TR 95-05, Svensk Kärnbränslehantering AB.

Laaksoharju M, Wallin B (eds.), 1997. Evolution of the groundwater chemistry at the Äspö Hard Rock Laboratory. Proceedings of the second Äspö International Geochemistry Workshop, June 6–7, 1995. SKB International Co-operation Report ISRN SKB-ICR-91/04-SE. ISSN 1104-3210 Stockholm, Sweden.

Laaksoharju M, Gurban I, Skårman C, 1998. Summary of the hydrochemical conditions at Aberg, Beberg and Ceberg. SKB TR 98-03, Svensk Kärnbränslehantering AB.

Laaksoharju M, Tullborg E-L, Wikberg P, Wallin B, Smellie J, 1999a. Hydrogeochemical conditions and evolution at Äspö HRL, Sweden. Applied Geochemistry Vol. 14, #7, 1999, Elsevier Science Ltd., pp835–859.

Laaksoharju M, Skårman C, Skårman E, 1999b. Multivariate Mixing and Mass-balance (M3) calculations, a new tool for decoding hydrogeochemical information. Applied Geochemistry Vol. 14, #7, 1999, Elsevier Science Ltd., pp861–871.

Laaksoharju M, Gurban I, Andersson C, 1999c. Indications of the origin and evolution of the groundwater at Palmottu. The Palmottu NaturalAnalogue Project. SKB TR 99-03, Svensk Kärnbränslehantering AB.

Laaksoharju M, 1999d. Groundwater Characterisation and Modelling: Problems, Facts and Possibilities. Dissertation TRITA-AMI-PHD 1031; ISSN 1400-1284; ISRN KTH/AMI/PHD 1031-SE; ISBN 91-7170-. Royal Institute of Technology, Stockholm, Sweden. Also as SKB TR-99-42, Svensk Kärnbränslehantering AB.

Laaksoharju M (ed.), Smellie J, Gimeno M, Auqué L, Gomez, Tullborg E-L, Gurban I, 2004. Hydrochemical evaluation of the Simpevarp area, model version 1.1. SKB R-04-16, Svensk Kärnbränslehantering AB.

Smellie J, Laaksoharju M, Tullborg E-L, 2002. Hydrochemical site descriptive model – a stategy for the model development during site investigation. SKB R-02-49, Svensk Kärnbränslehantering AB.

Smellie J, Karlsson F, 1996. A reappraisal of some Cigar-Lake issues of importance to performance assessment. SKB TR-96-08, Svensk Kärnbränslehantering AB.

Appendix 1

Water type classification of the Simpevarp samples by using AquaChem

These calculations are stored in the SKB database SIMONE.

Appendix 2

Measured data and M3 mixing calculations for Laxemar 1.2, bedrock data, model 5

These calculations are stored in the SKB database SIMONE.

Appendix 3

EC from DIFF measurements, measured Cl and calculated mixing proportions with model 5 along KLX02

These calculations are stored in the SKB database SIMONE.

Laxemar model 1.2.

Appendix 5

Coupled hydrogeological and solute transport modelling

Contribution to the model version 1.2

Jorge Molinero, Juan Ramón Raposo
Área de Ingeniería del Terreno, Universidade de Santiago de Compostela,
Escola Politécnica Superior, Lugo

September 2005

Contents

1	**Introduction**	383
2	**Visualization and spatial analysis of the hydrochemical database**	385
2.1	Description of the hydrochemical visualization tool	385
2.2	Visualization of near-suface hydrochemical database	388
2.3	Visualization of bedrock hydrochemical database	392
3	**Numerical modelling of groundwater flow, salinity and tritium transport**	411
3.1	Introduction	411
3.2	Model description	411
	3.2.1 Model domain	411
	3.2.2 Mathematical model	414
	3.2.3 Numerical discretization	415
3.3	Groundwater flow model	416
3.4	Decaying tritium transport model	423
4	**Conclusions**	429
5	**References**	431

1 Introduction

The work presented here constitutes an attempt to combine hydrogeological and hydrochemical analysis of the Laxemar subarea, within the framework of the study performed by the Hydrochemical Analitical Group (HAG, now known as ChemNet Group) supported by SKB. The Team of the University of Santiago de Compostela (USC), Spain, has contributed to the HAG activities since the Simpevarp model version 1.2 (May, 2004).

From the point of view of hydrochemical understanding of the site, there is very little new information for this modelling exercise, compared to the hydrochemical database available one year ago in the Simpevarp v. 1.2 model. However, a number of new boreholes and soil pipes are currently under operation which will contribute new information in the near future. The main objective of the present modelling stage was proposed to focus on setting-up, developing and testing new tools and methodologies for hydrochemical analyses and modelling, which could be used in future stages with new hydrochemical information.

It was determined that one of the weakest points of the hydrochemical analysis and, especially, for integration with hydrogeology, was related to the lack of spatial representation and visualization of available data. Hydrochemical modelling is usually made on a "water sample basis" with little (if any) analysis based on the spatial distribution of the information. Hydrochemical information used to be treated either by x-y plots (a given variable platted against chloride or depth, etc) or more sophisticated methods such as mass balance and statistical mixing models. However, these kinds of analyses make it often difficult to manage, simultaneously, information which corresponds to different hydrogeological and geographical settings, such as inland-coastal, recharge-discharge zones, etc.

The spatial analysis of hydrochemical information is not simple since there are few hydrochemical samples and they are located within a three-dimensional complex geo-hydrological framework in fractured crystalline bedrock. There are a number of commercial tools able to represent hydrochemical information in space, but usually they are intended to visualize either computed model results or geo-statistically interpolated trends, which are not appropriate when few data and/or highly heterogeneous and fractured media are analysed. This is why a specific visualization tool has been developed, which is described in Chapter 2. The visualization tool has the aim of representing "objectively" available hydrochemical and isotopic information, both in the near-surface and in the bedrock environments, combined with geographical information (topography, coast lines, etc), geometrical objects (such as boreholes and tunnel) and geo-hydrological information (deformation zones – hydraulic conductor domains). It is firmly believed that this kind of visual model can constitute a relevant contribution towards the definition of a sound hydrochemical conceptual model of the Laxemar subarea. In additon, it is also thought that 3D spatial visualization of hydrochemical information can also be useful for the task of integration and consistency assessment between hydrogeological and hydrochemical models.

Chapter 3 presents a summary of the main results of flow and transport numerical modelling. A two-step methodology has been developed and tested which allows fluid density-driven groundwater flow and reactive solute transport numerical modelling. The methodology has been applied to a simple 2D model which accounts for a large-scale (regional) domain with an accurate topographic representation of the site. Groundwater flow modelling coupled with transient salinity and decaying tritium transport has been performed and compared with field data. Some conclusions are drawn concerning to the use of tritium data, both in hydrogeological and hydrochemical models.

Finally, the main conclusions and possible future developments are summarized in Chapter 4.

2 Visualization and spatial analysis of the hydrochemical database

2.1 Description of the hydrochemical visualization tool

An application for hydrochemical visualization of Laxemar 1.2 database has been developed using OpenDX. OpenDX is an open product originated from a software product known as IBM Visualization System, Visualization Data Explorer, Data Explorer, or simply DX. This software was designed, marketed, and supported by IBM Visualization Systems as a product supported on all commercially available Unix workstations. It provides general-purpose, yet specialized, software to support the production of data visualization and analysis. DX is a specialized software system designed only to support visualization, not other types of programming or analysis. However, within the visualization niche DX is general purpose. It supports a broad range of facilities useful in the widest possible range of visualization applications, and is not tailored or customized to the more specific needs of any one limited application domain. Since its introduction by IBM Research in 1991, it is widely used in academia, industry and government worldwide for many research, design, commercial, education and operational endeavours such as aerospace and automotive engineering, chemistry, device design, earth and environmental sciences, finance, market research, medicine, petroleum exploration, space sciences, transportation and other disciplines. As of 5/24/99, IBM Visualization Data Explorer is now IBM Open Visualization Data Explorer, known as OpenDX. A world wide site for OpenDX community (users and developers) can be found at www.opendx.org.

According to /Thompson et al. 2001/, the OpenDX visualization environment is conceptually based on an underlying abstract data model, supported by three powerful visual programming support components. The first programming component is a graphical program editor that allows a user to create a visual program by using an interface to select program subcomponents, designate the order of their application, and define any parameter values they require. Second is a core set of supplied data transformations, each defined and encapsulated as an OpenDX module that takes specified inputs, uses other user-defined parameters, implements a specific data action, and outputs specific results. The third programming component implements user control over the computation of the visual program, based on a data-flow driven client-server execution model. In a simple single-processor execution mode, this facility allows the user to follow program execution by tracing the data flow. In a more computationally-intensive application, this approach allows the visualization to be divided into subcomponents that can be parcelled out for execution on multiple workstations or to the multiple processing elements of a modern supercomputer. The client-server execution model allows the user to easily distribute elements of the computation to multiple computer elements. This obviously helps to reduce overall processing time. More importantly, it can dramatically expand the size of data sets that can be effectively processed.

In visual programming terms, the OpenDX environment is designed to allow users to visualize both observed and simulated data. Developers can use the supplied facilities to create visual programs that provide imagery, along with interactive controls that allow users to directly manipulate the image display. For more advanced users, OpenDX also supplements the basic visual programming interface with other, more advanced features.

All the visual program development components are based on a very general, application-independent core data model supported by OpenDX. In essence, this data model is an N-dimensional abstract data space from which the OpenDX user takes 2-D and 3-D visual “snapshots” to create viewable images. This is in sharp contrast to more constrained data models that support only a 2-D or 3-D base model, onto which users must fit their data. The OpenDX data model is also purposely defined in a manner independent from particular encodings and data file formats. This distinction between the logical data model and the intricacies of particular file formats allows OpenDX to be flexible and adaptable, supporting data import from most applications and formats. Native OpenDX import facilities support various ways to read scientific data sets, allowing the data to be described by their dimensionality, value-type (e.g. real, complex, scalar, vector), location in space, and relationship to other data points.

By using this software environment, a visual program has been developed able to handle the Laxemar v. 1.2 database. This visualization tool has been programmed to be able to visualize hydrochemical and isotopic information both in the near-surface and in the bedrock environments, combined with geographical information (topography, coast lines, etc), geometrical objects (such as boreholes and tunnel) and geo-hydrological information (deformation zones – hydraulic conductor domains). The main structure of the visual program can be seen in Figure 2-1.The visual program contains several subprograms each processing independent datasets. The subprograms are made of modules, which can be regarded as traditional "subroutines", and send the results to the last subprogram named "visualizing". Figure 2-2 shows (just as an example) part of the structure of the

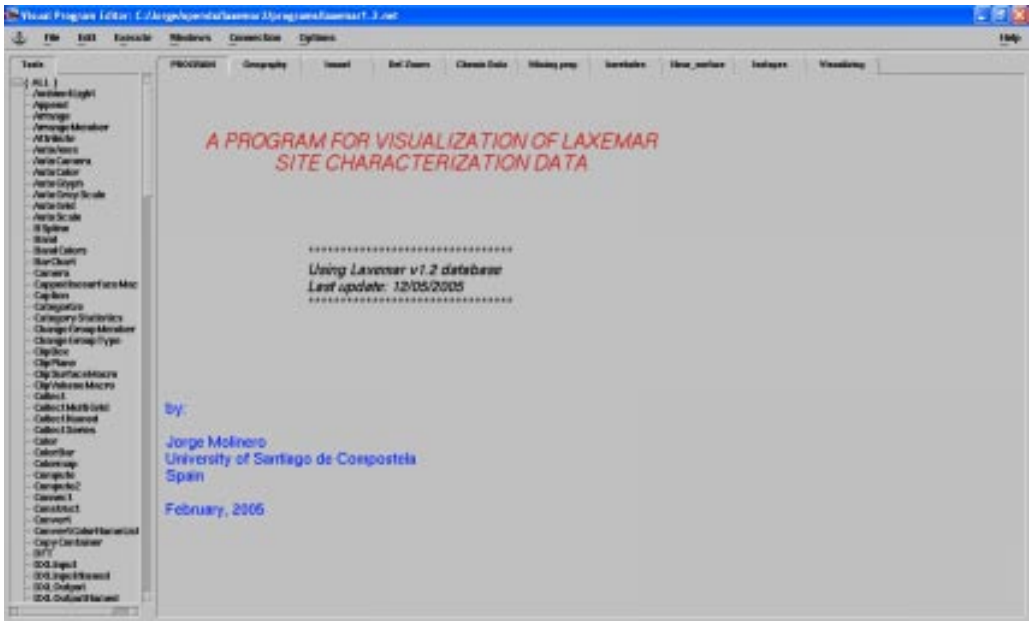

Figure 2-1. *Main structure of the visual program developed for visualization of the Laxemar v. 1.2 database. The program is made of 10 subprograms each one processing independent datasets.*

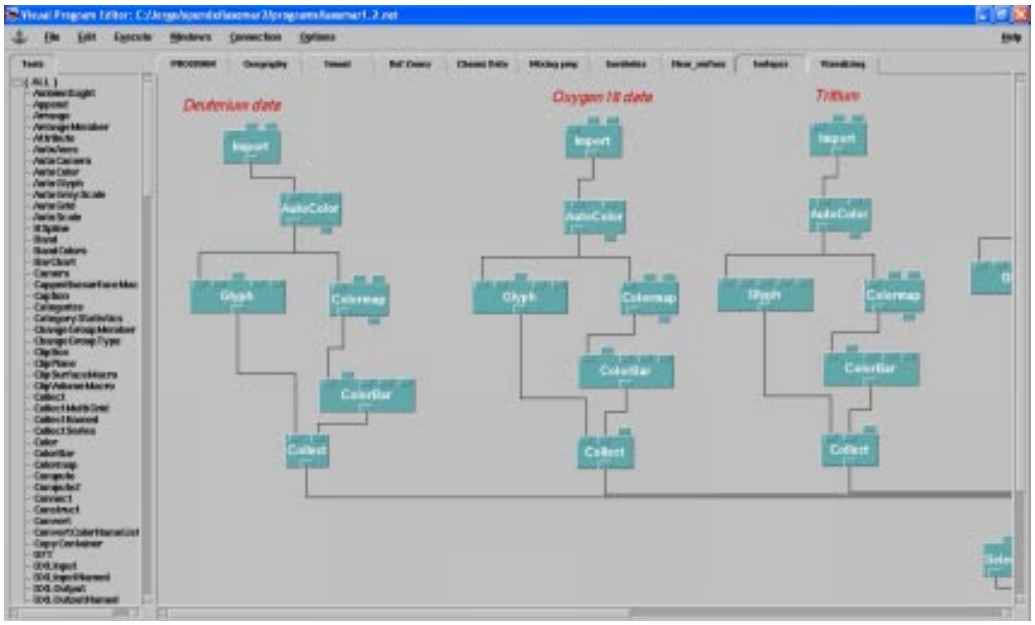

Figure 2-2. *Example of the subprogram "isotopes" for processing isotopic information. The subprogram is made of different modules ("subroutines"). Each module has a specific function and produces an output which constitutes the input for other modules.*

subprogram developed for visualization of isotopic data. The last subprogram can be regarded as the "main program", which collect all the outputs from the other subprograms and visualizes the information (Figure 2-3). The selection of the information to be visualized in each particular run of the visual program is user defined by means of several interactive control panels (Figure 2-4).

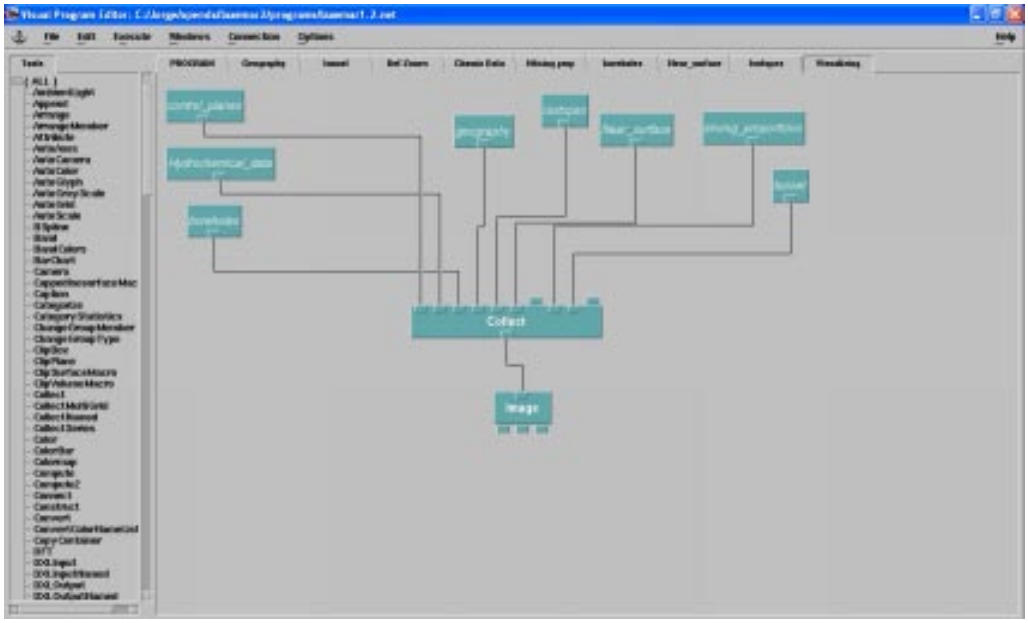

Figure 2-3. *The final subprogram visualizes the information processed in each subprogram.*

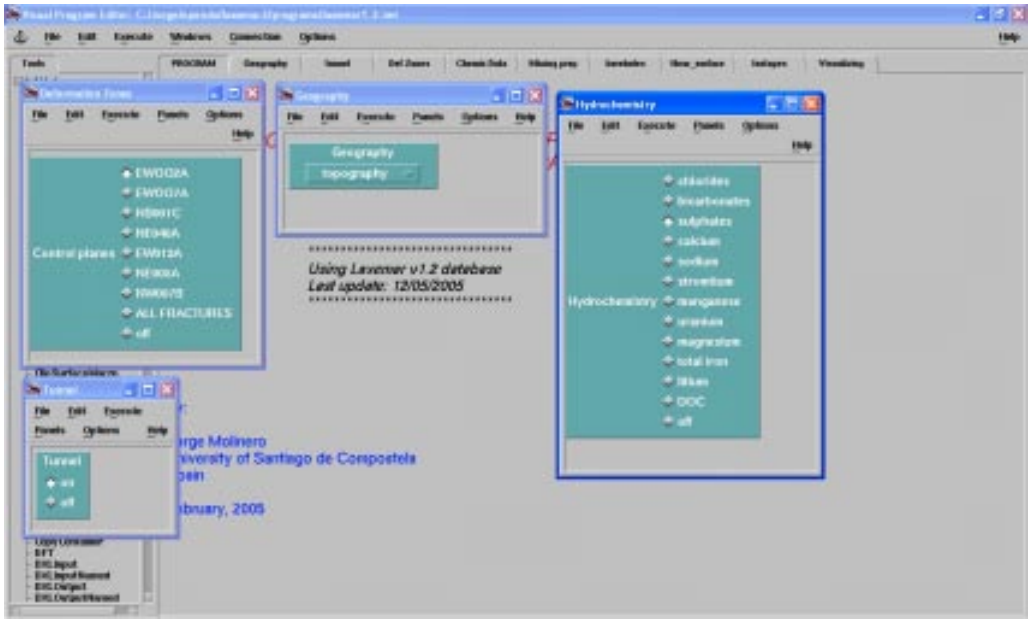

Figure 2-4. *The type of information to be visualized in a given run is defined by means of specific interactive control panels.*

2.2 Visualization of near-suface hydrochemical database

Figure 2-5 shows the location of all the available soil pipes in Laxemar and Simpevarp subareas, as they are named in the datafreeze of Laxemar 1.2.

Only those samples categorized as “representative samples” in the database have been included in the visualization of near-surface hydrochemistry. The amount of data is different depending on the type of element to be visualized (i.e there are more representative samples with chloride or bicarbonate data than tritium or ^{14}C, for instance).

Figure 2-6 shows chloride concentrations in soil pipes. It can be seen that near-surface groundwater samples are diluted, with chloride concentrations always lower than 150 mg/L. However, there is a clear influence of Baltic water in those soil pipes located close to the coast line (such as SSM00034

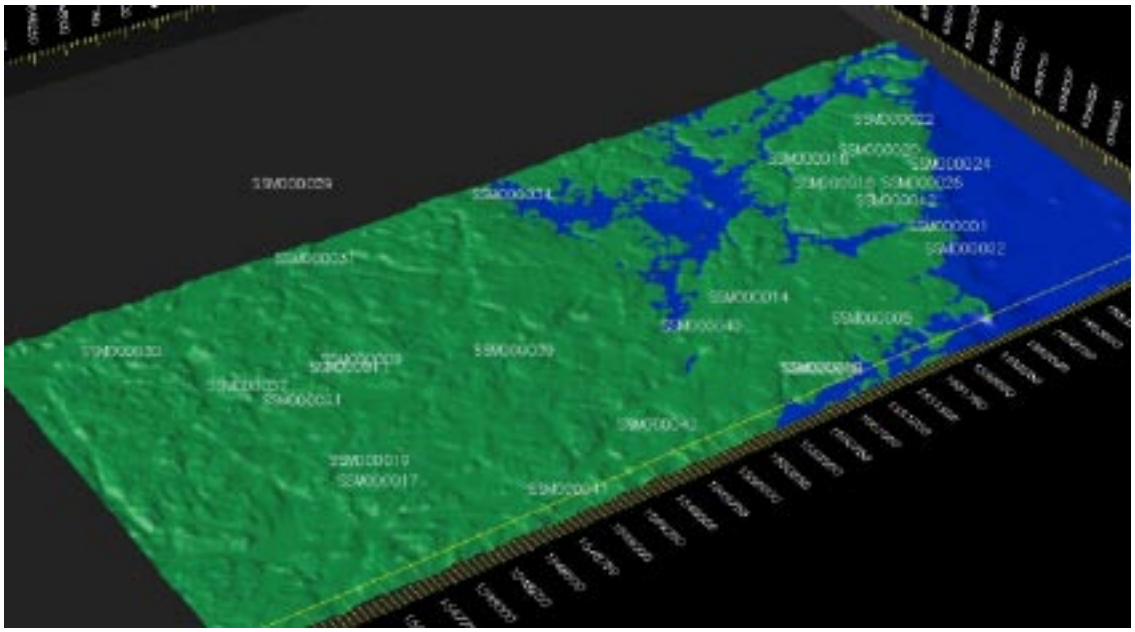

Figure 2-5. *Spatial location of soil pipes in the Laxemar v. 1.2 database.*

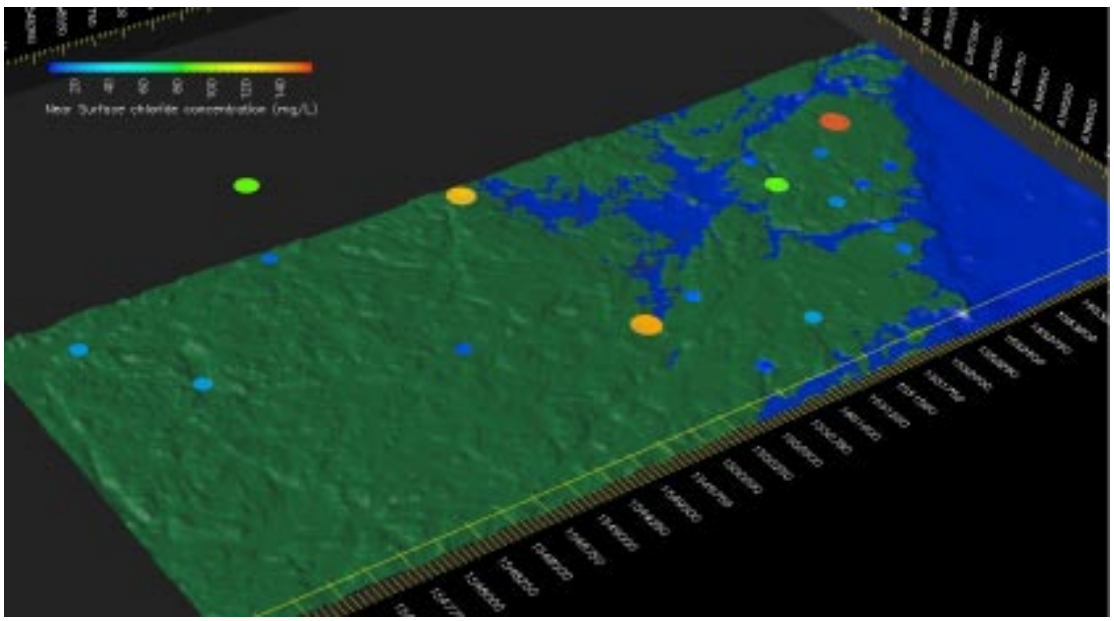

Figure 2-6. *Spatial distribution of chloride concentration in soil pipes. The maximum value is located in soil pipe SSM00022 at Ävrö.*

and SSM0040). An apparent anomaly to this general trend is observed in soil pipe SSM00022, located in Ävrö. This particular soil pipe is not located close to the coast line but inwards in the Ävrö Island. However it shows the highest chloride concentration of all the representative samples of soil pipes. This soil pipe also shows the highest concentrations of strontium, sodium and sulphates (among others) as can be seen in Figures 2-7, 2-8 and 2-9, respectively.

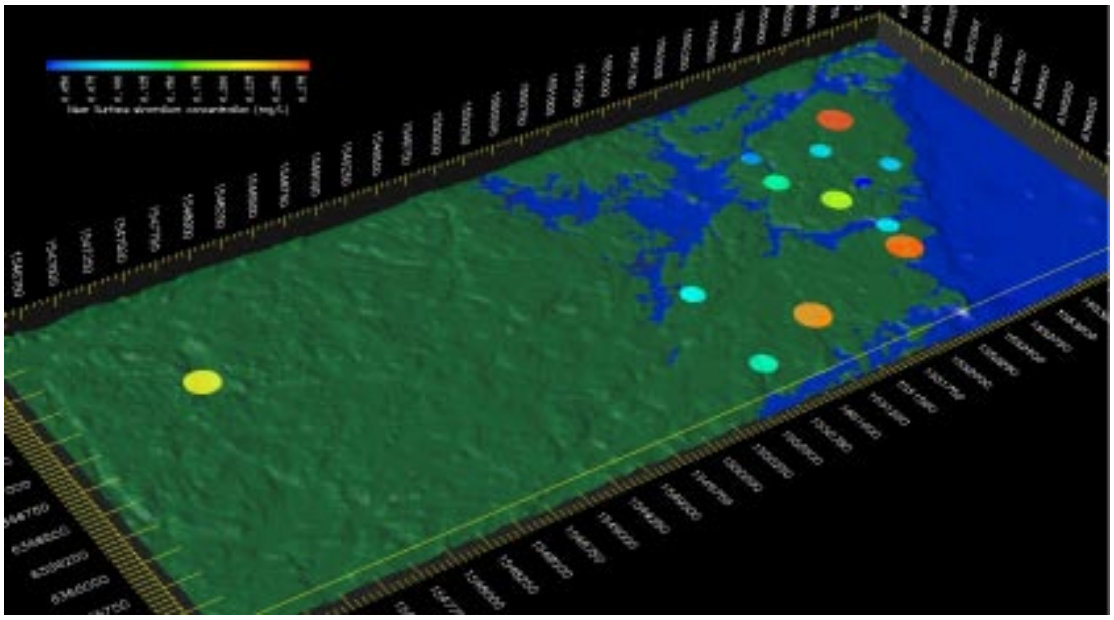

Figure 2-7. *Spatial distribution of stromtium concentration in soil pipes. The maximum value is located in soil pipe SSM00022 at Ävrö.*

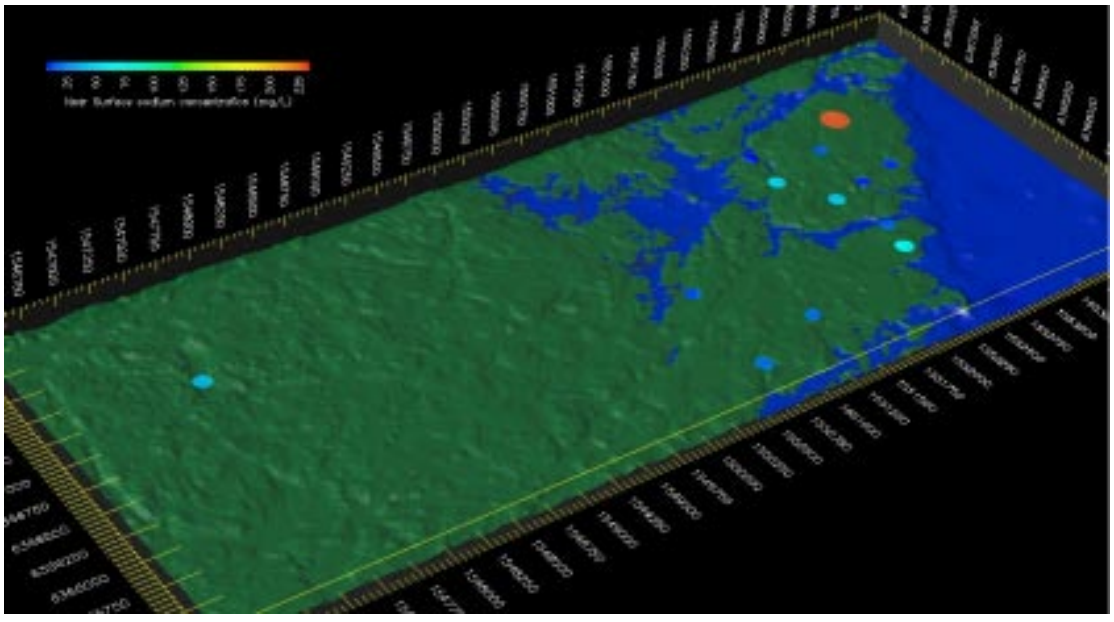

Figure 2-8. *Spatial distribution of sodium concentration in soil pipes. The maximum value is located in soil pipe SSM00022 at Ävrö.*

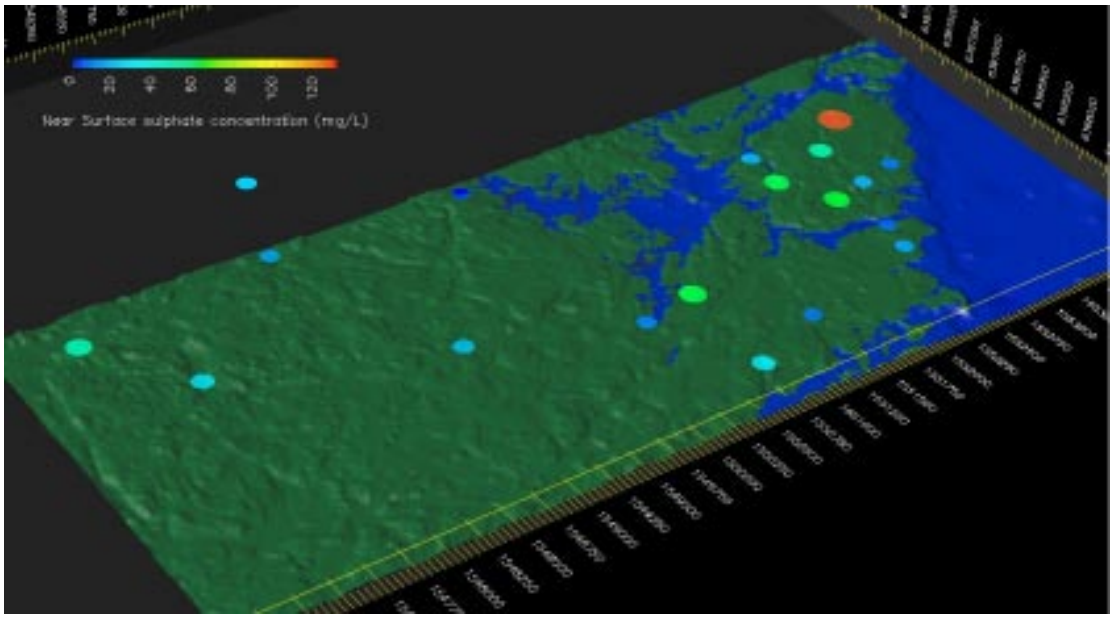

Figure 2-9. *Spatial distribution of sulphate concentration in soil pipes. The maximum value is located in soil pipe SSM00022 at Ävrö.*

Figure 2-10 shows the spatial distribution of bicarbonate in soil pipes. Bicarbonate is the dissolved component having the largest number of measurements in representative samples. It can be seen in Figure 2-10 that there is not an easily recognizable spatial trend for this component. The highest concentration of bicarbonate corresponds to soil pipe SSM00034, which is located on the coast line in front of Äspö, but other soil pipes located in the vicinity of the coast line show low concentrations. At inland positions in Laxemar, there are a number of soil pipes with low bicarbonate concentra-

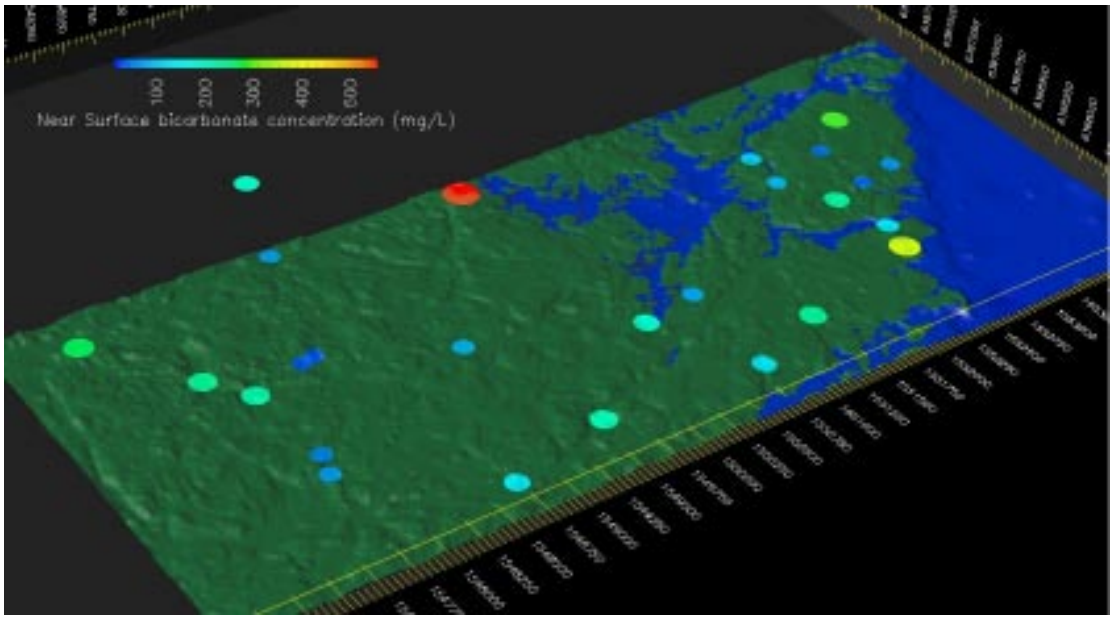

Figure 2-10. *Spatial distribution of bicarbonate concentration in soil pipes. There is not an easily recognizable spatial trend for this component.*

tions (such as SSM00031, SSM00009, SSM00011, SSM00019 and SSM00017) and other soil pipes located even more inwards in the mainland (SSM00030, SSM00037 and SSM00021) which show relatively high concentrations. Dissolved bicarbonate can be related with two main processes: calcite dissolution and organic matter oxidation. Then the spatial distribution of bicarbonate concentrations could be correlated with the local abundance of both calcite and organic matter. It can be expected that both compounds will be more abundant where Quaternary deposits and organic soils are thicker.

There are few representative samples in soil pipes having information on radioactive isotopes. Figures 2-11 and 2-12 show the spatial distribution of available measurements of ^{14}C and tritium, respectively. It can be recognized that soil pipe SSM00022 (Ävrö) shows clearly the lowest modern carbon contents and tritium activities.

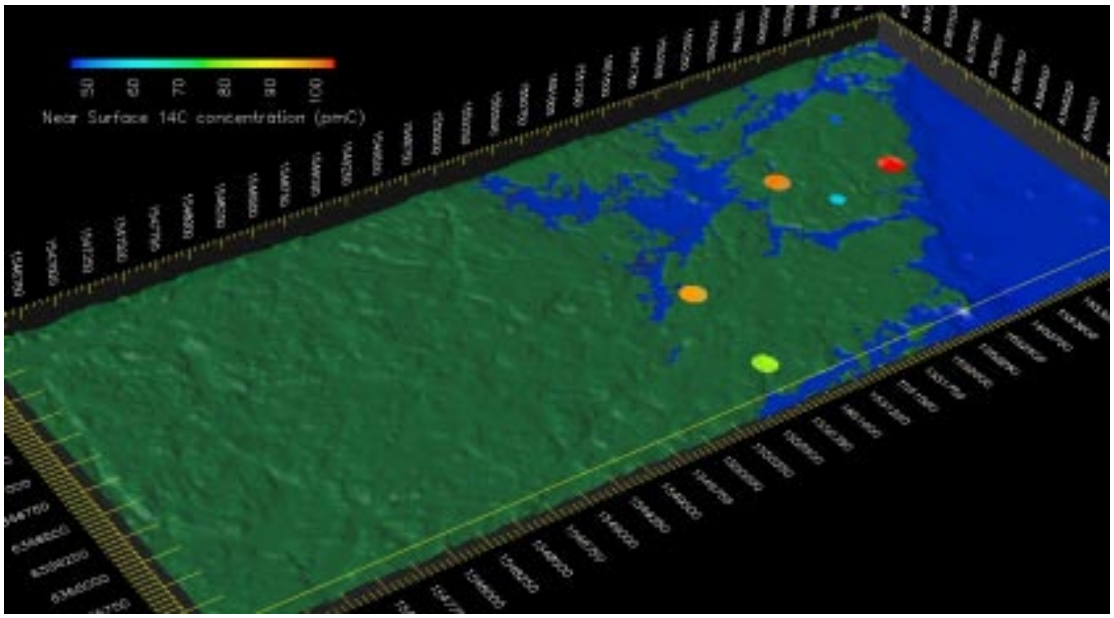

Figure 2-11. *Spatial distribution of 14C (pmC) in soil pipes. The minimum value is located in soil pipe SSM00022 at Ävrö.*

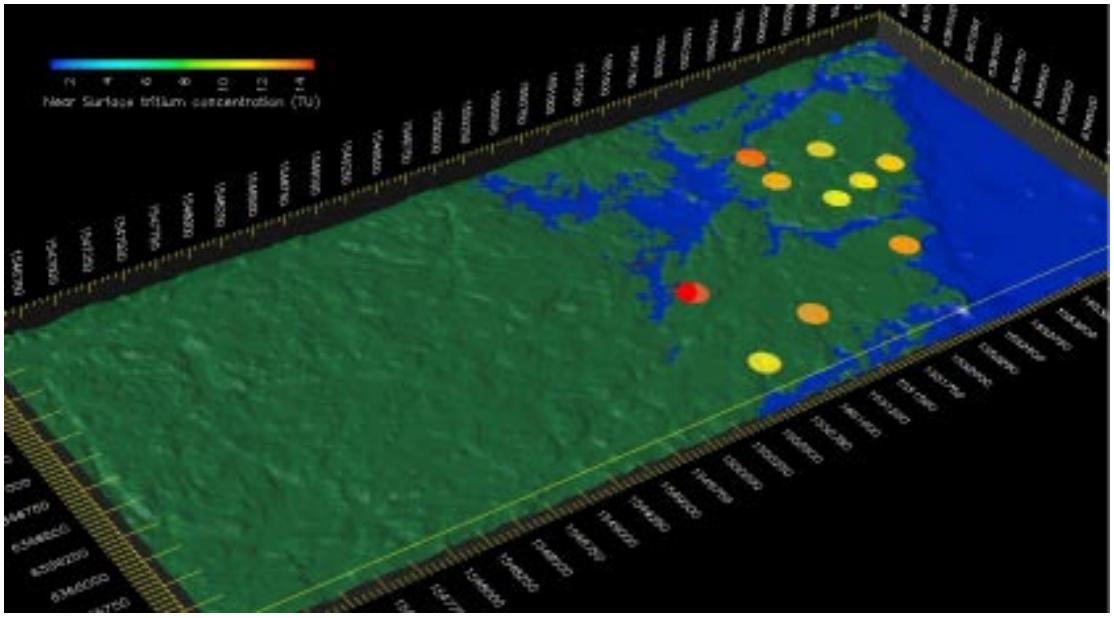

Figure 2-12. *Spatial distribution of tritium (TU) in soil pipes. The minimum value is located in soil pipe SSM00022 at Ävrö.*

From the previous analyses, it can be pointed out that soil pipe SSM0022 at Ävrö shows hydrochemical signatures consistent with the influence of older and more saline groundwater than the rest of the representative samples from soil pipes. These hydrogeochemical signatures at the near surface environment could constitute an indication of a groundwater discharge zone or stagnant older water that has been preserved under low permeable soil cover. This kind analysis will be combined with the quaternary geology and overburden description in future modelling phases. It is worth noting that, at the present time, there is no available isotopic information for soil pipes at the Laxemar subarea.

2.3 Visualization of bedrock hydrochemical database

Figure 2-13 shows a top view for the location of the main cored boreholes (from the point of view of the number of representative samples) available in Laxemar and Simpevarp subareas, as they are named in the datafreeze of Laxemar 1.2.

The main available cored boreholes are KLX01, KLX02, KLX03 and KLX04 at the Laxemar subarea and KSH01, KSH02, KSH03, KAV01, KAV04, KAS02, KAS03, KAS04 and KAS06 in the Simpevarp subarea. It is worth noting that several percussion boreholes contribute to the hydrochemical database with representative samples. The geometries of the percussion boreholes have not been included yet in the visual program (this work is now in progress), but all the representative samples available in the database, including percussion boreholes, have been taken into account for the hydrochemical visualization.

Figure 2-14 shows a bottom view (from the southwest) of the Laxemar and Simpevarp subareas, including the geometry of the main cored boreholes and the Äspö tunnel. It is thought that both boreholes and tunnel are a very useful reference for 3-D visualization of the bedrock hydrochemistry. It is worth noting that the geometry of the boreholes is not accurate but has been approximated from the coordinates of some water samples. This is the reason why Äspö boreholes do not reach the surface. It is expected to improve the definition of these geometrical features in future versions of the visual modelling.

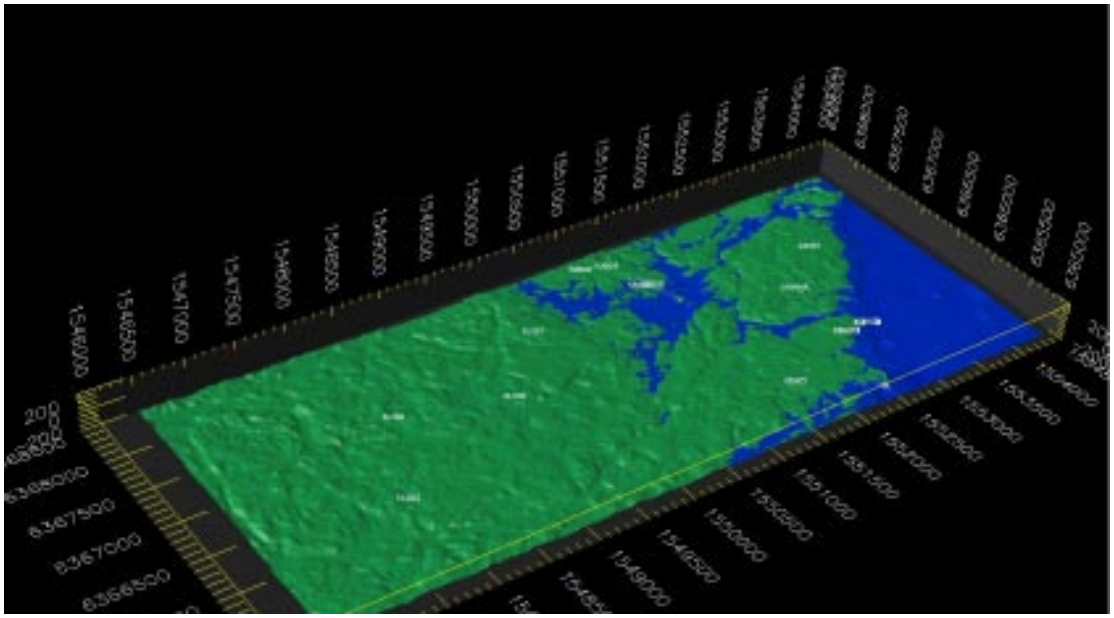

Figure 2-13. *Top-view of spatial location of the main cored boreholes in Laxemar v. 1.2 database.*

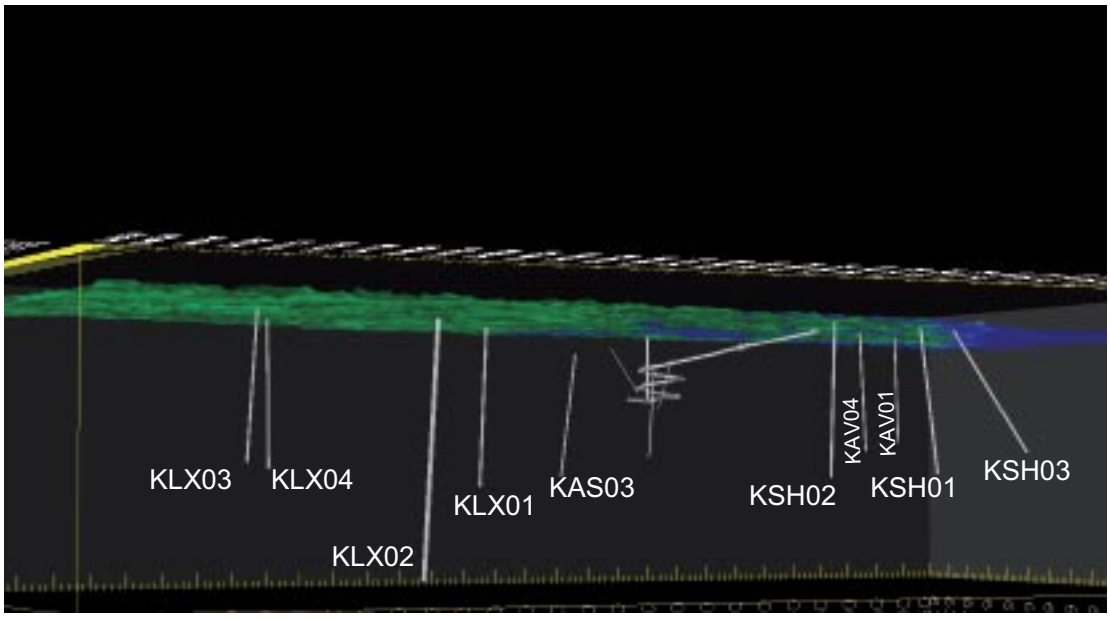

Figure 2-14. *Bottom-view (from the southwest) of Laxemar and Simpevarp subareas. Main cored boreholes, as well as the Äspö tunnel, have been included as geographical references in the visualization.*

The reason of including unrepresentative dissolved chlorides in KLX03 and KLX04 is to have a "first guess" of the salinity distribution at Laxemar subarea (notice that all the "representative knowledge" available up to now comes from KLX01 and KLX02). Figure 2-15 shows the occurrence of brine water at depth in Laxemar subarea. The brine has been detected in water samples of borehole KLX02 at a depth greater than 1,100 m. Figure 2-16 shows the same distribution of chloride concentration excluding the most saline waters of KLX02 boreholes. In this new visualization of chloride it is easier to notice the difference of salinity between the groundwater of Laxemar and Simpevarp subareas. Laxemar subarea represents a continental (inland) hydrogeological framework,

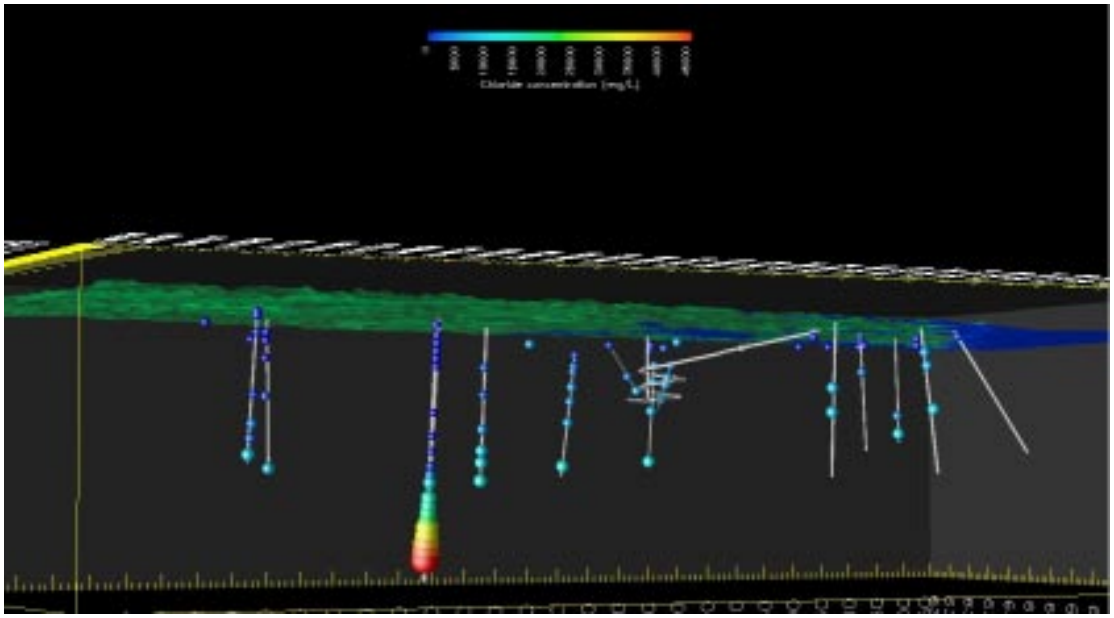

Figure 2-15. *Shows all the available representative chloride data in the bedrock samples, except for boreholes KLX03 and KLX04, where all available chloride data have been included (only for chloride visualization purposes).*

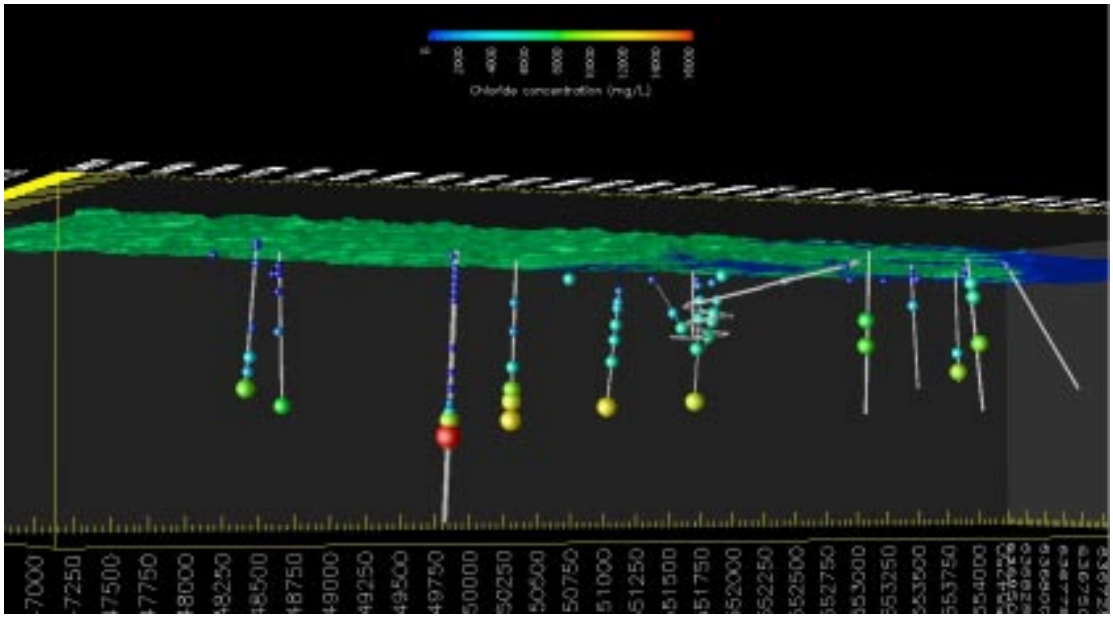

Figure 2-16. *Distribution of chloride concentrations at the bedrock under the Laxemar and Simpevarp subareas above 1,100 m (excluding the most saline waters in KLX02). Symbol size is proportional to the chloride concentration value.*

with a thick fresh water body reaching depths of nearly 1,000 m. However, the Simpevarp subarea represents a coastal hydrogeological framework where fresh water bodies are confined to the first 100–200 m of the bedrock.

According to the water classification used by /Laaksoharju et al. 2004/, four main hydrochemical water types have been identified in the Simpevarp area, named from type A to type D /Laaksoharju et al. 2004/.

Water Type A. This type comprises dilute groundwaters (< 1,000 mg/L Cl; 0.5–2.0 g/L TDS) mainly of Na-HCO_3 type present at shallow (< 200 m) depths at Simpevarp subarea, but at greater depths (0–900 m) at Laxemar subaraea. At both subareas the groundwaters are marginally oxidising close to the surface, but otherwise reducing. Figure 2-17 shows a visualization of the spatial distribution of water type A (diluted). This type of water is interpreted as related to a meteoric origin, and shows higher bicarbonate contents. Figure 2-18 shows the spatial distribution of bicarbonate concentrations. It can be seen that the higher values of bicarbonate concentrations coincides almost exactly with diluted groundwater (type A). The high bicarbonate concentration can be mainly attributed to the occurrence of organic matter oxidation coming from the soil layers at emerged lands.

Water Type B. This type comprises brackish groundwaters (1,000–6,000 mg/L Cl; 5–10 g/L TDS) present at shallow to intermediate (150–300 m) depths at Simpevarp subarea, but at greater depths (approx. 900–1,100 m) at Laxemar subarea. The origin of this water type could be different from one place to another. At Simpevarp subarea there is potentially some residual Littorina Sea (old marine) influence. In contrast, at the Laxemar subarea this water type could mainly be attributed to the influence (dispersion/diffusion) of deep brine water. Figure 2-19 shows a visualization of the spatial distribution of water type B (brackish).

The complex origin of this water type B can be better understood by analysing other hydrochemical information. Figure 2-20 shows the spatial distribution of magnesium in groundwater. It can be noticed that high magnesium concentrations are found in the Simpevarp subarea, exactly for the same water samples corresponding to water type B (brackish). However, water type B at the Laxemar subarea shows low magnesium contents compared to the Simpevarp subarea. Magnesium is not a conservative element. On the contrary, it is well known that Mg can be involved in cation exchange processes, mainly in fractures and fracture zones containing clay minerals. However, according to /Laaksoharju 1999/ the average magnesium concentration in Baltic water is 234 mg/L, while deep brine waters at KLX02 shows very low concentrations of magnesium (about 2 mg/l).

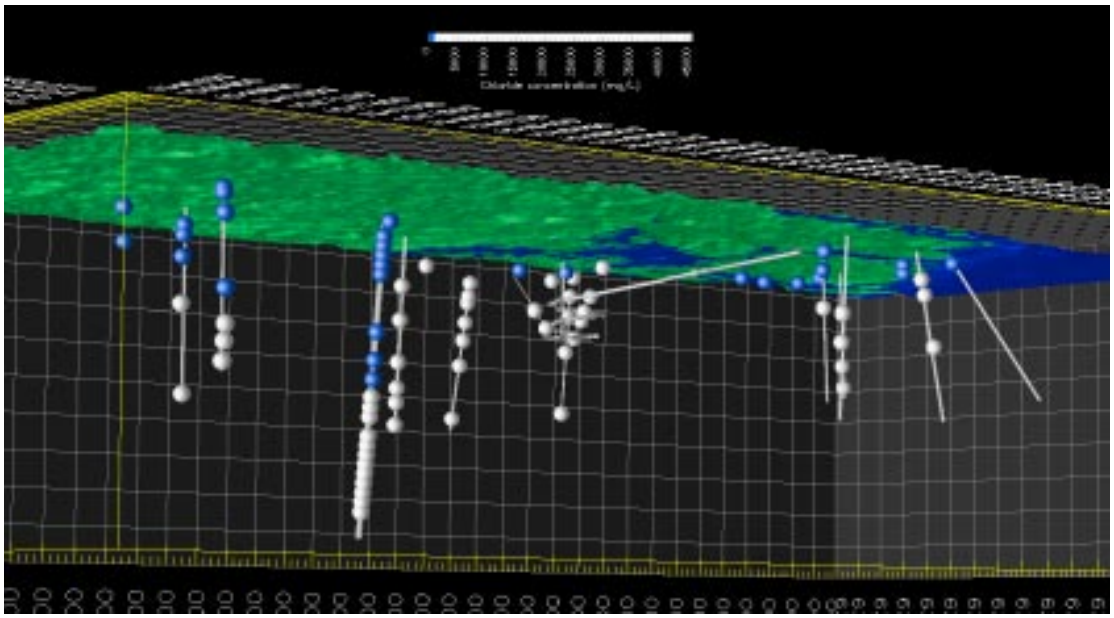

Figure 2-17. *Spatial distribution of water type A (diluted), which can be related to a meteoric origin. It can be noticed that this type of water reaches much higher depths at Laxemar subarea than at Simpevarp subarea.*

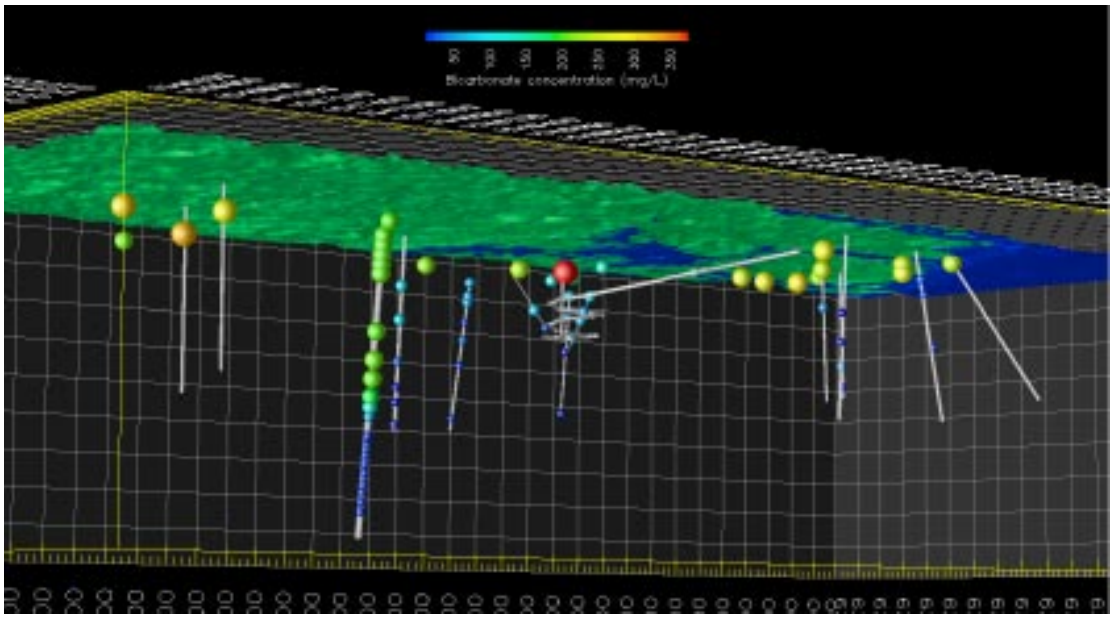

Figure 2-18. *Spatial distribution of bicarbonate concentrations. By comparing this figure with Figure 2-17 it can be noticed that diluted water (type A) show the highest bicarbonate concentrations, probably related with oxidation of organic matter from the surface soil layers.*

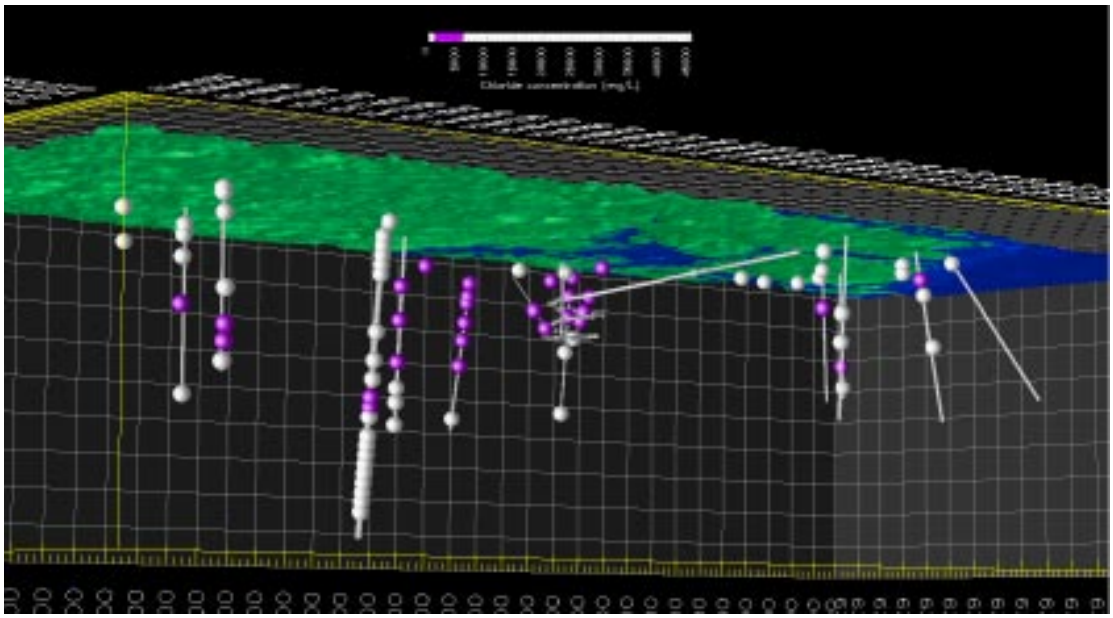

Figure 2-19. *Spatial distribution of water type B (brackish). This type of water is found at relatively shallow depths in Simpevarp subarea (mainly under Äspö), but also in Laxemar close to the coast (KLX01). Inland (KLX02-03-04) this type of water is found deeper, from 600 to 1,100 m.*

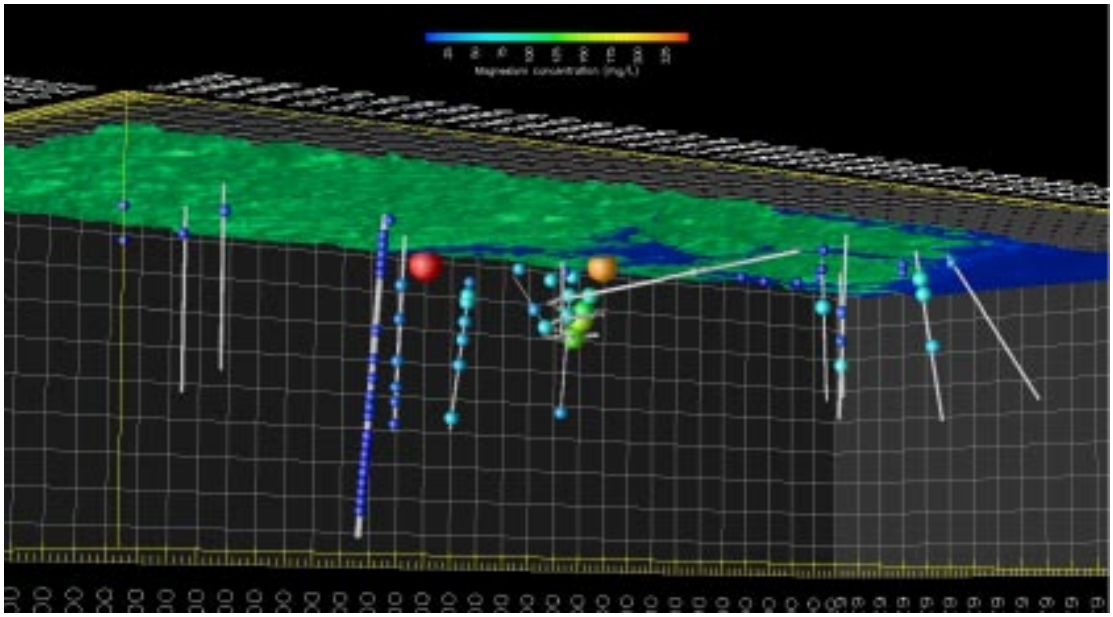

Figure 2-20. *Spatial distribution of dissolved magnesium in groundwater. It can be seen that maximum magnesium concentrations are found in the Simpevarp subarea, indicating a possible influence of older marine waters.*

This high contrast could be qualitatively useful to establish a difference between the salinity of the brackish waters at Laxemar and Simpevarp subareas. By comparing Figures 2-19 and 2-20 it can be seen that brackish waters at Laxemar are most likely related to the occurrence of a dispersion zone between deep saline waters and shallow diluted water of meteoric origin, while brackish waters of the Simpevarp subarea show an influence of marine waters. These marine waters must be older than the Baltic Sea, since nowadays there is no driving force for sea water to penetrate in the bedrock. It has been postulated that this old marine water was introduced into the bedrock at the Littorina sea stage, due to density driven flow caused by the presence of relict fresh glacial water deeper in the bedrock.

Water Type C. This type comprises saline groundwaters (6,000–20,000 mg/L Cl; 25–30 g/L TDS) present at intermediate depths (> 200–300 m) at the Simpevarp subarea, and at greater depths (> 1,000 m) at Laxemar subarea. Similarly to water type B, this type C shows different hydrochemical signatures from one place to another. At the Simpevarp subarea (but also at coastal Laxemar locations; i.e.KLX01) signatures of old marine influence can be recognized (see magnesium in Figure 2-20), together with glacial signatures (as will be shown latter on). On the contrary, at the Laxemar subarea this water type could mainly be attributed to the influence (dispersion/diffusion) of deep brine which is found adjacent in depth. Figure 2-21 shows a visualization of the spatial distribution of water type C (saline).

Glacial isotopic signatures have been postulated to be present in groundwater at different places of Scandinavian bedrock locations. According to /Laaksoharju 1999/, when the continental ice melted and retreated (about 13,000 years ago), glacial meltwater was hydraulically injected under considerable head pressure into the bedrock. The exact penetration depth of glacial water is uncertain but, according to /Svensson 1996/, a depth of several hundreds metres can be expected according to hydrogeological models.

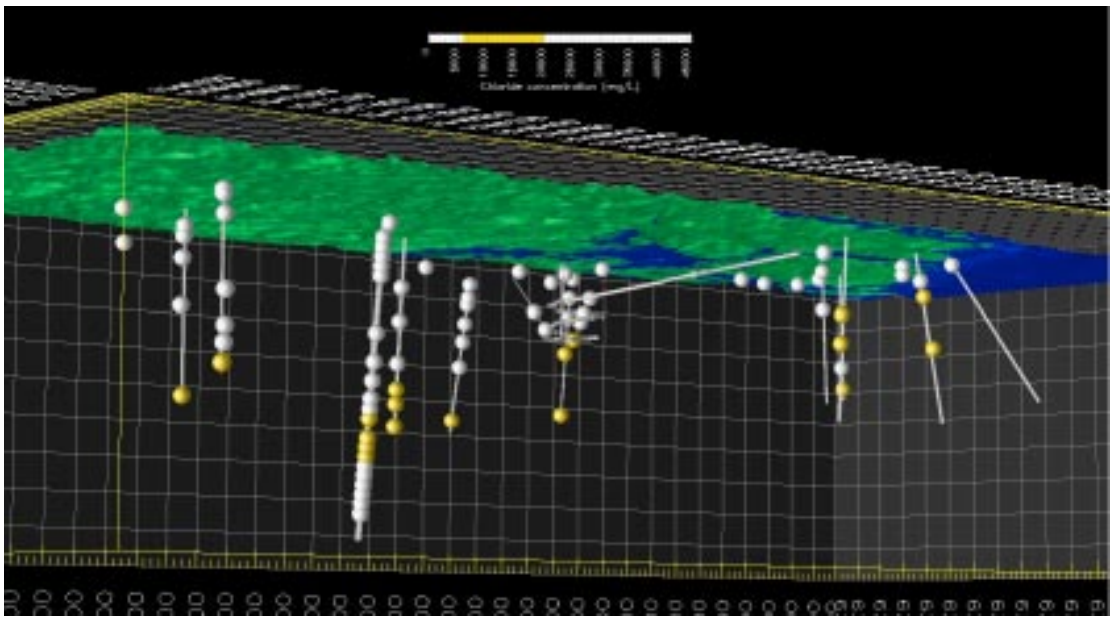

Figure 2-21. *Spatial distribution of water type C (saline). This type of water is found at shallow to intermediate depths in Simpevarp subarea, and deeper at Laxemar (800–1,200 m).*

The best tracers for glacial water signatures are assumed to be the stable isotopes 18-O and 2-H. According to /Laaksoharju 1999/, the isotopic composition for a Glacial end-member water is –21‰ SMOW for $\delta^{18}O$, and –158‰ SMOW for $\delta^{2}H$. The clearest glacial signature at the Simpevarp area was found under the Äspö island (KAS03) during the site characterization process before the construction of the tunnel. Figures 2-22 and 2-23 show the spatial distribution of ^{18}O and ^{2}H, respectively, of all the representative samples available in the Laxemar 1.2 database.

According to /Laaksoharju 1999/, meteoric reference water has a $\delta^{18}O$ of –10.2‰ and a $\delta^{2}H$ of –77.1‰. Marine reference water has a $\delta^{18}O$ of –5.9‰ and a $\delta^{2}H$ of –53.3‰. Finally, brine reference water has a $\delta^{18}O$ deviation of –8.9‰ and a $\delta^{2}H$ of 44.9‰. It can be seen that a there is a large

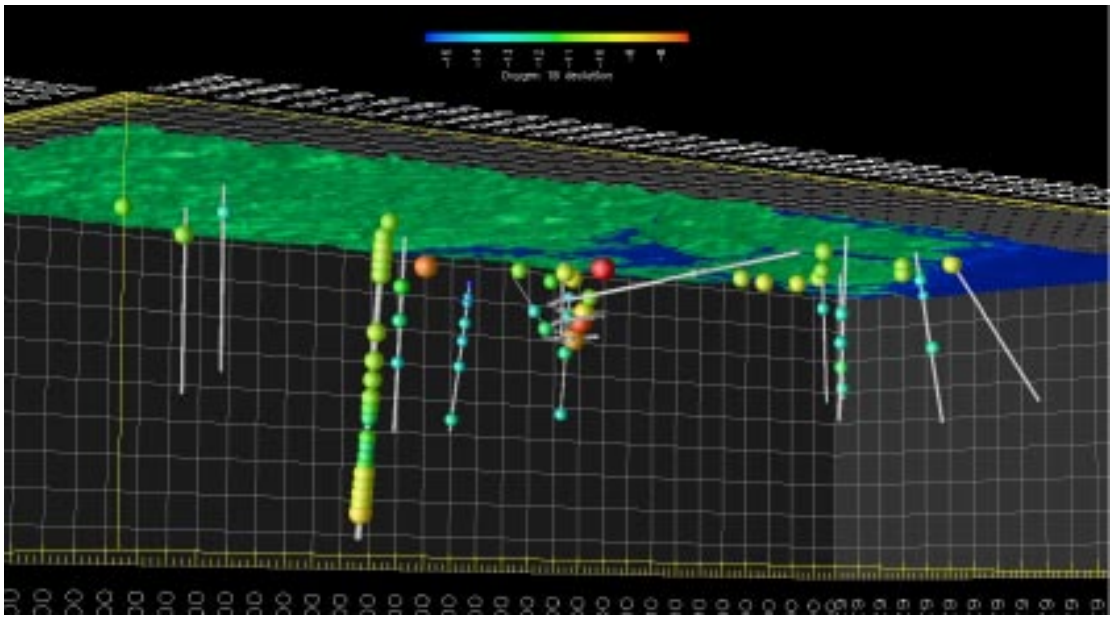

Figure 2-22. *Spatial distribution of ^{18}O deviations at Laxemar and Simpevarp subareas. A clear minimum value at KAS03 (under Äspö) can be seen which correspond to the Glacial Reference Water /Laaksoharju 1999/.*

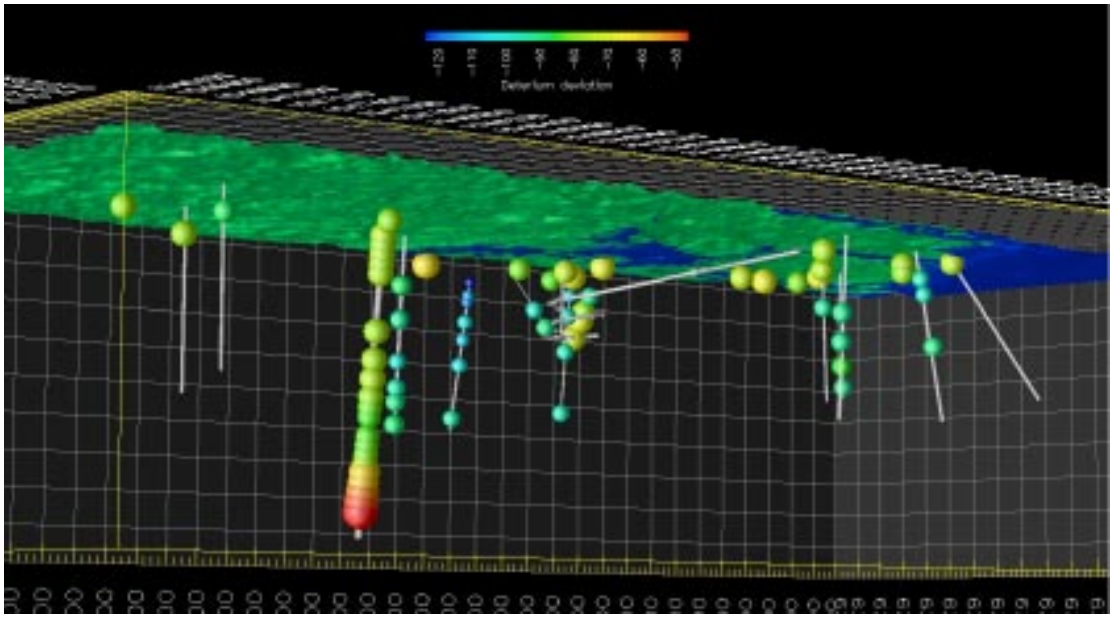

Figure 2-23. *Spatial distribution of ^{2}H deviations at Laxemar and Simpevarp subareas. A clear minimum value at KAS03 (under Äspö) can be seen which correspond to the Glacial Reference Water /Laaksoharju 1999/.*

constrast between a Glacial end-member water and the other possible end-members, in terms of the environmental stable isotopes. However, these numbers represent averages of values which can show considerable seasonal variations, such as occurs in recent meteoric precipitation. Figure 2-24 shows measured values of environmental stable isotopes in precipitation at Simpevarp area.

Looking at Figure 2-24, it can be seen that averaged values of stable isotopes in precipitation are consistent with the values proposed by /Laaksoharju 1999/ for meteoric reference water. However, seasonal variations can be important, since minimum isotopic values measured in precipitation (in winter) can be as low as the minimum values measured in groundwaters. Nevertheless, minimum isotopic values in groundwater correspond always to brackish or saline waters (see figures 2-19, 2-21, 2-22 and 2-23) and so, they can not correspond to fresh meteoric water that infiltrates the bedrock, but most probably correspond to glacial waters with (originally) lower deviations of ^{18}O and ^{2}H, which were mixed (dispersed/diffused) with more saline water.

Figures 2-25 and 2-26 show the spatial distribution of water samples with ^{18}O lower than –13‰ and ^{2}H lower than –90‰, respectively. Those "cutting values" are arbitrarily assumed, but help to visualize glacial signatures in brackish and saline groundwaters, according to the above reasoning.

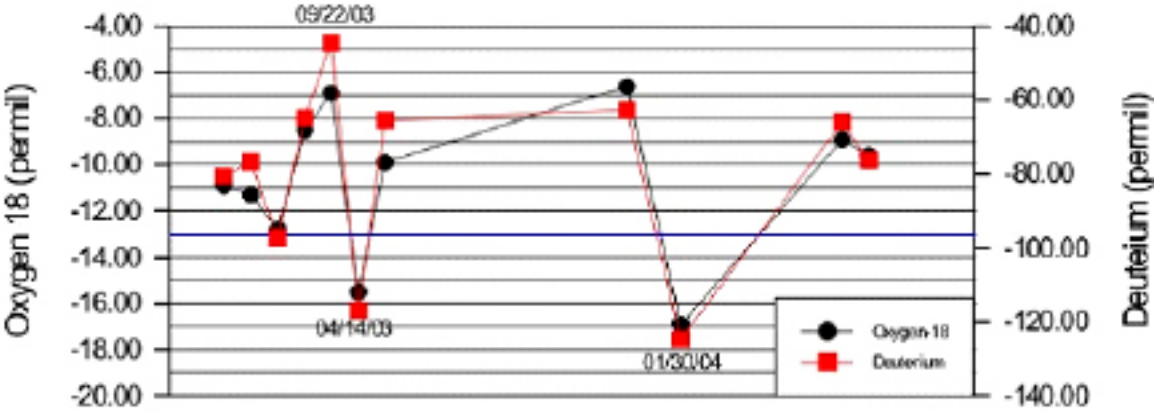

Figure 2-24. *Measured values of environmental stable isotopes in precipitation water at Simpevarp area. Blue line corresponds to the "cutting value" used latter in figures 2-25 and 2-26.*

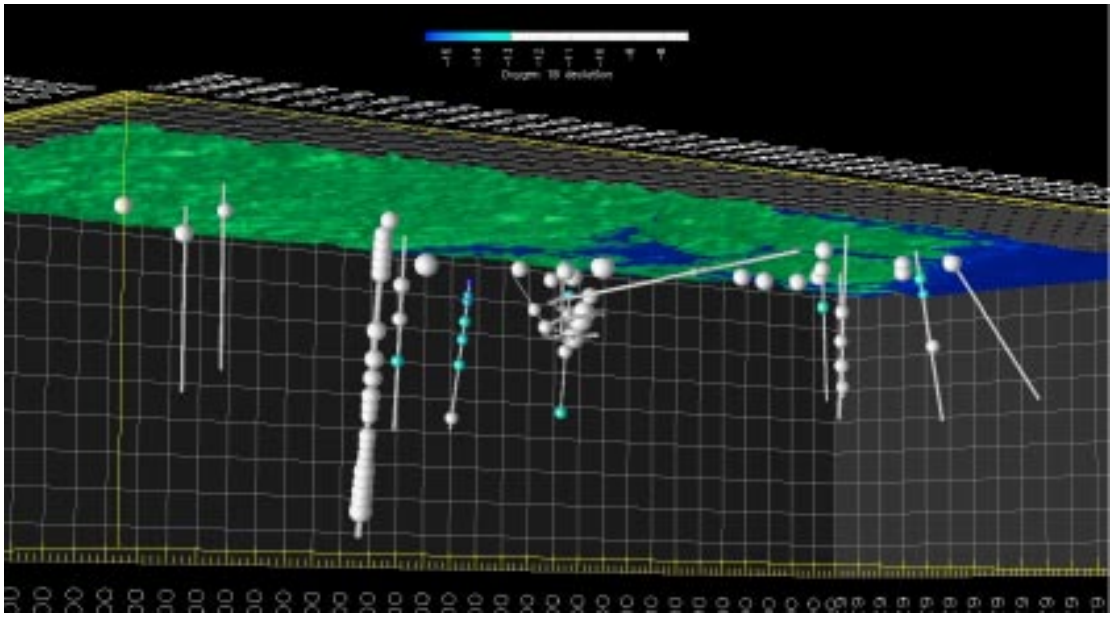

Figure 2-25. *Spatial distribution of $\delta^{18}O$ lower than –13‰.*

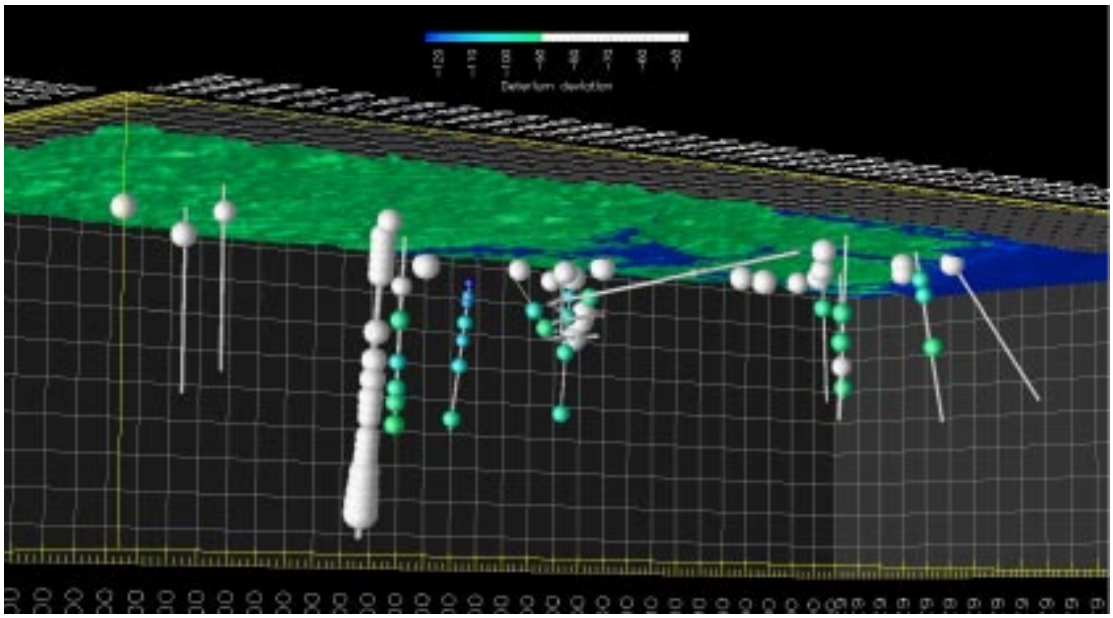

Figure 2-26. *Spatial distribution of δ^2H lower than –90‰.*

According to Figures 2-25 and 2-26, glacial isotopic signatures can be recognized clearly at the Simpevarp subarea, specially under the Äspö island and the Simpevarp peninsula. The clearest signature corresponds to borehole KAS03 at a shallow depth (about –120 m above sea level). At the Laxemar subarea, glacial signatures appear to be evident only close to the coast (KLX01) and deeper than in Simpevarp subarea. It is worth noting that all glacial signatures are found at groundwater type samples B and C (brackish or saline).

Water Type D. This type comprises highly saline groundwaters (> 20,000 mg/L Cl; to a maximum of ~ 70 g/L TDS) and have only been identified in one borehole at Laxemar (KLX02) at depths exceeding 1,200 m. Figure 2-27 shows a visualization of the spatial distribution of water type D (highly saline, also named "brine").

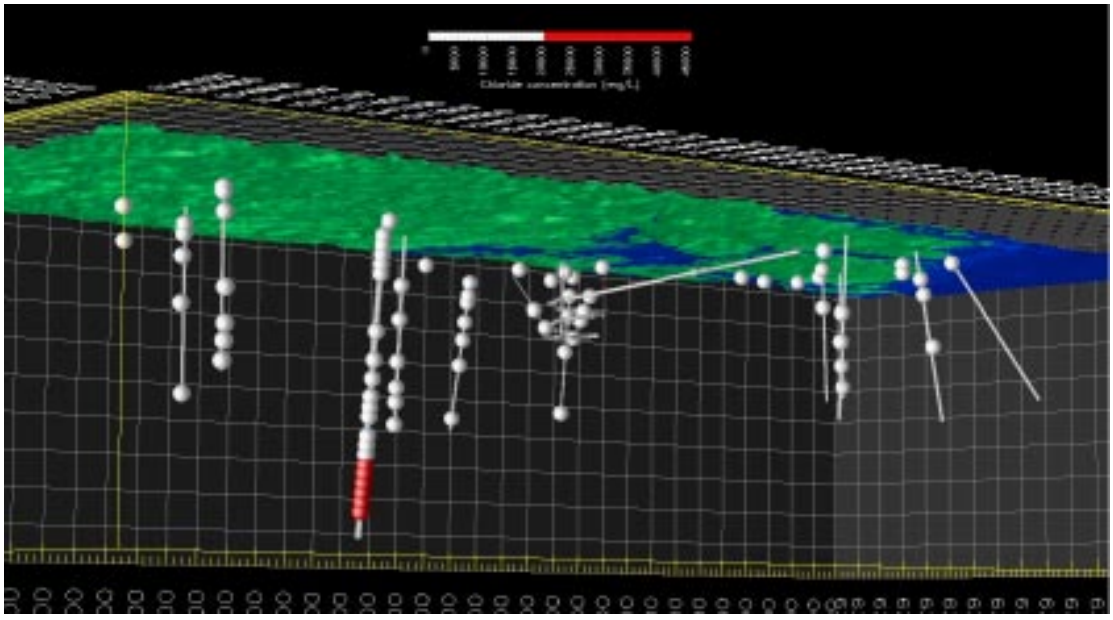

Figure 2-27. *Spatial distribution of water type D (highly saline). This type of water has been only found at borehole KLX02 (Laxemar), at depths from –1,200 to –1,600 m above sea level.*

Water samples of type D (highly saline) show also the highest concentrations of sulphates in bedrock groundwater (Figure 2-28).

Figures 2-29, 2-30 and 2-31 show different visualizations of the spatial distribution of the four water types in Laxemar and Simpevarp subareas. It can be seen that diluted water (type A) extends deeper at inland Laxemar positions compared to Laxemar coastal positions and the Simpevarp subarea, where diluted waters are only found at very shallow depths in the bedrock. On the contrary, brackish and saline waters (types B and C) are predominant at Laxemar coastal areas (KLX01) and at the Simpevarp subarea. Within the Simpevarp subarea, saline waters (type C) are found at much shallower depths under the Simpevarp Peninsula than under Äspö and Ävrö islands.

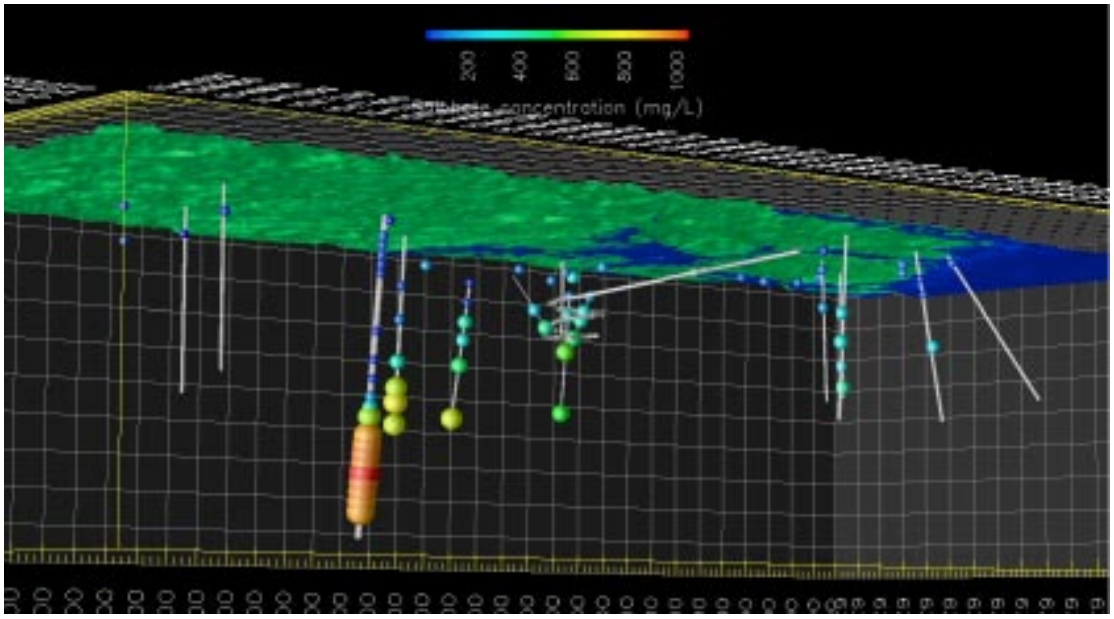

Figure 2-28. *Spatial distribution of dissolved sulphates at Laxemar and Simpevarp subareas.*

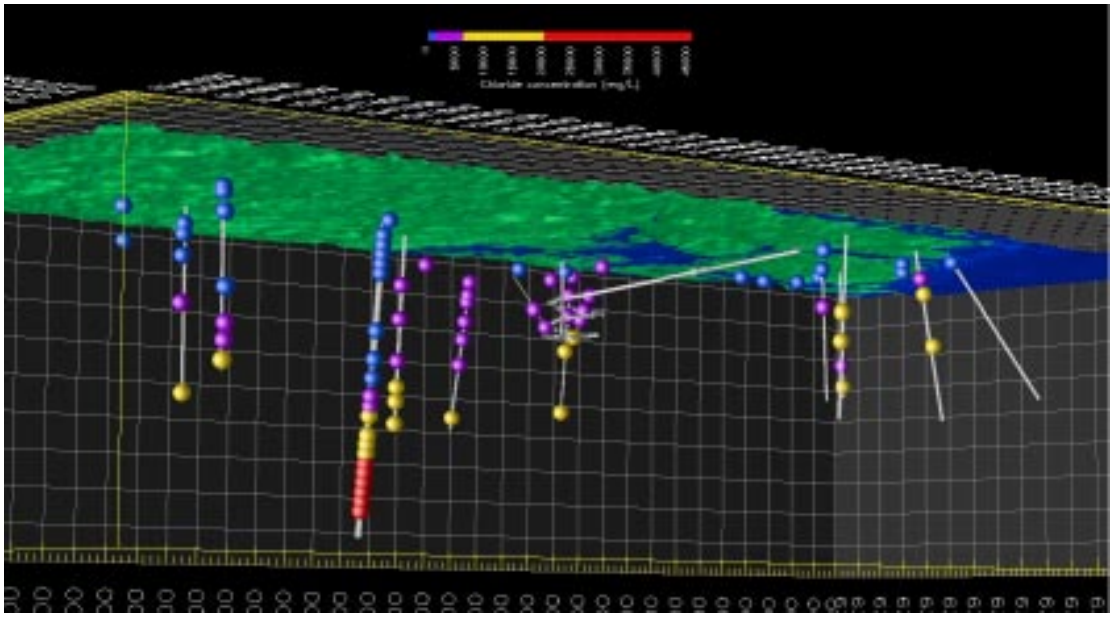

Figure 2-29. *Bottom view from the Southwest of the spatial distribution of water types in Laxemar and Simpevarp subareas. Water type A (blue), B (purple), C (yellow) and D (red).*

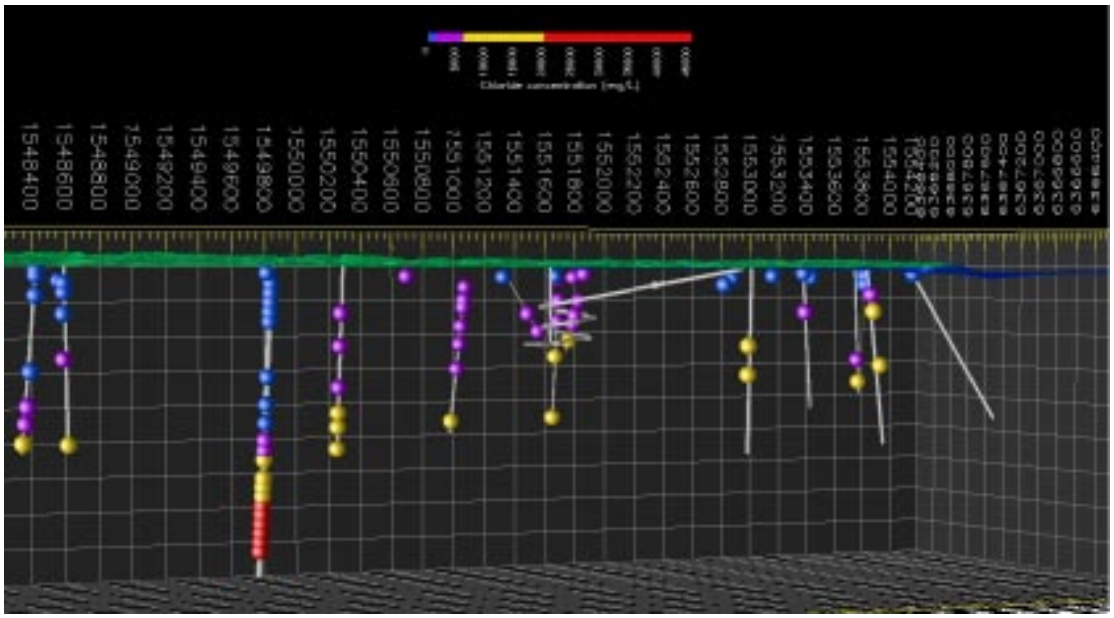

Figure 2-30. *South-frontal view of the spatial distribution of water types in Laxemar and Simpevarp subareas. Water type A (blue), B (purple), C (yellow) and D (red).*

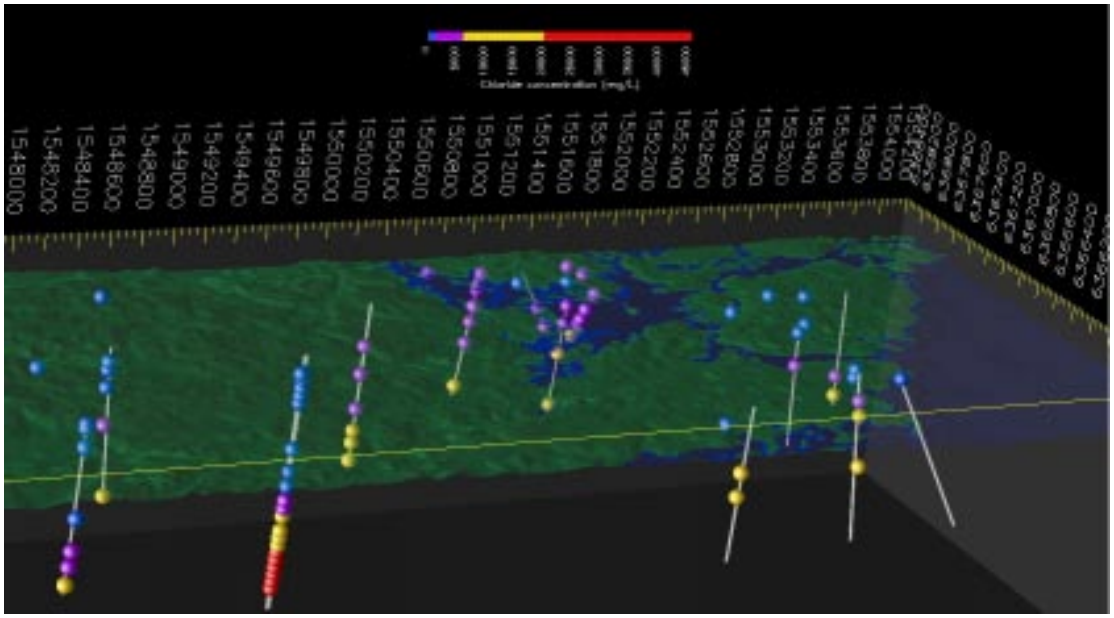

Figure 2-31. *Top view (with transparent terrain model) of the spatial distribution of water types in Laxemar and Simpevarp subareas. Water type A (blue), B (purple), C (yellow) and D (red).*

Water samples of type D (highly saline) show the highest concentrations of most dissolved species. Figures 2-32, 2-33, 3-34 and 2-35 show the spatial distribution of sodium, calcium, strontium and lithium, respectively.

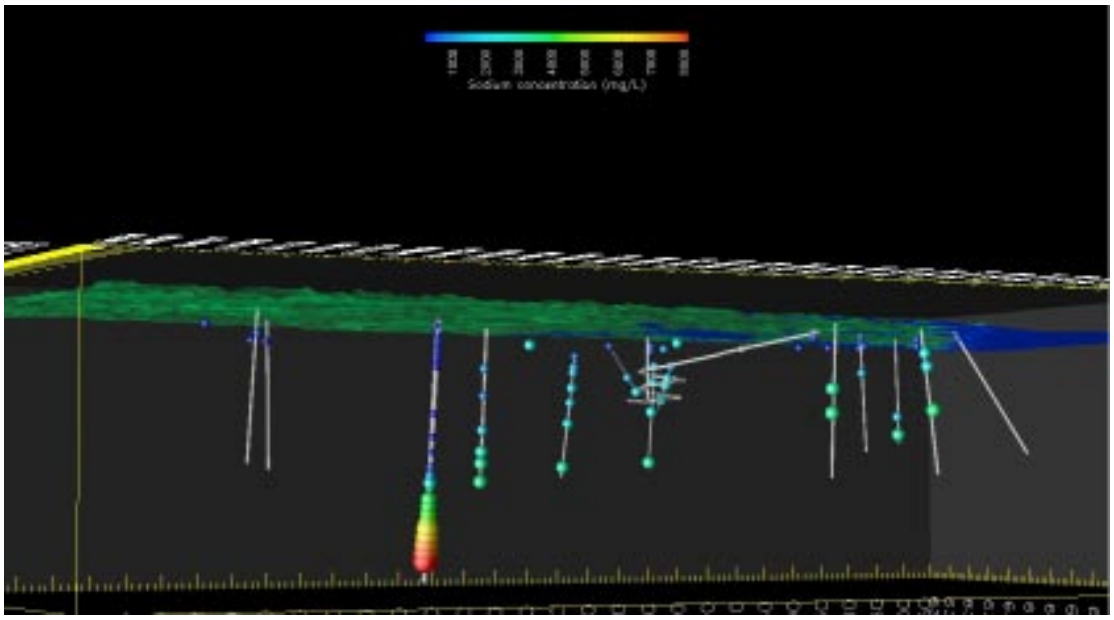

Figure 2-32. *Spatial distribution of dissolved sodium at Laxemar and Simpevarp subareas.*

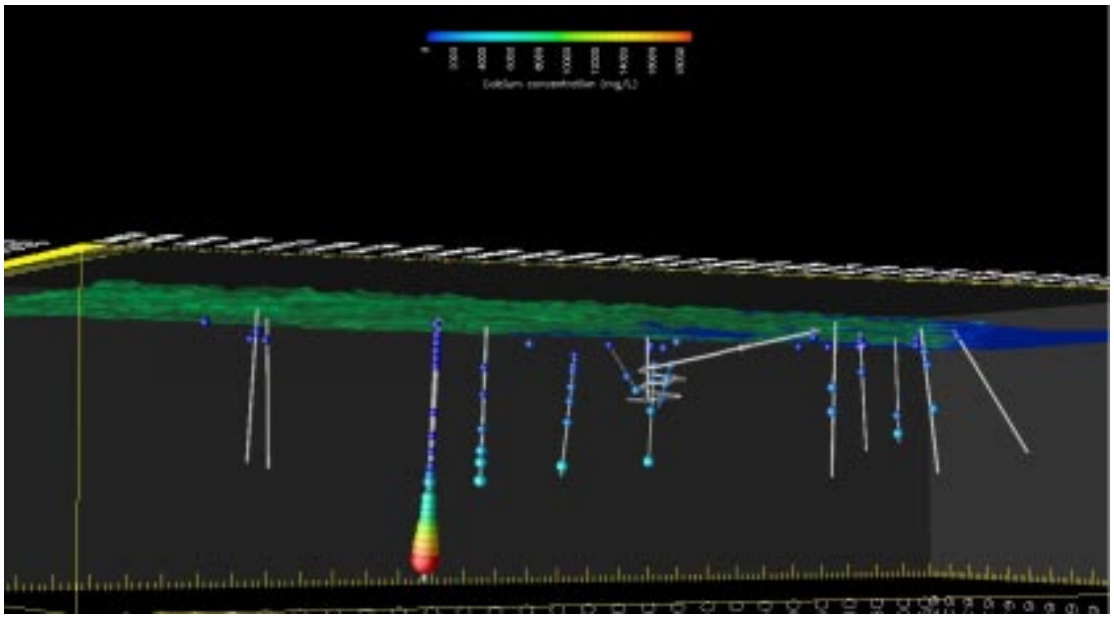

Figure 2-33. *Spatial distribution of dissolved calcium at Laxemar and Simpevarp subareas.*

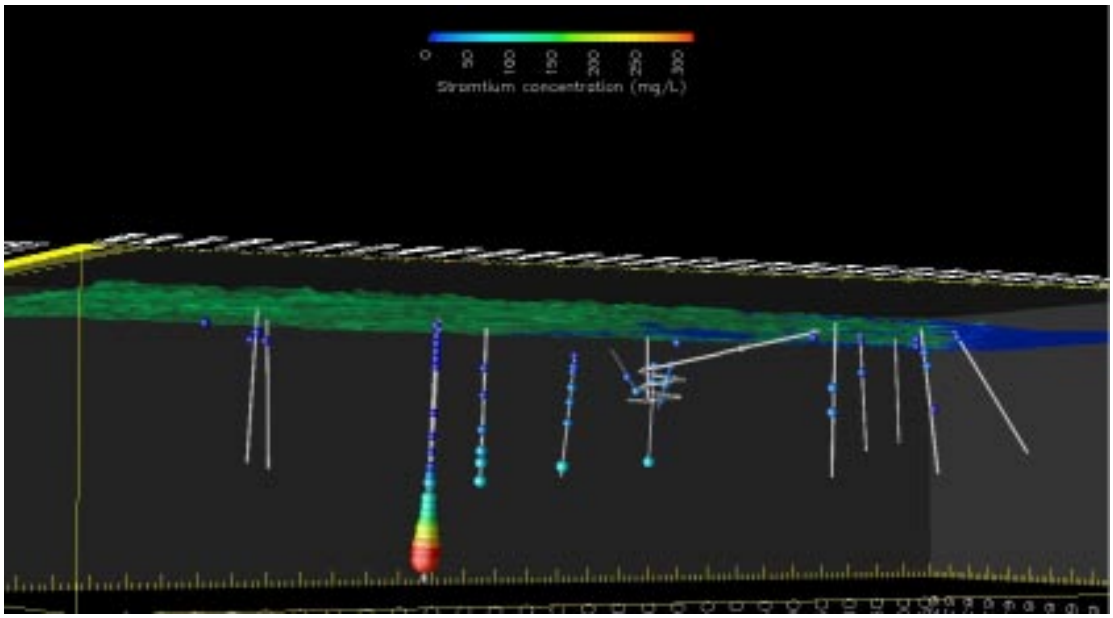

Figure 2-34. *Spatial distribution of dissolved strontium at Laxemar and Simpevarp subareas.*

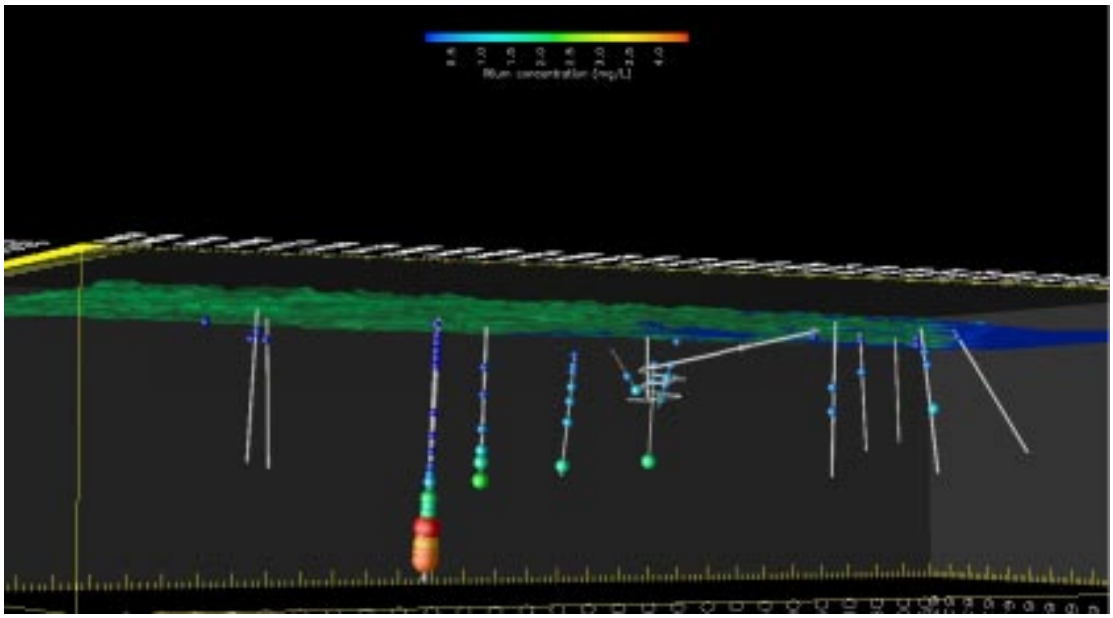

Figure 2-35. *Spatial distribution of dissolved lithium at Laxemar and Simpevarp subareas.*

It can be seen in the previous figures that most dissolved species show qualitative trends very similar to chlorides. This could be taken as an indication of the important role of physical transport processes (dispersion-diffusion; i.e mixing) in the hydrochemical nature of bedrock groundwater in Laxemar and Simpevarp subareas. Even the concentrations of some of the hydrochemical components which are known to be clearly involved in geochemical processes (such as calcium; Figure 2-32) are obviously masked by the influence of the mixing between different waters. It is thought that the concentration contrast between highly saline waters and the rest is so large, that very little mixing involving this end-member water would produce mass transfers higher than those

involved in some geochemical processes. However, this is not always the case. Some dissolved components, such as magnesium (see Figure 2-20), bicarbonate, iron and manganese show a very different spatial distribution. As it was discussed above, it has been postulated that magnesium is a good tracer for the marine influence of groundwater samples (even it is not a conservative solute), due to the fact that highly saline deep waters (type D) show very low concentrations compared with Baltic waters. Figure 2-36 shows the spatial distribution of dissolved manganese, which shows quite a similar trend to the observed distribution of magnesium. There is only a major difference which can be observed at the shallowest sample in borehole KSH03. This sample shows low relative concentration of magnesium but high relative concentration of manganese.

Apart from their intrinsic diluted nature, one of the best indicators of a meteoric influence of a groundwater sample is the concentration of bicarbonates. As shown in Figure 2-10, near-surface groundwater samples (soil pipes) show bicarbonate concentrations in the range 100 to 500 mg/L, with averaged values of about 200 mg/L). According to previous geochemical modelling /Gimeno et al. 2004/, the origin of bicarbonate in shallow waters could be due to two main processes: calcite dissolution and organic matter oxidation. The spatial distribution of dissolved bicarbonate in bedrock groundwater samples was shown in Figure 2-18.

By comparing Figures 2-17 and 2-18, it can be seen that all dilute water samples (Type A) show bicarbonate concentrations much higher than the rest of water samples of any water type. In fact, almost all diluted water samples in the bedrock show bicarbonate concentrations higher than 200 mg/L (mostly in the range from 200 to 300 mg/L).

Figure 2-37 shows the spatial distribution of dissolved (total) iron.

Unfortunately there is no representative sample at Laxemar fulfilling two requisites: a) being of type A (dilute) and b) having measurement of total dissolved iron. However, many of the representative samples available in Simpevarp subarea fulfil both requisites. By comparing Figures 2-37 and 2-18, it is possible to notice that maximum concentrations of dissolved iron have been measured at the shallowest positions in the bedrock, coinciding with those water samples being diluted and showing higher concentrations of bicarbonates.

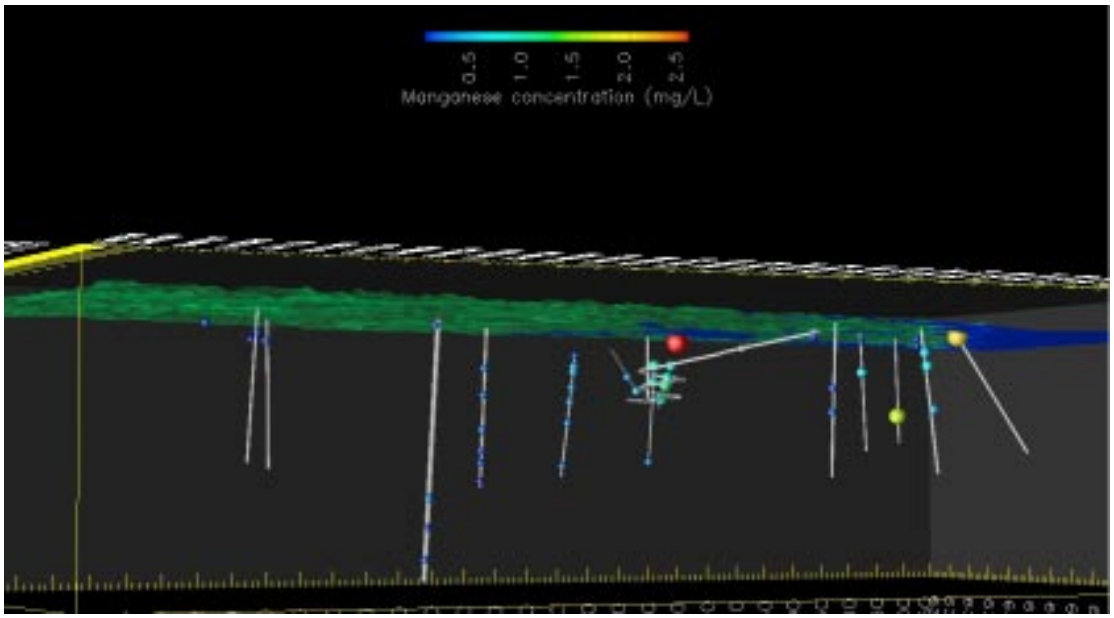

Figure 2-36. *Spatial distribution of dissolved manganese at Laxemar and Simpevarp subareas.*

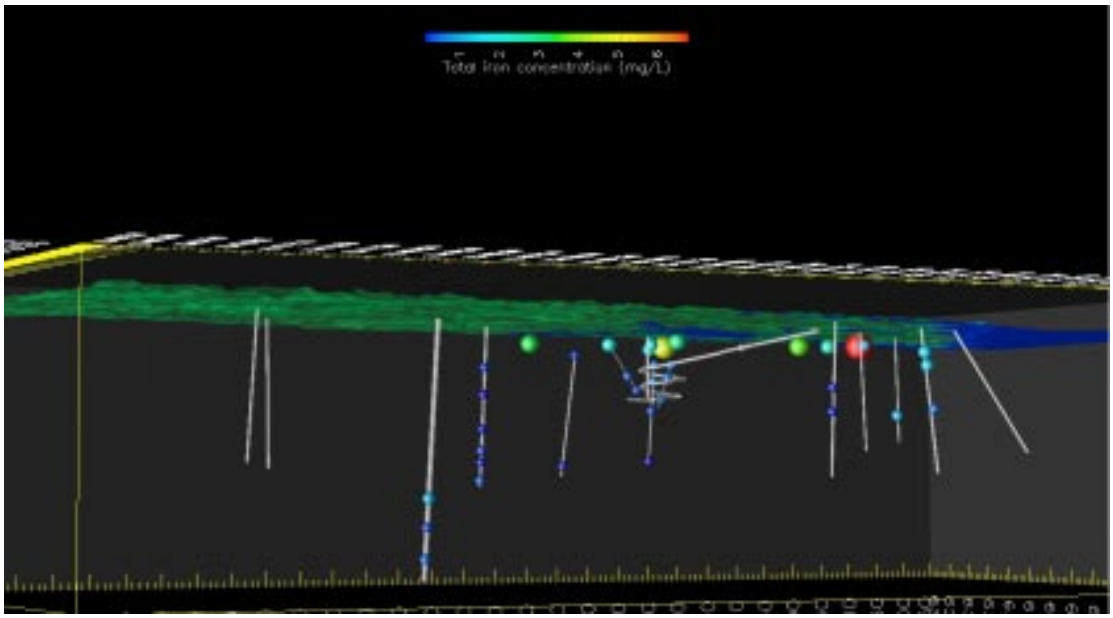

Figure 2-37. *Spatial distribution of iron (total) at Laxemar and Simpevarp subareas.*

It is worth noting that during the Redox Zone Experiment at the Äspö HRL /Banwart et al. 1995/ a large increase of bicarbonates was recorded at the tunnel after the intersection of a fracture zone at a depth of 70 m. Initially, the fracture zone was filled with saline native water, which was strongly diluted with fresh meteoric water once the tunnel intersected the fracture zone. Hydrogeochemical /Banwart et al. 1995, 1996/ and microbiological /Pedersen et al. 1995/ studies provide significant evidence supporting Fe (III) reduction as a respiration pathway for the oxidation of organic C in the fracture zone. /Tullborg and Gustafsson 1999/ report a large increase in ^{14}C activity measured in both dissolved organic and inorganic C during the experiment, thus providing other evidence for a source of young organic C in the groundwater. According to /Banwart et al. 1995, 1999/ and /Banwart 1999/, microbially-mediated anaerobic respiration of DOC, through the reduction of iron (III) minerals is the most likely hypothesis to explain such a measured increase of bicarbonates. It is known that both, ferric oxides and hydroxides minerals are present in the fracture zones of Äspö /Tullborg 1995/. More recently, /Molinero et al. 2004/ present a coupled hydrobiogeochemical model according to which the measured evolution of dissolved bicarbonates in the Redox Zone Experiment can be quantitatively explained by microbially-mediated organic matter oxidation and Fe (III) reduction, consistent with the known hydrogeological framework of the site.

Hydrogeologically, the Redox Zone Experiment mainly consisted of the flushing out and replacement of the initial brackish/saline water by the arrival of shallow fresh water of meteoric origin, due to the tunnel construction. This process is mostly the same as is happening in the shallower parts of the Laxemar and Simpevarp subareas since the emergence of the land above sea level (during the last 2,000 years, aprox.). Then, according to the observed concentrations of bicarbonate and iron in the diluted groundwater samples (Type A) of the Simpevarp subarea, microbially mediated oxidation of organic matter through the reduction of ferric minerals seems to be the most plausible hypothesis to explain the high bicarbonate concentrations of these groundwater samples. It is worth noting that both, soil pipes and some shallow bedrock groundwater samples at Simpevarp are undersaturated with respect to calcite /Gimeno et al. 2004, Molinero and Raposo 2004/ and, therefore, dissolution of calcite could also contribute to the observed bicarbonate concentrations in diluted groundwater. The visualization tool also has the capability of representing structural objects such as deformation zones. This capability is important for the establishment of conceptual models in a bedrock environment which is definitely affected by the presence of such features. Figure 2-38 shows a top view of the Simpevarp area with the main deformation zones considered so far. The visualized deformation zones are: EW002A, EW007A, NE040A, NE005A and EW013A. The selection of these 5 structural features was made taken into account the actual definition of the target area and the location of the boreholes in which representative hydrochemical information is available. In fact, for the case of the Laxemar subarea, deformation zones EW002A and EW007A are very important and well-defines features (named as “certain” in the geological model). NE040A is also an important structure as that it crosses the target Laxemar subarea. The geometry of discrete features (deformation zones) correspond to the structural model of Laxemar (version 1.2).

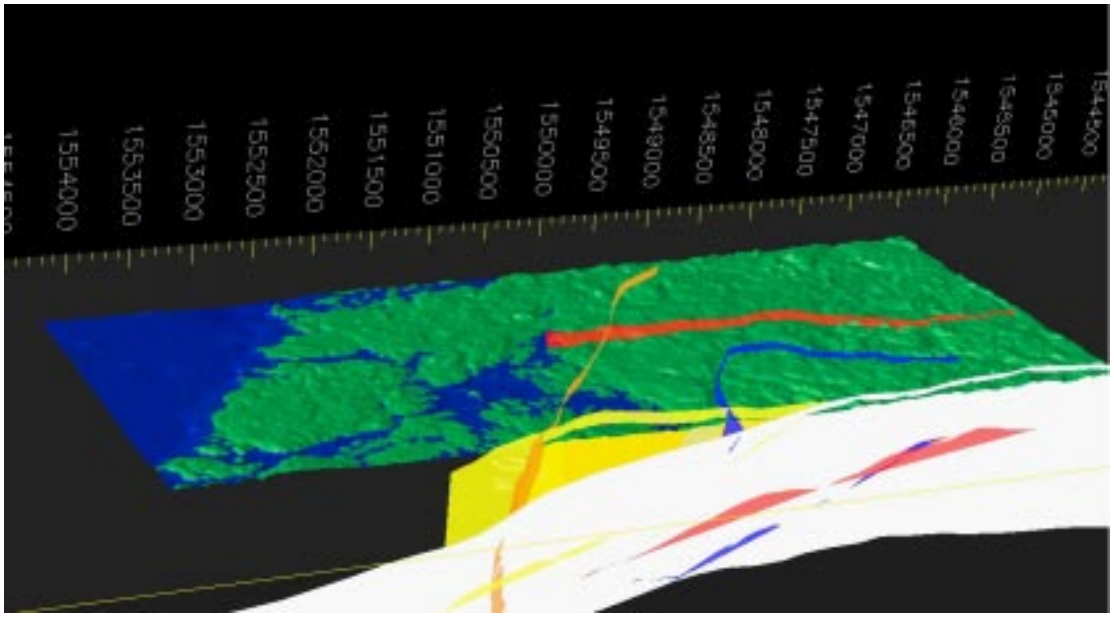

Figure 2-38. *Top view (from the north) of the Simpevarp area with the key deformation zones in the area. EW002A (white), EW007A (red), NE040A (blue), NE005A (orange) and EW013A (yellow).*

Including fracture zones in the visualization tool allows analysis of the possibility of "direct" hydrogeological connection between the different groundwater samples available in the database. Deformation zone EW002A (white in Figure 2-38) crosses KAS03 borehole under the Äspö Island and runs very close to the deeper saline water samples at KLX02 in Laxemar (see Figure 2-39).

Figure 2-40 shows deformation zone EW007A (red in Figure 2-38) which crosses borehole KLX02 and KLX04. It is worth remembering that the chloride concentration of KLX04 does not correspond to representative samples and should be used with care.

Figure 2-41 shows an interesting point. According to the current geometrical definition of deformation zones (geological model of Simpevarp 1.2), the fracture zone NE040A intersects KLX02 and KLX01 boreholes. It can be seen that both boreholes have a representative sample corresponding to the intersection with the deformation zone. The interesting point is that borehole KLX02 crosses the fracture zone deeper than KLX01 and both representative samples are relatively diluted, so they can be assumed as being part of the current dynamic fresh water body at Laxemar. The geographical location of both boreholes – KLX02 (inland) and KLX01 (nearer to the coast) – is consistent with a topographically-driven flow from the first to the second borehole. It is believed that these two representative groundwater samples fulfil the prerequisites for further analysis by inverse geochemical models and reactive solute transport models.

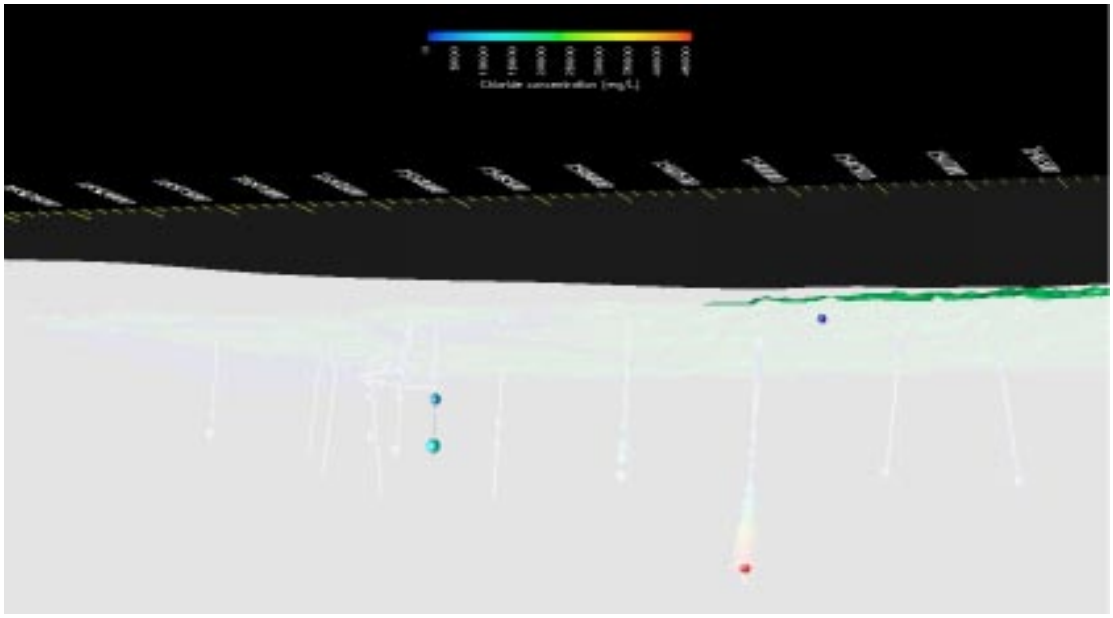

Figure 2-39. *Bottom view (from the north) of deformation zone EW002A and chloride concentrations in boreholes. This fracture zone crosses borehole KAS03 under Äspö and runs very close to the deeper part of KLX02 borehole in Laxemar.*

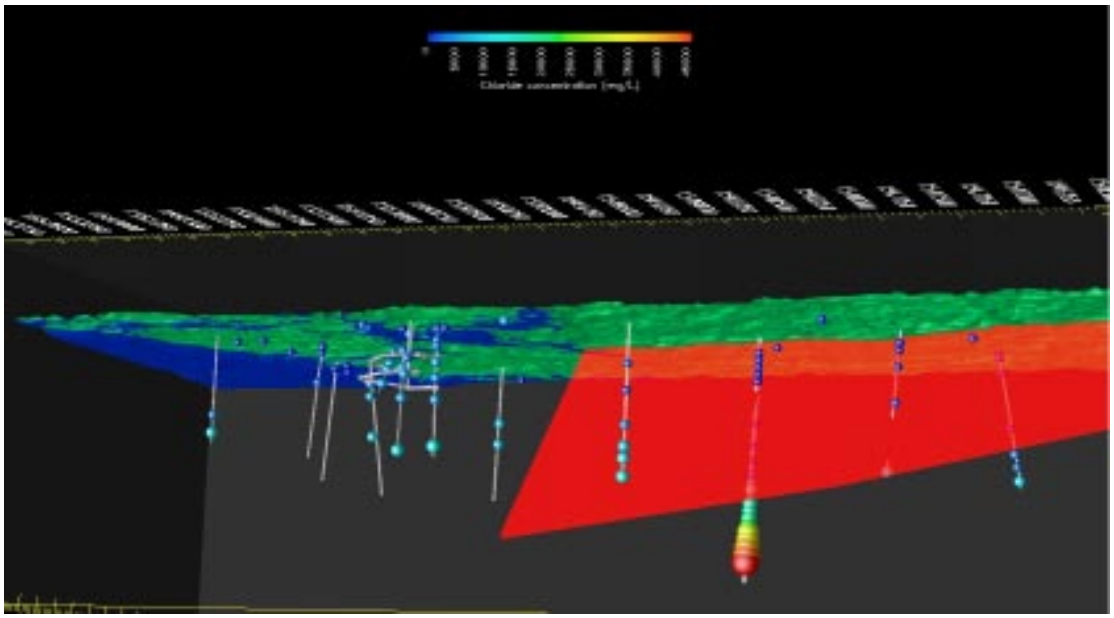

Figure 2-40. *Bottom-north view of deformation zone EW007A and chloride concentrations in boreholes. This fracture zone crosses borehole KLX02 and KLX04 at a deeper section. It should be remembered that measured chloride concentrations in KLX04 do not correspond to representative samples.*

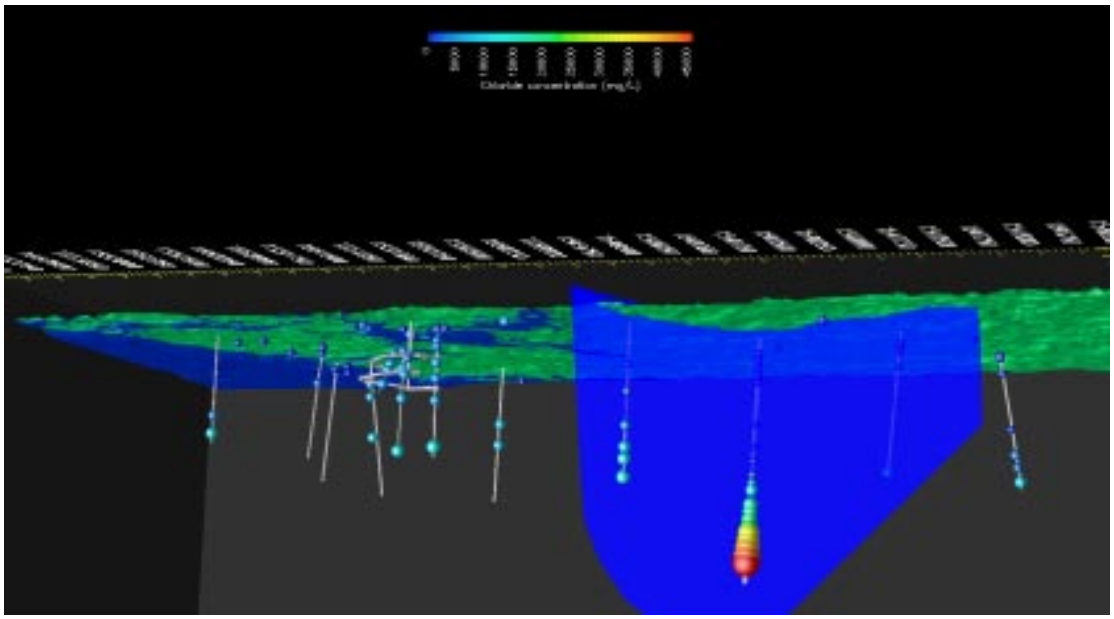

Figure 2-41. *Bottom-north view of deformation zone NE040A and chloride concentrations in boreholes. This fracture zone crosses borehole KLX02 (deeper and inland) and KLX01 (shallower and nearest to the coast).*

3 Numerical modelling of groundwater flow, salinity and tritium transport

3.1 Introduction

When modelling groundwater flow and solute transport, situations may arise where solute concentration is so high that its influence on fluid density is no longer negligible. Since fluid density, in turns, affects flow itself, this variation should be taken into account in order to properly describe the actual subsurface phenomena.

The latest version of SUTRA /Voss and Provost 2003/ is a finite-element-based code able to simulate fluid movement and transport of dissolved substances under saturated and unsaturated conditions, accounting for the variation of fluid density by the amount of solids dissolved. Although a powerful and reliable modeling tool, the code is unable to simulate reactive transport phenomena.

On the other hand, reactive transport can be simulated by other finite-element-based codes such as CORE2D /Samper et al. 2000/, which, in contrast to SUTRA, lacks the ability to account for fluid-density-dependent flow.

Therefore, a bridge is needed in order to couple both fluid-density-dependent flow and reactive transport in an efficient manner. In order to do so, modifications were needed in the SUTRA and CORE 2D codes. A program interface has been developed which allows the user to link computed outputs of SUTRA as inputs of CORE 2D.

In this way, the flow field with variation of fluid density is calculated with the SUTRA code. When the model arise a pseudo-steady state the velocity field can be considered as permanent. Then, this pseudo-steady state water velocity field is exported to the CORE code in order to calculate the reactive transport problem.

SUTRA and CORE source codes have been slightly modified to be compatible to solve, in two-steps, density dependent flow and reactive solute transport problems. The new versions of both codes (with the link interface), have been verified and tested by means of synthetic two-dimensional examples (see Appendix I).

The final aim is to perform coupled modelling of flow and reactive transport, in order to support hydrochemical interpretation of field data. It is expected that reactive transport modelling will provide a quantitative framework for testing alternative hydrochemical hypothesis and conceptual model of key hydrochemical processes. In the current model version, the first step has been to simulate conservative species (i.e. salinity). Tritium transport has been included in a second step in order to have an independent source of information about the behaviour of the fresh water hydrogeological system. It is expected that subsequent model version (2.1) will include reactive chemical solutes within a sound and realistic hydrogeological quantitative framework.

3.2 Model description

3.2.1 Model domain

Two-dimensional groundwater flow has been modeled along a profile perpendicular to the coastline (Figure 3-1). Its total length is 35 km, 28 km of which correspond to land surface and the remaining 7 km are under the sea.

The model profile ranges from the highest regional peaks to the sea level (Figure 3-2). Both lateral boundaries are considered to be impervious.

The profile studied has a depth of 2,000 m under sea level. The bottom boundary is also assumed to be impervious and to have a salt content of 0.1 g per g of water.

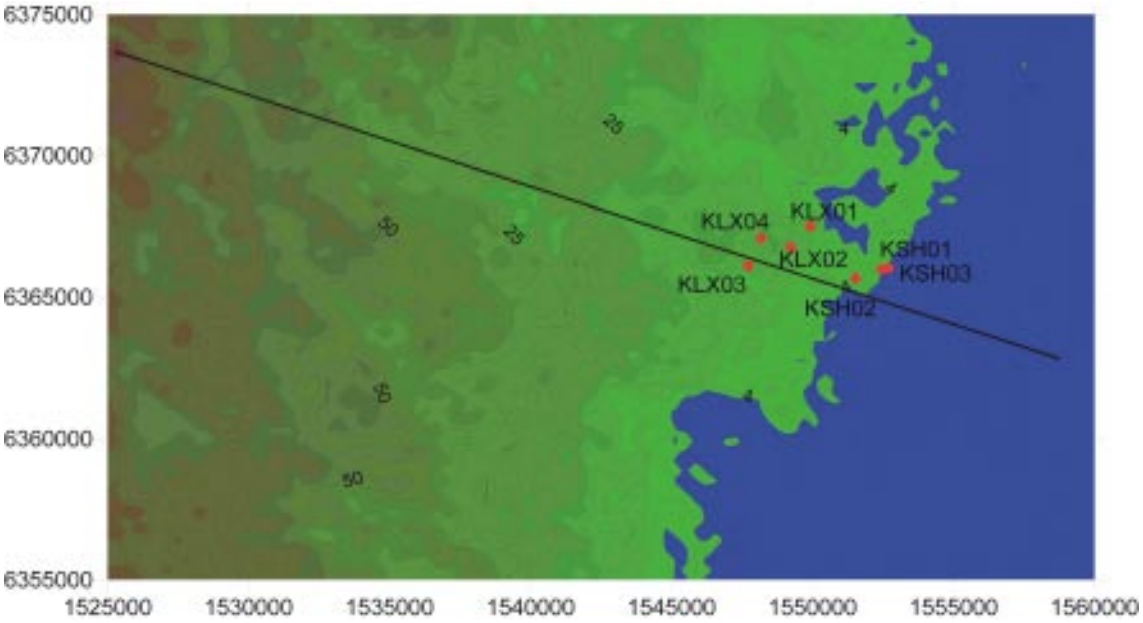

Figure 3-1. *Location of the modeled profile and main cored- boreholes at the Simpevarp area.*

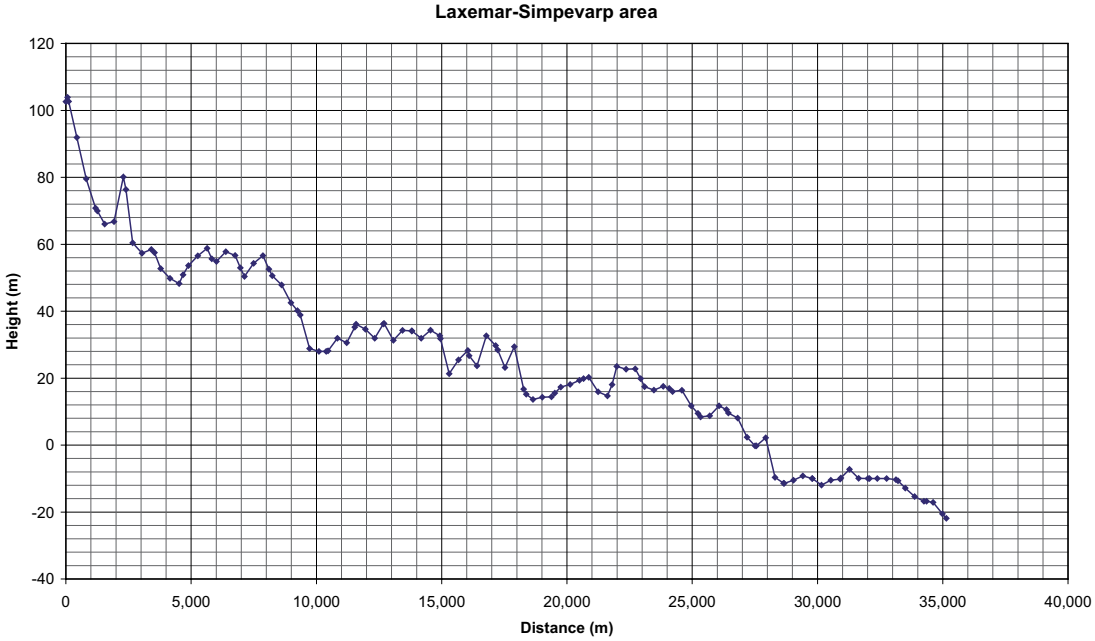

Figure 3-2. *Topographic profile of the domain (y-axis is in metre above sea level).*

Figure 3-3 shows hydraulic conductivity data measured at different depths at the Simpevarp area /Rhén et al. 1997/. Although it is not conclusive, a slight decrease of hydraulic conductivity with depth can be deduced from Figure 3-3. Data in Figure 3-3 was derived from hydraulic tests performed both at Äspö (the Simpevarp subarea) and Laxemar subarea. It is worth noting that new data of hydraulic conductivity and depth dependency in the Laxemar and Simpevarp subareas are being obtained within the framework of the site characterization activities. This new information will be available (analyzed/processed) in the Laxemar 1.2 report of the HydroNet Group. Then, it is planned to update the flow and transport models, including new hydrogeological information, in the next versions of the ChemNet activities.

Three zones of material have been considered along a vertical profile, in order to take into account the vertical heterogeneity of the bedrock (Figure 3-4). The upper layer extends up to 500 m under sea level. The intermediate layer reaches 1,100 m below sea level and the lower layer is 900-m-thick and reaches the bottom boundary. This heterogeneity is rather subjective, due to the current lack of field data. As it has been stated above, data on hydraulic conductivity and depth dependency will be incorporated into the model in the next model versions.

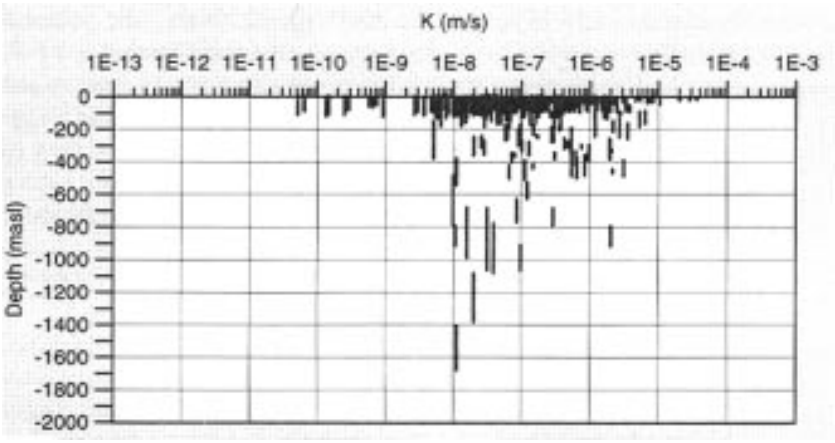

Figure 3-3. *Hydraulic conductivity distribution versus depth in Äspö and Laxemar /after Rhén et al. 1997/.*

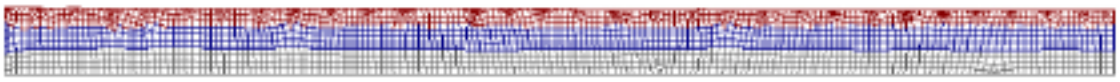

Figure 3-4. *Material zones in the finite elements mesh.*

3.2.2 Mathematical model

3.2.2.1 Fluid density-driven flow equation

Where groundwater density varies spatially, flow may be driven by difference either in fluid pressure or by unstable variations in fluid density. Density-driven flows are directed from dense regions of fluid toward less dense fluid regions.

The mechanisms of pressure and density driving forces for flow are expressed for SUTRA simulation by the general form of Darcy's Law. By combining Darcy's Law and the mass balance equation one has:

$$\left(\theta\rho S_{op}+\frac{\rho}{\phi}\frac{\partial\theta}{\partial p}\right)\frac{\partial p}{\partial t}+\left(\frac{\theta}{\phi}\frac{\partial\rho}{\partial c}\right)\frac{\partial c}{\partial t}-\nabla\cdot\left[\left(\frac{k\rho}{\mu}\right)\cdot(\nabla p-\rho g)\right]=Q_p \qquad \text{(Equation 3.1)}$$

where ρ is density, θ is the volumetric water content, S_{op} is specific pressure storativity, φ is porosity, p is pressure, g is gravity acceleration, k is intrinsic permeability tensor, μ is dynamic viscosity and Q_p is a fluid mass source.

Total fluid density is the sum of pure water density and solute volumetric concentration. The approximate density models employed by SUTRA are first order Taylor expansions in C (solute mass fraction) about a base density:

$$\rho(C)\cong\rho_0+\frac{\partial\rho}{\partial C}(C-C_0) \qquad \text{(Equation 3.2)}$$

where ρ_0 is the base fluid density at base concentration, C_0 (usually, $C_0 = 0$, and the base density is that of pure water). The factor $\frac{\partial\rho}{\partial C}$ is a constant value of density change with concentration. For mixtures of freshwater and seawater at 20°C, when C is the mass fraction of total dissolved solids, $C_0 = 0$ and $\rho_0 = 998.2$ kg/m3, then the factor is approx. 700 kg/m3 /Voss and Provost 2003/.

In the present model, water viscosity is assumed to be constant ($\mu_{T(20°C)} = 0.001$ kg/m*s).

3.2.2.2 Transport of conservative solutes

Dissolved species in saturated media are subject to transport processes. Main transport processes include advection, molecular diffusion and hydrodynamic dispersion.

The transport equation formulation used in this model is:

$$\nabla\cdot(\theta bD\nabla c)-bq\nabla c+r(c^*-c)+b\theta R=b\theta\frac{\partial c}{\partial t} \qquad \text{(Equation 3.3)}$$

where b is the transverse thickness of the cross-section, D is the dispersion tensor that lump the effects of molecular diffusion and hydrodynamic dispersion, c is solute concentration expressed as solute mass per unit fluid volume, q is the Darcy velocity, r is the fluid source term per unit surface area, c* is solute concentration in fluid sinks/sources and R is a chemical sink/source term.

3.2.2.3 Transport of solutes with decay

Some dissolved species can be subject to radioactive decay (for instance, Tritium). In this case, it is necessary to introduce this process into the transport equation.

The concentration of a radioactive species (P) suffering decay in the absence of another transport and chemical processes obeys the following equation:

$$c_P = c_P^o \exp(-\lambda_P t) \qquad \text{(Equation 3.4)}$$

where c^o_p is the initial concentration of the P species and λ_P is the decay constant of reaction.

The time variation of species P is given by:

$$\frac{dc_D}{dt} = \lambda_p c_P \qquad \text{(Equation 3.5)}$$

Introducing radioactive decay into the transport equation of the species P, gives:

$$\nabla \cdot (\theta b D \nabla c_P) - bq \nabla c_P + r\left(c_P^* - c_P\right) - \lambda_p b \theta c_p + b\theta R = b\theta \frac{\partial c_P}{\partial t} \qquad \text{(Equation 3.6)}$$

3.2.3 Numerical discretization

In the first stage of simulation, the domain under study was discretized into quadrilateral elements (Figure 3-5), as required by the latest version of SUTRA code /Voss and Provost 2003/. The characteristic dimensions of the elements were approx. 200 m each side, except close to the surface, where the mesh was refined. The final mesh consists of 2,145 elements and 2,371 nodes.

The initial time step adopted was of 105 seconds, which was increased ten times every 9,999 cycles, until a maximum length of 107 seconds was reached. The total time horizon of the simulation was 4,200 years.

On the other hand, triangular element meshes are required when working with CORE2D code /Samper et al. 2000/. Therefore, the original mesh was transformed into a triangular element mesh by dividing the quadrilateral elements in two (Figure 3-6). As a result, the number of elements of the new mesh increased to 4,290 elements whereas the number of nodes remained the same.

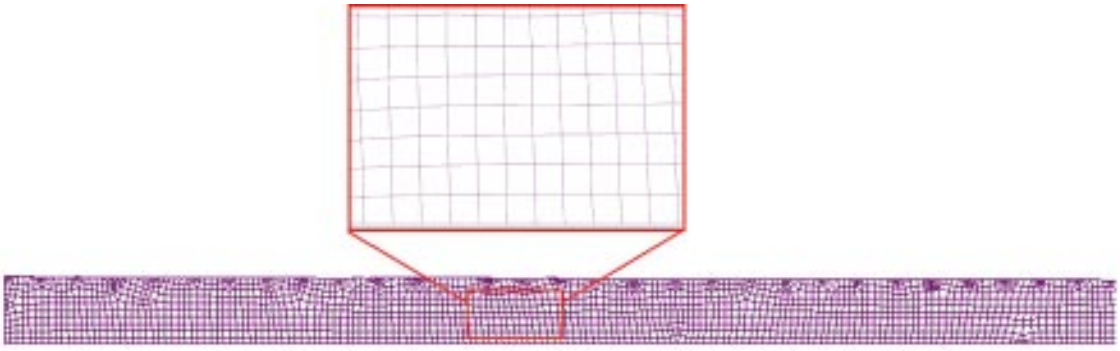

Figure 3-5. *Quadrilateral mesh of finite elements used for SUTRA code.*

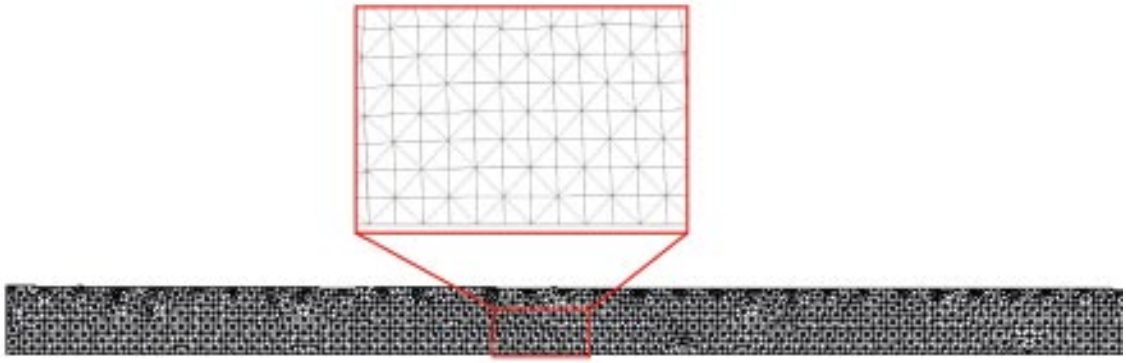

Figure 3-6. *Triangular mesh of finite elements used for CORE2D code.*

3.3 Groundwater flow model

Several calibration runs were performed in order to determine both the most appropriate boundary conditions and the equivalent key parameters, such as hydraulic conductivity and porosity. Calibration was made against measured salinity at KLX02, KLX03 and KSH02 boreholes.

The following boundary conditions were tested on the surface of the longitudinal profile:

- Dirichlet condition so that piezometric head equals the topographic level (hydrostatic pressure was assumed under the sea).
- Dirichlet condition so that piezometric head falls below the topographic level according to an exponential function (see Figure 3-7).
- Neumann condition so that recharge equals 10 mm/year.
- Mixed Neumann-Dirichlet condition: Neumann condition was applied over most of the domain so that recharge equals 10 mm/year. Dirichlet condition was applied at presumed discharge zones (valleys) by imposing piezometric head equals to topographic level.

The recharge rate adopted in this model, 10 mm/year, is based upon computed results obtained by the Hydronet Group, by means of the Darcytools code. Such computed results are shown in Figure 3-8. The recharge rate so obtained is consistent with other values computed in the framework of other groundwater flow models in the framework of the Äspö HRL /Molinero 2000, Molinero and Samper 2004/.

The prescribed (uncalibrated) parameters were:
Salt content at the bottom boundary: 0.1.
Salt content of the Baltic Sea: 0.034.
Salt content of recharge water: 2*E-5.
Longitudinal dispersivity = 200 m.
Transversal dispersivity = 100 m.

Porosity and permeability of each of the three material layers involved in the model were calibrated by a trial-and-error process. The initial guesses were taken from the Äspö area /Rhén et al. 1997/.

Table 3-1 lists the hydrogeologic parameters used in the groundwater flow runs performed with the SUTRA code. Runs A-1, A-2 and A-3 provide excessively high (unrealistic) recharge rates. On the other hand, run B-1 provides a water table above the topographic level, which is of course inadmissible. Finally, runs B-2 and B-3 provide realistic water tables in response to the recharge rate of 10 mm/year estimated in the zone. Of the latter runs, run B-3 provides the best fit compared to salt content measured at boreholes KLX02 and KSH02.

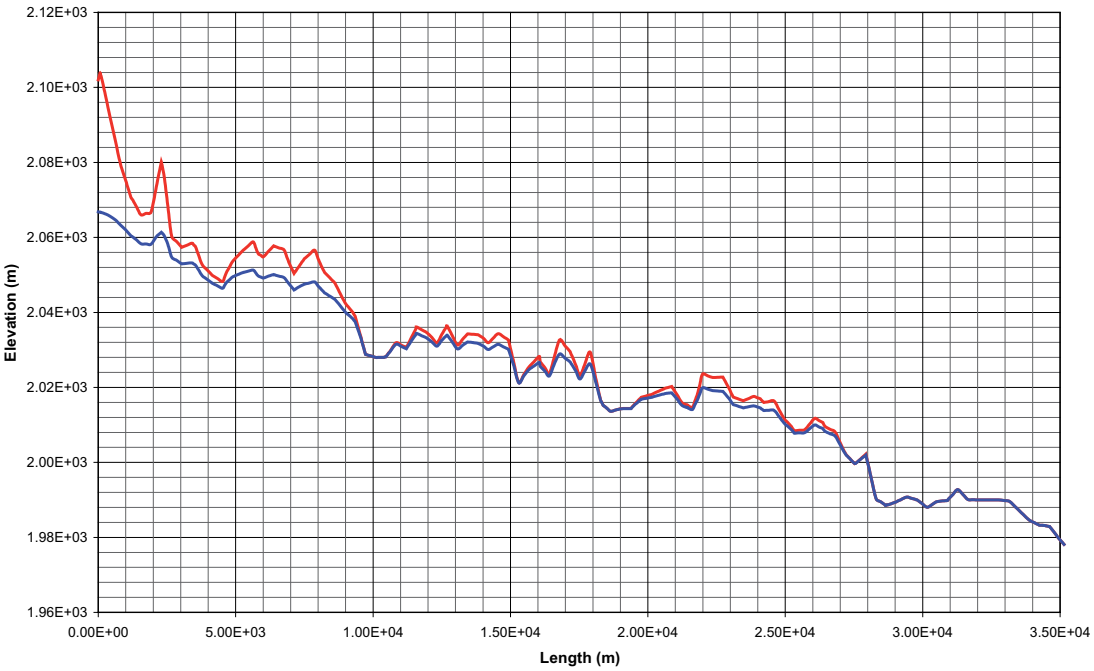

Figure 3-7. *Dirichlet-type boundary so that water table falls below the topographic level.*

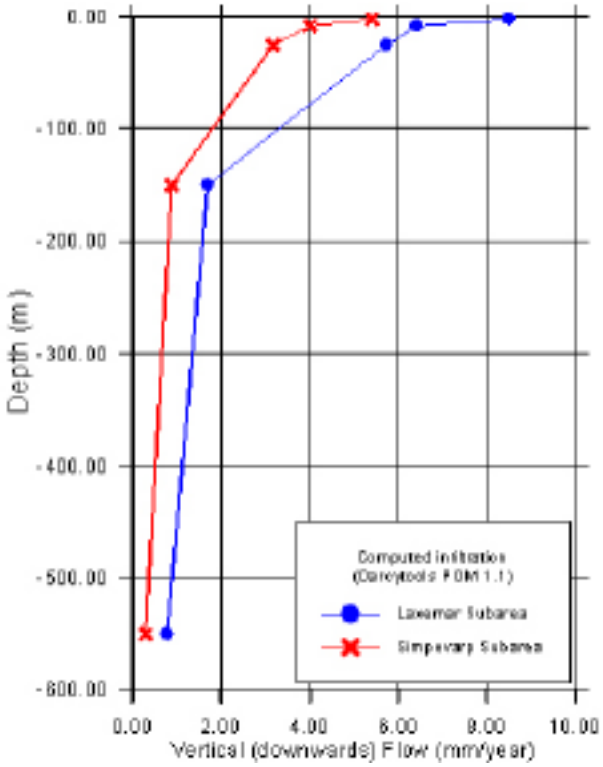

Figure 3-8. *Infiltration computed by Darcytools model Simpevarp v. 1.2 (Stigsson and Follin pers. comm.).*

Table 3-1. Hydrogeological description of runs. K1, K2 and K3 correspond to permeability values for the three material zones shown in Figure 3-4.

	k (m^2)	Φ	Boundary conditions	Comments
RUN A-1	$k_1 = 4.3\ 10^{-13}$ $k_2 = 8.5710^{-14}$ $k_3 = 5.0\ 10^{-14}$	0.001	Prescribed phreatic head equals topographic level.	Resulting recharge = 615 mm/year (unrealistic).
RUN A-2	$k_1 = 4.3\ 10^{-13}$ $k_2 = 8.5710^{-14}$ $k_3 = 5.0\ 10^{-14}$	0.001	Phreatic head slightly below topographic level.	Resulting recharge = 364 mm/year (unrealistic).
RUN A-3	$k_{1x} = 1.2910^{-13}$ $k_{1y} = 4.3\ 10^{-14}$ $k_{2x} = 2.5710^{-14}$ $k_{2y} = 8.5610^{-15}$ $k_{3x} = 1.5\ 10^{-14}$ $k_{3y} = 5.0\ 10^{-15}$	0.0001	Dirichlet condition Phreatic head equal topography.	Averaged parameters from Simpevarp v. 1.2 report. Resulting recharge = 120 mm/year (unrealistic).
RUN B-1	$k_1 = 4.3\ 10^{-13}$ $k_2 = 8.5710^{-14}$ $k_3 = 5.0\ 10^{-14}$	0.001	Neumann condition Q = 10 mm/year.	Resulting phreatic surface above topography level unrealistic).
RUN B-2	$k_{1x} = 1.2910^{-13}$ $k_{1y} = 4.3\ 10^{-14}$ $k_{2x} = 2.5710^{-14}$ $k_{2y} = 8.5610^{-15}$ $k_{3x} = 1.5\ 10^{-14}$ $k_{3y} = 5.0\ 10^{-15}$	0.0001	Mixed Neumann-Dirichlet condition.	Averaged parameters from Simpevarp V 1.2 report. Realistic phreatic surface.
RUN B-3	$k_1 = 4.3\ 10^{-13}$ $k_2 = 8.5710^{-14}$ $k_3 = 5.0\ 10^{-14}$	0.001	Mixed Neumann-Dirichlet condition.	Realistic phreatic surface. The best fit to measured alinities.

The groundwater flow model was calibrated by means of the salt content as measured at boreholes KLX02, KLX03 and KSH02. Figure 3-9 shows the fit obtained by Model Run A-1 using mean values of hydraulic conductivity and porosity, as reported for the Äspö area (see Table 3-1).

Recharge and discharge zones and their respective recharge rates, as obtained in run A-1, are shown in Figure 3-10. Even though groundwater salinity can be reasonably reproduced with this model run, the average recharge rate turned out to be 615 mm/year, which is clearly unrealistic and far above the 10 mm/year estimated for the area.

Figure 3-11 shows the fit obtained in run B-1 by imposing a recharge rate of 10 mm/year. As can be seen, the salt content calculated are more poorly estimated than with previous runs considered. The water table obtained is also unrealistic as it lies above the topographic level in the valleys (Figure 3-12).

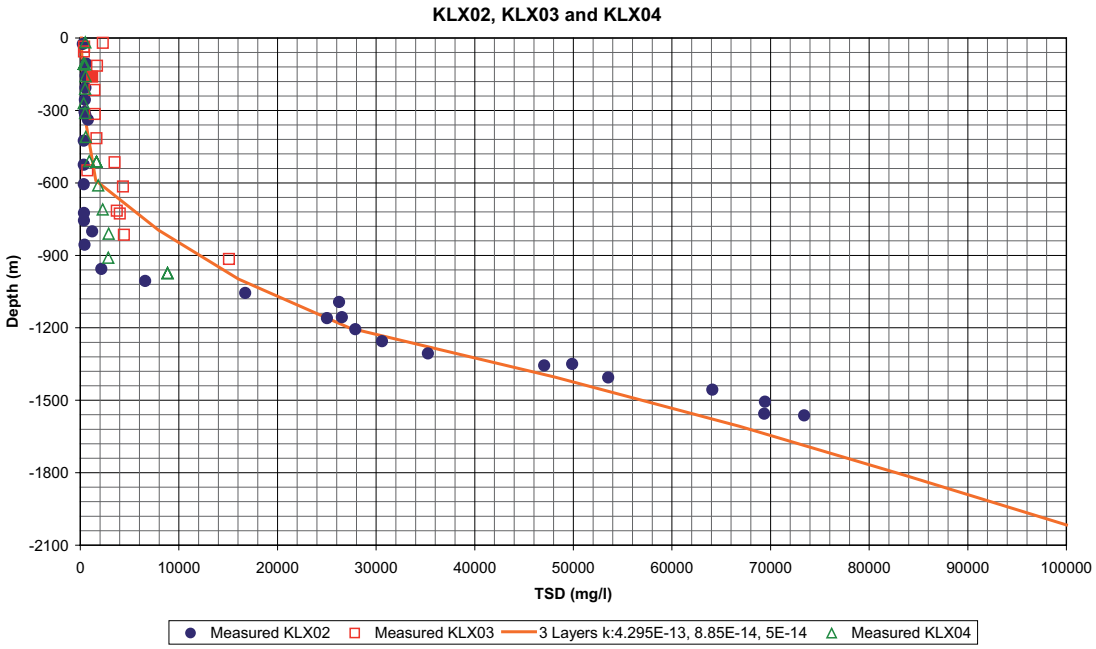

Figure 3-9. *Salt content calculated in run A-1 versus salt content measured in KLX02, KLX03 and KSH02. Unfilled symbols correspond to unrepresentative samples.*

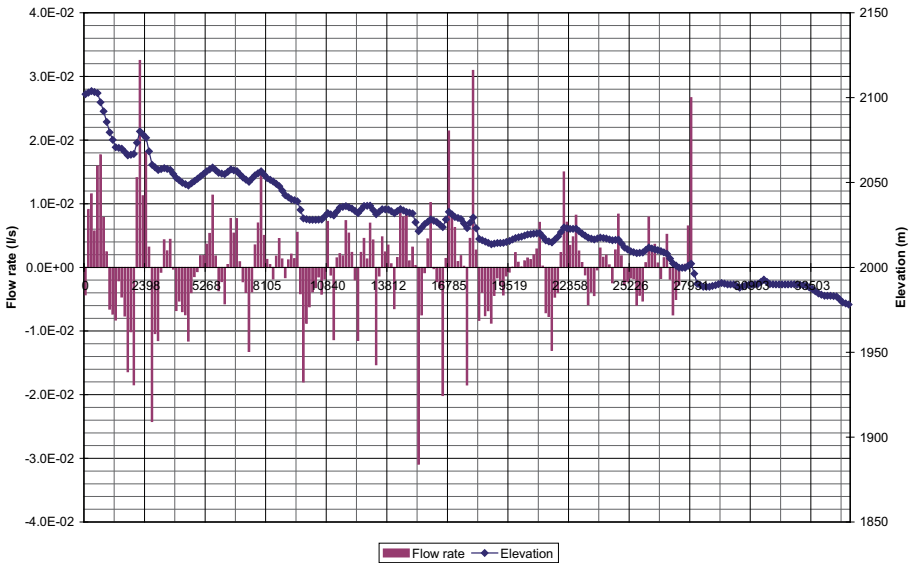

Figure 3-10. *Recharge and discharge rates (as simulated in run A-1) versus the topographic level.*

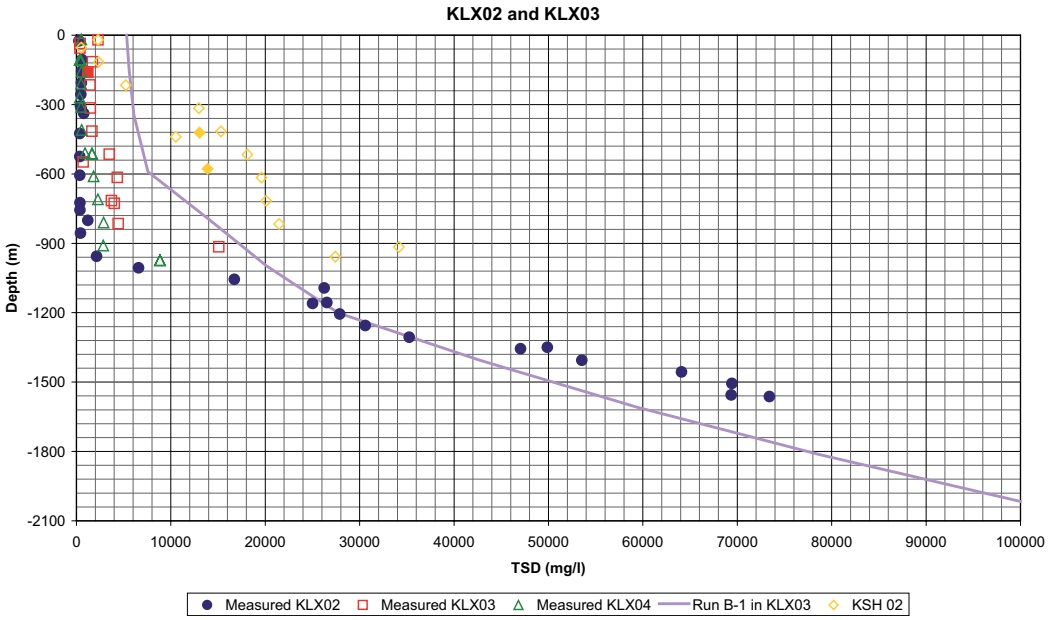

Figure 3-11. *Salt content calculated in run B-1 versus salt content measured in KLX-02, KLX03 and KSH02.*

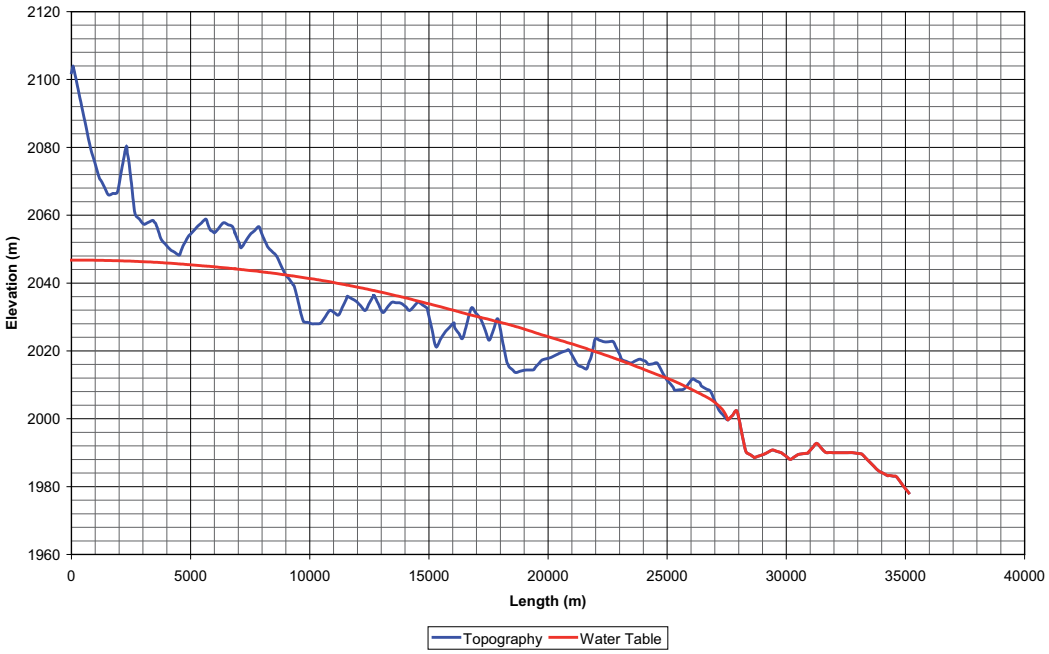

Figure 3-12. *Water table calculated under Neumann boundary condition (recharge rate = 10 mm/ year).*

A mixed Neumann-Dirichlet boundary condition is the one which best reproduces the salt content values observed at boreholes KLX02 and KLX03 as well as at KSH02. A recharge rate of 10 m m/year was imposed in those zones where recharge was observed in run A-1 (Figure 3-10) and the water table was fixed as equal to the topographic level in the presumed discharge zones (valleys). Under this boundary condition, the fit is enhanced by adopting the hydrogeologic parameters calibrated by means of the averaged values reported in Äspö (Figure 3-13), better than when adopting averaged values from the range provided by the Hydrogeological model pf Simpevarp 1.2 (Figure 3-14). In spite of the simplification adopted when assuming a two-dimensional flow pattern, in contrast to the actual three-dimensional flow field, the model is able to reproduce, with a reasonable accuracy, measured salt content profiles both at inland zones (borehole KLX02) and at coastal zones (borehole KSH02).

Figure 3-15 displays the phreatic surface calculated in run B-3. The computed water table looks realistic, always under the ground topography, for a given bedrock recharge of 10 mm/year, which is based upon computed results of the Hydronet Group (see Figure 3-8).

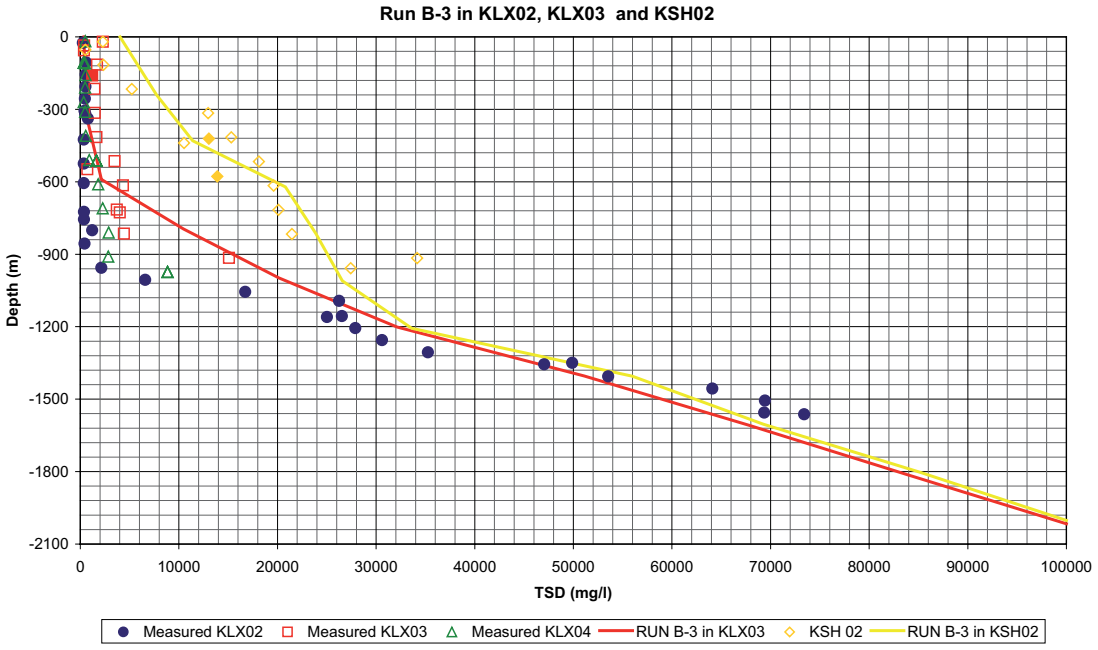

Figure 3-13. *Computed salinities with Model run B-3 versus salt content measured in KLX02, KLX03 and KSH02. Unfilled symbols correspond to unrepresentative samples. Filled symbols correspond to representative samples.*

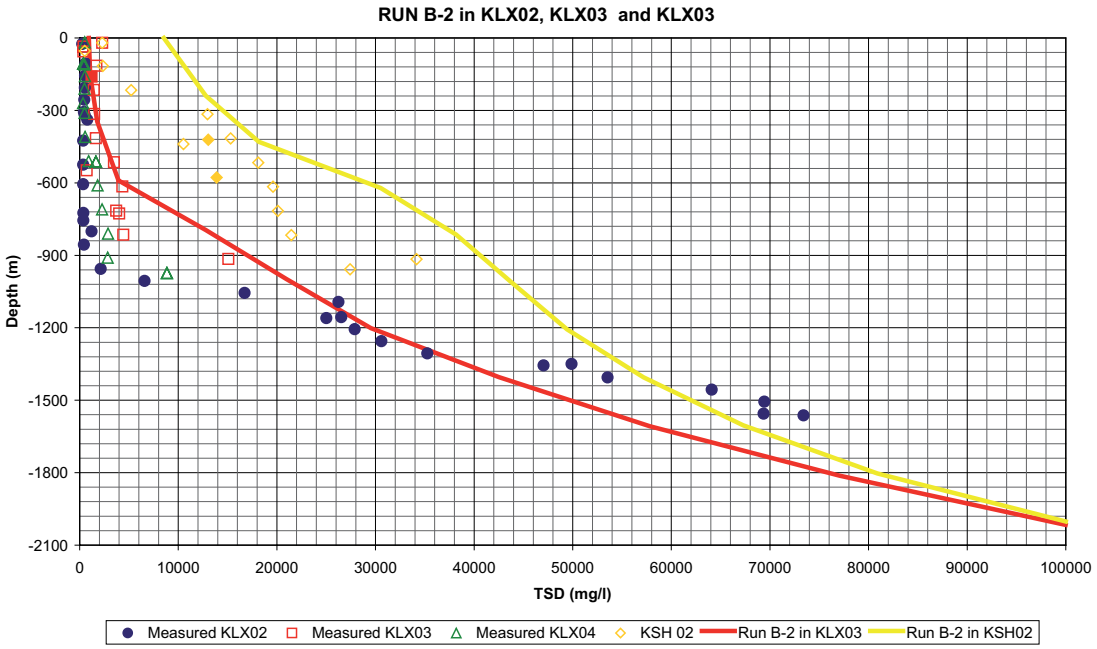

Figure 3-14. *Computed salinities with Model run B-2 versus salt content measured in KLX02, KLX03 and KSH02.*

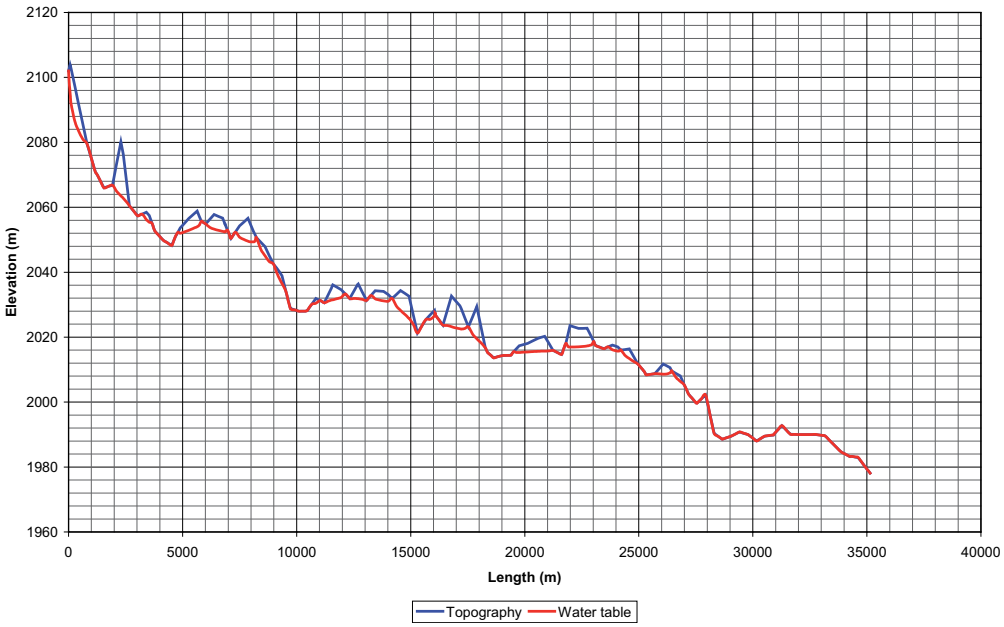

Figure 3-15. *Phreatic head versus topographic level in run B-3.*

3.4 Decaying tritium transport model

Groundwater recharged in the past decades and taking part in an active hydrological cycle is referred to as modern groundwater /Clark and Fritz 1997/. Tritium has become a standard tool for the definition and study of modern groundwater systems. The era of thermonuclear bomb testing in the atmosphere (1951–1976), provides the tritium input signal that defines modern water. Due to its natural decay, pre-bomb tritium input cannot be normally detected. Tritium-free groundwater is then considered to be "sub-modern" or old water /Clark and Fritz 1997/.

Tritium evolution within the Laxemar-Simpevarp aquifer can be simulated as a natural tracer test. The behaviour is not conservative since it is affected by radioactive decay, with a half-life of 12.43 years. The decay constant will be equal to ln2 divided by the half-life. In order to set up a model of groundwater flow and tritium transport, the input function of this environmental tracer is also needed. There is an excellent time series of tritium levels in precipitation measured at Ottawa, Ontario, which has become a classical reference for hydrogeologists. Such a good time characterization of rain water is not available in other places, such as Sweden, however. Figure 3-16 shows the Ottawa time series of tritium levels in rain water, as well as discrete values from 4 places in Sweden. All these data have been downloaded from the Isotope Hydrology Information System (the ISOHIS database; http://isohis.iaea.org) provided by the IAEA. It can be seen (Figure 3-16) that, even with relevant latitude difference, the Ottawa time series can be adopted as an appropriate description for atmospheric tritium in Sweden. Figure 3-16 also shows a step-wise function representing a "smoothed" tritium evolution. This step-wise function has been used as the input of tritium with the recharge (infiltrated) water for the numerical model of tritium transport at Laxemar-Simpevarp.

Initial conditions of tritium contents have been generated by a long-term run of the model, since year 0 to year 1950. The velocity field obtained in run B-3 with SUTRA code has been used as an input of CORE2D. Precipitation before 1950 is assumed to have a constant tritium content of 15 TU. Figure 3-17 shows simulated tritium contents in groundwater at year 1951. This distribution corresponds to the steady state prior to the nuclear bomb tests performed during the period 1951–1976.

Figure 3-18 shows the simulated tritium content in year 1970, after the maximum values of atmospheric tritium due to thermonuclear bombs. Contents of tritium in groundwater reach until 430 TU in Laxemar area at a depth of 500 m.

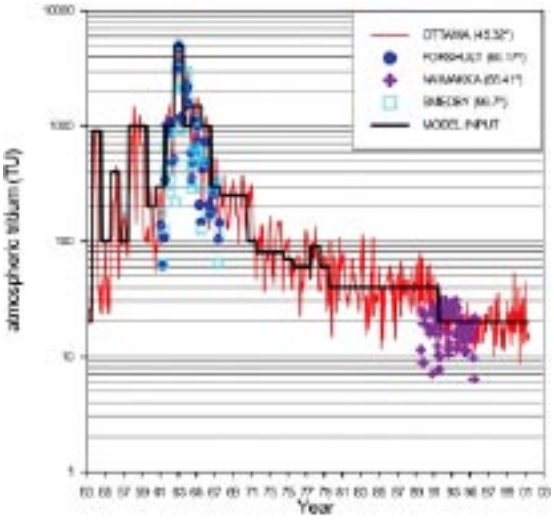

Figure 3-16. *Evolution of atmospheric tritium at Ottawa and 4 locations in Sweden /data from the ISOHIS database, IAEA 2001/. Step-wise function used as the model input signal is shown in solid black line.*

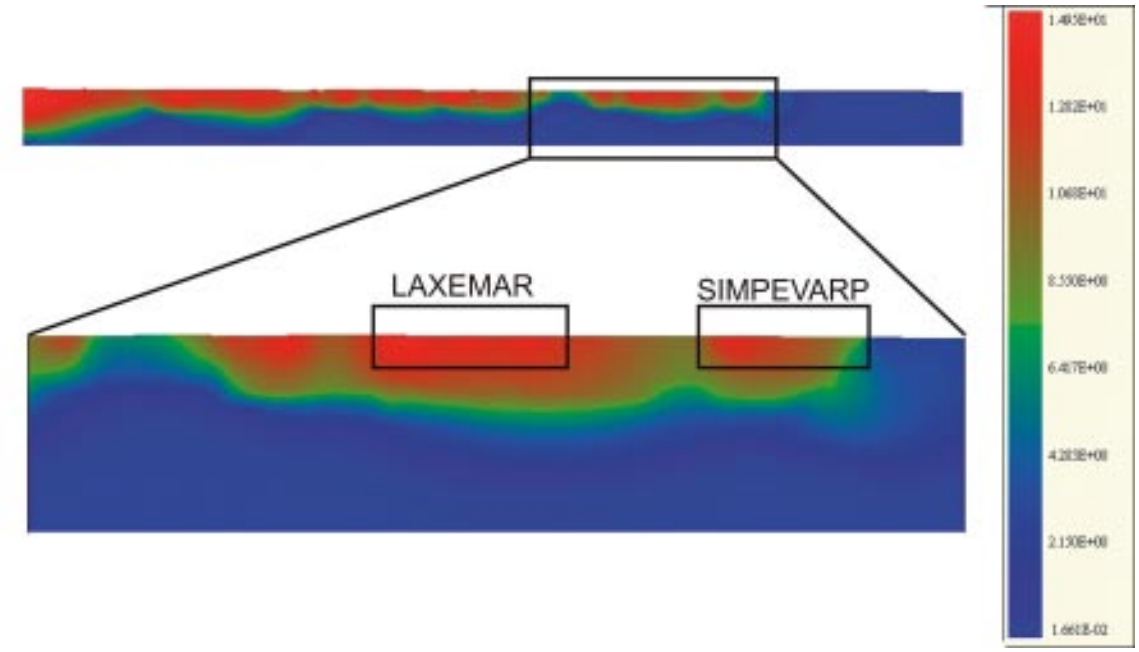

Figure 3-17. *Simulated tritium contents in Laxemar and Simpevarp subareas at year 1951.*

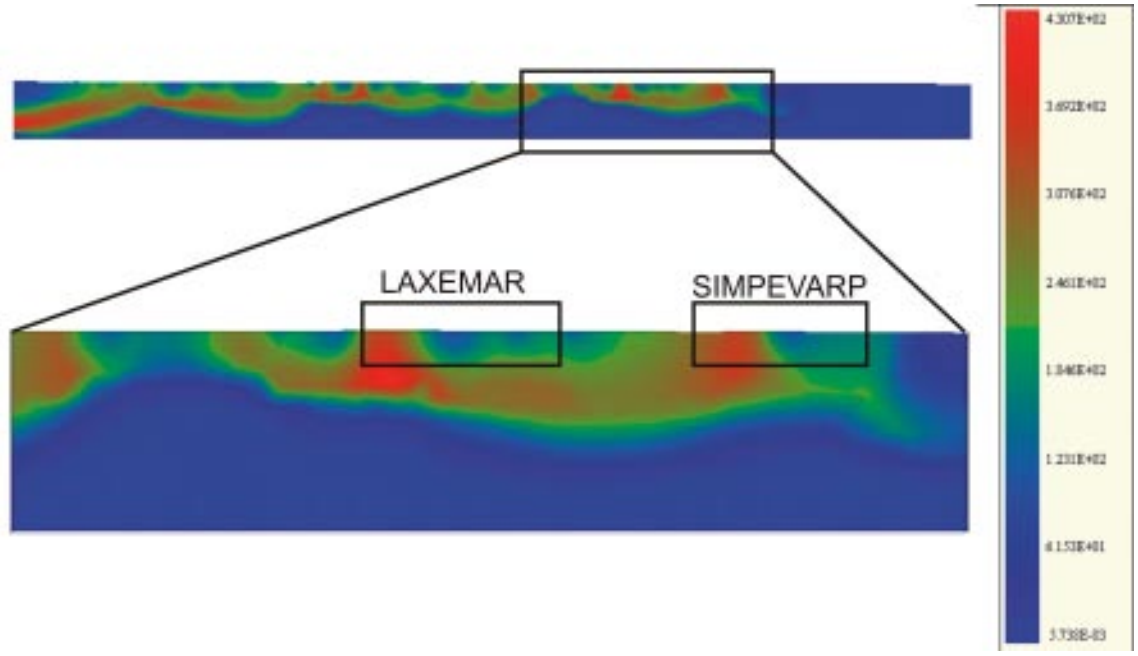

Figure 3-18. *Simulated tritium contents in Laxemar and Simpevarp subareas at year 1970.*

Figure 3-19 shows the simulated tritium content in year 1993. The advective front of "modern" water infiltrated during the 1950's–1970's can be seen in Laxemar area at a depth of about 800–900 m.

Figure 3-20 show computed and measured values of tritium activities at borehole KLX02 in year 1993.

A certain overestimation of tritium content is observed, which can be attributed to the fact that the upper soil layer is not considered in this model, thus imposing the effective bedrock recharge directly on the top boundary. As a result, the travel time from the surface to the massive rock is neglected, which gives rise to a lesser degree of radioactive decay.

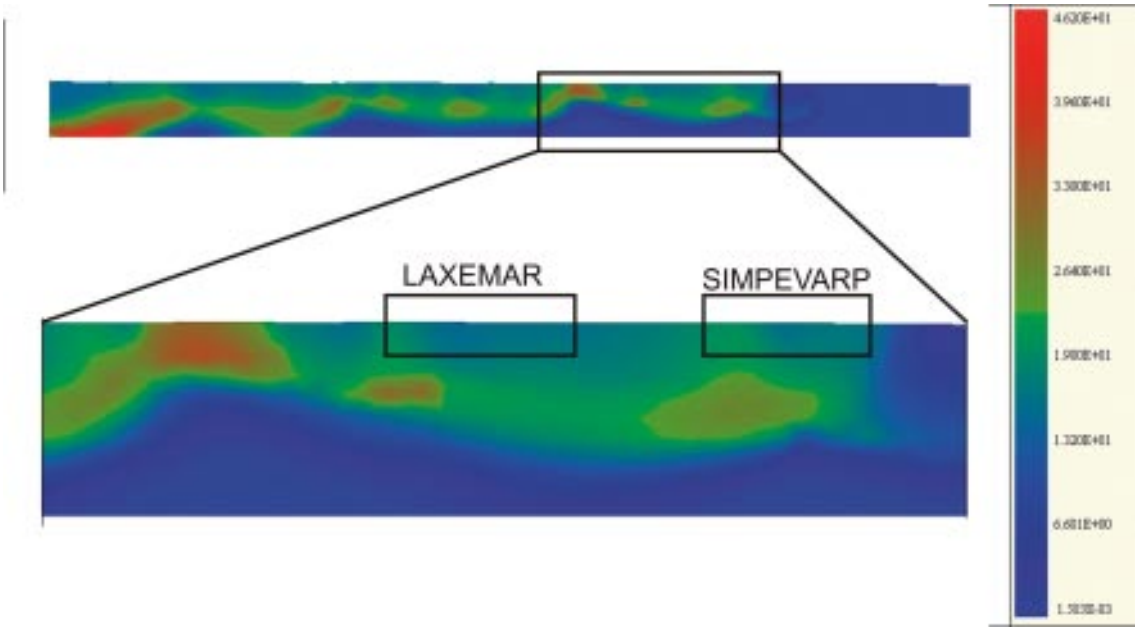

Figure 3-19. *Simulated tritium contents in Laxemar and Simpevarp subareas at year 1993.*

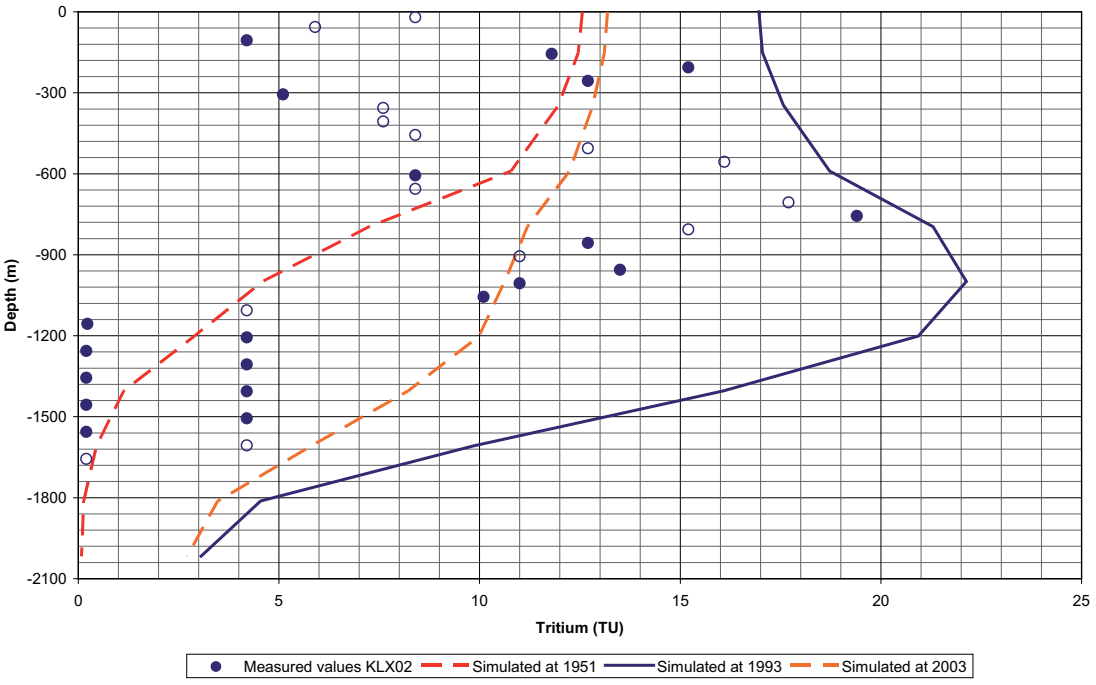

Figure 3-20. *A detail of Tritium evolution in KLX02 and KLX03 in 1951–2003 period.*

In spite of the rough representation of the actual domain, the model is able to provide tritium concentration patterns which are qualitatively comparable to those measured at borehole KLX02, with a concentration peak located at approx. 900 m of depth. This can be observed at Figure 3-20 where computed results of 1951, 1993 and 2003 have been plotted.

Care should be taken when dealing with tritium concentration data since, as was stated above, tritium distribution at a given time represents the result of the combined effect of both transport and radioactive decay. For instance, three-dimensional hydrogeological models, developed by the ConnectFlow Team in the framework of the Hydronet Group, are able to reproduce measured tritium activities in 2003 /see Hartley et al. 2005/. Their results could be regarded as an appropriate approach in light of the comparison with the measured values at boreholes KSH02 and KSH03A in 2003 (Figures 3-21 and 3-22). Nevertheless, the attempt to make a comparison with measured data at borehole KLX02 (Figure 3-23) shows a much poorer agreement. It is worth noting that model results shown in Figure 3-23 correspond to year 2005 whilst tritium data at KLX02 were measured (most of them) at 1993. Irrespective of any other consideration, computed and measured values at KLX02 /as presented in Hartley et al. 2005/ must necessarily fail in this comparison. As can be observed in Figure 3-20, the results obtained by a much simpler 2-D model are capable of reproducing qualitatively a tritium peak at a depth of 800–900 m in KLX02 at year 1993. Such a peak can also be observed in the measured tritium activities at KLX02 borehole (Figure 3-20).

It is worth noting that in the context of the ChemNet Group, correction of measured tritium data (in order to account for radioactive decay) has been used for normalizing tritium concentration to a given reference date (year 2000 usually). However, even though the method is strictly valid when applied to stagnant water, it lacks applicability whenever the actual conditions are such that fluid is in movement, as it is the case in Laxemar subarea.

The invalidity of the “normalization for decay” can be demonstrated by means of the two-dimensional model described above, which can simulate the spatial distribution of tritium in years 1993 and 2003. The numerical model presented here may be taken as a ‘synthetic reality’. This does not necessarily imply the ability to reproduce accurately the actual physicochemical processes taking place in the Simpevarp area but rather the ability to provide conceptual insight into the qualitative response of the system defined as the model domain. If this is the case, it should be noticed that the “synthetic reality” computed at 2003 is markedly different than the “synthetic reality” computed at 1993 and then normalized by decay to 2003 (Figure 3-24). As a consequence, the applicability of the normalization method can be putted in question and should be avoided in the future work of the ChemNet Group. Measured data “normalized” for decay do not account for solute transport and, “corrected” values are neither not representative for the actual date of measurement nor for the corrected date. The simultaneity of fluid movement and radioactive decay should always be considered together in a dynamic system such as Laxemar.

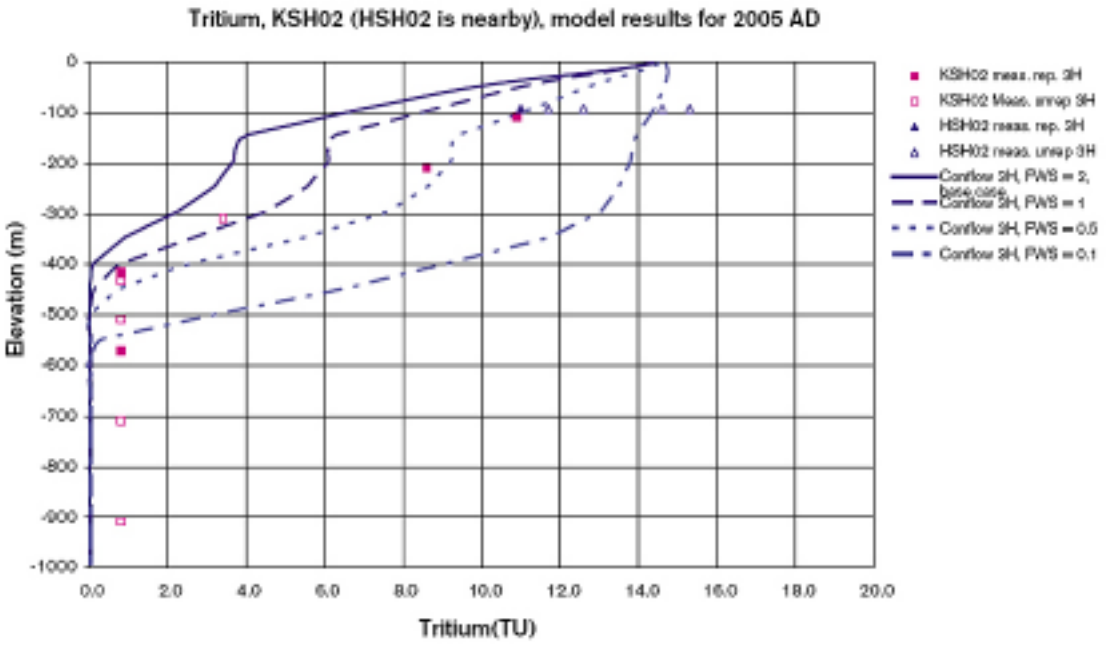

Figure 3-21. *Comparison of measured and computed tritium activities at KSH02 borehole /after Hartley et al. 2005/.*

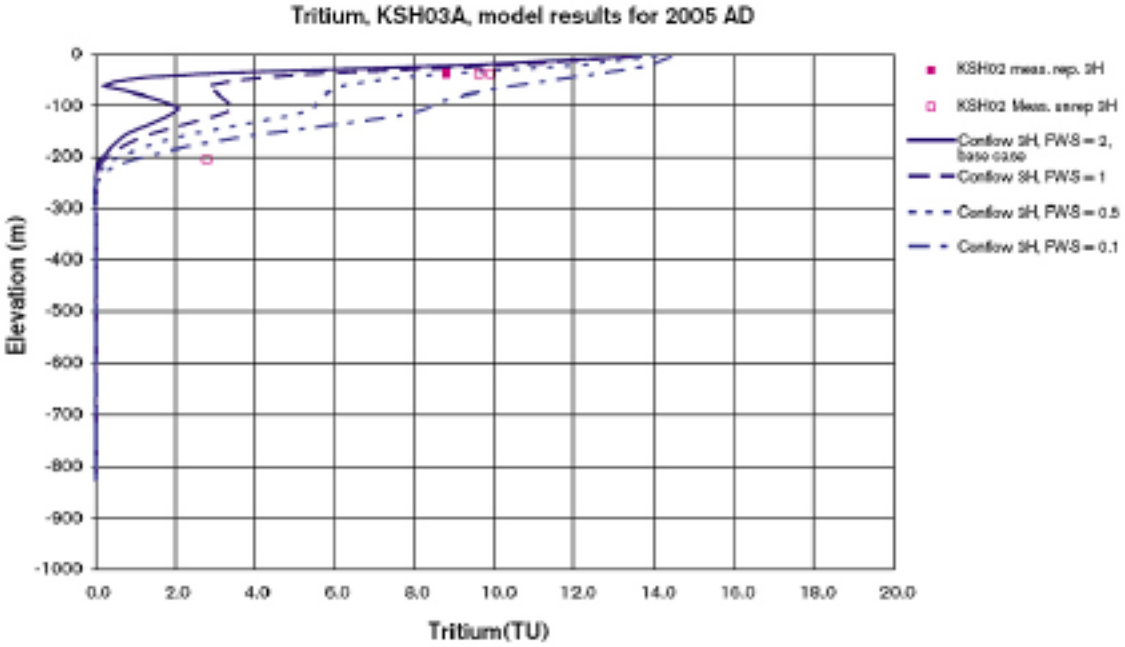

Figure 3-22. *Comparison of measured and computed tritium activities at KSH03 borehole /after Hartley et al. 2005/.*

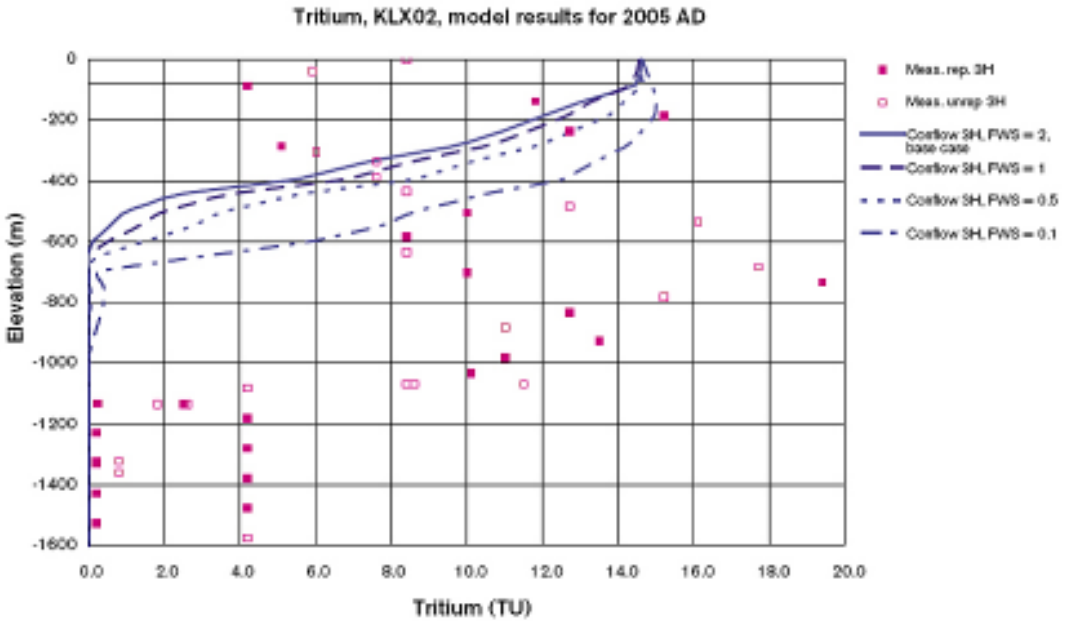

Figure 3-23. *Comparison of measured and computed tritium activities at KLX02 borehole /after Hartley et al. 2005/.*

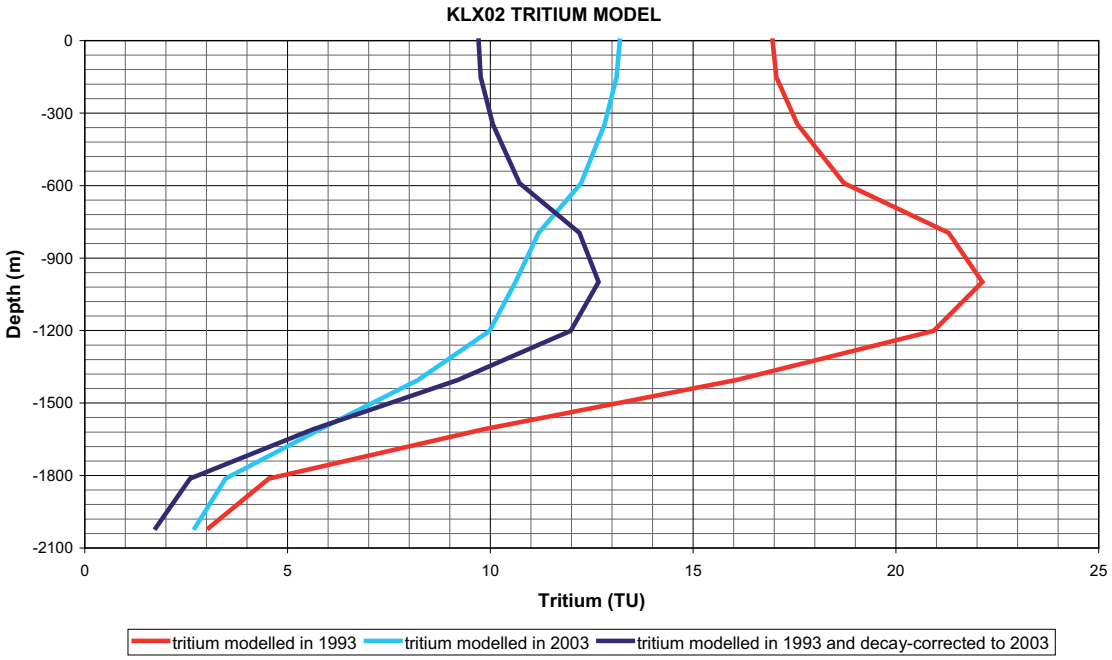

Figure 3-24. *Tritium distribution obtained by CORE2D (coupling flow and reactive transport) for years 1993 and 2003, compared to computed tritium at 1993 and then "normalized" to year 2003.*

4 Conclusions

A specific application for spatial analysis and visualization of hydrochemical information has been developed and applied to the Laxemar 1.2 database. This tool allows combination of hydrochemical and isotopic data, geographic and geometric references, and geo-hydrological discrete features.

Spatial analysis of the near-surface hydrochemical database reveals specific signatures consistent with the influence of older and more saline groundwater than the rest of the representative samples from soil pipes. These hydrogeochemical signatures at the near surface environment could constitute an indication of a groundwater discharge zone or stagnant older water that has been preserved under low permeable soil cover. It is worth noting that, at the present time, there is no available isotopic information for soil pipes at the Laxemar subarea.

Spatial analysis of the bedrock hydrochemical database indicates that dilute groundwaters of Na-HCO_3 type dominates at the Laxemar subarea reaching considerable depths, whilst this kind of water is confined to shallow depths at Simpevarp subarea. This is consistent with the hydrogeological framework of the site, where the dynamic fresh water body is thicker inland and much thinner at the coastal areas. In addition, diluted groundwater with higher bicarbonate concentrations coincides also with higher total iron concentrations. This observation could be attributed to microbially-mediated anaerobic respiration of DOC, through the reduction of iron (III) minerals, as it was postulated to explain the bicarbonate concentrations found in fresh waters during the Redox Zone Experiment of the Äspö HRL.

Brackish and saline groundwater is present at shallow to intermediate depth at the Simpevarp subarea, but at greater depths (down to 800–900 m) at the Laxemar subarea. The origin of these waters could be different from one place to another. At the Simpevarp subarea, brackish and saline waters show some residual marine signatures (Littorina) together with clear glacial isotopic signatures. In contrast, brackish and saline waters at Laxemar can be attributed to a relatively narrow dispersion zone between highly saline old and deep waters and diluted waters with recent (modern) meteoric origin.

A two-step methodology for numerical modelling of density-dependent flow and reactive solute transport has been developed and tested. The flow field with variation of fluid density is first calculated with the SUTRA code. The computed flow field and boundary flow rates are used as an input for the $CORE^{2D}$ code, which allows solving for reactive solute transport problems. This methodology has been applied to solve a 2D large-scale model with an accurate representation of the site topography. It is shown that, in spite of the 2D simplification of the flow pattern, the model is able to reproduce measured salinity trends both at inland and coastal zones of the Simpevarp area.

The numerical model has also been used to simulate the transient behaviour of dissolved tritium in groundwaters. Initial conditions of dissolved tritium have been generated by a long-term run of the model, prior to the nuclear bomb tests performed during 1953–1976. After that period, the Ottawa time series of atmospheric tritium has been adopted as the top boundary condition in the infiltration water.

A certain overestimation of tritium content is computed numerically, which is attributed to the fact that the upper soil layer is not considered in the present version of the numerical model, thus imposing the effective bedrock recharge directly on the top boundary. As a result, the travel time from the surface to the bedrock (including unsaturated zone) is neglected, which gives rise to a lesser degree of radioactive decay. However, in spite of all the inherent simplification in the modelling approach, a tritium peak located at a depth of about 900 m – at the equivalent position of KLX02 borehole – is computed. These computed results are in a qualitative agreement with the available observations performed at KLX02 in 1993.

Finally, the numerical model has been used to analyse the applicability of the normalization method that is being used regularly by ChemNet for handling tritium data. The invalidity of the “normalization for decay” method can be demonstrated by means of the coupled transport and decay model performed here. It is proposed to avoid correcting tritium measurements in the future.

5 References

Banwart S, Laaksoharju M, Pitkänen P, Snellman M, Wallin B, 1995. Development of a site scale model for reactive element dynamics. In: The Redox Experiment in Block Scale. Final Reporting of Results from the Three year Project. Chapter 6. Steven Banwart (ed). SKB PR-25-95-06, Svensk Kärnbränslehantering AB.

Banwart S, Tullborg E-L, Pedersen K, Gustafsson E, Laaksoharju M, Nilsson A-C, Wallin B, Wikberg P, 1996. Organic carbon oxidation induced by large-scale shallow water intrusion into a vertical fracture zone at the Äspö Hard Rock Laboratory (Sweden). Journal of Contaminant Hydrology, 21, 115–125.

Banwart S, 1999. Reduction of iron (III) minerals by natural organic matter in groundwater. Geochim. Cosmochim. Acta, 63, 2919–2928.

Banwart S, Gustafsson E, Laaksoharju M, 1999. Hydrological and reactive processes during rapid recharge to fracture zones. The Äspö large scale redox experiment. App. Geochem. 14, 873–892.

Clark I, Fritz P, 1997. Environmental Isotopes in Hydrogeology. Lewis Publishers. Boca Raton, Florida. 328 pp.

Gimeno M J, Auqué L, Gómez L, 2004. Explorative analyses and mass balance modelling. In: Hydrochemical evaluation of the Simpevarp area, model version 1.2. Appendix 2. SKB R-04-74, Svensk Kärnbränslehantering AB.

Hartley L, Hoch A, Hunter F, Jackson P, Marsic N, 2005. Regional simulations – Numerical modelling using ConnectFlow. Preliminary site description Simpevarp subarea – version 1.2. SKB R-05-12, Svensk Kärnbränslehantering AB.

Laaksoharju M, 1999. Groundwater characterisation and modelling: problems, facts and possibilities. Ph.D. dissertation. Department of Civil and Environmental Engineering. Royal Institute of Technology (KTH). Stockholm.

Laaksoharju M, Smellie J, Gimeno M, Auqué L, Gómez J, Tullborg E-L, Gurban I, 2004. Hydrogeochemical evaluation of the Simpevarp area, model version 1.1. SKB R 04-16, Svensk Kärnbränslehantering AB, 398 p.

Molinero J, 2000. Testing and Validation of Numerical Models of Groundwater Flow, Solute Transport and Chemical Reactions in Fractured Granites. PhD Thesis, Civil Engineering School, University of A Coruña, Spain. (Latter published as ENRESA Publicación Técnica 06/01).

Molinero J, Raposo J, 2004. Coupled hydrogeological and reactive transport modelling In: Hydrochemical evaluation of the Simpevarp area, model version 1.2. Appendix 6. SKB R-04-74, Svensk Kärnbränslehantering AB.

Molinero J, Samper J, 2004. Modeling Groundwater Flow and Solute Transport in Fracture Zones: Conceptual and Numerical Models of the Redox Zone Experiment at Äspö (Sweden). Journal of Hydraulic Research, 42, 157–172.

Molinero J, Samper J, Zhang G, Yang C B, 2004. Biogeochemical reactive transport model of the Redox Zone Experiment of the Äspö Hard Rock Laboratory in Sweden. Nuclear Technology, 148, (to appear in Nov. 2004), in press.

Pedersen K, Arlinger J, Jahromi N, Ekendahl S, Hallbeck L, 1995. Microbiological investigations. In: The Redox Experiment in Block Scale. Final Reporting of Results from the Three year Project. Chapter 7. Steven Banwart (ed). SKB PR-25-95-06, Svensk Kärnbränslehantering AB.

Rhén I, Bäckbom G, Gustafson G, Stanfors R, Wikberg P, 1997. Results from pre-investigations and detailed site characterization. Summary report. SKB TR 97-03, Svensk Kärnbränslehantering AB.

Samper J, Delgado J, Juncosa R, Montenegro L, 2000. CORE2D v 2.0: A Code for non-isothermal water flow and reactive solute transport. User's manual. ENRESA Technical report 06/2000.

Svensson U, 1996. SKB Palaeohydrogeological programme. Regional groundwater flow due to advancing and retreating glacier-scoping calculations. In: SKB Project Report U 96-35, Svensk Kärnbränslehantering AB.

Thompson D, Brown J, Ford R, 2001. OPENDX Paths to Visualization. Visualization and Imagery Solutions, Inc. 207 p.

Tullborg E-L, 1995. Mineralogical/Geochemical investigations in the Fracture Zone. In: The Redox Experiment in Block Scale. Final Reporting of Results from the Three year Project. Chapter 4. Steven Banwart (ed). SKB PR-25-95-06, Svensk Kärnbränslehantering AB.

Tullborg E-L, Gustafsson E, 1999. ^{14}C in biocarbonate and dissolved organics – a useful tracer? Applied Geochemistry, 14, 927–938.

Voss C I, Provost A M, 2003. SUTRA, A model for saturated-unsaturated variable-density ground-water flow with solute or energy transport. U.S. Geological Survey Water-Resources Investigations Report 02-4231, 250 p.

Appendix 6

Groundwater data for Laxemar 1.2

This data set is stored in the SKB database SIMONE.

The loggfile used in SICADA to create the data set is stored in the database SIMONE.

Appendix 7

Groundwater data from Nordic sites

This data set is stored in the SKB database SIMONE.